

# **Inducing the Chemodiversity of *Fucus vesiculosus*-Derived Fungi by OSMAC Strategy for Discovery of New Anticancer Leads**

## **Dissertation**

for the Academic Degree Dr. rer. nat.  
Faculty of Mathematics and Natural Sciences  
Christian-Albrechts-University Kiel  
GEOMAR Helmholtz Centre for Ocean Research Kiel

Presented by

**BICHENG FAN**

M.Sc in Microbiology and Biochemical Pharmacy  
China State Institute of Pharmaceutical Industry (CSIPI), Shanghai, China

Supervised by

**Prof. Dr. Deniz Tasdemir**

Kiel, 2020

First examiner: Prof. Dr. Deniz Tasdemir

Second examiner: Prof. Dr. Antje Labes

Defense date: 30/06/2020

## ACKNOWLEDGMENTS

Firstly and foremost I would like to express my sincere gratitude to my research supervisor Prof. Dr. Deniz Tasdemir for her continuous support of my Ph.D. study and related research, for her patience, motivation, and immense knowledge. Her guidance helped me in all the time of the research for this Ph.D. thesis. It was a great privilege and honor to work and study under her guidance. I would also like to thank her for her friendship and empathy. I would also like to thank Prof. Antje Labes for introducing me into marine fungi and helping to present my research outcomes as clearly as possible. I wish to express my most sincere gratitude to Dr. Martina Blümel for her continuous care, time, patience and daily supervision in microbiology part of my thesis for the last almost 4 years.

I would like to extend my thanks to Prof. Dr. Frank Sönnichsen and his group members Gitta Kohlmeyer-Yilmaz and Marion Höftmann for their kindly help in running NMR measurements. Also I want to thank to Prof. Dr. Alfonso Mangoni and his colleague Laura Grauso for carrying out DFT calculations in Italy in the unusual time of a coronavirus pandemic. Without your support, it would be impossible to progress with my research.

I am extremely grateful to Dr. Delphine Parrot, Dr. Pradeep Dewapriya and Dr. Fengjie Li, for their support in experimental design, dereplication, and structure elucidation. I would like to acknowledge the assistance of our technicians Jana Heumann and Arlette Wenzel-Storjohann for performing the anticancer assays. Also, I would like to express my sincere thanks to the whole GEOMAR Centre for Marine Biotechnology team. I have experienced four happy years of intense research, having a friendly and stimulating working environment in our research group.

I also express my gratitude to the China Scholarship Council (CSC) for their financial support, without which, this Ph.D. thesis would not have been possible. In addition, Christian-Albrecht University of Kiel (CAU) is also acknowledged for offering different courses, high quality student services and nice activities. I would also thank for Integrated School of Ocean Science (ISOS) for providing useful soft-skill training courses.

Finally, I would especially like to thank my parents for their love, care and sacrifices for educating and preparing me for my future. Last but not least, I am very much thankful to my wife Dan and my son Hongyi for their love, understanding and continuous support that enabled me to complete this research.



## Contents

<b>List of abbreviations</b> .....	<b>i</b>
<b>Summary</b> .....	<b>v</b>
<b>Zusammenfassung</b> .....	<b>vii</b>
<b>GENERAL INTRODUCTION</b> .....	<b>1</b>
<b>1. Marine fungi</b> .....	<b>3</b>
<b>2. Macroalgae-derived fungi</b> .....	<b>5</b>
2.1. Fungal abundance in macroalgae .....	5
2.2. Macroalgae-derived fungi as source of anticancer lead compounds discovery .....	6
2.3. Chemical prospecting of <i>Fucus</i> -derived fungi .....	8
<b>3. The fungal genus <i>Pyrenochaetopsis</i> sp.</b> .....	<b>9</b>
<b>4. Activation of silent biosynthetic gene clusters (BGCs)</b> .....	<b>11</b>
4.1. Approaches to activate silent BGCs for inducing chemical space.....	11
4.2. One-Strain-Many-Compounds (OSMAC).....	13
4.3. Application of OSMAC strategy to marine fungi .....	14
<b>5. Molecular networking-based metabolomics</b> .....	<b>17</b>
5.1. Advantages of molecular networking .....	17
5.2. Molecular networking as a dereplication tool.....	18
5.3. Bioactivity-based molecular networking for rapid discovery of bioactive natural products .....	19
<b>6. Research objective</b> .....	<b>21</b>
References.....	22
<b>II. RESULTS</b> .....	<b>31</b>
Chapter 1. Influence of OSMAC-Based Cultivation in Metabolome and Anticancer Activity of Fungi Associated with the Brown Alga <i>Fucus vesiculosus</i> .....	33
Chapter 2. Pyrenosetin A-C, New Decalinoylspirotetramic Acid Derivatives Isolated by Bioactivity-Based Molecular Networking from the Seaweed-Derived Fungus <i>Pyrenochaetopsis</i> sp. FVE-001 ....	61
Chapter 3. Pyrenosetin D, A New Pentacyclic Decalinoyltetramic Acid Derivative from the Algicolous Fungus <i>Pyrenochaetopsis</i> sp. FVE-087 .....	79
<b>III. DISCUSSION AND OUTLOOK</b> .....	<b>93</b>
<b>1. Discussion</b> .....	<b>95</b>
<b>2. Outlook</b> .....	<b>101</b>
References.....	103
<b>IV. APPENDIX</b> .....	<b>107</b>
1. Table 1. Natural products reported from algicolous fungi with anticancer potential .....	109
References.....	151
2. Strain list and MN data for Chapter 1 .....	157
3. Bioactivity data and NMR spectral data of Chapter 2 .....	200
4. NMR spectra and DFT calculation tables of Chapter 3 .....	217



**List of abbreviations**

<b>Abbreviation</b>	<b>Explanation</b>
22Rv1	Human prostate carcinoma cell line
5-Aza	5-Azacitidine
786-O	Hypertriploid renal carcinoma cell line
A2780	Human ovarian cancer cell line
A2780 CisR	Human ovarian cancer cell line-cisplatin resistant
A-375	Human malignant melanoma cell line
A-375-S2	Human malignant melanoma cell line-S2
A549	Human lung carcinoma cancer cell line
ACHN	Human renal cell carcinoma cell line
Balb3T3	Mouse fibroblast cell line
BALL-1	Human leukemic B cell line
BEL-7402	Human hepatocellular carcinoma cell line
BGC	Biosynthetic gene cluster
BGC823	Human gastric cancer cell line
BSY-1	Human breast cancer cell line
BT549	Human triple-negative breast cancer cell line
Caco-2	Human epithelial colorectal adenocarcinoma cell
CaMKIII	Calmodulin-dependent protein kinase III
CARD-FISH	Catalyzed reporter deposition fluorescent in situ hybridization
CHIKV	Chikungunya virus
CMF-ID	Competitive fragmentation modeling for metabolite identification
COSY	Correlation spectroscopy
CRISPR/Cas9	Clustered regularly interspaced short palindromic repeats/Cas9
CYP1A	Cytochrome P450, family 1, subfamily A, polypeptide 1
Cza	Czapek medium
DESI-IMS	Desorption electrospray ionization--imaging mass spectrometry
DFT	Density functional theory
DMS114	Human non-small cell lung cancer cell line
DNA	Deoxyribonucleic acid
DNP	Dictionary of natural products
DPPH	2,2-Diphenyl-1-picrylhydrazyl
Du145	Human prostate cancer cell line
EAC	Ehrlich-Lette ascites carcinoma cell line
EC <sub>50</sub>	Half effective concentration
ED <sub>50</sub>	Median effective dose
ETP	Epipolythiodiketopiperazine
FDA	U. S. Food and drug administration
GI50	Half maximal growth inhibition concentration
GNPS	Global Natural Products Social molecular networking
H125	Human non-small cell lung cancer cell line
H1975	Human non-small cell lung cancer cell line
H446	Human non-small cell lung cancer cell line
HCC-298	Human hepatocellular carcinoma cell line
HCC2998	Human colon adenocarcinoma cell line
HCT116	Human colon cancer cell line
HCT-15	Human colon adenocarcinoma cell line
HeLa	Human cervical cancer cell line
Hep1c1c7	Murine hepatoma cancer cell line
HepG2	Human hepatoma cancer cell line

LIST OF ABBREVIATIONS

HL-60	Human leukemia cancer cell line
HLE	Huma hepatoma cancer cell line
HM02	Gastric carcinoma cell line
HMBC	Heteronuclear multiple bond correlation
HMEC	Human mammary epithelial cell line
HSQC	Heteronuclear single quantum correlation
HT29	Human colon cancer cell line
Hub7	Human hepatoma cancer cell line
IC <sub>50</sub>	Half maximal inhibitory concentration
ISDB	<i>In-silico</i> database
K562	Human immortalised myelogenous leukemia cell line
KB	Human epidermoid carcinoma cell line
L1210	Murine lymphoma cell line
LC <sub>50</sub>	Median lethal concentration
LD <sub>50</sub>	Median lethal dose
LH1210	Murine lymphoma cancer cell line
LM3	Mouse mammary tumor cell line
LNCaP	Human prostate adenocarcinoma cell line
MAF	Marine algicolous fungi
MCF-7	Michigan cancer foundation-7, human immortalised cell line
MDA-MB-231	Human breast cancer cell line
MDA-MB-435	Human breast cancer cell line
MFNP	Marine fungal natural product
MIC	Minimum inhibitory concentration
MKN	Gastric adenocarcinoma cell line
MN	Molecular networking
Molt-4	Human acute lymphoblastic leukemia cancer cell line
mTOR	Mammalian target of rapamycin
NCI-H23	Human lung adenocarcinoma cancer cell line
NCI-H460	Human large-cell carcinoma cancer cell line
NCI-H522	Human non-small cell lung cancer cell line
NMR	Nuclear magnetic resonance
NOESY	Nuclear overhauser effect spectroscopy
NUGC-3	Human gastric carcinoma cancer cell line
OSMAC	One-Strain-Many-Compounds
OS-RC-2	Human renal carcinoma cancer cell line
OVCAR-3	Human ovarian carcinoma cancer cell line
P388	Murine leukemia cancer cell line
PANC-1	Human pancreatic cancer cell line
PC-3	Human prostate cancer cell line
PDM	Potato dextrose medium
PKS-NRPS	Polyketide synthase-nonribosomal peptide synthase
psu	Pfvractical salinity unit
PTK	Protein tyrosine kinase
SAHA	Suberoylanilide hydroxamic acid
SK-OV-3	Human ovarian cancer cell line
SM	Secondary metabolite
SMMC-7721	Human hepatocarcinoma cell line
SNB75	Human glioblastoma cell line
SPE	Solid-phase extraction
SW1353	Human chondrosarcoma cell line
SW-48	Human colonic adenocarcinoma cell line
SYM	Sucrose yeast medium
TBARS	Thiobarbituric acid reactive substances



## LIST OF ABBREVIATIONS

THP-1	Human leukemia monocytic cell line
U937	Human macrophage cell line
UMUC3	Human bladder cancer cell
UNPD	Universal natural products database
WM	Modified Wickerham medium

## LIST OF ABBREVIATIONS

## Summary

Algae-derived (algicolous) fungi has been regarded as an important source for discovery of novel bioactive natural products. As one of the most-widespread brown algae that occur in the shallow coastal regions of Baltic Sea, *Fucus vesiculosus* provides habitat for many invertebrates and vertebrates. However, the fungal community associated with *F. vesiculosus* has not been investigated for their chemical constituents or bioactivity potential. This Ph.D. project aimed to pursue a culture-based approach to isolate fungi from *F. vesiculosus* for discovery of new anticancer lead compounds. In order to induce the chemical space of fungi associated with *Fucus vesiculosus*, an OSMAC approach that included variations in media composition and culture regimes (liquid/solid) was applied. The crude extracts of ten fungal isolates showed anticancer bioactivities against at least one cancer cell line under one culture condition. MS/MS-based molecular networking (MN) combined with bioactivity mapping was applied to those crude extracts, allowing the identification and prioritization of two endophytic fungal strain, *Pyrenochaetopsis* sp. FVE-001 and FVE-087 with anticancer activity. Both strains were selected for large-scale fermentation followed by massive metabolomics analysis and chemical work-up.

For *Pyrenochaetopsis* sp. FVE-001, a modified Kupchan partition method was applied to crude extract to separate the crude extract into three subextracts. Bioactivity was tracked to the chloroform subextract, which was fractionated on a C18 solid-phase extraction (SPE) cartridge. The anticancer activity was mapped onto molecular networks (the so-called bioactivity-based MN), and with the aid of additional bioinformatics application, the anticancer activity of the compounds in the network was predicted. The compound isolation was carried out in a targeted manner from the bioactive fractions to yield three new decalinoylspirotetramic acid derivatives, pyrenosetins A-C, and a known decalin derivative, phomasetin. As expected, pyrenosetins A and B showed strong inhibitory potential against malignant melanoma cell A-375 with IC<sub>50</sub> values of 2.8 and 6.3 μM, respectively.

The bioactivity-guided isolation of the second *Pyrenochaetopsis* sp. FVE-087 strain yielded one new decalinoyltetramic acid derivative, pyrenosetin D, and two known compounds wakodecalines A and B. Pyrenosetin D possesses an unusual pentacyclic ring system, which is rare in nature. Bioassay results showed that pyrenosetins D exhibited moderate anticancer bioactivity against A-375 with IC<sub>50</sub> value of 77.5 μM, while wakodecalines A and B were inactive.

The current study represents a successful application of OSMAC in inducing new compounds with anticancer activity in algicolous fungi. Further combination of MN and additional information layers such as bioactivity data has successfully led to rapid purification of new compounds pyrenosetins A-D from two *Fucus vesiculosus*-derived *Pyrenochaetopsis* sp. strains. This is the first study focusing on secondary metabolites of algal-derived *Pyrenochaetopsis* sp.

## SUMMARY

## Zusammenfassung

Algen-assoziierte (algalic) Pilze sind als wichtige Quelle für die Entdeckung neuartiger bioaktiver Naturstoffe bekannt. Als eine der in den flachen Küstenregionen der Ostsee am weitesten verbreiteten Braunalgenarten bietet *Fucus vesiculosus* Lebensraum für viele Wirbellose und Wirbeltiere. Die mit *F. vesiculosus* assoziierte Pilzgemeinschaft wurde jedoch bisher nicht hinsichtlich ihres Potentials zur Produktion bioaktiver Sekundärmetabolite untersucht. Dieses Promotionsprojekt verfolgte einen kulturbasierten Ansatz zur Isolierung von Pilzen aus *F. vesiculosus* zur Entdeckung neuer Wirkstoffe gegen Krebs. Um eine Vergrößerung des Sekundärmetabolitspektrums der mit *F. vesiculosus* assoziierten Pilze zu erreichen, wurde ein OSMAC-Ansatz angewendet, der Variationen in Medienzusammensetzung und Kulturregime (flüssig/fest) umfasste. Im Ergebnis zeigten die Rohextrakte von 10 Pilzstämmen eine Induktion der Bioaktivität gegen mindestens eine Krebszelllinie bei einer bestimmten Kulturbedingung. MS/MS-basierte molekulare Netzwerke (MN) der Rohextrakte in Kombination mit einer Kartierung der krebszell-inhibierenden Bioaktivität resultierten in der Identifikation und Priorisierung zweier endophytischer Pilzstämmen, *Pyrenochaetopsis* sp. FVE-001 und FVE-087. Beide Stämme wurden für die Fermentation in großem Maßstab ausgewählt, gefolgt von einer massiven Metabolomics-Analyse und ihrer chemischen Aufarbeitung.

Für *Pyrenochaetopsis* sp. FVE-001 wurde eine modifizierte Kupchan-Partitionierung angewendet, um den Rohextrakt in drei Unterextrakte zu trennen. Die krebszell-inhibierende Bioaktivität wurde im Chloroform-Subextrakt detektiert, welcher auf einer C18-Festphasenextraktionspatrone fraktioniert wurde. Mit Hilfe bioaktivitätsbasierter molekularer Netzwerke konnte die Antikrebszell-Aktivität der Verbindungen im Netzwerk vorhergesagt werden. Darauf basierend erfolgte die Isolierung von Sekundärmetaboliten gezielt aus den bioaktiven Fraktionen und ergab drei neue Decalinoylspirotetraminsäurederivate, Pyrenosetine A-C, und ein bekanntes Decalinderivat, Phomasetin. Wie erwartet zeigten die Pyrenosetine A und B eine starke Inhibition gegen maligne Melanomzellen A-375 mit  $IC_{50}$ -Werten von 2,8 bzw. 6,3  $\mu$ M.

Die bioaktivitäts-geleitete Isolierung des zweiten *Pyrenochaetopsis* sp. -Stamms FVE-087 ergab ein neues Decalinoyltetraminsäurederivat, Pyrenosetin D sowie zwei bekannte Substanzen, Wakodecaline A und B. Die neue Verbindung Pyrenosetin D besitzt ein ungewöhnliches, in der Natur selten vorkommendes pentacyclisches Ringsystem. Ergebnisse der *in vitro* Bioassays zeigten, dass Pyrenosetin D eine moderate Bioaktivität gegen die Melanom-Zelllinie A-375 mit einem  $IC_{50}$ -Wert von 77,5  $\mu$ M aufwies, wohingegen die Wakodecaline A und B inaktiv waren.

Die aktuelle Arbeit stellt eine erfolgreiche Anwendung von OSMAC für die Induktion neuer Moleküle mit Antikrebs-Aktivität in algalen Pilzen dar. Des Weiteren hat die cheminformatische Kombination von MN mit zusätzlichen Informationsebenen aus Bioaktivitätsdaten erfolgreich zu einer schnellen und gezielten Isolierung der neuen Verbindungen Pyrenosetine A-D aus zwei mit *Fucus vesiculosus* assoziierten *Pyrenochaetopsis* sp. Stämmen beigetragen. Dies ist die erste Studie, die sich mit Sekundärmetaboliten von *Pyrenochaetopsis* sp. beschäftigt.

## ZUSAMMENFASSUNG

---

# I. GENERAL INTRODUCTION

---





## GENERAL INTRODUCTION

### 1. Marine fungi

Marine fungi represent a large ecological group of eukaryotic microorganisms. They are widely distributed in a variety of marine environments, ranging from deep-sea to coastal habitats and including water, sediments, ice covers, shallow sea rocks or associations with other organisms (Ogaki *et al.*, 2019; Rédou *et al.*, 2015; Zain ul Arifeen *et al.*, 2019). According to their lifestyle, marine fungi can be divided into two groups, namely obligate and facultative (Kohlmeyer and Kohlmeyer, 1979). Based on the currently accepted definition, obligate marine fungi are those living exclusively in the marine environment (e.g. *Ascochyta salicorniae*) (Osterhage *et al.*, 2000), while facultative marine fungi are those adapted to both marine and terrestrial or freshwater environments (e.g. *Aspergillus candidus*) (Rateb and Ebel, 2011; Vala, 2010). Recent molecular studies have revealed that marine habitats contain a vast array of obligate and facultative marine fungi, and these coexisting fungi represent one of the most underutilized biological resources for discovery of new species as well as of novel natural products (Jones *et al.*, 2015; Overy *et al.*, 2014; Reich and Labes, 2017). A high abundance of marine fungal species is reported in marine holobionts such as corals and sponges (Amend *et al.*, 2012; Li and Wang, 2009). Research on marine fungi can be traced back to 1915, with the identification of new fungi from the brown alga *Pelvetia* sp. (Sutherland, 1915). Until 2015, 1,112 marine fungal species belonging to 472 genera were reported from different marine habitats, with a slow but steady increase to 1,257 in 2019 (Jones *et al.*, 2019; Jones *et al.*, 2015). With regard to the large and yet underexplored marine habitat diversity including numerous holobionts, Jones *et al.* considered the current number of identified marine fungal species an underestimation and estimates > 10,000 marine fungal species in the marine environment (Jones, 2011; Jones *et al.*, 2015). Compared to other habitats, the marine environment features harsh conditions, and marine fungi are exposed to a number of stressors. High or very low salinity, low oxygen content, nutrient limitation but also eutrophication, potential desiccation due to water level differences (tides), high hydrostatic pressure, changes in UV radiation intensity, grazing, microbial competition with bacteria are only some potential stressors of marine fungi (Jones, 2000; Núñez-Pons *et al.*, 2018). Adaptation to these various stressors resulted in the evolution of sometimes unique gene clusters in marine fungi (Kumar *et al.*, 2018; Orsi *et al.*, 2015). This also affects their enzyme systems, leading to a remarkable chemical difference between marine and terrestrial fungi. Screening of carbohydrate-active enzymes and sugar transporters in the genome of the marine fungus *Calcarisporium* sp. revealed that the enzymes were specialized for algae and animal degradation, suggesting the adaption of its lifestyle to marine environment (Kumar *et al.*, 2018). Another result of this adaptation to challenges is the production of novel bioactive compounds (Ji and Wang, 2016; Petersen *et al.*, 2020). As an example, the marine fungus *Pestalotia* sp. produced the chlorinated benzophenone pestalone showing antibiotic activity in response to marine bacterial challenge (Figure 1a) (Cueto *et al.*, 2001). Since marine fungi remain largely unexplored for their potential as sources of bioactive natural products, there is a great need for seeking bioactive natural products from marine fungal resources.

## GENERAL INTRODUCTION

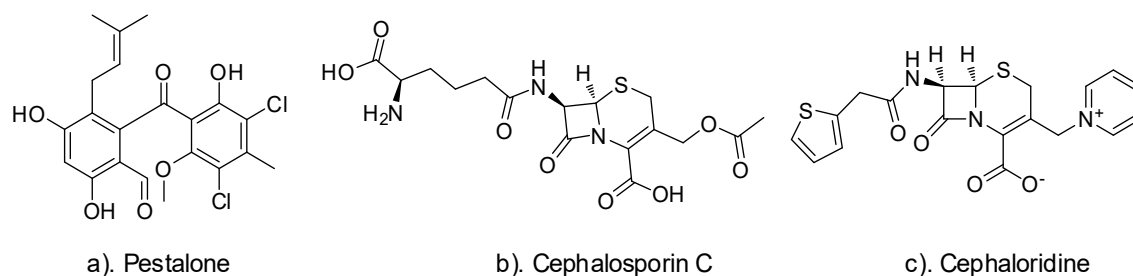


**Figure 1.** Structures of representative bioactive compounds associated with marine fungi. a). Pestalone (isolated from *Pestalotia* sp. co-cultured with marine bacteria) with antibiotic activity against methicillin-resistant *Staphylococcus aureus* and vancomycin-resistant *Enterococcus faecium*. b). Cephalosporin C (origin: *Acremonium chrysogenum*) c). Cephalosporin C-derived drug cephaloridine which is in clinical application as an antibiotic (against *Streptococcus*, *Staphylococcus* and *Pneumococcus* infections).

Marine fungi have long been neglected as a research subject, but nowadays they receive increasing attention for their ecological roles, their evolutionary complexity as well as for natural product prospecting (Gutiérrez *et al.*, 2011; Imhoff, 2016; Richards *et al.*, 2012). The total number of reports related to marine fungi increased from 10 papers in 1997 to around 500 publications in 2014 (Figure 2) (Overy *et al.*, 2014). This rise in interest of the scientific community was mainly due to the finding that marine fungi produce specific, structurally diverse metabolites, often with novel, pharmaceutically relevant bioactivities (Imhoff, 2016; König *et al.*, 2006). Those marine fungal natural products (MFNPs) have been regarded as promising resources for developing new drugs (Gomes *et al.*, 2015; Silber *et al.*, 2016). For example, the second generation  $\beta$ -lactam type natural antibiotic cephalosporin C (Figure 1b) was purified from the Mediterranean-seawater derived fungus *Acremonium chrysogenum*. It served as a lead compound for the development of the clinically used antibiotic cephaloridine (Figure 1c) (Bugni and Ireland, 2004; Murdoch *et al.*, 1964).

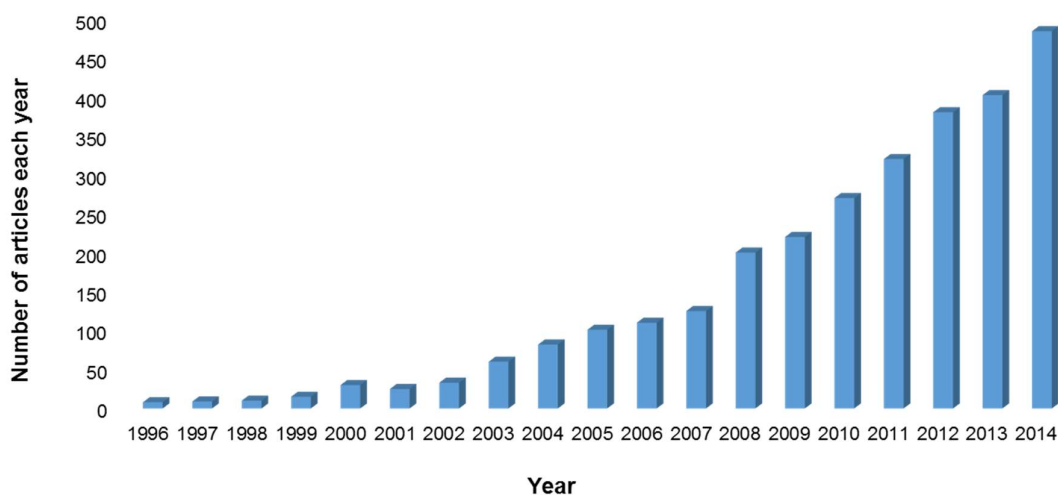


**Figure 2.** Development of scientific publications on marine fungi. The number of articles from 1996 until 2014 that include either the term ‘marine-derived fungi’ or ‘sponge-derived fungi’ in title, abstract, or keywords. Picture was adapted from Overy *et al.*, 2014.

## 2. Macroalgae-derived fungi

### 2.1. Fungal abundance in macroalgae

Macroalgae, or seaweeds, refer to a group of plant-like multicellular photosynthetic eukaryotes that include several types of organisms such as *Rhodophyta* (red), *Phaeophyta* (brown) and *Chlorophyta* (green) algae (Figure 3) (Madhusudan *et al.*, 2011). They are widely distributed mostly in shallow marine areas, ranging from tropical sea beaches to Antarctica. Seaweeds play an important role in the aquatic ecosystem by providing food and habitat for marine macrobiota (e.g. invertebrates and fishes) (Fulton *et al.*, 2019; Wikström and Kautsky, 2007). Recently, the close relationship between host and the microbiota intimately associated with these hosts physically but also functionally has been conceptualized as ‘holobiont’ (Egan *et al.*, 2013; Margulis, 1990; O’Malley, 2017). Similar to most marine holobionts, seaweeds harbor a diverse number and assemblage of microorganisms, such as bacteria, fungi, and viruses (Egan *et al.*, 2013). Fungi have been reported as common residents on the surfaces (epiphytes) or in the inner tissues as endophytes of different marine macroalgae (Abdel-Gawad *et al.*, 2014; Flewelling *et al.*, 2013b). In total, more than 150 fungal species were reported from diverse algal species, as reviewed by Ji and Wang (2016). Bioprospecting of endophytes from North Atlantic marine macroalgae resulted in the isolation of a total number of 632 fungal strains belonging to 79 different species. (Flewelling *et al.*, 2013b). Additionally, a study investigating the microbial diversity of algal surfaces from the Red Sea showed high taxonomic diversity of the fungal epiphytes including a wide range of fungal orders such as Capnodiales, Pleosporales and Hypocreales (Abdel-Gawad *et al.*, 2014). These reports impressively underline, that fungi are frequently found in different algal species, implying that they are important “associates” in marine algal holobionts.

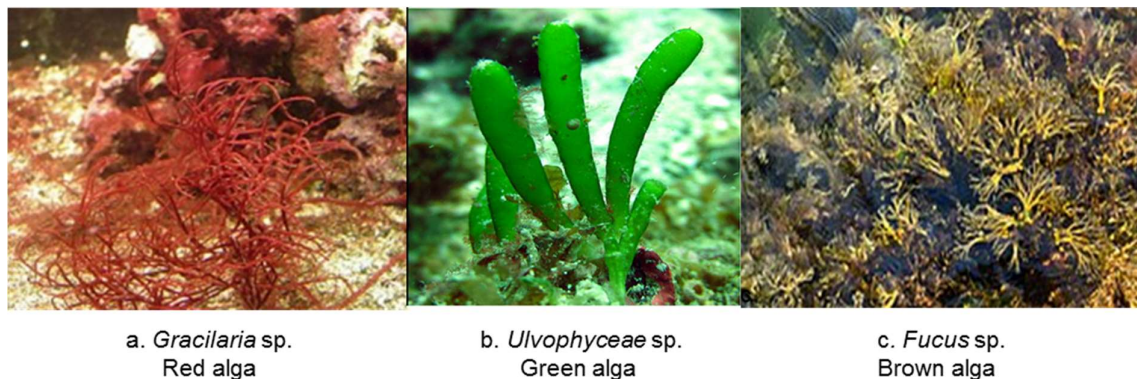


**Figure 3.** Representative species for the three groups of seaweeds (red, brown and green algae). a). Red alga *Gracilaria* sp. b). Green alga *Ulvophyceae* sp. c). Brown alga *Fucus* sp.

Interestingly, some fungi are obligate symbionts that are exclusively detected in the algal hosts. One example is a new *Acremonium* species termed *A. fuci*, which was isolated exclusively from *Fucus serratus* (Zuccaro *et al.*, 2004b). Notably, *A. fuci* only showed conidia germination in the presence of its host alga tissue or aqueous tissue homogenate (Zuccaro *et al.*, 2004b). This dependency of *A. fuci* spore germination on the host provides strong evidence for a symbiotic interaction between the alga and the fungus. *Vice versa*, the observed fungal diversity associated with macroalgae suggests that many fungal associates are critical for algal life in several aspects, such as nutrient cycling, development and chemical defense (Du *et al.*, 2019; Garbary and MacDonald, 1995; Vallet *et al.*, 2018). This is nicely exemplified by the role of a fungus for morphological development of the brown seaweed *Ascophyllum nodosum* (Garbary and MacDonald, 1995). After inoculated with ascospores of the endophyte *Mycosphaerella ascophylli*, the alga showed better growth condition, with longer thalli, greater

sporeling length and shorter rhizoids compared to non-infected control (Garbary and MacDonald, 1995). Although the current ecological role of marine algalicolous fungi (MAF) in associations with seaweeds is still incompletely understood, these complex interactions including nutrient transfer and hormonal regulation suggest a mutual adaptation process between algal host and fungi. The versatility of fungal-algal interaction also includes a positive or protective role of fungi in their host's life, especially in chemical defense. Reportedly, fungi produce bioactive metabolites to protect macroalgae from pathogen infestation (Vallet *et al.*, 2018). As an example, algal-derived fungi were found to be able to produce antifouling metabolites (Flewelling *et al.*, 2015; Overy *et al.*, 2014). Moreover, a recent study yielded several isolates from four brown algal species producing antibiotic metabolites active against protistan pathogens of the model brown alga *Ectocarpus siliculosus* (Vallet *et al.*, 2018). Among all 99 fungi isolated in the study, one *Phaeosphaeria* sp. AN596H derived from *Ascophyllum nodosum* produced a new pyrone pyrenocine S (Figure 4), showing activity against the algal-pathogenic oomycete *Eurychasma dicksonii* CCAP 418/3 at 0.1  $\mu\text{g}/\text{mL}$ . Additionally, the known pyrone type pyrenocines A and B displayed a strong antibiotic effect against all tested algal pathogens - *Eurychasma dicksonii* CCAP 418/3, *Anisolpidium ectocarpii* (CCAP 4001/1) and *Maullinia ectocarpii* (CCAP 1538/1) at 0.1  $\mu\text{g}/\text{mL}$  (Vallet *et al.*, 2018) (Figure 4). These results demonstrate that MAF have a high potential to produce bioactive small molecules protecting their host, and these small molecules have great potential in drug development.

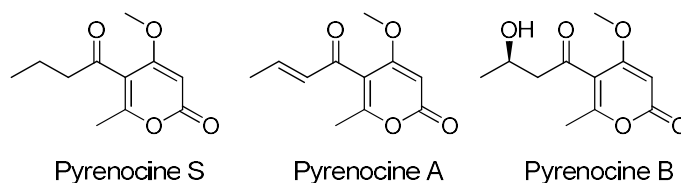


**Figure 4.** Structures of the chemical defense metabolite pyrenocines isolated from brown alga-derived *Phaeosphaeria* sp. AN596H.

## 2.2. Macroalgae-derived fungi as source of anticancer lead compounds discovery

Cancer is one of the major fatal diseases of the 21<sup>st</sup> century that has caused 18 million cases and about 10 million deaths in 2018 (Bray *et al.*, 2018). According to global demographic predictions, there will be an increase in the incidence of cancer with an estimated 20 million new annual cases by 2025 (Zugazagoitia *et al.*, 2016). Fortunately, continuous investments in anticancer research have notably varied treatment paradigms in past decades, e.g. surgery, chemotherapy, radiotherapy and immunotherapy (Arruebo *et al.*, 2011). Among those available methods, chemotherapy is still one of the most effective approaches for the treatment of different types of cancers. Despite the significant advances in anticancer drug development, strong side effects have been regarded as the biggest drawback of current chemotherapy agents, motivating the continuous search for effective cures with fewer side effects (Huang *et al.*, 2017). Terrestrial fungal natural products have contributed a number of novel molecules for the development of life-saving drugs (e.g. protein-bound polysaccharide K) (Jiménez-Medina *et al.*, 2008), while MFNPs and especially those produced by MAF have remained largely underexplored until the 1990s.

In 1993, the alkaloids communesins A and B (Figure 5a, b) were isolated from *Penicillium* sp. derived from the marine green alga *Enteromorpha intestinalis*. They showed strong anticancer bioactivity against the murine leukemia cancer cell line P388 with  $\text{ED}_{50}$  values of 3.5 and 4.5  $\mu\text{g}/\text{mL}$ , respectively (Numata *et al.*, 1993). The remarkable biological properties of these molecules have stimulated considerable interest in prospecting bioactive communesin derivatives from marine fungi

(Dalsgaard *et al.*, 2005; Jadulco *et al.*, 2004). Motivated by the isolation of the communesins, studies on discovering anticancer compounds from algicolous fungi experienced a boost. Between 1994 and 2004, investigations on the brown alga *Sargassum torile*-associated fungus *Leptosphaeria* sp. yielded another representative natural product family - the epipolythiodiketopiperazine (ETP) type leptosins - which so far includes 23 members (Takahashi *et al.*, 1994a; Takahashi *et al.*, 1994b; Yamada *et al.*, 2004; Yamada *et al.*, 2002). Leptosins are characterized by the incorporation of an intramolecular polysulfide bridge that forms different kinds of dimeric ETPs (Boyer *et al.*, 2013). All leptosins showed strong *in vitro* toxicity against P388 with ED<sub>50</sub> values ranging from 1.75 ng/mL to 1.40 µg/mL (Takahashi *et al.*, 1994a; Takahashi *et al.*, 1994b; Yamada *et al.*, 2004; Yamada *et al.*, 2002). Subsequent mechanistic studies on leptosins revealed inhibition of cancer cell growth through different ways: Yamada *et al.* found that leptosin M specifically inhibits the activity of the protein kinases PTK, CaMKIII and the human topoisomerase II to kill cancer cell lines, but did not exhibit any activity against topoisomerase I (Yamada *et al.*, 2002; Yanagihara *et al.*, 2005) (Figure 5c). A later study of leptosins C and F showed that they exhibit specific inhibition activity against both topoisomerase I and II leading to apoptosis induction in cancer cells (Yanagihara *et al.*, 2005) (Figure 5d, e).

In 1997, the naturally occurring secondary metabolite (SM) diketopiperazine halimide (also named phenylahistin, Figure 5f), was isolated from the fungus *Aspergillus* sp. associated to the marine green alga *Halimeda copiosa* collected off the Philippine (Fenical *et al.*, 2000; Kanoh *et al.*, 1997). It exhibited a strong *in vitro* growth inhibition profiles against the human lung carcinoma cancer cell line A549 and murine leukemia cancer cell line P388 (Fenical *et al.*, 2000; Fukumoto *et al.*, 2002; Kanoh *et al.*, 1997; Kanoh *et al.*, 1999a). In-depth analysis of its mechanism of action showed that halimide disturbs the microtubule network through interaction with the colchicine-binding site on tubulin, which is similar to vinca alkaloids and paclitaxel. Subsequent research on halimide focused on structural modifications, i.e. removing the chirality and optimizing its anticancer bioactivity. The structure modification effort led to the development of plinabulin (Kanoh *et al.*, 1999b) (Figure 5g). Plinabulin is a synthetic *tert*-butyl analogue of halimide. It blocks the polymerization of tubulin in cancer cells, which results in the disruption of the tumor blood supply to kill cancer cells (Cimino *et al.*, 2019). Plinabulin is subject to clinical studies for the treatment of non-small cell lung cancer and recently has been processed to the world-wide clinical trial phase III (Blayney *et al.*, 2019). Until now, plinabulin is the only anticancer agent derived from a MAF-sourced secondary metabolite in clinical trials.

In recent years, MAF-derived natural products represent one of the most relevant sources contributing to marine-derived new drug leads (Gomes *et al.*, 2015; Montaser and Luesch, 2011). Beyond showing *in vitro* anticancer activity in their natural, unmodified form, they also enlarge drug space through providing the basis for semi-synthetic analogs of lead compounds, as well as the natural product-inspired structural mimics (Kanoh *et al.*, 1999b). Recent technical advances in dereplication, purification and biological activity evaluation, have inspired an ongoing research interest in searching anticancer lead compounds from MAF (Hubert *et al.*, 2017; Teixeira *et al.*, 2019).

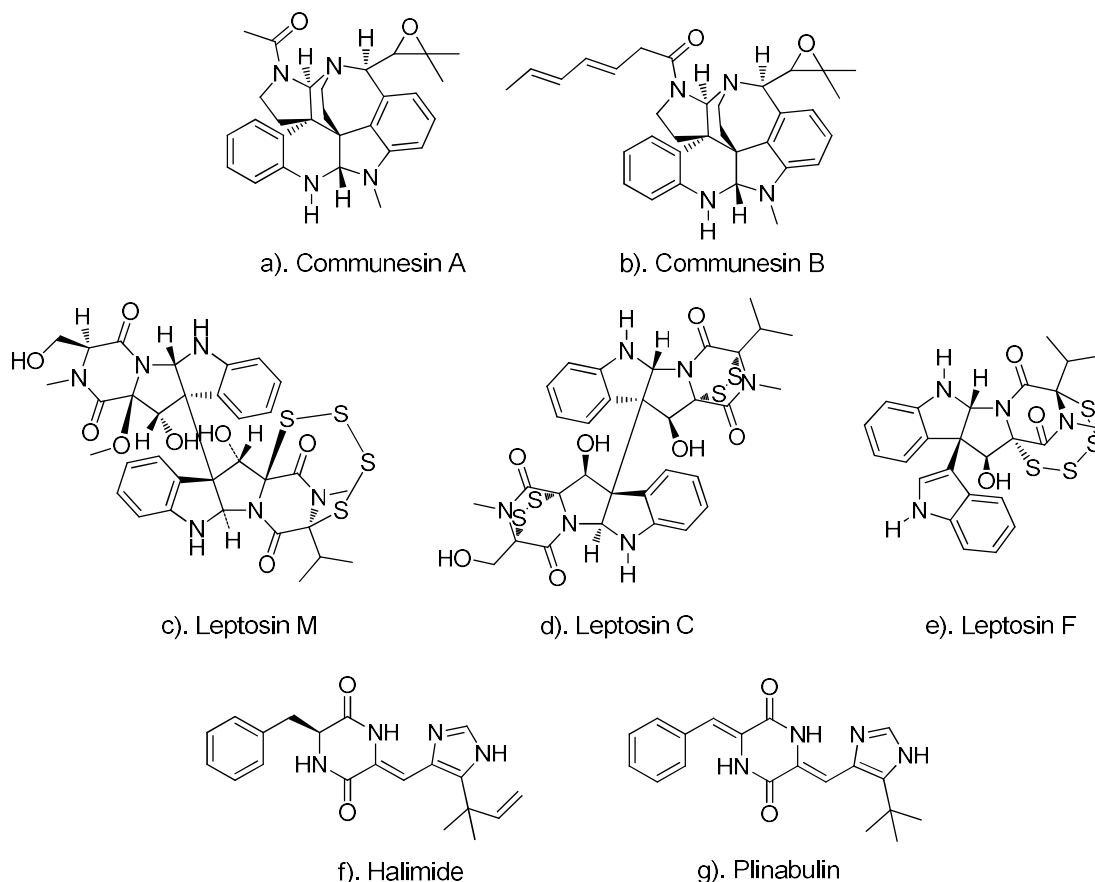


**Figure 5.** Structures of representative MAF-derived natural products. a-b). Communesins A and B isolated from *Penicillium* sp. c). Leptosin M isolated from *Leptosphaeria* sp, showing the inhibitive activity of the protein kinases PTK, CaMKIII and the human topoisomerase II. d-e). Leptosin C and F, reported from *Leptosphaeria* sp., within inhibitive activity of human topoisomerase I and II. f). Halimide isolated from *Aspergillus* sp., and g). Halimide-derived analogue plinabulin.

Continued isolation efforts have yielded a plethora of purified natural products with excellent anticancer bioactivities from fungal taxa collected from different algal hosts including green, red and brown algae (Elsebai *et al.*, 2011; Greve *et al.*, 2008; Sun *et al.*, 2012; Zhang *et al.*, 2016). Until late 2019, approximately 180 MAF-derived metabolites have been purified and reportedly showed activity against multiple cancer cell lines (Appendix Table 1). They belong to diverse chemical families such as polyketides, steroids, alkaloids, cyclodipeptides and macrodiolides (Lang *et al.*, 2006; Unsöld and Li, 2006; Usami *et al.*, 2002; Wang, 2012; Zhu *et al.*, 2009) (Appendix Table 1). However, most of the published studies on anticancer metabolites from MAF have focused on only a few genera, mainly *Penicillium*, *Aspergillus*, *Fusarium*, and *Leptosphaeria* (Choi *et al.*, 2019; Smetanina *et al.*, 2016; Takahashi *et al.*, 1994a; Usami *et al.*, 2002). The high diversity of seaweed-associated fungi (Abdel-Gawad *et al.*, 2014; Zuccaro *et al.*, 2004b) and the presence of yet understudied fungal genera besides the above-mentioned well-studied ones render MAF a promising resource for anticancer lead discovery.

### 2.3. Chemical prospecting of *Fucus*-derived fungi

The canopy-forming *Fucus* sp. is the most-widespread brown seaweed inhabiting the shallow coastal regions of northern Europe, including the Baltic Sea (Ardehed *et al.*, 2016; Malm and Kautsky, 2003). As one of the key species in many coastal marine environments, *Fucus* sp. often forms the basis

of species-rich ecosystems, including a rich mycobiome (Wikström and Kautsky, 2007; Zuccaro *et al.*, 2008; Zuccaro *et al.*, 2004a). Recently, a chemical imaging technique (Desorption Electrospray Ionization-Imaging Mass Spectrometry - DESI-IMS) revealed the presence of a rich surface metabolome in the bladderwrack *Fucus vesiculosus* including several fungal metabolites such as peptaibol emerimicins, alkaloid pestalamides and bis-indolyl benzenoid ochrindoles (Parrot *et al.*, 2019). These results provide further evidence for the important role of fungi in their host's chemical defense.

Discovery of bioactive natural products from *Fucus*-derived fungi started with the purification of polyketides 5-hydroxyramulosin and 7-methoxycoumarin (Figure 6a, b). They were produced by *Phoma* sp. derived from *Fucus spiralis*, and showed anticancer, antifungal and anti-HIV activities (Osterhage *et al.*, 2002; Santiago *et al.*, 2012). Since then, several other studies have found bioactive metabolites produced by *Fucus*-derived fungi. For example, a new isobenzofuranone derivative 4,5,6-trihydroxy-7-methylphthalide (Figure 6c) was produced by the fungus *Epicoccum* sp. isolated from *Fucus vesiculosus* collected on the North Sea coast (Abdel-Lateff *et al.*, 2003). The obtained compound was found to have considerable antioxidant activity, showing 95% radical scavenging effects at 25  $\mu\text{g/mL}$  in the 2,2-Diphenyl-1-picrylhydrazyl (DPPH) assay and inhibited the peroxidation of linolenic acid in the thiobarbituric acid reactive substances (TBARS) assay (62% inhibition at 37  $\mu\text{g/mL}$ ) (Abdel-Lateff *et al.*, 2003). Additionally, Flewelling and colleagues retrieved *Aspergillus fumigatus*, *Coniothyrium* sp. and *Penicillium* sp. isolates from *Fucus* sp. collected from the North Atlantic Ocean (Flewelling *et al.*, 2013a). Following initial antibacterial screening results, *Penicillium* sp. isolated from *Fucus spiralis* was selected for further chemical investigation. Bioassay-guided isolation of the selected *Penicillium* sp. yielded several metabolites such as the polyketides cladosporin, epiepoformin, phyllostine, and patulin showing antimicrobial activity (Flewelling *et al.*, 2013c) (Figure 6d-g). Patulin has been reported as a mycotoxin exhibiting toxicity to several cancer cell lines (Abastabar *et al.*, 2017). Although these examples suggest a high capacity of *Fucus* sp.-associated fungi for production of bioactive natural products, focus of these studies were antibiotic metabolites and hence, their potential for production of anticancer leads remains largely unexplored.

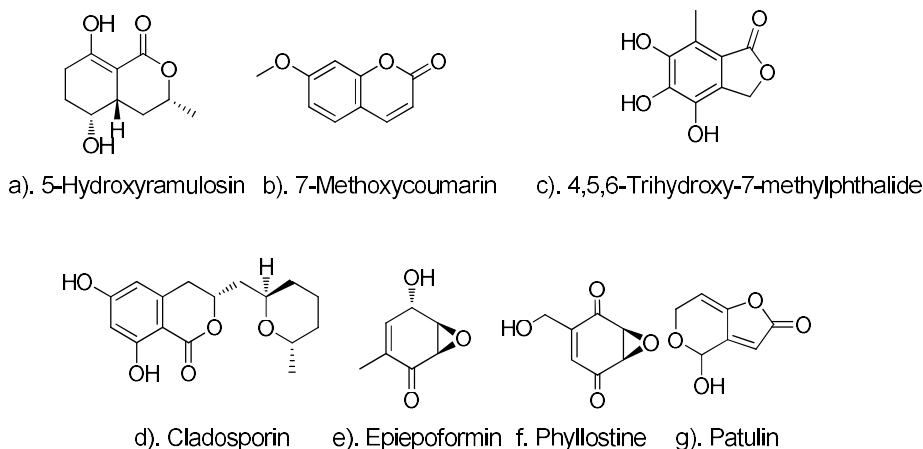


**Figure 6.** Structures of bioactive natural products reported from *Fucus*-derived fungal isolates. a-b). Compounds isolated from *Phoma* sp. originating from *F. spiralis*. c). New compound purified from *Epicoccum* sp. isolated from *F. vesiculosus*. d-g). Antibiotic compounds isolated from *Penicillium* sp. derived from *F. spiralis*.

### 3. The fungal genus *Pyrenochaetopsis* sp.

The genus *Pyrenochaetopsis* sp. taxonomically belongs to the fungal family Cucurbitariaceae (de

Gruyter *et al.*, 2010; Valenzuela-Lopez *et al.*, 2018) in the order Pleosporales, which is affiliated to the division Ascomycota. Recent studies showed that *Pyrenochaetopsis* sp. are widely distributed in diverse ecological niches, such as soil, plant-associated and airborne (de Gruyter *et al.*, 2010; de Gruyter *et al.*, 2013). *Pyrenochaetopsis* sp. has been previously isolated from the marine green alga *Flabellia petiolata* collected in the Mediterranean Sea (Gnavi *et al.*, 2017), suggesting that the marine environment also harbors fungi of this genus. Previously, often species of the genera *Pyrenochaetopsis* and *Phoma* were mixed, since morphological characters did not allow a clear distinction (de Gruyter *et al.*, 2010). Recent systematic analysis of the genus *Phoma* and the closely related genera *Pharaphoma*, *Pyrenochaeta*, *Herpotrichia*, *Pyrenochaetopsis* showed a genetic difference of *Pyrenochaetopsis* sp. from *Phoma* sp. (de Gruyter *et al.*, 2010) (Figure 7). Recently, several species previously regarded as *Phoma* sp. have been transferred to the genus *Pyrenochaetopsis* based on a combination of genetic and morphological characteristics (Chen *et al.*, 2015; de Gruyter *et al.*, 2010).

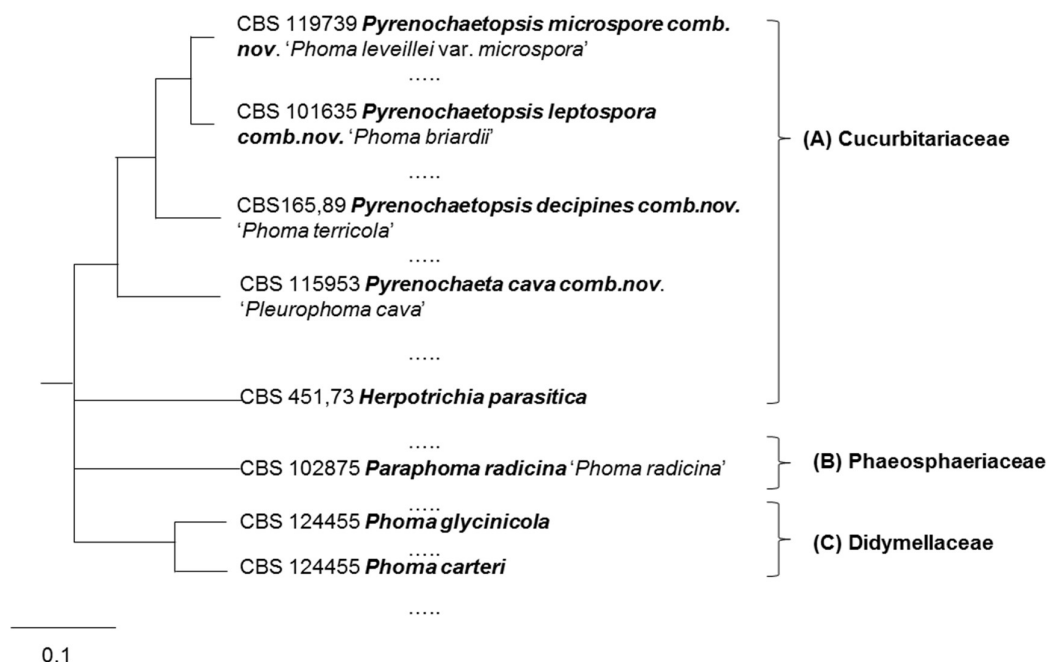


**Figure 7.** Phylogenetic species relationships in genus *Paraphoma*, *Herpotrichia*, *Pyrenochaeta*, *Pyrenochaetopsis* gen. nov. and *Phoma*. Consensus tree was adapted from de Gruyter *et al.* 2010. (A). Fungal family Cucurbitariaceae. (B). Fungal family Phaeosphaeriaceae. (C). Fungal family Didymellaceae.

Until now, the genus *Pyrenochaetopsis* sp. has not been studied extensively, especially regarding secondary metabolite production of species belonging to this genus. To our knowledge, to date only decalin derivatives such as phomasetin and wakodecalines have been isolated from the genus *Pyrenochaetopsis* sp. (Nogawa *et al.*, 2017) (Figure 8). The wakodecalines showed moderate antimalarial activity against *Plasmodium falciparum* 3D7, but were inactive against tested cancer cell lines (Nogawa *et al.*, 2017). Similarly, phomasetin has shown multiple bioactivities including antimalarial, toxic and anti-HIV bioactivity (Nogawa *et al.*, 2017; Singh *et al.*, 1998). Interestingly, phomasetin and wakodecalines contain the same *trans*-decalin skeleton, which was proposed to be biosynthesized by enzyme-catalyzed [4+2] cycloaddition (Kato *et al.*, 2018). The identification of biosynthetic gene clusters of *Pyrenochaetopsis* sp. revealed that the gene *phm7* was involved in the reaction and stereocontrol of [4+2] cycloaddition forming *trans*-decalin phomasetin, resulting in opposite chiral center configurations of phomasetin and equisetin (Kato *et al.*, 2018). Moreover, the



BGC screening of *Pyrenochaetopsis* sp. suggested that it had the potential to produce a high number of metabolites containing the ‘*trans*-decalin’ unit (Kato *et al.*, 2018). Hence, *Pyrenochaetopsis* sp. is supposed to be a promising strain for natural product discovery.

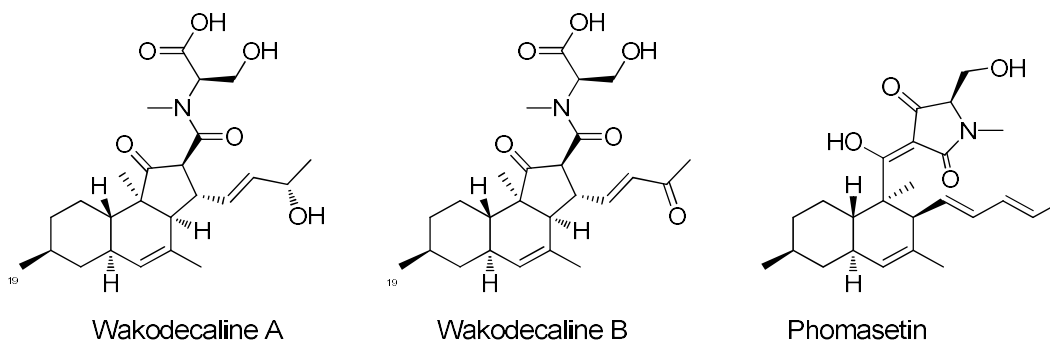


**Figure 8.** Structures of wakodecalines and phomasetin produced by *Pyrenochaetopsis* sp.

#### 4. Activation of silent biosynthetic gene clusters (BGCs)

##### 4.1. Approaches to activate silent BGCs for inducing chemical space

SMs are usually produced by enzymes that are encoded by co-localized genes organized in so-called BGCs (Keller *et al.*, 2005). However, the vast majority of fungal BGCs for SMs are either inactive or only active at a low expression level under standard laboratory culture conditions (Reen *et al.*, 2015) and are hence termed ‘silent’ or ‘cryptic’ BGCs. Their silence is mainly caused by a lack of environmental cues or stressors in standard lab culture conditions (Romano *et al.*, 2018; Rutledge and Challis, 2015). Thus, application of various approaches to activate these silent BGCs has become highly relevant in marine fungal research.

Until now, research on MFNPs has only touched the “tip of the iceberg” (Romano *et al.*, 2018). In order to achieve high chemical diversity of marine fungal metabolites, researchers have been continuously trying to evoke or enhance the expression of silent BGCs in marine fungi (Brakhage *et al.*, 2008; Reen *et al.*, 2015). Since the tremendous potential for SM production in many fungi has been observed by several genome-based studies (Rokas *et al.*, 2020; Rokas *et al.*, 2018), the development of techniques for both cultivation-dependent and -independent approaches to induce the production of marine fungal metabolites has become a rapidly developing field. There have been multiple approaches established to activate “silent” BGCs for marine fungal SM production. They can be divided into two major approaches: 1). Pleiotropic and 2). Pathway-specific methods (Rutledge and Challis, 2015) (Table 1). Pleiotropic approaches are generally technically simple and are therefore suitable for scaling up to high-throughput systems (Baral *et al.*, 2018). The term “pleiotropic approach” refers to methods changing a single cultivation parameter but leading to more than one observable change in the regulation of secondary metabolite pathways. Pleiotropic approaches include different methods such as variation of growth conditions, engineering of the transcription and translation machinery, manipulating global regulators and epigenetic perturbation (Table 1). Those approaches have been successfully applied to marine fungi for evoking or changing the expression of marine fungal silent BGCs (Chai *et al.*, 2012; Wang *et al.*, 2014a; Wu *et al.*, 2020). Pleiotropic approaches may activate more than one biosynthetic pathway and result in the production of new compounds belonging to different chemical families. As an example, Wu and co-workers applied two different epigenetic modifiers for triggering the production

## GENERAL INTRODUCTION

of bioactive metabolites from a marine-derived *Aspergillus versicolor* (Wu *et al.*, 2020). The fungus displayed different levels of chemical diversity when treated with the histone deacetylase inhibitor suberoylanilide hydroxamic acid (SAHA) and the DNA methyltransferase inhibitor 5-azacitidine (5-Aza). Furthermore, combination of 100  $\mu\text{M}$  SAHA and 100  $\mu\text{M}$  5-Aza led to an additive effect on the epigenetic regulation of the fungal SM production, which finally yielded two new nucleoside derivatives, kipukasins K and L (Figure 9a, b), as well as the new bisabolane sesquiterpene aspergillusene E (Figure 9c) (Wu *et al.*, 2020).

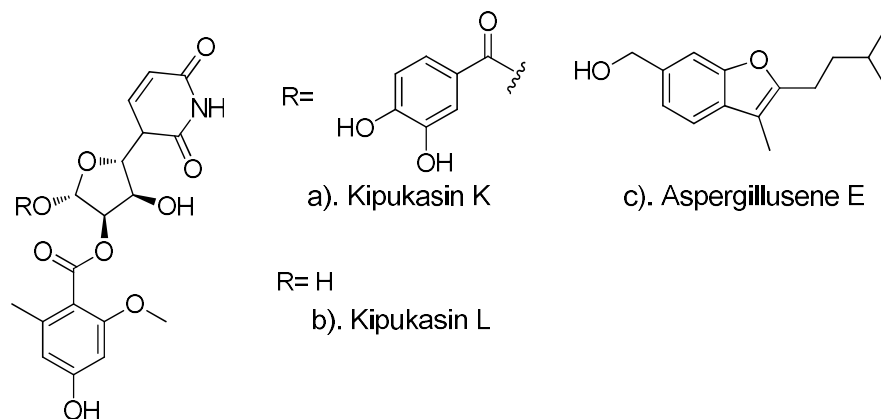


**Figure 9.** Structures of new secondary metabolites obtained from marine-derived *Aspergillus versicolor* after treatment with a pleiotropic approach (epigenetic modifiers).

In contrast to the pleiotropic approaches, pathway-specific strategies try to control the biosynthesis of certain types of compounds by targeting specific genes, but also regulatory elements such as activators, repressors or promoters. These strategies include multiple methods such as manipulating pathway-specific regulation, reporter-guided mutant selection, refactoring, heterologous expression and CRISPR/Cas9-based genome editing (Table 1). In general, pathway-specific strategies are designed based on a comprehensive understanding of the genes underlying SM production. Hence, compounds obtained after application of pathway-specific strategies highly matched to predicted structures (Bergmann *et al.*, 2007; Chiang *et al.*, 2009). However, due to the tight regulation of BGCs in pathway-specific strategies, those strategies often result in reduced chemical diversity compared to pleiotropic approaches (Rutledge and Challis, 2015).

**Table 1.** Different approaches used to activate silent BGCs (table was adapted from Rutledge and Challis *et al.*, 2015)

Approach	Principle of the method
<b>Pleiotropic methods</b>	
<b>Variation of growth conditions</b>	Subjection of a microorganism to a change in the environment in which it is growing (for example, by adding competing species, chemical elicitors or other additives) to induce changes in BGC expression
<b>Engineering the transcription and translation machinery</b>	Induction of mutations in RNA polymerase and ribosomal proteins to cause upregulation of BGC expression
<b>Manipulating global regulators</b>	Alteration of expression levels of pleiotropic transcriptional regulators to modulate BGC expression
<b>Epigenetic perturbation</b>	Use of mutagenesis or small-molecule inhibitors to disrupt chromatin structure and thus trigger global changes in gene expression
<b>Pathway-specific methods</b>	
<b>Manipulating pathway-specific regulators</b>	Identification of genes encoding putative pathway-specific transcription factors within a BGC of interest, followed by overexpression (for an activator) or deletion (for a repressor) of these genes as appropriate
<b>Reporter-guided mutant selection</b>	Genome-scale random mutagenesis to introduce genetic diversity, while coupling a target BGC to a promoter-reporter system that visualizes mutants in which target BGC transcription is activated
<b>Refactoring</b>	Replacement of the natural promoters within a BGC with constitutive or readily inducible promoters
<b>Heterologous expression</b>	Expression of an entire BGC in a heterologous host
<b>CRISPR/Cas9-based genome editing</b>	CRISPR/Cas9 mediated recognition and cleavage of specifically targeted DNA motifs to insert, delete, modify or replace BGCs

#### 4.2. One-Strain-Many-Compounds (OSMAC)

The above described pleiotropic approaches include the variation of cultivation conditions to trigger the production of SMs in fungi (Hemphill *et al.*, 2017; Meng *et al.*, 2017; Özkaya *et al.*, 2018). This approach of changing culture conditions for inducing microbial chemical production has been summarized as One-Strain-Many-Compounds (OSMAC) approach. It was conceptualized by Bode and co-workers, who found small changes in microbial culture conditions leading to variations in their SM production (Bode *et al.*, 2002). The basic theory underlying this approach is that one single strain has the genomic potential to produce diverse metabolites, but the actual production is restricted under standard culture conditions. This means, that the few metabolites produced in a certain culture condition reflect only a subset of the entire potential residing in the genome. By altering culture parameters such as temperature, aeration, salinity, and the shape of culture flasks in cultivation of the fungus *Aspergillus ochraceus*, Bode *et al.* succeeded in isolation of additional 15 metabolites (Bode *et al.*, 2002). This pioneering study highlighted the importance of exploring a single fungal strain by applying different culture conditions for production of new metabolites (Bode *et al.*, 2002). In the past decades, numerous studies have further provided evidence for the sensitivity of fungi towards changes in culture conditions (Abdelwahab *et al.*, 2018; Hewage *et al.*, 2014; Wang *et al.*, 2018). A plethora of abiotic cultivation parameters, including nutrient changes in carbon or nitrogen sources, salts, trace elements but also physical parameters (e.g. pH, shaking condition, temperature) could be optimized for inducing SM

production of fungi (Romano *et al.*, 2018) (Figure 10). Furthermore, the application of biotic challenges such as co-cultivation of microbes, e.g. bacteria & fungi have extended the OSMAC principle and have been successfully applied to fungi for the production of new types of SMs (Wang *et al.*, 2014b; Zhuravleva *et al.*, 2016) (Figure 10). In view of the difficulty simulate the real multispecies habitats of marine fungi, applying OSMAC approach to those fungi has been regarded as an essential method to induce their SM production (Gulder *et al.*, 2012; Leutou *et al.*, 2013).

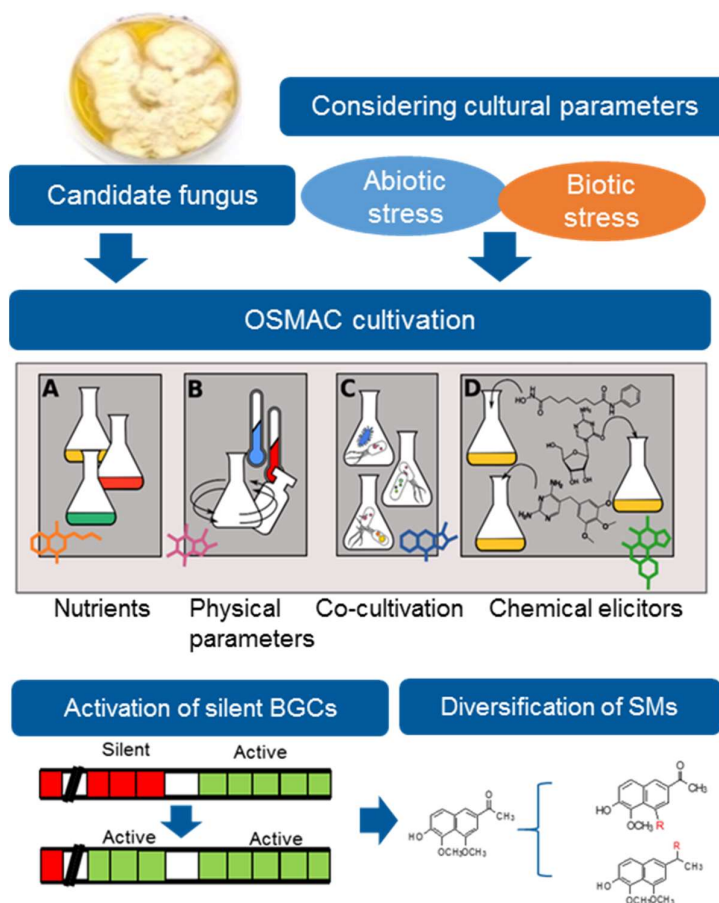


**Figure 10.** Overview of the “One-Strain-Many-Compounds” (OSMAC) approach to activate silent BGCs for the production of new metabolites. Modifiable parameters include (A). Nutrients; (B). Physical parameters; (C). Biological stressors induced by co-cultivation of more than one strain; (D). Chemical elicitors. (Picture modified based on Romano *et al.*, 2018 and Reen *et al.*, 2015)

#### 4.3. Application of OSMAC strategy to marine fungi

Beyond its application in bacteria and terrestrial fungi, the OSMAC approach has also been widely applied to marine fungi for new SM production (Meng *et al.*, 2017; Özkaya *et al.*, 2018; Wang *et al.*, 2014a). There are many parameters to be taken into account when designing OSMAC-based cultivation experiments. The effects of the supplied carbon source on microbial metabolism have been subject to continuous studies by both industry and research groups (Ruiz *et al.*, 2010; Sánchez *et al.*, 2010). One characteristic of microbial secondary metabolism is that it is usually tightly coupled with the growth phase, often commencing upon the stationary or resting phase (Calvo *et al.*, 2002). As reviewed by Sánchez and co-workers, the type of carbon source has important effects especially on secondary metabolism regulation such as polyketide biosynthesis (Sánchez *et al.*, 2010). There are two major types

of carbons - rapidly available carbon (e.g. glucose) and rather slowly used carbon (e.g. starch) used in the cultivation of marine fungi. Rapidly used carbon sources are often monosaccharides very well suited for fast microorganism growth, while slowly used carbon are polysaccharides that are considered as 'second-best' carbon resources for microorganisms (Sánchez *et al.*, 2010). Since glucose was reported to inhibit several enzymes involved in the SM production (Gutiérrez *et al.*, 1999), it is important to take different carbon resources into account when culturing any microorganism including fungi in the lab. The choice of the appropriate carbon source in the medium needs to be balanced between enabling good cell growth and favoring SM production. As a successful example, Lin *et al.* induced production of the new pentacyclic cytochalasan spicochalasin A as well as five novel cytochalasan aspochalasins and two known aspochalasins in the marine fungus *Spicaria elegans* by changing the carbon source in the culture medium from glucose to 2% starch (Lin *et al.*, 2009). Spicochalasin A (Figure 11a) showed moderate cytotoxicity against the human leukemic cancer cell line HL-60 with an IC<sub>50</sub> value of 19.9 µM, suggesting its potential as an anticancer agent (Lin *et al.*, 2009). Additional research showed that the application of different carbon sources to the cultivation of marine fungi changed both typology and titration of the produced metabolites (Camila Dos Santos Dias *et al.*, 2017).

Another important nutrient, the nitrogen source, also plays an important role in marine fungal growth and SM production. In particular, organic, amino acid-containing nitrogen sources play an important role in all peptide- but also amine- or amide- containing natural products as they provide major structural elements for the resulting SMs (Romano *et al.*, 2018). After changing the nitrogen source from inorganic NaNO<sub>3</sub> to a combination of arginine, asparagine and glutamic acid, the marine fungus *Asteromyces cruciatus* produced new pentapeptide lajollamide A showing weak antibacterial activity against Gram-positive bacteria at a concentration of 100 µM (Gulder *et al.*, 2012) (Figure 11b). The production of lajollamide A in *Asteromyces cruciatus* was implied to be strongly affected by nitrogen resource, since changing other cultural parameters (e.g. shaking condition, temperature) could not induce this productive shift (Gulder *et al.*, 2012). Analog to carbon, also the choice of nitrogen source in marine fungal cultivation needs to be well-balanced to enable cell growth on the one hand and on the other hand induce production of secondary metabolites. As reported by Miao *et al.*, nitrogen limitation (absence or minute concentrations of nitrogen) had negative effects on cell growth but positive effects on antibiotics production in the marine-derived fungus *Arthrinium c. f. saccharicola* (Miao *et al.*, 2006). Thus, low nitrogen concentrations seem to be one precondition for unlocking bioactive SM production of marine fungi. The carbon-nitrogen ratio should be considered when choosing cultivation media for inducing marine fungal SM production. In a study targeting the optimization of biosurfactant production from a sponge-derived *Aspergillus* sp., five different carbon-nitrogen ratios ranging from 5:1 to 1:5 were chosen. The results showed that the strain produced the highest amount of biosurfactant at a C:N ratio of 3:2 whereas the ratio at 1:5 yielded no biosurfactant production (Kiran *et al.*, 2009). The above-mentioned studies revealed the importance of nitrogen on SM production of marine fungi.

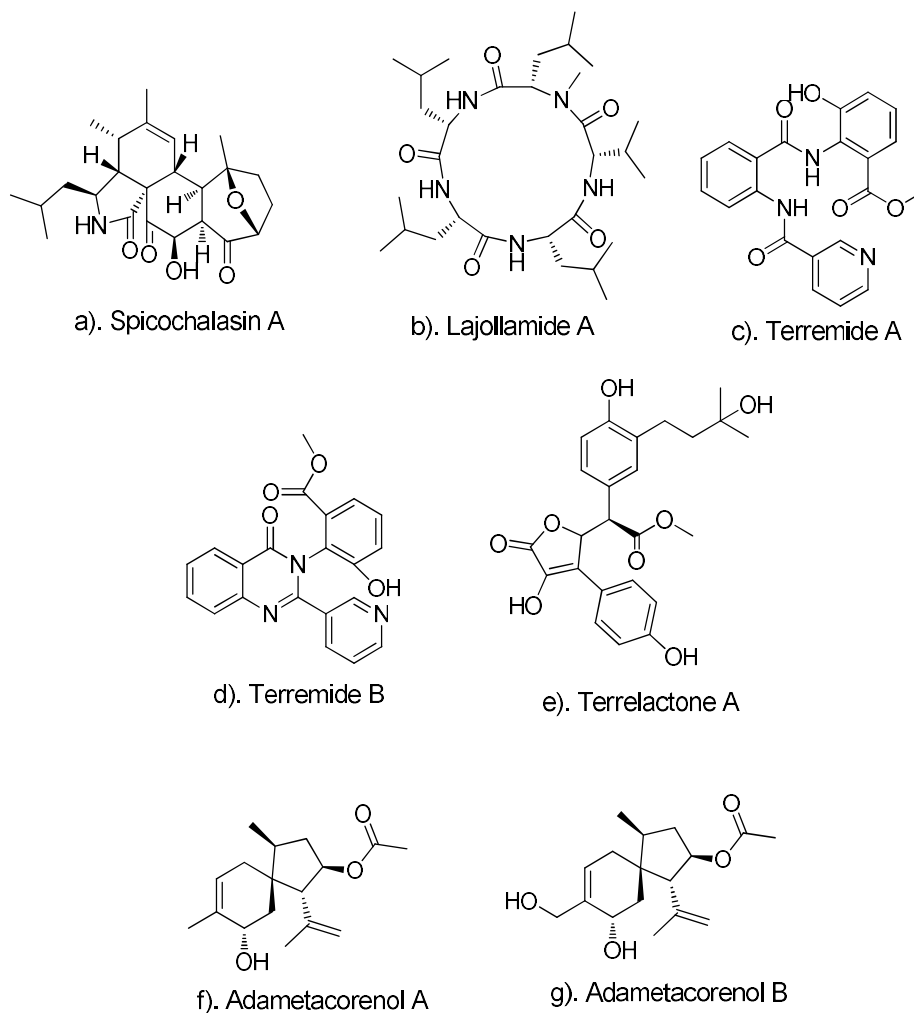


**Figure 11.** Structures of new compounds produced by marine fungi for adaption of OSMAC approach. a). New metabolite spicochalasin A produced by marine fungus *Spicaria elegans* after changing carbon resource in growth medium. b). New pentapeptide Lajollamide A purified from *Asteromyces cruciatus* after modification of nitrogen source in culture medium. c-e). Terremides A, B and terrelactone A purified from marine sediment-derived fungus *Aspergillus terreus* treated with high salt stress. f-g). New compounds Adametacorenols A and B purified from solid-phase culture extracts derived from marine fungus *Penicillium adamezioides* AS-53.

Marine fungi inhabit an environment with an average salinity of 3-3.5% (Li and Liu, 2019). In order to adapt to this comparably high salinity environment, marine fungi have developed several specific mechanisms such as generating osmotic potential and modifying enzyme systems (Clipson and Jennings, 1992; Kumar *et al.*, 2018; Rédou *et al.*, 2015). Production of SMs is one important strategie for salt adaptation (Wang *et al.*, 2011a; Wang *et al.*, 2011b). Hence, salt concentration needs to be considered when designing or selecting media for cultivation of marine fungi. For instance, Wang and colleagues applied three different salt concentrations - 0%, 3% and 10% in order to discover new bioactive compounds from the marine sediment-derived fungus *Aspergillus terreus*. Interestingly, the fungus produced three new alkaloids terremides A, B and polyketide terrelactone A (Figure 11c-e) only when cultured in the medium with the highest salt concentration (Wang *et al.*, 2011b). Moreover, the new compound terremide A showed antibacterial activity against *Pseudomonas aeruginosa* with minimum inhibitory concentration (MIC) value of 63.9  $\mu\text{M}$  and terremide B exhibited antibacterial

activity against *Enterobacter aerogenes* at a MIC value of 33.5  $\mu\text{M}$ . This study nicely demonstrates that salt stress is one of the dominant factors in activating silent BGCs for new SM production in marine fungi. Although salinity has been taken into account into biodiscovery studies on marine fungi, the effects of different salt types (e.g. NaCl alone or mixed inorganic salts) are still not well investigated.

While the above-mentioned studies have all attempted to optimize the culture media, a change of physical parameters also has drastic effects on the growth and chemical production of marine microorganisms. As recent studies on bacteria showed, changing the culture regime from liquid medium in flasks to agar-based medium on plates affected antibiotic production of a marine-derived *Streptomyces* strain, which produced antibiotically active metabolites only on agar (English *et al.*, 2017). Similarly, a shift of culture regime from liquid to solid in the marine-derived fungus *Penicillium adametzioides* AS-53 resulted in the production of two new acorane sesquiterpenes adametacorenols A and B (Figure 11f, g), which were not produced in liquid culture (Liu *et al.*, 2015). Furthermore, the secondary metabolite production of fungi is sensitive to several other physical culture features such as pH, temperature, aeration, shaking speed (Romano *et al.*, 2018).

Notwithstanding the numerous studies which have aimed to elicit the effects and results of activation of “silent” BGCs using the OSMAC principle, much remains yet to be investigated, particularly with regard to marine fungi. The OSMAC approach is still crucial to gain a better understanding of the induction of SM production in marine fungi.

## 5. Molecular networking-based metabolomics

### 5.1. Advantages of molecular networking

Loss of initial bioactivity or re-isolation of known compounds are common but sometimes costly pitfalls in microbial natural products discovery. Besides activation of silent BGCs for producing new SMs, dereplication and targeted isolation are indispensable steps in modern natural product discovery. Recently, an open-access platform named Global Natural Product Social molecular networking (GNPS) was established which represents a data-driven online platform for stockpile, analysis and dissemination of tandem mass (MS/MS) data. It enables community sharing of raw spectra, annotation of known compounds in complex mixtures, and collaborative curation of reference spectral data and experimental data (Wang *et al.*, 2016). The principle and workflow of molecular networking (MN)-based chemical analysis and isolation have been summarized by Wang *et al.* in 2016 (Figure 12). Implementation of MN has revolutionized natural product discovery in the field of dereplication, targeted isolation and structure elucidation (Fox Ramos *et al.*, 2019; Olivon *et al.*, 2017c; Yang *et al.*, 2013). Compared to traditional dereplication workflows, MN exhibits several advantages: 1). High accuracy of annotating known compounds; 2). Enabling a high-throughput dereplication of natural products by querying newly acquired MS/MS data against all reference spectra collected in GNPS spectral libraries; and 3). Visualizing not only known compounds but also structurally related analogues (Wang *et al.*, 2016).

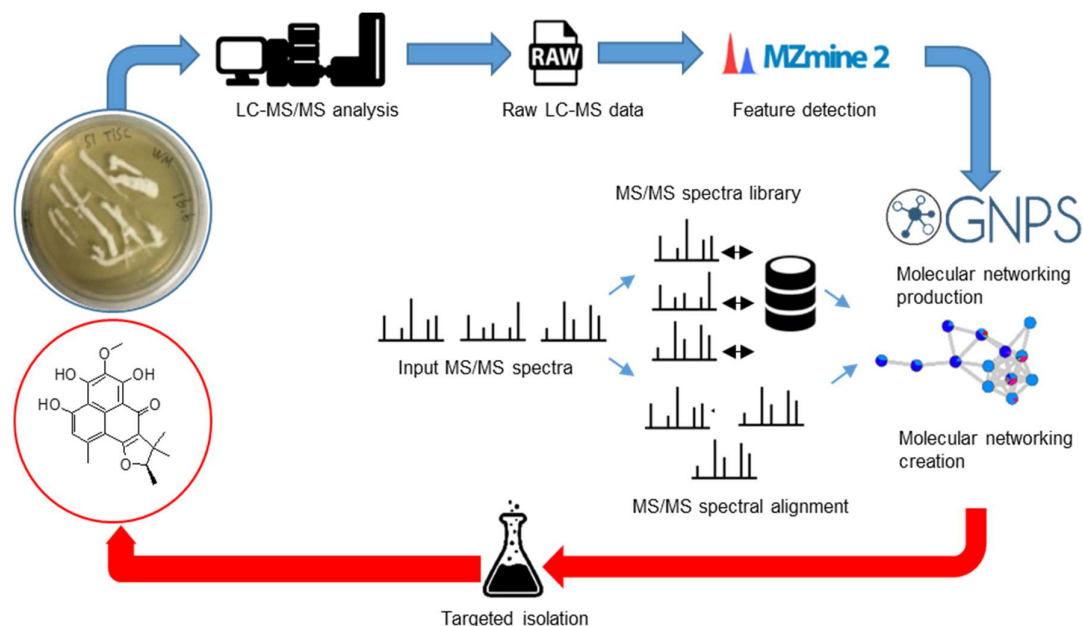


**Figure 12.** General workflow of GNPS-based chemical analysis and isolation (data was adapted from Wang *et al.* 2016). Identical tandem mass spectra of extracts are processed by analytical software (e.g. MZmine2). After uploading processed data to the GNPS website and searching against GNPS libraries for dereplication of known compounds, the map of related molecules is visualized as a MN online in GNPS or by using the publicly available software Cytoscape. The subsequent targeted isolation of potential new compounds is guided by MN.

Another remarkable advantage of GNPS lies in its continuous expansion of functions, thereby enabling researchers to select the appropriate tool for MS/MS data analysis among a variety of cheminformatic/database tools. Recently, GNPS has launched several newly developed analytical tools, such as *in-silico* tools, feature-based molecular networking, ReDU-MS<sup>2</sup>, GC-MS EI data analysis and MS<sup>2</sup>LDA-Motif database available on its website (<https://gnps.ucsd.edu/ProteoSAFe/static/gnps-splash.jsp>). These tools substantially enlarged the application field of MN. Moreover, GNPS is a ‘living library’, providing the newest annotated natural products using the automated comparison between included spectra and newly added datasets generated by its users (Fox Ramos *et al.*, 2019; Olivon *et al.*, 2017b; Wang *et al.*, 2016; Xu *et al.*, 2019). With the continued growth of GNPS spectral libraries, the number of matched known compounds in MN is expected to further increase over time, which further ameliorates the efficiency of natural products annotation.

## 5.2. Molecular networking as a dereplication tool

Mass spectrometry is a widely applied technology for analysis of crude extracts in natural product discovery studies. Resulting data are usually subject to manual comparison with public and commercially available natural product databases such as Dictionary of Natural Products (DNP), MarinLit and Reaxys to avoid re-isolation of known compounds (dereplication) (Nielsen *et al.*, 2011). MN has been confirmed to be a useful complement to the current MS-based dereplication (Yang *et al.*, 2013). In several cases, the GNPS workflow provided a fast dereplication process for analyzing complex crude extracts (Kang *et al.*, 2018; Maciá-Vicente *et al.*, 2018; Mohimani and Pevzner, 2016). The main superiority of using MN in dereplication is that it does not only identify known molecules from complex crude extracts, but it also captures related analogues, which challenged other dereplication strategies (Yang *et al.*, 2013). Hence, MN can be easily integrated into existing natural product discovery workflows to provide comprehensive guidance in the prospecting of new bioactive



substances.

Although GNPS has curated more than 70000 spectra corresponding to known compounds, this is still a small number compared to the current number of known natural products. Hence, some alternative and complementary methods have been developed to surpass the limitations imposed by GNPS libraries. As an example, Allard and colleagues have implemented an extensive *in-silico* database (ISDB) from more than 170,000 natural products included in the Universal Natural Products Database (UNPD) (Allard *et al.*, 2016). A total number of 170,602 compounds collected in UNPD have been fragmented *in silico* using the machine learning-based tool CMF-ID. This *in-silico* dereplication pipeline has been applied to dereplicate samples from various natural resources. For instance, application of UNPD-ISDB associated with MN resulted in the successful dereplication of marine-derived fungal co-cultivation extracts (Oppong-Danquah *et al.*, 2018). A total number of 1370 nodes, grouped into 66 different chemical clusters, were observed in MN. The UNPD-ISDB aided the dereplication process that successfully annotated several known compounds, such as peptide emerimicins and sesterterpene ophiobolins from co-cultivation-derived crude extracts.

### 5.3. Bioactivity-based molecular networking for rapid discovery of bioactive natural products

The application of MN can be further enriched by associating MN with different data types such as biological activity, cultivation parameters (e.g. culture media) and genome information (Crüsemann *et al.*, 2017; Mohimani and Pevzner, 2016; Nguyen *et al.*, 2013; Purves *et al.*, 2016). One important application is the combination of bioactivity data with MN to accelerate the biodiscovery process of putative bioactive natural products. The classical discovery process of bioactive natural compounds mainly relied on a bioactivity-based workflow, which can be generally described as an “extraction-bioassay-isolation-bioassay-elucidation-bioassay” cycle (Fox Ramos *et al.*, 2019). This traditional bioactivity-guided isolation has yielded several natural products which have resulted in FDA approved medicines for the treatment of numerous diseases (Noble, 1990; Oberlies and Kroll, 2004; Tu, 2011). However, it faces several challenges such as frequent rediscovery of known compounds, a time-consuming purification process and frequent loss of activity during bioassay-guided fractionation. MN combined with bioactivity data has emerged as a useful tool to overcome these drawbacks and it further has been proven to facilitate and accelerate the isolation process for targeted discovery of new bioactive natural products (Li *et al.*, 2018; Nothias *et al.*, 2018; Olivon *et al.*, 2017a).

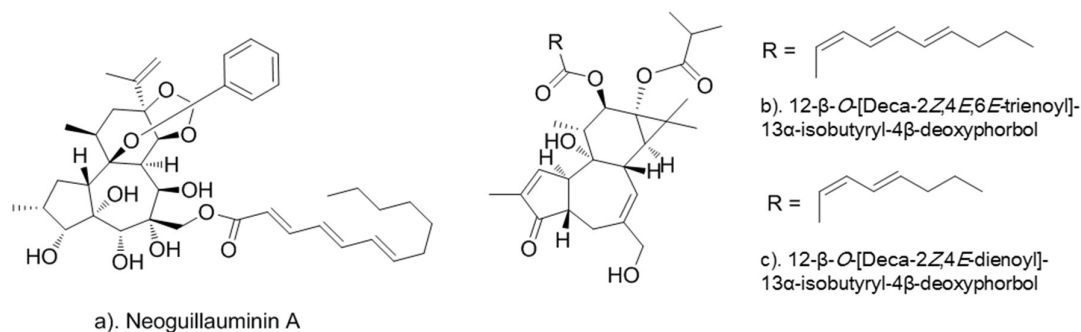


**Figure 13.** a) Neoguillauminin A isolated from two plants (*Bocquillonia nervosa* and *Neoguillauminia cleopatra*) based on ‘bioactivity mapping’ approach. b-c). Selective anti CHIKV deoxyphorbol esters isolated from *Euphorbia dendroides* (Euphorbiaceae) guided by bioactivity-based MN.

Combining bioassay results with MN generated the so-called “bioactivity mapping” (Olivon *et al.*, 2017a). Bioactivity mapping classifies crude extracts or fractions according to their activity level

(reported as  $IC_{50}/EC_{50}$  values) and then assigns different color tags to different bioactivity levels. This colorful mapping enables a simple visualization of nodes exclusively derived from bioactive extracts or fractions, thus enabling detection of potentially new bioactive scaffolds already at a very early stage of the analysis workflow. In a collection of 292 crude extracts from 107 New Caledonian Euphorbiaceae species, exploration of nodes frequently occurred in bioactive samples yielded the purification of a novel daphnane diterpene orthoester named neoguillauminin A from two plants (*Bocquillonia nervosa* and *Neoguillauminia cleopatra*). Neoguillauminin A showed anti-Chikungunya virus (CHIKV) bioactivity with  $EC_{50}$  value of  $17.7\mu\text{M}$  (Figure 13a). Furthermore, application of statistical methods (Pearson correlation coefficient) to MN resulted in the development of a “bioactivity-based molecular networking (MN)”, which was first introduced by Nothias *et al.* (2018). Bioactivity-based MN optimized the natural products isolation process by the following steps: 1). Acquiring LC-MS/MS data and modifying data using LC-MS feature-based software such as MZmine2, detecting and quantifying the ions detected in crude extracts/fractions; 2). Calculating bioactivity scores using Pearson correlation method, thus taking into account the intensity of detected ion peaks and bioactivity level of each subfraction; 3). Generating the MN using the GNPS derived feature-based platform, combining predicted bioactivity score and annotated dereplication in MN (Figure 14). This bioactivity-based MN approach has been applied to a latex extract from the plant *Euphorbia dendroides* (Euphorbiaceae) for reinvestigation of bioactive metabolites and yielded the isolation of two selective CHIKV replication inhibitors with half effective concentration ( $EC_{50}$ ) values of  $0.40\mu\text{M}$  and  $0.60\mu\text{M}$  (Nothias *et al.*, 2018) (Figure 13b-c). Compared to traditional bioactivity-guided isolation, the bioactivity mapping or bioactivity-based MN reduced the “fractionation-test” iterative cycle through targeting predicted bioactive molecules, considerably saving time and money (Figure 14). To our knowledge, bioactivity-based MN has not yet been applied for isolation of bioactive compounds from marine fungal extracts.

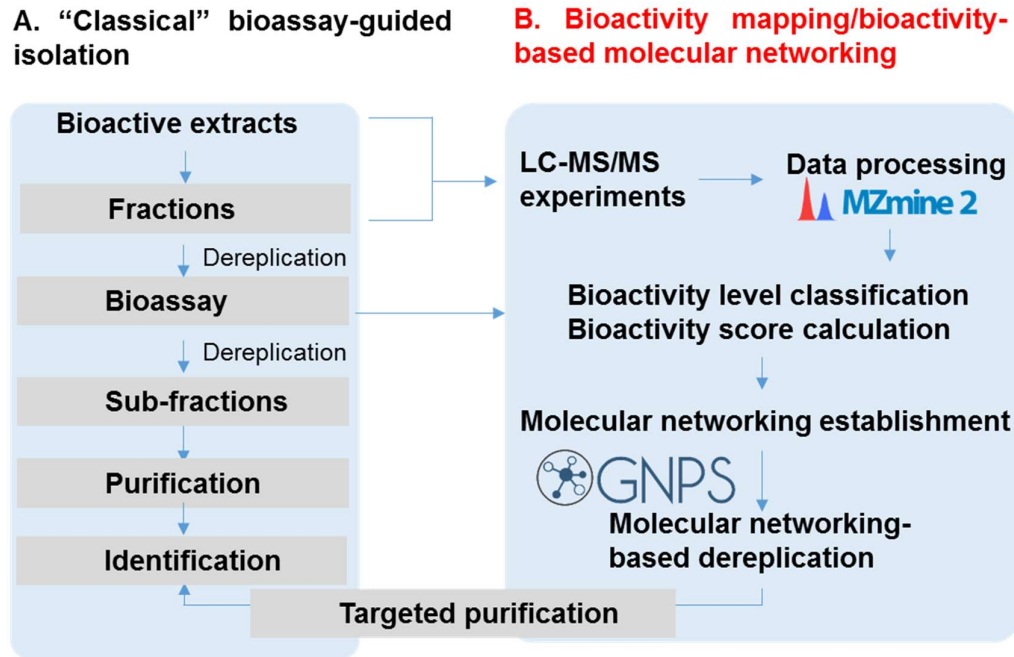


**Figure 14.** Comparison between traditional bioactivity-based workflow and bioactivity mapping/bioactivity-based molecular networking. (A). “Classical” bioassay-guided isolation (B). Bioactivity mapping/bioactivity-based molecular networking. Figure was adapted from Nothias *et al.*, 2018.

## 6. Research objective

MAF are prolific sources of new SMs with excellent bioactivities (Teixeira *et al.*, 2019; Zhang *et al.*, 2016). However, epiphytic and endophytic fungi derived from Baltic Sea *Fucus vesiculosus* were rarely studied for their biodiscovery potential as of yet. Until now, the distribution as well as the anticancer potential of fungi associated with *F. vesiculosus* has not yet been investigated. As indicated by a previous study (Parrot *et al.*, 2019), the fungal community associated with Baltic Sea *F. vesiculosus* showed great potential to produce new bioactive metabolites. Objective of this study was a biodiscovery approach targeting fungi associated to the brown algal species *F. vesiculosus*. Fungal isolates associated to the surface (epiphytes) and inner tissue (endophytes) of *F. vesiculosus* were studied for their potential to yield anticancer lead compounds. This is the first study investigating the fungal diversity associated to *Fucus vesiculosus*.

In order to activate silent BGCs for production of new SMs, the OSMAC approach was applied to 26 selected isolates to increase their chemical space. We aimed to test the applicability of molecular networking combined bioactivity in the biodiscovery workflow based on marine fungi. We applied a combination of bioactivity and MN on two different levels, i) bioactivity mapping of crude extracts for strain prioritization and ii) bioactivity-based MN on SPE fractions to enable a targeted isolation of novel compounds from the prioritized strains.

## References

- Abastabar, M., Akbari, A., Akhtari, J., Hedayati, M. T., Shokohi, T., Mehrad-Majd, H., Ghalehnoei, H., Ghasemi, S., 2017. *In vitro* antitumor activity of patulin on cervical and colorectal cancer cell lines. *Curr. Med. Mycol.* 3, 25-29. DOI: 10.18869/acadpub.cmm.3.1.25
- Abdel-Gawad, K. M., Hifney, A. F., Issa, A. A., Gomaa, M., 2014. Spatio-temporal, environmental factors, and host identity shape culturable-epibiotic fungi of seaweeds in the Red Sea, Egypt. *Hydrobiologia* 740, 37-49. DOI: 10.1007/s10750-014-1935-0
- Abdel-Lateff, A., Fisch, K. M., Wright, A. D., Konig, G. M., 2003. A new antioxidant isobenzofuranone derivative from the algicolous marine fungus *Epicoccum* sp. *Planta Med.* 69, 831-834. DOI: 10.1055/s-2003-43209
- Abdelwahab, M. F., Kurtán, T., Mándi, A., Müller, W. E. G., Fouad, M. A., Kamel, M. S., Liu, Z., Ebrahim, W., Daletos, G., Proksch, P., 2018. Induced secondary metabolites from the endophytic fungus *Aspergillus versicolor* through bacterial co-culture and OSMAC approaches. *Tetrahedron Lett.* 59, 2647-2652. DOI: 10.1016/j.tetlet.2018.05.067
- Allard, P.-M., Péresse, T., Bisson, J., Gindro, K., Marcourt, L., Pham, V. C., Roussi, F., Litaudon, M., Wolfender, J.-L., 2016. Integration of molecular networking and *in-silico* MS/MS fragmentation for natural products dereplication. *Anal. Chem.* 88, 3317-3323. DOI: 10.1021/acs.analchem.5b04804
- Amend, A. S., Barshis, D. J., Oliver, T. A., 2012. Coral-associated marine fungi form novel lineages and heterogeneous assemblages. *ISME J.* 6, 1291-1301. DOI: 10.1038/ismej.2011.193
- Ardehed, A., Johansson, D., Sundqvist, L., Schagerstrom, E., Zagrodzka, Z., Kovaltchouk, N. A., Bergstrom, L., Kautsky, L., Rafajlovic, M., Pereyra, R. T., Johannesson, K., 2016. Divergence within and among seaweed sibilings (*Fucus vesiculosus* and *F. radicans*) in the Baltic Sea. *PLOS ONE* 11, e0161266-e0161281. DOI: 10.1371/journal.pone.0161266
- Arruebo, M., Vilaboa, N., Sáez-Gutierrez, B., Lambea, J., Tres, A., Valladares, M., González-Fernández, Á., 2011. Assessment of the evolution of cancer treatment therapies. *Cancers* 3, 3279-3330. DOI: 10.3390/cancers3033279
- Baral, B., Akhgari, A., Metsä-Ketelä, M., 2018. Activation of microbial secondary metabolic pathways: Avenues and challenges. *Syst. Synth. Biol.* 3, 163-178. DOI: 10.1016/j.synbio.2018.09.001
- Bergmann, S., Schumann, J., Scherlach, K., Lange, C., Brakhage, A. A., Hertweck, C., 2007. Genomics-driven discovery of PKS-NRPS hybrid metabolites from *Aspergillus nidulans*. *Nat. Chem. Biol.* 3, 213-217. DOI: 10.1038/nchembio869
- Blayney, D. W., Huang, L., Mohanlal, R., 2019. A randomized phase 3 clinical trial of the combination of plinabulin (plin)+pegfilgrastim (peg) versus (vs) peg alone for tac (docetaxel, doxorubicin, cyclophosphamide) induced neutropenia (cin). *Blood* 134, 3590-3590. DOI: 10.1182/blood-2019-127310
- Bode, H. B., Bethe, B., Höfs, R., Zeeck, A., 2002. Big effects from small changes: Possible ways to explore nature's chemical diversity. *ChemBioChem* 3, 619-627. DOI: 10.1002/1439-7633(20020703)3:7<619::aid-cbic619>3.0.co;2-9
- Boyer, N., Morrison, K. C., Kim, J., Hergenrother, P. J., Movassaghi, M., 2013. Synthesis and anticancer activity of epipolythiodiketopiperazine alkaloids. *Chem. Sci.* 4, 1646-1657. DOI: 10.1039/C3SC50174D
- Brakhage, A. A., Schuemann, J., Bergmann, S., Scherlach, K., Schroeckh, V., Hertweck, C., 2008. Activation of fungal silent gene clusters: A new avenue to drug discovery. In: Petersen, F., Amstutz, R. (Eds.), *Natural Compounds as Drugs: Volume II*. Birkhäuser Basel, Basel, pp. 1-12. DOI: 10.1007/978-3-7643-8595-8\_1
- Bray, F., Ferlay, J., Soerjomataram, I., Siegel, R. L., Torre, L. A., Jemal, A., 2018. Global cancer statistics 2018: GLOBOCAN estimates of incidence and mortality worldwide for 36 cancers in 185 countries. *CA: Cancer J. Clin.* 68, 394-424. DOI: 10.3322/caac.21492
- Bugni, T. S., Ireland, C. M., 2004. Marine-derived fungi: A chemically and biologically diverse group of microorganisms. *Nat. Prod. Rep.* 21, 143-163. DOI: 10.1039/b301926h
- Calvo, A. M., Wilson, R. A., Bok, J. W., Keller, N. P., 2002. Relationship between secondary metabolism and fungal development. *Microbiol. Mol. Biol. Rev.* 66, 447-459. DOI: 10.1128/mmb.66.3.447-459.2002
- Camila Dos Santos Dias, A., Couzinet-Mossion, A., Ruiz, N., Le Bellec, M., Gentil, E., Wielgosz-Collin,

- G., Bertrand, S., 2017. Sugar induced modification in glycolipid production in *Acremonium* sp. revealed by LC-MS lipidomic approach. *Curr. Biotechnol.* 6, 227-237. DOI: 10.2174/2211550105666160922130029
- Chai, Y.-J., Cui, C.-B., Li, C.-W., Wu, C.-J., Tian, C.-K., Hua, W., 2012. Activation of the dormant secondary metabolite production by introducing gentamicin-resistance in a marine-derived *Penicillium purpurogenum* G59. *Mar. Drugs* 10, 559-582. DOI: 10.3390/md10030559
- Chen, Q., Jiang, J. R., Zhang, G. Z., Cai, L., Crous, P. W., 2015. Resolving the *Phoma* enigma. *Stud. Mycol.* 82, 137-217. DOI: 10.1016/j.simyco.2015.10.003
- Chiang, Y.-M., Szewczyk, E., Davidson, A. D., Keller, N., Oakley, B. R., Wang, C. C. C., 2009. A gene cluster containing two fungal polyketide synthases encodes the biosynthetic pathway for a polyketide, asperfuranone, in *Aspergillus nidulans*. *J. Am. Chem. Soc.* 131, 2965-2970. DOI: 10.1021/ja8088185
- Choi, B.-K., Trinh, P. T. H., Lee, H.-S., Choi, B.-W., Kang, J. S., Ngoc, N. T. D., Van, T. T. T., Shin, H. J., 2019. New ophiobolin derivatives from the marine fungus *Aspergillus flocculosus* and their cytotoxicities against cancer cells. *Mar. Drugs* 17, 346. DOI: 10.3390/md17060346
- Cimino, P. J., Huang, L., Du, L., Wu, Y., Bishop, J., Dalsing-Hernandez, J., Kotlarczyk, K., Gonzales, P., Carew, J., Nawrocki, S., Jordan, M. A., Wilson, L., Lloyd, G. K., Wirsching, H. G., 2019. Plinabulin, an inhibitor of tubulin polymerization, targets KRAS signaling through disruption of endosomal recycling. *Biomed. Rep.* 10, 218-224. DOI: 10.3892/br.2019.1196
- Clipson, N. J. W., Jennings, D. H., 1992. *Dendryphiella salina* and *Debaryomyces hansenii*: Models for ecophysical adaptation to salinity by fungi that grow in the sea. *Can. J. Bot.* 70, 2097-2105. DOI: 10.1139/b92-260
- Crüsemann, M., O'Neill, E. C., Larson, C. B., Melnik, A. V., Floros, D. J., da Silva, R. R., Jensen, P. R., Dorrestein, P. C., Moore, B. S., 2017. Prioritizing natural product diversity in a collection of 146 bacterial strains based on growth and extraction protocols. *J. Nat. Prod.* 80, 588-597. DOI: 10.1021/acs.jnatprod.6b00722
- Cueto, M., Jensen, P. R., Kauffman, C., Fenical, W., Lobkovsky, E., Clardy, J., 2001. Pestalone, a new antibiotic produced by a marine fungus in response to bacterial challenge. *J. Nat. Prod.* 64, 1444-1446. DOI: 10.1021/np0102713
- Dalsgaard, P. W., Blunt, J. W., Munro, M. H. G., Frisvad, J. C., Christophersen, C., 2005. Communesins G and H, new alkaloids from the psychrotolerant fungus *Penicillium rivulum*. *J. Nat. Prod.* 68, 258-261. DOI: 10.1021/np0496461
- de Gruyter, J., Woudenberg, J. H. C., Aveskamp, M. M., Verkley, G. J. M., Groenewald, J. Z., Crous, P. W., 2010. Systematic reappraisal of species in *Phoma* section *Paraphoma*, *Pyrenochaeta* and *Pleurophoma*. *Mycologia* 102, 1066-1081. DOI: 10.3852/09-240
- de Gruyter, J., Woudenberg, J. H. C., Aveskamp, M. M., Verkley, G. J. M., Groenewald, J. Z., Crous, P. W., 2013. Redisposition of *Phoma*-like anamorphs in Pleosporales. *Stud. Mycol.* 75, 1-36. DOI: 10.3114/sim0004
- Du, Z.-Y., Zienkiewicz, K., Vande Pol, N., Ostrom, N. E., Benning, C., Bonito, G. M., 2019. Algal-fungal symbiosis leads to photosynthetic mycelium. *eLife* 8, e47815-e47836. DOI: 10.7554/eLife.47815
- Egan, S., Harder, T., Burke, C., Steinberg, P., Kjelleberg, S., Thomas, T., 2013. The seaweed holobiont: Understanding seaweed-bacteria interactions. *FEMS Microbiol. Rev.* 37, 462-476. DOI: 10.1111/1574-6976.12011
- Elsebai, M. F., Natesan, L., Kehraus, S., Mohamed, I. E., Schnakenburg, G., Sasse, F., Shaaban, S., Gütschow, M., König, G. M., 2011. HLE-inhibitory alkaloids with a polyketide skeleton from the marine-derived fungus *Coniothyrium cereale*. *J. Nat. Prod.* 74, 2282-2285. DOI: 10.1021/np2004227
- English, A. L., Boufridi, A., Quinn, R. J., Kurtböke, D. I., 2017. Evaluation of fermentation conditions triggering increased antibacterial activity from a near-shore marine intertidal environment-associated *Streptomyces* species. *Syst. Synth. Biol.* 2, 28-38. DOI: 10.1016/j.synbio.2016.09.005
- Fenical, W., Jensen, P. R., Cheng, X. C., 2000. Halimide, a cytotoxic marine natural product, and derivatives thereof. World Intellectual Property Organization.
- Flewelling, A., J., Johnson, J. A., Gray, C. A., 2013a. Isolation and bioassay screening of fungal endophytes from North Atlantic marine macroalgae. *Bot. Mar.* 56, 287-297. DOI: 10.1515/bot-2012-

0224

- Flewelling, A. J., Currie, J., Gray, C. A., Johnson, J. A., 2015. Endophytes from marine macroalgae: Promising sources of novel natural products. *Curr. Sci.* 109, 88-111. Web: [www.jstor.org/stable/24905694](http://www.jstor.org/stable/24905694)
- Flewelling, A. J., Ellsworth, K. T., Sanford, J., Forward, E., Johnson, J. A., Gray, C. A., 2013b. Macroalgal endophytes from the Atlantic coast of Canada: A potential source of antibiotic natural products? *Microorganisms* 1, 175-187. DOI: 10.3390/microorganisms1010175
- Flewelling, A. J., Johnson, J. A., Gray, C. A., 2013c. Antimicrobials from the marine algal endophyte *Penicillium* sp. *Nat. Prod. Commun.* 8, 373-374. DOI: 10.1177/1934578X1300800324
- Fox Ramos, A. E., Evanno, L., Poupon, E., Champy, P., Beniddir, M. A., 2019. Natural products targeting strategies involving molecular networking: Different manners, one goal. *Nat. Prod. Rep.* 36, 960-980. DOI: 10.1039/C9NP00006B
- Fukumoto, K., Kohno, S., Kanoh, K., Asari, T., Kawashima, H., Sekiya, H., Ohmizo, K., Harada, T., 2002. Phenylahistin and the phenylahistin analogs, a new class of anti-tumor compounds. United States Patent.
- Fulton, C. J., Abesamis, R. A., Berkström, C., Depczynski, M., Graham, N. A. J., Holmes, T. H., Kulbicki, M., Noble, M. M., Radford, B. T., Tano, S., Tinkler, P., Wernberg, T., Wilson, S. K., 2019. Form and function of tropical macroalgal reefs in the Anthropocene. *Funct. Ecol.* 33, 989-999. DOI: 10.1111/1365-2435.13282
- Garbary, D. J., MacDonald, K. A., 1995. The ascophyllum/polysiphonia/mycosphaerella symbiosis. IV. mutualism in the ascophyllum/mycosphaerella interaction. *Bot. Mar.* 38, 221-225. DOI: 10.1515/botm.1995.38.1-6.221
- Gnavi, G., Garzoli, L., Poli, A., Prigione, V., Burgaud, G., Varese, G. C., 2017. The culturable mycobiota of *Flabellia petiolata*: First survey of marine fungi associated to a Mediterranean green alga. *PLOS ONE* 12, e0175941-e0175960. DOI: 10.1371/journal.pone.0175941
- Gomes, N. G. M., Lefranc, F., Kijjoa, A., Kiss, R., 2015. Can some marine-derived fungal metabolites become actual anticancer agents? *Mar. Drugs* 13, 3950-3991. DOI: 10.3390/md13063950
- Greve, H., Schupp, P. J., Eguereva, E., Kehraus, S., Kelter, G., Maier, A., Fiebig, H.-H., König, G. M., 2008. Apralactone A and a new stereochemical class of curvularins from the marine fungus *Curvularia* sp. *Eur. J. Org. Chem.* 2008, 5085-5092. DOI: 10.1002/ejoc.200800522
- Gulder, T. A. M., Hong, H., Correa, J., Egereva, E., Wiese, J., Imhoff, J. F., Gross, H., 2012. Isolation, structure elucidation and total synthesis of lajollamide A from the marine fungus *Asteromyces cruciatus*. *Mar. Drugs* 10, 2912-2935. DOI: 10.3390/md10122912
- Gutiérrez, M. H., Pantoja, S., Tejos, E., Quiñones, R. A., 2011. The role of fungi in processing marine organic matter in the upwelling ecosystem off Chile. *Mar. Biol.* 158, 205-219. DOI: 10.1007/s00227-010-1552-z
- Gutiérrez, S., Marcos, A. T., Casqueiro, J., Kosalková, K., Fernández, F. J., Velasco, J., Martín, J. F., 1999. Transcription of the *pcbAB*, *pcbC* and *penDE* genes of *Penicillium chrysogenum* AS-P-78 is repressed by glucose and the repression is not reversed by alkaline pHs. *Microbiology* 145, 317-324. DOI: 10.1099/13500872-145-2-317
- Hemphill, C. F. P., Sureechatchaiyan, P., Kassack, M. U., Orfali, R. S., Lin, W., Daletos, G., Proksch, P., 2017. OSMAC approach leads to new fusarielin metabolites from *Fusarium tricinctum*. *J. Antibiot.* 70, 726-732. DOI: 10.1038/ja.2017.21
- Hewage, R. T., Aree, T., Mahidol, C., Ruchirawat, S., Kittakoop, P., 2014. One-strain-many-compounds (OSMAC) method for production of polyketides, azaphilones, and an isochromanone using the endophytic fungus *Dothideomycete* sp. *Phytochemistry* 108, 87-94. DOI: 10.1016/j.phytochem.2014.09.013
- Huang, C.-Y., Ju, D.-T., Chang, C.-F., Muralidhar Reddy, P., Velmurugan, B. K., 2017. A review on the effects of current chemotherapy drugs and natural agents in treating non-small cell lung cancer. *Biomedicine (Taipei)* 7, 12-23. DOI: 10.1051/bmdcn/2017070423
- Hubert, J., Nuzillard, J.-M., Renault, J.-H., 2017. Dereplication strategies in natural product research: How many tools and methodologies behind the same concept? *Phytochem. Rev.* 16, 55-95. DOI: 10.1007/s11101-015-9448-7
- Imhoff, J. F., 2016. Natural products from marine fungi-still an underrepresented resource. *Mar. Drugs* 14, 19. DOI: 10.3390/md14010019

- Jadulco, R., Edrada, R. A., Ebel, R., Berg, A., Schaumann, K., Wray, V., Steube, K., Proksch, P., 2004. New communesin derivatives from the fungus *Penicillium* sp. derived from the Mediterranean sponge *Axinella verrucosa*. *J. Nat. Prod.* 67, 78-81. DOI: 10.1021/np030271y
- Ji, N.-Y., Wang, B.-G., 2016. Mycochemistry of marine algicolous fungi. *Fungal Divers.* 80, 301-342. DOI: 10.1007/s13225-016-0358-9
- Jiménez-Medina, E., Berruguilla, E., Romero, I., Algarra, I., Collado, A., Garrido, F., Garcia-Lora, A., 2008. The immunomodulator PSK induces *in vitro* cytotoxic activity in tumour cell lines via arrest of cell cycle and induction of apoptosis. *BMC Cancer* 8, 78. DOI: 10.1186/1471-2407-8-78
- Jones, E. B. G., 2011. Are there more marine fungi to be described? *Bot. Mar.* 54, 343. DOI: 10.1515/bot.2011.043
- Jones, E. B. G., Pang, K.-L., Abdel-Wahab, M. A., Scholz, B., Hyde, K. D., Boekhout, T., Ebel, R., Rateb, M. E., Henderson, L., Sakayaroj, J., Suetrong, S., Dayarathne, M. C., Kumar, V., Raghukumar, S., Sridhar, K. R., Bahkali, A. H. A., Gleason, F. H., Norphanphoun, C., 2019. An online resource for marine fungi. *Fungal Divers.* 96, 347-433. DOI: 10.1007/s13225-019-00426-5
- Jones, E. B. G., Suetrong, S., Sakayaroj, J., Bahkali, A. H., Abdel-Wahab, M. A., Boekhout, T., Pang, K.-L., 2015. Classification of marine bascomycota, basidiomycota, blastocladiomycota and chytridiomycota. *Fungal Divers.* 73, 1-72. DOI: 10.1007/s13225-015-0339-4
- Jones, E. G., 2000. Marine fungi: some factors influencing biodiversity. *Fungal Divers.* 4, 53-73.
- Kang, K. B., Park, E. J., da Silva, R. R., Kim, H. W., Dorrestein, P. C., Sung, S. H., 2018. Targeted isolation of neuroprotective dicoumaroyl neolignans and lignans from *Sageretia theezans* using *in silico* molecular network annotation propagation-based dereplication. *J. Nat. Prod.* 81, 1819-1828. DOI: 10.1021/acs.jnatprod.8b00292
- Kanoh, K., Kohno, S., Asari, T., Harada, T., Katada, J., Muramatsu, M., Kawashima, H., Sekiya, H., Uno, I., 1997. (-)-Phenylahistin: A new mammalian cell cycle inhibitor produced by *Aspergillus ustus*. *Bioorg. Med. Chem. Lett.* 7, 2847-2852. DOI: 10.1016/S0960-894X(97)10104-4
- Kanoh, K., Kohno, S., Katada, J., Takahashi, J., Uno, I., 1999a. (-)-Phenylahistin arrests cells in mitosis by inhibiting tubulin polymerization. *J. Antibiot.* 52, 134-141. DOI: 10.7164/antibiotics.52.134
- Kanoh, K., Kohno, S., Katada, J., Takahashi, J., Uno, I., Hayashi, Y., 1999b. Synthesis and biological activities of phenylahistin derivatives. *Bioorg. Med. Chem.* 7, 1451-1457. DOI: 10.1016/S0968-0896(99)00059-0
- Kato, N., Nogawa, T., Takita, R., Kinugasa, K., Kanai, M., Uchiyama, M., Osada, H., Takahashi, S., 2018. Control of the stereochemical course of [4+2] cycloaddition during trans-decalin formation by Fsa2-family enzymes. *Angew. Chem. Int. Ed.* 57, 9754-9758. DOI: 10.1002/anie.201805050
- Keller, N. P., Turner, G., Bennett, J. W., 2005. Fungal secondary metabolism-from biochemistry to genomics. *Nat. Rev. Microbiol.* 3, 937-947. DOI: 10.1038/nrmicro1286
- Kiran, G. S., Hema, T. A., Gandhimathi, R., Selvin, J., Thomas, T. A., Rajeetha Ravji, T., Natarajaseenivasan, K., 2009. Optimization and production of a biosurfactant from the sponge-associated marine fungus *Aspergillus ustus* MSF3. *Colloids Surf. B: Biointerfaces* 73, 250-256. DOI: 10.1016/j.colsurfb.2009.05.025
- Kohlmeyer, J., Kohlmeyer, E., 1979. *Marine mycology: the higher fungi*. Academic Press, New York. DOI: 10.1016/C2013-0-10998-1
- König, G. M., Kehraus, S., Seibert, S. F., Abdel-Lateff, A., Müller, D., 2006. Natural products from marine organisms and their associated microbes. *ChemBioChem* 7, 229-238. DOI: 10.1002/cbic.200500087
- Kumar, A., Sørensen, J. L., Hansen, F. T., Arvas, M., Syed, M. F., Hassan, L., Benz, J. P., Record, E., Henrissat, B., Pöggeler, S., Kempken, F., 2018. Genome sequencing and analyses of two marine fungi from the North Sea unraveled a plethora of novel biosynthetic gene clusters. *Sci. Rep.* 8, 10187. DOI: 10.1038/s41598-018-28473-z
- Lang, G., Mitova, M. I., Ellis, G., van der Sar, S., Phipps, R. K., Blunt, J. W., Cummings, N. J., Cole, A. L. J., Munro, M. H. G., 2006. Bioactivity profiling using HPLC/microtiter-plate analysis: Application to a New Zealand marine alga-derived fungus, *Gliocladium* sp. *J. Nat. Prod.* 69, 621-624. DOI: 10.1021/np0504917
- Leutou, A. S., Yun, K., Kang, J. S., Son, B. W., 2013. Induced production of methyl bromodihydroxyphenyl acetates by the marine-derived fungus *Aspergillus* sp. *Chem. Pharm. Bull.* 61, 483-485. DOI: 10.1248/cpb.c12-01048

- Li, D., Liu, S., 2019. Chapter 9-Seawater quality detection. In: Li, D., Liu, S. (Eds.), *Water Quality Monitoring and Management*. Academic Press, pp. 233-249. DOI: 10.1016/B978-0-12-811330-1.00009-0
- Li, F., Janussen, D., Peifer, C., Pérez-Victoria, I., Tasdemir, D., 2018. Targeted isolation of tsitsikammamines from the Antarctic deep-sea sponge *Latrunculia biformis* by molecular networking and anticancer activity. *Mar. Drugs* 16, 268. DOI: 10.3390/md16080268
- Li, Q., Wang, G., 2009. Diversity of fungal isolates from three Hawaiian marine sponges. *Microbiol. Res.* 164, 233-241. DOI: 10.1016/j.micres.2007.07.002
- Lin, Z., Zhu, T., Wei, H., Zhang, G., Wang, H., Gu, Q., 2009. Spicochalsin A and new aspochalasins from the marine-derived fungus *Spicaria elegans*. *Eur. J. Org. Chem.* 2009, 3045-3051. DOI: 10.1002/ejoc.200801085
- Liu, Y., Li, X.-M., Meng, L.-H., Jiang, W.-L., Xu, G.-M., Huang, C.-G., Wang, B.-G., 2015. Bisthiodiketopiperazines and acorane sesquiterpenes produced by the marine-derived fungus *Penicillium adametzioides* AS-53 on different culture media. *J. Nat. Prod.* 78, 1294-1299. DOI: 10.1021/acs.jnatprod.5b00102
- Maciá-Vicente, J. G., Shi, Y.-N., Cheikh-Ali, Z., Grün, P., Glynou, K., Kia, S. H., Piepenbring, M., Bode, H. B., 2018. Metabolomics-based chemotaxonomy of root endophytic fungi for natural products discovery. *Environ. Microbiol.* 20, 1253-1270. DOI: 10.1111/1462-2920.14072
- Madhusudan, C., Manoj, S., Rahul, K., Rishi, C. M., 2011. Seaweeds: A diet with nutritional, medicinal and industrial value. *Res. J. Med. Plant* 5, 153-157. DOI: 10.3923/rjmp.2011.153.157
- Malm, T., Kautsky, L., 2003. Differences in life-history characteristics are consistent with the vertical distribution pattern of *Fucus serratus* and *Fucus vesiculosus* (Fucales, phaeophyceae) in the central Baltic Sea. *J. Phycol.* 39, 880-887. DOI: 10.1046/j.1529-8817.2003.02115.x
- Margulis, L., 1990. Words as battle cries: Symbiogenesis and the new field of endocytobiology. *BioScience* 40, 673-677. DOI: 10.2307/1311435
- Meng, L.-H., Li, X.-M., Liu, Y., Xu, G.-M., Wang, B.-G., 2017. Antimicrobial alkaloids produced by the mangrove endophyte *Penicillium brocae* MA-231 using the OSMAC approach. *RSC Adv.* 7, 55026-55033. DOI: 10.1039/C7RA12081H
- Miao, L., Kwong, T. F. N., Qian, P.-Y., 2006. Effect of culture conditions on mycelial growth, antibacterial activity, and metabolite profiles of the marine-derived fungus *Arthrinium c. f. saccharicola*. *Appl. Microbiol. Biot.* 72, 1063-1073. DOI: 10.1007/s00253-006-0376-8
- Mohimani, H., Pevzner, P. A., 2016. Dereplication, sequencing and identification of peptidic natural products: From genome mining to peptidogenomics to spectral networks. *Nat. Prod. Rep.* 33, 73-86. DOI: 10.1039/C5NP00050E
- Montaser, R., Luesch, H., 2011. Marine natural products: A new wave of drugs? *Future Med. Chem.* 3, 1475-1489. DOI: 10.4155/fmc.11.118
- Murdoch, J. M., Speirs, C. F., Geddes, A. M., Wallace, E. T., 1964. Clinical trial of cephaloridine (ceporin), a new broad-spectrum antibiotic derived from cephalosporin C. *Br. Med. J.* 2, 1238-1240. DOI: 10.1136/bmj.2.5419.1238
- Nguyen, D. D., Wu, C.-H., Moree, W. J., Lamsa, A., Medema, M. H., Zhao, X., Gavilan, R. G., Aparicio, M., Atencio, L., Jackson, C., Ballesteros, J., Sanchez, J., Watrous, J. D., Phelan, V. V., van de Wiel, C., Kersten, R. D., Mehnaz, S., De Mot, R., Shank, E. A., Charusanti, P., Nagarajan, H., Duggan, B. M., Moore, B. S., Bandeira, N., Palsson, B. Ø., Pogliano, K., Gutiérrez, M., Dorrestein, P. C., 2013. MS/MS networking guided analysis of molecule and gene cluster families. *PNAS* 110, E2611-E2620. DOI: 10.1073/pnas.1303471110
- Nielsen, K. F., Månsson, M., Rank, C., Frisvad, J. C., Larsen, T. O., 2011. Dereplication of microbial natural products by LC-DAD-TOFMS. *J. Nat. Prod.* 74, 2338-2348. DOI: 10.1021/np200254t
- Noble, R. L., 1990. The discovery of the vinca alkaloids-chemotherapeutic agents against cancer. *Biochem. Cell. Biol.* 68, 1344-1351. DOI: 10.1139/o90-197
- Nogawa, T., Kato, N., Shimizu, T., Okano, A., Futamura, Y., Takahashi, S., Osada, H., 2017. Wakodecalines A and B, new decaline metabolites isolated from a fungus *Pyrenochaetopsis* sp. RK10-F058. *J. Antibiot.* 71, 123-128. DOI: 10.1038/ja.2017.103
- Nothias, L.-F., Nothias-Esposito, M., da Silva, R., Wang, M., Protsyuk, I., Zhang, Z., Sarvepalli, A., Leyssen, P., Touboul, D., Costa, J., Paolini, J., Alexandrov, T., Litaudon, M., Dorrestein, P. C., 2018. Bioactivity-based molecular networking for the discovery of drug leads in natural product bioassay-



- guided fractionation. *J. Nat. Prod.* 81, 758-767. DOI: 10.1021/acs.jnatprod.7b00737
- Numata, A., Takahashi, C., Ito, Y., Takada, T., Kawai, K., Usami, Y., Matsumura, E., Imachi, M., Ito, T., Hasegawa, T., 1993. Communesins, cytotoxic metabolites of a fungus isolated from a marine alga. *Tetrahedron Lett.* 34, 2355-2358. DOI: 10.1016/S0040-4039(00)77612-X
- Núñez-Pons, L., Avila, C., Romano, G., Verde, C., Giordano, D., 2018. UV-Protective compounds in marine organisms from the Southern Ocean. *Mar. Drugs* 16, 336. DOI: 10.3390/md16090336
- O'Malley, M. A., 2017. From endosymbiosis to holobionts: Evaluating a conceptual legacy. *J. Theor. Biol.* 434, 34-41. DOI: 10.1016/j.jtbi.2017.03.008
- Oberlies, N. H., Kroll, D. J., 2004. Camptothecin and taxol: Historic achievements in natural products research. *J. Nat. Prod.* 67, 129-135. DOI: 10.1021/np030498t
- Ogaki, M. B., de Paula, M. T., Ruas, D., Pellizzari, F. M., García-Laviña, C. X., Rosa, L. H., 2019. Marine fungi associated with Antarctic macroalgae. In: Castro-Sowinski, S. (Ed.), *The ecological role of micro-organisms in the Antarctic environment*. Springer International Publishing, Cham, pp. 239-255. DOI: 10.1007/978-3-030-02786-5\_11
- Olivon, F., Allard, P.-M., Koval, A., Righi, D., Genta-Jouve, G., Neyts, J., Apel, C., Pannecouque, C., Nothias, L.-F., Cachet, X., Marcourt, L., Roussi, F., Katanaev, V. L., Touboul, D., Wolfender, J.-L., Litaudon, M., 2017a. Bioactive natural products prioritization using massive multi-informational molecular networks. *ACS Chem. Biol.* 12, 2644-2651. DOI: 10.1021/acscchembio.7b00413
- Olivon, F., Grelier, G., Roussi, F., Litaudon, M., Touboul, D., 2017b. MZmine2 data-preprocessing to enhance molecular networking reliability. *Anal. Chem.* 89, 7836-7840. DOI: 10.1021/acs.analchem.7b01563
- Olivon, F., Roussi, F., Litaudon, M., Touboul, D., 2017c. Optimized experimental workflow for tandem mass spectrometry molecular networking in metabolomics. *Anal. Bioanal. Chem.* 409, 5767-5778. DOI: 10.1007/s00216-017-0523-3
- Opong-Danquah, E., Parrot, D., Blümel, M., Labes, A., Tasdemir, D., 2018. Molecular networking-based metabolome and bioactivity analyses of marine-adapted fungi co-cultivated with phytopathogens. *Front. Microbiol.* 9, 2072. DOI: 10.3389/fmicb.2018.02072
- Orsi, W. D., Richards, T. A., Santoro, A. E., 2015. Cellular maintenance processes that potentially underpin the survival of subseafloor fungi over geological timescales. *Estuar. Coast. Shelf Sci.* 164, A1-A9. DOI: 10.1016/j.ecss.2015.04.009
- Osterhage, C., Kaminsky, R., König, G. M., Wright, A. D., 2000. Ascosalipyrrolidinone A, an antimicrobial alkaloid, from the obligate marine fungus *Ascochyta salicorniae*. *J. Org. Chem.* 65, 6412-6417. DOI: 10.1021/jo000307g
- Osterhage, C., König, G. M., Jones, P. G., Wright, A. D., 2002. 5-Hydroxyramulosin, a new natural product produced by *Phoma tropica*, a marine-derived fungus isolated from the alga *Fucus spiralis*. *Planta Med.* 68, 1052-1054. DOI: 10.1055/s-2002-35670
- Overy, D. P., Bayman, P., Kerr, R. G., Bills, G. F., 2014. An assessment of natural product discovery from marine (sensu strictu) and marine-derived fungi. *Mycology* 5, 145-167. DOI: 10.1080/21501203.2014.931308
- Özkaya, F. C., Ebrahim, W., El-Neketi, M., Tansel Tanrikul, T., Kalscheuer, R., Müller, W. E. G., Guo, Z., Zou, K., Liu, Z., Proksch, P., 2018. Induction of new metabolites from sponge-associated fungus *Aspergillus carneus* by OSMAC approach. *Fitoterapia* 131, 9-14. DOI: 10.1016/j.fitote.2018.10.008
- Parrot, D., Blümel, M., Utermann, C., Chianese, G., Krause, S., Kovalev, A., Gorb, S. N., Tasdemir, D., 2019. Mapping the surface microbiome and metabolome of brown seaweed *Fucus vesiculosus* by amplicon sequencing, integrated metabolomics and imaging techniques. *Sci. Rep.* 9, 1061-1077. DOI: 10.1038/s41598-018-37914-8
- Petersen, L.-E., Kellermann, M. Y., Schupp, P. J., 2020. Secondary metabolites of marine microbes: From natural products chemistry to chemical ecology. In: Jungblut, S., Liebich, V., Bode-Dalby, M. (Eds.), *YOUMARES 9 - The Oceans: Our Research, Our Future: Proceedings of the 2018 conference for YOUnG MARine RESEARCHer in Oldenburg, Germany*. Springer International Publishing, Cham, pp. 159-180. DOI: 10.1007/978-3-030-20389-4\_8
- Purves, K., Macintyre, L., Brennan, D., Hreggviðsson, G. Ó., Kuttner, E., Ásgeirsdóttir, M. E., Young, L. C., Green, D. H., Edrada-Ebel, R., Duncan, K. R., 2016. Using molecular networking for microbial secondary metabolite bioprospecting. *Metabolites* 6, 2. DOI: 10.3390/metabo6010002
- Rateb, M. E., Ebel, R., 2011. Secondary metabolites of fungi from marine habitats. *Nat. Prod. Rep.* 28,

## GENERAL INTRODUCTION

- 290-344. DOI: 10.1039/C0NP00061B
- Rédou, V., Navarri, M., Meslet-Cladière, L., Barbier, G., Burgaud, G., 2015. Species richness and adaptation of marine fungi from deep-subseafloor sediments. *Appl. Environ. Microbiol.* 81, 3571-3583. DOI: 10.1128/aem.04064-14
- Reen, F. J., Romano, S., Dobson, A. D. W., Gara, F., 2015. The sound of silence: Activating silent biosynthetic gene clusters in marine microorganisms. *Mar. Drugs* 13, 4754-4783. DOI: 10.3390/md13084754
- Reich, M., Labes, A., 2017. How to boost marine fungal research: A first step towards a multidisciplinary approach by combining molecular fungal ecology and natural products chemistry. *Mar. Genomics* 36, 57-75. DOI: 10.1016/j.margen.2017.09.007
- Richards, T. A., Jones, M. D. M., Leonard, G., Bass, D., 2012. Marine fungi: Their ecology and molecular diversity. *Annu. Rev. Mar. Sci.* 4, 495-522. DOI: 10.1146/annurev-marine-120710-100802
- Rokas, A., Mead, M. E., Steenwyk, J. L., Raja, H. A., Oberlies, N. H., 2020. Biosynthetic gene clusters and the evolution of fungal chemodiversity. *Nat. Prod. Rep.* DOI: 10.1039/C9NP00045C
- Rokas, A., Wisecaver, J. H., Lind, A. L., 2018. The birth, evolution and death of metabolic gene clusters in fungi. *Nat. Rev. Microbiol.* 16, 731-744. DOI: 10.1038/s41579-018-0075-3
- Romano, S., Jackson, S. A., Patry, S., Dobson, A. D. W., 2018. Extending the “One-Strain-Many-Compounds” (OSMAC) pinciple to mrine mcroorganisms. *Mar. Drugs* 16, 244. DOI:10.3390/md16070244
- Ruiz, B., Chávez, A., Forero, A., García-Huante, Y., Romero, A., Sánchez, M., Rocha, D., Sánchez, B., Rodríguez-Sanoja, R., Sánchez, S., Langley, E., 2010. Production of microbial secondary metabolites: Regulation by the carbon source. *Crit. Rev. Microbiol.* 36, 146-167. DOI: 10.3109/10408410903489576
- Rutledge, P. J., Challis, G. L., 2015. Discovery of microbial natural products by activation of silent biosynthetic gene clusters. *Nat. Rev. Microbiol.* 13, 509-523. DOI: 10.1038/nrmicro3496
- Sánchez, S., Chávez, A., Forero, A., García-Huante, Y., Romero, A., Sánchez, M., Rocha, D., Sánchez, B., Avalos, M., Guzmán-Trampe, S., Rodríguez-Sanoja, R., Langley, E., Ruiz, B., 2010. Carbon source regulation of antibiotic production. *J. Antibiot.* 63, 442-459. DOI: 10.1038/ja.2010.78
- Santiago, C., Fitchett, C., Munro, M. H., Jalil, J., Santhanam, J., 2012. Cytotoxic and antifungal activities of 5-hydroxyramulosin, a compound produced by an endophytic fungus isolated from *Cinnamomum mollisimum*. *Evid-based. compl. alt.* 2012, 689310-689315. DOI: 10.1155/2012/689310
- Silber, J., Kramer, A., Labes, A., Tasdemir, D., 2016. From discovery to production: Biotechnology of marine fungi for the production of new antibiotics. *Mar. Drugs* 14, 137. DOI:10.3390/md14070137
- Singh, S. B., Zink, D. L., Goetz, M. A., Dombrowski, A. W., Polishook, J. D., Hazuda, D. J., 1998. Equisetin and a novel opposite stereochemical homolog phomasetin, two fungal metabolites as inhibitors of HIV-1 integrase. *Tetrahedron Lett.* 39, 2243-2246. DOI: 10.1016/S0040-4039(98)00269-X
- Smetanina, O. F., Yurchenko, A. N., Ivanets, E. V., Kirichuk, N. N., Khudyakova, Y. V., Yurchenko, E. A., Afiyatullo, S. S., 2016. Metabolites of the marine fungus *Penicillium citrinum* associated with a brown alga *Padina* sp. *Chem. Nat. Compd.* 52, 111-112. DOI: 10.1007/s10600-016-1560-4
- Sun, H.-F., Li, X.-M., Meng, L., Cui, C.-M., Gao, S.-S., Li, C.-S., Huang, C.-G., Wang, B.-G., 2012. Asperolides A-C, tetranorlabdane diterpenoids from the marine alga-derived endophytic fungus *Aspergillus wentii* EN-48. *J. Nat. Prod.* 75, 148-152. DOI: 10.1021/np2006742
- Sutherland, G. K., 1915. New marine fungi on *Pelvetia*. *New Phytol.* 14, 33-42. DOI: 10.1111/j.1469-8137.1915.tb07171.x
- Takahashi, C., Numata, A., Ito, Y., Matsumura, E., Araki, H., Iwaki, H., Kushida, K., 1994a. Leptosins, antitumour metabolites of a fungus isolated from a marine alga. *Perkin Trans. 1*, 1859-1864. DOI: 10.1039/P19940001859
- Takahashi, C., Numata, A., Matsumura, E., Minoura, K., Eto, H., Shingu, T., Ito, T., Hasegawa, T., 1994b. Leptosins I and J, cytotoxic substances produced by a *Leptosphaeria* sp. Physico-chemical properties and structures. *J. Antibiot.* 47, 1242-1249. DOI: 10.7164/antibiotics.47.1242
- Teixeira, T. R., Santos, G. S. d., Armstrong, L., Colepicolo, P., Deboni, H. M., 2019. Antitumor potential of seaweed derived-endophytic fungi. *Antibiotics* 8, 205. DOI: 10.3390/antibiotics8040205

- Tu, Y., 2011. The discovery of artemisinin (qinghaosu) and gifts from Chinese medicine. *Nat. Med.* 17, 1217-1220. DOI: 10.1038/nm.2471
- Unsöld, I. A., Li, S.-M., 2006. Reverse prenyltransferase in the biosynthesis of fumigaclavine C in *Aspergillus fumigatus*: Gene expression, purification, and characterization of fumigaclavine C synthase FGAPT1. *ChemBioChem* 7, 158-164. DOI: 10.1002/cbic.200500318
- Usami, Y., Aoki, S., Hara, T., Numata, A., 2002. New dioxopiperazine metabolites from a *Fusarium* species separated from a marine alga. *J. Antibiot.* 55, 655-659. DOI: 10.7164/antibiotics.55.655
- Vala, A. K., 2010. Tolerance and removal of arsenic by a facultative marine fungus *Aspergillus candidus*. *Bioresour. Technol.* 101, 2565-2567. DOI: 10.1016/j.biortech.2009.11.084
- Valenzuela-Lopez, N., Cano-Lira, J. F., Guarro, J., Sutton, D. A., Wiederhold, N., Crous, P. W., Stchigel, A. M., 2018. Coelomycetous dothideomycetes with emphasis on the families Cucurbitariaceae and Didymellaceae. *Stud. Mycol.* 90, 1-69. DOI: 10.1016/j.simyco.2017.11.003
- Vallet, M., Strittmatter, M., Murúa, P., Lacoste, S., Dupont, J., Hubas, C., Genta-Jouve, G., Gachon, C. M. M., Kim, G. H., Prado, S., 2018. Chemically-mediated interactions between macroalgae, their fungal endophytes, and protistan pathogens. *Front. Microbiol.* 9, 3161-3161. DOI: 10.3389/fmicb.2018.03161
- Wang, F.-W., 2012. Bioactive metabolites from *Guignardia* sp., an endophytic fungus residing in *Undaria pinnatifida*. *Chin. J. Nat. Medicines* 10, 72-76. DOI: 10.1016/S1875-5364(12)60016-8
- Wang, H., Eze, P. M., Höfert, S.-P., Janiak, C., Hartmann, R., Okoye, F. B. C., Esimone, C. O., Orfali, R. S., Dai, H., Liu, Z., Proksch, P., 2018. Substituted L-tryptophan-L-phenyllactic acid conjugates produced by an endophytic fungus *Aspergillus aculeatus* using an OSMAC approach. *RSC Adv.* 8, 7863-7872. DOI: 10.1039/C8RA00200B
- Wang, M., Carver, J. J., Phelan, V. V., Sanchez, L. M., Garg, N., Peng, Y., Nguyen, D. D., Watrous, J., Kaponov, C. A., Luzzatto-Knaan, T., Porto, C., Bouslimani, A., Melnik, A. V., Meehan, M. J., Liu, W.-T., Crüseman, M., Boudreau, P. D., Esquenazi, E., Sandoval-Calderón, M., Kersten, R. D., Pace, L. A., Quinn, R. A., Duncan, K. R., Hsu, C.-C., Floros, D. J., Gavilan, R. G., Kleigrewe, K., Northen, T., Dutton, R. J., Parrot, D., Carlson, E. E., Aigle, B., Michelsen, C. F., Jelsbak, L., Sohlenkamp, C., Pevzner, P., Edlund, A., McLean, J., Piel, J., Murphy, B. T., Gerwick, L., Liaw, C.-C., Yang, Y.-L., Humpf, H.-U., Maansson, M., Keyzers, R. A., Sims, A. C., Johnson, A. R., Sidebottom, A. M., Sedio, B. E., Klitgaard, A., Larson, C. B., Boya P, C. A., Torres-Mendoza, D., Gonzalez, D. J., Silva, D. B., Marques, L. M., Demarque, D. P., Pociute, E., O'Neill, E. C., Briand, E., Helfrich, E. J. N., Granatosky, E. A., Glukhov, E., Ryffel, F., Houson, H., Mohimani, H., Kharbush, J. J., Zeng, Y., Vorholt, J. A., Kurita, K. L., Charusanti, P., McPhail, K. L., Nielsen, K. F., Vuong, L., Elfeki, M., Traxler, M. F., Engene, N., Koyama, N., Vining, O. B., Baric, R., Silva, R. R., Mascuch, S. J., Tomasi, S., Jenkins, S., Macherla, V., Hoffman, T., Agarwal, V., Williams, P. G., Dai, J., Neupane, R., Gurr, J., Rodríguez, A. M. C., Lamsa, A., Zhang, C., Dorrestein, K., Duggan, B. M., Almaliti, J., Allard, P.-M., Phapale, P., Nothias, L.-F., Alexandrov, T., Litaudon, M., Wolfender, J.-L., Kyle, J. E., Metz, T. O., Peryea, T., Nguyen, D.-T., VanLeer, D., Shinn, P., Jadhav, A., Müller, R., Waters, K. M., Shi, W., Liu, X., Zhang, L., Knight, R., Jensen, P. R., Palsson, B. Ø., Pogliano, K., Linington, R. G., Gutiérrez, M., Lopes, N. P., Gerwick, W. H., Moore, B. S., Dorrestein, P. C., Bandeira, N., 2016. Sharing and community curation of mass spectrometry data with Global Natural Products Social Molecular Networking. *Nat. Biotechnol.* 34, 828-837. DOI: 10.1038/nbt.3597
- Wang, W.-J., Li, D.-Y., Li, Y.-C., Hua, H.-M., Ma, E.-L., Li, Z.-L., 2014a. Caryophyllene sesquiterpenes from the marine-derived fungus *Ascotricha* sp. ZJ-M-5 by the One-Strain-Many-Compounds strategy. *J. Nat. Prod.* 77, 1367-1371. DOI: 10.1021/np500110z
- Wang, Y., Lu, Z., Sun, K., Zhu, W., 2011a. Effects of high salt stress on secondary metabolite production in the marine-derived fungus *Spicaria elegans*. *Mar. Drugs* 9, 535-542. DOI: 10.3390/md9040535
- Wang, Y., Wang, L., Zhuang, Y., Kong, F., Zhang, C., Zhu, W., 2014b. Phenolic polyketides from the co-cultivation of marine-derived *Penicillium* sp. WC-29-5 and *Streptomyces fradiae* 007. *Mar. Drugs* 12, 2079-2088. DOI: 10.3390/md12042079
- Wang, Y., Zheng, J., Liu, P., Wang, W., Zhu, W., 2011b. Three new compounds from *Aspergillus terreus* PT06-2 grown in a high salt medium. *Mar. Drugs* 9, 1368-1378. DOI: 10.3390/md9081368
- Wikström, S. A., Kautsky, L., 2007. Structure and diversity of invertebrate communities in the presence and absence of canopy-forming *Fucus vesiculosus* in the Baltic Sea. *Estuar. Coast. Shelf Sci.* 72, 168-176. DOI: 10.1016/j.ecss.2006.10.009

- Wu, J.-S., Yao, G.-S., Shi, X.-H., Rehman, S. U., Xu, Y., Fu, X.-M., Zhang, X.-L., Liu, Y., Wang, C.-Y., 2020. Epigenetic agents trigger the production of bioactive nucleoside derivatives and bisabolane sesquiterpenes from the marine-derived fungus *Aspergillus versicolor*. *Front. Microbiol.* 11, 1-9. DOI: 10.3389/fmicb.2020.00085
- Xu, S., Wang, J.-J., Wei, Y., Deng, W.-W., Wan, X., Bao, G.-H., Xie, Z., Ling, T.-J., Ning, J., 2019. Metabolomics based on UHPLC-orbitrap-MS and Global Natural Product Social Molecular Networking reveals effects of time scale and environment of storage on the metabolites and taste quality of raw Pu-erh tea. *J. Agric. Food Chem.* 67, 12084-12093. DOI: 10.1021/acs.jafc.9b05314
- Yamada, T., Iwamoto, C., Yamagaki, N., Yamanouchi, T., Minoura, K., Hagishita, S., Numata, A., 2004. Leptosins O-S, cytotoxic metabolites of a strain of *Leptosphaeria* sp. isolated from a marine alga. *Heterocycles* 63, 641-653. DOI: 10.3987/COM-03-9967
- Yamada, T., Iwamoto, C., Yamagaki, N., Yamanouchi, T., Minoura, K., Yamori, T., Uehara, Y., Andoh, T., Umemura, K., Numata, A., 2002. Leptosins M-N<sub>1</sub>, cytotoxic metabolites from a *Leptosphaeria* species separated from a marine alga. Structure determination and biological activities. *Tetrahedron* 58, 479-487. DOI: 10.1016/S0040-4020(01)01170-X
- Yanagihara, M., Sasaki-Takahashi, N., Sugahara, T., Yamamoto, S., Shinomi, M., Yamashita, I., Hayashida, M., Yamanoha, B., Numata, A., Yamori, T., Andoh, T., 2005. Leptosins isolated from marine fungus *Leptosphaeria* species inhibit DNA topoisomerases I and/or II and induce apoptosis by inactivation of Akt/protein kinase B. *Cancer Sci.* 96, 816-824. DOI: 10.1111/j.1349-7006.2005.00117.x
- Yang, J. Y., Sanchez, L. M., Rath, C. M., Liu, X., Boudreau, P. D., Bruns, N., Glukhov, E., Wodtke, A., de Felicio, R., Fenner, A., Wong, W. R., Linington, R. G., Zhang, L., Debonsi, H. M., Gerwick, W. H., Dorrestein, P. C., 2013. Molecular networking as a dereplication strategy. *J. Nat. Prod.* 76, 1686-1699. DOI: 10.1021/np400413s
- Zain ul Arifeen, M., Ma, Y.-N., Xue, Y.-R., Liu, C.-H., 2019. Deep-sea fungi could be the new arsenal for bioactive molecules. *Mar. Drugs* 18, 9. DOI: 10.3390/md18010009
- Zhang, P., Li, X., Wang, B.-G., 2016. Secondary metabolites from the marine algal-derived endophytic fungi: Chemical diversity and biological activity. *Planta Med.* 82, 832-842. DOI: 10.1055/s-0042-103496
- Zhu, T. J., Du, L., Hao, P. F., Lin, Z. J., Gu, Q. Q., 2009. Citrinal A, a novel tricyclic derivative of citrinin, from an algicolous fungus *Penicillium* sp. i-1-1. *Chin. Chem. Lett.* 20, 917-920. DOI: 10.1016/j.ccllet.2009.03.009
- Zhuravleva, O. I., Kirichuk, N. N., Denisenko, V. A., Dmitrenok, P. S., Yurchenko, E. A., Min'ko, E. M., Ivanets, E. V., Afiyatullof, S. S., 2016. New diorcinol J produced by co-cultivation of marine fungi *Aspergillus sulphureus* and *Isaria felina*. *Chem. Nat. Compd.* 52, 227-230. DOI: 10.1007/s10600-016-1601-z
- Zuccaro, A., Schoch, C. L., Spatafora, J. W., Kohlmeyer, J., Draeger, S., Mitchell, J. I., 2008. Detection and identification of fungi intimately associated with the brown seaweed *Fucus serratus*. *Appl. Environ. Microbiol.* 74, 931-941. DOI: 10.1128/aem.01158-07
- Zuccaro, A., Schulz, B., Mitchell, J. I., 2004a. Molecular detection of ascomycetes associated with *Fucus serratus*. *Mycol. Res.* 107, 1451-1466. DOI: 10.1017/S0953756203008657
- Zuccaro, A., Summerbell, R. C., Gams, W., Schroers, H.-J., Mitchell, J. I., 2004b. A new *Acremonium* species associated with *Fucus* spp., and its affinity with a phylogenetically distinct marine *Emericellopsis* clade. *Stud. Mycol.* 50, 283-297. DOI: ci.nii.ac.jp/naid/10027837088/
- Zugazagoitia, J., Guedes, C., Ponce, S., Ferrer, I., Molina-Pinelo, S., Paz-Ares, L., 2016. Current challenges in cancer treatment. *Clin. Ther.* 38, 1551-1566. DOI: 10.1016/j.clinthera.2016.03.026

---

## II. RESULTS

---



# Chapter 1


**Influence of OSMAC-Based Cultivation in Metabolome and Anticancer Activity of Fungi Associated with the Brown Alga *Fucus vesiculosus***

## RESULTS



Article

# Influence of OSMAC-Based Cultivation in Metabolome and Anticancer Activity of Fungi Associated with the Brown Alga *Fucus vesiculosus*

Bicheng Fan <sup>1</sup>, Delphine Parrot <sup>1</sup>, Martina Blümel <sup>1</sup>, Antje Labes <sup>1,†</sup> and Deniz Tasdemir <sup>1,2,\*</sup> 

<sup>1</sup> GEOMAR Centre for Marine Biotechnology (GEOMAR-Biotech), Research Unit Marine Natural Products Chemistry, GEOMAR Helmholtz Centre for Ocean Research Kiel, Am Kiel-Kanal 44, 24106 Kiel, Germany; bfan@geomar.de (B.F.); delphine.parrot@gmail.com (D.P.); mbluemel@geomar.de (M.B.); antje.labes@hs-flensburg.de (A.L.)

<sup>2</sup> Faculty of Mathematics and Natural Sciences, Kiel University, Christian-Albrechts-Platz 4, 24118 Kiel, Germany

\* Correspondence: dtasdemir@geomar.de; Tel.: +49-431-600-4430

† Current address: Flensburg University of Applied Sciences, Department Energy and Biotechnology, Kanzleistraße 91-93, 24943 Flensburg, Germany.

Received: 6 January 2019; Accepted: 16 January 2019; Published: 19 January 2019



**Abstract:** The fungi associated with marine algae are prolific sources of metabolites with high chemical diversity and bioactivity. In this study, we investigated culture-dependent fungal communities associated with the Baltic seaweed *Fucus vesiculosus*. Altogether, 55 epiphytic and endophytic fungi were isolated and identified. Twenty-six strains were selected for a small-scale One-Strain-Many-Compounds (OSMAC)-based fermentation in four media under solid and liquid culture regimes. In total, 208 fungal EtOAc extracts were tested for anticancer activity and general cytotoxicity. Ten most active strains (i.e., 80 extracts) were analyzed for their metabolome by molecular networking (MN), *in-silico* MS/MS fragmentation analysis (ISDB-UNPD), and manual dereplication. Thirty-six metabolites belonging to 25 chemical families were putatively annotated. The MN clearly distinguished the impact of culture conditions in chemical inventory and anticancer activity of the fungal extracts that was often associated with general toxicity. The bioactivity data were further mapped into MN to seek metabolites exclusively expressed in the active extracts. This is the first report of cultivable fungi associated with the Baltic *F. vesiculosus* that combined an OSMAC and an integrated MN-based untargeted metabolomics approaches for efficient assessment and visualization of the impact of the culture conditions on chemical space and anticancer potential of the fungi.

**Keywords:** Marine fungi; *Fucus vesiculosus*; OSMAC; molecular network; metabolomics; dereplication; bioactivity mapping

## 1. Introduction

Marine fungi are found in all habitats and make a significant contribution to marine environments, e.g., by decomposition of substrates and animal remains. Marine fungi are regarded as saprotrophs, parasites, or symbionts (epiphytic and endophytic), as a consequence of the evolution of fungal cell biology and feeding strategies [1–3]. Recent culture-dependent studies reveal that fungi establish a symbiotic association with marine macroalgae (seaweeds) [1–3]. The sedentary lifestyle and the lack of an immune system have led to the evolution of a seaweed holobiont, in which macroalga and its associated microbiota, including fungi, jointly exercise to enhance the tolerance to abiotic and biotic stresses [4]. The algicolous fungi have been shown to produce diverse types of secondary metabolites, presumably contributing to the fitness of its host. Some of these metabolites have demonstrated

bioactivities, e.g., antioxidant, antimicrobial, and cytotoxic [5–7] that are beneficial to human health. A prominent example is halimide, a diketopiperazine obtained from an *Aspergillus* sp. isolated from the green alga *Halimeda copiosa* [8]. Plinabulin (NPI-2358) is a synthetic tert-butyl analog of halimide and the only marine fungal metabolite-based compound that has entered clinical trials (currently in Phase III) to date [9]. This clearly highlights the potential of seaweed-derived fungi as a valuable source for discovery of anticancer lead compounds.

Recent bioinformatic approaches in the genomics field points out a significant discrepancy between the number of secondary metabolite biosynthetic gene clusters (BGCs) and the actual number of chemically characterized compounds obtained from microorganisms. This stems from the so-called ‘silent’ or ‘cryptic’ BGCs that are not expressed under standard laboratory conditions due to a lack of essential natural stimuli for activation of secondary metabolite BGCs [10]. Hence, fermentation of microorganisms in artificial laboratory conditions represents a major limitation in microbial drug discovery. Culture-based strategies such as OSMAC (One-Strain-Many-Compounds) or co-cultivation are vital to evoke the expression of silent BGCs to produce new compounds [11]. The OSMAC approach is highly efficient for induction of chemical diversity by variation of cultivation parameters [12]. It has been successfully applied to stimulate the production of several new marine fungal secondary metabolites, exemplified by lajollamide A, a new pentapeptide produced by the marine green alga-derived fungus *Asteromyces cruciatus* [13]. This observation, in addition to numerous other OSMAC-based cultivation studies on microorganisms, suggest that variation of culture conditions is a promising approach for enhancing the chemical space of alga-derived fungi.

MS/MS based Global Natural Products Social Molecular Networking (GNPS) is a platform, which enables rapid and automated mass spectral mining of large number of samples. It groups similar compounds based on similarities of their MS/MS fragmentation patterns and links known and unknown compounds belonging to the same molecular family in networks [14]. This approach not only substantially accelerates dereplication capabilities and enhances annotation rates, but also delivers more in-depth information on chemical inventory of biological organisms [15]. Integration of MN with *in-silico* fragmentation pattern database (Universal Natural Product Database (ISDB-UNPD)) further speeds up the tedious dereplication processes [16]. A few recent studies have used molecular networks (MN) for optimizing the culture conditions and the extraction methods for bacterial natural products [17]. MN also offers the possibility to map additional information over the network. The integration of bioactivity data of crude extracts and fractions obtained therefrom with MN is gaining popularity for prioritization of bioactive extracts and targeted isolation of bioactive metabolites from botanical sources [18].

The canopy-forming seaweed *Fucus vesiculosus* L. (bladder wrack) is the most-widespread brown alga in the shallow coastal regions of the Baltic Sea [19]. It serves as a primary producer providing food and shelter for marine animals [20]. Previous studies conducted on this seaweed indicate its rich chemistry and various bioactivities [21]. In a recent study, we investigated seasonal variations in the metabolome of the Baltic Sea *F. vesiculosus* and its impact on antioxidant, anticancer and antimicrobial activity profile of the *F. vesiculosus* extracts [22]. However, the associated microbiota of this seaweed or their biotechnological potential has remained poorly investigated. The fungi derived from the North Atlantic *F. vesiculosus* were tested for antibacterial and antifungal activity [6,7]. An isobenzofuranone derivative with antioxidative activity was reported from an *Epicoccum* sp. isolated from the North Sea *F. vesiculosus* [23]. The present study aimed at identification of cultivable fungal communities associated with the Baltic *F. vesiculosus*. By using an OSMAC approach, the isolated epi- and endophytic fungi were grown in, altogether, eight solid and liquid-based culture media. The generated extracts were tested for their anticancer and cytotoxic properties and the selected ones were dereplicated by an untargeted LC-MS/MS-based molecular network using automated (GNPS and ISDB-UNPD) [14,16] and classical manual dereplication methods. The UPLC-MS/MS based MN revealed different culture conditions to lead to significant differences in chemical inventory and bioactivity of the extracts. The bioactivity data combined with MN allowed the detection of specific metabolites in the anticancer

or toxic extracts. This is the first study on fungi associated with the Baltic Sea *F. vesiculosus* applying an untargeted metabolomics study integrated with OSMAC and bioactivity mapping.

## 2. Results

### 2.1. Isolation of Fungi

In total, 87 fungal strains were obtained (Table S1). Of which, 55 strains were isolated and identified from *F. vesiculosus* collected at Kiel Fjord (Baltic Sea, Germany), while 32 fungi originated from its surrounding environment, i.e.,—sediment (30 isolates) and seawater (2 isolates) controls. Four solid media (indicated by an “S” in the medium name), i.e., modified Wickerham medium (WM-S), Potato Dextrose medium (PDM-S), Glucose Yeast Peptone medium (GYP-S), and Glucose Casein medium (GCM-S) were used for their isolation. The highest number of fungal isolates was retrieved from WM-S medium (21 isolates), followed by PDM-S (15 isolates), GCM-S (10 isolates), and GYP-S (9 isolates) (Figure 1A and Figure S1). Overall, 11 epiphytic and 44 endophytic fungi were obtained from algal thalli after surface sterilization (Figure 1B). Sanger sequencing of the PCR-amplified ITS1-5.8S rRNA gene-ITS2 region allowed identification of 39 *Penicillium* sp. that constituted the largest fraction (71%) of the fungi. In general, a considerable fungal diversity was obtained with 10 strains belonging to seven fungal genera (identified at the genus level). Six isolates were identified only to a higher taxonomic (i.e., order) level (Figure 2). *Penicillium* was the predominant genus in both endophytic and epiphytic fungi. *Gibellulopsis* sp. was isolated from both endophytic and epiphytic communities. The endophytic fungi showed a four-fold higher abundance (44 isolates) and represented by five specific genera, i.e., *Acremonium*, *Trichoderma*, *Cadophora*, *Wallemia*, and *Emericellopsis* (Figure 3A). The media used had a great impact on the diversity of the isolated fungi. For example, four fungal genera (*Acremonium*, *Fusarium*, *Trichoderma* and *Wallemia*) were exclusively isolated from WM-S medium (Figure S2A). Other media also produced unique isolates, e.g., *Cadophora* sp. was only retrieved from GYP-S medium (Figure S2B). Both *Emericellopsis* sp. (WM-S and PDM-S, Figure S2A,C) and *Gibellulopsis* sp. were isolated from two different media (WM-S and GCM-S, Figure S2A,D). *Penicillium* species were obtained from all media, with PDM-S and GCM-S yielding the highest numbers (14 and 9 isolates, respectively) (Figure S2C,D).

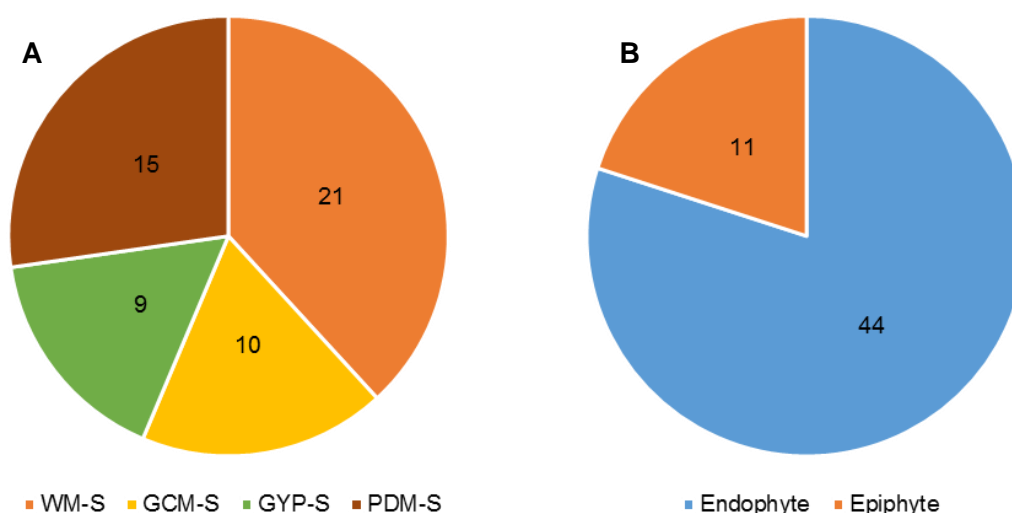


**Figure 1.** The number of identified fungal isolates from *Fucus vesiculosus*. (A) The number of fungal strains isolated from single solid medium (S). WM-S = modified Wickerham medium, PDM-S: Potato Dextrose medium, GCM-S; Glucose Casein medium, GYP-S; and Glucose Yeast Peptone medium. (B) The origin of fungi from *F. vesiculosus* microhabitats.

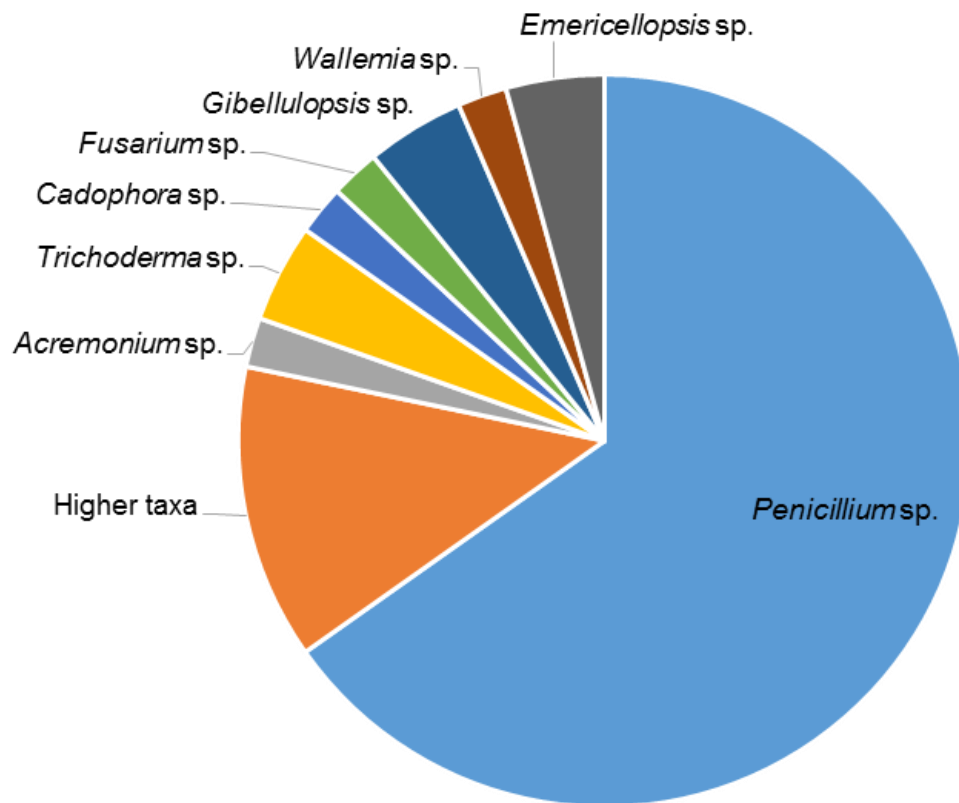
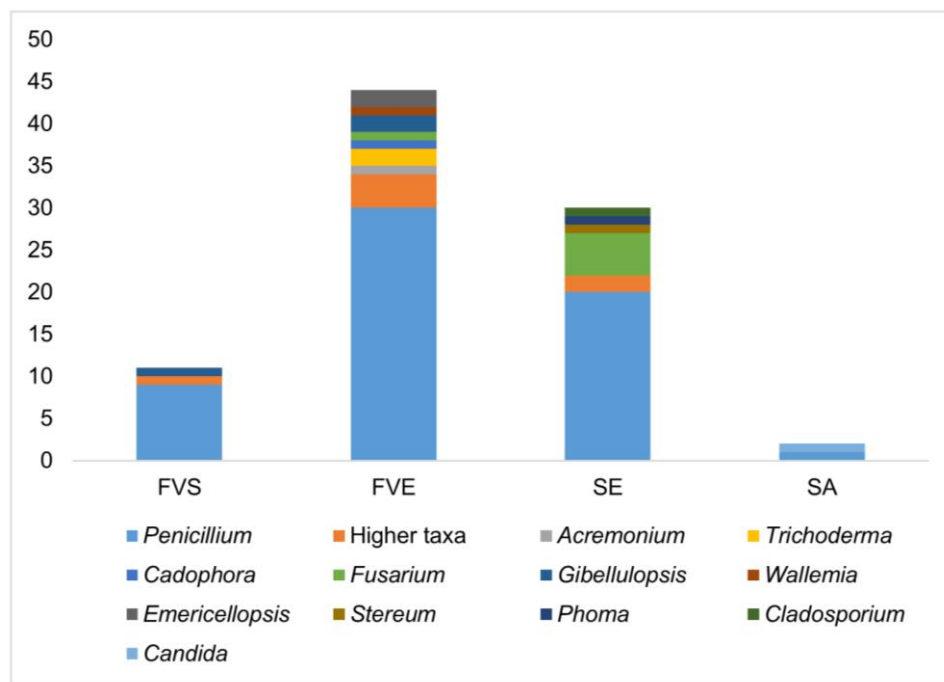


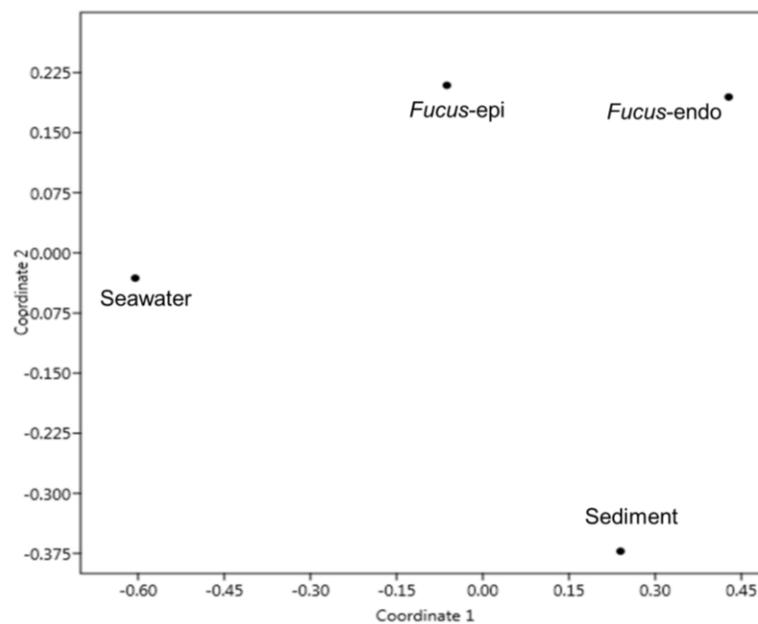
**Figure 2.** Taxonomical diversity of 55 fungal genera isolated from *F. vesiculosus* (excluding sediment and seawater). Strains that were not identified to genus level were indicated with 'Higher taxa'.

The sediment control sample yielded 30 fungal strains, while only two isolates were retrieved from the seawater (Figure 3A). The genus *Penicillium* was also dominant among sediment isolates, accounting for 67% of the isolated strains (20 out of 30), followed by *Fusarium* sp. (5 isolates). Three genera, *Phoma*, *Cladosporium*, and *Stereum* were represented by one species each in sediment samples. Two other sediment-derived strains were only identified at order level (Figure 3A, Table S1). The seawater control yielded one *Penicillium* sp. and one *Candida* sp. Figure 3A depicts the comparative diversity of fungal isolates from *F. vesiculosus* and its surrounding habitats.

Several fungal genera, i.e., *Acremonium*, *Gibellulopsis*, *Trichoderma*, *Wallemia*, *Cadophora*, and *Emericellopsis* were exclusive to *F. vesiculosus*. The fungal communities isolated from different origins were compared by a 2D MDS plot to visualize their similarity (Figure 3B). All *Fucus*-derived fungal communities (*Fucus*-epi and *Fucus*-endo in Figure 3B) clustered more closely, showing a clear differentiation to those deriving from seawater and sediment controls.



(A)



(B)

**Figure 3.** (A) Comparison of taxonomical diversity of the fungal isolates isolated from *F. vesiculosus* and its surrounding habitat. FVS = *F. vesiculosus* surface epiphytes, FVE = *F. vesiculosus* endophytes, SE = sediment, SA = seawater. (B) 2D MDS plot (Bray Curtis Similarity index) showing differences in the origin of fungi. MDS plot is based on a presence/absence of fungal genera (all 87 identified isolates).

## 2.2. OSMAC Cultivation, Extraction and Anticancer Assays

Twenty-three endophytic and three epiphytic fungal strains (Table 1) deriving from *F. vesiculosus* thalli were selected for subsequent small-scale fermentation using an OSMAC approach. The strain selection criteria were: (i) genetic diversity at genus or order level and (ii) morphology differences in colony (especially *Penicillium* sp.). Four different culture media, PDM, WM, Sucrose Yeast Medium (SYM), and Czapek (Cza) were selected based on variations they offer with respect to carbon source

and salt concentration. Additionally, the solid (“S”, agar plates, static) and liquid (“L”, 300 mL flasks, shaking at 120 rpm) culture regimes were applied in order to enhance the chemical diversity of the selected strains. The temperature was set to 22 °C in all samples. A simple coding system including the strain number, growth medium, and culture regime was used to describe the extracts (e.g., 1PDM-L).

**Table 1.** The list of 26 *F. vesiculosus*-derived fungal isolates selected for OSMAC-based cultivation. Strain I.D. numbers correspond to those used in strain collection in Table S1. Closest relative identification showing high sequence similarity according to NCBI GenBank by BLAST and the original isolation medium are displayed. \* Strain could not be identified to genus level, but to a higher taxa (order) level.

Strain I.D.	Epiphytic/Endophytic Fungus	Closest Taxonomical Relative	Sequence Similarity (%)	Isolation Solid Medium
1 *	Endophytic	Pleosporales (order)	100	WM-S
11	Epiphytic	<i>Gibellulopsis</i> sp.	100	GCM-S
12	Endophytic	<i>Acremonium</i> sp.	99	WM-S
35	Endophytic	<i>Cadophora malorum</i>	100	GYP-S
37 *	Endophytic	Hypocreales (order)	99	GYP-S
38	Endophytic	<i>Penicillium biourgeianum</i>	100	WM-S
50	Endophytic	<i>Penicillium</i> sp.	99	PDM-S
55	Endophytic	<i>Penicillium glabrum</i>	100	PDM-S
56	Endophytic	<i>Penicillium</i> sp.	100	WM-S
58	Endophytic	<i>Fusarium graminearum</i>	96	WM-S
59 *	Endophytic	Glomerellales (order)	100	WM-S
61	Endophytic	<i>Penicillium brevicompactum</i>	100	PDM-S
62	Endophytic	<i>Penicillium brevicompactum</i>	100	PDM-S
67	Endophytic	<i>Gibellulopsis nigrescens</i>	100	WM-S
68	Endophytic	<i>Penicillium</i> sp.	100	WM-S
78	Endophytic	<i>Penicillium</i> sp.	100	PDM-S
81	Endophytic	<i>Wallemia muriae</i>	100	WM-S
82	Endophytic	<i>Emericellopsis</i> sp.	99	WM-S
84 *	Endophytic	Hypocreales (order)	100	WM-S
86	Endophytic	<i>Emericellopsis terricola</i>	99	PDM-S
87 *	Endophytic	Pleosporales (order)	99	WM-S
89	Endophytic	<i>Trichoderma</i> sp.	100	WM-S
91	Endophytic	<i>Penicillium virgatum</i>	100	GCM-S
96	Epiphytic	<i>Penicillium brevicompactum</i>	100	GYP-S
104	Epiphytic	<i>Penicillium chrysogenum</i>	100	WM-S
122	Endophytic	<i>Penicillium brevicompactum</i>	100	GCM-S

The selected strains were cultured, and overall, under eight different conditions, for two weeks and subsequently extracted with EtOAc to yield 208 crude extracts. These extracts were profiled for their in vitro activity against six cancer cell lines (liver cancer cell line HepG2, colorectal adenocarcinoma cell line HT29, malignant melanoma cell line A375, colon cancer cell line HCT116, lung carcinoma cell line A549, human breast cancer line MDA-MB231) and for toxicity against the noncancerous human keratinocyte cell line (HaCaT). Twenty-six samples that showed >90% growth inhibition at the initial test concentration (200 µg/mL) against at least one cancer line were selected and further tested for determination of their IC<sub>50</sub> values. A threshold in anticancer activity (IC<sub>50</sub> value ≤ 100 µg/mL against at least one cancer line) was set as a second filter for further prioritization of the extracts. Hence, 10 endophytic strains complying with this criterium were selected and grown in four liquid and four solid culture conditions to generate 80 extracts. Of these, only 16 extracts, all deriving from endophytic strains (Table 2) inhibited at least one cancer cell line with an IC<sub>50</sub> value of ≤ 100 µg/mL, whereas the remaining 64 were inactive (IC<sub>50</sub> > 100 µg/mL). Notably, 14 of the 16 fungal extracts that showed anticancer activity (IC<sub>50</sub> values 2–100 µg/mL) also inhibited the growth of HaCaT cells with similar IC<sub>50</sub> values, indicating a general toxicity. Only two crude extracts (1PDM-L and 58Cza-S) were active against cancer cell lines (IC<sub>50</sub> values 39–98 µg/mL) and possessed no toxicity against HaCaT cell lines at 100 µg/mL concentration (Table 2). All sixteen extracts were selected for further studies.

**Table 2.** List of 16 extracts deriving from 10 fungi with IC<sub>50</sub> values ≤ 100 µg/mL against at least one cancer line. Crude extracts were tested against six cancer cell lines (human liver cancer cell line HepG2, human colorectal adenocarcinoma cell line HT29, human malignant melanoma cell line A375, human colon cancer cell line HCT116, human lung carcinoma cell line A549 and human breast cancer line MDA-MB231) and the non-cancerous human keratinocyte cell line HaCaT. Stand.: Standard for positive control (doxorubicin). Strain I.D. corresponds to strain collection I.D. in Table S1.

Strain I.D.	Taxonomic ID	Medium & Regime	IC <sub>50</sub> Value (µg/mL)						
			HepG2	HT29	A375	HCT116	A549	MDA-MB231	HaCaT
1	Pleosporales	PDM-L	47	39	>100	>100	98	49	>100
35	<i>Cadophora malorum</i>	PDM-L	15	50	4	6	16	35	5
37	Hypocreales	PDM-L	11	27	5	7	18	7	8
50	<i>Penicillium</i> sp.	PDM-L	11	100	8	8	15	7	9
		PDM-S	6	16	29	8	10	2	2
		Cza-S	>100	>100	53	23	23	6	4
56	<i>Penicillium</i> sp.	PDM-L	43	36	66	>100	42	35	69
		Cza-L	100	100	63	>100	40	32	32
58	<i>Fusarium graminearum</i>	PDM-L	74	69	72	74	85	78	78
		PDM-S	69	63	59	69	71	62	44
		Cza-S	65	79	52	65	74	74	>100
59	Glomerellales	PDM-S	>100	>100	42	32	83	14	30
68	<i>Penicillium</i> sp.	PDM-L	10	32	8	7	10	5	8
		PDM-S	12	18	28	6	9	3	3
78	<i>Penicillium</i> sp.	PDM-L	17	21	15	25	19	9	10
87	Pleosporales	PDM-L	43	35	56	91	36	30	60
Stand.			14.9	3	0.13	10.6	31.4	15.2	10

The composition of the medium, as well as the culture regime, had a profound impact in bioactivity and toxicity of the fungi (Table 2). For example, the crude extracts of strains 1 (order Pleosporales), 35 (*Cadophora malorum*), 37 (order Hypocreales), 78 (*Penicillium* sp.), and 87 (order Pleosporales), inhibited the cancer cell lines only when fermented in liquid PDM medium (PDM-L). Similarly, strain 59 (order Glomerellales), cultivated only in PDM-S, displayed activity against four cancer cell lines, particularly against MDA-MB231 cells (IC<sub>50</sub> value 14 µg/mL, Table 2). The remaining strains were either active in both liquid and solid cultures of one medium (e.g., *Penicillium* sp.—strain 68 in PDM), or in multiple media and culture conditions, e.g., strain 56 (*Penicillium* sp.) and strain 58 (*Fusarium graminearum*) (Table 2). In the case of strain 50 (*Penicillium* sp.), the extracts deriving from PDM-L and PDM-S media showed higher potency in comparison to that deriving from the Cza-S medium.

### 2.3. Evaluation of the Chemical Diversity Using Molecular Network Approach

An UPLC-QToF-MS/MS based comparative untargeted metabolomics study (in positive ionization mode) was carried out on those 10 initially selected strains (Figure S3). To ascertain the impact of media and culture regime on the chemical profile, as well as to detect potentially specific metabolites produced in the bioactive samples, 80 EtOAc extracts (10 strains grown in 8 culture conditions) were subjected to MN-based metabolomics analysis. The MS/MS data of the extracts were analyzed using the publicly available Global Natural Products Social Molecular Networking (GNPS) platform (<https://gnps.ucsd.edu>) [14] combined with both *in-silico* MS/MS database (ISDB-UNPD) [16] and manual dereplication employing multiple databases (Dictionary of Natural Products (DNP) [24], Scifinder [25], and Chempidder [26]). The global MN revealed 4782 nodes in total, of which 1700 were clustered in 255 chemical families, whereas the remaining single nodes were considered as unique chemistries without link to others. Some nodes represent adducts, thus, not all network nodes correspond to a single molecule. In the MN, 25 different chemical families were annotated (Figures 4, 6 and 7 and Table S2), including various types of alkaloids, polyketides, peptides, lipids, amino acid derivatives, dihydroxyanthraquinones, bile acids, polyenes, and binaphthoquinones. Characteristic information for all annotated peak ions to known metabolites (retention time, MS, MS/MS fragmentation, molecular formula, biological source and structure) is displayed in Table S2. The global MN of fungal extracts based on culture regime and growth media are shown in Figures 4A and 6A, respectively. The global MN-derived Euler and Venn diagrams

(Figures 4B and 6B) display node (ion) distribution in different culture conditions, as discussed below. The chemical composition of each individual strain is displayed in a separate MN (Figures S4–S23).

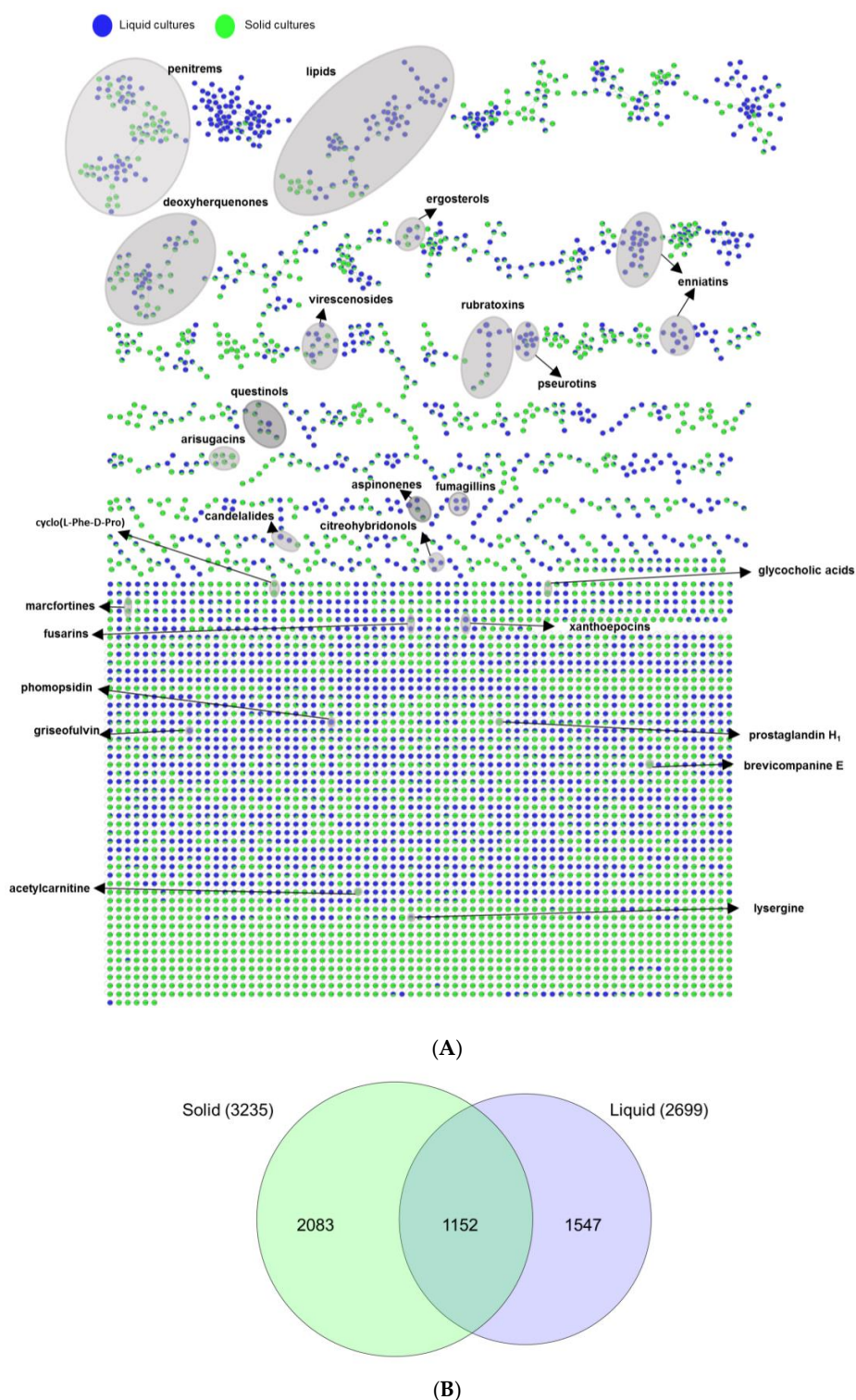


**Figure 4.** (A) Global molecular network of the extracts of 10 fungal strains grown in liquid and solid culture regimes. See Table S2 for annotated molecules. Green nodes: Ions detected in solid culture extracts. Blue nodes: Ions detected in liquid culture extracts. Grey loop: Nodes annotated as putatively known chemical clusters. (B) Euler diagram of the specific and shared ions detected in liquid and solid culture extracts.



### 2.3.1. Impact of Culture Regime on Chemical Diversity

The effect of culture regime (liquid versus solid) was ascertained by comparing liquid and solid culture groups from the MN (Figure 4A). The Euler diagram derived from MN (Figure 4B) pointed out to clear differences in the chemical profile of the liquid and solid culture extracts. In total 4782 nodes (ions) were identified. The extracts deriving from the solid cultures (in total 3235 nodes) and the liquid cultures (in total 2699 nodes) had only 1152 nodes in common, indicating <24% similarity of total 4782 nodes (Figure 4B). Approximately, 32% of the total nodes (i.e., 1547 specific nodes) were expressed exclusively in the liquid culture extracts, while 2083 nodes ( $\approx$ 43%) in the solid culture extracts. The comparison of the liquid and solid culture-derived fungal extracts clearly points out a differential chemistry. The observed metabolic differences suggest activation of different BGCs under different culture regimes.

Annotation efforts of the chemical inventory of the extracts revealed only a few metabolites to be common in both liquid and solid cultures, e.g., the aminolipid family (7–11) and aromatic polyketide deoxyherquenone (25) (Figure 4A, Table S2) in both Cza-L and Cza-S media. Interestingly, several metabolites were mapped to only one culture regime. For example, the cyclic depsipeptide enniatin B<sub>1</sub> (34) (Figure 4A and Figure S6) was detected only in liquid culture conditions. Importantly, their production was dependent on the culture regime, but was not much affected by the growth media. In addition to induction of different chemical families in individual culture regimes, we also observed production of compounds in both culture regimes. A good example is the aromatic polyketide family (21, 25, 29) that was detected in multiple extracts of strain 68 (*Penicillium* sp., Table S2). Deoxyherquenone (25,  $m/z$  [M + H]<sup>+</sup> 357.1544) was present in all liquid and solid culture extracts, whereas its analogues atrovenetinone (29,  $m/z$  [M + H]<sup>+</sup> 341.1123) and atrovenetin (21,  $m/z$  [M + H]<sup>+</sup> 343.1276) were exclusive to liquid culture regimes. As shown in Figure 5, with 22 nodes observed in liquid culture-based extracts and 13 nodes in solid extracts of the strain 68, liquid culture conditions clearly led to a higher chemical diversity for this molecular family, clearly demonstrating the impact of the culture regime on variable chemical composition of the same strain.

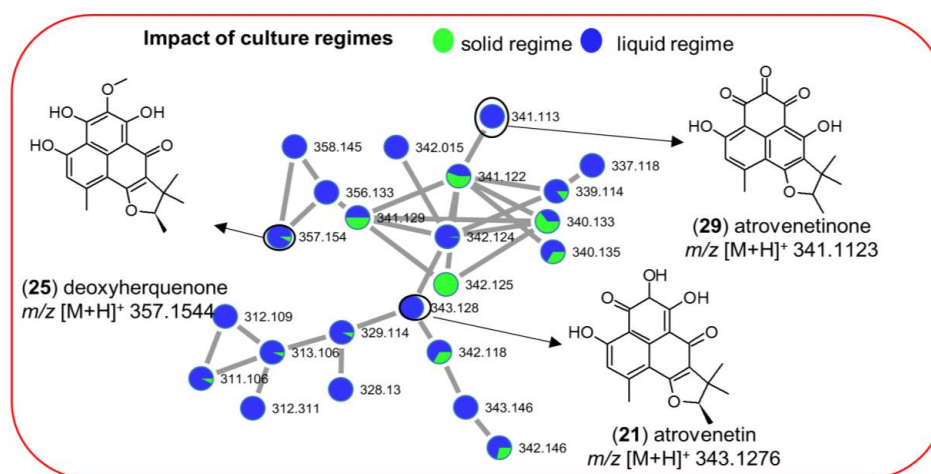


**Figure 5.** MN of the aromatic polyketide family detected in strain 68 (*Penicillium* sp.) extracts. Green: Ions detected in solid extracts. Blue: Ions detected in liquid extracts.

### 2.3.2. Impact of Culture Media on Chemical Diversity

Next, we investigated the influence of culture media on the extracts of 10 selected strains (Figure 6A). The global MN-derived Venn diagram (Figure 6B) displays the distribution of altogether 4782 detected nodes. Notably, the Cza medium contained the highest number of nodes (2820), whereas the lowest number of nodes (1615) was detected in the WM medium. The Venn diagram also clearly indicated unique expression of significant numbers of nodes in one single culture medium. For example, 1476 of all nodes (ions) were specifically mapped to the Cza medium, corresponding

to 31% of in total 4782 nodes. Significantly lower levels of nodes that were found to be exclusive to other media, i.e., 487 (PDM), 441 (SYM), and 370 (WM) (Figure 6B). These results confirmed that the chemical composition and other characteristics (e.g., selected carbon resource) of the growth media had a significant effect on the chemical machinery of the fungi derived from *F. vesiculosus*. The inspection of Table 2 indicated that most of the bioactive extracts that inhibited the growth of the cancer cell lines derived from the liquid PDM medium. Three extracts obtained from the Czapek culture also showed activities with lower potency.

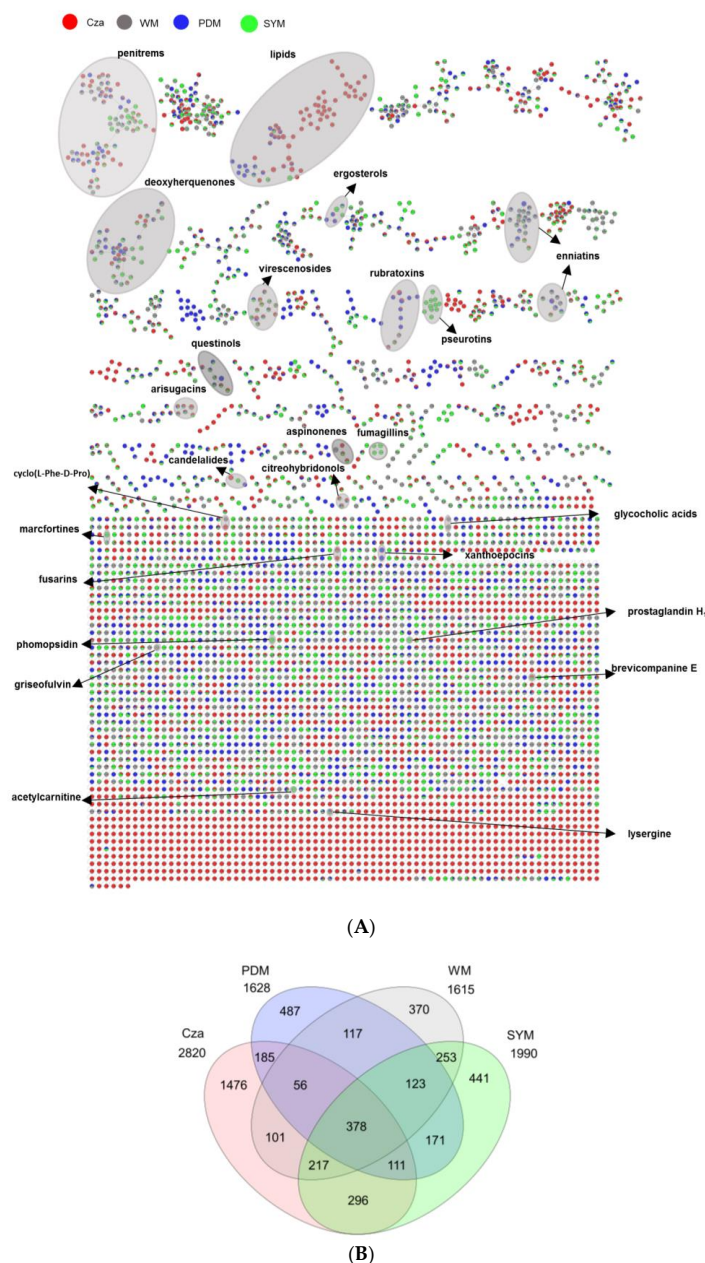


**Figure 6.** (A) Global MN of crude extracts of 10 fungal strains originating from 4 media (Cza, PDM, SYM, WM). See Table S2 for annotated molecules. Red: Nodes detected in Cza extracts. Blue: Nodes detected in PDM extracts. Green: Nodes detected in SYM extracts. Grey nodes: Nodes detected WM medium extracts. Grey loop: Nodes annotated as putatively known chemical clusters. (B) Venn diagram comparing the number of ions detected in different media. Cza (pink), PDM (blue), WM (grey), and SYM (green). Numbers of shared ions and specific ions only produced in one media-based extract were shown in differently shaded areas, while the total number of ions detected in each medium extract is shown underneath the medium name.

The global MN of the crude extracts deriving from different media (Figure 6A) indicated variations in chemical diversity of the extracts. The annotated natural product clusters included e.g., fumagillin (26) type meroterpenoid mycotoxins, which were only expressed by strain 35 (*Cadophora malorum*) in SYM-L (Figure 6A, Figure S6 and Table S2), while the small binaphthoquinone family represented only by xanthoepocin (19) and bisdehydroxanthomegnin (20) that was exclusively mapped to PDM-L extract of strain 59 (order Glomerellales) (Figure 6A, Figure S16 and Table S2). Another striking example was the aminolipid family (7–11) produced by the same strain 59. This very large molecular cluster was expressed in both liquid and solid Cza media, with 52 of total 71 analogues with  $m/z$  ranging from 300 to 1300 Da exclusively mapped to the Cza medium (Table S2, Figure S24). The identification of this rare lipid family was based on the database search in GNPS, with a high spectral similarity score ( $>0.7$ ) to our experimental MS/MS fragmentation pattern. The inspection of Figures 4 and 6, the Supplementary Figures S4–S23 and Table S2 shows that, with the exception of the amide alkaloid pseurotin A (6) and the polyketide deoxyherquenone (25), all annotated chemical families/compounds are produced by one single strain often in one or more growth media. In most cases, both culture regime and culture media had an effect on chemical production, in which 15 of the total 36 known metabolites were exclusively annotated in one single culture medium under one single culture regime (Table S2). This was exemplified by the amino acid derivative acetylcarnitine (1, SYM-S) (Figure S5), the tetrahydrofuranone polyketide griseofulvin (15, WM-L) (Figure S18), and the indole diterpenoid penitrem B (30, SYM-S) (Figure S19). Despite the use of an integrated and detailed metabolomics approach, we were able to annotate only a few nodes to known compounds. This may suggest potential novelty of the remaining compounds.

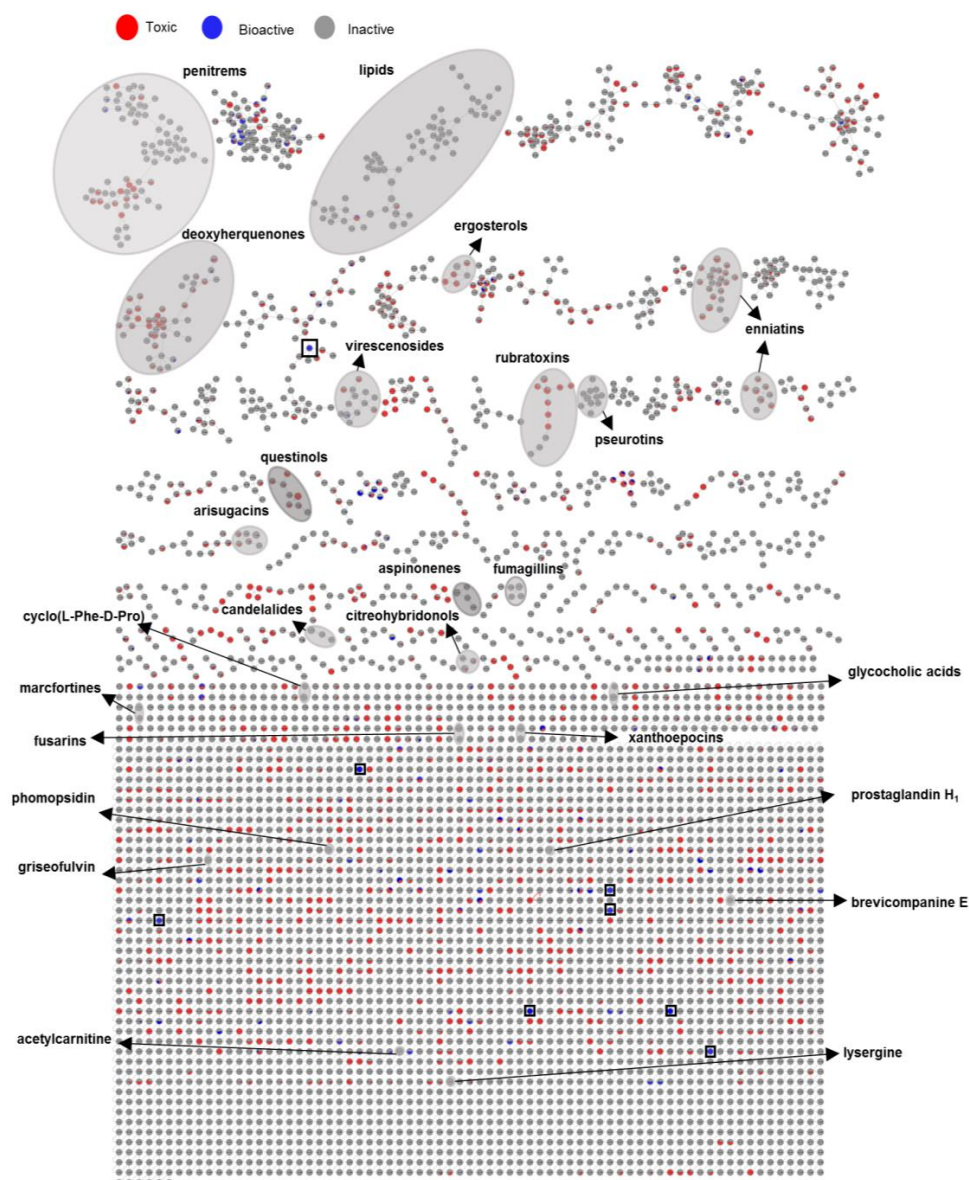
### 2.3.3. Bioactivity Mapping

As a last step, we mapped the bioactivity data ( $IC_{50}$  values) of altogether 80 extracts over the MN and searched for a link between spectral molecular networks and their anticancer activity (or toxicity). To this end, we classified the fungal extracts into three groups based on their anticancer activity ( $IC_{50}$  values), assigned them a specific color tag, and applied this color mapping to all nodes to establish a visible MN (Figure 7A). Thus i) 64 extracts that did not kill any cancer cell line in preliminary testing ( $IC_{50} > 100 \mu\text{g/mL}$ , see Section 2.2) were regarded as ‘inactive’ (tagged in grey), ii) 14 extracts that exhibited anticancer activity towards at least one cancer cell line and general toxicity to HaCaT cells with  $IC_{50}$  values  $< 100 \mu\text{g/mL}$  were treated as ‘toxic’ (tagged in red) and iii) 2 crude extracts (1PDM-L and 58Cza-S) that were devoid of toxicity against HaCaT cells ( $IC_{50} > 100 \mu\text{g/mL}$ ) and killed at least one cancer cell line ( $IC_{50} < 100 \mu\text{g/mL}$ ) were regarded as ‘bioactive’ (tagged in blue) (Figure 7A). Then, we explored the networks and compared the chemical composition of all three classes with different color mapping to all nodes in the MN. The rationale behind it is that if certain clusters/nodes are uniquely present in an extract, these compounds may possibly be responsible for the observed bioactivity and this extract(s) can be prioritized for further bioactivity-guided isolation studies.

As shown in the Euler diagram (Figure 7B), altogether 4452 nodes were detected in the inactive extracts, 2207 nodes in the toxic extracts, while the two bioactive extracts collectively comprised 175 nodes. Respectively, 2499 and 295 nodes were exclusive to the inactive and the toxic extracts. The bioactive extracts had only eight nodes that were specifically produced in them, but shared 27 nodes with the toxic and 68 with inactive extracts. Seventy-two nodes were common to all extracts.

The combination of massive MN with activity mapping allowed an easy visual inspection of the networks and their inhibitory activity against cancerous and non-cancerous cell lines. As shown in Figure 7A, the MN revealed eight fully exclusive (completely blue) ions for bioactive extracts 1PDM-L and 58Cza-S, five of which belonging to 1PDM-L and three of which belonging to 58Cza-S. Only one of these nodes identified from 1PDM-L ( $m/z$   $[M + H]^+$  428.2081,  $C_{25}H_{34}NO_5$ ) was embedded in a large molecular cluster containing 38 nodes (Figure 7A and Figure S25). The remaining seven were single nodes (single compound-single molecular family, Figure 7A), four of which being exclusive to 1PDM-L ( $m/z$   $[M + Na]^+$  452.2278 ( $C_{25}H_{35}NO_5Na$ ),  $m/z$   $[M + H]^+$  469.2242 ( $C_{27}H_{33}O_7$ ),  $m/z$   $[M + H]^+$  463.2679

( $C_{26}H_{39}O_7$ ),  $m/z$   $[M + H]^+$  939.6554 ( $C_{55}H_{91}N_2O_{10}$ ) and 3 nodes being exclusive to 58Cza-S ( $m/z$   $[M + H]^+$  232.1525 ( $C_{11}H_{22}NO_4$ ),  $m/z$   $[M + H]^+$  681.3819 ( $C_{31}H_{57}N_2O_{14}$ ), and  $m/z$   $[M + H]^+$  685.3978 ( $C_{32}H_{61}O_{15}$ )). None of these eight nodes found a match to any known compound in databases, hence represent potentially new compounds that may be responsible or contributing to the bioactivity of these extracts. On the other hand, the blue nodes were also common to a number of networks that were toxic. This may suggest that the observed toxicity and anticancer activity is dependent on their final concentration in the extract and the chemical structure of the individual compounds and/or their molecular clusters. The fully toxic ions (fully red nodes) were represented by small networks and a number of single nodes. However, similar to bioactive samples, the toxicity was also embedded in many inactive (grey) networks. As expected, there were many fully inactive molecular clusters, but a large number of clusters included toxic and/or bioactive nodes, again pointing to general phenomenon of toxicity associated with anticancer activity.



(A)

Figure 7. Cont.

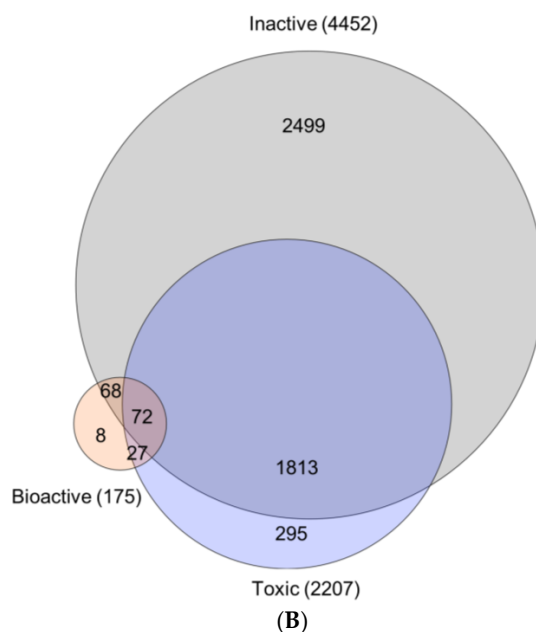


**Figure 7.** (A) Bioactivity ( $IC_{50}$  values) mapped to global MN of the extracts of 10 fungal strains (80 extracts). See Table S2 for annotated molecules. Red node: Ions detected in toxic samples ( $IC_{50} < 100 \mu\text{g/mL}$  towards both cancerous and non-cancerous HaCaT cell lines). Grey node: Ions detected in inactive samples ( $IC_{50} > 100 \mu\text{g/mL}$  towards cancer cell lines). Blue node: Ions detected in bioactive samples ( $IC_{50} \leq 100 \mu\text{g/mL}$  towards cancer cell lines and  $IC_{50} > 100 \mu\text{g/mL}$  to HaCaT cell line). Grey loop: Nodes annotated as putatively known chemical clusters. Black squares: Eight nodes exclusively detected in bioactive (fully blue) extracts. (B) Euler diagram showing the specific and the shared ions in crude extracts. Red: Nodes detected in toxic samples. Grey: Nodes detected in inactive samples. Blue: Nodes detected in bioactive samples. Numbers of shared ions and specific ions are shown in differently shaded areas. The total number of ions for each group of extract is given in brackets.

### 3. Discussion

#### 3.1. Fungal Isolation

Only a few studies have investigated endophytic fungi associated with the seaweed genus *Fucus* and their metabolites with antioxidant and antibiotic activities [6,7]. In this study, we isolated fungal assemblages present on the surface and in the inner tissues of the Baltic Sea *F. vesiculosus*. Isolation media (mostly favoring the growth of Ascomycetes) used herein were similar to those used for obtaining endophytic fungi from the North Sea *F. serratus* [1,27]. In accordance with previous studies, our isolates were also dominated by *Penicillium* sp. that are common in macroalgae [28]. The abundance of *Penicillium* sp. (39 isolates) in our study was even higher than that (14 isolates) observed in the previous study [1]. Reportedly, the abundance of *Penicillium* sp. in macroalgae is negatively correlated with water temperature [29]. Low water temperatures ( $8.3 \text{ }^{\circ}\text{C}$ ) during our sampling campaign may provide a possible explanation for the higher abundance of *Penicillium* sp. *Vice versa*, the abundance of another very common genus in macroalgae, *Aspergillus*, is reportedly positively correlated with increasing temperatures [29], which may underlie the absence of *Aspergillus* sp. in our study. Zuccaro et al. [1] isolated only a few (5 isolates) *Aspergillus* sp. during their study on *F. serratus* for a full calendar year, suggesting an overall low abundance of the genus *Aspergillus* in *Fucus* species.

In addition, we identified four genera *Acremonium*, *Gibellulopsis*, *Trichoderma*, and *Emericellopsis* (Figure 3A) from the Baltic *F. vesiculosus*. Since they are absent in the sediment or seawater samples, they can be regarded as specific to the seaweed. These genera have also been isolated from the

North Sea *F. serratus* samples [1]. A *Cadophora* sp. has previously been reported from the green alga *Enteromorpha* sp. [30], but not from any brown algae before. In the present study, we identified an endophytic *Wallemia* sp. This fungal genus is generally considered as xerophilic (adapted to dry conditions or high salinity) [31], and has previously been obtained from air, soil, dried food, and salt. To our knowledge, this is the first report of this genus being associated with a marine alga. The seawater control sample yielded a *Candida* sp., which is commonly found in seawater [32]. Finally, we isolated three fungal strains, *Cladosporium* sp., *Phoma* sp. and *Stereum* sp., that were exclusive to sediment surrounding *F. vesiculosus* (Figure 3A). *Cladosporium* and *Phoma* species are very common molds in sediment samples [33]. *Stereum* species belong to mycobiota of trees and known for wood-destroying and carbon recycling properties of arid forest ecosystems [34], but has never been isolated from a marine sediment before.

Interestingly, two known plant pathogens i.e., *Cadophora malorum* and *Fusarium graminearum* were also isolated from the inner tissues of *F. vesiculosus*. The presence of potential phytopathogens in macroalgae has already been described [1,27]. Those endophytes live in a healthy host resuming a saprophytic growth only during senescence of the hosts [1]. While their ecological role in *F. vesiculosus* remains elusive, these fungal genera that produce bioactive compounds, such as the hydroxylated sclerosporin derivatives reported from *Cadophora malorum* [30], may be involved in the well-being of the marine algae.

It is widely accepted that *Fucus* sp. employs various mechanisms to control their surface biofilm and microbiota. This includes mechanical means, i.e., cuticle shedding [35], production of reactive oxygen species (ROS) [36], and the release of secondary metabolites, such as the carotenoid fucoxanthin, onto the algal surface [37,38]. Such regulatory mechanisms of epiphytic control may underlie the 4-fold lower abundance of epiphytic fungi (11 isolates) compared to endophytic fungi (44 isolates). The diversity of epiphytic fungi was also poor and only three genera, *Gibellulopsis* (1 isolate), *Phoma* (1 isolate), and *Penicillium* (9 isolates) represented the cultivable epiphytic fungal community. Notably, none of the epiphytic fungi showed growth inhibitory activity against cancer cell lines in initial screenings, and hence, were not prioritized for in-depth metabolomics and IC<sub>50</sub> determinations.

### 3.2. Evaluation of Chemical Diversity Under Different Culture Conditions

OSMAC is regarded as an essential method for activating silent BGCs to enhance the chemical diversity of microorganisms [39]. Here, we applied for the first time an OSMAC-based cultivation approach to *F. vesiculosus*-derived fungal strains, 10 of which inhibited the growth of multiple cancer cell lines in vitro. The UPLC-HRMS/MS-based untargeted metabolomics study by employing MN on 16 fungal extracts deriving from 10 selected fungal isolates revealed an enhanced chemical diversity, as shown in their respective MNs (Figures S4–S23). As discussed below, MNs provided opportunities to identify known compounds/molecular families and putatively new molecular families and to assess differences due to changes in the culture regime and the growth media. Overall, 36 metabolites belonging to 25 clusters were putatively identified, spanning from simple amino acids, fatty acid derivatives (including sphingolipids, aminolipids, aminoglycolipids), various types of alkaloids and polyketides, terpenoids, meroterpenoids, and steroids.

In this study, liquid and solid culture extracts only shared 24% nodes and more than 30% nodes were produced only under one single culture regime (Figure 4B). In-depth MN studies revealed that 16 putatively identified metabolites were exclusive to liquid culture regimes and 11 to solid regimes (Table S2). A similar MN-based metabolomics study conducted on marine bacterial extracts confirmed the strong impact of the culture regime on chemical diversity in which only 7% of the nodes were shared [17]. The differences in chemical production under different culture conditions may stem from changes in physical parameters, e.g., shaking that increases the availability of oxygen. As reviewed by Papagianni et al. [40], the production of metabolites in different morphological and physiological conditions is unique for each fungus. In this study, we applied shaking (120 rpm) to the liquid cultures, while the solid cultures were grown statically. Previous research on fungal

antibiotics showed that fungi formed mycelial mat under static conditions and dispersed mycelia under shaking condition. The chemical production was affected by different mycelial growth conditions [41]. Our results confirmed differential biosynthesis of various types of metabolites in liquid (1547 specific nodes) and solid (2083 specific nodes) cultures (Figure 4B). Another factor affecting the fungal growth and metabolome is the availability of oxygen. The lack of oxygen in solid media has been shown to lead to impairment of the fungal growth and decreased production of fungal metabolites [42]. Conversely, shaking (in liquid conditions) facilitates aeration and the uptake of oxygen, thereby promoting fungal growth and potential accumulation of bioactive metabolites. While a lower number of nodes were expressed in the liquid culture extracts (i.e., 1547 specific nodes versus 2083 nodes in the solid extracts, 32 versus 43%, respectively) the liquid culture regime appeared more favorable for the expression of bioactive/cytotoxic metabolites than the solid regime. Many fungal mycotoxins, such as the enniatin type cyclic depsipeptides (31, 34, 36) (produced by strain 35), fumagillins (26), and the diterpene glycoside virescenside E (35) (produced by strain 1), were exclusively expressed in liquid culture extracts. Ten of the total 16 active extracts with activity against cancer cell lines derive from liquid growth media and only six strains showed bioactivity against cancer cell lines when grown under solid static condition (Table 2). Expression of specific fungal metabolites under shaking has previously been observed by Guo and co-workers [43] where the switch of the culture condition of a *Penicillium* sp. from static to shaking led to the biosynthesis of five new nitrogen-containing sorbicillinoids [44]. Analogously, we detected 16 specific metabolites in liquid culture extracts, exemplified by the antifungal polyketide griseofulvin (Figure S18).

The culture media also played a significant role in the chemical diversity of the *F. vesiculosus* associated fungi. The Venn diagram (Figure 6B) showed that Cza medium provided not only chemically the most diverse extracts with the highest numbers of nodes (2820), but also the highest number of nodes (1476) exclusively produced in this medium. MN annotated specific metabolites that were produced in a single medium i.e., Cza (4, 8, 9, 10, 11, 32), PDM (5, 19, 20), SYM (1, 14, 26, 28, 30, 33), and WM (2, 12, 15) (Table S2). Annotation of metabolites that can be mapped exclusively to a certain medium suggests activation of silent BGCs due to varying culture parameters. This metabolism shift may be due to different nutrients used in this study, e.g., carbon, trace elements and salt. For example, Cza is the only medium containing sucrose (as carbon source) and trace metals (e.g.,  $Mg^{2+}$ ) at the same time. The influence of carbon source on fungal metabolism is well known. For example only sucrose has stimulated the production of antibiotic metabolite bikaverin in *Fusarium fujikuroi* [45]. In the current work, the linear aminolipid family (7–11) produced by strain 59 (Table S2, Figure S24) was exclusively detected in the sucrose-containing medium Cza. Chatzifragkou and co-workers (2010) showed that carbon source affects the lipid production in fungi and the highest oleic acid concentration was obtained when a sucrose-based medium was used [46]. Additional research showed several enzymes that are involved in the regulation of lipid synthesis, e.g., ATP citrate lyase, were dependent of  $Mg^{2+}$  for their activities [47,48]. The use of Cza as medium for culturing the strain 59 (order Glomerellales) resulted in the highest number of metabolites (2820 nodes) and highest percentage (31%) of compounds unique to this medium, as a response to the presence of specific nutrients, e.g., trace elements and sucrose.

PDM was the only medium containing a mixed carbon source, i.e., the polymer starch and the monomer dextrose. The anti-inflammatory metabolite dihydroxyanthraquinone questinol (5) [49] was previously isolated from the marine derived fungus *Eurotium amstelodami* incubated in a starch-based SWS medium. The strain 50 (*Penicillium* sp.) exclusively produced this compound in the starch containing medium PDM (Figure S10), pointing out the importance of the polymeric starch as carbon resource. The total number of nodes in PDM extracts was 1628, of which 487 were exclusive to this medium. Only a few nodes mapped to PDM were annotated to known metabolites, this suggests that fungal strains are able to produce a rich number of putative new natural products when cultured in a PDM medium. Importantly, most of the extracts with growth inhibitory activity against cancerous (and non-cancerous) cell lines were grown in solid or liquid PDM (Table 2). Thus, all 10 strains showed

low  $IC_{50}$  values ( $<100 \mu\text{g/mL}$ ) against cancer cell lines in PDM (six fungi only in PDM-L, one fungus only in PDM-S, and three strains—50, 58, and 68 in both PDM-L and PDM-S) (Table 2).

The third medium, SYM, contained sucrose and yeast extract as nutrient provider. These two components appeared suitable for production of mycotoxins. There were altogether 1990 nodes detected in SYM extracts, with 441 nodes being exclusive. Previous research on *Aspergillus flavus* showed that the absence of yeast extract led to silencing of mycotoxin production in fungi [44]. In the present study, several known fungal mycotoxins families, such as the small cluster of fumagillin family (26 produced by strain 35, Figure S6) and a very large cluster of penitrem family (30, produced by strain 68, Figure S19) were assigned to be exclusive to SYM by analysis of the MN.

The last medium, WM contains high concentrations of salt (NaCl 30 g/L). As shown in Figure 6B, 1615 nodes in total were observed in WM extracts, 370 of these being specific to this medium. One such compound is griseofulvin (15), a chlorinated tetrahydrofuranone polyketide produced by the strain 68 (Figure S18). Griseofulvin was only annotated from the 68WM-L extract, potentially as a response to high  $Cl^+$  concentration. Glucose is an excellent carbon resource for fungal growth, however, it may repress the transcription of biosynthetic genes, such as *pcbAB*, *pcbC*, and *penDE* in *Penicillium* sp. [50] resulting in a poor metabolite diversity. Finally the presence of salts may impair the growth of some fungi, leading to a poor chemical composition. This could be another factor contributing to the low chemical diversity and lack of bioactivity of the crude extracts derived from salt-containing media, SYM and WM.

It is important to mention that the chemical production of strains was not only affected by the culture regime but also by the culture media. The most striking example is represented by the indole diterpenoid penitrem B (30). A previous study showed that penitrems were only produced under static conditions and enhanced production occurs upon addition of sucrose and yeast extract into medium [51]. Accordingly, we detected the penitrem B (30), exclusively, in solid SYM culture of strain 68 (*Penicillium* sp.) (Figure S19). This indicates that both culture regime and culture media strongly affect fungal chemical diversity of the fungi. Our research that employed detailed metabolomics by MN and bioactivity testing underlines the complexity of the media effect on fungal metabolism and bioactivity as a result of it. Overall, the OSMAC approach applied here suggests PDM-L as the best culture condition for a high chemical diversity coupled with cancer growth inhibitory activity in *F. vesiculosus*-derived fungi. While the Cza medium provided the highest chemical diversity and exclusiveness in metabolites, only a few extracts deriving from this medium showed generally low anticancer activity associated with toxicity. It is very likely that these extracts/induced compounds have other biological activities, which warrants further screenings in future.

### 3.3. Bioactivity

Based on the proven anticancer potential of algal-derived fungi [9], we focused on the assessment of the anticancer activity and general toxicity of *F. vesiculosus* derived fungi. An  $IC_{50}$  value  $\leq 100 \mu\text{g/mL}$  was set to define the bioactivity of the crude extracts. The changes in the fungal metabolism due to composition of the culture medium and/or the culture regime played a very important role in the observed bioactivity of the crude extracts. Hence, out of 80 extracts, only 16 fulfilled the  $IC_{50}$  value criterium ( $\leq 100 \mu\text{g/mL}$ ). Some extracts showed significant variations in their potency against different cancer cells. For example, 50Cza-S was inactive against HepG2 and HT29 cells, but showed good  $IC_{50}$  values against other cancerous cell lines, in particular towards MDA-MB231. However, the majority of the extracts suffered from the lack of selectivity, as their anticancer activity was often comparable to their general toxicity towards non-cancerous HaCaT cells. As exemplified by doxorubicin, the standard drug used as a positive control herein (Table 2), toxicity is a well-known general side effect of anticancer drugs. Only two extracts 1PDM-L and 58Cza-S lacked toxicity at the highest test concentrations ( $IC_{50} > 100 \mu\text{g/mL}$ ), but their anticancer effect was also moderate.



Our dereplication study indicated the presence of some known chemical families, including mycotoxins, in the fungal extracts. Indeed, we annotated 11 individual mycotoxins belonging to eight chemical families that were previously reported as fungal mycotoxins. These include the amide alkaloid pseurotin A (6), polyketide griseofulvin (15), polyene fusarin C (16), bis-anhydrides rubratoxins A (18) and B (17), meroterpenoid fumagillin (26), indole diterpenoid penitrem B (30), cyclic depsipeptides enniatins B, B<sub>1</sub>, and A (31, 34, 36), and the diterpene glycoside virescenoside E (35). Several mycotoxins with demonstrated anticancer and/or cytotoxic activities (the existing literature mostly measured their anticancer activity without assessing their toxicity) were detected, and their bioactivity was often dependent on the culture conditions. Rubratoxins are common mycotoxins of *Penicillium* sp. [52,53] with specific protein phosphatase A2 inhibitory and anticancer/antimetastasis activities [54]. Rubratoxins A (18,  $m/z$  [M + H]<sup>+</sup> 521.1890) and B (17,  $m/z$  [M + H]<sup>+</sup> 519.1832) were only annotated in the toxic PDM-L and Cza-L extracts of strain 50 (*Penicillium* sp.) (Table S2, Figure S10). This molecular cluster contained four additional unannotated nodes ( $m/z$  [M + H]<sup>+</sup> 598.1872, 577.1812, 767.2503, and 768.2531), which were only induced in this strain when incubated in PDM-L medium (Figure S10). These results suggest that culture conditions enhance the expression of fungal BGCs to induce biosynthesis of certain molecular families with new, potentially bioactive congeners. Enniatin type mycotoxins (31, 34, 36) with known anticancer properties [55] were also abundant in the toxic PDM-L extract of strain 35 (*Cadophora malorum*) (Figure S6). Other mycotoxin families, e.g., fumagillins (26) and pseurotins (6) with known anticancer/cytotoxic activity were expressed in 35SYM-L and 78WM-S, which lacked anticancer activity. The bioactivity mapping further proved this, as many toxic/anticancer mycotoxin clusters (fumagillins, pseurotins, penitrems, etc) were detected in grey colored networks belonging to inactive extracts. This may stem from their low concentrations in the extract and/or overall chemical composition of these extracts.

MN has found successful applications in drug discovery, in the form of bioactivity mapping and bioactivity-based MN for prioritization of extracts and targeted isolation of bioactive natural products [17,56]. In this study, we applied OSMAC approach with varied growth media and culture regime and mapped its results on MN for assessing both bioactivity and molecular profile of the extracts. The crude extracts were classified into three different groups based on their IC<sub>50</sub> values ( $\leq 100$   $\mu\text{g}/\text{mL}$ ) and toxicity to HaCaT. The layout assigned color tags to each group, which allowed i) rapid and efficient visualization and analysis of molecular clusters, and ii) analysis of whether these specific cluster of nodes were restricted to certain strain, growth medium, or culture regime. By using this visible network, we attempted to detect unique metabolites produced in bioactive samples. Toxicity is the main limitation in anticancer drug discovery. Accordingly, 14 extracts showed significant toxicity whereas the extracts derived from the strain 1 (order Pleosporales) in PDM-L and strain 58 (*Fusarium graminearum*) in Cza-S media showed moderate anticancer potential with no toxicity at 100  $\mu\text{g}/\text{mL}$ . MN-based bioactivity mapping identified 8 unannotated nodes to be exclusively present in these two extracts, indicating their potential impact in the observed activity. Then, we attempted to annotate known metabolites in these bioactive extracts. The only secondary metabolite we could annotate in the 1PDM-L extract was the diterpene glycoside virescenoside E (35, Figure S4), which is regarded as a fungal mycotoxin [57]. This compound belonged to a small, four-membered molecular cluster, however, none of the compounds in this cluster were unique to 1PDM-L, so their significant contribution to bioactivity is unclear. We were unable to dereplicate any nodes in the other selectively active extract 58Cza-S. However, we found one significant cluster in this crude extract (Figure S26) that was distributed in all three groups of extracts (inactive, toxic and bioactive). Dereplication efforts on three nodes specific to 58Cza-S, i.e.,  $m/z$  [M + H]<sup>+</sup> 401.3221, [M + H]<sup>+</sup> 403.3355, [M + H]<sup>+</sup> 419.3300, and their MS spectral fragments did not match any known compounds in the databases used. These three compounds are closely related and may potentially represent new metabolites.

Besides the mycotoxins described above, a few other dereplicated metabolites reportedly exerting anticancer activity were mapped to toxic or inactive extracts. For example, ergosterol (28), the major steroidal constituent of fungal membranes with inhibitory activity against several cancer cell lines [58]

was detected in the inactive 35SYM-L extract (Figure S6). Phomopsidin (**33**) is a polyketide that interacts with microtubules [59]. This compound that was embedded in a small molecular family was annotated and originated from the inactive sample 87SYM-L (Figure S22). We also observed various chemical families without reported anticancer activity. This was exemplified by the sesterterpenoid citreohybridonol (**13**,  $m/z$  501.2903,  $[M + H]^+$ ) identified from strain 68 (*Penicillium* sp.) grown in several solid-liquid media, however only the 68PDM-S showed activity associated with strong toxicity (Table S2, Figure S18).

In conclusion, we have isolated and identified, for the first time, a diverse cultivable fungal community associated with the Baltic Sea *F. vesiculosus*. The use of an OSMAC approach combined with efficient and modern tools such as MN coupled with bioactivity mapping, enabled the identification of optimal culture conditions and clear visual comparison of the chemical diversity and bioactivity of the extracts. Based on this important information, strain 1 (order Pleosporales) was prioritized for large-scale fermentation to be followed by purification and structure elucidation of its bioactive components.

## 4. Materials and Methods

### 4.1. General Experimental Procedures

EtOAc (used for fungal extraction) was purchased from VWR International GmbH, Hannover, Germany. UPLC grade methanol, acetonitrile and water used for UPLC/MS analysis were purchased from BiosolveChimie, Dieuze, France. Formic acid (UPLC/MS optigrade) was obtained from LGC Standards Promochem®, Wesel, Germany. UPLC-QToF-MS/MS analyses were carried out on an ACQUITY UPLC I-Class System coupled to the Xevo G2-XS QToF Mass Spectrometer (Waters®, Milford, MA, USA). Czapek broth, yeast extracts and malt extracts were purchased from BD Bioscience, Sparks, NE, USA. Agar was purchased from Applichem, Darmstadt, Germany. Peptone from soymeal and glucose were purchased from Merck, Darmstadt, Germany. Potato extract was from Sigma-Aldrich, Schnellendorf, Germany. Sucrose was purchased from Handelsmarken, Offenburg, Germany. Casein hydrolysate was purchased from Carl Roth, Karlsruhe, Germany.

### 4.2. Sampling and Isolation of Fungi

All fungi were isolated and identified from *F. vesiculosus* (Class: Phaeophyceae, Order: Fucales, Family: Fucaeae) specimens collected in Falckenstein Beach (54°23'22.6" N, 10°11'26.4" E), Kiel Fjord, Baltic Sea, Germany in December 2015 (pH 7, water temperature 8.3 °C). For isolation of fungal strains, four solid media were used: modified Wickerham medium (WM: NaCl 30 g, glucose 10 g, peptone from soymeal 5 g, yeast extract 3 g, malt extract 3 g, agar 15 g for 1 L), Glucose Yeast Peptone medium (GPY: glucose monohydrate 1 g, peptone 0.5 g, yeast extract 0.1 g, sodium chloride 15 g, agar 15 g for 1 L; pH 7.2), Potato Dextrose medium (PDM: Potato extract 4 g, dextrose 20 g, agar 15 g for 1 L; pH 5.6), and Glucose Casein medium (GCM: casein hydrolysate 2.5 g, glucose 40 g, MgSO<sub>4</sub> 0.1 g, KH<sub>2</sub>PO<sub>4</sub> 1.8 g, agar 15 g for 1 L pH 6.8) [60,61]. All media were enriched with 100 µg/mL streptomycin and 100 µg/mL of penicillin to suppress bacterial growth. Before plating, the macroalgal specimens were washed three times with sterilized saline solution (0.9 g/L NaCl). Epibionts were obtained from the surface of conceptacles, stipe, and holdfast regions by sterile cotton swabs. For isolation of endophytic fungi, the algal surface was disinfected by 40% ethanol and 1% sodium hypochlorite for 1 min [62]. Algal tissues from conceptacles, stipe and holdfast regions were cut into approximately 4 mm × 1 mm fragments. Each fragment was put into a 2 mL innuSPEED lysis tube type S containing 0.4–0.6 mm ceramic beads (Analytik Jena, Jena, Germany) and 600 µL of sterilized 0.9% saline. Samples were homogenized for about 2 min at 15 Hertz (15/s) with the RetschMM200 mixer mill (RetschGmbH, Haan, Germany) to release the endophytes from tissue to saline. Low speed mixing was pursued in order to prevent destruction of the endophytic fungal cells. After homogenization, two dilutions of mixture (containing endophyte fungi and saline), namely 10<sup>-1</sup> and 10<sup>-2</sup> were prepared. An aliquot (100 µL) of the dilutions

as well as of the undiluted sample were inoculated on the above-mentioned 4 agar media and spread evenly using drigalski spatula. Surface sterilized tissues of *F. vesiculosus* was swabbed again and incubated on the same 4 solid media to evaluate the effects of surface sterilization. Samples were incubated for 14 days at 22 °C and checked for fungal growth twice per week. Fungal colonies were transferred to new plates and incubated until pure cultures were obtained. For cryopreservation, the pure fungal strains were transferred to cryobank tubes (MAST Diagnostica, Reinfeld, Germany) and stored at −100 °C following the manufacturer's instructions.

#### 4.3. Identification of Fungal Strains

Fungal communities were identified based on the nuclear ribosomal internal transcribed spacer (ITS) region containing the ITS1 and ITS2 regions, which frame the 5.8S rRNA gene. The ITS region is generally accepted as a universal phylogenetic marker for fungi [63]. DNA extraction was performed according to the protocol published previously [64]. PCR amplification was performed using primers ITS1F and ITS4R, in a total reaction volume of 25 µL, consisting of 1 µL of template DNA, 1 µL of each primer (concentration: 10 µM), 12.5 µL Dream Taq Master mix (ThermoFisherScientific, Schwerte, Germany), and 9.5 µL DNA free water (ThermoFisher Scientific, Schwerte, Germany). DNA free water was used as negative control for PCR. The following protocol was used in a Biometra T1 thermocycler for amplification: initial denaturation for 85 s at 94 °C, followed by 30 cycles of denaturation of DNA at 94 °C for 35 s, primer annealing at 55 °C for 55 s, and elongation for 3 min at 72 °C. A final elongation step for 10 min at 72 °C completed the PCR. The correct length of PCR products was checked by gel electrophoresis on a 1% agarose gel run for 20 min at a voltage of 120 V in 1× TBE buffer, taking 100 bp plus DNA ladder (Thermo Scientific™ GeneRuler™, Sunnyvale, CA, USA) length standard. PCR products were submitted for Sanger sequencing to the Institute of Clinical Molecular Biology (IKMB) at Kiel University applying the same primers as used for PCR. Obtained sequences were checked for quality and trimmed using Chromas Pro (Technelysium Pty Ltd., South Brisbane, Australia). Sequences were then compared to the NCBI Genbank (<https://www.ncbi.nlm.nih.gov/genbank/>) using the Nucleotide BLAST function. Sequences were stored at GenBank and the accession numbers are displayed in Table S1. An MDS plot showing differences between samples (seawater, sediment, *Fucus* epiphytic, *Fucus* endophytic) was generated using the statistical software PAST based on a presence/absence matrix of identified fungal genera in 87 identified isolates [65].

#### 4.4. OSMAC-Based Cultivation of Fungi

The fungi were incubated in four different media, which were chosen based on variations in their carbon and nitrogen sources and salt concentration: The modified Wickerham medium (WM), Czapek medium (Cza: sucrose 30 g, KH<sub>2</sub>PO<sub>4</sub> 1 g, MgSO<sub>4</sub> 0.5 g, KCl 0.5 g, Fe<sub>2</sub>(SO<sub>4</sub>)<sub>3</sub> 0.01 g for 1 L; pH 7.3), Potato Dextrose medium (PDM), and Sucrose Yeast medium (SYM: sucrose 20 g, yeast extract 10 g, NaCl 10 g for 1L; pH 5.2) [61]. These media were selected in order to provide different nutrient regimes to activate biosynthetic gene clusters [12]. Each fungal strain was incubated in all four media by applying two different culture regimes (solid and liquid). The solid culturing contained 15 g/L agar as solidifying agent and liquid media (100 mL medium in 300 mL Erlenmeyer flasks). Solid cultures were incubated at 22 °C for 14 days in the dark under static conditions. The liquid cultures were incubated on an orbital shaker (VKS-75 control, Edmund Bühler, Hechingen, Germany) agitating at 120 rpm at 22 °C for 14 days in the dark.

#### 4.5. Extraction

For extraction of the liquid cultures, 100 mL of culture broth were mixed with the same volume of EtOAc by means of an ultra-turrax (Micra, Mülheim, Germany) at 19,000 rpm. The mycelia were filtered by folded filter cellulose membrane type 113P (100% cellulose membrane 210 mm, Carl Roth, Karlsruhe, Germany). The filtrate was collected into a glass separatory funnel and left for phase separation. The lower (water) phase was discarded. 40 mL of Milli-Q water (Arium®

Water Purification Systems, Sartorius, Germany) was added to the organic phase to remove salts and water-soluble compounds. After phase separation, the water phase was discarded, and the EtOAc phase was transferred into 40 mL glass tubes. The extracts were evaporated to dryness by a Speed-Vac concentrator (RVC2-33, Martin Christ Gefriertrocknungsanlagen, Osterode am Harz, Germany). The dissolved crude extracts were re-dissolved in 2.5 mL MeOH and transferred into 4 mL pre-weighted HPLC vials (amber glass, VWR, International GmbH, Hannover, Germany). For chemical analysis, 0.1 mg/mL of extract was prepared in an ULC/MS grade MeOH and transferred into 1.5 mL vials (amber glass, VWR, International GmbH, Hannover, Germany). The dissolved extracts were filtered through 0.20 µm PTFE syringe filter (Carl Roth, Karlsruhe, Germany) before injection. Solid fungal cultures were sliced into small pieces (approximately 1 cm<sup>2</sup>) with a flat spatula and transferred into a 250 mL glass flask and homogenized with 100 mL EtOAc by means of an ultra-turrax at 19,000 rpm for 30 s. The extraction process for solid cultures followed the same steps as applied for liquid cultures. The media blanks were prepared by extracting liquid and solid media using the same protocol.

#### 4.6. Chemical Analysis

##### 4.6.1. UPLC-QToF-MS/MS Analysis

The extracts were prepared at final concentration of 0.1 mg/mL and injected (2 µL) into an Acquity UPLC HSS T3 column (High Strength Silica C18, 1.8 µm, 2.1 × 100 mm, Waters®) operating at 40 °C. A mobile phase system (A: 0.1% formic acid in 99.9% ULC/MS grade water and B: 0.1% formic acid in 99.9% acetonitrile) was pumped at a flow rate of 0.6 mL/min using the following linear gradient: initial, 99% A–1% B; 0–11.5 min, 0% A–100% B; 11.5–12.5 min 0% A–100% B, and finally a column reconditioning phase until 15 min. The total run time was 15 min. MS and MS/MS spectra, in positive mode, were recorded during the UPLC run with the following conditions: capillary voltage: 0.8 kV, sample cone voltage: 40.0 V, source temperature: 150 °C, desolvation temperature: 550 °C, cone gas flow: 50 L/h and desolvation gas flow: 1200 L/h. A scan range was performed from 50 to 1600 Da, MS<sup>2</sup> fragmentation was achieved with ramp collision energy (CE): Low CE from 6–60 eV and a high CE of 9–80 eV. The solvent (MeOH) and non-inoculated blank media were used as controls. MS and MS<sup>2</sup> data were acquired and analyzed with MassLynx® software (Waters®, V4.1, Waters, Milford, MA, USA).

##### 4.6.2. Molecular Network and Data Analysis

All MS/MS data were converted from files (.raw) to mzXML file format using the ProteoWizard tool MSConvert (version 3.0.10051, Vanderbilt University, Nashville, TE, USA) [66]. The data were uploaded to GNPS server ([gnps.ucsd.edu](https://gnps.ucsd.edu)) [14] by using FileZilla (<https://filezilla-project.org/>) [67]. All mzXML data were analyzed using the molecular networking workflow. A molecular network was created using the online workflow at GNPS. The data was filtered by removing all MS/MS peaks within +/− 17 Da of the precursor *m/z*. The data were then clustered with MS-Cluster with a parent mass tolerance of 0.1 Da and a MS/MS fragment ion tolerance of 0.1 Da to create consensus spectra. Further, consensus spectra that contained less than 2 spectra were discarded. A network was then created where the edges were filtered to have a cosine score above 0.65 and more than 6 matched peaks. Further edges between two nodes were kept in the network if and only if each of the nodes appeared in each other's respective top 10 most similar nodes. The spectra in the network were then searched against GNPS spectral libraries. The library spectra were filtered in the same manner as the input data. All matches kept between network spectra and library spectra were required to have a score above 0.65 and at least 6 matched peaks. The clustered data were downloaded and imported into Cytoscape® (version 3.5.1, Institute for Systems Biology, Seattle, WA, USA) [68] and visualized using import network and table, individual (selfloop) nodes without neighbors were also displayed in molecular network. Nodes derived from the blank media and methanol blank as well as solvent

nodes were subtracted. Self-loop nodes (single node without link to others) were also displayed in molecular network. Venn diagram and Euler diagram were drawn by Venn and Euler Diagrams app available as a plugin for Cytoscape®. To improve the dereplication, the *in-silico* MS/MS database based on the Universal Natural Products Database (UNDP) was integrated into the MN following the workflow from Allard et al. [16] The parent mass was selected as dereplication prefilter. Setting was as following: Top\_K\_Result was used to return maximal number of results. Parameters were selected as following: PM tolerance = 0.05, score threshold = 0.2, Top K Result = 3. Only natural products reported isolated from fungal resources were selected as putative hits. The manual annotation was done by using the multiple databases, such as Dictionary of Natural Products (DNP) [24], Scifinder (<https://www.cas.org/products/scifinder>) [25] and ChempSpider [26] based on *m/z* value, ppm shift.

#### 4.7. Anticancer Activity

The crude extracts were initially tested *in vitro* against 6 human cancer cell lines; liver cancer cell line HepG2 (DSMZ, Braunschweig, Germany), colorectal adenocarcinoma cell line HT-29 (DSMZ, Braunschweig, Germany), malignant melanoma cell line A-375 (CLS, Eppelheim, Germany), colon cancer cell line HCT-116 (DSMZ, Braunschweig, Germany), lung carcinoma cell line A549 (CLS, Eppelheim, Germany), human breast cancer line MDA-MB-231 (CLS, Eppelheim, Germany), and the non-cancerous human keratinocyte line HaCaT (CLS, Eppelheim, Germany) at a concentration of 200 µg/mL. The antitumoral activity of the crude extracts was evaluated by monitoring the metabolic activity using the CellTiterBlue Cell Viability Assay (Promega, Mannheim, Germany). HepG2, HT-29 and HaCaT cells were cultivated in RPMI medium, A549 and MDA-MB-231 cells in DMEM:Ham's F12 medium (1:1) supplemented with 15mM HEPES and A-375 and HCT-116 cells in DMEM medium supplemented with 4.5 g/L D-Glucose and 110 mg/L sodium pyruvate. All media were supplemented with L-Glutamine, 10% fetal bovine serum, 100 U/mL penicillin, and 100 mg/mL streptomycin. The cultures were maintained at 37 °C under a humidified atmosphere and 5% CO<sub>2</sub>. The cell lines were transferred every 3 or 4 days. For experimental procedure, the cells were seeded in 96 well plates at a concentration of 10,000 cells per well. A stock solution of 40 mg/mL in DMSO was prepared of each extract. After 24 h incubation, the medium was removed from the cells and 100 µl fresh medium containing the test samples was added. Each sample was prepared in duplicate once. Doxorubicin as a standard therapeutic drug was used as positive control, 0.5% DMSO and growth media were used as controls. Following compound addition, plates were cultured at 37 °C for 24 h. Afterwards, the assay was performed according to the manufacturer's instructions and measured using the microplate reader Tecan Infinite M200 at excitation 560 nm and emission of 590 nm. For the determination of IC<sub>50</sub> values, a dilution series of the extracts was prepared and tested, as described before. The IC<sub>50</sub> values were calculated by Excel as the concentration that shows 50% inhibition of the viability on the basis of a negative control (no compound) and compared with the positive control (doxorubicin).

**Supplementary Materials:** The following are available online at <http://www.mdpi.com/1660-3397/17/1/67/s1>, Table S1: Identification of 87 fungal strains from *F. vesiculosus* and its surrounding environment (sediment and seawater). Table S2: Putatively identified compounds from 80 culture extracts. Figures S1–S2: Strains isolated and identified from *F. vesiculosus* and its surroundings. Figure S3: Workflow for the OSMAC study based on the 55 fungal isolates derived from *F. vesiculosus*. Figure S4–S23: Annotated molecular network for crude extracts of different strains under different culture regime and culture media. Figure S24: Molecular network of the aminolipid family of strain 59 (order Glomerellales) extracts. Figure S25. Molecular network of unannotated cluster containing one specific node. Figure S26: Molecular network of unannotated cluster containing 3 specific nodes in 58Cza-S.

**Author Contributions:** B.F., A.L. and D.T. designed research; B.F. and D.P. conducted experiments; B.F., D.P., M.B. and D.T. analyzed data; B.F., D.P., M.B., A.L. and D.T. wrote the draft of the paper. D.T. finalized the manuscript and supervised this work.

**Funding:** This research was supported by a scholarship from the China Scholarship Council (CSC) to Bicheng Fan.

**Acknowledgments:** We thank Arlette Wenzel-Storjohann for performing the anticancer assays. The Institute of Clinical Molecular Biology (IKMB) at Kiel University is kindly acknowledged for Sanger sequencing.

**Conflicts of Interest:** The authors declare no conflicts of interest.

## References

1. Zuccaro, A.; Schoch, C.L.; Spatafora, J.W.; Kohlmeyer, J.; Draeger, S.; Mitchell, J.I. Detection and identification of fungi intimately associated with the brown seaweed *Fucus serratus*. *Appl. Environ. Microbiol.* **2008**, *74*, 931–941. [[CrossRef](#)] [[PubMed](#)]
2. Loque, C.P.; Medeiros, A.O.; Pellizzari, F.M.; Oliveira, E.C.; Rosa, C.A.; Rosa, L.H. Fungal community associated with marine macroalgae from Antarctica. *Polar Biol.* **2010**, *33*, 641–648. [[CrossRef](#)]
3. Harvey, J.B.J.; Goff, L.J. Genetic covariation of the marine fungal symbiont *Haloguignardia irritans* (Ascomycota, Pezizomycotina) with its algal hosts *Cystoseira* and *Halidrys* (Phaeophyceae, Fucales) along the west coast of North America. *Fungal Biol.* **2010**, *114*, 82–95. [[CrossRef](#)] [[PubMed](#)]
4. Egan, S.; Harder, T.; Burke, C.; Steinberg, P.; Kjelleberg, S.; Thomas, T. The seaweed holobiont: Understanding seaweed–bacteria interactions. *FEMS Microbiol. Rev.* **2013**, *37*, 462–476. [[CrossRef](#)] [[PubMed](#)]
5. Sarasan, M.; Puthumana, J.; Job, N.; Han, J.; Lee, J.-S.; Philip, R. Marine algicolous endophytic fungi—a promising drug resource of the era. *J. Microbiol. Biotechnol.* **2017**, *27*, 1039–1052. [[PubMed](#)]
6. Flewelling, A.J.; Johnson, J.A.; Gray, C.A. Isolation and bioassay screening of fungal endophytes from North Atlantic marine macroalgae. *Bot. Mar.* **2013**, *56*, 287–297. [[CrossRef](#)]
7. Flewelling, A.J.; Ellsworth, K.T.; Sanford, J.; Forward, E.; Johnson, J.A.; Gray, C.A. Macroalgal endophytes from the Atlantic coast of Canada: A potential source of antibiotic natural products? *Microorganisms* **2013**, *1*, 175–187. [[CrossRef](#)]
8. Fenical, W.; Jensen, P.R.; Cheng, X.C. Halimide, a Cytotoxic Marine Natural Product, and Derivatives Thereof. U.S. Patent US6358957B1, 30 May 2000.
9. Gomes, N.G.; Lefranc, F.; Kijjoa, A.; Kiss, R. Can some marine-derived fungal metabolites become actual anticancer agents? *Mar. Drugs* **2015**, *13*, 3950–3991. [[CrossRef](#)]
10. Romano, S.; Jackson, S.; Patry, S.; Dobson, A. Extending the “One Strain Many Compounds” (OSMAC) principle to marine microorganisms. *Mar. Drugs* **2018**, *16*, 244. [[CrossRef](#)]
11. Reen, F.J.; Romano, S.; Dobson, A.D.; O’Gara, F. The sound of silence: Activating silent biosynthetic gene clusters in marine microorganisms. *Mar. Drugs* **2015**, *13*, 4754–4783. [[CrossRef](#)]
12. Bode, H.B.; Bethe, B.; Höfs, R.; Zeeck, A. Big effects from small changes: Possible ways to explore nature’s chemical diversity. *ChemBioChem* **2002**, *3*, 619–627. [[CrossRef](#)]
13. Gulder, T.; Hong, H.; Correa, J.; Egereva, E.; Wiese, J.; Imhoff, J.; Gross, H. Isolation, structure elucidation and total synthesis of lajollamide A from the marine fungus *Asteromyces cruciatus*. *Mar. Drugs* **2012**, *10*, 2912–2935. [[CrossRef](#)] [[PubMed](#)]
14. Wang, M.; Carver, J.J.; Phelan, V.V.; Sanchez, L.M.; Garg, N.; Peng, Y.; Nguyen, D.D.; Watrous, J.; Kapono, C.A.; Luzzatto-Knaan, T.; et al. Sharing and community curation of mass spectrometry data with Global Natural Products Social Molecular Networking. *Nat. Biotechnol.* **2016**, *34*, 828–837. [[CrossRef](#)] [[PubMed](#)]
15. Yang, J.Y.; Sanchez, L.M.; Rath, C.M.; Liu, X.; Boudreau, P.D.; Brunns, N.; Glukhov, E.; Wodtke, A.; De Felicio, R.; Fenner, A. Molecular networking as a dereplication strategy. *J. Nat. Prod.* **2013**, *76*, 1686–1699. [[CrossRef](#)] [[PubMed](#)]
16. Allard, P.-M.; Péresse, T.; Bisson, J.; Gindro, K.; Marcourt, L.; Pham, V.C.; Roussi, F.; Litaudon, M.; Wolfender, J.-L. Integration of molecular networking and *in-silico* MS/MS fragmentation for natural products dereplication. *Anal. Chem.* **2016**, *88*, 3317–3323. [[CrossRef](#)] [[PubMed](#)]
17. Crüsemann, M.; O’Neill, E.C.; Larson, C.B.; Melnik, A.V.; Floros, D.J.; da Silva, R.R.; Jensen, P.R.; Dorrestein, P.C.; Moore, B.S. Prioritizing natural product diversity in a collection of 146 bacterial strains based on growth and extraction protocols. *J. Nat. Prod.* **2016**, *80*, 588–597. [[CrossRef](#)] [[PubMed](#)]
18. Olivon, F.; Allard, P.-M.; Koval, A.; Righi, D.; Genta-Jouve, G.; Neyts, J.; Apel, C.; Pannecouque, C.; Nothias, L.-F.; Cachet, X. Bioactive natural products prioritization using massive multi-informational molecular networks. *ACS Chem. Biol.* **2017**, *12*, 2644–2651. [[CrossRef](#)] [[PubMed](#)]
19. Ardehed, A.; Johansson, D.; Sundqvist, L.; Schagerström, E.; Zagrodzka, Z.; Kovaltchouk, N.A.; Bergström, L.; Kautsky, L.; Rafajlovic, M.; Pereyra, R.T.; et al. Divergence within and among seaweed siblings (*Fucus vesiculosus* and *F. radicans*) in the Baltic Sea. *PLoS ONE* **2016**, *11*, e0161266–e0161281. [[CrossRef](#)] [[PubMed](#)]

20. Pereira, L. A review of the nutrient composition of selected edible seaweeds. In *Seaweed: Ecology, Nutrient Composition and Medicinal Uses*; Nova Science: Coimbra, Portugal, 2011; pp. 15–47.
21. Zenthoefer, M.; Geisen, U.; Hofmann-Peiker, K.; Fuhrmann, M.; Kerber, J.; Kirchhöfer, R.; Hennig, S.; Peipp, M.; Geyer, R.; Piker, L. Isolation of polyphenols with anticancer activity from the Baltic Sea brown seaweed *Fucus vesiculosus* using bioassay-guided fractionation. *J. Appl. Phycol.* **2017**, *29*, 2021–2037. [[CrossRef](#)]
22. Heavisides, E.; Rouger, C.; Reichel, A.; Ulrich, C.; Wenzel-Storjohann, A.; Sebens, S.; Tasdemir, D. Seasonal variations in the metabolome and bioactivity profile of *Fucus vesiculosus* extracted by an optimised, pressurised liquid extraction protocol. *Mar. Drugs* **2018**, *16*, 503. [[CrossRef](#)]
23. Abdel-Lateff, A.; Fisch, K.M.; Wright, A.D.; König, G.M. A new antioxidant isobenzofuranone derivative from the algicolous marine fungus *Epicoccum* sp. *Planta Med.* **2003**, *69*, 831–834. [[PubMed](#)]
24. Whittle, M.; Willett, P.; Klaffke, W.; van Noort, P. Evaluation of similarity measures for searching the dictionary of natural products database. *J. Chem. Inf. Comput. Sci.* **2003**, *43*, 449–457. [[CrossRef](#)] [[PubMed](#)]
25. Ridley, D.D. Introduction to structure searching with SciFinder Scholar. *J. Chem. Educ.* **2001**, *78*, 559–560. [[CrossRef](#)]
26. Little, J.L.; Williams, A.J.; Pshenichnov, A.; Tkachenko, V. Identification of “Known unknowns” utilizing accurate mass data and ChemSpider. *J. Am. Soc. Mass Spectrom.* **2012**, *23*, 179–185. [[CrossRef](#)] [[PubMed](#)]
27. Zuccaro, A.; Schulz, B.; Mitchell, J.I. Molecular detection of ascomycetes associated with *Fucus serratus*. *Mycol. Res.* **2004**, *107*, 1451–1466. [[CrossRef](#)]
28. Godinho, V.M.; Furbino, L.E.; Santiago, I.F.; Pellizzari, F.M.; Yokoya, N.S.; Pupo, D.; Alves, T.M.A.; Junior, P.A.S.; Romanha, A.J.; Zani, C.L.; et al. Diversity and bioprospecting of fungal communities associated with endemic and cold-adapted macroalgae in Antarctica. *ISME J.* **2013**, *7*, 1434–1451. [[CrossRef](#)]
29. Abdel-Gawad, K.M.; Hifney, A.F.; Issa, A.A.; Gomaa, M. Spatio-temporal, environmental factors, and host identity shape culturable-epibiotic fungi of seaweeds in the Red Sea, Egypt. *Hydrobiologia* **2014**, *740*, 37–49. [[CrossRef](#)]
30. Almeida, C.; Eguereva, E.; Kehraus, S.; Siering, C.; König, G.M. Hydroxylated sclerosporin derivatives from the marine-derived fungus *Cadophora malorum*. *J. Nat. Prod.* **2010**, *73*, 476–478. [[CrossRef](#)] [[PubMed](#)]
31. Zalar, P.; De Hoog, G.S.; Schroers, H.-J.; Frank, J.M.; Gunde-Cimerman, N. Taxonomy and phylogeny of the xerophilic genus *Wallemia* (*Wallemiomycetes* and *Wallemiales*, cl. et ord. nov.). *Anton Leeuw* **2005**, *87*, 311–328. [[CrossRef](#)]
32. Cornax, R.; Moriñigo, M.A.; Romero, P.; Borrego, J.J. Survival of pathogenic microorganisms in seawater. *Curr. Microbiol.* **1990**, *20*, 293–298. [[CrossRef](#)]
33. Nagahama, T.; Takahashi, E.; Nagano, Y.; Abdel-Wahab, M.A.; Miyazaki, M. Molecular evidence that deep-branching fungi are major fungal components in deep-sea methane cold-seep sediments. *Environ. Microbiol.* **2011**, *13*, 2359–2370. [[CrossRef](#)] [[PubMed](#)]
34. Tura, D.; Zmitrovich, I.V.; Wasser, S.P.; Nevo, E. The genus *Stereum* in Israel. *Mycotaxon* **2008**, *106*, 109–126.
35. Rickert, E.; Lenz, M.; Barboza, F.R.; Gorb, S.N.; Wahl, M. Seasonally fluctuating chemical microfouling control in *Fucus vesiculosus* and *Fucus serratus* from the Baltic Sea. *Mar. Biol.* **2016**, *163*, 203–215. [[CrossRef](#)]
36. Weinberger, F. Pathogen-induced defense and innate immunity in macroalgae. *Biol. Bull.* **2007**, *213*, 290–302. [[CrossRef](#)] [[PubMed](#)]
37. Sivagnanam, S.; Yin, S.; Choi, J.; Park, Y.; Woo, H.; Chun, B. Biological properties of fucoxanthin in oil recovered from two brown seaweeds using supercritical CO<sub>2</sub> extraction. *Mar. Drugs* **2015**, *13*, 3422–3442. [[CrossRef](#)] [[PubMed](#)]
38. Lachnit, T.; Fischer, M.; Künzel, S.; Baines, J.F.; Harder, T. Compounds associated with algal surfaces mediate epiphytic colonization of the marine macroalga *Fucus vesiculosus*. *FEMS Microbiol. Ecol.* **2013**, *84*, 411–420. [[CrossRef](#)] [[PubMed](#)]
39. Hewage, R.T.; Aree, T.; Mahidol, C.; Ruchirawat, S.; Kittakoop, P. One strain-many compounds (OSMAC) method for production of polyketides, azaphilones, and an isochromanone using the endophytic fungus *Dothideomycete* sp. *Phytochemistry* **2014**, *108*, 87–94. [[CrossRef](#)] [[PubMed](#)]
40. Papagianni, M. Fungal morphology and metabolite production in submerged mycelial processes. *Biotechnol. Adv.* **2004**, *22*, 189–259. [[CrossRef](#)] [[PubMed](#)]

41. Bigelis, R.; He, H.; Yang, H.Y.; Chang, L.-P.; Greenstein, M. Production of fungal antibiotics using polymeric solid supports in solid-state and liquid fermentation. *J. Ind. Microbiol. Biotechnol.* **2006**, *33*, 815–826. [[CrossRef](#)] [[PubMed](#)]
42. Nout, M.J.R.; Bonants-van Laarhoven, T.M.G.; de Jongh, P.; de Koster, P.G. Ergosterol content of *Rhizopus oligosporus* NRRL 5905 grown in liquid and solid substrates. *Appl. Microbiol. Biotechnol.* **1987**, *26*, 456–461. [[CrossRef](#)]
43. Guo, W.; Peng, J.; Zhu, T.; Gu, Q.; Keyzers, R.A.; Li, D. Sorbicillamines A–E, nitrogen-containing sorbicillinoids from the deep-sea-derived fungus *Penicillium* sp. F23–2. *J. Nat. Prod.* **2013**, *76*, 2106–2112. [[CrossRef](#)] [[PubMed](#)]
44. Davis, N.D.; Diener, U.L.; Eldridge, D.W. Production of aflatoxins B<sub>1</sub> and G<sub>1</sub> by *Aspergillus flavus* in a semisynthetic medium. *Appl. Microbiol.* **1966**, *14*, 378–380. [[PubMed](#)]
45. Rodríguez-Ortiz, R.; Mehta, B.J.; Avalos, J.; Limón, M.C. Stimulation of bikaverin production by sucrose and by salt starvation in *Fusarium fujikuroi*. *Appl. Microbiol. Biotechnol.* **2010**, *85*, 1991–2000. [[CrossRef](#)] [[PubMed](#)]
46. Chatzifragkou, A.; Fakas, S.; Galiotou-Panayotou, M.; Komaitis, M.; Aggelis, G.; Papanikolaou, S. Commercial sugars as substrates for lipid accumulation in *Cunninghamella echinulata* and *Mortierella isabellina* fungi. *Eur. J. Lipid Sci. Technol.* **2010**, *112*, 1048–1057. [[CrossRef](#)]
47. Måhlén, A. Purification and some properties of ATP citrate lyase from *Penicillium spiculisporum*. *Eur. J. Biochem.* **1973**, *36*, 342–346. [[CrossRef](#)]
48. Muhid, F.; Nawati, W.; Kader, A.J.A.; Yusoff, W.M.W.; Hamid, A.A. Effects of metal ion concentrations on lipid and gamma linolenic acid production by *Cunninghamella* sp. 2A1. *Online J. Biol. Sci.* **2008**, *8*, 62–67. [[CrossRef](#)]
49. Yang, X.; Kang, M.-C.; Li, Y.; Kim, E.-A.; Kang, S.-M.; Jeon, Y.-J. Anti-inflammatory activity of questinol isolated from marine-derived fungus *Eurotium amstelodami* in lipopolysaccharide-stimulated RAW 264.7 macrophages. *J. Microbiol. Biotechnol.* **2014**, *24*, 1346–1353. [[CrossRef](#)] [[PubMed](#)]
50. Gutiérrez, S.; Marcos, A.T.; Casqueiro, J.; Kosalková, K.; Fernández, F.J.; Velasco, J.; Martín, J.F. Transcription of the *pcbAB*, *pcbC* and *penDE* genes of *Penicillium chrysogenum* AS-P-78 is repressed by glucose and the repression is not reversed by alkaline pHs. *Microbiology* **1999**, *145*, 317–324. [[CrossRef](#)]
51. Wagener, R.E.; Davis, N.D.; Diener, U.L. Penitrem A and roquefortine production by *Penicillium commune*. *Appl. Environ. Microbiol.* **1980**, *39*, 882–887.
52. Nagashima, H. Cytotoxic effects of rubratoxin B on cultured cells. *JSM Mycotoxins* **1996**, *1996*, 57–61. [[CrossRef](#)]
53. Moss, M.O.; Wood, A.B.; Robinson, F.V. The structure of rubratoxin A, a toxic metabolite of *Penicillium rubrum*. *Tetrahedron Lett.* **1969**, *10*, 367–370. [[CrossRef](#)]
54. Wada, S.-I.; Usami, I.; Umezawa, Y.; Inoue, H.; Ohba, S.-I.; Someno, T.; Kawada, M.; Ikeda, D. Rubratoxin A specifically and potently inhibits protein phosphatase 2A and suppresses cancer metastasis. *Cancer Sci.* **2010**, *101*, 743–750. [[CrossRef](#)] [[PubMed](#)]
55. Ivanova, L.; Skjerve, E.; Eriksen, G.S.; Uhlig, S. Cytotoxicity of enniatins A, A<sub>1</sub>, B, B<sub>1</sub>, B<sub>2</sub> and B<sub>3</sub> from *Fusarium avenaceum*. *Toxicon* **2006**, *47*, 868–876. [[CrossRef](#)] [[PubMed](#)]
56. Nothias, L.-F.; Nothias-Esposito, M.; da Silva, R.; Wang, M.; Protsyuk, I.; Zhang, Z.; Sarvepalli, A.; Leyssen, P.; Touboul, D.; Costa, J.; et al. Bioactivity-based molecular networking for the discovery of drug leads in natural product bioassay-guided fractionation. *J. Nat. Prod.* **2018**, *81*, 758–767. [[CrossRef](#)] [[PubMed](#)]
57. Mefteh, F.B.; Daoud, A.; Bouket, A.C.; Thissera, B.; Kadri, Y.; Cherif-Silini, H.; Eshelli, M.; Alenezi, F.N.; Vallat, A.; Oszako, T. Date palm trees root-derived endophytes as fungal cell factories for diverse bioactive metabolites. *Int. J. Mol. Sci.* **2018**, *19*, 1986. [[CrossRef](#)]
58. Wu, H.-Y.; Yang, F.-L.; Li, L.-H.; Rao, Y.K.; Ju, T.-C.; Wong, W.-T.; Hsieh, C.-Y.; Pivkin, M.V.; Hua, K.-F.; Wu, S.-H. Ergosterol peroxide from marine fungus *Phoma* sp. induces ROS-dependent apoptosis and autophagy in human lung adenocarcinoma cells. *Sci. Rep.* **2018**, *8*, 17956–17969. [[CrossRef](#)]
59. Kobayashi, H.; Meguro, S.; Yoshimoto, T.; Namikoshi, M. Absolute structure, biosynthesis, and anti-microtubule activity of phomopsidin, isolated from a marine-derived fungus *Phomopsis* sp. *Tetrahedron* **2003**, *59*, 455–459. [[CrossRef](#)]
60. Silber, J.; Ohlendorf, B.; Labes, A.; Erhard, A.; Imhoff, J.F. Calcarides A–E, antibacterial macrocyclic and linear polyesters from a *Calcarisporium* strain. *Mar. Drugs* **2013**, *11*, 3309–3323. [[CrossRef](#)]
61. Atlas, R.M. *Handbook of Microbiological Media*, 4th ed.; CRC Press: Boca Raton, FL, USA, 2010; pp. 1654–1657.



62. Schulz, B.; Wanke, U.; Draeger, S.; Aust, H.J. Endophytes from herbaceous plants and shrubs: Effectiveness of surface sterilization methods. *Mycol. Res.* **1993**, *97*, 1447–1450. [[CrossRef](#)]
63. Schoch, C.L.; Seifert, K.A.; Huhndorf, S.; Robert, V.; Spouge, J.L.; Levesque, C.A.; Chen, W. Nuclear ribosomal internal transcribed spacer (ITS) region as a universal DNA barcode marker for fungi. *Proc. Natl. Acad. Sci. USA* **2012**, *109*, 6241–6246. [[CrossRef](#)]
64. Wiese, J.; Ohlendorf, B.; Blümel, M.; Schmaljohann, R.; Imhoff, J.F. Phylogenetic identification of fungi isolated from the marine sponge *Tethya aurantium* and identification of their secondary metabolites. *Mar. Drugs* **2011**, *9*, 561–585. [[CrossRef](#)] [[PubMed](#)]
65. Hammer, Ě.; Harper, D.; Ryan, P. PAST: Paleontological statistics software package for education and data analysis. *Palaeontol. Electron.* **2001**, *4*, 9.
66. Chambers, M.C.; Maclean, B.; Burke, R.; Amodei, D.; Ruderman, D.L.; Neumann, S.; Gatto, L.; Fischer, B.; Pratt, B.; Egertson, J. A cross-platform toolkit for mass spectrometry and proteomics. *Nat. Biotechnol.* **2012**, *30*, 918–920. [[CrossRef](#)] [[PubMed](#)]
67. Woodraska, D.; Sanford, M.; Xu, D. Security mutation testing of the FileZilla FTP server. In Proceedings of the 2011 ACM Symposium on Applied Computing, TaiChung, Taiwan, 21–24 March 2011; pp. 1425–1430.
68. Shannon, P.; Markiel, A.; Ozier, O.; Baliga, N.S.; Wang, J.T.; Ramage, D.; Amin, N.; Schwikowski, B.; Ideker, T. Cytoscape: A software environment for integrated models of biomolecular interaction networks. *Genome Res.* **2003**, *13*, 2498–2504. [[CrossRef](#)]



© 2019 by the authors. Licensee MDPI, Basel, Switzerland. This article is an open access article distributed under the terms and conditions of the Creative Commons Attribution (CC BY) license (<http://creativecommons.org/licenses/by/4.0/>).



## Chapter 2

**Pyrenosetin A-C, New Decalinoylspirotetramic Acid  
Derivatives Isolated by Bioactivity-Based Molecular  
Networking from the Seaweed-Derived Fungus  
*Pyrenochaetopsis* sp. FVE-001**

## RESULTS

Article

# Pyrenosetins A–C, New Decalinoylspirotetramic Acid Derivatives Isolated by Bioactivity-Based Molecular Networking from the Seaweed-Derived Fungus *Pyrenochaetopsis* sp. FVE-001

Bicheng Fan <sup>1</sup>, Pradeep Dewapriya <sup>1</sup> , Fengjie Li <sup>1</sup> , Martina Blümel <sup>1</sup>  and Deniz Tasdemir <sup>1,2,\*</sup> 

<sup>1</sup> GEOMAR Centre for Marine Biotechnology (GEOMAR-Biotech), Research Unit Marine Natural Products Chemistry, GEOMAR Helmholtz Centre for Ocean Research Kiel, Am Kiel-Kanal 44, 24106 Kiel, Germany; bfan@geomar.de (B.F.); pdewapriya@geomar.de (P.D.); fli@geomar.de (F.L.); mbluemel@geomar.de (M.B.)

<sup>2</sup> Faculty of Mathematics and Natural Sciences, Kiel University, Christian-Albrechts-Platz 4, 24118 Kiel, Germany

\* Correspondence: dtasdemir@geomar.de; Tel.: +49-431-600-4430

Received: 5 December 2019; Accepted: 9 January 2020; Published: 11 January 2020



**Abstract:** Marine algae represent a prolific source of filamentous fungi for bioprospecting. In continuation of our search for new anticancer leads from fungi derived from the brown alga *Fucus vesiculosus*, an endophytic *Pyrenochaetopsis* sp. FVE-001 was selected for an in-depth chemical analysis. The crude fungal extract inhibited several cancer cell lines in vitro, and the highest anticancer activity was tracked to its CHCl<sub>3</sub>-soluble portion. A bioactivity-based molecular networking approach was applied to C18-SPE fractions of the CHCl<sub>3</sub> subextract to predict the bioactivity scores of metabolites in the fractions and to aid targeted purification of anticancer metabolites. This approach led to a rapid isolation of three new decalinoylspirotetramic acid derivatives, pyrenosetins A–C (1–3) and the known decalin tetramic acid phomasetin (4). The structures of the compounds were elucidated by extensive NMR, HR-ESIMS, FT-IR spectroscopy, [α]<sub>D</sub> and Mosher's ester method. Compounds 1 and 2 showed high anticancer activity against malignant melanoma cell line A-375 (IC<sub>50</sub> values 2.8 and 6.3 μM, respectively), in line with the bioactivity predictions. This is the first study focusing on secondary metabolites of a marine-derived *Pyrenochaetopsis* sp. and the second investigation performed on the member of the genus *Pyrenochaetopsis*.

**Keywords:** marine fungus; pyrenosetin; phomasetin; *Pyrenochaetopsis* sp.; *Fucus vesiculosus*; bioactivity-based molecular networking; decalin tetramic acid

## 1. Introduction

Macroalgae (seaweeds) are regarded as holobionts due to their complex epiphytic and endophytic microbiota [1]. Seaweed-derived fungi are emerging as a promising source of novel bioactive secondary metabolites for marine bioprospecting. For example, plinabulin, the synthetic *tert*-butyl analog of diketopiperazine halimide, which derives from the seaweed-derived fungus *Aspergillus* sp. [2] is currently undergoing phase III clinical trials for treatment of non-small cell lung cancer [2,3]. Over the past decades, fungi associated with brown algal genus *Fucus* have gained attention as an untapped source of fungal biodiversity [4,5]. A previous study by Flewelling et al. showed *Fucus*-associated fungi to produce antimicrobial compounds [6]. Further studies have shown that *Fucus*-derived fungi produced secondary metabolites belonging to diverse structural classes and exhibited further bioactivities. For example, the culture broth of *Fucus spiralis*-derived fungus *Phoma*

sp. yielded the polyketide 5-hydroxyramulosin and 7-methoxycoumarin, which showed anticancer, antifungal and anti-HIV activities [7,8]. Another study by Lateff et al. (2003) reported a new, antioxidant isobenzofuranone derivative from *Epicoccum* sp. associated with *Fucus vesiculosus* [9]. However, a systematic research exploring bioactive metabolites from fungi associated with *Fucus* sp. is still missing.

Mass spectrometry-based molecular networking (MN) in conjunction with the publicly available web-platform Global Natural Products Social Molecular Network (GNPS) serves as an automated tool for mining large volumes of mass spectra. MN uses an untargeted metabolomics approach that powerfully processes the tandem mass spectrometry (MS/MS) fragmentation data. It is a vector-based workflow that calculates cosine scores (between 0 and 1) to determine the degree of similarity between the MS<sup>2</sup> fragments. These fragment ions (nodes) will then be organized into relational networks depending on their similarity [10]. MN has been employed for rapid and successful dereplication of known compounds from complex natural extracts [11,12]. Another advantage of MN is the possibility for incorporation of additional information, such as the bioactivity data, over the network. The bioactivity mapping or bioactivity-based MN have been effectively applied in natural product research on both crude extracts and fractions obtained therefrom [13,14]. In the latter, a further bioinformatic program is employed to predict the bioactivity score of molecules according to their relative abundance in the fractions. Bioactivity-based MN (B-B MN) approach, hence assists rapid prioritization and targeted isolation of bioactive compounds, thereby accelerating natural product biodiversity efforts.

*Fucus vesiculosus* is a habitat forming brown alga commonly found in the shallow coastal regions of Europe. In a recent study, we profiled the surface microbiome and metabolome of the Baltic *F. vesiculosus* and identified primary and secondary metabolites, including many fungal metabolites from its surface and inner tissues by massive MN coupled with DESI-imaging mass spectrometry [15]. We also reported the isolation and identification of epiphytic and endophytic fungal communities associated with *F. vesiculosus*, and applied an OSMAC approach to assess the impact of culture conditions on chemical space and anticancer potential of these filamentous fungi [12]. A fungal strain belonging to the order Pleosporales showed anticancer activity with lower toxicity to non-cancerous cells when cultivated in liquid potato dextrose medium (PDM) [12]. In the continuation of this project, we have now identified this fungus as a *Pyrenochaetopsis* sp. (strain FVE-001) by building a phylogenetic tree and comparing relationship with closely related fungal species. We further focused on isolation and characterization of its anticancer constituents. For this aim, we applied a B-B MN workflow [14] on the C18-SPE fractions obtained from the CHCl<sub>3</sub> subextract of the fungus for prioritization of the active fractions and targeted isolation of new bioactive compounds. This approach enabled rapid identification of three new and one known decalinoyl tetramic acid derivatives, 1–4. Herein we outline the isolation, structure elucidation and anticancer activities of the compounds 1–4.

## 2. Results

### 2.1. Strain Isolation and Identification

The endophytic fungus FVE-001 was isolated from the thallus of *Fucus vesiculosus* collected at Kiel Fjord (Baltic Sea, Germany) [12]. The initial Sanger sequencing of the PCR-amplified ITS1-5.8S rRNA gene-ITS2 region yielded a total length of 297 bp fragment, which only enabled its identification at order level, i.e., Pleosporales [12]. In order to further confirm the taxonomic identity of the fungus, the same genomic DNA extract was re-amplified and sequenced for ITS1-5.8S-ITS2 genes to yield a 394 bp length PCR fragment. The sequence result was subjected to NCBI Blast analysis that showed 100% sequence similarity to *Phoma* sp. and 99% sequence similarity to closely related strain, *Pyrenochaetopsis microspore*. In order to further validate the taxonomy of the fungus FVE-001, a phylogenetic tree was constructed with 14 related strains from the NCBI database. As shown in Figure 1, the phylogenetic tree suggested the fungus FVE-001 to be closely related to *Phoma* sp. However, in the phylogenetic

tree, FVE-001 did not cluster with the typical *Phoma* sp., i.e., *Phoma neerlandica* and *Phoma herbarum*. Further investigation revealed that the closely related *Phoma* strains MUT 5460, MUT 5462 and MUT 5465 (Figure 1) have now been reclassified as *Pyrenochaetopsis leptospora* in the UNITE database (<https://unite.ut.ee/sh/SH1525086.08FU#fndtn-panel1>) [16]. This confirmed that the fungus FVE-001 to be a *Pyrenochaetopsis* sp.

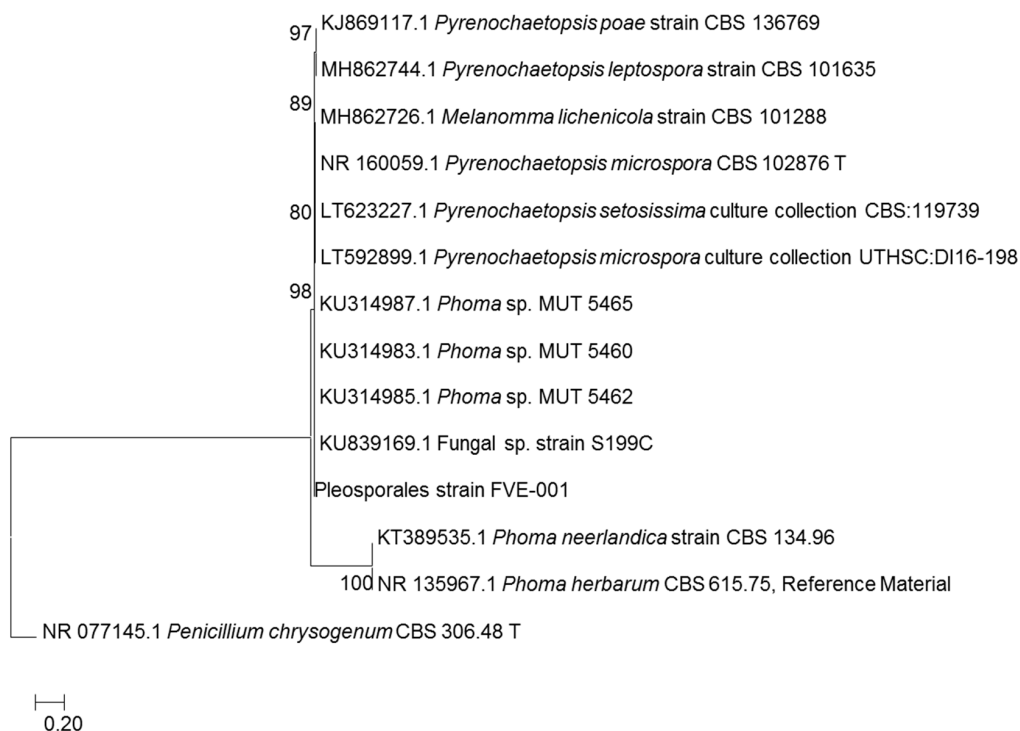


**Figure 1.** Molecular phylogenetic analysis by maximum likelihood method.

## 2.2. Cultivation, Extraction, Bioactivity Test and Molecular Networking

Based on the results of our One-Strain-Many-Compounds (OSMAC) study [12], the fungus *Pyrenochaetopsis* sp. FVE-001 was cultivated at 22 °C for 14 days under shaking (120 rpm) in 2 L flasks, each containing 800 mL PDM liquid medium. The EtOAc extract of the culture broth (12 L in total) was evaporated, and subjected to a modified Kupchan partition to yield *n*-hexane (KH), CHCl<sub>3</sub> (KC) and aqueous MeOH (KM) subextracts. All three subextracts were tested against five human cancer cell lines (malignant melanoma A-375; lung carcinoma A-549; colorectal adenocarcinoma HT-29; colorectal carcinoma HCT-116 and breast cancer MB-231), plus against non-cancerous human keratinocyte cell HaCaT for assessing their cytotoxicity. The KC subextract showed the highest activity against all cancer cell lines (>75% cell growth inhibition at 100 µg/mL) (Table S1), and was selected for in-depth chemical investigations. It was subjected to solid phase extraction (SPE) on a C18 Sep-Pak cartridge (10% gradient elution from 0% to 100% methanol) to yield 11 fractions. Fractions 5–7 exhibited a promising activity with high rates of growth inhibition (up to 99% at 100 µg/mL, Table S1). The fraction 8 showed a moderate inhibition rate (43%) against malignant melanoma cell line A-375 while the rest of the fractions had no activity (Table S1). In order to investigate their chemical profiles, all 11 fractions were analyzed by tandem UPLC-QToF-MS/MS (positive ion mode) metabolomics using MN. To facilitate the bioassay-guided isolation of anticancer metabolites, we integrated the bioactivity and the MS/MS (MS<sup>2</sup>) data of the fractions using the B-B MN workflow [14]. Briefly, the acquired MS<sup>2</sup> data was processed using MZmine2 toolbox to detect and assess relative quantification of LC-MS/MS spectral features (ions) across the chromatographic fractions. The processed data was used to calculate a bioactivity score using the Pearson correlation coefficient (*r*) between feature intensity, i.e., the molecule's relative abundance calculated from the LC-MS peak (area under the curve) across the fraction, and the anticancer activity

of each fraction. The nodes with higher  $r$  ( $>0.75$ ) and lower  $p$  ( $<0.05$ ) values indicated the presence of most active metabolites in fractions 5–7. Since this approach only allowed using single bioactivity data per analysis, activity results against melanoma cancer cell line A-375 was used to calculate bioactivity scores. Finally, the processed data was analyzed on the GNPS platform and visualized by Cytoscape®.

The B-B MN of the SPE fractions obtained from the KC subextract of *Pyrenochaetopsis* sp. FVE-001 is displayed in Figure 2. A total of 175 nodes forming seven different chemical clusters were identified after removal of nodes from chromatography solvents and the medium. The node size in Figure 2 indicates the statistical significance of bioactivity score, i.e., the largest nodes represent molecules with strong Pearson correlation ( $r > 0.75$ ) and a significance ( $p < 0.05$ ). Since the  $r$  value has linear correlation between the molecule's relative abundance and the level of the bioactivity, the B-B MN directly visualizes the relative bioactivity of the detected molecules. The relative abundance of the detected molecules in the each fraction is shown in each node with a pie chart diagram (colors corresponding to the bioactivity level of each fraction, i.e., red for samples with inhibition rate  $>90\%$ , pink for samples with inhibition rate 90–75%, light pink for samples with inhibition rate 75–20% and grey for inactive samples). In total, 10.3% (18 of total 175 nodes) of molecules showed a statistically significant bioactivity score ( $r > 0.75$  and  $p < 0.05$ ). This approach enabled us to narrow down the potentially active metabolites to 18 nodes (out of 56 nodes) that were detected in the highly active fractions 5–7.

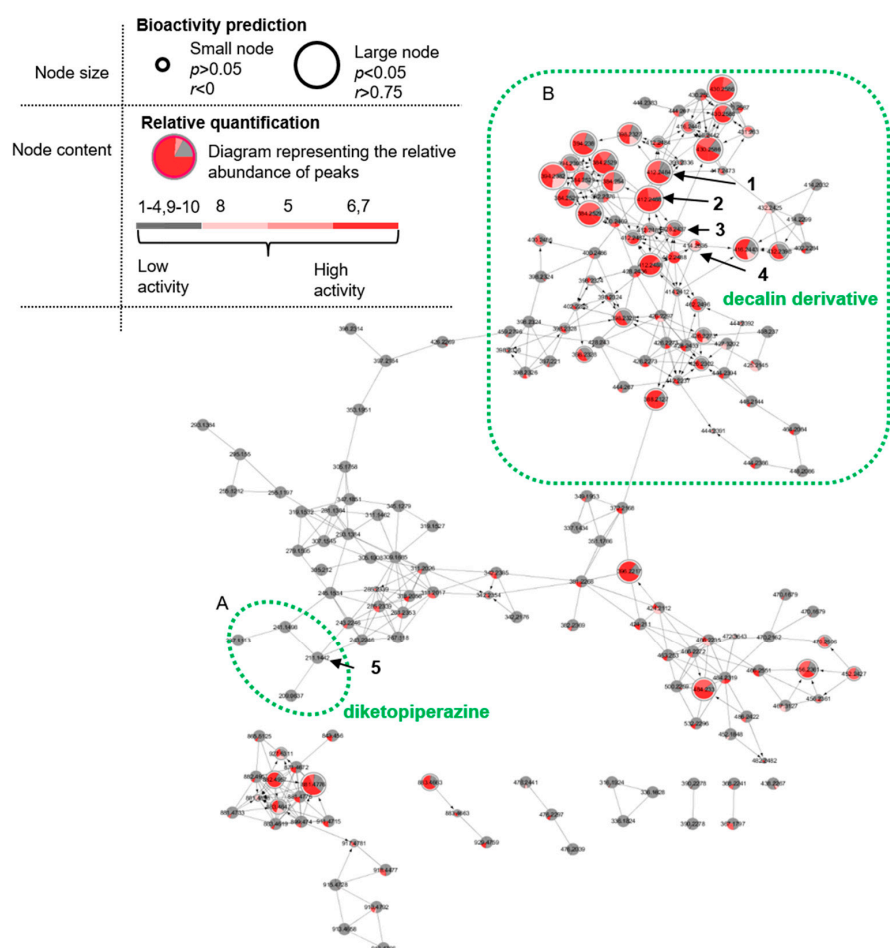


**Figure 2.** Bioactivity-based molecular networking of SPE fractions obtained from chloroform subextract of *Pyrenochaetopsis* sp. FVE-001. (A) Subcluster of diketopiperazine chemical family detected in MN. (B) Subcluster of decalin family detected in MN. 1–4: Decalinoyltetramic acid derivatives, 5: known diketopiperazine cyclo-(leu-pro).



A detailed analysis of the MN permitted the annotation of several fungal metabolites to different molecular families (Figure 2). The biggest cluster with 144 nodes consisted of several subclusters (e.g., **A** and **B**). The node with the precursor ion  $m/z$  211.1442 ( $[M + H]^+$ ,  $C_{11}H_{19}N_2O_2$ ) in subcluster **A** showed a close MS/MS spectral matching with GNPS spectral library and was annotated as the known diketopiperazine cyclo-(leu-pro) (**5**) [17]. Three related nodes in subcluster **A** at  $m/z$  209.0637, 241.1498 and 237.1113 that clustered with **5** were also identified as structurally related diketopiperazines. The subcluster **B**, which contains the most of the potential bioactive metabolites revealed a node ( $m/z$  414.2645  $[M + H]^+$ ,  $C_{25}H_{36}NO_4$ ) suggestive of the known fungal metabolite phomasetin (**4**) [18] (Figure 3). This was further confirmed by diagnostic MS/MS fragments corresponding to the loss of the olefinic side chain of the decalin moiety ( $m/z$  346.2017 and 328.1915) and the cleavage of the tetramic acid moiety ( $m/z$  271.2062 and 243.2113). No additional spectral annotation could be retrieved from GNPS library for other related nodes in the subcluster **B**. However, detailed analysis of MS/MS fragmentation patterns suggested that molecules in subcluster **B** are closely related to phomasetin (**4**). The subcluster **B** consisted of the highest number of potentially active nodes (15 of total 18 nodes). Based on the significant bioactivity score of nodes at  $m/z$  412.2484 (**1**) ( $[M - H_2O + H]^+$ ) and 412.2488 (**2**) ( $[M - H_2O + H]^+$ ) ( $r$  values of 0.79, 0.93 and  $p$  values of  $2.2 \times 10^{-3}$  and  $1.30 \times 10^{-5}$ , respectively) and their close similarity to phomasetin (**4**), we carried out a targeted isolation of these putatively bioactive molecules. In addition, a related molecule with  $m/z$  428.2434  $[M + H]^+$  (**3**) with low bioactivity score ( $r$  value 0.45) was also targeted due to the high probability to be an analogue of the most active metabolites.

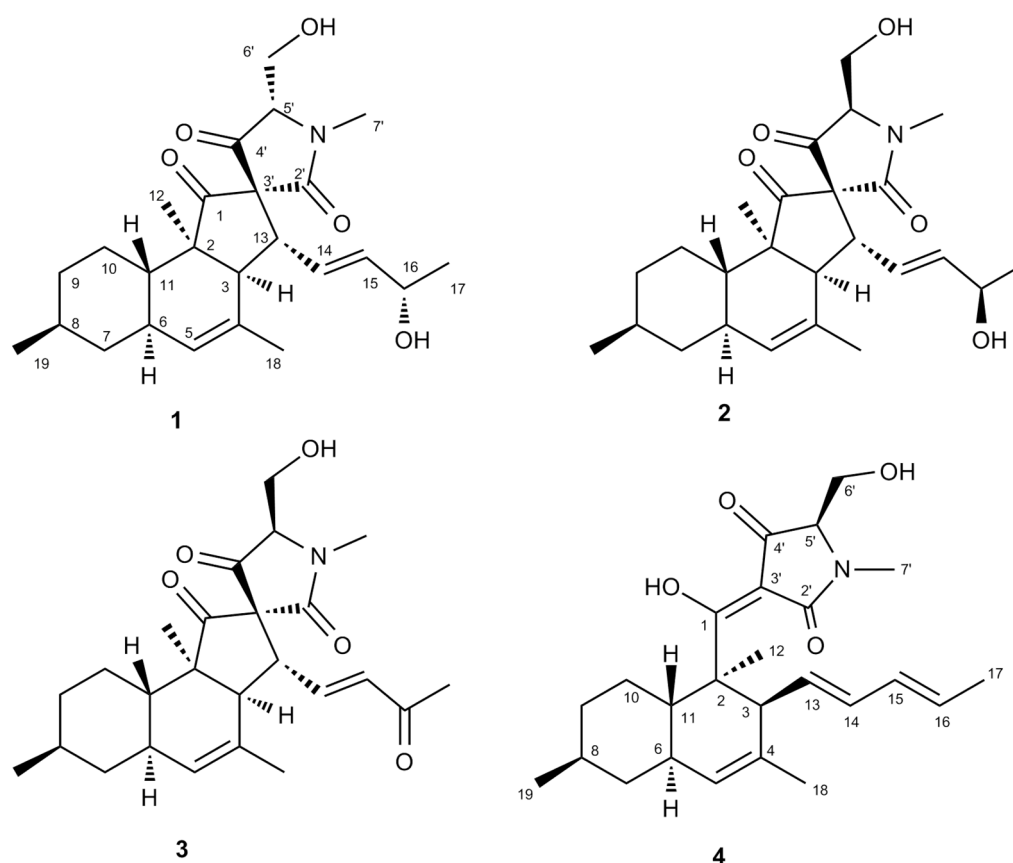


**Figure 3.** Chemical structures of compounds 1–4.

### 2.3. Purification and Structure Elucidation

The comprehensive analysis of the B-B MN revealed fractions 5 and 6 to have the highest relative abundance of targeted molecules. Based on this, fractions 5 and 6 were combined (106 mg altogether) and subjected to RP-HPLC separation to afford three new compounds, **1–3** (Figure 3). The known

metabolite phomasetin (**4**) (Figure 3), which was previously identified by MS/MS based dereplication (see above), was isolated from fraction 7. The chemical structure of phomasetin (**4**) was confirmed by comparing its HRMS, NMR (Tables 1 and 2) and  $[\alpha]_D$  data with those reported in the literature [19].

Compound **1** was isolated as a colorless oil. HR-ESIMS spectrum of **1** contained a molecular ion peak at  $m/z$  430.2592  $[M + H]^+$  consistent with the molecular formula  $C_{25}H_{35}NO_5$  requiring 9 degrees of unsaturation (Figure S7). The FT-IR spectrum implied the presence of hydroxyl and carbonyl groups (3249–3554, 1683 and 1721  $cm^{-1}$ , respectively) (Figure S8). The  $^{13}C$ -NMR data (Table 2, Figure S2) comprised 25 carbon signals, including four olefinic carbons at  $\delta_C$  127.3, 128.1, 131.8 and 138.8 along with three carbonyl groups at  $\delta_C$  168.6, 207.2 and 213.3. The  $^1H$  NMR and DEPT-HSQC spectra of **1** (Table 1, Figures S1 and S3) contained signals corresponding to five methyl groups, of which two are secondary ( $\delta_H$  1.19, d,  $J = 6.4$  Hz, H<sub>3</sub>-17;  $\delta_H$  0.90, d,  $J = 6.5$  Hz, H<sub>3</sub>-19), one tertiary ( $\delta_H$  0.98, s, H<sub>3</sub>-12), one olefinic ( $\delta_H$  1.73, br s, H<sub>3</sub>-18) and one being an *N*-methyl ( $\delta_H$  3.10, s, H<sub>3</sub>-7'). The DEPT-HSQC spectrum also confirmed the presence of four diastereotopic methylene protons corresponding to H<sub>2</sub>-7 ( $\delta_H$  0.86 and 1.78), H<sub>2</sub>-9 ( $\delta_H$  1.01 and 1.72), H<sub>2</sub>-10 ( $\delta_H$  1.04 and 1.42) and the oxymethylene H<sub>2</sub>-6' ( $\delta_H$  4.09, dd,  $J = 12.2, 2.6$  Hz and  $\delta_H$  3.92, dd,  $J = 12.3, 4.8$  Hz). Further detected were ten complex methine protons, six of which appearing at  $\delta_H$  2.57 (H-3, d,  $J = 11.4$  Hz),  $\delta_H$  1.43 (H-8, m),  $\delta_H$  1.82 (H-6, m),  $\delta_H$  1.63 (H-11, m),  $\delta_H$  3.44 (H-13, dd,  $J = 11.4, 8.6$  Hz) and  $\delta_H$  3.57 (H-5', dd,  $J = 4.8, 2.6$  Hz). The seventh (oxy) methine proton appeared at  $\delta_H$  4.24 (H-16, m). The remaining three methine protons were olefinic; two appeared as part of an AB system at  $\delta_H$  5.75 (H-14, dd,  $J = 15.4, 8.6$  Hz) and  $\delta_H$  5.71 (H-15, dd,  $J = 15.4, 4.8$  Hz), while the final olefinic methine (H-5) emerged as a broad singlet at  $\delta_H$  5.24 (Figure S1). The  $^1H$ - $^1H$  COSY spectrum of **1** (Figure S4) led to the establishment of three spin systems. As shown in Figure 4A, the shortest spin system belonged to a hydroxyethyl group including H-5' and H-6', while the second spin system was represented by a 16-hydroxypentenyl group (H-13 to H<sub>3</sub>-17). The largest and third COSY spin network corresponded to a substituted methylcyclohexane moiety, starting with the secondary methyl H<sub>3</sub>-19 and ending with the olefinic H-5 (Figure 4A and Figure S4). Diagnostic HMBC correlations (Figure 4A and Figure S5) observed from H-3 to C-2, C-4, C-11; from H-5 to C-3, C-7 and C-11; from H-7 to C-5, C-8 and C-9 and from H-11 to C-2, C-6, C-7, C-9 and C-10 permitted the establishment of the bicyclic partial structure, i.e., the unsaturated decalin moiety (rings A-B, Figure 4A). The olefinic methyl H<sub>3</sub>-18 was assigned to C-4 based on the substantial HMBC cross peaks seen from H<sub>3</sub>-18 to C-4, C-5 and C-3. The secondary methyl H<sub>3</sub>-19 was already placed at C-8 by COSY data and HMBC cross-peaks from H<sub>3</sub>-19 to C-7, C-8 and C-9 further confirmed its assignment. The tertiary methyl H<sub>3</sub>-12 had to be attached at C-2 on the basis of multiple HMBC correlations of H<sub>3</sub>-12 with C-1, C-2, C-3 and C-11. Additional correlations, i.e., COSY (between H-3 and H-13, H-13 and H-14) and HMBC (between H-3 with C-13, C-14 and C-15), confirmed the attachment of the 16-hydroxypentenyl side chain at C-3 of the decalin ring (Figure 4A, Figures S4 and S5). Further HMBC correlations from H-5' to C-2', C-4' and from H<sub>3</sub>-7' to C-2' and C-5' established the terminal *N*-methyl tetramic acid structure (ring D) (Figure 4A and Figure S5). The long-range (HMBC) couplings detected between H-13/C-3' and H-13/C-2' confirmed the connectivity of tetramic acid ring to decalin moiety through a spiro carbon, C-3' (Figure 4A and Figure S5). A key long range coupling between H<sub>3</sub>-12/C-1 and H<sub>3</sub>-12/C-2 and H-3/C-12 clearly assigned the carbonyl group ( $\delta_C$  213.3) at C-1. This completed the final ring system, C (Figure 4A).

Table 1. <sup>1</sup>H NMR data of compounds 1–4 at 600 MHz.

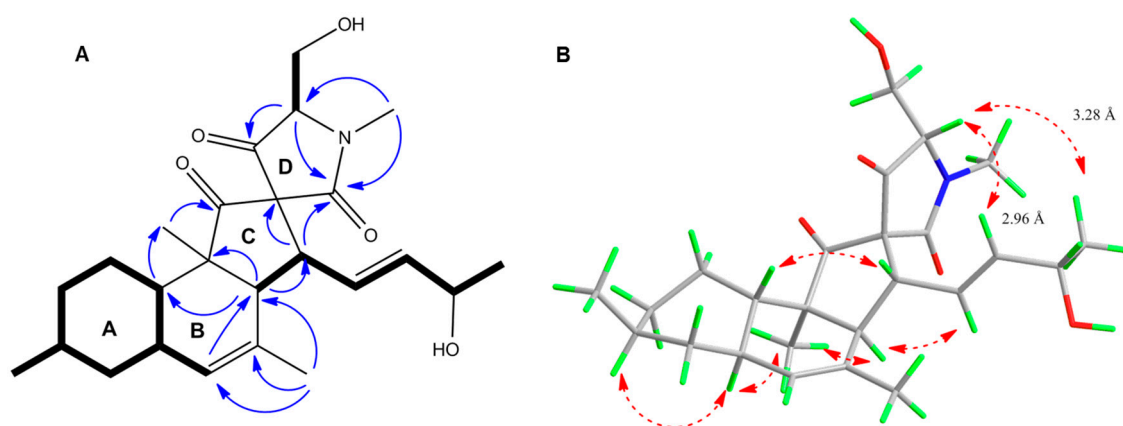
No.	1 <sup>a</sup>	2 <sup>a</sup>	3 <sup>a</sup>	4 <sup>b</sup>
	$\delta_{\text{H}}$ , Mult (J in Hz)	$\delta_{\text{H}}$ , Mult (J in Hz)	$\delta_{\text{H}}$ , Mult (J in Hz)	$\delta_{\text{H}}$ , Mult (J in Hz)
1	-	-	-	-
2	-	-	-	-
3	2.57, d (11.4)	2.73, d (11.4)	2.66, d (11.3)	3.17, br d (9.4)
4	-	-	-	-
5	5.24, br s	5.22, br s	5.28, br.s	5.22, br s
6	1.82, m	1.82, m	1.83, m	1.84, m
7	1.78, m	1.80, m	1.82, m	1.82, m
	0.86, m	0.84, m	0.88, m	0.86, m
8	1.43, m	1.44, m	1.44, m	1.51, m
9	1.72, m	1.73, m	1.73, m	1.76, m
	1.01, m	0.93, m	0.99, m	1.04, m
10	1.42, m	1.40, m	1.41, m	1.97, m
	1.04, m	1.07, qd (12.8,3.4)	1.04, m	1.06, m
11	1.63, m	1.42, m	1.64, td (11.0, 2.7)	1.64 m
12	0.98, s	1.00, s	1.01, s	1.38, br s
13	3.44, dd (11.4, 8.6)	3.26, dd (11.4, 9.4)	3.57, dd (11.4, 9.8)	5.27, dd (13.6, 10.5)
14	5.75, dd (15.4, 8.6)	5.97, dd (15.3, 9.4)	6.85, dd (15.9, 9.8)	5.78, dd (14.6, 10.5)
15	5.71, dd (15.4, 4.8)	5.50, dd (15.3, 8.0)	6.18, d (15.9)	5.91, t (12.8)
16	4.24, m	4.18, m	-	5.56, dq (14.2, 6.8)
17	1.19, d (6.4)	1.19, d (6.2)	2.22, s	1.67, d (6.8)
18	1.73, br s	1.69, br s	1.68, br s	1.55, t (1.9)
19	0.90, d (6.5)	0.91, d (6.5)	0.90, d (6.2)	0.91, d (6.5)
2'	-	-	-	-
3'	-	-	-	-
4'	-	-	-	-
5'	3.57, dd (4.8, 2.6)	3.94, dd (2.7, 1.9)	3.61, dd (4.9, 2.7)	3.61, t (2.7)
6'	4.09, dd (12.2, 2.6)	4.08, m	4.10, m	3.87, m
	3.92, dd (12.3, 4.8)	3.86, dd (12.4, 2.7)	3.94, m	3.81, m
7'	3.10, s	3.07, s	3.11, s	2.97, brs
6'-OH			2.74, m	

<sup>a</sup> Recorded in CDCl<sub>3</sub>, <sup>b</sup> Recorded in CD<sub>3</sub>CN.

The relative configuration of the stereogenic centers within **1** was established mainly by NOESY data (Figure 4B and Figure S6). The NOESY correlations observed between H-6/H-8, H-6/H<sub>3</sub>-12, H<sub>3</sub>-12/H-3 and H-11/H-13 revealed the *trans* junction of the decalin ring, the  $\alpha$ -orientation of H-3, H-6, H-8, H<sub>3</sub>-12 and the  $\beta$ -orientation of H-11, H-13 and H<sub>3</sub>-19 methyl group (Figure 4B). The large coupling constant ( $J_{14,15} = 15.4$  Hz) and the NOESY correlation detected between H-13 and H-15 indicated the *E*-geometry of the double bond at  $\Delta^{14(15)}$ . The NOE correlations and the distances (Å) between relevant protons on the Chem3D optimized model of **1** assisted the assignment of the relative stereochemistry at C-5' in the tetramic acid portion (Figure 4B, Table S3). The NOE cross-peaks detected between H-5'/H-15 (distance 2.96 Å) and H-5'/H-17 (distance 3.28 Å) indicated H-5' to be  $\beta$ -oriented. The absolute configuration of C-16 was determined by Mosher's ester method [20]. The compound **1** was converted to 16-(*S*)-MTPA methyl ester (**6**) and 16-(*R*)-MTPA methyl ester (**7**) using (*S*)- and (*R*)-MTPA chloride (Figures S25 and S26). The differences of <sup>1</sup>H NMR chemical shifts around C-16 of **6** and **7** were measured (Table S2, Figure S29). The results of  $\Delta\delta$  ( $\delta_{\text{S}} - \delta_{\text{R}}$ ) for H-14 (0.08), H-15 (0.07) and H<sub>3</sub>-17 (−0.08) suggested the absolute configuration at C-16 to be *S*. Thus, we propose the trivial name pyrenosetin A for compound **1**.

**Table 2.**  $^{13}\text{C}$  NMR data of compounds 1–4 at 150 MHz.

Position	1 <sup>a</sup>	2 <sup>a</sup>	3 <sup>a</sup>	4 <sup>b</sup>
	$\delta_{\text{C}}$	$\delta_{\text{C}}$	$\delta_{\text{C}}$	$\delta_{\text{C}}$
1	213.3 (C)	209.8 (C)	212.1 (C)	197.6 (C)
2	54.8 (C)	54.1 (C)	54.7 (C)	49.9 (C)
3	53.6 (CH)	52.8 (CH)	53.6 (CH)	50.2 (CH)
4	131.8 (C)	132.3 (C)	130.9 (C)	132.4 (C)
5	128.1 (CH)	127.6 (CH)	128.8 (CH)	127.1 (CH)
6	37.6 (CH)	37.6 (CH)	37.6 (CH)	40.1 (CH)
7	41.9 (CH <sub>2</sub> )	42.0 (CH <sub>2</sub> )	41.8 (CH <sub>2</sub> )	43.1 (CH <sub>2</sub> )
8	33.0 (CH)	32.9 (CH)	32.9 (CH)	34.3 (CH)
9	35.3 (CH <sub>2</sub> )	35.3 (CH <sub>2</sub> )	35.2 (CH <sub>2</sub> )	36.6 (CH <sub>2</sub> )
10	25.3 (CH <sub>2</sub> )	25.3 (CH <sub>2</sub> )	25.2 (CH <sub>2</sub> )	29.0 (CH <sub>2</sub> )
11	37.4 (CH)	38.0 (CH)	37.4 (CH)	40.6 (CH)
12	15.0 (CH <sub>3</sub> )	15.2 (CH <sub>3</sub> )	15.2 (CH <sub>3</sub> )	14.2 (CH <sub>3</sub> )
13	51.5 (CH)	51.0 (CH)	50.6 (CH)	131.6 (CH)
14	127.3 (CH)	130.5 (CH)	144.4 (CH)	133.4 (CH)
15	138.8 (CH)	137.8 (CH)	133.9 (CH)	132.1 (CH)
16	67.9 (CH)	69.0 (CH)	197.6 (C)	129.2 (CH)
17	23.5 (CH <sub>3</sub> )	22.9 (CH <sub>3</sub> )	27.6 (CH <sub>3</sub> )	18.1 (CH <sub>3</sub> )
18	24.2 (CH <sub>3</sub> )	23.9 (CH <sub>3</sub> )	23.7 (CH <sub>3</sub> )	22.5 (CH <sub>3</sub> )
19	22.4 (CH <sub>3</sub> )	22.4 (CH <sub>3</sub> )	22.4 (CH <sub>3</sub> )	22.7 (CH <sub>3</sub> )
2'	168.6 (C)	168.6 (C)	167.8 (C)	178.1 (C)
3'	73.1 (C)	73.8 (C)	72.7 (C)	101.6 (C)
4'	207.2 (C)	205.0 (C)	206.4 (C)	191.5 (C)
5'	69.8 (CH)	69.4 (CH)	69.8 (CH)	68.8 (CH)
6'	60.3 (CH <sub>2</sub> )	58.3 (CH <sub>2</sub> )	60.3 (CH <sub>2</sub> )	59.6 (CH <sub>2</sub> )
7'	28.3 (CH <sub>3</sub> )	27.7 (CH <sub>3</sub> )	28.5 (CH <sub>3</sub> )	27.4 (CH <sub>3</sub> )

<sup>a</sup> Recorded in CDCl<sub>3</sub>, <sup>b</sup> Recorded in CD<sub>3</sub>CN.**Figure 4.** (A) Key COSY (bold), HMBC (blue) correlations within 1. (B) NOESY (red) correlations and distances between H-5', H-15 and H<sub>3</sub>-17 shown on the Chem3D optimized model of 1.

Compound 2 was isolated as an optically active colorless oil. Its molecular formula C<sub>25</sub>H<sub>35</sub>NO<sub>5</sub> deduced by HR-ESIMS ( $m/z$  452.2401 [M + Na]<sup>+</sup>) was found to be the same as 1 (Figure S15). A close inspection of its FT-IR, 1D and 2D NMR spectra (Figures S9–S14 and S16) revealed that 2 had the same 2D structure as 1. As depicted in Tables 1 and 2, 1D NMR spectra of 2 however contained slight changes in chemical shifts of H-14 (1  $\delta_{\text{H}}$  5.75 and 2  $\delta_{\text{H}}$  5.97) and C-14 (1  $\delta_{\text{C}}$  127.3 and 2  $\delta_{\text{C}}$  130.5); H-15 (1  $\delta_{\text{H}}$  5.71 and 2  $\delta_{\text{H}}$  5.50) and C-15 (1  $\delta_{\text{C}}$  138.8 and 2  $\delta_{\text{C}}$  137.8); and H-16 (1  $\delta_{\text{H}}$  4.24 and 2  $\delta_{\text{H}}$  4.18) and C-16 (1  $\delta_{\text{C}}$  67.9 and 2  $\delta_{\text{C}}$  69.0). These differences were indicative of an opposite (*R*) stereochemistry at C-16. The absolute configuration of C-16 was investigated by Mosher's method. The chemical shift differences [ $\Delta\delta(\delta_{\text{S}}-\delta_{\text{R}})$ ] in the <sup>1</sup>H-NMR of the MTPA esters (8 and 9) for H-14 (−0.01), H-15 (−0.13) and

H<sub>3</sub>-17 (+0.04) suggested a 16-*R* absolute configuration, which was opposite to **1** (Table S2, Figures S27, S28 and S30). The absence of any NOESY correlation between H-5' and H-15 or between H-5' and H-17 suggested the  $\alpha$ -orientation of H-5'. The distances calculated on the 3D structure of compound **2** (with both  $\alpha$ - and  $\beta$ -epimers of H-5') (Table S3) supported this assignment. Based on the NOESY spectrum (Figure S14), the relative configuration of all other chiral centers within **2** was identified to be the same as in compound **1**. We suggest the trivial name pyrenosetin B for compound **2**.

HR-ESIMS analysis of compound **3** revealed a molecular ion ( $m/z$  428.2434 [M + H]<sup>+</sup>) that corresponded to a molecular formula C<sub>25</sub>H<sub>33</sub>NO<sub>5</sub> (Figure S23). This requires 10 degrees of unsaturation. The FT-IR, 1D and 2D NMR data of **3** closely resembled compounds **1** and **2** (Figures S17–S22 and S24). The two most striking differences were the absence of H-16 oxymethine resonance in the <sup>1</sup>H-NMR spectrum of **2**, and the appearance of an additional carbonyl singlet at  $\delta_C$  197.6 (C-16) in its <sup>13</sup>C-NMR spectrum (Tables 1 and 2, Figures S17 and S18). This clearly suggested **3** to be an oxidized analog of **1** and **2**. The conversion of the secondary methyl group H<sub>3</sub>-17 into a highly deshielded singlet at  $\delta_H$  2.22 (Table 1) indicated that the hydroxyl group at C-16 was replaced by a ketone function. The remarkable shift of H-14 and H-15 protons to downfield up to +0.8 and 1.0 ppm, respectively, further supported this assumption (Table 1). Clear HMBC correlations from H-14, H-15 and H<sub>3</sub>-17 to C-16 provided the final proof for the presence of a carbonyl function at C-16. The planar structure of **3** was confirmed by detailed analysis of <sup>1</sup>H, <sup>13</sup>C, DEPT-HSQC, COSY and HMBC data (Figures S17–S22). The relative configuration of the chiral centers at C-3, C-6, C-8, C-11, C-2, C-13, C-3' and C-5' within **3** was deduced to be the same as in **2** by analyzing its NOESY spectrum (Figure S22) and distances between proton pairs H-5'/H-15 and H-5'/H-17 (Table S3). We suggest the trivial name pyrenosetin C for compound **3**.

#### 2.4. Biological Activity of Compounds 1–4

Compounds **1–4** were tested against the human malignant melanoma cancer cells (A-375). As shown in Table 3, compounds **1** and **2** showed the highest anticancer activity with IC<sub>50</sub> values of 2.8 and 6.3  $\mu$ M, respectively. Compound **3** and the known metabolite **4** were less potent (IC<sub>50</sub> 140.3 and 37.3  $\mu$ M). The general toxicity of the isolated metabolites was assessed against the human keratinocyte cell line HaCaT. Interestingly the IC<sub>50</sub> values of **1**, **3** and **4** against HaCaT cells were very similar to their IC<sub>50</sub> values against melanoma cells, indicating them to be non-selectively toxic. However, compound **2** exerted lower toxicity towards HaCaT cells (IC<sub>50</sub> 35.0  $\mu$ M) with a relatively better selectivity index around 5.6 (calculated by dividing IC<sub>50</sub> value against HaCaT cells / IC<sub>50</sub> value against A-375 cells) compared to other three fungal metabolites.

**Table 3.** In vitro activity of compounds **1–4** against human malignant melanoma cell line (A-375) and non-cancerous keratinocyte cell line (HaCaT). The IC<sub>50</sub> values are in  $\mu$ M. Positive control: Doxorubicin.

Compound	A-375 Cells	HaCaT Cells
<b>1</b>	2.8 ( $\pm$ 0.0)	4.2 ( $\pm$ 0.0)
<b>2</b>	6.3 ( $\pm$ 0.0)	35.0 ( $\pm$ 0.0)
<b>3</b>	140.3 ( $\pm$ 0.9)	142.9 ( $\pm$ 1.4)
<b>4</b>	37.3 ( $\pm$ 0.1)	45.0 ( $\pm$ 0.2)
Positive control	0.6 ( $\pm$ 0.0)	22.1 ( $\pm$ 2.9)

### 3. Discussion

Phylogenetic tree analysis confirmed the fungus FVE-001 to be a *Pyrenochaetopsis* sp. The genus *Pyrenochaetopsis* has previously been reported as a close relative of *Pyrenochaeta*, which is a member of the family Cucurbitariaceae. The genus *Pyrenochaetopsis* shows genetic similarity to the genus *Phoma*, but their conidiogenesis is considered to be significantly different [21,22]. The chemical machinery of the genus *Pyrenochaetopsis* has not received much attention so far. To our knowledge, only one chemical study has been performed on terrestrial soil fungus *Pyrenochaetopsis* sp., reporting the isolation of phomasetin (**4**) and two new decalinoyl tetramic acids, wakodecalines A and B [18]. A very recent study

by Kato et al. (2018) has identified the biosynthetic gene cluster of phomasetin in a *Pyrenochaetopsis* sp. RK10-F058 [23]. The wakodecalines A and B showed moderate antimalarial activity against the *Plasmodium falciparum* 3D7, but were inactive against cancer cell lines [18]. Phomasetin (4) has been reported from few fungal genera, e.g., *Phoma* and *Pyrenochaetopsis*. It exerts anti-HIV and antitumor activities against cancer cell lines such as HeLa and HL-60 [18,19]. In this study phomasetin showed weak antitumor activity, which was associated with general toxicity.

The major drawbacks of the traditional bioassay-guided isolation process include its time consuming nature and the re-isolation of known compounds. Molecular network-based metabolomics is emerging as an efficient method in identification of chemical inventory of biological organisms and dereplication of natural products from crude extracts [11,24]. In our previous work, we used OSMAC approach to investigate chemical diversity and anticancer activity of fungi associated with *Fucus vesiculosus* [12] where we mapped the anticancer activity data of large number of fungal extracts over the MN and searched for a link between spectral molecular networks and their anticancer activity [12]. One fungus from this study that was identified herein as *Pyrenochaetopsis* sp. FVE-001 (order Pleosporales) was selected for work-up, based on its anticancer activity. The combination of both bioassay-guided fractionation and MN approaches in the form of B-B MN allowed the rapid isolation of three new compounds 1–3. As expected, pyrenosetins A (1) and B (2) had the highest anticancer activity, supporting the bioactivity scores obtained by B-B MN at fractionation stage. Pyrenosetin B (2) that differs from 1 by the stereochemistry of the C-16 hydroxyl group displayed less pronounced anticancer activity but also lower toxicity. The replacement of the OH group at C-16 with a keto function in pyrenosetin C (3) was not favorable for bioactivity, leading to a low IC<sub>50</sub> value against A-375 cells. This indicates that the presence of an OH group at C-16 impacts the anticancer and toxic potential of pyrenosetins A–C.

Compounds 1–3 possess unique decalinoylspirotetramic acid structures characterized by a *trans*-decalin ring, a fused spiro system with a carbonyl unit (cyclopentanone) and a terminal tetramic acid moiety. Bioactive natural products containing *trans*-decalin ring are common in fungi (e.g., genera *Fusarium*, *Penicillium* and *Alternaria*) [25], however, molecules containing a decalin ring with a terminal tetramic acid structure linked through a spiro ring are rare in Nature. Some known examples include fusarisetins A and B from a soil-derived *Fusarium* sp., fusarisetins C–D from a marine-derived *Fusarium* sp. [26,27], altercrasins A–E from a sea urchin-derived *Alternaria* sp. [28]. Wakodecalines A and B obtained from the terrestrial soil fungus *Pyrenochaetopsis* sp. RK10-F058 possess a *N*-methylated serine moiety instead of the terminal tetramic acid ring [18]. Interestingly some *Fusarium* sp. [29] contain equisetin, the enantiomeric homolog of phomasetin, which possesses totally opposite stereochemistry in all chiral centers. Such compounds have been proposed to be mixed biosynthesis products of PKS and NRPS pathways [23]. Despite the structural similarities, biosynthesis of decalin derivatives is highly controlled by stereospecific enzymes [19,30]. A recent study by Kato et al. (2018) reported that the stereospecific enzyme *fas2* determines the formation of the *trans*-decalin ring in equisetin (and fusarisetin), while *phm7* enzyme controls the biosynthesis of the *trans*-decalin ring in the enantiomeric homolog phomasetin (4) [23]. In this study, we isolated phomasetin (4) and three new related metabolites 1–3 from *Pyrenochaetopsis* sp. FVE-001. This is the first chemical study carried out on a marine-derived *Pyrenochaetopsis* sp. and the second investigation performed on a member of the genus *Pyrenochaetopsis*. Although the anticancer activity the compounds 1 and 2 is associated with cytotoxicity, a medicinal chemistry approach in future may improve their potency and selectivity.

## 4. Material and Methods

### 4.1. General Procedures

NMR spectra were recorded on a Bruker AV 600 spectrometer (600 and 150 MHz for <sup>1</sup>H- and <sup>13</sup>C-NMR, respectively, Bruker®, Billerica, MA, USA) or a Bruker Avance III spectrometer (500 and 125 MHz for <sup>1</sup>H- and <sup>13</sup>C-NMR, respectively). The residual solvent signals were used as

internal references:  $\delta_{\text{H}}$  7.26/ $\delta_{\text{C}}$  77.2 ppm ( $\text{CDCl}_3$ ),  $\delta_{\text{H}}$  1.94/ $\delta_{\text{C}}$  118.3 and  $\delta_{\text{C}}$  1.3 ( $\text{CD}_3\text{CN}$ ). 4-Dimethyl-4-silapentane-1-sulfonic acid (DSS) was used as internal standard. High-resolution MS<sup>2</sup> data were recorded on a Xevo G2-XS QToF Mass Spectrometer (Waters<sup>®</sup>, Milford, MA, USA) coupled to a Waters Acquity I-Class UPLC system). HR-ESIMS was recorded on a Bruker microTOF II-High-performance TOF-MS system equipped with an electrospray ionization source. Solid phase extraction (SPE) was performed on the Chromabond C18 SPE cartridges (6 mL/2000 mg, Macherey-Nagel, Duren, Germany). HPLC separations were performed on a VWR Hitachi Chromaster system (VWR International, Allison Park, PA, USA) consisting of a 5430 diode array detector (VWR International, Allison Park, PA, USA), a 5310 column oven, a 5260 autosampler and a 5110 pump combined in parallel with a VWR Evaporative Light Scattering Detector (ELSD 90). Routine HPLC separations were performed on semipreparative (Onyx, 100 × 10 mm, Phenomenex, Torrance, CA, USA) C18 monolithic column, analytic (SeQuant<sup>®</sup>, 250 × 4.6 mm, Merck, Darmstadt, Germany) ZIC-HILIC column and analytic (Synergi<sup>™</sup>, 4  $\mu\text{m}$ , 250 × 4.6 mm, Phenomenex) polar-RP 80 Å LC column. The water used was MilliQ-water produced by in-house Arium<sup>®</sup> Water Purification Systems (Sartorius, Germany). EtOAc, *n*-hexane, methanol and acetonitrile were purchased from VWR International GmbH (Hannover, Germany). Potato extract and dextrose that were used for culture medium were purchased from Sigma-Aldrich (Schnellendorf, Germany) and from Merck, respectively. Agar was purchased from Applichem (Darmstadt, Germany). (S)- and (R)-MTPA chloride were purchased from Merck. The 3D structures of compounds 1–3 were obtained by using ChemBio3D Ultra 12.0 software (PerkinElmer, Waltham, MA, USA).

#### 4.2. Strain Identification and Cultivation

The fungal strain was isolated from *Fucus vesiculosus* specimens collected in Falckenstein Beach (54°23'22.6" N, 10°11'26.4" E), Kiel Fjord, Baltic Sea, Germany in December 2015 [12]. The fungus was identified using ITS-5.8s rRNA sequencing to species level through building phylogenetic tree (Figure 1). The evolutionary history was inferred by using the Maximum Likelihood method based on the General Time Reversible model [31]. The percentage of trees in which the associated taxa clustered together is shown next to the branches. Initial tree(s) for the heuristic search were obtained automatically by applying Neighbor-Join and BioNJ algorithms to a matrix of pairwise distances estimated using the Maximum Composite Likelihood (MCL) approach, and then selecting the topology with superior log likelihood value. A discrete Gamma distribution was used to model evolutionary rate differences among sites (5 categories (+G, parameter = 0.8198)). The rate variation model allowed for some sites to be evolutionarily invariable ([+I], 37.97% sites). The tree is drawn to scale, with branch lengths measured in the number of substitutions per site. The analysis involved 14 nucleotide sequences. Evolutionary analyses were conducted in MEGA7 [32]. The fungal sample was deposited at the GEOMAR-Biotech laboratory (Kiel, Germany). The strain was cultured on potato dextrose agar (PDA: potato extract 4 g, dextrose 20 g, agar 15g for 1 L, pH 5.6). After 3 days of pre-culturing, the conidia was inoculated in 500 mL cylindrical flasks containing 100 mL of seed medium (PDM: potato extract 4 g, dextrose 20 g for 1 L; pH 5.6) incubated at 22 °C for 7 days on a rotary shaker at 120 rpm.

#### 4.3. Extraction and Isolation

The 12 L of culture broth was partitioned with the same volume of EtOAc twice. The resulting organic extract was evaporated *in vacuo* to afford light yellow oily extract (2.66 g). The crude extract was subjected to a modified Kupchan partition to yield three subextracts, namely *n*-hexane (KH, 1.99 g),  $\text{CHCl}_3$  (KC, 345.4 mg) and aqueous MeOH (KM, 68.7 mg). Briefly, the crude extract was dissolved in 500 mL aqueous methanol (90% MeOH) and partitioned against *n*-hexane (KH, 2 × 500 mL). The MeOH content of the aq. MeOH phase was increased to 30% before partitioning against  $\text{CHCl}_3$  (KC, 2 × 500 mL). The KC subextract showed relatively high anticancer bioactivity against all five cancer cell lines (>75% inhibition rate at 100  $\mu\text{g}/\text{mL}$ ) and was fractionated on a Chromabond C18 SPE cartridge. A 10% stepwise gradient elution with MeOH:  $\text{H}_2\text{O}$  mixtures (0% to 100%) afforded 11

fractions (fraction 0–10). Anticancer activity was tracked to fractions 5–7. The fraction 5 (92.7 mg) and fraction 6 (13.3 mg) were combined and subjected to semi-preparative RP–HPLC, eluting with MeCN:H<sub>2</sub>O (40% isocratic MeCN over 28 min, and gradual increase to 60% by 40 min, flow 3.0 mL/min) to yield 7 subfractions (fraction 5.1 to 5.7). Subfraction 5.4 contained the pure compound **1** (2.4 mg, *t*<sub>R</sub> 16.5 min). Fraction 5.7 (3.6 mg) was rechromatographed by RP–HPLC (isocratic mixture H<sub>2</sub>O: MeCN (45:55, flow 1.0 mL/min) to yield **2** (1.2 mg, *t*<sub>R</sub> 8.0 min) and **3** (0.8 mg, *t*<sub>R</sub> 9.5 min). The fraction 7 (25.4 mg) was subjected to a semi-prep. RP–HPLC (65% isocratic MeCN over 30 min, and gradual decrease to 60% MeCN to 60%MeCN by 35 min, flow 3.0 mL/min) to yield 5 subfractions (fraction 7.1–7.5). Fraction 7.4 (12.9 mg) was separated on HPLC equipped with an analytical HPLC column (Synergi™, 250 × 4.6 mm, Phenomenex) using MeCN:H<sub>2</sub>O (50% isocratic MeCN over 6 min and gradual increase to 78% MeCN by 12 min (flow 1.0 mL/min)) to yield **4** (1.4 mg, *t*<sub>R</sub> 6.5 min) in a pure state.

*Pyrenosetin A (1)*: Colorless oil;  $[\alpha]_{\text{D}}^{22} +30$  (c 0.10, MeOH); IR (oil)  $\nu_{\text{max}}$  3554, 3249, 2952, 2875, 1721, 1683, 1456, 1378, 1271 cm<sup>-1</sup>; <sup>1</sup>H-NMR (CDCl<sub>3</sub>, 600 MHz) and <sup>13</sup>C-NMR (CDCl<sub>3</sub>, 150 MHz), Tables 1 and 2; HR-ESIMS found *m/z* [M + H]<sup>+</sup> 430.2592, C<sub>25</sub>H<sub>36</sub>NO<sub>5</sub>, calculated for 430.2588.

*Pyrenosetin B (2)*: Colorless oil;  $[\alpha]_{\text{D}}^{22} +13$  (c 0.10, MeOH); IR (oil)  $\nu_{\text{max}}$  3550, 3185, 2944, 2862, 1726, 1675, 1456, 1378, 1249 cm<sup>-1</sup>; <sup>1</sup>H-NMR (CDCl<sub>3</sub>, 600 MHz) and <sup>13</sup>C-NMR (CDCl<sub>3</sub>, 150 MHz), Tables 1 and 2; HR-ESIMS found *m/z* [M + Na]<sup>+</sup> 452.2401 C<sub>25</sub>H<sub>35</sub>NO<sub>5</sub>Na, calculated for 452.2407.

*Pyrenosetin C (3)*: Colorless oil;  $[\alpha]_{\text{D}}^{22} +12$  (c 0.10, MeOH); IR (oil)  $\nu_{\text{max}}$  3559, 3259, 2952, 2858, 1726, 1683, 1451, 1369, 1253 cm<sup>-1</sup>; <sup>1</sup>H-NMR (CDCl<sub>3</sub>, 600 MHz) and <sup>13</sup>C-NMR (CDCl<sub>3</sub>, 150 MHz), Tables 1 and 2; HR-ESIMS found *m/z* [M + H]<sup>+</sup> 428.2434, C<sub>25</sub>H<sub>34</sub>NO<sub>5</sub>, calculated for 428.2431.

*Phomasetin (4)*: Colorless oil;  $[\alpha]_{\text{D}}^{22} +116$  (c 0.15, CDCl<sub>3</sub>); <sup>1</sup>H-NMR (CD<sub>3</sub>CN, 600 MHz) and <sup>13</sup>C-NMR (CD<sub>3</sub>CN, 150 MHz), Tables 1 and 2; HR-ESIMS found *m/z* [M + H]<sup>+</sup> 414.2645, C<sub>25</sub>H<sub>36</sub>NO<sub>4</sub>, calculated for 414.2639.

#### 4.4. UHPLC-QToF-MS/MS Analysis and Molecular Networking

The SPE fractions derived from the KC subextract were analyzed on an ACQUITY UPLC I-Class System coupled to the Waters® Xevo G2-XS QToF Mass Spectrometer equipped with an electrospray ionization (ESI) source operating with a mass range of *m/z* 50–1600 Da. The 0.1 mg/mL MeOH solution of each fraction was filtered through a 0.2 μm PTFE syringe filter (Carl Roth, Karlsruhe, Germany) and then injected (injection volume: 0.2 μL) into the system that equipped with Acquity UPLC HSS T3 column (High Strength Silica C18, 1.8 μm, 100 × 2.1 mm I.D., Waters®) operating at 40 °C. Separation was achieved with a binary LC solvent system controlled by MassLynx® (version 4.1) using mobile phase A (99%) water/ 0.1 % formic acid (ULC/MS grade) and B 99.9% ACN/ 0.1% formic acid (ULC/MS grade), pumped at a rate of 0.6 mL/ min with the following gradient: initial, 1% B; 0.0–6.0 min to 30% B; 6.0–11.5 min to 100% B; 11.5–13.5 min 100% B, and a column reconditioning phase until 15 min.

ESI conditions were set with the capillary voltage at 0.8 kV, sample cone voltage at 40.0 V, source temperature at 150 °C, desolvation temperature at 550 °C, cone gas flow in 50 L/h and desolvation gas flow in 1200 L/h. MS/MS setting was a ramp collision energy (CE): low CE from 6 eV to 60 eV and high CE from 9 eV to 80 eV. As a control, solvent (methanol) was injected. MassLynx® (Waters®, V4.1) was used to analyze the achieved MS and MS<sup>2</sup> data.

The raw data were converted to mzXML file format using MSConvert (version 3.0.10051, Vanderbilt University, Nashville, TN, USA). The resulting mzXML data were processed in MZmine2 (version 2.32). Mass lists were created using the mass detection module with a noise level of 1500 counts for MS<sup>1</sup> and 10 counts for MS<sup>2</sup>. The chromatogram builder module was used to create peak lists with a scan retention time from 0.01 min to 13.0 min, a minimum retention time of 0.01 min, a minimum peak height of 10,000 counts and an *m/z* tolerance of 0.01 Da or 10 ppm. The peak lists were deconvoluted using the local minimum search algorithm with the following parameters: chromatographic threshold 0.01%, search minimum in RT range 0.20, minimum relative height 0.01%, minimum absolute height



1000 counts, minimum ratio of peak top/edge 2, peak duration range 0.01–3 min. For MS<sup>2</sup> scan pairing, the *m/z* range was set to 0.05 Da and retention time range to 0.2 min. Furthermore, the deconvoluted peak lists were deisotoped with the following parameters: *m/z* tolerance 0.02 or 10 ppm, retention time tolerance 0.01 min and maximum charge 2. The deisotoped peak lists were aligned through using the Join aligner module with an *m/z* tolerance of 0.01 Da or 10 ppm and a retention time tolerance of 0.2 min. Weight for *m/z* and retention time were both set to 50. The aligned peak list was filtered to exclude peaks derived from solvent and peaks with *m/z* lower than 125 Da. The peak ID's were lastly reset and the peak list was exported as mgf file for GNPS analysis. The reset peak list was exported as CSV table file for bioactivity score analysis.

The adjusted mgf files were uploaded to GNPS for molecular networking analysis. A molecular network was created with the feature based molecular networking work flow (<https://ccms-ucsd.github.io/GNPSDocumentation/featurebasedmolecularnetworking/>) on the GNPS website (<http://gnps.ucsd.edu>) [33]. The data was filtered by removing all MS/MS fragment ions within  $\pm 17$  Da of the precursor *m/z*. MS/MS spectra were window filtered by choosing only the top 6 fragment ions in the  $\pm 50$  Da window throughout the spectrum. The precursor ion mass tolerance was set to 0.02 Da and a MS/MS fragment ion tolerance of 0.02 Da. A network was then created where edges were filtered to have a cosine score above 0.65 and more than 6 matched peaks. Further, edges between two nodes were kept in the network if and only if each of the nodes appeared in each other's respective top 10 most similar nodes. Finally, the maximum size of a molecular family was set to 250, and the lowest scoring edges were removed from molecular families until the molecular family size was below this threshold. The spectra in the network were then searched against GNPS spectral libraries. The library spectra were filtered in the same manner as the input data. All matches kept between network spectra and library spectra were required to have a score above 0.65 and at least 6 matched peaks. The CSV table generated from MZmine2 (ver. 2.32) was input to R studio (version 1.1.463) to calculate the bioactivity score based on the workflow reported by Nothias et al. [14]. The obtained bioactivity score list and GNPS data were downloaded and imported into Cytoscape<sup>®</sup> (version 3.5.1, Institute for Systems Biology, Seattle, WA, USA) to generate the bioactivity-based molecular networking.

#### 4.5. Mosher's Esterification

##### 4.5.1. Preparation of 16-(S) MTPA Ester 6 and 16-(R)-MTPA Ester 7

To a solution of **1** (1.1 mg, 2.1  $\mu$ mol) in abs. pyridine (0.3 mL), (S)-MTPA chloride (3.2 mg, 12.6  $\mu$ mol) was added, and the reaction mixture was stirred at room temperature for 12 h. Subsequently 1.0 mL water was added to the reaction mixture and extracted using CH<sub>2</sub>Cl<sub>2</sub>. The organic layer was evaporated under reduced pressure, and the residue was purified by RP-HPLC eluted with MeCN:H<sub>2</sub>O (gradient from 50:50 to 100:0 in 10 min, 100:0 in 10 to 15 min, and from 100:0 to 50:50 in 15 to 21 min, flow 1.0 mL/min) to afford 16-(S)-MTPA ester **6** (0.7 mg, *t<sub>R</sub>* 12.0 min) as a colorless oil. The 16-(R)-MTPA ester **7** was prepared from **1** using (R)-MTPA chloride in pyridine employing the same procedure. The 16-(R)-MTPA ester **7** (0.5 mg, *t<sub>R</sub>* 11.9 min) was a colorless oil. Both **6** and **7** were dissolved in CDCl<sub>3</sub> and analysed by <sup>1</sup>H-NMR spectroscopy.

##### 4.5.2. Preparation of 16-(S) MTPA Ester 8 and 16-(R)-MTPA Ester 9

Compound **8** and **9**, respectively, were individually prepared from **2** using either with (S)-MTPA chloride) or (R)-MTPA chloride. The same procedure used for preparation of **6** was employed. Both 16-(S)-MTPA ester **8** (0.3 mg, *t<sub>R</sub>* 11.3 min) and 16-(R)-MTPA ester **9** (0.3 mg, *t<sub>R</sub>* 11.2 min) were colorless oils. They were dissolved in CDCl<sub>3</sub> and analysed by <sup>1</sup>H-NMR spectroscopy.

#### 4.6. Bioactivity Assays

The crude extracts were initially tested in vitro against 5 human cancer cell lines: colorectal adenocarcinoma cell line HT-29 (DSMZ, Braunschweig, Germany), malignant melanoma cell line

A-375 (CLS, Eppelheim, Germany), colon cancer cell line HCT-116 (DSMZ), lung carcinoma cell line A-549 (CLS, Eppelheim, Germany), human breast cancer line MB-231 (CLS), and the non-cancerous human keratinocyte line HaCaT (CLS) at a concentration of 100 µg/mL. The antitumoral activity of the crude extracts was evaluated by monitoring the metabolic activity using the CellTiterBlue Cell Viability Assay (Promega, Mannheim, Germany). HT-29 and HaCaT cells were cultivated in RPMI medium, A-549 and MB-231 cells in DMEM: Ham's F12 medium (1:1) supplemented with 15 mM HEPES and A-375 and HCT-116 cells in DMEM medium supplemented with 4.5 g/L D-Glucose and 110 mg/L sodium pyruvate. All media were supplemented with L-Glutamine, 10% fetal bovine serum, 100 U/mL penicillin, and 100 mg/mL streptomycin. The cultures were maintained at 37 °C under a humidified atmosphere and 5% CO<sub>2</sub>. The cell lines were transferred every 3 or 4 days. For experimental procedure, the cells were seeded in 96 well plates at a concentration of 10,000 cells per well. A stock solution of 40 mg/mL in DMSO was prepared of each extract. After 24 h incubation, the medium was removed from the cells and 100 µL fresh medium containing the test samples was added. Each sample was prepared in duplicate once. Doxorubicin as a standard therapeutic drug was used as positive control, 0.5% DMSO and growth media were used as controls. Following compound addition, plates were cultured at 37 °C for 24 h. Afterwards, the assay was performed according to the manufacturer's instructions and measured using the microplate reader Tecan Infinite M200 at excitation 560 nm and emission of 590 nm. For determination of IC<sub>50</sub> values, a dilution series of the extracts was prepared and tested, as described before for the crude extract. The IC<sub>50</sub> values were calculated by Excel as the concentration that shows 50% inhibition of the viability on the basis of a negative control (no compound) and compared with the positive control (doxorubicin).

**Supplementary Materials:** The supplementary are available online at <http://www.mdpi.com/1660-3397/18/1/47/s1>, Bioactivity results of different KC fractions against cancer and HaCaT cell lines; NMR, HR-ESIMS and FT-IR spectra of compounds 1–3. <sup>1</sup>H NMR spectra of MTPA esters 6–9.

**Author Contributions:** Design of the work, D.T. and B.F.; extraction, purifications of compounds, B.F.; data analysis, B.F., F.L., P.D. and D.T.; strain identification M.B. and B.F.; writing original manuscript, B.F., P.D., D.T.; supervision, D.T. All authors have read and agreed to the published version of the manuscript.

**Funding:** This research received no external funding.

**Acknowledgments:** BF thanks the China Scholarship Council for a Ph.D. scholarship. We are grateful to Arlette Wenzel-Storjohann and Jana Heumann for performing anticancer assays. We acknowledge financial support by Land Schleswig-Holstein within the funding program Open Access Publikationsfonds.

**Conflicts of Interest:** The authors declare no conflict of interest.

## References

1. Egan, S.; Harder, T.; Burke, C.; Steinberg, P.; Kjelleberg, S.; Thomas, T. The seaweed holobiont: Understanding seaweed–bacteria interactions. *FEMS Microbiol. Rev.* **2013**, *37*, 462–476. [[CrossRef](#)] [[PubMed](#)]
2. Fenical, W.; Jensen, P.R.; Cheng, X.C. Halimide, a Cytotoxic Marine Natural Product, and Derivatives Thereof. U.S. Patent US6358957B1, 30 May 2000.
3. Cimino, P.J.; Huang, L.; Du, L.; Wu, Y.; Bishop, J.; Dalsing-Hernandez, J.; Kotlarczyk, K.; Gonzales, P.; Carew, J.; Nawrocki, S. Plinabulin, an inhibitor of tubulin polymerization, targets KRAS signaling through disruption of endosomal recycling. *Biomed. Rep.* **2019**, *10*, 218–224. [[CrossRef](#)] [[PubMed](#)]
4. Zuccaro, A.; Schulz, B.; Mitchell, J.I. Molecular detection of ascomycetes associated with *Fucus serratus*. *Mycol. Res.* **2004**, *107*, 1451–1466. [[CrossRef](#)] [[PubMed](#)]
5. Zuccaro, A.; Schoch, C.L.; Spatafora, J.W.; Kohlmeyer, J.; Draeger, S.; Mitchell, J.I. Detection and identification of fungi intimately associated with the brown seaweed *Fucus serratus*. *Appl. Environ. Microbiol.* **2008**, *74*, 931–941. [[CrossRef](#)] [[PubMed](#)]
6. Flewelling, A.J.; Johnson, J.A.; Gray, C.A. Isolation and bioassay screening of fungal endophytes from North Atlantic marine macroalgae. *Bot. Mar.* **2013**, *56*, 287–297. [[CrossRef](#)]
7. Osterhage, C.; König, G.M.; Jones, P.G.; Wright, A.D. 5-Hydroxyramulosin, a new natural product produced by *Phoma tropica*, a marine-derived fungus isolated from the alga *Fucus spiralis*. *Planta Med.* **2002**, *68*, 1052–1054. [[CrossRef](#)]

8. Santiago, C.; Fitchett, C.; Munro, M.H.G.; Jalil, J.; Santhanam, J. Cytotoxic and antifungal activities of 5-hydroxyramulosin, a compound produced by an endophytic fungus isolated from *Cinnamomum mollissimum*. *Evid. Based Complement. Altern. Med.* **2012**, *2012*, 689310. [[CrossRef](#)]
9. Abdel-Lateff, A.; Fisch, K.M.; Wright, A.D.; König, G.M. A new antioxidant isobenzofuranone derivative from the algicolous marine fungus *Epicoccum* sp. *Planta Med.* **2003**, *69*, 831–834.
10. Quinn, R.A.; Nothias, L.F.; Vining, O.; Meehan, M.; Esquenazi, E.; Dorrestein, P.C. Molecular networking as a drug discovery, drug metabolism, and precision medicine strategy. *Trends Pharmacol. Sci.* **2017**, *38*, 143–154. [[CrossRef](#)]
11. Yang, J.Y.; Sanchez, L.M.; Rath, C.M.; Liu, X.; Boudreau, P.D.; Bruns, N.; Glukhov, E.; Wodtke, A.; de Felicio, R.; Fenner, A.; et al. Molecular networking as a dereplication strategy. *J. Nat. Prod.* **2013**, *76*, 1686–1699. [[CrossRef](#)]
12. Fan, B.; Parrot, D.; Blümel, M.; Labes, A.; Tasdemir, D. Influence of OSMAC-based cultivation in metabolome and anticancer activity of fungi associated with the brown alga *Fucus vesiculosus*. *Mar. Drugs* **2019**, *17*, 67. [[CrossRef](#)] [[PubMed](#)]
13. Olivon, F.; Allard, P.M.; Koval, A.; Righi, D.; Genta-Jouve, G.; Neyts, J.; Apel, C.; Pannecouque, C.; Nothias, L.F.; Cachet, X.; et al. Bioactive natural products prioritization using massive multi-informational molecular networks. *ACS Chem. Biol.* **2017**, *12*, 2644–2651. [[CrossRef](#)]
14. Nothias, L.F.; Nothias-Esposito, M.; da Silva, R.; Wang, M.; Protsyuk, I.; Zhang, Z.; Sarvepalli, A.; Leyssen, P.; Touboul, D.; Costa, J.; et al. Bioactivity-based molecular networking for the discovery of drug leads in natural product bioassay-guided fractionation. *J. Nat. Prod.* **2018**, *81*, 758–767. [[CrossRef](#)]
15. Parrot, D.; Blümel, M.; Utermann, C.; Chianese, G.; Krause, S.; Kovalev, A.; Gorb, S.N.; Tasdemir, D. Mapping the surface microbiome and metabolome of brown seaweed *Fucus vesiculosus* by amplicon sequencing, integrated metabolomics and imaging techniques. *Sci. Rep.* **2019**, *9*, 1061. [[CrossRef](#)] [[PubMed](#)]
16. Kõljalg, U.; Larsson, K.H.; Abarenkov, K.; Nilsson, R.H.; Alexander, I.J.; Eberhardt, U.; Erland, S.; Høiland, K.; Kjølner, R.; Larsson, E.; et al. UNITE: A database providing web-based methods for the molecular identification of ectomycorrhizal fungi. *New Phytol.* **2005**, *166*, 1063–1068. [[CrossRef](#)] [[PubMed](#)]
17. Yamamoto, K.; Hayashi, M.; Murakami, Y.; Araki, Y.; Otsuka, Y.; Kashiwagi, T.; Shimamura, T.; Ukeda, H. Development of LC-MS/MS analysis of cyclic dipeptides and its application to tea extract. *Biosci. Biotechnol. Biochem.* **2016**, *80*, 172–177. [[CrossRef](#)] [[PubMed](#)]
18. Nogawa, T.; Kato, N.; Shimizu, T.; Okano, A.; Futamura, Y.; Takahashi, S.; Osada, H. Wakodecalines A and B, new decaline metabolites isolated from a fungus *Pyrenochaetopsis* sp. RK10-F058. *J. Antibiot.* **2017**, *71*, 123–128. [[CrossRef](#)]
19. Singh, S.B.; Zink, D.L.; Goetz, M.A.; Dombrowski, A.W.; Polishook, J.D.; Hazuda, D.J. Equisetin and a novel opposite stereochemical homolog phomasetin, two fungal metabolites as inhibitors of HIV-1 integrase. *Tetrahedron Lett.* **1998**, *39*, 2243–2246. [[CrossRef](#)]
20. Hoye, T.R.; Jeffrey, C.S.; Shao, F. Mosher ester analysis for the determination of absolute configuration of stereogenic (chiral) carbinol carbons. *Nat. Protoc.* **2007**, *2*, 2451–2458. [[CrossRef](#)]
21. Papizadeh, M.; Soudi, M.R.; Amini, L.; Wijayawardene, N.N.; Hyde, K.D. *Pyrenochaetopsis tabarestanensis* (Cucurbitariaceae, Pleosporales), a new species isolated from rice farms in north Iran. *Phytotaxa* **2017**, *297*, 15–28. [[CrossRef](#)]
22. de Gruyter, J.; Woudenberg, J.H.C.; Aveskamp, M.M.; Verkley, G.J.M.; Groenewald, J.Z.; Crous, P.W. Systematic reappraisal of species in *Phoma* section *Paraphoma*, *Pyrenochaeta* and *Pleurophoma*. *Mycologia* **2010**, *102*, 1066–1081. [[CrossRef](#)] [[PubMed](#)]
23. Kato, N.; Nogawa, T.; Takita, R.; Kinugasa, K.; Kanai, M.; Uchiyama, M.; Osada, H.; Takahashi, S. Control of the stereochemical course of [4+2] cycloaddition during *trans*-decalin formation by Fsa2-family enzymes. *Angew. Chem. Int. Ed.* **2018**, *57*, 9754–9758. [[CrossRef](#)] [[PubMed](#)]
24. Fox Ramos, A.E.; Evanno, L.; Poupon, E.; Champy, P.; Beniddir, M.A. Natural products targeting strategies involving molecular networking: Different manners, one goal. *Nat. Prod. Rep.* **2019**, *36*, 960–980. [[CrossRef](#)] [[PubMed](#)]
25. Li, G.; Kusari, S.; Spiteller, M. Natural products containing ‘decalin’ motif in microorganisms. *Nat. Prod. Rep.* **2014**, *31*, 1175–1201. [[CrossRef](#)]

26. Jang, J.H.; Asami, Y.; Jang, J.P.; Kim, S.O.; Moon, D.O.; Shin, K.S.; Hashizume, D.; Muroi, M.; Saito, T.; Oh, H. Fusarisetin A, an acinar morphogenesis inhibitor from a soil fungus, *Fusarium* sp. FN080326. *J. Am. Chem. Soc.* **2011**, *133*, 6865–6867. [[CrossRef](#)]
27. Zhao, D.; Han, X.; Wang, D.; Liu, M.; Gou, J.; Peng, Y.; Liu, J.; Li, Y.; Cao, F.; Zhang, C. Bioactive 3-decalinoyltetramic acids derivatives from a marine-derived strain of the fungus *Fusarium equiseti* D39. *Front. Microbiol.* **2019**, *10*, 1285–1294. [[CrossRef](#)]
28. Yamada, T.; Tanaka, A.; Nehira, T.; Nishii, T.; Kikuchi, T. Altercrasins A–E, decalin derivatives, from a sea-urchin-derived *Alternaria* sp.: Isolation and structural analysis including stereochemistry. *Mar. Drugs* **2019**, *17*, 218. [[CrossRef](#)]
29. Liu, S.Z.; Yan, X.; Tang, X.X.; Lin, J.G.; Qiu, Y.K. New bis-alkenoic acid derivatives from a marine-derived fungus *Fusarium solani* H915. *Mar. Drugs* **2018**, *16*, 483. [[CrossRef](#)]
30. Kato, N.; Nogawa, T.; Hirota, H.; Jang, J.H.; Takahashi, S.; Ahn, J.S.; Osada, H. A new enzyme involved in the control of the stereochemistry in the decalin formation during equisetin biosynthesis. *Biochem. Biophys. Res. Commun.* **2015**, *460*, 210–215. [[CrossRef](#)]
31. Waddell, P.J.; Steel, M.A. General time-reversible distances with unequal rates across sites: Mixing  $\Gamma$  and inverse gaussian distributions with invariant sites. *Mol. Phylogenet. Evol.* **1997**, *8*, 398–414. [[CrossRef](#)]
32. Kumar, S.; Stecher, G.; Tamura, K. Mega7: Molecular evolutionary genetics analysis version 7.0 for bigger datasets. *Mol. Biol. Evol.* **2016**, *33*, 1870–1874. [[CrossRef](#)]
33. Wang, M.; Carver, J.J.; Phelan, V.V.; Sanchez, L.M.; Garg, N.; Peng, Y.; Nguyen, D.D.; Watrous, J.; Kapono, C.A.; Luzzatto-Knaan, T.; et al. Sharing and community curation of mass spectrometry data with Global Natural Products Social Molecular Networking. *Nat. Biotechnol.* **2016**, *34*, 828–837. [[CrossRef](#)]



© 2020 by the authors. Licensee MDPI, Basel, Switzerland. This article is an open access article distributed under the terms and conditions of the Creative Commons Attribution (CC BY) license (<http://creativecommons.org/licenses/by/4.0/>).

## Chapter 3

**Pyrenosetin D, A New Pentacyclic Decalinoyltetramic Acid Derivative from the Algicolous Fungus *Pyrenochaetopsis* sp. FVE-087**

## RESULTS

Article

# Pyrenosetin D, a New Pentacyclic Decalinoyltetramic Acid Derivative from the Algicolous Fungus *Pyrenochaetopsis* sp. FVE-087

Bicheng Fan<sup>1</sup>, Pradeep Dewapriya<sup>1</sup> , Fengjie Li<sup>1</sup> , Laura Grauso<sup>2</sup> , Martina Blümel<sup>1</sup> , Alfonso Mangoni<sup>3</sup>  and Deniz Tasdemir<sup>1,4,\*</sup> 

<sup>1</sup> GEOMAR Centre for Marine Biotechnology (GEOMAR-Biotech), Research Unit Marine Natural Products Chemistry, GEOMAR Helmholtz Centre for Ocean Research Kiel, Am Kiel-Kanal 44, 24106 Kiel, Germany; bfan@geomar.de (B.F.); pdewapriya@geomar.de (P.D.); fli@geomar.de (F.L.); mbluemel@geomar.de (M.B.)

<sup>2</sup> Dipartimento di Agraria, Università degli Studi di Napoli Federico II, via Università 100, 80055 Portici (NA), Italy; laura.grauso@unina.it

<sup>3</sup> Dipartimento di Farmacia, Università degli Studi di Napoli Federico II, via Domenico Montesano 49, 80131 Napoli, Italy; alfonso.mangoni@unina.it

<sup>4</sup> Faculty of Mathematics and Natural Sciences, Kiel University, Christian-Albrechts-Platz 4, 24118 Kiel, Germany

\* Correspondence: dtasdemir@geomar.de; Tel.: +49-431-600-4430

Received: 28 April 2020; Accepted: 24 May 2020; Published: 26 May 2020



**Abstract:** The fungal genus *Pyrenochaetopsis* is commonly found in soil, terrestrial, and marine environments, however, has received little attention as a source of bioactive secondary metabolites so far. In a recent work, we reported the isolation and characterization of three new anticancer decalinoyltetramic acid derivatives, pyrenosetins A–C, from the Baltic *Fucus vesiculosus*-derived endophytic fungus *Pyrenochaetopsis* sp. FVE-001. Herein we report a new pentacyclic decalinoylspirotetramic acid derivative, pyrenosetin D (**1**), along with two known decalin derivatives wakodecalines A (**2**) and B (**3**) from another endophytic strain *Pyrenochaetopsis* FVE-087 isolated from the same seaweed and showed anticancer activity in initial screenings. The chemical structures of the purified compounds were elucidated by comprehensive analysis of HR-ESIMS, FT-IR,  $[\alpha]_D$ , 1D and 2D NMR data coupled with DFT calculations of NMR parameters and optical rotation. Compounds **1–3** were evaluated for their anticancer and toxic potentials against the human malignant melanoma cell line (A-375) and the non-cancerous keratinocyte cell line (HaCaT). Pyrenosetin D (**1**) showed toxicity towards both A-375 and HaCaT cells with IC<sub>50</sub> values of 77.5 and 39.3  $\mu$ M, respectively, while **2** and **3** were inactive. This is the third chemical study performed on the fungal genus *Pyrenochaetopsis* and the first report of a pentacyclic decalin ring system from the fungal genus *Pyrenochaetopsis*.

**Keywords:** *Pyrenochaetopsis*; pyrenosetin; marine fungus; decalinoyltetramic acid; *Fucus vesiculosus*; anticancer

## 1. Introduction

Seaweeds harbor diverse microbial communities, such as bacteria, fungi, bacteriophage, and viruses, forming a complex holobiont [1–3]. Endophytic fungi are one of the predominant microbial communities associated with seaweeds and are gaining growing interest as a source of small molecule natural products with high chemical diversity and wide-ranging bioactivity profiles [4]. Over the past decades, several structurally unique metabolites from different classes of natural products, such as polyketides [5], terpenes [6], steroids [7], non-ribosomal peptides [8], and alkaloids [9] were

reported from seaweed-derived (algicolous) fungi, with multiple bioactivities, including anticancer [7], antibiotic [9], and antioxidant [10].

Fungal metabolites with a 'decalin ring system' represent a large group of architecturally complex structural scaffolds [11]. The decalin ring system is usually substituted with, e.g., a terpene side chain [12] or  $\gamma$ -lactam [13], pyrone [14], diene [15], pyrrolizidine [16], and tetramic acid rings [17]. Decalin derivatives are also intriguing for their remarkable biological activities, including anticancer [18], antiviral [19], and antimicrobial [20]. So far, several decalin derivatives with multiple ring systems (e.g., tricyclic ring system [21]) or rare functional groups (e.g., deoxytetramic acid [17]) have been isolated from different algicolous fungi. As an example, *Ascochyta salicorniae*, an endophytic fungus derived from the green seaweed *Ulva* sp. yielded ascosalipyrrolidinones A and B, unusual decalin derivatives with an ether function on the terminal tetramic acid [17]. Ascosalipyrrolidinone A is a potent antiplasmodial agent that inhibits both the drug-resistant and the drug-sensitive *Plasmodium falciparum* strains K<sub>1</sub> and NF<sub>54</sub> (IC<sub>50</sub> 736 and 378 ng/mL, respectively). It also shows antimicrobial and tyrosine kinase inhibiting activities [17].

As part of our on-going project aiming to investigate the cultivable mycobiome of seaweeds, we have previously isolated 55 epiphytic and endophytic fungi from the Baltic brown alga *Fucus vesiculosus* [22]. In-depth chemical investigation of the endophytic fungus *Pyrenochaetopsis* sp. FVE-001 by using a bioactivity-based molecular networking approach led to the rapid isolation and characterization of three new decalinoylspirotetramic acid derivatives pyrenosetins A–C and the known decalin phomasetin [23]. All four compounds showed notable activity against human malignant melanoma cancer cells (A-375) [23]. In the continuation of our search for new anticancer metabolites from *Fucus vesiculosus*-associated fungi, a second strain of *Pyrenochaetopsis* sp. FVE-087 attracted our attention. In preliminary screenings, the crude extract of this strain also exerted potent anticancer activity [22]. Chemical work-up of this endophyte monitored by anticancer activity against the same melanoma cell line (A-375) resulted in the purification of a new pentacyclic decalinoyltetramic acid derivative, pyrenosetin D (1), along with two known decalins wakodecaline A (2) and wakodecaline B (3). In this study, we report the isolation, detailed structure elucidation, the anticancer activity, and the toxicity of compounds 1–3.

## 2. Results

### 2.1. Strain Identification and Cultivation

The endophytic fungus FVE-087 (GenBank accession number: MH881502) was isolated from the inner thallus of the brown alga *Fucus vesiculosus* collected at Kiel Fjord (Baltic Sea, Germany). The initial taxonomic study of FVE-087 revealed its taxonomical identity at order level, i.e., Pleosporales [22]. The re-amplification of ITS1-5.8S rRNA gene-ITS2 region yielded a longer 408 bp fragment, which enabled its identification at the genus level. A phylogenetic tree was constructed using the nucleotide sequences for related strains (obtained from NCBI database) including the previously identified *Pyrenochaetopsis* sp. FVE-001 from the same seaweed, indicating that the fungus FVE-087 was a close relative of the co-existing fungus *Pyrenochaetopsis* sp. FVE-001. Based on the phylogenetic tree analysis (Figure S1), the strain FVE-087 was confirmed to be a *Pyrenochaetopsis* sp. The fungus FVE-087 was cultivated in the same manner as described in our previous study [23], i.e., in liquid potato dextrose medium (PDM) at 22 °C for 14 days under continuous shaking.

### 2.2. Extraction, Bioactivity Testing, and Isolation

The culture broth (24 L) was extracted with EtOAc. The crude EtOAc extract of the fungus was subjected to a modified Kupchan partitioning scheme to yield *n*-hexane (KH), CHCl<sub>3</sub> (KC), and aqueous MeOH (KM) subextracts. All three subextracts were tested for their activity against five cancer cell lines; malignant melanoma (A-375), lung carcinoma (A-549), colorectal adenocarcinoma (HT-29), colorectal carcinoma (HCT-116), and breast cancer cell line (MDA-MB-231). The KC subextract showed the



highest inhibitory activity against all tested cell lines (>84% cell growth inhibition at 100  $\mu\text{g}/\text{mL}$ ) and was selected for a detailed chemical work-up. The KC subextract was fractionated on a C18 SPE cartridge using a 10% gradient of MeOH in water. This yielded 11 subfractions, and the anticancer activity was tracked to late fractions 7–9 (Table S6). Reversed-phase HPLC purification of the fractions 7 and 8, monitored by the anticancer activity against malignant melanoma (A-375) cells, afforded compounds 1–3 (Figure 1).

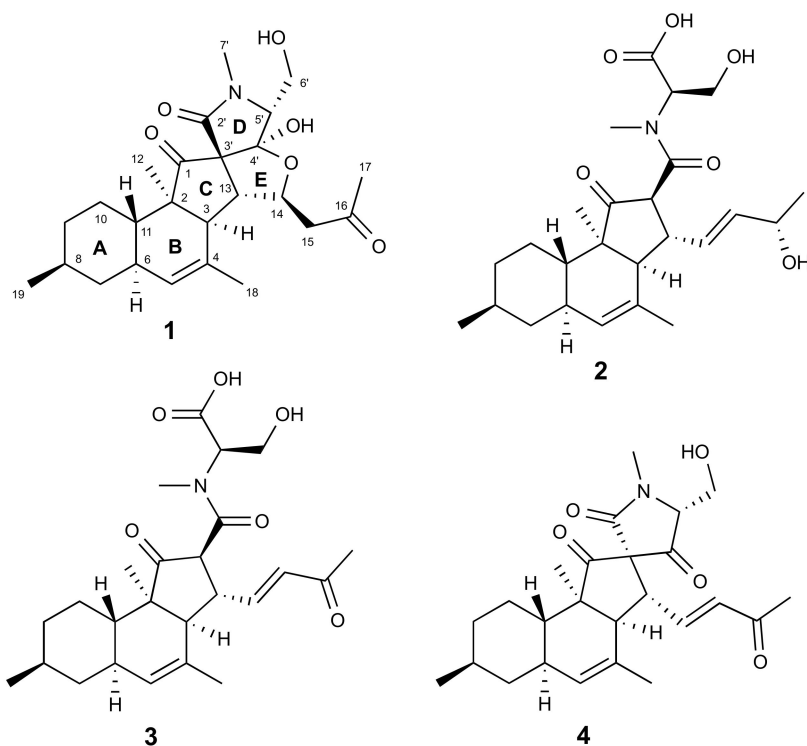


**Figure 1.** Chemical structures of compounds 1–4.

### 2.3. Structure Elucidation

Compound 1 was obtained as a colorless oil. The molecular formula  $\text{C}_{25}\text{H}_{35}\text{NO}_6$  that required nine degrees of unsaturation (DoU) was assigned based on the HR-ESIMS spectrum of 1 (Figure S10). The FT-IR spectrum (Figure S11) indicated the presence of hydroxyl ( $\nu_{\text{max}}$  3226–3560  $\text{cm}^{-1}$ ), carbonyl ( $\nu_{\text{max}}$  1679 and 1734  $\text{cm}^{-1}$ ) and aliphatic ether ( $\nu_{\text{max}}$  1064 and 1159  $\text{cm}^{-1}$ ) functions. Comprehensive analysis of the  $^1\text{H}$  NMR data in conjunction with the DEPT-HSQC spectrum ( $\text{CD}_3\text{CN}$ , Table 1, Figures S4 and S6) revealed the presence of five methyl groups, including one secondary ( $\text{H}_3$ -19,  $\delta_{\text{H}}$  0.89, d,  $J = 6.6$  Hz), one tertiary ( $\text{H}_3$ -12,  $\delta_{\text{H}}$  0.88, s), one olefinic ( $\text{H}_3$ -18,  $\delta_{\text{H}}$  1.76, br s), one methylketone ( $\text{H}_3$ -17,  $\delta_{\text{H}}$  2.09, s), plus an *N*-methyl ( $\text{H}_3$ -7',  $\delta_{\text{H}}$  2.86, s) signal. In addition, also observed were five pairs of diastereotopic methylene protons, namely  $\text{H}_2$ -7 ( $\delta_{\text{H}}$  0.75, q,  $J = 11.9$  Hz and 1.82, m),  $\text{H}_2$ -9 ( $\delta_{\text{H}}$  0.83, dq,  $J = 2.7, 12.6$  Hz and 1.71, m),  $\text{H}_2$ -10 ( $\delta_{\text{H}}$  1.02, m and 1.29, dq,  $J = 12.9, 3.0$  Hz),  $\text{H}_2$ -15 ( $\delta_{\text{H}}$  2.52, dd,  $J = 16.2, 9.4$  Hz and  $\delta_{\text{H}}$  2.70, dd,  $J = 16.2, 3.1$  Hz), and the oxymethylene protons of  $\text{H}_2$ -6' ( $\delta_{\text{H}}$  3.79, dd,  $J = 11.6, 6.4$  Hz and  $\delta_{\text{H}}$  3.86, dd,  $J = 11.6, 4.1$  Hz). The  $^1\text{H}$  NMR spectrum also comprised signals belonging to eight methine protons; this included six aliphatic methine protons which were assigned to H-3 ( $\delta_{\text{H}}$  2.32, d,  $J = 10.0$  Hz), H-6 ( $\delta_{\text{H}}$  1.84, m), H-8 (1.44, m), H-11 (1.48, ddd,  $J = 11.8, 10.5, 2.7$  Hz), H-13 ( $\delta_{\text{H}}$  2.67, dd,  $J = 10.1, 3.4$  Hz), H-5' ( $\delta_{\text{H}}$  3.44, dd,  $J = 7.0, 4.1$  Hz), plus one olefinic methine proton that appeared as a broad singlet at  $\delta_{\text{H}}$  5.25 (H-5) and an oxymethine proton that resonated at  $\delta_{\text{H}}$  4.90 (H-14, dt,  $J = 9.3, 3.3$  Hz) (Table 1). The  $^{13}\text{C}$  NMR spectrum of 1 (Table 1, Figure S5) contained 25 signals accounting for three carbonyls  $\delta_{\text{C}}$  170.2 (C-2'), 206.8 (C-16), and 213.2 (C-1), and two olefinic carbons at

$\delta_C$  128.0 (C-5), and 133.2 (C-4), accounting for four DoU. This indicated **1** to be a pentacyclic compound. Comparison of the NMR data of **1** with those of tetracyclic decalinoylspirotetramic acid derivatives pyrenosetins A–C [23] indicated close similarities. Thus, **1** was identified as a pyrenosetin-type decalinoylspirotetramic acid with an additional ring system.

**Table 1.**  $^1\text{H}$  NMR (600 MHz) and  $^{13}\text{C}$  NMR (150 MHz) data of compound **1** ( $\text{CD}_3\text{CN}$ ).

No.	<b>1</b>	
	$\delta_{\text{H}}$ , mult (J in Hz)	$\delta_{\text{C}}$
1	-	213.2
2	-	56.4
3	2.32, d (10.0)	54.8
4	-	133.2
5	5.25, br s	128.0
6	1.84, m	37.7
7	eq ax	42.9
	0.75, q (11.9)	
8	1.44, m	33.5
9	eq ax	36.0
	0.83, dq (2.7, 12.6)	
10	eq ax	25.8
	1.29, dq (12.9, 3.0)	
	1.02, m	
11	1.48, ddd (11.8, 10.5, 2.7)	37.9
12	0.88, s	14.2
13	2.67, dd (10.1, 3.4)	57.0
14	4.90, dt (9.3, 3.3)	83.7
15	a b	50.3
	2.70, dd (16.2, 3.1)	
	2.52, dd (16.2, 9.4)	
16	-	206.8
17	2.09, s	30.8
18	1.76, br s	23.2
19	0.89, d (6.6)	22.5
2'	-	170.2
3'	-	75.3
4'	-	110.3
5'	3.44, dd (7.0, 4.1)	68.3
6'	a b	60.4
	3.86, dd (11.6, 4.1)	
	3.79, dd (11.6, 6.4)	
7'	2.86, s	29.5

In order to identify the position of the fifth ring system and the complete planar structure of **1**, we undertook DQF-COSY and HMBC experiments. The  $^1\text{H}$ - $^1\text{H}$  COSY spectrum of **1** comprised three spin systems (a–c) (Figure 2A and Figure S7). The largest spin system (a) started with the olefinic proton H-5 that coupled with H-6, then included the methyl substituted cyclohexane moiety that terminated with the H-11. The latter proton was in turn coupled with H-6, while H<sub>3</sub>-19 coupled with H-8, completing the structure of the ring **A** with a secondary methyl group attached at C-8. Further detected in the COSY spectrum was a short spin system (b) that corresponded to a hydroxyethyl group (H-5' to H-6'). The final proton network (c) covered the protons of H-3, H-13, H-14, and H<sub>2</sub>-15 (Figure 2A and Figure S7).

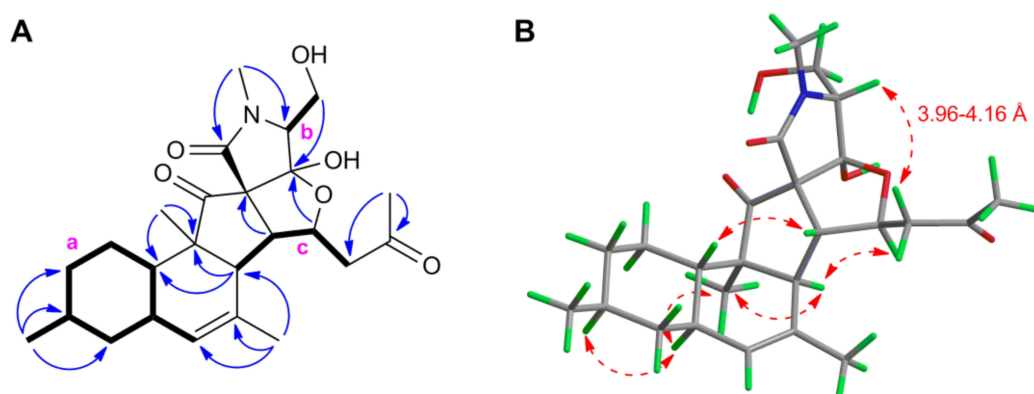


**Figure 2.** (A) Key COSY (**bold**) and HMBC (**blue**) correlations within **1**. **a–c**: Spin systems extracted from the COSY spectrum. (B) NOESY (**red**) correlations on the lowest-energy DFT conformer of **1**.

In-depth analysis of the  $^1\text{H}$ - $^{13}\text{C}$  HMBC data (Figure 2A and Figure S8) enabled to assemble the three COSY spin systems with quaternary carbons and heteroatoms, hence completing the full structure of **1**. Firstly, the position of the  $\text{H}_3$ -19 at C-8 (ring **A**) was further confirmed by the HMBC correlations between  $\text{H}_3$ -19 with C-7, C-8, and C-9. The ring **B** of the unsaturated decalin moiety was constructed on the basis of the HMBC cross-peaks observed from H-3 to C-2, C-4, C-5, and C-11, from H-5 to C-3 and C-11, and from the olefinic methyl group  $\text{H}_3$ -18 to C-3, C-4, and C-5. The tertiary methyl  $\text{H}_3$ -12 was assigned to C-2 based on the key HMBC correlations from  $\text{H}_3$ -12 to C-2, C-3, and C-11. Additional HMBC correlations between  $\text{H}_3$ -12/C-1, H-3/C-3', and H-13/C-3' confirmed the spiro (cyclopentanone) ring system **C** (Figure 2A). The ring **D** comprising of an *N*-methyl tetramic acid was built with the aid of the HMBC correlations between H-5'/C-2', H-5'/C-4', H-6'/C-4', H-6'/C-5',  $\text{H}_3$ -7'/C-2',  $\text{H}_3$ -7'/C-5'. The upfield chemical shift of C-4' ( $\delta_{\text{C}}$  110.3) in comparison to other pyrenosetins, such as pyrenosetin **C** (**4**) suggested the presence in **1** of an acetal or hemiacetal rather than a ketone function. The connection of the ring **D** at C-3' of the ring **C** was evident due to further HMBC cross-peak seen between H-5'/C-3'.

Pyrenosetins **A–C** bear a C-16 oxygenated butyl substitution with a double bond  $\Delta^{14(15)}$  in the side chain (attached at C-13) [23]. The comparison of the  $^1\text{H}$  and  $^{13}\text{C}$  NMR data of **1** from C-13 to C-15 (Table 1) with those of pyrenosetin **C** (**4**) [23] clearly showed that **1** lacks the double bond at C-14. Instead, the H-14 was converted to an oxymethine signal ( $\delta_{\text{H}}$  4.90) that showed a diagnostic HMBC coupling with C-4' (Figure 2A and Figure S8). This fact, in addition to above mentioned COSY correlations between H-13/H-14 and H-14/H<sub>2</sub>-15 confirmed the fifth tetrahydrofuran ring (**E**). Final HMBC correlations from  $\text{H}_3$ -17 to C-15 ( $\delta_{\text{C}}$  50.3) and C-16 ( $\delta_{\text{C}}$  206.8) completed the side chain that ended with a methylketone. Thus, the pentacyclic 2D structure of **1** was established as shown in Figure 1.

The relative configuration of the stereogenic centers within **1** was deduced based on NOESY correlations and coupling constant analysis (Figure 2B and Figure S9). The two large axial-axial couplings experienced by H-11 (ddd,  $J = 11.8, 10.5,$  and  $2.7$  Hz) established the *trans* junction between rings **A** and **B**. The observed NOESY correlations between H-3/ $\text{H}_3$ -12, H-3/H-14, H-6/H-8, H-6/ $\text{H}_3$ -12, and H-11/H-13 indicated the  $\alpha$ -orientation of H-3, H-6, H-8,  $\text{H}_3$ -12, H-14, and the  $\beta$ -orientation of H-11, H-13, and the  $\text{H}_3$ -19 methyl group. This left three stereogenic centers (C-3', C-4', and C-5') in the tetramic acid moiety to be assigned.

Assignment of configuration at C-3' and C-4' was based on the high geometric strain of *trans*-5,5-fused ring systems, which are known to be less stable than their *cis* counterparts by more than 6 kcal/mol [24]. As the hemiacetal function at C-4' would readily open in case of steric strain, the possibility of strained *trans* junctions between rings **C** and **E** and/or between rings **E** and **D** was ruled out, and the requirement of *cis* junctions between rings **C**, **E**, and **D** defined configurations at

C-3' and C-4' as depicted in structure 1. The configuration at C-5' was suggested by a very weak NOE correlation between H-5' and H-15b ( $\delta_{\text{H}}$  2.52) (Figure 2B).

As the determined configuration at C-3' was opposite to that found in the other pyrenosetin analogues (including compound 4), and configuration at C-5' was only based on a single weak NOE correlation, the structure of 1 was validated using DFT prediction of NMR parameters. Compound 1, its epimer at C-3', namely 3'-*epi*-1 (which has also opposite configuration at C-4', to keep the *cis* junction between rings D and E), and its epimer at C-5', namely 5'-*epi*-1 were considered for calculations (see Supplementary Figure S2 for structures, and Materials and Methods Section for details on computational methods). After a molecular dynamics-based conformational search, conformers were optimized at the B3LYP/TZVP/SMD level; then,  $^1\text{H}$  and  $^{13}\text{C}$  isotropic shieldings were calculated, respectively, at the WP04/aug-cc-pVDZ/PCM and mPW1PW91/6-311+G(2d,p) levels of theory, and scaled to chemical shifts using the linear regression method [25]. Calculations on 3'-*epi*-1 were soon stopped, because optimized conformers showed energies constantly higher than 1 by more than 10 kcal/mol (as expected, because of the strained *trans* junction between rings C and E) and root-mean-square deviations (RMSD) of  $^{13}\text{C}$  NMR chemical shifts of rings C, D, and E constantly over 6 ppm. In contrast, chemical shifts calculated for compound 1 were in excellent agreement with the experimental values (RMSD of 1.66 ppm for  $^{13}\text{C}$  and 0.076 for  $^1\text{H}$ ). While this results provided solid support to the overall structure of 1 and to configurations at C-3' and C-4', they did not support the assignment of the configuration at C-5', because chemical shifts of 5'-*epi*-1 also showed a comparable agreement with the experiment (RMSD of 1.69 ppm for  $^{13}\text{C}$  and 0.077 ppm for  $^1\text{H}$ ) (Figure S3). Even restricting the comparison to atoms of ring D and/or using DP4+ analysis [26], no clear-cut answer about configuration at C-5' could be obtained from the predicted chemical shifts. Therefore, coupling constants were examined.

Analysis of structures 1 and 5'-*epi*-1 showed that the main difference between the two compounds was expected in the  $^1\text{H}$ - $^{13}\text{C}$  coupling constants of H-5'. In particular, the coupling constant between H-5' and C-2' was calculated as 4.3 Hz for 1 and 0.6 Hz for 5'-*epi*-1 (Table S5). When not measured directly,  $^1\text{H}$ - $^{13}\text{C}$  coupling constants can be estimated from the intensity of the corresponding HMBC peaks, an intense peak indicating a relatively large  $J_{\text{CH}}$  [27]. The prominent correlation peak observed between H-5' and C-2' was not consistent with the small 0.6 Hz coupling constant predicted for 5'-*epi*-1, and conclusively determined the relative stereochemistry of pyrenosetin D as in structure 1. Finally, the observed weak NOE correlation between H-5 and H-15b was in good agreement with the distance between 3.96 and 4.16 Å of these protons measured for the DFT optimized conformers of 1 (Figure 2B).

The absolute configuration of compound 1 was determined on the basis of its predicted optical rotation (OR). DFT prediction of OR is a valuable, although not as general, alternative to ECD for determining the absolute configuration of natural products, and can be reliably used for this purpose provided that (i) the magnitude of the measured OR is not close to zero and (ii) the sign of the calculated OR is the same for all, or at least for most conformers [28]. The OR of compound 1 was predicted at the B3LYP/TZVP/PCM(MeOH) level of theory; the calculated  $[\alpha]_{\text{D}}$  (as the Boltzmann average of individual conformers) was -104, compared to the experimental value -56. In addition, the OR values calculated for individual conformers were all negative, and with similar magnitude. These results strongly supported the absolute configuration of pyrenosetin D as shown in Figure 1.

The known compounds 2 and 3 were identified as wakodecalines A and B (Figure 1), respectively, based on their HR-ESIMS and MS/MS data, plus by comparison of their 1D/2D NMR and  $[\alpha]_{\text{D}}$  data with those reported in the literature [29].

#### 2.4. Bioactivity Tests

Due to the limited availability, compounds 1–3 were tested for their inhibitory activity against only one cancer cell line, i.e., the human malignant melanoma cell line (A-375). The general toxicity of the isolated metabolites was assessed against the human keratinocyte cells (HaCaT). Compound 1 exhibited moderate anticancer activity against the A-375 cells ( $\text{IC}_{50}$  value 77.5  $\mu\text{M}$ ), but it was also

toxic towards the HaCaT cells ( $IC_{50}$  value of 39.3  $\mu M$ ). The known compounds **2** and **3** did not exert anticancer or toxic effects, even at the highest test concentration of 200  $\mu M$ .

### 3. Discussion

*Pyrenochaetopsis* is a ubiquitous fungal genus found in both terrestrial and marine environments [30,31]. However, the members of this genus have remained almost fully unexplored for their bioactive secondary metabolites. To our knowledge, the very first chemical study was published in 2017 by Nogawa et al. on a *Pyrenochaetopsis* sp. isolated from a soil sample collected in Japan [29]. This work reported wakodecalines A, B, two new tricyclic decalin derivatives with a spiro pentanone ring (C) and *N*-methylated terminal serine moiety as well as phomasetin, a known decalin compound with a terminal tetramic acid function [29]. The lack of any other investigation in the literature on chemical constituents or biological activity has initiated our interest into this unexplored fungal taxon. In a very recent study, we demonstrated that, when cultured in liquid potato dextrose medium, the algicolous *Pyrenochaetopsis* sp. FVE-001 produces pyrenosetins A–C, new tetracyclic decalin derivatives with good activity against malignant melanoma cells (A-375) [23]. In addition, also isolated and identified from this fungus was the known compound phomasetin [23].

The ‘decalin’ moiety is a common structural motif in an array of marine fungal natural products [13,32,33]. It has been proposed that the decalin ring serves as a primary ring system or a scaffold to form polycyclic metabolites, with bicyclic decalins being the most common [11,13,32–35]. The chemical investigation of the marine sponge-derived fungus *Trichoderma harzianum* in 1993 led to the isolation of the first bicyclic decalin derivative trichoharzin isolated from a marine fungus. Trichoharzin contains rare alkyl and acyl moieties [36]. So far, more than 50 decalin derivatives have been reported from marine fungi [11,13,32–37]. The marine-derived bicyclic decalin derivatives often incorporate additional ring systems, e.g., pyrone [37], cyclopentanone [13], and tetramic acid [34] to lead tricyclic [35,37], tetracyclic [13], and pentacyclic scaffolds [34]. Of all, tetramic acid represents one of the most common substituents [13,34,38]. Pyrenosetins A–C, which we recently reported from *Pyrenochaetopsis* sp. FVE-001, an endophyte of the Baltic brown alga *Fucus vesiculosus*, represent one of the most complex tetracyclic decalinoylspirotetramic acids reported to date [23]. Such complex decalin scaffold is rare in fungi. To our knowledge, only a few fungal genera such as *Fusarium* sp. [34,39], *Alternaria* sp. [13], *Diaporthe* sp. [40], and *Pyrenochaetopsis* sp. [23] have been reported to produce such type of unique molecules. Decalinoyltetramic acid derivatives are also intriguing for remarkable biological activities they exhibit. For example, altercrasins D and E isolated from sea-urchin-derived *Alternaria* sp., have shown potent activity against murine P388 leukemia, human HL-60 leukemia, and murine L1210 leukemia cell lines [13]. However, most of the decalin derivatives suffer from poor selectivity, i.e., they also possess toxicity towards non-cancerous cells. This is a common characteristic of mycotoxins [34,41].

Our previous research on pyrenosetins highlighted the importance of the side chain attached at C-13 for their bioactivity [23]; both the anticancer activity and the general toxicity were significantly reduced with the oxidation of the C-16 hydroxyl group to a ketone. Notably, wakodecalines (**2** and **3**) that lack the terminal tetramic acid moiety did not show any bioactivity against A-375 cells, even at the highest test concentrations. This suggests that both side chain and the tetramic acid moiety are crucial for bioactivity of the decalin derivatives. Additionally, the presence of the additional tetrahydrofuran ring as found in **1** may be improving the activity against A-375 cells ( $IC_{50}$  77.5  $\mu M$ ) when compared to the anticancer activity of pyrenosetin C on the same cell line ( $IC_{50}$  140.3  $\mu M$ ) [23]. A previous study showed that fusarisetin A that possesses a tetrahydrofuran ring exhibits higher activity against the invasive breast cancer cell line MDA-MB-231 than its precursor equisetin [42].

In conclusion, a new cytotoxic pentacyclic decalinoylspirotetramic acid derivative, pyrenosetin D (**1**) and two known and non-toxic tricyclic metabolites, wakodecalines A (**2**) and B (**3**), were purified from the algicolous fungus *Pyrenochaetopsis* sp. To our knowledge, only fusarisetins that were isolated from *Fusarium* sp. possess somehow similar pentacyclic skeleton [34,39]. This is the third study

performed on the chemical constituents of the fungal genus *Pyrenochaetopsis* and the first report of a pentacyclic decalin ring system from *Pyrenochaetopsis* species. Further investigation of the anticancer activity, selectivity, and mechanism of cytotoxic action of our metabolites might expand our knowledge of the structure–activity relationship of decalinoyltetramic acid derivatives.

#### 4. Materials and Methods

##### 4.1. General Procedures

FT-IR spectra were recorded on a PerkinElmer Spectrum Two FT-IR spectrometer (PerkinElmer, Boston, MA, USA). Specific rotation ( $[\alpha]_D$ ) values were measured in MeOH on a Jasco P-2000 polarimeter (Jasco, Pfungstadt, Germany). NMR data were recorded on a Bruker AV 600 spectrometer (600 and 150 MHz for  $^1\text{H}$  and  $^{13}\text{C}$  NMR, respectively, Bruker®, Billerica, MA, USA). The residual solvent signals were detected in NMR spectra as internal references:  $\delta_{\text{H}}$  1.94/ $\delta_{\text{C}}$  118.3 and  $\delta_{\text{C}}$  1.3 ( $\text{CD}_3\text{CN}$ ). 4-Dimethyl-4-silapentane-1-sulfonic acid (DSS) was used as an internal standard. HRESIMS was recorded on a microTOF II-high-performance TOF-MS system (Bruker®, Billerica, MA, USA) equipped with an electrospray ionization source. Solid-phase extraction (SPE) was performed on a C18 cartridge (50  $\mu\text{m}$ , 65 Å, Phenomenex, 411 Madrid Avenue, Torrance, CA, USA). HPLC separations were performed on a VWR Hitachi Chromaster system (VWR International, Allison Park, PA, USA) consisting of a 5430 diode array detector (VWR International, Allison Park, PA, USA), a 5310 column oven, a 5260 autosampler, and a 5110 pump. The eluents used for HPLC separations were milli Q water (A) and MeCN (B). Routine HPLC separations were performed on a semi-preparative C18 monolithic column (Onyx, 100  $\times$  10 mm, Phenomenex, Torrance, CA, USA) and an analytical synergi polar-RP 80 Å LC column (250  $\times$  4.6 mm, Phenomenex, Torrance, CA, USA). The organic solvents used for chemical analysis were of HPLC grade (ITW Reagents, Germany). An in-house Arium® Water Purification Systems (Sartorius, Germany) was used for the preparation of milli Q water. Solvents used in extraction, Kupchan partition, and purification (including EtOAc, *n*-hexane, MeOH and MeCN) were purchased from VWR International GmbH (Hannover, Germany). Potato extract and dextrose that used for fungal cultivation were purchased from Sigma-Aldrich (Schnellendorf, Germany) and Merck (Darmstadt, Germany), respectively. Agar was purchased from Applichem (Darmstadt, Germany).

##### 4.2. Strain Identification and Cultivation

The fungal strain *Pyrenochaetopsis* sp. FVE-087 (GenBank accession number: MH881502) was obtained from *Fucus vesiculosus* specimens that were collected in Falckenstein Beach (54°23'22.6'' N, 10°11'26.4'' E), Kiel Fjord, Baltic Sea, in December 2015, Germany [22]. The fungus was identified by morphological observation, analysis of the ITS1-5.8S rRNA gene-ITS2 region and by building a phylogenetic tree with 14 related strains including the *Pyrenochaetopsis* sp. FVE-001, using the method described in our previous work [23]. The initial cultures were maintained on potato dextrose agar plates (PDA: potato extract 4 g, dextrose 20 g, agar 15g for 1 L, pH 5.6). After 3 days of pre-cultivation, pieces of mycelia were cut into small segments and aseptically inoculated into an Erlenmeyer flask (300 mL) that contained 100 mL of potato dextrose broth media (PDM: potato extract 4 g, dextrose 20 g for 1 L; pH 5.6). After 7 days inoculation, 1 mL liquid seed was added into Erlenmeyer flasks (2 L), each containing 800 mL PDM. A 24 L culture broth was fermented at 22 °C for 14 days on a rotary shaker at 120 rpm.

##### 4.3. Extraction and Isolation

The culture broth was partitioned against the same volume of EtOAc twice at room temperature. The EtOAc phase was evaporated to dryness under reduced pressure to afford 17.64 g yellow oily extract. The extract was subjected to a modified Kupchan partition scheme to yield three subextracts, *n*-hexane (KH, 6.93 g),  $\text{CHCl}_3$  (KC, 4.57 g), and aqueous MeOH (KM, 440.5 mg). All three subextracts were tested for their bioactivity against five cancer cell lines and non-cancerous cell line HaCaT. The KC

subextract showed high anticancer bioactivity against all five cancer cell lines (>84% inhibition rate at 100 µg/mL) and was fractionated on a C18-SPE column eluting with 10% stepwise gradient of MeOH in water (0–100%) to afford 11 fractions (F0–F10). Anticancer bioactivity was tracked to fractions F7–F9 (Table S6). The fraction 7 (F7, 138 mg) was subjected to semi-preparative RP–HPLC equipped with an Onyx monolithic C18 column. Elution with a gradient MeCN:H<sub>2</sub>O mixture (25–35% MeCN over 30 min, flow 3.0 mL/min) yielded eight subfractions (F7-1 to F7-8). The F7-7 (10.8 mg) was further purified by RP–HPLC on an analytical synergi polar-RP 80 Å column eluting with MeCN:H<sub>2</sub>O (52% isocratic MeCN over 19 min, flow 1.0 mL/min) to yield wakodecaline B (**3**, 2.4 mg, *t<sub>R</sub>* 8.8 min) and pyrenosetin D (**1**, 1.2 mg, *t<sub>R</sub>* 10.3 min). The subfraction 8 (F8, 369.6 mg) was chromatographed by RP–HPLC equipped with Onyx monolithic C18 column using MeCN:H<sub>2</sub>O mixtures (40% isocratic MeCN over 28 min and gradual increase to 60% MeCN by 40 min, flow 3.0 mL/min) to yield 14 subfractions (F8-1 to 14). Wakodecaline A (**2**) was tracked to F8-3 (7 mg). This fraction was subjected to RP–HPLC on an analytical synergi polar-RP 80 Å LC column using an isocratic mixture of MeCN:H<sub>2</sub>O (45:55) (flow 1.0 mL/min) to yield wakodecaline A (**2**, 2.9 mg, *t<sub>R</sub>* 9.5 min).

*Pyrenosetin D* (**1**): Colorless oil;  $[\alpha]_D^{20}$   $-56$  (*c* 0.10, MeOH); IR (oil)  $\nu_{\max}$  3226–3560, 2947, 2921, 1734, 1679, 1460, 1406, 1377, 1159, 1064  $\text{cm}^{-1}$ . <sup>1</sup>H NMR (CD<sub>3</sub>CN, 600 MHz) and <sup>13</sup>C NMR (CD<sub>3</sub>CN, 150 MHz) are shown in Table 1; HR-ESIMS found *m/z* 446.2520 [M + H]<sup>+</sup>, C<sub>25</sub>H<sub>36</sub>NO<sub>6</sub>, calculated for 446.2537.

#### 4.4. Computational Details

Conformational search for **1** and 5′-*epi*-**1** was based on a 10-ns molecular dynamics (MD) simulation at 600 K as previously described [43]. The MD simulation generated 101 and 102 different conformers for **1** and 5′-*epi*-**1**, respectively, within 5 kcal/mol from the lowest energy conformer. Optimizations of geometries from MD were performed using density functional theory (DFT) with the Gaussian 16 program [44], the B3LYP functional, the 6-31G(d,p) basis set, and the SMD model for the solvent, ACN. This resulted in 15 and 17 conformers for **1** and 5′-*epi*-**1**, respectively, within 3 kcal/mol from the lowest energy conformer. Finally, these conformers were further optimized at the B3LYP/TZVP/SMD level of theory, giving a final set of 10 significantly populated (population > 1% at 298 K) conformers for **1** and 11 significantly populated conformers for 5′-*epi*-**1**. Vibrational frequency analysis revealed no imaginary frequencies, confirming that all conformers were in a true energy minimum. The Cartesian coordinates and relative energies of the conformers are reported in Tables S1 and S2. These conformational ensembles were used for all the subsequent calculations.

NMR isotropic shieldings of **1** and 5′-*epi*-**1** were calculated using WP04/aug-cc-pVDZ/PCM for <sup>1</sup>H and mPW1PW91/6-311+G(2d,p) for <sup>13</sup>C, which have been shown to be most accurate levels of theory, among those tested, for NMR data acquired in CD<sub>3</sub>CN [45]. Average shieldings were obtained by Boltzmann statistics based on internal energies of conformers. Finally, shieldings were scaled to chemical shifts using linear regression [25]. The results are reported in Tables S3 and S4. Coupling constants were calculated at the B3LYP/6-31G(d,p) level and using the keyword "mixed", which augments the basis set for the calculation of the Fermi Contact term, and averaged by Boltzmann statistics. The results are reported in Table S4.

Optical rotations of DFT-optimized conformer of **1** were calculated using TDDFT at the B3LYP/TZVP/PCM(MeOH) level; the results can be found in Table S1. The Boltzmann mean of individual optical rotations gave  $[\alpha]_D = -105$ .

#### 4.5. Biological Assays

The bioactivity tests were performed as described previously [23]. The crude extract, the subextracts and the SPE fractions of the KC subextract were tested in vitro against five human cancer cell lines: colorectal adenocarcinoma cell line HT-29 (DSMZ, Braunschweig, Germany), malignant melanoma cell line A-375 (CLS, Eppelheim, Germany), colon cancer cell line HCT-116 (DSMZ, Braunschweig, Germany), lung carcinoma cell line A-549 (CLS, Eppelheim, Germany), human breast cancer line MDA-MB-231 (CLS, Eppelheim, Germany), as well as for the non-cancerous human keratinocyte

line HaCaT (CLS, Eppelheim, Germany) at a concentration of 100 µg/mL. The bioactivity of the extracts was evaluated by monitoring the metabolic activity using the CellTiterBlue Cell Viability Assay (Promega, Mannheim, Germany). HT-29 and HaCaT cells were cultivated in RPMI medium, A-549 and MDA-MB-231 cells in DMEM:Ham's F12 medium (1:1) supplemented with 15mM HEPES and A-375 and HCT-116 cells in DMEM medium supplemented with 4.5 g/L D-Glucose and 110 mg/L sodium pyruvate. All media were supplemented with L-glutamine, 10% fetal bovine serum, 100 U/mL penicillin, and 100 mg/mL streptomycin. The cultures were maintained at 37 °C under a humidified atmosphere and 5% CO<sub>2</sub>. The cell lines were transferred every 3 or 4 days. For the experimental procedure, the cells were seeded in 96-well plates at a concentration of 10,000 cells per well. A stock solution of 40 mg/mL in DMSO was prepared for each extract. After 24 h incubation, the medium was removed from the cells and 100 µL fresh medium containing the test samples was added. Each sample was prepared in duplicate once. Doxorubicin as a standard therapeutic drug was used as a positive control, 0.5% DMSO and growth media were used as negative controls. Following compound addition, plates were cultured at 37 °C for 24 h. Afterward, the assay was performed according to the manufacturer's instructions and measured using the microplate reader Tecan Infinite M200 at excitation 560 nm and emission of 590 nm. For determination of IC<sub>50</sub> values, a dilution series of the extracts were prepared and tested, as described before for the crude extract. The IC<sub>50</sub> values were calculated by Excel as the concentration that shows 50% inhibition of the viability based on a negative control (no compound) and compared with the positive control (doxorubicin).

**Supplementary Materials:** The following are available online at <http://www.mdpi.com/1660-3397/18/6/281/s1>; NMR, HRESIMS, and FT-IR spectra of compound 1. Tables with detailed information of computational results.

**Author Contributions:** Design of the work, D.T. and B.F.; extraction, purifications of compounds, B.F.; data analysis, B.F., F.L., P.D. and D.T.; computational studies, L.G. and A.M.; strain identification M.B. and B.F.; writing the original manuscript, B.F., P.D., D.T.; supervision, D.T. All authors have read and agreed to the published version of the manuscript.

**Funding:** B.F. is the recipient of a China Scholarship Council Ph.D. scholarship. A.M was supported by Regione Campania, PO FESR 2014-2020, O.S. 1.2, Project "Campania Oncoterapie" No. B61G18000470007.

**Acknowledgments:** We are grateful to Arlette Wenzel-Storjohann and Jana Heumann for performing anticancer assays. We acknowledge financial support by DFG within the funding programm Open Access Publizieren.

**Conflicts of Interest:** The authors declare no conflict of interest.

## References

1. Flewelling, A.J.; Johnson, J.A.; Gray, C.A. Isolation and bioassay screening of fungal endophytes from North Atlantic marine macroalgae. *Bot. Mar.* **2013**, *56*, 287–297. [[CrossRef](#)]
2. Zuccaro, A.; Schoch, C.L.; Spatafora, J.W.; Kohlmeyer, J.; Draeger, S.; Mitchell, J.I. Detection and identification of fungi intimately associated with the brown seaweed *Fucus serratus*. *Appl. Environ. Microbiol.* **2008**, *74*, 931–941. [[CrossRef](#)] [[PubMed](#)]
3. Egan, S.; Harder, T.; Burke, C.; Steinberg, P.; Kjelleberg, S.; Thomas, T. The seaweed holobiont: Understanding seaweed–bacteria interactions. *FEMS Microbiol. Rev.* **2013**, *37*, 462–476. [[CrossRef](#)] [[PubMed](#)]
4. Zhang, P.; Li, X.; Wang, B.-G. Secondary metabolites from the marine algal-derived endophytic fungi: Chemical diversity and biological activity. *Planta Med.* **2016**, *82*, 832–842. [[CrossRef](#)] [[PubMed](#)]
5. Son, B.W.; Choi, J.S.; Kim, J.C.; Nam, K.W.; Kim, D.-S.; Chung, H.Y.; Kang, J.S.; Choi, H.D. Parasitenone, a new epoxycyclohexenone related to gabosine from the marine-derived fungus *Aspergillus parasiticus*. *J. Nat. Prod.* **2002**, *65*, 794–795. [[CrossRef](#)] [[PubMed](#)]
6. Almeida, C.; Elsaedi, S.; Kehraus, S.; König, G.M. Novel bisabolane sesquiterpenes from the marine-derived fungus *Verticillium tenerum*. *Nat. Prod. Commun.* **2010**, *5*, 507–510. [[CrossRef](#)] [[PubMed](#)]
7. Cui, C.-M.; Li, X.-M.; Meng, L.; Li, C.-S.; Huang, C.-G.; Wang, B.-G. 7-Nor-ergosterolide, a pentalactone-containing norsteroid and related steroids from the marine-derived endophytic *Aspergillus ochraceus* EN-31. *J. Nat. Prod.* **2010**, *73*, 1780–1784. [[CrossRef](#)]
8. Komatsu, K.; Shigemori, H.; Kobayashi, J. Dictyonamides A and B, new peptides from marine-derived fungus. *J. Org. Chem.* **2001**, *66*, 6189–6192. [[CrossRef](#)]



9. Du, F.-Y.; Li, X.-M.; Li, C.-S.; Shang, Z.; Wang, B.-G. Cristatumins A–D, new indole alkaloids from the marine-derived endophytic fungus *Eurotium cristatum* EN-220. *Bioorg. Med. Chem. Lett.* **2012**, *22*, 4650–4653. [[CrossRef](#)]
10. Abdel-Lateff, A.; Klemke, C.; König, G.M.; Wright, A.D. Two new xanthone derivatives from the algicolous marine fungus *Wardomyces anomalus*. *J. Nat. Prod.* **2003**, *66*, 706–708. [[CrossRef](#)]
11. Li, G.; Kusari, S.; Spiteller, M. Natural products containing ‘decalin’ motif in microorganisms. *Nat. Prod. Rep.* **2014**, *31*, 1175–1201. [[CrossRef](#)] [[PubMed](#)]
12. Sobolevskaya, M.P.; Leshchenko, E.V.; Hoai, T.P.T.; Denisenko, V.A.; Dyshlovoy, S.A.; Kirichuk, N.N.; Khudyakova, Y.V.; Kim, N.Y.; Berdyshev, D.V.; Pislyagin, E.A.; et al. Pallidopenillines: Polyketides from the alga-derived fungus *Penicillium thomii* Maire KMM 4675. *J. Nat. Prod.* **2016**, *79*, 3031–3038. [[CrossRef](#)] [[PubMed](#)]
13. Yamada, T.; Tanaka, A.; Nehira, T.; Nishii, T.; Kikuchi, T. Altercrasins A–E, decalin derivatives, from a sea-urchin-derived *Alternaria* sp.: Isolation and structural analysis including stereochemistry. *Mar. Drugs* **2019**, *17*, 218. [[CrossRef](#)] [[PubMed](#)]
14. Jenkins, K.M.; Toske, S.G.; Jensen, P.R.; Fenical, W. Solanapyrones E–G, antialgal metabolites produced by a marine fungus. *Phytochemistry* **1998**, *49*, 2299–2304. [[CrossRef](#)]
15. Nguyen, H.P.; Zhang, D.; Lee, U.; Kang, J.S.; Choi, H.D.; Son, B.W. Dehydroxychlorofusarielin B, an antibacterial polyoxygenated decalin derivative from the marine-derived fungus *Aspergillus* sp. *J. Nat. Prod.* **2007**, *70*, 1188–1190. [[CrossRef](#)] [[PubMed](#)]
16. Nogawa, T.; Kawatani, M.; Uramoto, M.; Okano, A.; Aono, H.; Futamura, Y.; Koshino, H.; Takahashi, S.; Osada, H. Pyrrolizilactone, a new pyrrolizidinone metabolite produced by a fungus. *J. Antibiot.* **2013**, *66*, 621–623. [[CrossRef](#)]
17. Osterhage, C.; Kaminsky, R.; König, G.M.; Wright, A.D. Ascosalipyrrolidinone A, an antimicrobial alkaloid, from the obligate marine fungus *Ascochyta salicorniae*. *J. Org. Chem.* **2000**, *65*, 6412–6417. [[CrossRef](#)]
18. Yamada, T.; Mizutani, Y.; Umebayashi, Y.; Inno, N.; Kawashima, M.; Kikuchi, T.; Tanaka, R. Tandyukisin, a novel ketoaldehyde decalin derivative, produced by a marine sponge-derived *Trichoderma harzianum*. *Tetrahedron Lett.* **2014**, *55*, 662–664. [[CrossRef](#)]
19. Singh, S.B.; Zink, D.L.; Goetz, M.A.; Dombrowski, A.W.; Polishook, J.D.; Hazuda, D.J. Equisetin and a novel opposite stereochemical homolog phomasetin, two fungal metabolites as inhibitors of HIV-1 integrase. *Tetrahedron Lett.* **1998**, *39*, 2243–2246. [[CrossRef](#)]
20. Alfatafta, A.A.; Gloer, J.B.; Scott, J.A.; Malloch, D. Apiosporamide, a new antifungal agent from the coprophilous fungus *Apiospora montagnei*. *J. Nat. Prod.* **1994**, *57*, 1696–1702. [[CrossRef](#)]
21. Duong, T.-H.; Nguyen, H.-H.; Le, T.-T.; Tran, T.-N.; Sichaem, J.; Nguyen, T.-T.; Nguyen, T.-P.; Mai, D.-T.; Nguyen, H.-H.; Le, H.-D. Subnudatones A and B, new *trans*-decalin polyketides from the cultured lichen mycobionts of *Pseudopyrenula subnudata*. *Fitoterapia* **2020**, *142*, 104512–104526. [[CrossRef](#)]
22. Fan, B.; Parrot, D.; Blümel, M.; Labes, A.; Tasdemir, D. Influence of OSMAC-based cultivation in metabolome and anticancer activity of fungi associated with the brown alga *Fucus vesiculosus*. *Mar. Drugs* **2019**, *17*, 67. [[CrossRef](#)]
23. Fan, B.; Dewapriya, P.; Li, F.; Blümel, M.; Tasdemir, D. Pyrenosetins A–C, new decalinoylspirotetramic acid derivatives isolated by bioactivity-based molecular networking from the seaweed-derived fungus *Pyrenochaetopsis* sp. FVE-001. *Mar. Drugs* **2020**, *18*, 47. [[CrossRef](#)] [[PubMed](#)]
24. Carey, F.A.; Sundberg, R.J. *Advanced Organic Chemistry*, 3rd ed.; Plenum Press: New York, NY, USA, 1990; p. 158.
25. Moosmann, P.; Ueoka, R.; Grauso, L.; Mangoni, A.; Morinaka, B.I.; Gugger, M.; Piel, J. Cyanobacterial *ent*-sterol-like natural products from a deviated ubiquinone pathway. *Angew. Chem. Int. Ed. Engl.* **2017**, *56*, 4987–4990. [[CrossRef](#)]
26. Grimblat, N.; Zanardi, M.M.; Sarotti, A.M. Beyond DP4: An improved probability for the stereochemical assignment of isomeric compounds using quantum chemical calculations of NMR shifts. *J. Org. Chem.* **2015**, *80*, 12526–12534. [[CrossRef](#)] [[PubMed](#)]
27. Ciminiello, P.; Dell’Aversano, C.; Dello Iacovo, E.; Fattorusso, E.; Forino, M.; Grauso, L.; Tartaglione, L. Stereochemical studies on ovatoxin-a. *Chem. Eur. J.* **2012**, *18*, 16836–16843. [[CrossRef](#)]
28. Grauso, L.; Teta, R.; Esposito, G.; Menna, M.; Mangoni, A. Computational prediction of chiroptical properties in structure elucidation of natural products. *Nat. Prod. Rep.* **2019**, *36*, 1005–1030. [[CrossRef](#)] [[PubMed](#)]

29. Nogawa, T.; Kato, N.; Shimizu, T.; Okano, A.; Futamura, Y.; Takahashi, S.; Osada, H. Wakodecalines A and B, new decaline metabolites isolated from a fungus *Pyrenochaetopsis* sp. RK10-F058. *J. Antibiot.* **2017**, *71*, 123–128. [[CrossRef](#)] [[PubMed](#)]
30. De Gruyter, J.; Woudenberg, J.H.C.; Aveskamp, M.M.; Verkley, G.J.M.; Groenewald, J.Z.; Crous, P.W. Redisposition of *Phoma*-like anamorphs in Pleosporales. *Stud. Mycol.* **2013**, *75*, 1–36. [[CrossRef](#)]
31. De Gruyter, J.; Woudenberg, J.H.C.; Aveskamp, M.M.; Verkley, G.J.M.; Groenewald, J.Z.; Crous, P.W. Systematic reappraisal of species in *Phoma* section *Paraphoma*, *Pyrenochaeta* and *Pleurophoma*. *Mycologia* **2010**, *102*, 1066–1081. [[CrossRef](#)]
32. Klemke, C.; Kehraus, S.; Wright, A.D.; König, G.M. New secondary metabolites from the marine endophytic fungus *Apiospora montagnei*. *J. Nat. Prod.* **2004**, *67*, 1058–1063. [[CrossRef](#)] [[PubMed](#)]
33. Wu, B.; Wiese, J.; Labes, A.; Kramer, A.; Schmaljohann, R.; Imhoff, J.F. Lindgomycin, an unusual antibiotic polyketide from a marine fungus of the Lindgomycetaceae. *Mar. Drugs* **2015**, *13*, 4617–4632. [[CrossRef](#)] [[PubMed](#)]
34. Zhao, D.; Han, X.; Wang, D.; Liu, M.; Gou, J.; Peng, Y.; Liu, J.; Li, Y.; Cao, F.; Zhang, C. Bioactive 3-decalinoyltetramic acids derivatives from a marine-derived strain of the fungus *Fusarium equiseti* D39. *Front. Microbiol.* **2019**, *10*, 1285. [[CrossRef](#)]
35. Afiyatulloev, S.S.; Leshchenko, E.V.; Berdyshev, D.V.; Sobolevskaya, M.P.; Antonov, A.S.; Denisenko, V.A.; Popov, R.S.; Pivkin, M.V.; Udovenko, A.A.; Pisyagin, E.A.; et al. Zosteropenillines: Polyketides from the marine-derived fungus *Penicillium thomii*. *Mar. Drugs* **2017**, *15*, 46. [[CrossRef](#)] [[PubMed](#)]
36. Kobayashi, M.; Uehara, H.; Matsunami, K.; Aoki, S.; Kitagawa, I. Trichoharzin, a new polyketide produced by the imperfect fungus *Trichoderma harzianum* separated from the marine sponge *Micale cecilia*. *Tetrahedron Lett.* **1993**, *34*, 7925–7928. [[CrossRef](#)]
37. Ma, Y.; Li, J.; Huang, M.; Liu, L.; Wang, J.; Lin, Y. Six new polyketide decalin compounds from mangrove endophytic fungus *Penicillium aurantiogriseum* 328#. *Mar. Drugs* **2015**, *13*, 6306–6318. [[CrossRef](#)] [[PubMed](#)]
38. Yamada, T.; Kikuchi, T.; Tanaka, R. Altercrasin A, a novel decalin derivative with spirotetramic acid, produced by a sea urchin-derived *Alternaria* sp. *Tetrahedron Lett.* **2015**, *56*, 1229–1232. [[CrossRef](#)]
39. Jang, J.-H.; Asami, Y.; Jang, J.-P.; Kim, S.-O.; Moon, D.O.; Shin, K.-S.; Hashizume, D.; Muroi, M.; Saito, T.; Oh, H. Fusarisetin A, an acinar morphogenesis inhibitor from a soil fungus, *Fusarium* sp. FN080326. *J. Am. Chem. Soc.* **2011**, *133*, 6865–6867. [[CrossRef](#)]
40. Pornpakakul, S.; Roengsumran, S.; Deechangvipart, S.; Petsom, A.; Muangsin, N.; Ngamrojnavanich, N.; Sriubolmas, N.; Chaichit, N.; Ohta, T. Diaporthichalasin, a novel CYP3A4 inhibitor from an endophytic *Diaporthe* sp. *Tetrahedron Lett.* **2007**, *48*, 651–655. [[CrossRef](#)]
41. Pitt, J.L.; Miller, J.D. A concise history of mycotoxin research. *J. Agric. Food Chem.* **2017**, *65*, 7021–7033. [[CrossRef](#)]
42. Xu, J.; Caro-Diaz, E.J.E.; Lacoske, M.H.; Hung, C.-I.; Jamora, C.; Theodorakis, E.A. Fusarisetin A: Scalable total synthesis and related studies. *Chem. Sci.* **2012**, *3*, 3378–3386. [[CrossRef](#)] [[PubMed](#)]
43. Grauso, L.; Li, Y.; Scarpato, S.; Shulha, O.; Rárová, L.; Strnad, M.; Teta, R.; Mangoni, A.; Zidorn, C. Structure and conformation of zosteraphenols, tetracyclic diarylheptanoids from the seagrass *Zostera marina*: An NMR and DFT Study. *Org. Lett.* **2020**, *22*, 78–82. [[CrossRef](#)] [[PubMed](#)]
44. Frisch, M.J.; Trucks, G.W.; Schlegel, H.B.; Scuseria, G.E.; Robb, M.A.; Cheeseman, J.R.; Scalmani, G.; Barone, V.; Petersson, G.A.; Nakatsuji, H.; et al. *Gaussian 16. Revision C.01.*; Gaussian, Inc.: Wallingford, CT, USA, 2019.
45. Pierens, G.K. <sup>1</sup>H and <sup>13</sup>C NMR scaling factors for the calculation of chemical shifts in commonly used solvents using density functional theory. *J. Comput. Chem.* **2014**, *35*, 1388–1394. [[CrossRef](#)] [[PubMed](#)]



---

### III. DISCUSSION AND OUTLOOK

---



## 1. Discussion

Marine fungi are important microbial associates of various marine macroorganisms, including sponges, echinoderms, vertebrates, seagrasses and macroalgae (Abdel-Gawad *et al.*, 2014; Höller *et al.*, 2001; Li and Wang, 2009; Richards *et al.*, 2012; Wainwright *et al.*, 2018). Macroalgae contribute approximately one-third of all marine fungal isolates and hence constitute an important study object for marine fungal biodiversity and biodiscovery research (Balabanova *et al.*, 2018; Ji and Wang, 2016). With regard to *Fucus*, a key brown seaweed genus in Northern hemisphere coastal ecosystems, previous molecular and culture-based studies have contributed to understanding the fungal community associated to *F. serratus* (Zuccaro *et al.*, 2008; Zuccaro *et al.*, 2004). Further, molecular and metabolomic evidence (based on CARD-FISH and a comparative surface metabolome study) suggests a metabolically active fungal community associated to *F. vesiculosus* (Parrot *et al.*, 2019). However, the present study (Chapter 1) represents the first report of cultivable fungi associated with Baltic *F. vesiculosus* for anticancer biodiscovery. After publication of Chapter 1, another study was published examining the fungal community associated to *Fucus* sp. yielding 13 genera from 22 fungal isolates (Patyshakuliyeva *et al.*, 2020).

In this study, 55 fungal isolates were obtained from Baltic Sea *F. vesiculosus* belonging to 8 genera and 3 higher taxonomic levels (e.g. order level). Six fungal genera including *Acremonium*, *Gibellulopsis*, *Trichoderma*, *Emericellopsis*, *Wallemia* and *Cadophora* were exclusively isolated from *F. vesiculosus*, but not from seawater or sediment references. The genera *Acremonium*, *Gibellulopsis*, and *Trichoderma* are rather generalists and common in marine environments (Jones *et al.*, 2009). In the genus *Emericellopsis* two distinct ecological clades are known, one containing terrestrial isolates and the other consisting of predominantly marine representatives suggesting an adaptation to the marine habitat of the latter clade (Grum-Grzhimaylo *et al.*, 2013). All of them have been previously reported associated to *F. serratus* (Zuccaro *et al.*, 2008). The genus *Wallemia*, a cosmopolitan xerophilic fungus was previously isolated from soil, salts and seafloor (Oleinikova *et al.*, 2010; Zalar *et al.*, 2005) but not from macroalgae. Unlike the other isolates, which all belong to Ascomycota, *Wallemia* sp. is a basidiomycete (Zalar *et al.*, 2005). *Wallemia ichthyophaga* serves as a model halophilic fungus, so an adaptation to the marine environment is highly probable (Janja *et al.*, 2011). The genus *Cadophora* was previously isolated from the green alga *Enteromorpha* sp. (Almeida *et al.*, 2010) and also from other marine substrata (Rämä *et al.*, 2014). The genus *Cadophora* contains several terrestrial plant pathogens such as *C. malorum* or *C. luteo-olivacea*, but their role in the marine realm remains unknown (Rämä *et al.*, 2014). We therefore conclude that all obtained isolates from *F. vesiculosus* in this study represent facultative marine fungi. We did not obtain any obligate marine fungi, which may be due to the low number of isolates but also to the selection of a brackish environment like the Baltic Sea as a study site. Compared to fully marine conditions (35 psu), the Baltic Sea has a reduced salinity (15-18 psu in Kiel Bight) potentially promoting the presence of facultative marine fungi over obligately marine representatives.

Although some genera were only isolated from the alga, we do not regard them as specific to *F. vesiculosus*, because all have been reported from other marine environments including other macroalgae. A recently published study (Patyshakuliyeva *et al.*, 2020) also isolated *Penicillium* and *Trichoderma* sp. from a *Fucus* sp., but also detected fungi of the ascomycete genera *Cladosporium*, *Clonostachys*, *Rhizopus*, *Epicoccum*, *Aspergillus*, *Alternaria*, *Engyodontium*, *Exophiala* and the basidiomycete genera *Symmetrospora*, *Cryptococcus* and *Leucosporidium*, which could not be isolated in this study. *Vice versa*, Patyshakuliyeva *et al.* (2020) did not observe many genera isolated during our study. Different

## DISCUSSION AND OUTLOOK

isolation media, sampling season, salinity of the *Fucus* sp. habitat and a different algal species explain the observed differences, but also show that isolation-based studies reflect only a snapshot of the entire fungal community. A non-culture-based mycobiome study is needed to allow conclusive evidence on the entire fungal species inventory associated to *Fucus* sp. and potential host-specificity of *Fucus* associated fungi. In conclusion, our results (Chapter 1) suggest that Baltic Sea *F. vesiculosus* represents a promising resource for the isolation of facultative marine fungi.

Out of the 55 *Fucus*-derived isolates, 26 fungi were selected for a small-scale fermentation based on their genetic diversity and morphological differences. In order to stimulate the expression of silent BGCs and to enlarge chemical space, an OSMAC approach has been applied to these 26 fungal isolates. Cultivation media and culture regimes were varied with the aim to explore potential anticancer natural products. The observed *in vitro* anticancer bioactivity (IC<sub>50</sub> values < 100 µg/ml) of 10 (out of 26) strains against at least one cancer cell line under at least one culture condition underlines the importance of OSMAC for biodiscovery studies. Interestingly, all of these 10 strains were endophytes of *F. vesiculosus*. In contrast, none of the *Fucus*-epiphytes showed anticancer bioactivity when culture conditions were changed. A recent study on anticancer potential of Indian algal endophytes showed similar patterns (Kamat *et al.*, 2020). As reviewed by Ji and Wang, algal endophytes appeared to be more prolific producers of new metabolites (almost 50%) than algal epiphytes (ca. 30%, Ji and Wang, 2016). There is a scientific consensus, that algal endophytes are a prolific source of bioactive natural products (Sarasan *et al.*, 2017; Teixeira *et al.*, 2019). However, a systematic approach to understand the biology of alga-endophyte interaction is still lacking. Compared to the algal surface, there must be a tight interaction between algal internal tissue and endophytes, which stimulate endophytes to contribute to host's defense by producing secondary metabolites (Maciá-Vicente *et al.*, 2018). This may explain the high capacity of endophytes to produce bioactive SMs.

It is difficult to predict the effects of any OSMAC approach on SM production. For biodiscovery, early dereplication and strain prioritization are however crucial. Therefore, molecular networking (MN) was integrated with multi-informational data (i.e. culture regimes, culture media and bioactivity results) to observe chemical changes of the 10 selected fungal strains (Chapter 1). Previously, MN has been applied to 146 marine bacteria for analyzing the effects of culture regime, culture media, sampling site and extraction method on chemical production (Crüsemann *et al.*, 2017), proving the suitability of this approach for biodiscovery studies. This strategy enables assessment of chemical differences following changes in culture regime and growth media at extract stage, generating a global metabolome, which can be used as a roadmap for future isolation prioritization. MN confirmed that the 10 selected strains produced diverse types of secondary metabolites under different culture conditions, including polyketides, alkaloids, cyclic depsipeptides and lipids. Simultaneously, MN clearly demonstrated that culture regime change had a significant impact on those 10 strains' secondary metabolite production. Several metabolites were mapped to only one culture regime, e.g. cyclic depsipeptide enniatin B<sub>1</sub> was restricted to liquid cultures. *Vice versa*, the indole diterpenoid penitrem B was only produced by *Penicillium* sp. FVE-68 in sucrose yeast medium (SYM) on agar plates but not in liquid culture. Moreover, 9 of the 10 strains produced toxic/anticancer metabolites only in liquid culture regime. These different performances of chemical production in liquid and solid media suggest that those fungi were particularly sensitive to culture regime changes. Reasons for this differential production include different levels of aeration of the culture (Nout *et al.*, 1987) as well as different mycelium structures in liquid (dispersed mycelia) and solid (mycelial mat) medium (Bigelis *et al.*, 2006). Consequently, a change of culture regime is expected to affect the chemical inventory of marine fungi and was observed previously (Guo *et al.*, 2013). The present study confirms the important effect of the cultivation regime on the metabolome of marine fungi.

In parallel, the MN showed the important effect of the medium on the chemical production of those 10 *Fucus*-associated fungi. Several metabolites were exclusively detected in extracts of specific media, e.g. dihydroxyanthraquinone questinol in potato dextrose medium (PDM), and chlorinated tetrahydrofuranone polyketide griseofulvin in modified Wickerham medium (WM). The different media reflect different nutrient regimes with respect to carbon and salt. Bioactivity results showed that PDM seems to be the best medium for inducing the production of anticancer/toxic metabolites, since all 10 strains showed strong anticancer/toxic activity against tested cell lines when cultured in PDM. Moreover, MN revealed a number of unannotated clusters/nodes specifically induced in PDM-derived crude extracts. The major difference between PDM and other media applied in this study is the carbon resource. PDM is the only medium featuring a combination of polysaccharides (potato starch) and monosaccharides (dextrose) as slowly and fast available organic carbon sources. These results suggest that the type of carbon source played a core role in inducing bioactive metabolites production of *Fucus*-derived fungi. This is in perfect accordance with other studies reporting a successful induction of novel secondary metabolite production, supporting the core role of carbon for marine fungal metabolism (Lin *et al.*, 2009; Romano *et al.*, 2018). Notably, none of the 10 selected strains showed any anticancer bioactivity after cultivation on NaCl-containing medium (SYM or WM). These results further indicate that the selected fungi are facultative marine fungi not requiring salt and suggest that salt may impair the production of bioactive metabolites. This thesis further highlights the importance of OSMAC approaches for the optimization of cultivation conditions.

Identification of potentially bioactive natural products at early stages (e.g. crude extracts level) is crucially important for natural product discovery. To facilitate the dereplication process and allow an early prioritization of fungal strains, for the first time the combination of bioactivity data and MN in “bioactivity mapping” was applied to marine fungal crude extracts (Chapter 1). The bioactivity mapping was established by embedding bioactivity data into MN, and aimed at highlighting potential bioactive molecules in crude extracts (Olivon *et al.*, 2017). Besides annotation of known compounds to avoid the time-consuming re-isolation, bioactivity mapping could be used as an indicator for the selection of potentially active compounds (Olivon *et al.*, 2017). In this study, bioactivity mapping was performed by visualizing the MS-derived clusters in MN followed by color-tagging of each node detected in samples showing different bioactivity (Chapter 1). Guided by bioactivity mapping, several mycotoxins were annotated in MN, such as the bis-anhydride rubratoxins (Moss *et al.*, 1971) and the cyclic depsipeptide enniatins (Jestoi, 2008). These potent molecules are thought to be responsible for the observed bioactivity of many crude extracts derived from *Fucus*-associated fungi against human cancer and non-cancer cell lines. Usually, mycotoxins lack selective anticancer bioactivity but show a general cytotoxicity (Pitt and Miller, 2017). Since inselectivity restricts their application in drug discovery, strains exhibiting general cytotoxicity to all tested cell lines were not prioritized for the following large-scale fermentation. Instead, we focused on those extracts showing more selective toxicity against cancer cell lines. Thus, the *Fucus*-endophyte *Pyrenochaetopsis* sp. FVE-001, which showed bioactivity against several different cancer cell line types such as HepG2 (human hepatoma cancer cell line), HT29 (human colon cancer cell line), A549 (human lung carcinoma cancer cell line) and MDA-MB-231 (human breast cancer cell line) at 100 µg/ml in PDM liquid medium was selected for following large-scale fermentation (Chapter 2). The comparative bioactivity mapping of FVE-001 (Chapter 1) including all OSMAC-derived crude extracts interestingly revealed five nodes exclusively in PDM-L, i.e.  $m/z$  [M+H]<sup>+</sup> 428.2081 belonging to a large unidentified cluster containing 38 nodes as well as four single nodes with  $m/z$  [M+H]<sup>+</sup> 463.2679,  $m/z$  [M+H]<sup>+</sup> 469.2242,  $m/z$  [M+H]<sup>+</sup> 939.6554 and  $m/z$  [M+Na]<sup>+</sup> 452.2278. Those nodes could not be annotated to any known natural product suggesting their chemical novelty and potential as new anticancer metabolites. The bioactivity mapping of crude extracts showed obvious differences between bioactive samples and non-bioactive samples and annotated potential

## DISCUSSION AND OUTLOOK

interesting candidates for isolation at an early stage and thus substantially helped prioritization.

Another endophytic strain FVE-087 showing similar morphology but higher chemical complexity than FVE-001 was also selected for chemical investigation (Chapter 3). Initial genetic identification of FVE-001 and FVE-087 only enabled the classification at order level (order: Pleosporales). Re-amplification and sequencing for ITS1-5.8S-ITS2 genes along with phylogenetic tree construction identified both strains as *Pyrenochaetopsis* sp. To our knowledge, there is only one study focusing on secondary metabolite production of *Pyrenochaetopsis* sp. collected from Japanese soil samples (Nogawa *et al.*, 2017). Therefore, this yet underexplored genus is considered to be a valuable candidate for the discovery of novel bioactive natural products. Large-scale fermentation and extraction yielded 2.66g crude extract from *Pyrenochaetopsis* sp. FVE-001 (Chapter 2) and 17.64g oily extract from *Pyrenochaetopsis* sp. FVE-087 (Chapter 3). After sequential extraction with *n*-hexane (KH), chloroform (KC) and methanol (KM) for both crude extracts, anticancer bioactivity and the toxicity of obtained subfractions were evaluated. The anticancer bioactivity was tracked to the KC fractions of both FVE-001 and FVE-087. Thus, the purification process was focused on 345.4mg and 4.57g KC subextracts derived from FVE-001 and FVE-087, respectively. In order to accelerate the compound purification process, another metabolomic tool combining bioactivity and MN was applied. Bioactivity-based MN was applied to SPE subfractions derived from *Pyrenochaetopsis* sp. FVE-001 KC fraction. It applies the Pearson correlation coefficient to fractions with different bioactivity levels (Nothias *et al.*, 2018). Compared to the bioactivity mapping, the bioactivity-based MN integrates the measurement of linear correlation between peak area detected in the mass chromatogram and bioactivity data into MN (Nothias *et al.*, 2018). It enabled a prediction of the bioactivity score of nodes detected in MN through calculating their *p* and *r* values and further guide the bioactivity-based targeted isolation. Based on the bioactivity score, three new decalinoylspirotetramic acid derivatives, namely pyrenosetins A-C (**1-3**) and one known compound phomasetin (**4**) were targeted and purified from FVE-001 (Chapter 2, Figure 1). Motivated by this study, bioactivity-guided isolation of second strain *Pyrenochaetopsis* sp. FVE-087 yielded another new decalinoyltetramic acid derivative, pyrenosetin D (**5**) along with two known decalins wakodecalines A (**6**,) and B (**7**) (Chapter 3, Figure 1).

This study represents the first application of bioactivity-based MN to marine fungi for biodiscovery. In the bioactivity-based MN, the decalinoylspirotetramic acid derivatives pyrenosetins A (**1**) and B (**2**) were annotated as nodes with high bioactivity scores, displaying *r* values of 0.79, 0.93 and *p* values of  $2.2 \times 10^{-5}$  and  $1.30 \times 10^{-5}$ , respectively. These high predicted bioactivity scores suggest a high anticancer potential of **1** and **2**. Confirming the prediction, **1** and **2** showed high toxicity against the malignant melanoma cell line A-375 with IC<sub>50</sub> values of 2.8 and 6.3 μM, respectively. More interestingly, **2** exhibited selective bioactivity against A-375 (IC<sub>50</sub> value = 6.3 μM) but lower toxicity to HaCaT (IC<sub>50</sub> value = 35.0 μM). Experimental bioassay results verified the predictions; beyond this, bioactivity-based MN allowed targeted compound isolation, hence rendering it a powerful tool for substantially facilitating the biodiscovery process.

The pure compound pyrenosetin C (**3**) exhibited weak anticancer bioactivity against the melanoma cell line A-375 (140.3 μM) as well as low toxicity to HaCaT (142.9 μM). From a structural point of view, **2** differs from **1** only in the stereochemistry of the C-16 hydroxyl group, while **3** contains a ketone group at C-16. The differences in their bioactivity suggested that the presence of a hydroxyl group at C-16 had impact on anticancer activity and toxicity of pyrenosetins. Phomasetin (**4**) was previously reported from fungal genera *Phoma* and *Pyrenochaetopsis* with anti-HIV activity and cytotoxicity (Nogawa *et al.*, 2017; Singh *et al.*, 1998). In this study, phomasetin (**4**) exhibited activity against A-375 and HaCaT with almost identical IC<sub>50</sub> values of 37.5 and 45.0 μM respectively, suggesting a general



toxicity.

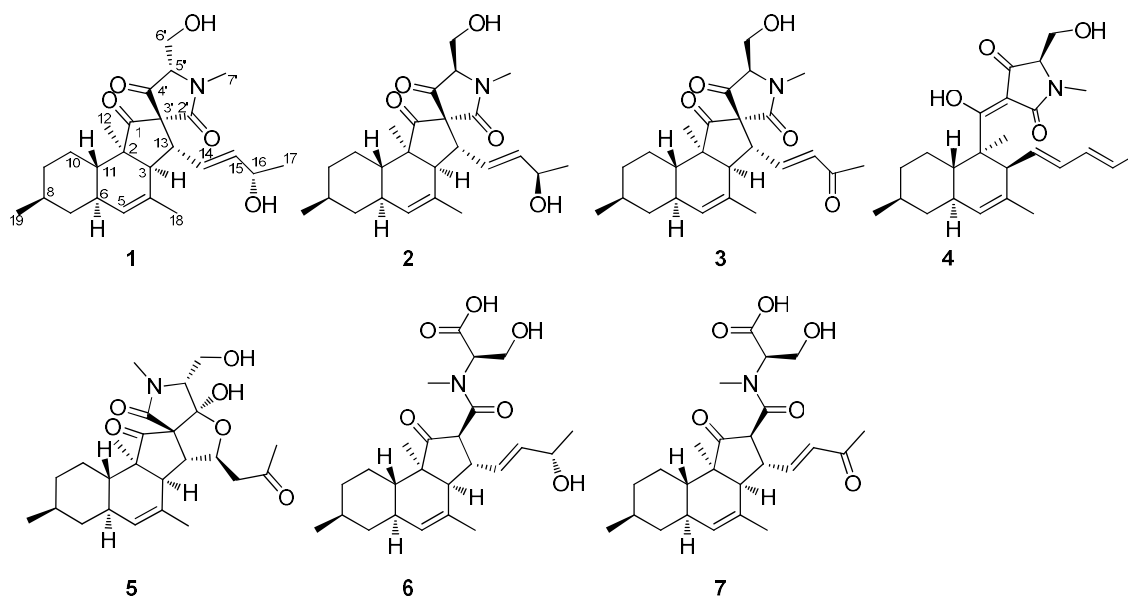


**Figure 1.** Compounds purified from *Fucus vesiculosus*-derived fungi *Pyrenochaetopsis* sp. FVE-001 and FVE-087 during this study. **1-3.** New decalinoylspirotetramic acid derivatives pyrenosetin A-C isolated from *Pyrenochaetopsis* sp. FVE-001. **4.** Known decalin phomasetin isolated from *Pyrenochaetopsis* sp. FVE-001. **5.** New decalinoyltetramic acid derivative pyrenosetin D isolated from *Pyrenochaetopsis* sp. FVE-087. **6-7.** Known decalins wakodecalines A-B isolated from *Pyrenochaetopsis* sp. FVE-087.

Similar to FVE-001, KC subfraction of strain *Pyrenochaetopsis* sp. FVE-087 also exhibited high anticancer bioactivity. The bioactivity-guided isolation process yielded three compounds from this subfraction, including one new decalinoyltetramic acid derivative - namely pyrenosetin D (**5**) and two known decalin derivatives - wakodecalines A (**6**) and B (**7**). NMR-based structure elucidation showed that compound **5** contained a complex pentacyclic motif with ten stereocenters. This pentacyclic ring system comprised a *trans*-decalin moiety (6/6) and a tricyclic moiety (5/5/5). To our knowledge, only *Fusarium* sp. was previously reported to produce structurally similar decalin derivatives fusarisetin A – B (Jang *et al.*, 2011; Zhao *et al.*, 2019). The NOE spectrum assisted determination of the relative configuration of **5** between decalin skeleton and the side chain. However, there were still three stereogenic centers (C-3', C-4' and C-5') left to be assigned. Since compound **5** could not be purified in enough amounts for crystallization, a density functional theory (DFT) calculation of NMR chemical shifts was performed to determine the relative configuration at C-3', C-4' and C-5', shown in Figure 1. This approach, together with the coupling constant analyses and prediction of optical rotation values confirmed the structure of **5** as shown in Figure 1. DFT calculation of NMR parameters is an emerging method and has been previously applied to marine-derived metabolites for determination of their absolute configurations (Grauso *et al.*, 2020). The present study represents the first example for the application of this method to algal-derived fungal metabolites to overcome the difficulty in determining the configuration of compounds with multiple stereocenters. Compound **5** exhibited weak activity against A-375 with IC<sub>50</sub> 77.5 μM. Although **5** had the same cyclopentanone fused decalin skeleton and ketone group at C-16 as **3**, they displayed different bioactivity against A-375 (**3**, 140.3 μM and **5**, 77.5 μM). This difference suggested the importance of tetrahydrofuran ring in **5** with regard to anticancer bioactivity. Moreover, **6** and **7**, which lack the terminal tetramic acid moiety did not exhibit any bioactivity against A-375 cells up to 200 μM. This suggested that the tetramic acid moiety is important

## DISCUSSION AND OUTLOOK

for anticancer bioactivity.

All isolated compounds obtained during this study contained a decalin ring as the skeleton. The ‘decalin’ moiety has been found in an array of marine natural products from marine fungi. The marine-derived decalin derivatives represent a big group of architecturally complex structural scaffolds, which contain multiple ring systems ranging from bicyclic to pentacyclic rings (Li *et al.*, 2014a; Wu *et al.*, 2015; Yamada *et al.*, 2019). They show diverse bioactivities, such as anticancer (Zhuravleva *et al.*, 2012), phytotoxic (Zhao *et al.*, 2019), and antibiotic (Nguyen *et al.*, 2007). The compounds obtained in this study were polyketide type decalin derivatives most probably biosynthesized by an enzymatic intramolecular Diels-Alder cycloaddition (Kato *et al.*, 2015; Kato *et al.*, 2018). All pyrenosetins and wakodecalines contained a cyclopentanone fused decalin skeleton that is rare in nature. To our knowledge, only a few compounds, e.g. altercrasins A-C (Yamada *et al.*, 2019) and fusarisetins A-D (Zhao *et al.*, 2019) have been reported as natural products with a similar planar skeleton. This study enlarged the space of marine-derived decalins with multiple ring systems. As reported, the stereochemistry of *trans*-decalin formation is enzymatically controlled (e.g. Fsa2 and its analogues) encoded by BGCs (e.g. *fsa*) (Kato *et al.*, 2015). Previous genome analysis of soil-derived *Pyrenochaetopsis* sp. RK10-F058 revealed the importance of the *phm* gene cluster in the biosynthesis of phomasetin (Kato *et al.*, 2018). As reported from Kato *et al.*, *phm* encoding a PKS-NRPS hybrid enzyme determined the stereoselectivity of decalin formation of phomasetin, making its decalin unit opposite to that of equisetin (Kato *et al.*, 2018). Since pyrenosetins are structurally related to phomasetin, it is reasonable to assume that gene cluster *phm* and its homologues are involved in the synthesis of pyrenosetins, leading to the opposite stereochemistry between pyrenosetins versus fusarisetins and altercrasins. Genome sequencing and BGC analysis of *Pyrenochaetopsis* sp. FVE-001 and FVE-087 would further help to understand the formation and stereochemistry of those pyrenosetins in the future.

## 2. Outlook

This study aimed at investigating the biological diversity of *Fucus vesiculosus*-derived fungal isolates, and prospecting new anticancer lead compounds from them. A total of 55 fungal isolates were obtained from Baltic Sea *Fucus vesiculosus*. Application of OSMAC approach to 26 selected *Fucus*-derived strains successfully induced the production of anticancer/toxic compounds under at least one certain cultural condition in 10 endophytic strains. Following strain prioritization and targeted isolation due to the application of new bioinformatic tool (MN) with predictive power, two *Fucus*-derived *Pyrenochaetopsis* sp. have yielded four new decalin derivatives (**1-3**, **5**) and three known compounds (**4**, **6-7**). Compounds **1-5** showed anticancer bioactivity against A-375 with IC<sub>50</sub> values ranging from 2.8 to 140.3  $\mu$ M. Results from this thesis suggest that *Fucus*-derived fungi are a good resource for bioprospecting and natural product discovery. Future research activities in this direction should include the following aspects:

- Collection of a larger number of *Fucus* samples

Chemical diversity is mirrored by the biodiversity of marine fungal isolates (Ji and Wang, 2016; Saleem *et al.*, 2007). Thus, it is important to obtain diverse fungal samples for the selection of interesting candidates for chemical and bioactivity profiling. Increasing the biological diversity of fungi by using different media, culture conditions, or increasing the sampling size is an important aspect. In this study, 8 genera and 3 higher taxonomic levels of fungi were achieved from three *F. vesiculosus* specimens from a single sampling site, suggesting that *F. vesiculosus* is a promising candidate for bioprospection. However, we did not obtain any strain belonging to the genus *Aspergillus*, which has been isolated from several other *Fucus* sp. before (Zuccaro *et al.*, 2008). Moreover, an intensified isolation effort including multiple sampling sites, other *Fucus* species or other brown algae may afford potentially obligate marine fungi, which we were unable to retrieve although they have been reported from diverse algal hosts (Ji and Wang, 2016).

- Integration of genomics and OSMAC

In this study, we evaluated the influence of nutrient and culture regimes on the metabolism of *Fucus*-associated fungal isolates. Future studies could include further OSMAC approaches, e.g. addition of epigenetic modifiers, different amino acids, host extracts, to name a few, may lead induction of even more interesting chemistry. Furthermore, genomics studies could be incorporated into the optimization of OSMAC approach through monitoring the expression of BGCs under different cultural conditions (Romano *et al.*, 2018). Moreover, genome-scale biological models would be integrated with OSMAC-based cultivation to predict the production of secondary metabolites under certain cultural conditions (Xu *et al.*, 2018).

- Broad bioactivity screenings

Fungal natural products were frequently reported to possess multiple biological activities (Ji and Wang, 2016; Saleem *et al.*, 2007), i.e. one compound may represent a lead compound in different target diseases. This is exemplified by rapamycin, which has been applied in clinical treatment to prevent organ transplant rejection. Moreover, rapamycin exhibited a strong inhibitory effect on the mammalian target of rapamycin (mTOR) signaling pathway, which regulates cell growth, cell proliferation, cell motility and plays an important role in mammalian metabolism. It has been approved by the FDA for lymphangioliomyomatosis, a rare, progressive lung disease caused by abnormal activation of the mTOR signaling pathway in humans (Li *et al.*, 2014b). This may also hold true for compounds isolated

## DISCUSSION AND OUTLOOK

from *Pyrenochaetopsis* sp. FVE-001 and FVE-087. Beyond the observed anticancer activity, they should be also evaluated for their antifungal, antibacterial, antifouling activities to probe their biotechnological potential.

## References

- Abdel-Gawad, K. M., Hifney, A. F., Issa, A. A., Gomaa, M., 2014. Spatio-temporal, environmental factors, and host identity shape culturable-epibiotic fungi of seaweeds in the Red Sea, Egypt. *Hydrobiologia* 740, 37-49. DOI: 10.1007/s10750-014-1935-0
- Almeida, C., Eguereva, E., Kehraus, S., Siering, C., König, G. M., 2010. Hydroxylated sclerosporin derivatives from the marine-derived fungus *Cadophora malorum*. *J. Nat. Prod.* 73, 476-478. DOI: 10.1021/np900608d
- Balabanova, L., Slepchenko, L., Son, O., Tekutyeva, L., 2018. Biotechnology potential of marine fungi degrading plant and algae polymeric substrates. *Front. Microbiol.* 9. DOI: 10.3389/fmicb.2018.01527
- Bigelis, R., He, H., Yang, H. Y., Chang, L.-P., Greenstein, M., 2006. Production of fungal antibiotics using polymeric solid supports in solid-state and liquid fermentation. *J. Ind. Microbiol. Biotechnol.* 33, 815-826. DOI: 10.1007/s10295-006-0126-z
- Crüseemann, M., O'Neill, E. C., Larson, C. B., Melnik, A. V., Floros, D. J., da Silva, R. R., Jensen, P. R., Dorrestein, P. C., Moore, B. S., 2017. Prioritizing natural product diversity in a collection of 146 bacterial strains based on growth and extraction protocols. *J. Nat. Prod.* 80, 588-597. DOI: 10.1021/acs.jnatprod.6b00722
- Grauso, L., Li, Y., Scarpato, S., Shulha, O., Rárová, L., Strnad, M., Teta, R., Mangoni, A., Zidorn, C., 2020. Structure and conformation of zosteraphenols, tetracyclic diarylheptanoids from the seagrass *Zostera marina*: An NMR and DFT study. *Org. Lett.* 22, 78-82. DOI: 10.1021/acs.orglett.9b03964
- Grum-Grzhimaylo, A. A., Georgieva, M. L., Debets, A. J. M., Bilanenko, E. N., 2013. Are alkalitolerant fungi of the *Emericellopsis* lineage (Bionectriaceae) of marine origin? *IMA Fungus* 4, 213-228. DOI: 10.5598/imafungus.2013.04.02.07
- Guo, W., Peng, J., Zhu, T., Gu, Q., Keyzers, R. A., Li, D., 2013. Sorbicillamines A-E, nitrogen-containing sorbicillinoids from the deep-sea-derived fungus *Penicillium* sp. F23-2. *J. Nat. Prod.* 76, 2106-2112. DOI: 10.1021/np4006647
- Höller, U., Wright, A. D., MatthÉE, G. F., König, G. M., Draeger, S., Aust, H.-J., Schulz, B., 2001. Fungi from marine sponges: Diversity, biological activity and secondary metabolites. *Mycol. Res.* 104, 1354-1365. DOI: 10.1017/S0953756200003117
- Jang, J.-H., Asami, Y., Jang, J.-P., Kim, S.-O., Moon, D. O., Shin, K.-S., Hashizume, D., Muroi, M., Saito, T., Oh, H., 2011. Fusarisetin A, an acinar morphogenesis inhibitor from a soil fungus, *Fusarium* sp. FN080326. *J. Am. Chem. Soc.* 133, 6865-6867. DOI: 10.1021/ja1110688
- Janja, Z., Polona, Z., Kristina, S. i., Nina, G.-C., 2011. Xerophilic fungal genus *Wallemia*: Bioactive inhabitants of marine solar salterns and salty food. *Zb. Matice. Srp. Priir. Nauk.* DOI: 10.2298/zmspn1120007z
- Jestoi, M., 2008. Emerging *Fusarium*-mycotoxins fusaproliferin, beauvericin, enniatins, and moniliformin - a review. *Crit. Rev. Food Sci. Nutr.* 48, 21-49. DOI: 10.1080/10408390601062021
- Ji, N.-Y., Wang, B.-G., 2016. Mycochemistry of marine algicolous fungi. *Fungal Divers.* 80, 301-342. DOI: /10.1007/s13225-016-0358-9
- Jones, E. B. G., Sakayaroj, J., Suetrong, S., Somrithipol, S., Pang, K. L., 2009. Classification of marine Ascomycota, anamorphic taxa and Basidiomycota. *Fungal Divers.* 35, 1-187.
- Kamat, S., Kumari, M., Taritla, S., Jayabaskaran, C., 2020. Endophytic fungi of marine alga from Konkan Coast, India - a rich source of bioactive material. *Front. Mar. Sci.* 7. DOI: 10.3389/fmars.2020.00031
- Kato, N., Nogawa, T., Hirota, H., Jang, J.-H., Takahashi, S., Ahn, J. S., Osada, H., 2015. A new enzyme involved in the control of the stereochemistry in the decalin formation during equisetin biosynthesis. *Biochem. Biophys. Res. Commun.* 460, 210-215. DOI: 10.1016/j.bbrc.2015.03.011
- Kato, N., Nogawa, T., Takita, R., Kinugasa, K., Kanai, M., Uchiyama, M., Osada, H., Takahashi, S., 2018. Control of the stereochemical course of [4+2] cycloaddition during trans-decalin formation by Fsa2-family enzymes. *Angew. Chem. Int. Ed.* 57, 9754-9758. DOI: 10.1002/anie.201805050
- Li, G., Kusari, S., Spiteller, M., 2014a. Natural products containing 'decalin' motif in microorganisms. *Nat. Prod. Rep.* 31, 1175-1201. DOI: 10.1039/C4NP00031E
- Li, J., Kim, Sang G., Blenis, J., 2014b. Rapamycin: One drug, many effects. *Cell Metab.* 19, 373-379. DOI: 10.1016/j.cmet.2014.01.001

## DISCUSSION AND OUTLOOK

- Li, Q., Wang, G., 2009. Diversity of fungal isolates from three Hawaiian marine sponges. *Microbiol. Res.* 164, 233-241. DOI: 10.1016/j.micres.2007.07.002
- Lin, Z., Zhu, T., Wei, H., Zhang, G., Wang, H., Gu, Q., 2009. Spicochalasin A and new aspochalasins from the marine-derived fungus *Spicaria elegans*. *Eur. J. Org. Chem.* 2009, 3045-3051. DOI: 10.1002/ejoc.200801085
- Maciá-Vicente, J. G., Shi, Y.-N., Cheikh-Ali, Z., Grün, P., Glynou, K., Kia, S. H., Piepenbring, M., Bode, H. B., 2018. Metabolomics-based chemotaxonomy of root endophytic fungi for natural products discovery. *Environ. Microbiol.* 20, 1253-1270. DOI: 10.1111/1462-2920.14072
- Moss, M. O., Robinson, F. V., Wood, A. B., 1971. Rubratoxins. *J. Chem. Soc. C.*, 619-624. DOI: 10.1039/J39710000619
- Nguyen, H. P., Zhang, D., Lee, U., Kang, J. S., Choi, H. D., Son, B. W., 2007. Dehydroxychlorofusarielin B, an antibacterial polyoxygenated decalin derivative from the marine-derived fungus *Aspergillus* sp. *J. Nat. Prod.* 70, 1188-1190. DOI: 10.1021/np060552g
- Nogawa, T., Kato, N., Shimizu, T., Okano, A., Futamura, Y., Takahashi, S., Osada, H., 2017. Wakodecalines A and B, new decaline metabolites isolated from a fungus *Pyrenochaetopsis* sp. RK10-F058. *J. Antibiot.* 71, 123-128. DOI: 10.1038/ja.2017.103
- Nothias, L.-F., Nothias-Esposito, M., da Silva, R., Wang, M., Protsyuk, I., Zhang, Z., Sarvepalli, A., Leyssen, P., Touboul, D., Costa, J., Paolini, J., Alexandrov, T., Litaudon, M., Dorrestein, P. C., 2018. Bioactivity-based molecular networking for the discovery of drug leads in natural product bioassay-guided fractionation. *J. Nat. Prod.* 81, 758-767. DOI: 10.1021/acs.jnatprod.7b00737
- Nout, M. J. R., Bonants-van Laarhoven, T. M. G., de Jongh, P., de Koster, P. G., 1987. Ergosterol content of *Rhizopus oligosporus* NRRL 5905 grown in liquid and solid substrates. *Appl. Microbiol. Biot.* 26, 456-461. DOI: 10.1007/BF00253532
- Oleinikova, G. K., Navrazhnykh, Y. A., Pivkin, M. V., Menzorova, N. I., Kuznetsova, T. A., 2010. Free fatty acids from the marine fungi *Cladosporium cladosporioides*, *Talaromyces wortmanii* and *Wallemia sebi*. *Chem. Nat. Compd.* 46, 446-447. DOI: 10.1007/s10600-010-9638-x
- Olivon, F., Allard, P.-M., Koval, A., Righi, D., Genta-Jouve, G., Neyts, J., Apel, C., Pannecouque, C., Nothias, L.-F., Cachet, X., Marcourt, L., Roussi, F., Katanaev, V. L., Touboul, D., Wolfender, J.-L., Litaudon, M., 2017. Bioactive natural products prioritization using massive multi-informational molecular networks. *ACS Chem. Biol.* 12, 2644-2651. DOI: 10.1021/acschembio.7b00413
- Parrot, D., Blümel, M., Utermann, C., Chianese, G., Krause, S., Kovalev, A., Gorb, S. N., Tasdemir, D., 2019. Mapping the surface microbiome and metabolome of brown seaweed *Fucus vesiculosus* by amplicon sequencing, integrated metabolomics and imaging techniques. *Sci. Rep.* 9, 1061-1077. DOI: 10.1038/s41598-018-37914-8
- Patyshakuliyeva, A., Falkoski, D. L., Wiebenga, A., Timmermans, K., de Vries, R. P., 2020. Macroalgae derived fungi have high abilities to degrade algal polymers. *Microorganisms* 8, 52. DOI: 10.3390/microorganisms8010052
- Pitt, J. I., Miller, J. D., 2017. A concise history of mycotoxin research. *J. Agric. Food Chem.* 65, 7021-7033. DOI: 10.1021/acs.jafc.6b04494
- Rämä, T., Nordén, J., Davey, M. L., Mathiassen, G. H., Spatafora, J. W., Kausrud, H., 2014. Fungi ahoy! Diversity on marine wooden substrata in the high North. *Fungal Ecol.* 8, 46-58. DOI: 10.1016/j.funeco.2013.12.002
- Richards, T. A., Jones, M. D. M., Leonard, G., Bass, D., 2012. Marine fungi: Their ecology and molecular diversity. *Annu. Rev. Mar. Sci.* 4, 495-522. DOI: 10.1146/annurev-marine-120710-100802
- Romano, S., Jackson, S. A., Patry, S., Dobson, A. D. W., 2018. Extending the “One-Strain-Many-Compounds” (OSMAC) principle to marine microorganisms. *Mar. Drugs* 16, 244. DOI:10.3390/md16070244
- Saleem, M., Ali, M. S., Hussain, S., Jabbar, A., Ashraf, M., Lee, Y. S., 2007. Marine natural products of fungal origin. *Nat. Prod. Rep.* 24, 1142-1152. DOI: 10.1039/B607254M
- Sarasan, M., Puthumana, J., Job, N., Han, J., Lee, J. S., Philip, R., 2017. Marine algicolous endophytic fungi - a promising drug resource of the era. *J. Microbiol. Biotechnol.* 27, 1039-1052. DOI: 10.4014/jmb.1701.01036
- Singh, S. B., Zink, D. L., Goetz, M. A., Dombrowski, A. W., Polishook, J. D., Hazuda, D. J., 1998. Equisetin and a novel opposite stereochemical homolog phomasetin, two fungal metabolites as

- inhibitors of HIV-1 integrase. *Tetrahedron Lett.* 39, 2243-2246. DOI: 10.1016/S0040-4039(98)00269-X
- Teixeira, T. R., Santos, G. S. d., Armstrong, L., Colepicolo, P., Deboni, H. M., 2019. Antitumor potential of seaweed derived-endophytic fungi. *Antibiotics* 8, 205. DOI:10.3390/antibiotics8040205
- Wainwright, B. J., Zahn, G. L., Arlyza, I. S., Amend, A. S., 2018. Seagrass-associated fungal communities follow Wallace's line, but host genotype does not structure fungal community. *J. Biogeogr.* 45, 762-770. DOI: 10.1111/jbi.13168
- Wu, B., Wiese, J., Labes, A., Kramer, A., Schmaljohann, R., Imhoff, J. F., 2015. Lindgomycin, an unusual antibiotic polyketide from a marine fungus of the lindgomycetaceae. *Mar. Drugs* 13, 4617-4632. DOI: 10.3390/md13084617
- Xu, N., Ye, C., Liu, L., 2018. Genome-scale biological models for industrial microbial systems. *Appl. Microbiol. Biot.* 102, 3439-3451. DOI: 10.1007/s00253-018-8803-1
- Yamada, T., Tanaka, A., Nehira, T., Nishii, T., Kikuchi, T., 2019. Altercrasins A-E, decalin derivatives, from a sea-urchin-derived *Alternaria* sp.: Isolation and structural analysis including stereochemistry. *Mar. Drugs* 17, 218. DOI: 10.3390/md17040218
- Zalar, P., Sybren de Hoog, G., Schroers, H.-J., Frank, J. M., Gunde-Cimerman, N., 2005. Taxonomy and phylogeny of the xerophilic genus *Wallemia* (*Wallemiomycetes* and *Wallemiales*, cl. et ord. nov.). *Antonie van Leeuwenhoek* 87, 311-328. DOI: 10.1007/s10482-004-6783-x
- Zhao, D., Han, X., Wang, D., Liu, M., Gou, J., Peng, Y., Liu, J., Li, Y., Cao, F., Zhang, C., 2019. Bioactive 3-decalinoyltetramic acids derivatives from a marine-derived strain of the fungus *Fusarium equiseti* D39. *Front. Microbiol.* 10, 1285. DOI: 10.3389/fmicb.2019.01285
- Zhuravleva, O. I., Afiyatullo, S. S., Vishchuk, O. S., Denisenko, V. A., Slinkina, N. N., Smetanina, O. F., 2012. Decumbenone C, a new cytotoxic decaline derivative from the marine fungus *Aspergillus sulphureus* KMM 4640. *Arch. Pharm. Res.* 35, 1757-1762. DOI: 10.1007/s12272-012-1007-9
- Zuccaro, A., Schoch, C. L., Spatafora, J. W., Kohlmeyer, J., Draeger, S., Mitchell, J. I., 2008. Detection and identification of fungi intimately associated with the brown seaweed *Fucus serratus*. *Appl. Environ. Microbiol.* 74, 931-941. DOI: 10.1128/aem.01158-07
- Zuccaro, A., Schulz, B., Mitchell, J. I., 2004. Molecular detection of ascomycetes associated with *Fucus serratus*. *Mycol. Res.* 107, 1451-1466. DOI: 10.1017/S0953756203008657

## DISCUSSION AND OUTLOOK



---

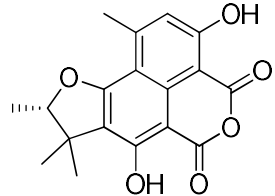
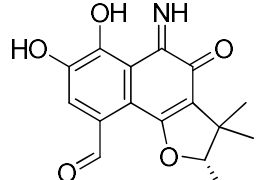
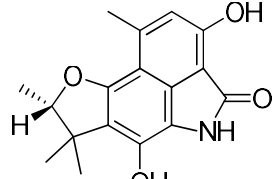
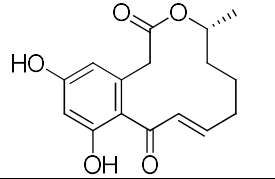
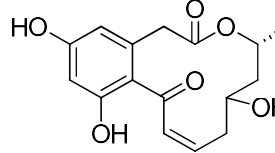
## IV. APPENDIX

---

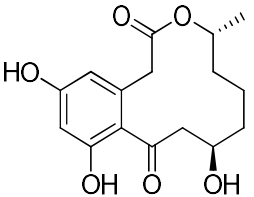
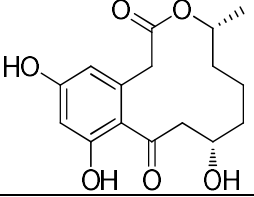
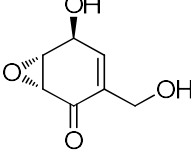
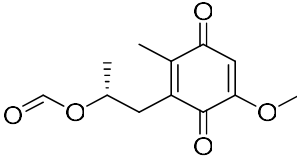


APPENDIX

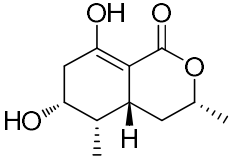
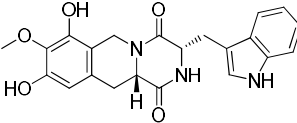
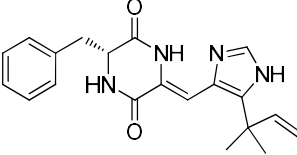
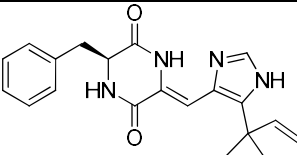
**1. Table 1. Natural products reported from algicolous fungi with anticancer potential**

Compound name	Structure	Chemical family	Resources (fungal resource)	Bioactivity	Reference
(-)-Sclerodin		Polyketide	Green alga <i>Enteromorpha</i> sp. ( <i>Coniothyrium cereale</i> )	Toxicity against cancer cell line: HLE: IC <sub>50</sub> = 10.9 μM	(Nazir <i>et al.</i> , 2015)
(-)-Cereoaldomine		Polyketide	Green alga <i>Enteromorpha</i> sp. ( <i>Coniothyrium cereale</i> )	Toxicity against cancer cell line: HLE: IC <sub>50</sub> = 3.01 μM	(Elsebai <i>et al.</i> , 2011; Nazir <i>et al.</i> , 2015)
(-)-Cereolactam		Polyketide	Green alga <i>Enteromorpha</i> sp. ( <i>Coniothyrium cereale</i> )	Toxicity against cancer cell line: HLE: IC <sub>50</sub> = 9.28 μM	(Elsebai <i>et al.</i> , 2011; Nazir <i>et al.</i> , 2015)
(+)-(10E,15R)-10,11-Dehydrocurvularin		Macrolide	Red alga <i>Acanthophora spicifera</i> ( <i>Curvularia</i> sp.)	Toxicity to 36 human tumor cell lines: mean IC <sub>50</sub> = 1.25 μM	(Greve <i>et al.</i> , 2008)
(+)-(10E,15R)-13-Hydroxy-10,11-dehydrocurvularin		Macrolide	Red alga <i>Acanthophora spicifera</i> ( <i>Curvularia</i> sp.)	Toxicity to 36 human tumor cell lines: mean IC <sub>50</sub> = 30.06 μM	(Greve <i>et al.</i> , 2008)

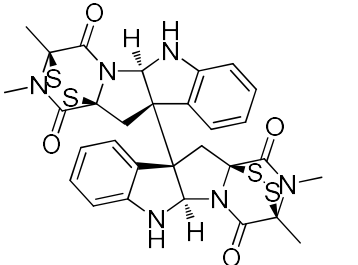
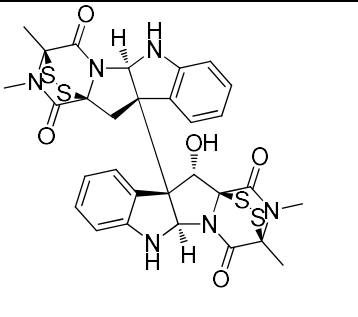
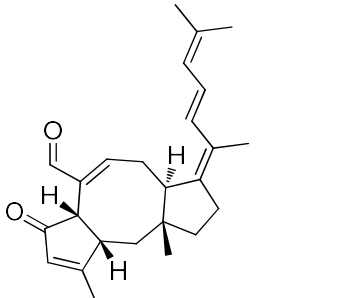
APPENDIX

(+)-(11R,15R)-11-Hydroxycurvularin		Macrolide	Red alga <i>Acanthophora spicifera</i> ( <i>Curvularia</i> sp.)	Toxicity to 36 human tumor cell lines: Mean IC <sub>50</sub> = 12.99 μM	(Greve <i>et al.</i> , 2008)
(+)-(11S,15R)-11-Hydroxycurvularin		Macrolide	Red alga <i>Acanthophora spicifera</i> ( <i>Curvularia</i> sp.)	Toxicity to 36 human tumor cell lines: mean IC <sub>50</sub> = 6.09 μM	(Greve <i>et al.</i> , 2008)
(+)–Epieoxydon		Epoxyquinone	Red alga <i>Polysiphonia violacea</i> ( <i>Apiospora montagnei</i> )	Toxicity against cancer cell line: HM02: GI <sub>50</sub> = 0.7 μg/mL HepG2 GI <sub>50</sub> = 0.75 μg/mL MCF-7 GI <sub>50</sub> = 1.5 μg/mL	(Klemke <i>et al.</i> , 2004)
			Green alga <i>Enteromorpha intestinalis</i> ( <i>Penicillium</i> sp. OUPS-79)	Toxicity against cancer cell line: P388: ED <sub>50</sub> = 0.2 μg/mL	(Iwamoto <i>et al.</i> , 1999)
(+)–Formylanserine B		Polyketide	Brown alga <i>Padina</i> sp. ( <i>Penicillium citrinum</i> )	Toxicity against cancer cell line: EAC: ED <sub>50</sub> = 35.7 μM	(Smetanina <i>et al.</i> , 2016)
			-	Toxicity against cancer cell line: MDA-MB-435: IC <sub>50</sub> = 2.9 μg/mL	(Gautschi <i>et al.</i> , 2004)

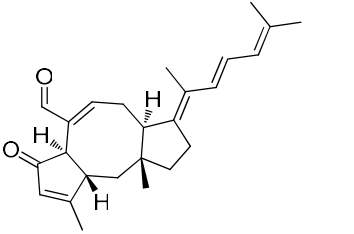
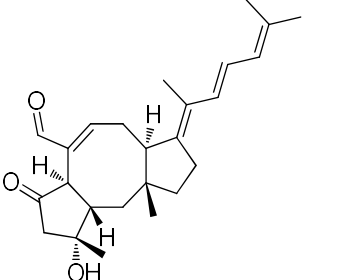
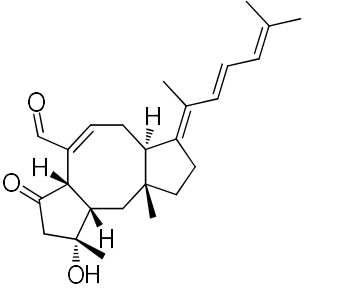
APPENDIX

(3 <i>R</i> ,4 <i>aR</i> ,5 <i>S</i> ,6 <i>R</i> )-6-Hydroxy-5-methylramulosin		Polyketide	Green alga <i>Codium fragile</i> ( <i>Valsa ceratosperma</i> )	65% growth inhibition against HeLa at 50 µg/mL	(El-Beih <i>et al.</i> , 2007)
(3 <i>S</i> , 11 <i>aS</i> )-3- [(1 <i>H</i> -Indol-3-yl) Methyl]-7,9- dihydroxy-8-methoxy- 2,3,11,11 <i>a</i> -tetrahydro- 6 <i>H</i> - pyrazino [1,2- <i>b</i> ] isoquinoline-1,4-dione		Diketopiperazine alkaloid	Green alga <i>Enteromorpha tubulosa</i> ( <i>Aspergillus flavus</i> c-f-3)	Toxicity against cancer cell line: HL-60: IC <sub>50</sub> = 36.5 µg/mL	(Lin <i>et al.</i> , 2008)
( <i>R</i> )-Phenylahistin		Diketopiperazine alkaloid	Unidentified alga ( <i>Aspergillus ustus</i> NSC-F038)	Toxicity against cancer cell line: P388: IC <sub>50</sub> = 3.8 µM	(Kano <i>et al.</i> , 1997)
(S)-Phenylahistin (Halimide)		Diketopiperazine alkaloid	Unidentified alga ( <i>Aspergillus ustus</i> NSC-F038)	Toxicity against cancer cell line: P388: IC <sub>50</sub> = 3.5 µM	(Kano <i>et al.</i> , 1997)
				Toxicity against cancer cell line: A549: IC <sub>50</sub> = 0.3 µM	(Kano <i>et al.</i> , 1999)
			Green alga <i>Halimedia copiosa</i> ( <i>Aspergillus</i> sp. CNC139)	Toxicity against cancer cell lines: HCT116: IC <sub>50</sub> = 1.0 µM A2780: IC <sub>50</sub> = 0.8 µM	(Fenical <i>et al.</i> , 2000b)
				Anti-proliferative activity against 38 cancer cell lines with GI <sub>50</sub> values ranging from 2.3 ×10 <sup>-7</sup> M to 4.0 ×10 <sup>-5</sup> M	(Fukumoto <i>et al.</i> , 2002)

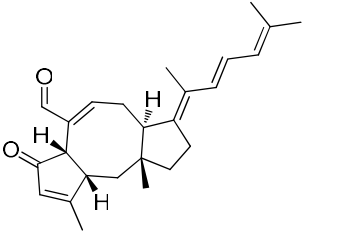
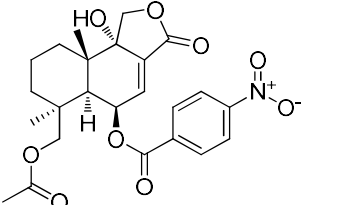
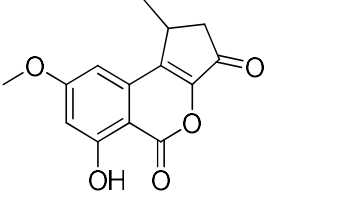
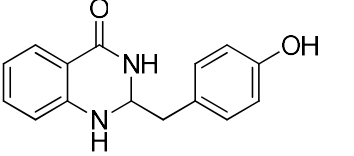
APPENDIX

<p>11,11'-Dideoxyverticillin A</p>		<p>Epidithiodioxopiperazine</p>	<p>Green alga <i>Avrainbillea longicaulis</i> (<i>Penicillium</i> sp. CNC-350)</p>	<p>Toxicity against cancer cell line: HCT116: IC<sub>50</sub> = 30 ng/mL</p>	<p>(Son <i>et al.</i>, 1999)</p>
<p>11'-Deoxyverticillin A</p>		<p>Epidithiodioxopiperazine</p>	<p>Green alga <i>Avrainbillea longicaulis</i> (<i>Penicillium</i> sp. CNC-350)</p>	<p>Toxicity against cancer cell line: HCT116: IC<sub>50</sub> = 30 ng/mL</p>	<p>(Son <i>et al.</i>, 1999)</p>
<p>14,15-Dehydro-(Z)-14-ophiobolin G</p>		<p>Sesterpenoid</p>	<p>Brown alga <i>Padina</i> sp. (<i>Aspergillus flocculosus</i>)</p>	<p>Cytotoxicity against 6 cancer cell lines: HCT-15: GI<sub>50</sub> = 1.67 μM NUGC-3: GI<sub>50</sub> = 1.53 μM NCI-H23: GI<sub>50</sub> = 1.84 μM ACHN: GI<sub>50</sub> = 2.01 μM PC-3: GI<sub>50</sub> = 1.60 μM MDA-MB-231: GI<sub>50</sub> = 1.75 μM</p>	<p>(Choi <i>et al.</i>, 2019)</p>

APPENDIX

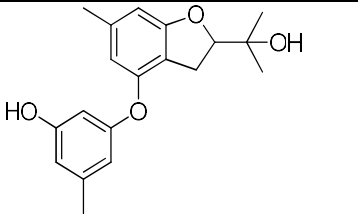
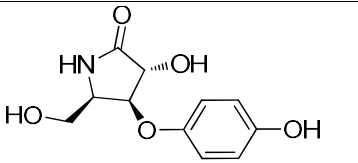
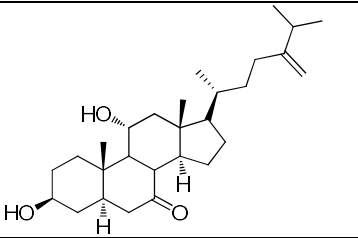
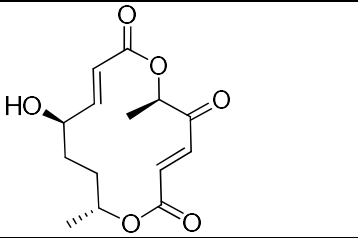
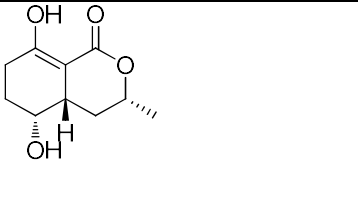
14,15-Dehydro-6-epi-ophiobolin G		Sesterpenoid	Brown alga <i>Padina</i> sp. ( <i>Aspergillus flocculosus</i> )	Cytotoxicity against 6 cancer cell lines: HCT-15: GI <sub>50</sub> = 0.96 μM NUGC-3: GI <sub>50</sub> = 0.88 μM NCI-H23: GI <sub>50</sub> = 1.40 μM ACHN: GI <sub>50</sub> = 1.14 μM PC-3: GI <sub>50</sub> = 1.00 μM MDA-MB-231: GI <sub>50</sub> = 1.05 μM	(Choi <i>et al.</i> , 2019)
14,15-Dehydro-6-epi-ophiobolin K		Sesterpenoid	Brown alga <i>Padina</i> sp. ( <i>Aspergillus flocculosus</i> )	Cytotoxicity against 6 cancer cell lines: HCT-15: GI <sub>50</sub> = 0.21 μM NUGC-3: GI <sub>50</sub> = 0.19 μM NCI-H23: GI <sub>50</sub> = 0.24 μM ACHN: GI <sub>50</sub> = 0.24 μM PC-3: GI <sub>50</sub> = 1.00 μM MDA-MB-231: GI <sub>50</sub> = 0.14 μM	(Choi <i>et al.</i> , 2019)
14,15-Dehydro-ophiobolin K		Sesterpenoid	Brown alga <i>Padina</i> sp. ( <i>Aspergillus flocculosus</i> )	Cytotoxicity against 6 cancer cell lines: HCT-15: GI <sub>50</sub> = 0.44 μM NUGC-3: GI <sub>50</sub> = 0.50 μM NCI-H23: GI <sub>50</sub> = 0.61 μM ACHN: GI <sub>50</sub> = 0.53 μM PC-3: GI <sub>50</sub> = 0.47 μM MDA-MB-231: GI <sub>50</sub> = 0.63 μM	(Choi <i>et al.</i> , 2019)

APPENDIX

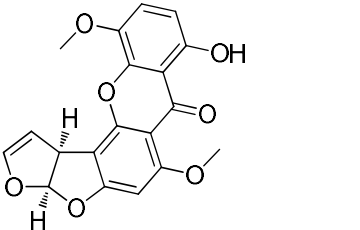
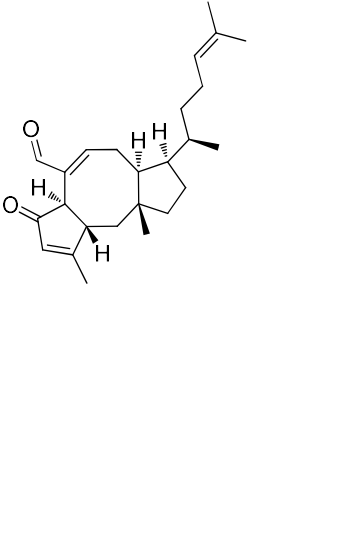
<p>14,15-Dehydro-ophiobolin G</p>		<p>Sesterpenoid</p>	<p>Brown alga <i>Padina</i> sp. (<i>Aspergillus flocculosus</i>)</p>	<p>Cytotoxicity against 6 cancer cell lines:  HCT-15: GI<sub>50</sub> = 1.24 μM  NUGC-3: GI<sub>50</sub> = 1.07 μM  NCI-H23: GI<sub>50</sub> = 1.50 μM  ACHN: GI<sub>50</sub> = 1.40 μM  PC-3: GI<sub>50</sub> = 1.38 μM  MDA-MB-231: GI<sub>50</sub> = 1.35 μM</p>	<p>(Choi <i>et al.</i>, 2019)</p>
<p>14-O-Acetylinsulicolide A</p>		<p>Sesquiterpenoid</p>	<p>Red alga <i>Coelarthrum</i> sp. (<i>Aspergillus ochraceus</i> Jcma1F17)</p>	<p>Cytotoxicity against cancer cell lines:  ACHN: IC<sub>50</sub> = 4.1 μM;  OS-RC-2: IC<sub>50</sub> = 5.3 μM;  786-O: IC<sub>50</sub> = 2.3 μM</p>	<p>(Tan <i>et al.</i>, 2018)</p>
<p>1-Deoxyrubralactone</p>		<p>Polyketide</p>	<p>Unknown alga (Undetermined fungus HJ33moB)</p>	<p>Inhibitor of Eukaryotic DNA polymerases (pols) β and κ:  Eukaryotic DNA polymerases (pols) β: IC<sub>50</sub> = 11.9 μM  Eukaryotic DNA polymerases (pols) κ: IC<sub>50</sub> = 59.8 μM</p>	<p>(Naganuma <i>et al.</i>, 2008)</p>
<p>2-(4-Hydroxybenzyl)quinazolin-4(3H)-one</p>		<p>Quinazolinone</p>	<p>Brown alga <i>Sargassum palladium</i> (<i>Penicillium chrysogenum</i> EN-118)</p>	<p>Cytotoxicity against cancer cell lines:  Du145: IC<sub>50</sub> = 8 μg/mL;  A549: IC<sub>50</sub> = 20 μg/mL;  HeLa: IC<sub>50</sub> = 20 μg/mL</p>	<p>(An <i>et al.</i>, 2013)</p>



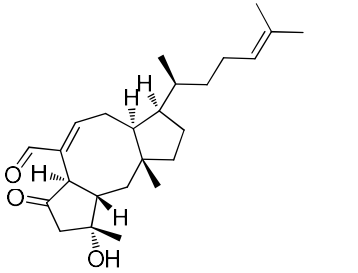
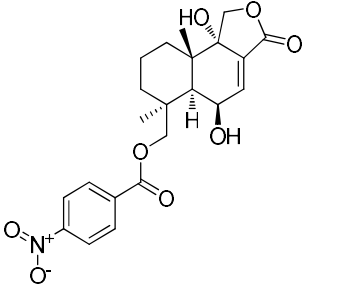
APPENDIX

<p>3-(2-(1-Hydroxy-1-methyl-ethyl)-6-Methyl-2,3-dihydrobenzofuran-4-yloxy)-5-methylphenol</p>		<p>Dihydrobenzofuran derivative</p>	<p>Unidentified alga (<i>Aspergillus tennessensis</i>)</p>	<p>Cytotoxicity against cancer cell line: THP-1: IC<sub>50</sub> = 7.0 µg/mL</p>	<p>(Li <i>et al.</i>, 2018)</p>
<p>3-Hydroxy-5-(hydroxymethyl)-4-(4'-hydroxyphenoxy)pyrrolidin-2-one</p>		<p>Pyrrolidine derivative</p>	<p>Green alga <i>Codium fragile</i> (<i>Gibberella zeae</i>)</p>	<p>Cytotoxicity against cancer cell lines at 10 µM: A549: 61.8% inhibitory rate BEL-7402: 17.6% inhibitory rate</p>	<p>(Liu <i>et al.</i>, 2011)</p>
<p>3β,11α-Dihydroxyergosta-8,24(28)-dien-7-one</p>		<p>Steroid</p>	<p>Brown alga <i>Sargassum kjellmanianum</i> (<i>Aspergillus ochraceus</i> EN-31)</p>	<p>Cytotoxicity against cancer cell line: SMMC-7721: IC<sub>50</sub> = 28.0 µg/mL</p>	<p>(Cui <i>et al.</i>, 2010b)</p>
<p>4-Keto-clonostachydiol</p>		<p>Macrodiolide</p>	<p>Brown alga <i>Durvillaea antarctica</i> (<i>Gliocladium</i> sp.)</p>	<p>Cytotoxicity against cancer cell line: P388: IC<sub>50</sub> = 0.55 µM</p>	<p>(Lang <i>et al.</i>, 2006)</p>
<p>5-Hydroxyramulosin</p>		<p>Polyketide</p>	<p>Brown alga <i>Fucus spiralis</i> (<i>Phoma tropica</i>)</p>	<p>-</p>	<p>(Osterhage <i>et al.</i>, 2002)</p>
			<p>-</p>	<p>Cytotoxicity against cancer cell line: P388: IC<sub>50</sub> = 2.1 µg/mL</p>	<p>(Santiago <i>et al.</i>, 2012)</p>

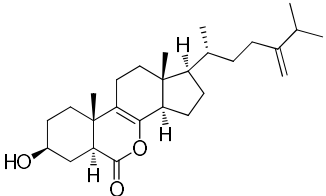
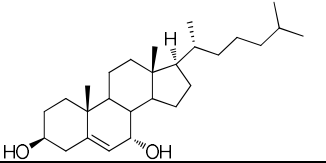
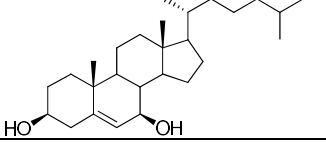
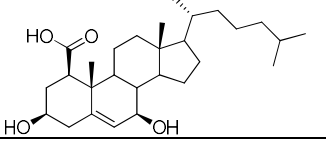
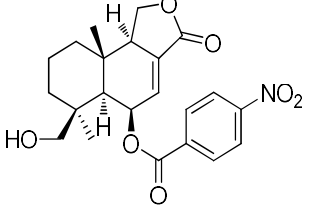
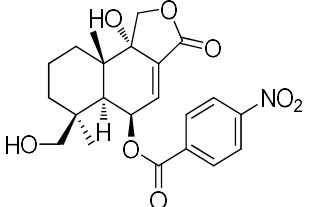
APPENDIX

<p>5-Methoxysterigmatocystin</p>		<p>Polyketide</p>	<p>Brown alga <i>Sargassum</i> (<i>Aspergillus</i> BM-05 and BM-05ML)</p>	<p>Cytotoxicity against cancer cell lines: K562: IC<sub>50</sub> = 13.4 μM HCT116: IC<sub>50</sub> = 4.4 μM A2780: IC<sub>50</sub> = 51.0 μM</p>	<p>(Ebada <i>et al.</i>, 2014a)</p>
<p>6-Epi-ophiobolin N</p>		<p>Sesterpenoid</p>	<p>Brown alga <i>Padina</i> sp. (<i>Aspergillus flocculosus</i>)</p>	<p>Cytotoxicity against 6 cancer cell lines: HCT-15: GI<sub>50</sub> = 0.30 μM NUGC-3: GI<sub>50</sub> = 0.22 μM NCI-H23: GI<sub>50</sub> = 0.22 μM ACHN: GI<sub>50</sub> = 0.23 μM PC-3: GI<sub>50</sub> = 0.20 μM MDA-MB-231: GI<sub>50</sub> = 0.21 μM</p>	<p>(Choi <i>et al.</i>, 2019)</p>

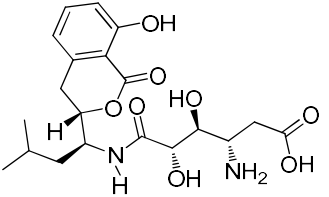
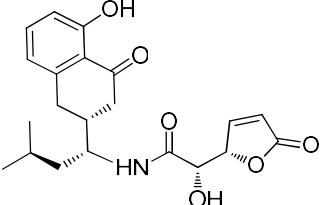
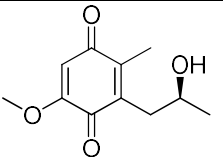
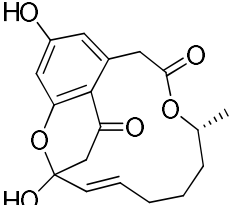
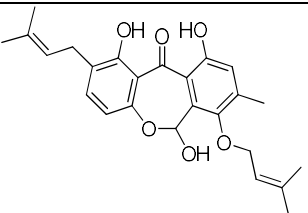
APPENDIX

<p>6-Epi-ophiobolin C</p>		<p>Sesterpenoid</p>	<p>Brown alga <i>Padina</i> sp. (<i>Aspergillus flocculosus</i>)</p>	<p>Cytotoxicity against 6 cancer cell lines: HCT-15: GI<sub>50</sub> = 0.24 μM NUGC-3: GI<sub>50</sub> = 0.22 μM NCI-H23: GI<sub>50</sub> = 0.24 μM ACHN: GI<sub>50</sub> = 0.43 μM PC-3: GI<sub>50</sub> = 0.27 μM MDA-MB-231: GI<sub>50</sub> = 0.19 μM</p>	<p>(Choi <i>et al.</i>, 2019)</p>
<p>6β,9α-Dihydroxy-14-<i>p</i>-nitrobenzoylcinnamolide</p>		<p>Nitrobenzoyl sesquiterpenoid</p>	<p>-</p> <p>Red alga <i>Coelarthrum</i> sp. (<i>Aspergillus ochraceus</i> Jcma1F17)</p>	<p>Cytotoxicity against cancer cell lines: H1975: IC<sub>50</sub> = 2.08 μM U937: IC<sub>50</sub> = 1.95 μM K562: IC<sub>50</sub> = 4.33 μM BGC823: IC<sub>50</sub> = 2.32 μM Molt-4: IC<sub>50</sub> = 2.39 μM MCF-7: IC<sub>50</sub> = 4.25 μM A549: IC<sub>50</sub> = 2.41 μM HeLa: IC<sub>50</sub> = 6.12 μM HL-60: IC<sub>50</sub> = 2.44 μM Hub7: IC<sub>50</sub> = 3.28 μM</p> <p>Cytotoxicity against cancer cell lines: ACHN: IC<sub>50</sub> = 11 μM; OS-RC-2: IC<sub>50</sub> = 8.2 μM; 786-O: IC<sub>50</sub> = 4.3 μM</p>	<p>(Fang <i>et al.</i>, 2014)</p> <p>(Tan <i>et al.</i>, 2018)</p>

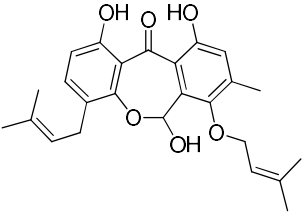
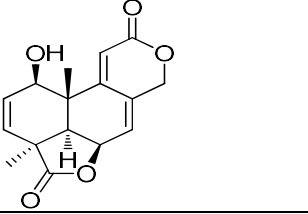
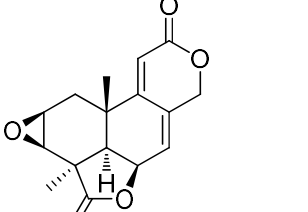
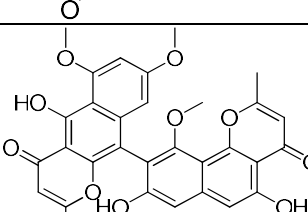
APPENDIX

7-Nor-ergosterolide		Steroid	Brown alga <i>Sargassum kjellmanianum</i> ( <i>Aspergillus ochraceus</i> EN-31)	Cytotoxicity against cancer cell lines: NCI-H460: IC <sub>50</sub> = 5.0 µg/mL SMMC-7721: IC <sub>50</sub> = 7.0 µg/mL SW1990: IC <sub>50</sub> = 28.0 µg/mL	(Cui <i>et al.</i> , 2010b)
7α-Hydroxycholesterol		Steroid	Brown alga <i>Sargassum</i> sp. ( <i>Aspergillus</i> BM-05 and BM-05ML)	Antiproliferative activity against K562, HCT116, A2780, A2780 CisR with IC <sub>50</sub> values from 10.0 to 100.0 µM	(Ebada <i>et al.</i> , 2014b)
7β-Hydroxycholesterol		Steroid	Brown alga <i>Sargassum</i> sp. <i>Aspergillus</i> BM-05 and BM-05ML)	Antiproliferative activity against K562, HCT116, A2780, A2780 CisR with IC <sub>50</sub> values from 10.0 to 100.0 µM	(Ebada <i>et al.</i> , 2014b)
7β-Hydroxycholesterol-1β-carboxylic acid		Steroid	Brown alga <i>Sargassum</i> sp. <i>Aspergillus</i> BM-05 and BM-05ML)	Antiproliferative activity against K562, HCT116, A2780, A2780 CisR with IC <sub>50</sub> values from 10.0 to 100.0 µM	(Ebada <i>et al.</i> , 2014b)
9-Deoxyinsulicolide A		Sesquiterpenoid	Red alga <i>Coelarthrum</i> sp. ( <i>Aspergillus ochraceus</i> Jcma1F17)	Cytotoxicity against cancer cell lines: ACHN: IC <sub>50</sub> = 25 µM OS-RC-2: IC <sub>50</sub> = 30 µM 786-O: IC <sub>50</sub> = 20 µM	(Tan <i>et al.</i> , 2018)
9α,14-Dihydroxy-6β-p-nitrobenzoylcinnamolid		Sesquiterpenoid	Green alga <i>Penicillus captitatus</i> ( <i>Aspergillus versicolor</i> )	Cytotoxicity against cancer cell lines: HCC-298: LD <sub>50</sub> = 0.53 µg/mL HCT116: LD <sub>50</sub> = 0.44 µg/mL SNB75: LD <sub>50</sub> = 0.44 µg/mL BT549: LD <sub>50</sub> = 0.27 µg/mL	(Belofsky <i>et al.</i> , 1998)

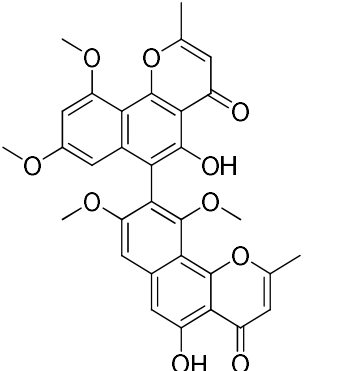
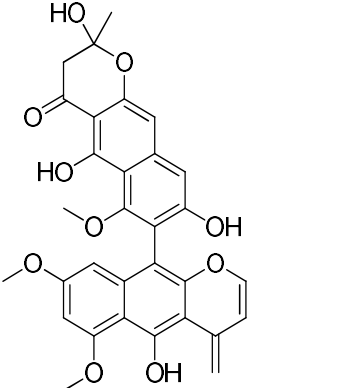
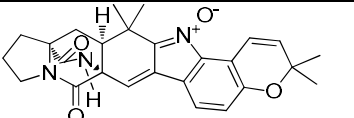
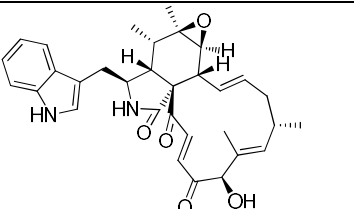
APPENDIX

AI-77-B		Polyketide	Unkown alga ( <i>Alternaria tenuis</i> Sg17-1)	Cytotoxicity against cancer cell lines: A375-S2: IC <sub>50</sub> = 0.3 mM HeLa: IC <sub>50</sub> = 0.05 mM	(Huang <i>et al.</i> , 2006)
AI-77-F		Polyketide	Unkown alga ( <i>Alternaria tenuis</i> Sg17-1)	Cytotoxicity against cancer cell line: HeLa: IC <sub>50</sub> = 0.4 mM	(Huang <i>et al.</i> , 2006)
Anserinone B		Benzoquinone derivatives	Brown alga <i>Padina</i> sp. ( <i>Penicillium citrinum</i> )	Cytotoxicity against cancer cell line: Ehrlich carcinoma cell: ED <sub>50</sub> = 46.1 μM	(Smetanina <i>et al.</i> , 2016)
Apralactone A		Macrolide	Red alga <i>Acanthophora spicifera</i> ( <i>Curvularia</i> sp.)	Toxicity to 36 human tumor cell lines: mean IC <sub>50</sub> = 9.87 μM	(Greve <i>et al.</i> , 2008)
Arugosin A		Benzophenone derivative	Unknown green alga ( <i>Emericella nidulans</i> var. <i>acristata</i> )	Toxicity against 7 tumor cell lines growth at 10 μg/mL	(Kralj <i>et al.</i> , 2006)

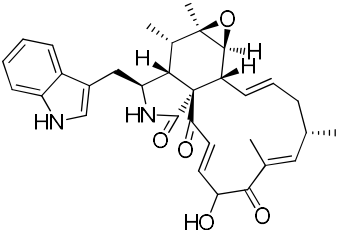
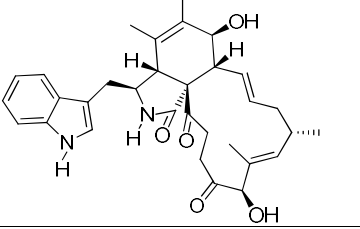
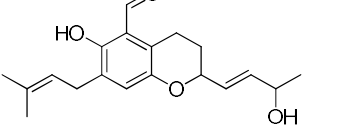
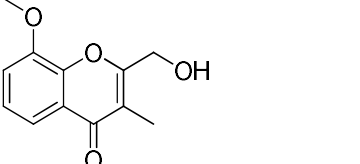
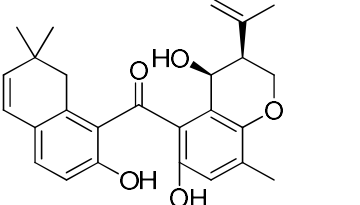
APPENDIX

Arugosin B		Benzophenone derivative	Unknown green alga ( <i>Emericella nidulans</i> var. <i>acristata</i> )	Toxicity against 7 tumor cell lines growth at 10 µg/mL	(Kralj <i>et al.</i> , 2006)
Asperolide A		Tetranorlabdane diterpenoid	Brown alga <i>Sargassum</i> ( <i>Aspergillus wentii</i> EN-48)	Cytotoxicity against cancer cell line: HeLa: IC <sub>50</sub> = 97 µM HepG2: IC <sub>50</sub> = 63 µM NCI-H460: IC <sub>50</sub> = 42 µM SMMC-7721: IC <sub>50</sub> = 52 µM SW1990: IC <sub>50</sub> = 69 µM	(Sun <i>et al.</i> , 2012)
Asperolide B		Tetranorlabdane diterpenoid	Brown alga <i>Sargassum</i> ( <i>Aspergillus wentii</i> EN-48)	Toxicity Cytotoxicity against cancer cell line: HeLa: IC <sub>50</sub> = 56 µM MCF-7: IC <sub>50</sub> = 63 µM MDA-MB-231: IC <sub>50</sub> = 35 µM NCI-H460: IC <sub>50</sub> = 63 µM SW1990: IC <sub>50</sub> = 69 µM	(Sun <i>et al.</i> , 2012)
Asperpyrone A		Dimeric naphtho-γ-pyrone	Brown alga <i>Leathesia nana</i> ( <i>Aspergillus</i> sp. XNM-4)	Cytotoxicity against PANC-1, A549, MDA-MB-231, Caco-2, and SK-OV-3 at 50 µM	(Xu <i>et al.</i> , 2019)

APPENDIX

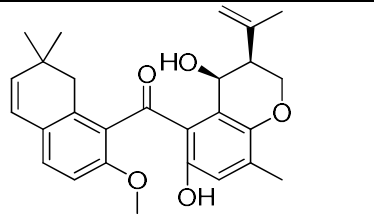
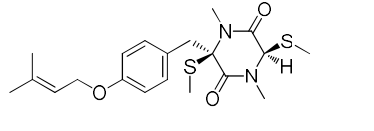
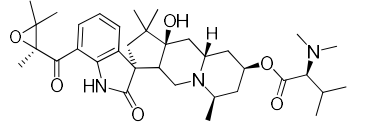
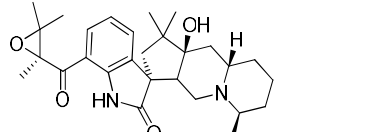
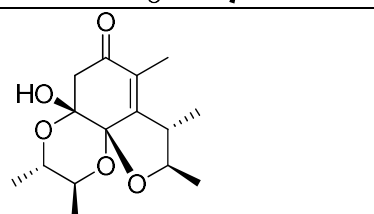
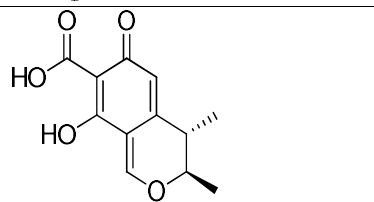
Asperpyrone B		Dimeric naphtho- $\gamma$ -pyrone	Brown alga <i>Leathesia nana</i> ( <i>Aspergillus</i> sp. XNM-4)	Cytotoxicity against PANC-1, A549, MDA-MB-231, Caco-2, and SK-OV-3 at 50 $\mu$ M	(Xu <i>et al.</i> , 2019)
Aurasperone F		Dimeric naphtho- $\gamma$ -pyrone	Brown alga <i>Leathesia nana</i> ( <i>Aspergillus</i> sp. XNM-4)	Cytotoxicity against PANC-1, A549, MDA-MB-231, Caco-2, and SK-OV-3 at 50 $\mu$ M	(Xu <i>et al.</i> , 2019)
Avrainvillamide		Diketopiperazine	Green alga <i>Avrainvillea</i> sp. ( <i>Aspergillus</i> sp. CNC358)	Cytotoxicity against cancer cell line: HCT116: IC <sub>50</sub> = 2.0 $\mu$ g/mL	(Fenical <i>et al.</i> , 2000a)
Chaetoglobosin A		Indole alkaloid	Green alga <i>Enteromorpha intestinalis</i> ( <i>Penicillium</i> sp.)	Cytotoxicity against cancer cell line: P388: ED <sub>50</sub> = 0.6 $\mu$ g/mL	(Numata <i>et al.</i> , 1996)

APPENDIX

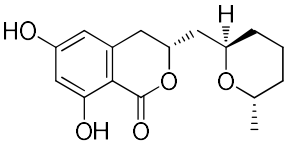
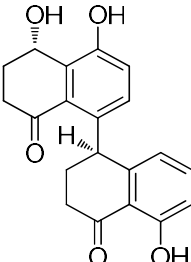
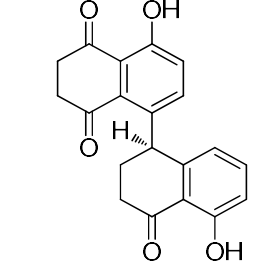
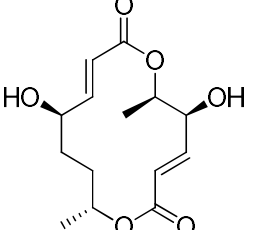
Chaetoglobosin F		Indole alkaloid	Green alga <i>Enteromorpha intestinalis</i> ( <i>Penicillium</i> sp.)	Cytotoxicity against cancer cell line: P388: ED <sub>50</sub> = 0.9 µg/mL	(Numata <i>et al.</i> , 1996)
Chaetoglobosin O		Indole alkaloid	Green alga <i>Enteromorpha intestinalis</i> ( <i>Penicillium</i> sp. OUPS-79)	Cytotoxicity against cancer cell line: P388: ED <sub>50</sub> = 2.4 µg/mL	(Iwamoto <i>et al.</i> , 2001)
Chaetopyranin		Benzaldehyde derivative	Red alga <i>Polysiphonia urceolata</i> ( <i>Chaetomium globosum</i> )	Cytotoxicity against cancer cell lines: HMEC: IC <sub>50</sub> = 15.4 µg/mL SMMC-7721: IC <sub>50</sub> = 28.5 µg/mL A549: IC <sub>50</sub> = 39.1 µg/mL	(Wang <i>et al.</i> , 2006)
Chromanone A		Chromone	Green alga <i>Ulva</i> sp. ( <i>Penicillium</i> sp.)	Inhibit CYP1A activity up to 60% of the stimulated-CYP1A in Hepa1c17	(Gamal-Eldeen <i>et al.</i> , 2009)
Chryxanthone A		Benzophenone	Red alga <i>Grateloupia turuturu</i> ( <i>Penicillium chrysogenum</i> AD-1540)	Cytotoxicity against cancer cell lines: A549: IC <sub>50</sub> = 41.7 µM BT549: IC <sub>50</sub> = 20.4 µM HeLa: IC <sub>50</sub> = 23.5 µM HepG2: IC <sub>50</sub> = 33.6 µM MCF-7: IC <sub>50</sub> = 46.4 µM	(Zhao <i>et al.</i> , 2018)



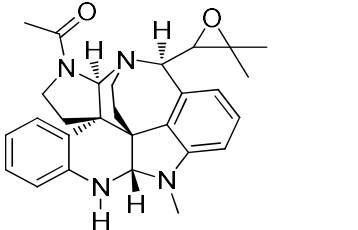
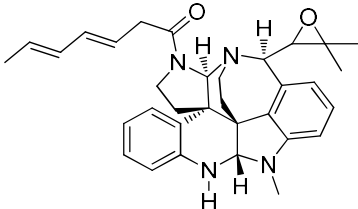
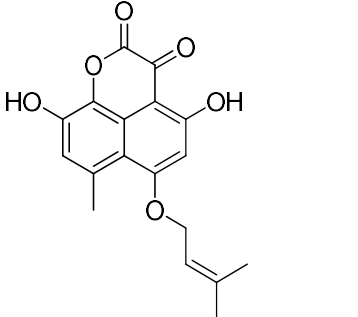
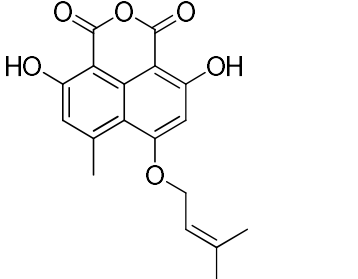
APPENDIX

Chryxanthone B		Benzophenone	Red alga <i>Grateloupia turuturu</i> ( <i>Penicillium chrysogenum</i> AD-1540)	Cytotoxicity against cancer cell lines: A549: IC <sub>50</sub> = 20.4 μM THP-1: IC <sub>50</sub> = 41.1 μM	(Zhao <i>et al.</i> , 2018)
<i>Cis</i> -bisdehthiodi (methylthio) silvatin		Cyclodipeptide	Red alga <i>Carpopeltis affinis</i> ( <i>Fusarium chlamyosporum</i> OUPS-N124)	Cytotoxicity against cancer cell line: P388: ED <sub>50</sub> = 7.7 μg/mL	(Usami <i>et al.</i> , 2002)
Citrinadin A		Pentacyclic indolinone	Red alga <i>Actinotrichia fragilis</i> ( <i>Penicillium citrinum</i> (N059))	Cytotoxicity against cancer cell lines: L1210: ED <sub>50</sub> = 6.2 μg/mL KB: ED <sub>50</sub> = 10 μg/mL	(Mugishima <i>et al.</i> , 2005) (Tsuda <i>et al.</i> , 2004)
Citrinadin B		Pentacyclic indolinone	Red alga <i>Actinotrichia fragilis</i> ( <i>Penicillium citrinum</i> )	Cytotoxicity against cancer cell line: L1210: IC <sub>50</sub> = 10 μg/mL	(Mugishima <i>et al.</i> , 2005)
Citrinal A		Polyketide	Green alga <i>Blidingia minima</i> ( <i>Penicillium</i> sp. i-1-1)	Cytotoxicity against cancer cell lines: A549: IC <sub>50</sub> = 80.7 μmol/L HL-60: IC <sub>50</sub> = 143.1 μmol/L	(Zhu <i>et al.</i> , 2009)
Citrinin		Polyketide	Green alga <i>Blidingia minima</i> ( <i>Penicillium</i> sp. i-1-1)	Cytotoxicity against cancer cell lines: A549: IC <sub>50</sub> = 43.5 μmol/L HL-60 = 62.5 μmol/L	(Zhu <i>et al.</i> , 2009)

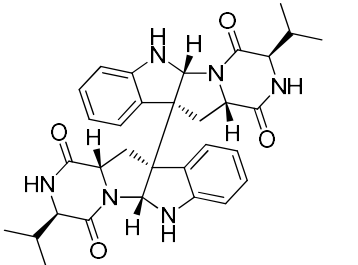
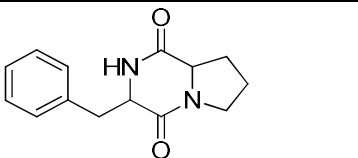
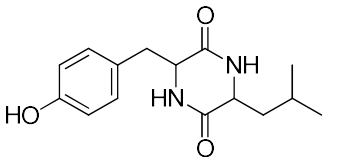
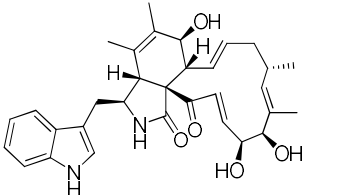
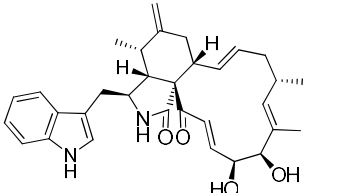
APPENDIX

Cladosporin		Polyketide	Brown alga <i>Fucus spiralis</i> ( <i>Penicillium</i> sp.)	-	(Flewelling <i>et al.</i> , 2013)
			-	-79% antitumor induction in <i>Agrobacterium tumefaciens</i> potato disc assay at 25 µg/disc	(Bryant <i>et al.</i> , 1994)
Cladosporol C		Polyketide	Red alga <i>Laurencia okamurai</i> ( <i>Cladosporium cladosporioides</i> EN-399)	Cytotoxicity against cancer cell line: H446: IC <sub>50</sub> = 4 µM	(Li <i>et al.</i> , 2017)
Cladosporol H		Polyketide	Red alga <i>Laurencia okamurai</i> ( <i>Cladosporium cladosporioides</i> EN-399)	Cytotoxicity against cancer cell lines: A549: IC <sub>50</sub> = 5.0 µM Hub7: IC <sub>50</sub> = 1.0 µM LM3: IC <sub>50</sub> = 4.1 µM	(Li <i>et al.</i> , 2017)
Clonostachydiol		Macrodiolide	Brown alga <i>Durvillaea antarctica</i> ( <i>Gliocladium</i> sp.)	Cytotoxicity against cancer cell line: P388: IC <sub>50</sub> = 25 µM	(Lang <i>et al.</i> , 2006)

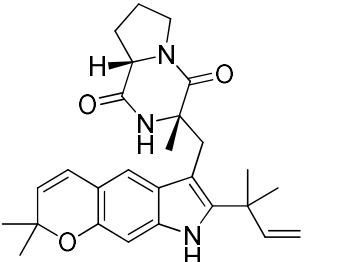
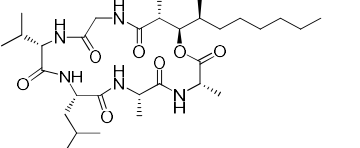
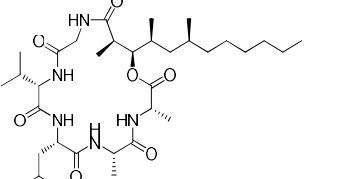
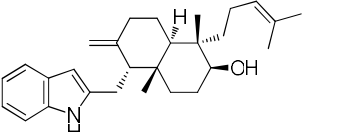
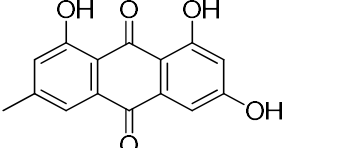
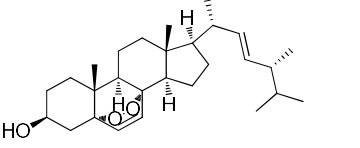
APPENDIX

Communesin A		Alkaloid	Green alga <i>Enteromorpha intestinalis</i> ( <i>Penicillium</i> sp.)	Cytotoxicity against cancer cell line: P388: ED <sub>50</sub> = 3.5 µg/mL	(Numata <i>et al.</i> , 1993)
Communesin B		Alkaloid	Green alga <i>Enteromorpha intestinalis</i> ( <i>Penicillium</i> sp.)	Cytotoxicity against cancer cell line: P388: ED <sub>50</sub> = 0.45 µg/mL	(Numata <i>et al.</i> , 1993)
Conioscleroderolide		Phenalenone derivative	Green alga <i>Enteromorpha</i> sp. ( <i>Coniothyrium cereale</i> )	Cytotoxicity against cancer cell line: HLE IC <sub>50</sub> = 13.3 µM	(Nazir <i>et al.</i> , 2015)
Coniosclerodin		Phenalenone derivative	Green alga <i>Enteromorpha</i> sp. ( <i>Coniothyrium cereale</i> )	Cytotoxicity against cancer cell line: HLE IC <sub>50</sub> = 7.2 µM	(Nazir <i>et al.</i> , 2015)

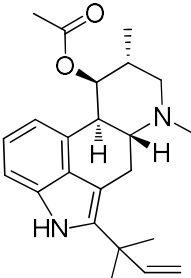
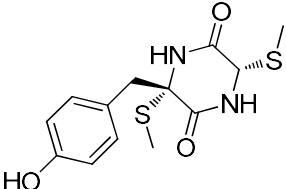
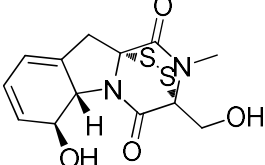
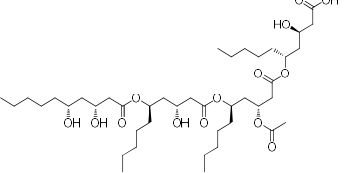
APPENDIX

Cristatumin E		Pyrrolidinoindoline diketopiperazin	Green alga <i>Enteromorpha prolifera</i> ( <i>Eurotium herbariorum</i> HT-2)	Cytotoxicity against cancer cell line: K562: IC <sub>50</sub> = 8.3 μmol/L	(Li <i>et al.</i> , 2013b)
Cyclo-(Phe-Pro)		Diketopiperazine	Green alga <i>Undaria pinnatifida</i> ( <i>Guignardia</i> sp.)	Cytotoxicity against cancer cell line: KB: IC <sub>50</sub> = 10 μg/mL	(Wang, 2012)
Cyclo-(Tyr-Leu)		Diketopiperazine	Green alga <i>Undaria pinnatifida</i> ( <i>Guignardia</i> sp.)	Cytotoxicity against cancer cell line: KB: IC <sub>50</sub> = 10 μg/mL	(Wang, 2012)
Cytoglobosin C		Indole alkaloid	Green alga <i>Ulva pertusa</i> ( <i>Chaetomium globosum</i> QEN-14)	Cytotoxicity against cancer cell line: A549: IC <sub>50</sub> = 2.26 μM	(Cui <i>et al.</i> , 2010a)
Cytoglobosin D		Indole alkaloid	Green alga <i>Ulva pertusa</i> ( <i>Chaetomium globosum</i> QEN-14)	Cytotoxicity against cancer cell line: A549: IC <sub>50</sub> = 2.55 μM	(Cui <i>et al.</i> , 2010a)

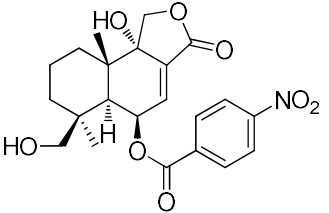
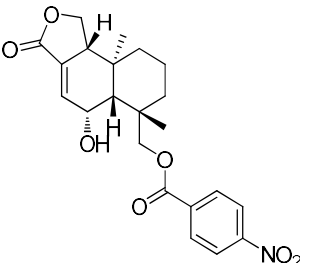
APPENDIX

Dihydrocarneamide A		Prenylated indole alkaloid	Red alga <i>Grateloupia turuturu</i> ( <i>Paecilomyces variotii</i> EN-291)	Cytotoxicity against cancer cell line: NCI-H460: IC <sub>50</sub> = 69.3 μmol/L	(Zhang <i>et al.</i> , 2015)
Emericellamide A		Cyclic depsipeptide	Green alga <i>Halimeda</i> sp. ( <i>Emericella</i> sp. CNL-878)	Cytotoxicity against cancer cell line: HCT116: IC <sub>50</sub> = 23 μM	(Oh <i>et al.</i> , 2007)
Emericellamide B		Cyclic depsipeptide	Green alga <i>Halimeda</i> sp. ( <i>Emericella</i> sp. CNL-878)	Cytotoxicity against cancer cell line: HCT116: IC <sub>50</sub> = 40 μM	(Oh <i>et al.</i> , 2007)
emindole DA		Indole diterpene	Unkonwn green alga ( <i>Emericella nidulans</i> var. <i>acristata</i> )	Toxicity against 36 tumor cell lines: mean IC <sub>50</sub> = 5.5 μg/mL	(Kralj <i>et al.</i> , 2006)
Emodine		Anthraquinone	Green alga <i>Halimeda opuntia</i> ( <i>Aspergillus versicolor</i> )	Weak anticancer bioactivity against HCT116 at 250 μg/disk	(Hawas <i>et al.</i> , 2012)
Ergosterol peroxide		Steroid	Green alga <i>Undaria pinnatifida</i> ( <i>Guignardia</i> sp.)	Cytotoxicity against cancer cell line: KB: = IC <sub>50</sub> 20 μg/mL	(Wang, 2012)
			Brown alga <i>Sargassum</i> sp. <i>Aspergillus</i> BM-05 and BM-05ML)	Antiproliferative activity against K562, HCT116, A2780, A2780 cisR with	(Ebada <i>et al.</i> , 2014b)

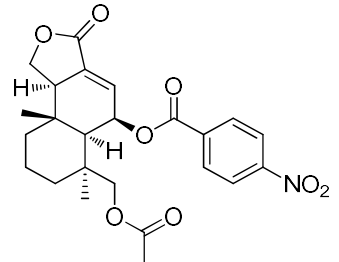
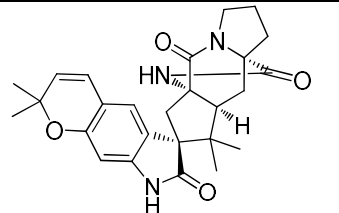
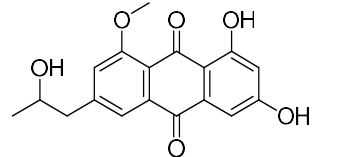
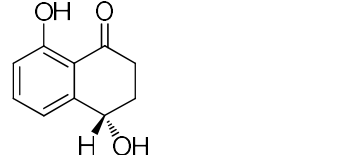
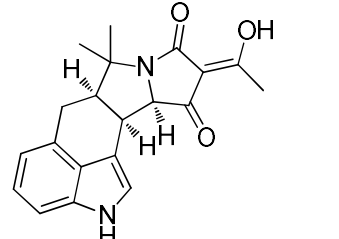
APPENDIX

Fumigaclavine C		Indole alkaloid	Unknown green alga ( <i>Aspergillus fumigatus</i> )	IC <sub>50</sub> values from 10 to 100 μM Inducing apoptosis in MCF-7 cell at 60 μM	(Li <i>et al.</i> , 2013a)
Fusaperazine A		Dioxopiperazine	Red alga <i>Carpopeltis affinis</i> ( <i>Fusarium chlamyosporum</i> OUPS-N124)	Cytotoxicity against cancer cell line: P388: ED <sub>50</sub> = 22.8 μg/mL	(Usami <i>et al.</i> , 2002)
Gliotoxin		Diketopiperazine	Unknown brown alga ( <i>Aspergillus</i> sp. YL-6)	Toxicity on HeLa and human SW1353 cells with inhibition rates 94% and 83% at 10 μM	(Nguyen <i>et al.</i> , 2014)
Halymecin A		Mannosyl lipid	Red alga <i>Halymenia dilatata</i> ( <i>Fusarium</i> sp. FE-71-1)	Cytotoxicity against cancer cell lineS: HeLa S3 = IC <sub>50</sub> 6 μg/mL Balb3T3 = IC <sub>50</sub> 7 μg/mL	(Chen <i>et al.</i> , 1996)

APPENDIX

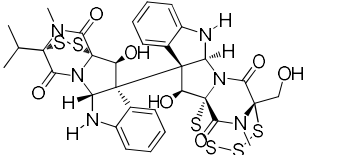
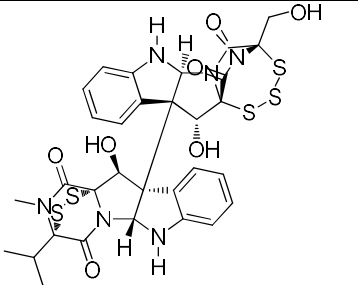
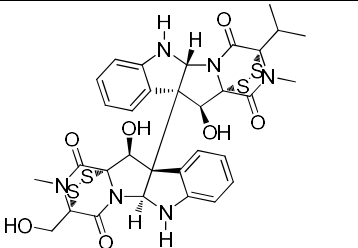
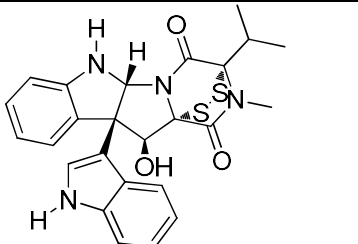
Insulicolide A		Nitrobenzoyl sesquiterpenoid	Unidentified green alga ( <i>Aspergillus insulicola</i> )	-	(Rahbæk <i>et al.</i> , 1997)
			Red alga <i>Coelarthrum</i> sp. ( <i>Aspergillus ochraceus</i> Jcma1F17)	Cytotoxicity against ACHN IC <sub>50</sub> = 1.5 µM OS-RC-2 IC <sub>50</sub> = 1.5 µM 786-O IC <sub>50</sub> = 0.89 µM	(Tan <i>et al.</i> , 2018)
				Cytotoxicity against cancer cell lines: H1975: IC <sub>50</sub> = 4.63 µM U937: IC <sub>50</sub> = 3.97 µM K562: IC <sub>50</sub> = 4.76 µM BGC823: IC <sub>50</sub> = 2.78 µM Molt-4: IC <sub>50</sub> = 2.11 µM MCF-7: IC <sub>50</sub> = 6.08 µM A549: IC <sub>50</sub> = 2.86 µM HeLa: IC <sub>50</sub> = 6.35 µM HL-60: IC <sub>50</sub> = 2.34 µM Hub7: IC <sub>50</sub> = 2.35 µM	(Fang <i>et al.</i> , 2014)
Insulicolide B		Nitrobenzoyl sesquiterpenoid	Red alga <i>Coelarthrum</i> sp. ( <i>Aspergillus ochraceus</i> Jcma1F17)	Cytotoxicity against cancer cell lines: ACHN: IC <sub>50</sub> = 30 µM OS-RC-2: IC <sub>50</sub> = 23 µM 786-O IC <sub>50</sub> = 24 µM	(Tan <i>et al.</i> , 2018)

APPENDIX

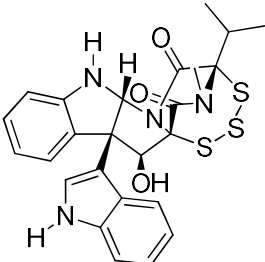
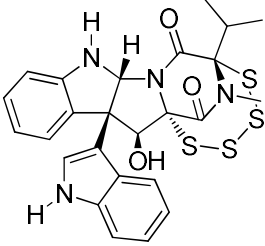
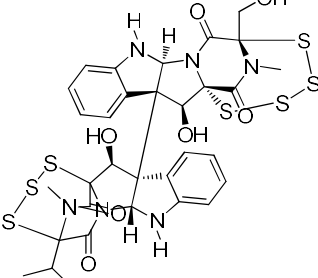
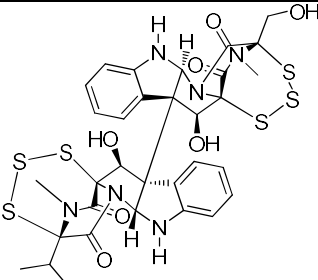
Insulicolide C		Nitrobenzoyl sesquiterpenoid	Red alga <i>Coelarthrum</i> sp. ( <i>Aspergillus ochraceus</i> Jcma1F17)	Cytotoxicity against cancer cell lines: ACHN: IC <sub>50</sub> = 13 μM OS-RC-2: IC <sub>50</sub> = 11 μM 786-O IC <sub>50</sub> = 14 μM	(Tan <i>et al.</i> , 2018)
Iso-notoamide B		Prenylated indole alkaloid	Red alga <i>Grateloupia turuturu</i> ( <i>Paecilomyces variotii</i> EN-291)	Cytotoxicity against cancer cell line: NCI-H460: IC <sub>50</sub> = 55.9 μmol/L	(Zhang <i>et al.</i> , 2015)
Isorhodoptilometrin-1-methyl ether		Anthraquinone	Green alga <i>Halimeda opuntia</i> ( <i>Aspergillus versicolor</i> )	Weak anticancer bioactivity against LH1210, H125 and HepG2 at 350, 300, 400 μg/disk	(Hawas <i>et al.</i> , 2012)
Isosclerone		Polyketide	Unknown green alga ( <i>Aspergillus fumigatus</i> )	Cytotoxicity against cancer cell line: MCF-7: IC <sub>50</sub> = 60 μM	(Li <i>et al.</i> , 2014)
Iso-α-cyclopiazonic acid		Ergoline alkaloid	Green alga <i>Enteromorpha tubulosa</i> ( <i>Aspergillus flavus</i> c-f-3)	Cytotoxicity against cancer cell lines: HL-60: IC <sub>50</sub> = 90 μM MoLT-4: IC <sub>50</sub> = 68.6 μM A-549: IC <sub>50</sub> = 42.2 μM	(Lin <i>et al.</i> , 2009)



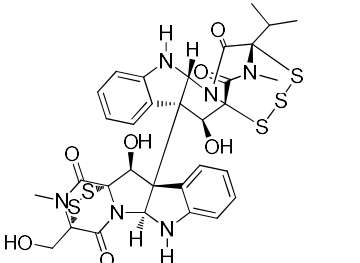
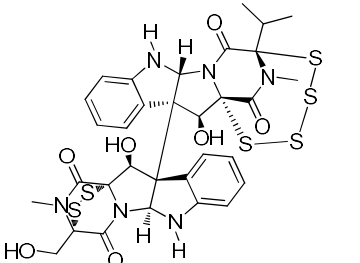
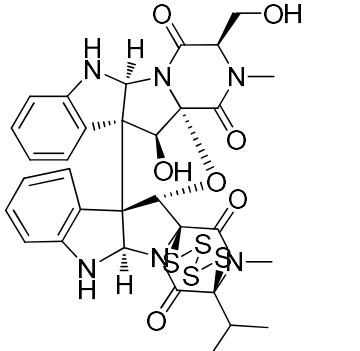
APPENDIX

Leptosin A		Epipolythiodioxopiperazine	Brown alga <i>Sargassum tortile</i> ( <i>Leptosphaeria</i> sp.)	Cytotoxicity against cancer cell line: P388: IC <sub>50</sub> = 1.85 ng/mL	(Takahashi <i>et al.</i> , 1994a)
Leptosin B		Epipolythiodioxopiperazine	Brown alga <i>Sargassum tortile</i> ( <i>Leptosphaeria</i> sp.)	Cytotoxicity against cancer cell line: P388: IC <sub>50</sub> = 2.40 ng/mL	(Takahashi <i>et al.</i> , 1994a)
Leptosin C		Epipolythiodioxopiperazine	Brown alga <i>Sargassum tortile</i> ( <i>Leptosphaeria</i> sp.)	Cytotoxicity against cancer cell line: P388: IC <sub>50</sub> = 1.75 ng/mL	(Takahashi <i>et al.</i> , 1994a)
Leptosin D		Epipolythiodioxopiperazine	Brown alga <i>Sargassum tortile</i> ( <i>Leptosphaeria</i> sp.)	Cytotoxicity against cancer cell line: P388: IC <sub>50</sub> = 86 ng/mL	(Takahashi <i>et al.</i> , 1994a)

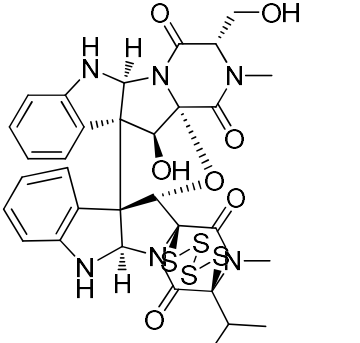
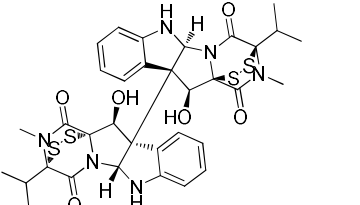
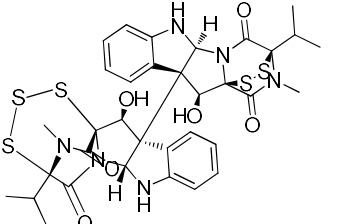
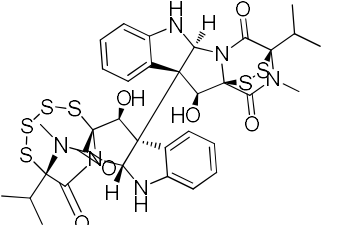
APPENDIX

Leptosin E		Epipolythiodioxopiperazine	Brown alga <i>Sargassum tortile</i> ( <i>Leptosphaeria</i> sp.)	Cytotoxicity against cancer cell line: P388: IC <sub>50</sub> = 46 ng/mL	(Takahashi <i>et al.</i> , 1994a)
Leptosin F		Epipolythiodioxopiperazine	Brown alga <i>Sargassum tortile</i> ( <i>Leptosphaeria</i> sp.)	Cytotoxicity against cancer cell line: P388: IC <sub>50</sub> = 56 ng/mL	(Takahashi <i>et al.</i> , 1994a)
Leptosin G		Epipolythiodioxopiperazine	Brown alga <i>Sargassum tortile</i> ( <i>Leptosphaeria</i> sp.)	Cytotoxicity against cancer cell line: P388: IC <sub>50</sub> = 4.6 ng/mL	(Takahashi <i>et al.</i> , 1995b)
Leptosin G <sub>1</sub>		Epipolythiodioxopiperazine	Brown alga <i>Sargassum tortile</i> ( <i>Leptosphaeria</i> sp.)	Cytotoxicity against cancer cell line: P388: ED <sub>50</sub> = 4.3 ng/mL	(Takahashi <i>et al.</i> , 1995b)

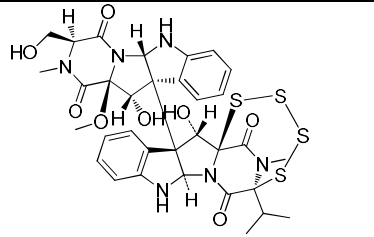
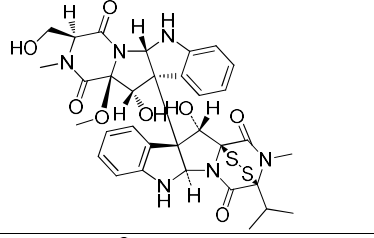
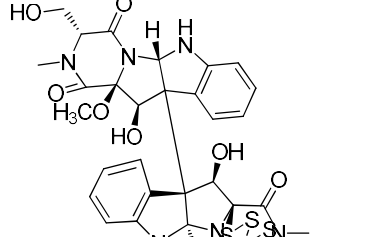
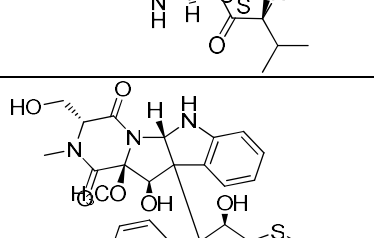
APPENDIX

Leptosin G <sub>2</sub>		Epipolythiodioxopiperazine	Brown alga <i>Sargassum tortile</i> ( <i>Leptosphaeria</i> sp.)	Cytotoxicity against cancer cell line: P388: ED <sub>50</sub> = 4.4 ng/mL	(Takahashi <i>et al.</i> , 1995b)
Leptosin H		Epipolythiodioxopiperazine	Brown alga <i>Sargassum tortile</i> ( <i>Leptosphaeria</i> sp.)	Cytotoxicity against cancer cell line: P388: ED <sub>50</sub> = 3.0 ng/mL	(Takahashi <i>et al.</i> , 1995b)
Leptosin I		Epipolythiodioxopiperazine	Brown alga <i>Sargassum tortile</i> ( <i>Leptosphaeria</i> sp.)	Cytotoxicity against cancer cell line: P388: ED <sub>50</sub> = 1.13 µg/mL	(Takahashi <i>et al.</i> , 1994b)

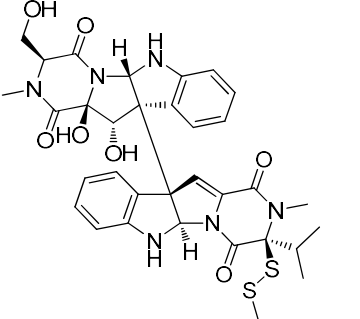
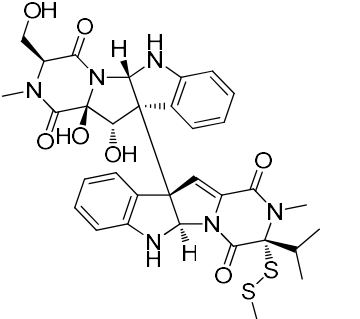
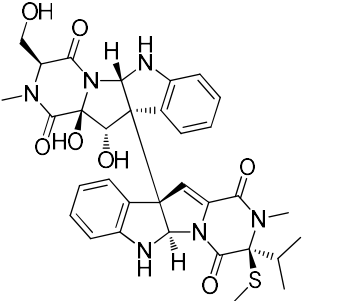
APPENDIX

Leptosin J		Epipolythiodioxopiperazine	Brown alga <i>Sargassum tortile</i> ( <i>Leptosphaeria</i> sp.)	Cytotoxicity against cancer cell line: P388: ED <sub>50</sub> = 1.25 µg/mL	(Takahashi <i>et al.</i> , 1994b)
Leptosin K		Epipolythiodioxopiperazine	Brown alga <i>Sargassum tortile</i> ( <i>Leptosphaeria</i> sp.)	Cytotoxicity against cancer cell line: P388: ED <sub>50</sub> = 3.8 ng/mL	(Takahashi <i>et al.</i> , 1995a)
Leptosin K <sub>1</sub>		Epipolythiodioxopiperazine	Brown alga <i>Sargassum tortile</i> ( <i>Leptosphaeria</i> sp.)	Cytotoxicity against cancer cell line: P388: ED <sub>50</sub> = 2.8 ng/mL	(Takahashi <i>et al.</i> , 1995a)
Leptosin K <sub>2</sub>		Epipolythiodioxopiperazine	Brown alga <i>Sargassum tortile</i> ( <i>Leptosphaeria</i> sp.)	Cytotoxicity against cancer cell line: P388: ED <sub>50</sub> = 2.1 ng/mL	(Takahashi <i>et al.</i> , 1995a)

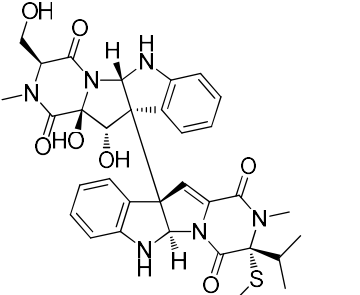
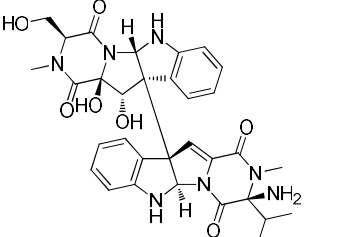
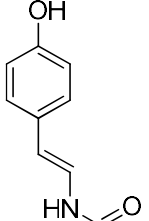
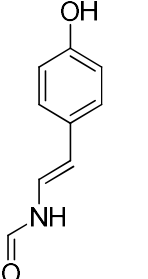
APPENDIX

Leptosin M		Epipolythiodioxopiperazine	Brown alga <i>Sargassum tortile</i> ( <i>Leptosphaeria</i> sp.)	Cytotoxicity against cancer cell line: P388: ED <sub>50</sub> = 1.05 µg/mL	(Yamada <i>et al.</i> , 2002)
Leptosin M <sub>1</sub>		Epipolythiodioxopiperazine	Brown alga <i>Sargassum tortile</i> ( <i>Leptosphaeria</i> sp.)	Cytotoxicity against cancer cell line: P388: ED <sub>50</sub> = 1.40 µg/mL	(Yamada <i>et al.</i> , 2002)
Leptosin N		Epipolythiodioxopiperazine	Brown alga <i>Sargassum tortile</i> ( <i>Leptosphaeria</i> sp.)	Cytotoxicity against cancer cell line: P388: ED <sub>50</sub> = 0.18 µg/mL	(Yamada <i>et al.</i> , 2002)
Leptosin N <sub>1</sub>		Epipolythiodioxopiperazine	Brown alga <i>Sargassum tortile</i> ( <i>Leptosphaeria</i> sp.)	Cytotoxicity against cancer cell line: P388: ED <sub>50</sub> = 0.19 µg/mL	(Yamada <i>et al.</i> , 2002)

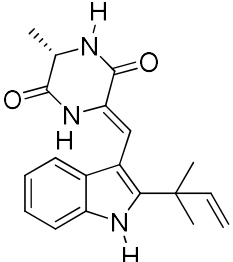
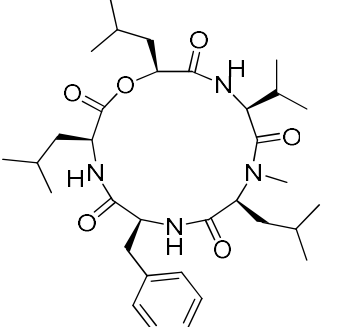
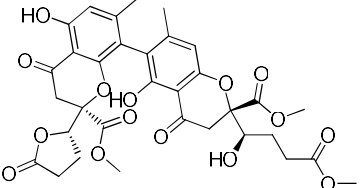
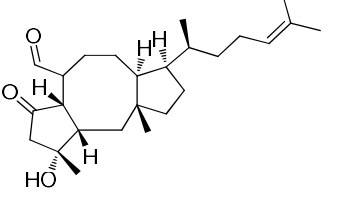
APPENDIX

Leptosin O	 <p>The chemical structure of Leptosin O is a complex polythiodioxopiperazine. It features a central piperazine ring system with multiple sulfur atoms (S) and carbonyl groups (C=O). The structure includes a phenyl ring, a hydroxyl group (OH), and a methyl group (CH3). The stereochemistry is indicated with wedges and dashes.</p>	Epipolythiodioxopiperazine	Brown alga <i>Sargassum tortile</i> ( <i>Leptosphaeria</i> sp.)	Cytotoxicity against cancer cell line: P388: ED <sub>50</sub> = 1.1 µg/mL Moderate cytotoxicity againsts 39 human cancer cell lines with mean log GI <sub>50</sub> -4.01M	(Yamada <i>et al.</i> , 2004)
Leptosin P	 <p>The chemical structure of Leptosin P is a complex polythiodioxopiperazine, very similar to Leptosin O. It features a central piperazine ring system with multiple sulfur atoms (S) and carbonyl groups (C=O). The structure includes a phenyl ring, a hydroxyl group (OH), and a methyl group (CH3). The stereochemistry is indicated with wedges and dashes.</p>	Epipolythiodioxopiperazine	Brown alga <i>Sargassum tortile</i> ( <i>Leptosphaeria</i> sp.)	Cytotoxicity against cancer cell line: P388: ED <sub>50</sub> = 0.1 µg/mL	(Yamada <i>et al.</i> , 2004)
Leptosin Q	 <p>The chemical structure of Leptosin Q is a complex polythiodioxopiperazine, very similar to Leptosin O and P. It features a central piperazine ring system with multiple sulfur atoms (S) and carbonyl groups (C=O). The structure includes a phenyl ring, a hydroxyl group (OH), and a methyl group (CH3). The stereochemistry is indicated with wedges and dashes.</p>	Epipolythiodioxopiperazine	Brown alga <i>Sargassum tortile</i> ( <i>Leptosphaeria</i> sp.)	Cytotoxicity against cancer cell line: P388: ED <sub>50</sub> = 14.8 µg/mL	(Yamada <i>et al.</i> , 2004)

APPENDIX

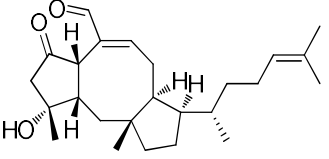
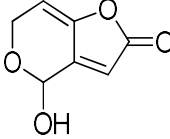
<p>Leptosin R</p>		<p>Epipolythiodioxopiperazine</p>	<p>Brown alga <i>Sargassum tortile</i> (<i>Leptosphaeria</i> sp.)</p>	<p>Cytotoxicity against cancer cell line: P388: ED<sub>50</sub> = 15.2 µg/mL</p>	<p>(Yamada <i>et al.</i>, 2004)</p>
<p>Leptosin S</p>		<p>Epipolythiodioxopiperazine</p>	<p>Brown alga <i>Sargassum tortile</i> (<i>Leptosphaeria</i> sp.)</p>	<p>Cytotoxicity against cancer cell line: P388: ED<sub>50</sub> = 10.1 µg/mL; cytotoxicity againsts 39 human cancer cell lines with mean log GI<sub>50</sub> -4.01M</p>	<p>(Yamada <i>et al.</i>, 2004)</p>
<p>N-[(2E)-(4-Hydroxyphenyl)ethenyl]formamide</p>		<p>Alkaloid</p>	<p>Brown alga <i>Sargassum palladium</i> (<i>Penicillium chrysogenum</i> EN-118)</p>	<p>Cytotoxicity against cancer cell lines: Du145: IC<sub>50</sub> = 8 µg/mL A549: IC<sub>50</sub> = 20 µg/mL HeLa: IC<sub>50</sub> = 20 µg/mL</p>	<p>(An <i>et al.</i>, 2013)</p>
<p>N-[(2Z)-(4-Hydroxyphenyl)acetyl]formamide</p>		<p>Alkaloid</p>	<p>Brown alga <i>Sargassum palladium</i> (<i>Penicillium chrysogenum</i> EN-118)</p>	<p>Cytotoxicity against cancer cell lines: Du145: IC<sub>50</sub> = 8 µg/mL A549: IC<sub>50</sub> = 20 µg/mL HeLa: IC<sub>50</sub> = 20 µg/mL</p>	<p>(An <i>et al.</i>, 2013)</p>

APPENDIX

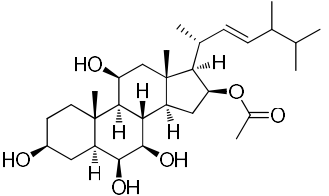
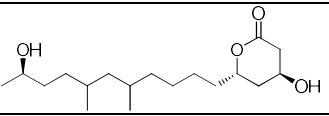
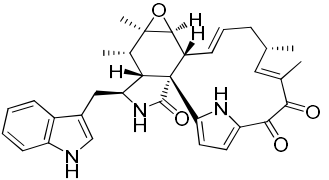
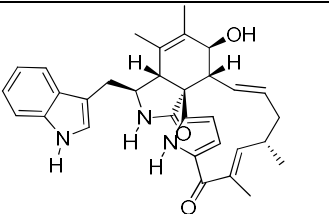
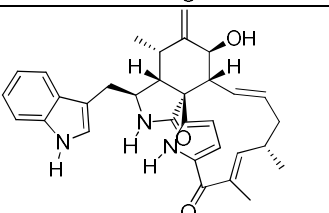
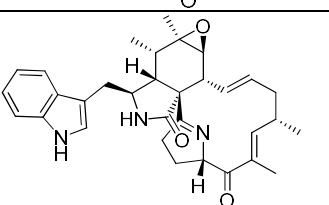
<p>Neochinulin A</p>		<p>Indole alkaloid</p>	<p>Red alga <i>Lomentaria catenata</i> (<i>Microsporium</i> sp.)</p>	<p>Inhibition rate higher than 50% against HeLa cells at 100 <math>\mu</math>M</p>	<p>(Wijsekara <i>et al.</i>, 2013)</p>
<p>N-methylsansalvamide</p>		<p>Cyclic depsipeptide</p>	<p>Green alga <i>Avrainvillea</i> sp. (<i>Fusarium</i> CNL-619)</p>	<p>Cytotoxicity against NCI human tumor: <math>GI_{50}</math> = 8.3 <math>\mu</math>M</p>	<p>(Cueto <i>et al.</i>, 2000)</p>
<p>Noduliprevenone</p>		<p>Polyketide</p>	<p>Unknown Mediterranean alga (<i>Nodulisporium</i> sp.)</p>	<p>inhibitor of CYP1A activity in vitro, with an <math>IC_{50}</math> value of <math>6.5 \pm 1.6</math> <math>\mu</math>M</p>	<p>(Pontius <i>et al.</i>, 2008)</p>
<p>Ophiobolin N</p>		<p>Sesterpenoid</p>	<p>Brown alga <i>Padina</i> sp. (<i>Aspergillus flocculosus</i>)</p>	<p>Cytotoxicity against 6 cancer cell lines: HCT-15: <math>GI_{50}</math> = 0.30 <math>\mu</math>M NUGC-3: <math>GI_{50}</math> = 0.22 <math>\mu</math>M NCI-H23: <math>GI_{50}</math> = 0.22 <math>\mu</math>M ACHN: <math>GI_{50}</math> = 0.23 <math>\mu</math>M PC-3: <math>GI_{50}</math> = 0.20 <math>\mu</math>M MDA-MB-231: <math>GI_{50}</math> = 0.21 <math>\mu</math>M</p>	<p>(Choi <i>et al.</i>, 2019)</p>



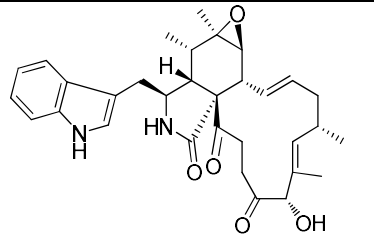
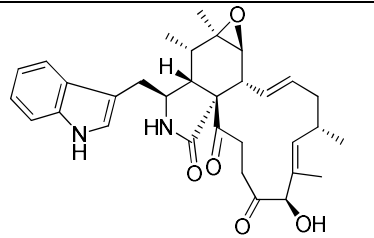
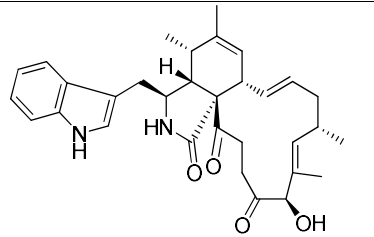
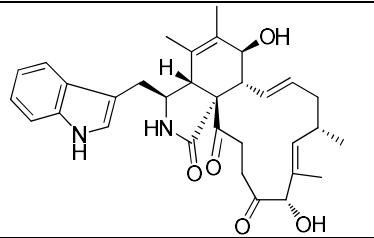
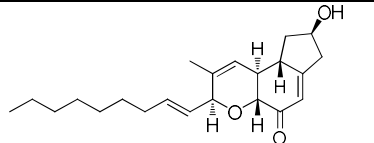
APPENDIX

Ophiobolin C		Sesterpenoid	Brown alga <i>Padina</i> sp. ( <i>Aspergillus flocculosus</i> )	Cytotoxicity against 6 cancer cell lines: HCT-15: GI <sub>50</sub> = 0.21 μM NUGC-3: GI <sub>50</sub> = 0.20 μM NCI-H23: GI <sub>50</sub> = 0.16 μM ACHN: GI <sub>50</sub> = 0.20 μM PC-3: GI <sub>50</sub> = 0.36 μM MDA-MB-231: GI <sub>50</sub> = 0.22 μM	(Choi <i>et al.</i> , 2019)
Patulin		Polyketide	Brown alga <i>Fucus spiralis</i> ( <i>Penicillium</i> sp.)	-	(Flewelling <i>et al.</i> , 2013)
			Green alga <i>Enteromorpha intestinalis</i> ( <i>Penicillium</i> sp. OUPS-79)	Cytotoxicity against cancer cell line: P388: ED <sub>50</sub> = 0.06 μg/mL BSY-1: ED <sub>50</sub> = 0.34 μg/mL MCF-7: ED <sub>50</sub> = 0.65 μg/mL HCC2998: ED <sub>50</sub> = 1.54 μg/mL NCI-H522: ED <sub>50</sub> = 0.30 μg/mL DMS114: ED <sub>50</sub> = 0.57 μg/mL OVCAR-3: ED <sub>50</sub> = 0.37 μg/mL MKN: ED <sub>50</sub> = 0.39 μg/mL	(Iwamoto <i>et al.</i> , 1999)
				66% antitumor induction in <i>Agrobacterium tumefaciens</i> potato disc assay at 25 μg/disc	(Bryant <i>et al.</i> , 1994)
				SW-48: 55% inhibition rate at 4 μM HeLa: 65% inhibition rate at 4 μM	(Abastabar <i>et al.</i> , 2017)

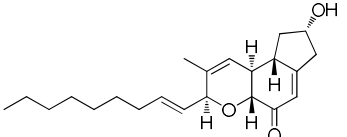
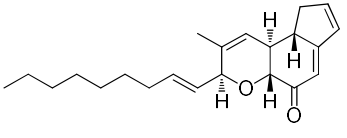
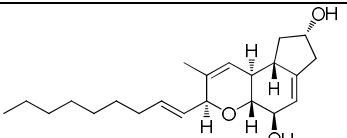
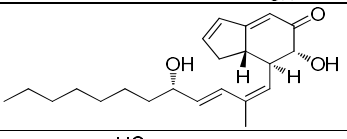
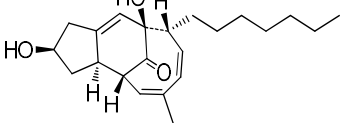
APPENDIX

Penicisteroid A		Polyoxygenated steroid	Red alga <i>Laurencia</i> sp. ( <i>penicillium chrysogenum</i> QEN-24S)	Cytotoxicity against cancer cell lines: HeLa: IC <sub>50</sub> = 15 µg/mL SW1990: IC <sub>50</sub> = 31 µg/mL NCI-H460: IC <sub>50</sub> = 40 µg/mL	(Gao <i>et al.</i> , 2011b)
Penicitide A		Polyketide	Red alga <i>Laurencia</i> sp. ( <i>Penicillium chrysogenum</i> QEN-24S)	Cytotoxicity against cancer cell line: HepG2 IC <sub>50</sub> = 32 µg/mL	(Gao <i>et al.</i> , 2011a)
Penochalasin A		Indole alkaloid	Green alga <i>Enteromorpha intestinalis</i> ( <i>Penicillium</i> sp.)	Cytotoxicity against cancer cell line: P388: ED <sub>50</sub> = 0.4 µg/mL	(Numata <i>et al.</i> , 1996)
Penochalasin B		Indole alkaloid	Green alga <i>Enteromorpha intestinalis</i> ( <i>Penicillium</i> sp.)	Cytotoxicity against cancer cell line: P388: ED <sub>50</sub> = 0.3 µg/mL	(Numata <i>et al.</i> , 1996)
Penochalasin C		Indole alkaloid	Green alga <i>Enteromorpha intestinalis</i> ( <i>Penicillium</i> sp.)	Cytotoxicity against cancer cell line: P388: ED <sub>50</sub> = 0.5 µg/mL	(Numata <i>et al.</i> , 1996)
Penochalasin D		Indole alkaloid	Green alga <i>Enteromorpha intestinalis</i> ( <i>Penicillium</i> sp. OUPS-79)	Cytotoxicity against cancer cell line: P388: ED <sub>50</sub> = 3.2 µg/mL	(Iwamoto <i>et al.</i> , 2001)

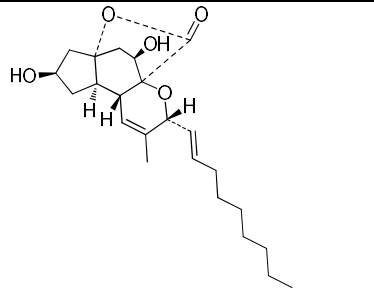
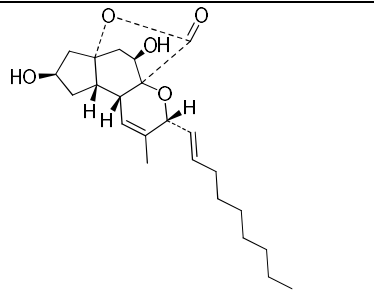
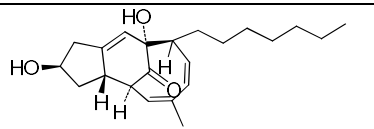
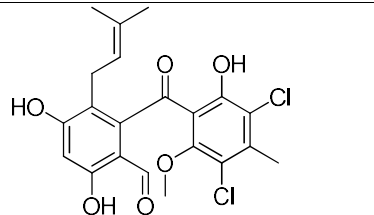
APPENDIX

Penochalasin E		Indole alkaloid	Green alga <i>Enteromorpha intestinalis</i> ( <i>Penicillium</i> sp. OUPS-79)	Cytotoxicity against cancer cell line: P388: ED <sub>50</sub> = 2.1 µg/mL	(Iwamoto <i>et al.</i> , 2001)
Penochalasin F		Indole alkaloid	Green alga <i>Enteromorpha intestinalis</i> ( <i>Penicillium</i> sp. OUPS-79)	Cytotoxicity against cancer cell line: P388: ED <sub>50</sub> = 1.8 µg/mL	(Iwamoto <i>et al.</i> , 2001)
Penochalasin G		Indole alkaloid	Green alga <i>Enteromorpha intestinalis</i> ( <i>Penicillium</i> sp. OUPS-79)	Cytotoxicity against cancer cell line: P388: ED <sub>50</sub> = 1.9 µg/mL	(Iwamoto <i>et al.</i> , 2001)
Penochalasin H		Indole alkaloid	Green alga <i>Enteromorpha intestinalis</i> ( <i>Penicillium</i> sp. OUPS-79)	Cytotoxicity against cancer cell line: P388: ED <sub>50</sub> = 2.8 µg/mL	(Iwamoto <i>et al.</i> , 2001)
Penostatin A		Polyketide	Green alga <i>Enteromorpha intestinalis</i> ( <i>Penicillium</i> sp. OUPS-79)	Cytotoxicity against cancer cell line: P388: ED <sub>50</sub> = 0.8 µg/mL	(Iwamoto <i>et al.</i> , 1999; Takahashi <i>et al.</i> , 1996)

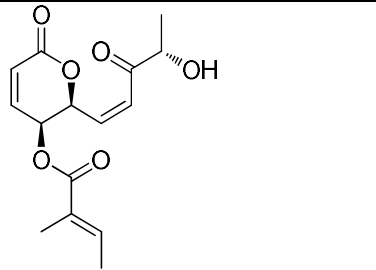
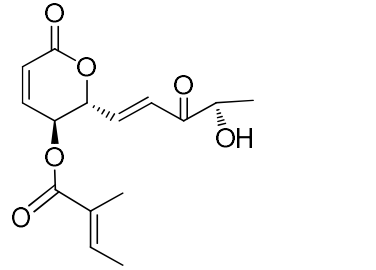
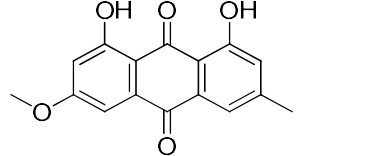
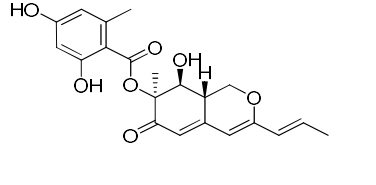
APPENDIX

Penostatin B		Polyketide	Green alga <i>Enteromorpha intestinalis</i> ( <i>Penicillium</i> sp. OUPS-79)	Cytotoxicity against cancer cell line: P388: ED <sub>50</sub> = 1.2 µg/mL	(Iwamoto <i>et al.</i> , 1999; Takahashi <i>et al.</i> , 1996)
Penostatin C		Polyketide	Green alga <i>Enteromorpha intestinalis</i> ( <i>Penicillium</i> sp. OUPS-79)	Cytotoxicity against cancer cell line: P388: ED <sub>50</sub> = 1.0 µg/mL BSY-1: ED <sub>50</sub> = 2.0 µg/mL MCF-7: ED <sub>50</sub> = 1.6 µg/mL HCC2998: ED <sub>50</sub> = 2.0 µg/mL NCI-H522: ED <sub>50</sub> = 2.5 µg/mL DMS114: ED <sub>50</sub> = 2.4 µg/mL OVCAR-3: ED <sub>50</sub> = 1.7 µg/mL MKN: ED <sub>50</sub> = 1.0 µg/mL	(Iwamoto <i>et al.</i> , 1999; Takahashi <i>et al.</i> , 1996)
Penostatin D		Polyketide	Green alga <i>Enteromorpha intestinalis</i> ( <i>Penicillium</i> sp. OUPS-79)	Cytotoxicity against cancer cell line: P388: ED <sub>50</sub> = 11.0 µg/mL	(Iwamoto <i>et al.</i> , 1999; Takahashi <i>et al.</i> , 1996)
Penostatin E		Polyketide	Green alga <i>Enteromorpha intestinalis</i> ( <i>Penicillium</i> sp. OUPS-79)	Cytotoxicity against cancer cell line: P388: ED <sub>50</sub> = 0.9 µg/mL	(Iwamoto <i>et al.</i> , 1998; Iwamoto <i>et al.</i> , 1999)
Penostatin F		Polyketide	Green alga <i>Enteromorpha intestinalis</i> ( <i>Penicillium</i> sp. OUPS-79)	Cytotoxicity against cancer cell line: P388: ED <sub>50</sub> = 1.4 µg/mL	(Iwamoto <i>et al.</i> , 1998)

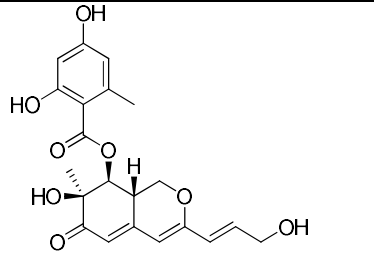
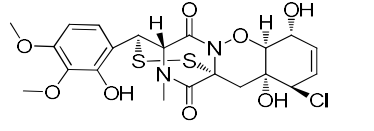
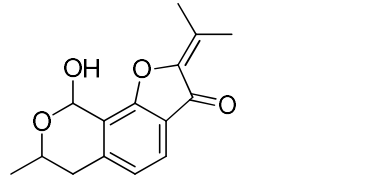
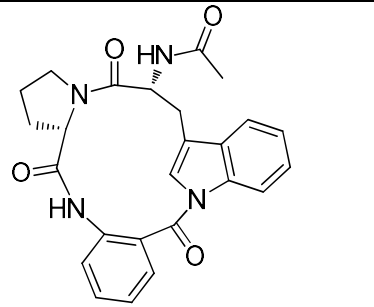
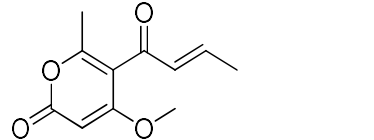
APPENDIX

Penostatin G		Polyketide	Green alga <i>Enteromorpha intestinalis</i> ( <i>Penicillium</i> sp. OUPS-79)	Cytotoxicity against cancer cell line: P388: ED <sub>50</sub> = 0.5 µg/mL	(Iwamoto <i>et al.</i> , 1998)
Penostatin H		Polyketide	Green alga <i>Enteromorpha intestinalis</i> ( <i>Penicillium</i> sp. OUPS-79)	Cytotoxicity against cancer cell line: P388: ED <sub>50</sub> = 0.8 µg/mL	(Iwamoto <i>et al.</i> , 1998)
Penostatin I		Polyketide	Green alga <i>Enteromorpha intestinalis</i> ( <i>Penicillium</i> sp. OUPS-79)	Cytotoxicity against cancer cell line: P388: ED <sub>50</sub> = 1.2 µg/mL	(Iwamoto <i>et al.</i> , 1998)
Pestalone		Chlorinated benzophenone	Brown alga <i>Rosenvingea</i> sp. ( <i>Pestalotia</i> sp. CNL-365)	Toxicity to 60 cancer cell lines: mean GI <sub>50</sub> = 6.0 µM	(Cueto <i>et al.</i> , 2001)

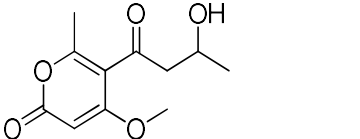
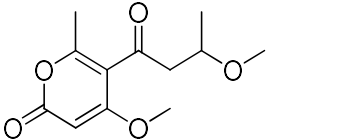
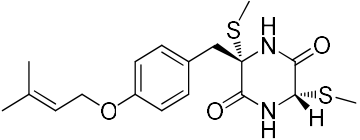
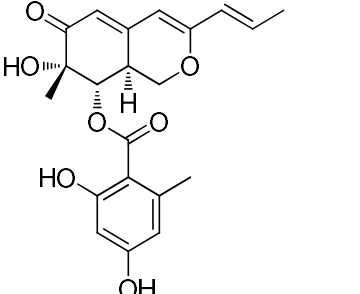
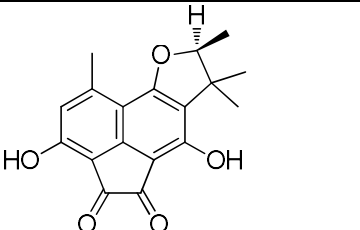
APPENDIX

Phomopsolide A		Tiglic acid	Green alga <i>Chlorella vulgaris</i> Beyerinck ( <i>Penicillium clavigerum</i> )	Cytotoxicity against cancer cell lines: HeLa S3: IC <sub>50</sub> = 6.3 μM UMUC3: IC <sub>50</sub> = 6.5 μM	(Stierle <i>et al.</i> , 2014)
Phomopsolide C		Tiglic acid	Green alga <i>Chlorella vulgaris</i> Beyerinck ( <i>Penicillium clavigerum</i> )	Cytotoxicity against cancer cell lines: HeLa S3: IC <sub>50</sub> = 3.6 μM UMUC3: IC <sub>50</sub> = 2.2 μM	(Stierle <i>et al.</i> , 2014)
Physcion		Anthraquinone	Red alga <i>Lomentaria catenata</i> ( <i>Microsporium</i> sp. MFS-YL)	Toxicity against HeLa with inhibition rate higher than 60% at 100 μM	(Wijsekara <i>et al.</i> , 2014)
Pinophilin A		Polyketide	Green alga <i>Ulva fasciata</i> ( <i>Penicillium pinophilum</i> Hedgcok)	Cytotoxicity against cancer cell lines: A549: GI <sub>50</sub> = 52.5 μM BALL-1: GI <sub>50</sub> = 50.2 μM HCT-116: GI <sub>50</sub> = 51.3 μM HeLa: GI <sub>50</sub> = 55.6 μM NUGC-3: GI <sub>50</sub> = 54.7 μM	(Myobatake <i>et al.</i> , 2012)

APPENDIX

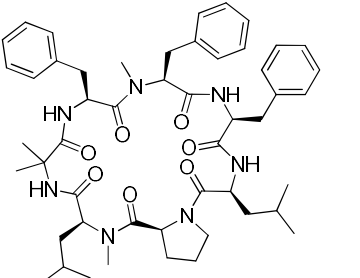
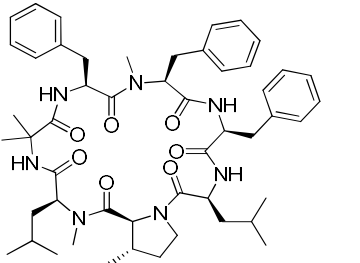
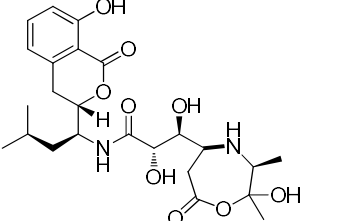
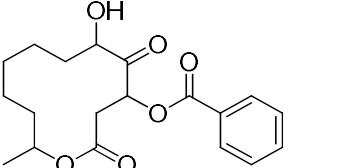
Pinophilin B		Polyketide	Green alga <i>Ulva fasciata</i> ( <i>Penicillium pinophilum</i> Hedgcok)	Cytotoxicity against cancer cell lines: A549 : GI <sub>50</sub> = 93.1 μM BALL-1: GI <sub>50</sub> = 90.4 μM HCT-116: GI <sub>50</sub> = 92.5 μM HeLa: GI <sub>50</sub> = 99.0 μM NUGC-3: GI <sub>50</sub> = 96.8 μM	(Myobatake <i>et al.</i> , 2012)
N-methylpretrichoderamide B		Epidithiodiketopiperazine	Brown alga <i>Padina</i> sp. ( <i>Penicillium</i> sp. KMM 4672)	Cytotoxicity against cancer cell line: 22Rv1: IC <sub>50</sub> = 0.51 μM PC-3: IC <sub>50</sub> = 5.11 μM LNCaP: IC <sub>50</sub> = 1.76 μM	(Yurchenko <i>et al.</i> , 2016)
Pseudodeflectusin		Isochroman derivative	Brown alga <i>Sargassum fusiform</i> ( <i>Aspergillus pseudodeflectus</i> )	Cytotoxicity against cancer cell line: HL-60: LD <sub>50</sub> = 39 μM	(Ogawa <i>et al.</i> , 2004)
Psychrophilin E		Cyclic tripeptide	Brown alga <i>Sargassum Aspergillus</i> BM-05 and BM-05ML)	Cytotoxicity against cancer cell lines: K562: IC <sub>50</sub> = 67.8 μM HCT116: IC <sub>50</sub> = 28.5 μM A2780: IC <sub>50</sub> = 27.3 μM A2780cisR: IC <sub>50</sub> = 49.4 μM	(Ebada <i>et al.</i> , 2014a)
Pyrenocine A		Pyrone	Brown alga <i>Sargassum ringgoldianum</i> ( <i>Penicillium waksmanii</i> Zaleski OUPS-N133)	Cytotoxicity against cancer cell line: P388: ED <sub>50</sub> = 0.16 μg/mL	(Amagata <i>et al.</i> , 1998)

APPENDIX

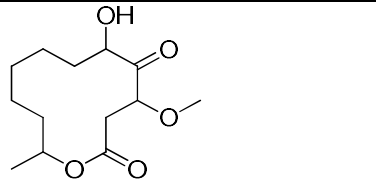
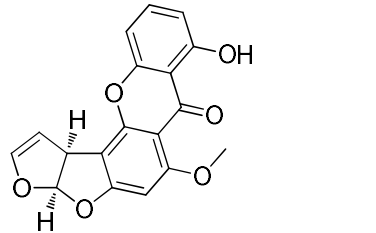
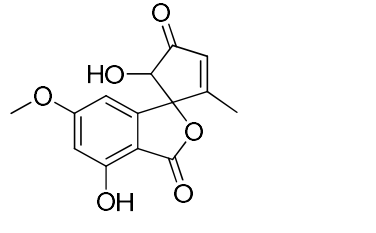
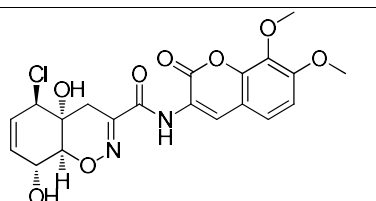
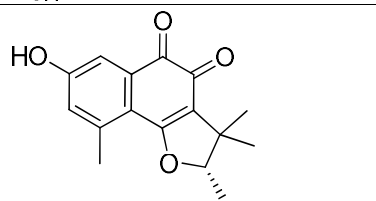
Pyrenocine B		Pyrone	Brown alga <i>Sargassum ringgoldianum</i> ( <i>Penicillium waksmanii</i> Zaleski OUPS-N133)	Cytotoxicity against cancer cell line: P388: ED <sub>50</sub> = 1.4 µg/mL	(Amagata <i>et al.</i> , 1998)
Pyrenocine E		Pyrone	Brown alga <i>Sargassum ringgoldianum</i> ( <i>Penicillium waksmanii</i> Zaleski OUPS-N133)	Cytotoxicity against cancer cell line: P388: ED <sub>50</sub> = 1.3 µg/mL	(Amagata <i>et al.</i> , 1998)
Sch 54794		Cyclodipeptide	Red alga <i>Carpopeltis affinis</i> ( <i>Fusarium chlamydosporum</i> OUPS-N124)	Cytotoxicity against cancer cell line: P388: ED <sub>50</sub> = 21.5 µg/mL	(Usami <i>et al.</i> , 2002)
Sch 725680		Hydrogenated azaphilone	Green alga <i>Ulva fasciata</i> ( <i>Penicillium pinophilum</i> Hedgcok)	Cytotoxicity against cancer cell lines: A549: GI <sub>50</sub> = 65.7 µM BALL-1: GI <sub>50</sub> = 62.0 µM HCT-116: GI <sub>50</sub> = 64.6 µM HeLa: GI <sub>50</sub> = 68.8 µM NUGC-3: GI <sub>50</sub> = 66.4 µM	(Myobatake <i>et al.</i> , 2012)
(-)-Sclerodione		Polyketide	Green alga <i>Enteromorpha</i> sp. ( <i>Coniothyrium cereale</i> )	Cytotoxicity against cancer cell line: mouse fibroblast cell: IC <sub>50</sub> = 6.4 µM	(Nazir <i>et al.</i> , 2015)



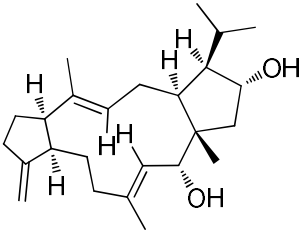
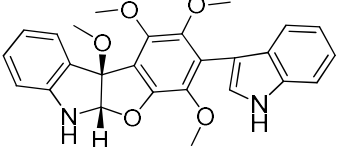
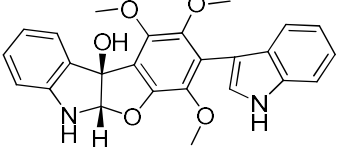
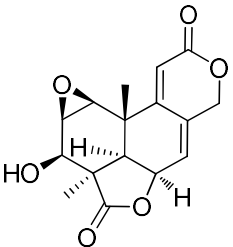
APPENDIX

Scytalidamide A		Cyclic heptapeptide	Green alga <i>Halimeda</i> sp. ( <i>Sytilidium</i> sp. CNC-310)	Cytotoxicity against cancer cell line: HCT116: IC <sub>50</sub> = 2.7 μM	(Tan <i>et al.</i> , 2003)
Scytalidamide B		Cyclic heptapeptide	Green alga <i>Halimeda</i> sp. ( <i>Sytilidium</i> sp. CNC-310)	Cytotoxicity against cancer cell line: HCT116: IC <sub>50</sub> = 11.0 μM	(Tan <i>et al.</i> , 2003)
Sg17-1-4		Polyketide	Unkown alga ( <i>Alternaria tenuis</i> )	Cytotoxicity against cancer cell line: A375-S2: IC <sub>50</sub> = 0.1 mM HeLa: IC <sub>50</sub> = 0.02 mM	(Huang <i>et al.</i> , 2006)
Sporiolide A		Macrolide	Brown alga <i>Actinotrichia fragilis</i> ( <i>Cladosporium</i> sp.)	Cytotoxicity against cancer cell line: L1210: IC <sub>50</sub> = 0.13 μg/mL	(Shigemori <i>et al.</i> , 2004)

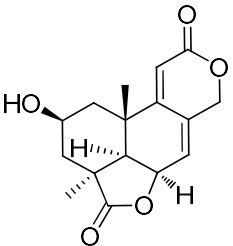
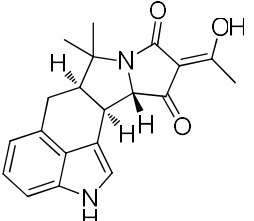
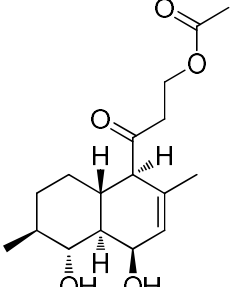
APPENDIX

Sporiolide B		Macrolide	Brown alga <i>Actinotrichia fragilis</i> ( <i>Cladosporium</i> sp.)	Cytotoxicity against cancer cell line: L1210: IC <sub>50</sub> = 0.81 µg/mL	(Shigemori <i>et al.</i> , 2004)
Sterigmatocystin		Polyketide	Brown alga <i>Sargassum</i> ( <i>Aspergillus</i> (BM-05 and BM-05ML))	Cytotoxicity against cancer cell lines: K562: IC <sub>50</sub> = 57.0 µM HCT116: IC <sub>50</sub> = 10.3 µM A2780: IC <sub>50</sub> = 30.6 µM A2780cisR: IC <sub>50</sub> = 95.5 µM	(Ebada <i>et al.</i> , 2014a)
Talaroflavone		Polyketide	Unknown alga (Undetermined fungus HJ33moB)	Inhibitor of Eukaryotic DNA polymerases (pols) β and κ : Eukaryotic DNA polymerases (pols) β: IC <sub>50</sub> = 16.3 µM Eukaryotic DNA polymerases (pols) κ: IC <sub>50</sub> = 86.5 µM	(Naganuma <i>et al.</i> , 2008)
Trichodermamide B		Dipeptide	Green alga <i>Halimeda</i> ( <i>Trichoderma virens</i> CNK266)	Cytotoxicity against cancer cell line: HCT116: IC <sub>50</sub> = 0.32 µg/mL	(Garo <i>et al.</i> , 2003)
(-)-Trypethelone		Polyketide	Green alga <i>Enteromorpha</i> sp. ( <i>Coniothyrium cereale</i> )	Cytotoxicity against cancer cell line: mouse fibroblast cell: IC <sub>50</sub> = 7.5 µM	(Nazir <i>et al.</i> , 2015)

APPENDIX

Variculanol		Sesterterpenoid	Green alga <i>Halimeda opuntia</i> ( <i>Aspergillus versicolor</i> )	Weak anticancer bioactivity against Hep G2 at 300 µg/disk	(Hawas <i>et al.</i> , 2012)
Varioloid A		Indole alkaloid	Red alga <i>Grateloupia turuturu</i> ( <i>Paecilomyces variotii</i> EN-291)	Cytotoxicity against cancer cell lines: A549: IC <sub>50</sub> = 3.5 µg/mL HCT116: IC <sub>50</sub> = 6.4 µg/mL HepG2: IC <sub>50</sub> = 2.5 µg/mL	(Zhang <i>et al.</i> , 2016)
Varioloid B		Indole alkaloid	Red alga <i>Grateloupia turuturu</i> ( <i>Paecilomyces variotii</i> EN-291)	Cytotoxicity against cancer cell lines: A549: IC <sub>50</sub> = 4.6 µg/mL HCT116: IC <sub>50</sub> = 8.8 µg/mL HepG2: IC <sub>50</sub> = 6.2 µg/mL	(Zhang <i>et al.</i> , 2016)
Wentilactone A		Tetranorlabdane diterpenoid	Brown alga <i>Sargassum</i> ( <i>Aspergillus wentii</i> EN-48)	Cytotoxicity against cancer cell lines: HeLa: IC <sub>50</sub> = 52 µM HepG2: IC <sub>50</sub> = 35 µM MCF-7: IC <sub>50</sub> = 69 µM NCI-H460: IC <sub>50</sub> = 28 µM SMMC-7721: IC <sub>50</sub> = 28 µM SW 1990: IC <sub>50</sub> = 42 µM	(Sun <i>et al.</i> , 2012)

APPENDIX

<p>Wentilactone B</p>		<p>Tetranorlabdane diterpenoid</p>	<p>Brown alga <i>Sargassum</i> (<i>Aspergillus wentii</i> EN-48)</p>	<p>Cytotoxicity against cancer cell lines:                  HeLa: IC<sub>50</sub> = 42 μM                  HepG2: IC<sub>50</sub> = 38 μM                  MCF-7: IC<sub>50</sub> = 56 μM                  NCI-H460: IC<sub>50</sub> = 24 μM                  SMMC-7721: IC<sub>50</sub> = 17 μM                  SW 1990: IC<sub>50</sub> = 24 μM</p>	<p>(Sun <i>et al.</i>, 2012)</p>
<p>α-Cyclopiazonic acid</p>		<p>Ergoline alkaloid</p>	<p>Green alga <i>Enteromorpha tubulosa</i> (<i>Aspergillus flavus</i> c-f-3)</p>	<p>Cytotoxicity against cancer cell lines:                  HL-60: IC<sub>50</sub> = 2.4 μM                  MoLT-4: IC<sub>50</sub> = 12.3 μM                  A549: IC<sub>50</sub> = 21.5 μM</p>	<p>(Lin <i>et al.</i>, 2009)</p>
<p>Pallidopenilline G</p>		<p>Polyketide</p>	<p>Brown alga <i>Sargassum pallidum</i> (<i>Penicillium thomii</i> KMM 4675)</p>	<p>Cytotoxicity against cancer cell line:                  22Rv1: IC<sub>50</sub> = 9.8 μM</p>	<p>(Sobolevskaya <i>et al.</i>, 2016)</p>

## APPENDIX

### References

- Abastabar, M., Akbari, A., Akhtari, J., Hedayati, M. T., Shokohi, T., Mehrad-Majd, H., Ghalehnoei, H., Ghasemi, S., 2017. *In vitro* antitumor activity of patulin on cervical and colorectal cancer cell lines. *Curr. Med. Mycol.* 3, 25-29. DOI: 10.18869/acadpub.cmm.3.1.25
- Amagata, T., Minoura, K., Numata, A., 1998. Cytotoxic metabolites produced by a fungal strain from a *Sargassum* alga. *J. Antibiot.* 51, 432-434. DOI: 10.7164/antibiotics.51.432
- An, C.-Y., Li, X.-M., Li, C.-S., Gao, S.-S., Shang, Z., Wang, B.-G., 2013. Triazoles and other *N*-containing metabolites from the marine-derived endophytic fungus *Penicillium chrysogenum* EN-118. *Helv. Chim. Acta.* 96, 682-687. DOI: 10.1002/hlca.201200433
- Belofsky, G. N., Jensen, P. R., Renner, M. K., Fenical, W., 1998. New cytotoxic sesquiterpenoid nitrobenzoyl esters from a marine isolate of the fungus *Aspergillus versicolor*. *Tetrahedron* 54, 1715-1724. DOI: 10.1016/S0040-4020(97)10396-9
- Bryant, F. O., Cutler, H. G., Parker, S. R., 1994. Effect of fungal natural products in an *Agrobacterium tumefaciens* potato disc assay. *J. Nat. Prod.* 57, 640-643. DOI: 10.1021/np50107a012
- Chen, C., Imamura, N., Nishijima, M., Adachi, K., Sakai, M., Sano, H., 1996. Halymecins, new antimicrobial substances produced by fungi isolated from marine algae. *J. Antibiot (Tokyo)* 49, 998-1005. DOI: 10.7164/antibiotics.49.998
- Choi, B.-K., Trinh, P. T. H., Lee, H.-S., Choi, B.-W., Kang, J. S., Ngoc, N. T. D., Van, T. T. T., Shin, H. J., 2019. New ophiobolin derivatives from the marine fungus *Aspergillus flocculosus* and their cytotoxicities against cancer cells. *Mar. Drugs* 17, 346. DOI: 10.3390/md17060346
- Cueto, M., Jensen, P. R., Fenical, W., 2000. *N*-Methylsalsalvamide, a cytotoxic cyclic depsipeptide from a marine fungus of the genus *Fusarium*. *Phytochemistry* 55, 223-226. DOI: 10.1016/S0031-9422(00)00280-6
- Cueto, M., Jensen, P. R., Kauffman, C., Fenical, W., Lobkovsky, E., Clardy, J., 2001. Pestalone, a new antibiotic produced by a marine fungus in response to bacterial challenge. *J. Nat. Prod.* 64, 1444-1446. DOI: 10.1021/np0102713
- Cui, C.-M., Li, X.-M., Li, C.-S., Proksch, P., Wang, B.-G., 2010a. Cytochalasins A-G, cytochalasans from a marine-derived endophytic fungus, *Chaetomium globosum* QEN-14. *J. Nat. Prod.* 73, 729-733. DOI: 10.1021/np900569t
- Cui, C.-M., Li, X.-M., Meng, L., Li, C.-S., Huang, C.-G., Wang, B.-G., 2010b. 7-Nor-ergosterolide, a pentalactone-containing norsteroid and related steroids from the marine-derived endophytic *Aspergillus ochraceus* EN-31. *J. Nat. Prod.* 73, 1780-1784. DOI: 10.1021/np100386q
- Ebada, S. S., Fischer, T., Hamacher, A., Du, F.-Y., Roth, Y. O., Kassack, M. U., Wang, B.-G., Roth, E. H., 2014a. Psychrophilin E, a new cyclotriptide, from co-fermentation of two marine alga-derived fungi of the genus *Aspergillus*. *Nat. Prod. Res.* 28, 776-781. DOI: 10.1080/14786419.2014.880911
- Ebada, S. S., Fischer, T., Klaffen, S., Hamacher, A., Roth, Y. O., Kassack, M. U., Roth, E. H., 2014b. A new cytotoxic steroid from co-fermentation of two marine alga-derived micro-organisms. *Nat. Prod. Res.* 28, 1241-1245. DOI: 10.1080/14786419.2014.895730
- El-Beih, A. A., Kato, H., Ohta, T., Tsukamoto, S., 2007. (3*R*,4*aR*,5*S*,6*R*)-6-Hydroxy-5-methylramulosin: A new ramulosin derivative from a marine-derived sterile mycelium. *Chem. Pharm. Bull.* 55, 953-954. DOI: 10.1248/cpb.55.953
- Elsebai, M. F., Natesan, L., Kehraus, S., Mohamed, I. E., Schnakenburg, G., Sasse, F., Shaaban, S., Gütschow, M., König, G. M., 2011. HLE-inhibitory alkaloids with a polyketide skeleton from the marine-derived fungus *Coniothyrium cereale*. *J. Nat. Prod.* 74, 2282-2285. DOI: 10.1021/np2004227
- Fang, W., Lin, X., Zhou, X., Wan, J., Lu, X., Yang, B., Ai, W., Lin, J., Zhang, T., Tu, Z., Liu, Y., 2014. Cytotoxic and antiviral nitrobenzoyl sesquiterpenoids from the marine-derived fungus *Aspergillus ochraceus* Jcm1F17. *MedChemComm* 5, 701-705. DOI: 10.1039/C3MD00371J
- Fenical, W., Jensen, P. R., Cheng, X. C., 2000a. Avrainvillamide, a cytotoxic marine natural product, and derivatives thereof. United States Patent
- Fenical, W., Jensen, P. R., Cheng, X. C., 2000b. Halimide, a cytotoxic marine natural product, and derivatives thereof. World Intellectual Property Organization.

## APPENDIX

- Flewelling, A. J., Johnson, J. A., Gray, C. A., 2013. Antimicrobials from the marine algal endophyte *Penicillium* sp. *Nat. Prod. Commun.* 8, 373-374. DOI: 10.1177/1934578X1300800324
- Fukumoto, K., Kohno, S., Kanoh, K., Asari, T., Kawashima, H., Sekiya, H., Ohmizo, K., Harada, T., 2002. Phenylahistin and the phenylahistin analogs, a new class of anti-tumor compounds. United States Patent.
- Gamal-Eldeen, A. M., Abdel-Lateff, A., Okino, T., 2009. Modulation of carcinogen metabolizing enzymes by chromanone A; a new chromone derivative from algicolous marine fungus *Penicillium* sp. *Environ. Toxicol. Pharmacol.* 28, 317-322. DOI: 10.1016/j.etap.2009.05.010
- Gao, S.-S., Li, X.-M., Du, F.-Y., Li, C.-S., Proksch, P., Wang, B.-G., 2011a. Secondary metabolites from a marine-derived endophytic fungus *Penicillium chrysogenum* QEN-24S. *Mar. Drugs* 9, 59-70. DOI: 10.3390/md9010059
- Gao, S.-S., Li, X.-M., Li, C.-S., Proksch, P., Wang, B.-G., 2011b. Penicisteroids A and B, antifungal and cytotoxic polyoxygenated steroids from the marine alga-derived endophytic fungus *Penicillium chrysogenum* QEN-24S. *Bioorg. Med. Chem. Lett.* 21, 2894-2897. DOI: 10.1016/j.bmcl.2011.03.076
- Garo, E., Starks, C. M., Jensen, P. R., Fenical, W., Lobkovsky, E., Clardy, J., 2003. Trichodermamides A and B, cytotoxic modified dipeptides from the marine-derived fungus *Trichoderma virens*. *J. Nat. Prod.* 66, 423-426. DOI: 10.1021/np0204390
- Gautschi, J. T., Amagata, T., Amagata, A., Valeriote, F. A., Mooberry, S. L., Crews, P., 2004. Expanding the strategies in natural product studies of marine-derived fungi: A chemical investigation of *Penicillium* obtained from deep water sediment. *J. Nat. Prod.* 67, 362-367. DOI: 10.1021/np030388m
- Greve, H., Schupp, P. J., Eguereva, E., Kehraus, S., Kelter, G., Maier, A., Fiebig, H.-H., König, G. M., 2008. Apralactone A and a new stereochemical class of curvularins from the marine fungus *Curvularia* sp. *Eur. J. Org. Chem.* 2008, 5085-5092. DOI: 10.1002/ejoc.200800522
- Hawas, U. W., El-Beih, A. A., El-Halawany, A. M., 2012. Bioactive anthraquinones from endophytic fungus *Aspergillus versicolor* isolated from Red Sea algae. *Arch. Pharm. Res.* 35, 1749-1756. DOI: 10.1007/s12272-012-1006-x
- Huang, Y.-F., Li, L.-H., Tian, L., Qiao, L., Hua, H.-M., Pei, Y.-H., 2006. Sg17-1-4, a novel isocoumarin from a marine fungus *Alternaria tenuis* Sg17-1. *J. Antibiot.* 59, 355-357. DOI: 10.1038/ja.2006.50
- Iwamoto, C., Minoura, K., Hagishita, S., Nomoto, K., Numata, A., 1998. Penostatins F–I, novel cytotoxic metabolites from a *Penicillium* species separated from an *Enteromorpha* marine alga. *Perkin Trans. 1*, 449-456. DOI: 10.1039/A706853K
- Iwamoto, C., Minoura, K., Oka, T., Ohta, T., Hagishita, S., Numata, A., 1999. Absolute stereostructures of novel cytotoxic metabolites, penostatins A–E, from a *Penicillium* species separated from an *Enteromorpha* alga. *Tetrahedron* 55, 14353-14368. DOI: 10.1016/S0040-4020(99)00884-4
- Iwamoto, C., Yamada, T., Ito, Y., Minoura, K., Numata, A., 2001. Cytotoxic cytochalasans from a *Penicillium* species separated from a marine alga. *Tetrahedron* 57, 2997-3004. DOI: 10.1016/S0040-4020(01)00153-3
- Kanoh, K., Kohno, S., Asari, T., Harada, T., Katada, J., Muramatsu, M., Kawashima, H., Sekiya, H., Uno, I., 1997. (-)-Phenylahistin: A new mammalian cell cycle inhibitor produced by *Aspergillus ustus*. *Bioorg. Med. Chem. Lett.* 7, 2847-2852. DOI: 10.1016/S0960-894X(97)10104-4
- Kanoh, K., Kohno, S., Katada, J., Takahashi, J., Uno, I., 1999. (-)-Phenylahistin arrests cells in mitosis by inhibiting tubulin polymerization. *J. Antibiot.* 52, 134-141. DOI: 10.7164/antibiotics.52.134
- Klemke, C., Kehraus, S., Wright, A. D., König, G. M., 2004. New secondary metabolites from the marine endophytic fungus *Apiospora montagnei*. *J. Nat. Prod.* 67, 1058-1063. DOI: 10.1021/np034061x
- Kralj, A., Kehraus, S., Krick, A., Eguereva, E., Kelter, G., Maurer, M., Wortmann, A., Fiebig, H.-H., König, G. M., 2006. Arugosins G and H: Prenylated polyketides from the marine-derived fungus *Emericella nidulans* var. *acristata*. *J. Nat. Prod.* 69, 995-1000. DOI: 10.1021/np050454f
- Lang, G., Mitova, M. I., Ellis, G., van der Sar, S., Phipps, R. K., Blunt, J. W., Cummings, N. J., Cole, A. L. J., Munro, M. H. G., 2006. Bioactivity profiling

## APPENDIX

- using HPLC/microtiter-plate analysis: Application to a New Zealand marine alga-derived fungus, *Gliocladium* sp. J. Nat. Prod. 69, 621-624. DOI: 10.1021/np0504917
- Li, H.-L., Li, X.-M., Mándi, A., Antus, S., Li, X., Zhang, P., Liu, Y., Kurtán, T., Wang, B.-G., 2017. Characterization of cladospores from the marine alga-derived endophytic fungus *Cladosporium cladosporioides* EN-399 and configurational revision of the previously reported cladospore derivatives. J. Org. Chem. 82, 9946-9954. DOI: 10.1021/acs.joc.7b01277
- Li, Y.-X., Himaya, S. W. A., Dewapriya, P., Kim, H. J., Kim, S.-K., 2014. Anti-proliferative effects of isosclerone isolated from marine fungus *Aspergillus fumigatus* in MCF-7 human breast cancer cells. Process Biochem. 49, 2292-2298. DOI: 10.1016/j.procbio.2014.08.016
- Li, Y.-X., Himaya, S. W. A., Dewapriya, P., Zhang, C., Kim, S.-K., 2013a. Fumigaclavine C from a marine-derived fungus *Aspergillus fumigatus* induces apoptosis in MCF-7 breast cancer cells. Mar. Drugs 11, 5063-5086. DOI: 10.3390/md11125063
- Li, Y., Sun, K.-L., Wang, Y., Fu, P., Liu, P.-P., Wang, C., Zhu, W.-M., 2013b. A cytotoxic pyrrolidinoindoline diketopiperazine dimer from the algal fungus *Eurotium herbariorum* HT-2. Chin. Chem. Lett. 24, 1049-1052. DOI: 10.1016/j.cclet.2013.07.028
- Li, Z.-X., Wang, X.-F., Ren, G.-W., Yuan, X.-L., Deng, N., Ji, G.-X., Li, W., Zhang, P., 2018. Prenylated diphenyl ethers from the marine alga-derived endophytic fungus *Aspergillus tennesseensis*. Molecules 23, 2368. DOI: 10.3390/molecules23092368
- Lin, A.-Q., Du, L., Fang, Y.-C., Wang, F.-Z., Zhu, T.-J., Gu, Q.-Q., Zhu, W.-M., 2009. Iso- $\alpha$ -cyclopiazonic acid, a new natural product isolated from the marine-derived fungus *Aspergillus flavus* C-F-3. Chem. Nat. Compd. 45, 677-680. DOI: 10.1007/s10600-009-9433-8
- Lin, A.-Q., Fang, Y.-C., Zhu, T.-J., Gu, Q.-Q., Zhu, W.-M., 2008. A new diketopiperazine alkaloid isolated from an algicolous *Aspergillus flavus* strain. Pharmazie 63, 323-324. DOI: 10.1691/ph.2008.7700
- Liu, X.-H., Tang, X.-Z., Miao, F.-P., Ji, N.-Y., 2011. A new pyrrolidine derivative and steroids from an algicolous *Gibberella zeae* strain. Nat. Prod. Commun. 6, 1243-1246. DOI: 10.1177/1934578x1100600908
- Mugishima, T., Tsuda, M., Kasai, Y., Ishiyama, H., Fukushi, E., Kawabata, J., Watanabe, M., Akao, K., Kobayashi, J. i., 2005. Absolute stereochemistry of citrinadins A and B from marine-derived fungus. J. Org. Chem. 70, 9430-9435. DOI: 10.1021/jo051499o
- Myobatake, Y., Takeuchi, T., Kuramochi, K., Kuriyama, I., Ishido, T., Hirano, K., Sugawara, F., Yoshida, H., Mizushima, Y., 2012. Pinophilins A and B, inhibitors of mammalian A-, B-, and Y-Family DNA polymerases and human cancer cell proliferation. J. Nat. Prod. 75, 135-141. DOI: 10.1021/np200523b
- Naganuma, M., Nishida, M., Kuramochi, K., Sugawara, F., Yoshida, H., Mizushima, Y., 2008. 1-Deoxyrubralactone, a novel specific inhibitor of families X and Y of eukaryotic DNA polymerases from a fungal strain derived from sea algae. Bioorg. Med. Chem. 16, 2939-2944. DOI: 10.1016/j.bmc.2007.12.044
- Nazir, M., El Maddah, F., Kehraus, S., Egereva, E., Piel, J., Brachmann, A. O., König, G. M., 2015. Phenalenones: insight into the biosynthesis of polyketides from the marine alga-derived fungus *Coniothyrium cereale*. Org. Biomol. Chem. 13, 8071-8079. DOI: 10.1039/c5ob00844a
- Nguyen, V.-T., Lee, J. S., Qian, Z.-J., Li, Y.-X., Kim, K.-N., Heo, S.-J., Jeon, Y.-J., Park, W. S., Choi, I.-W., Je, J.-Y., Jung, W.-K., 2014. Gliotoxin isolated from marine fungus *Aspergillus* sp. induces apoptosis of human cervical cancer and chondrosarcoma cells. Mar. Drugs 12, 69-87. DOI: 10.3390/md12010069.
- Numata, A., Takahashi, C., Ito, Y., Minoura, K., Yamada, T., Matsuda, C., Nomoto, K., 1996. Penochalasin, a novel class of cytotoxic cytochalasins from a *Penicillium* species separated from a marine alga: structure determination and solution conformation. Perkin Trans. 1, 239-245. DOI: 10.1039/P19960000239
- Numata, A., Takahashi, C., Ito, Y., Takada, T., Kawai, K., Usami, Y., Matsumura, E., Imachi, M., Ito, T., Hasegawa, T., 1993. Communesins, cytotoxic metabolites of a fungus isolated from a marine alga. Tetrahedron Lett. 34, 2355-2358. DOI: 10.1016/S0040-4039(00)77612-X
- Ogawa, A., Murakami, C., Kamisuki, S., Kuriyama, I., Yoshida, H., Sugawara, F., Mizushima, Y., 2004. Pseudodeflectusin, a novel isochroman derivative from *Aspergillus pseudodeflectus* a parasite of the sea weed, *Sargassum fusiform*, as a selective human cancer cytotoxin. Bioorg. Med. Chem. Lett. 14, 3539-3543.

## APPENDIX

- DOI: 10.1016/j.bmcl.2004.04.050
- Oh, D.-C., Kauffman, C. A., Jensen, P. R., Fenical, W., 2007. Induced production of emericellamides A and B from the marine-derived fungus *Emericella* sp. in competing co-culture. *J. Nat. Prod.* 70, 515-520. DOI: 10.1021/np060381f
- Osterhage, C., König, G. M., Jones, P. G., Wright, A. D., 2002. 5-Hydroxyramulosin, a new natural product produced by *Phoma tropica*, a marine-derived fungus isolated from the alga *Fucus spiralis*. *Planta Med.* 68, 1052-1054. DOI: 10.1055/s-2002-35670
- Pontius, A., Krick, A., Kehraus, S., Foegen, S. E., Müller, M., Klimo, K., Gerhäuser, C., König, G. M., 2008. Noduliprevenone: A novel heterodimeric chromanone with cancer chemopreventive potential. *Chem-Eur. J.* 14, 9860-9863. DOI: 10.1002/chem.200801574
- Rahbæk, L., Christophersen, C., Frisvad, J., Bengaard, H. S., Larsen, S., Rassing, B. R., 1997. Insulicolide A: A new nitrobenzoyloxy-substituted sesquiterpene from the marine fungus *Aspergillus insulicola*. *J. Nat. Prod.* 60, 811-813. DOI: 10.1021/np970142f
- Santiago, C., Fitchett, C., Munro, M. H., Jalil, J., Santhanam, J., 2012. Cytotoxic and antifungal activities of 5-hydroxyramulosin, a compound produced by an endophytic fungus isolated from *Cinnamomum mollissimum*. *Evid-based. compl. alt.* 2012, 689310-689315. DOI: 10.1155/2012/689310
- Shigemori, H., Kasai, Y., Komatsu, K., Tsuda, M., Mikami, Y., Kobayashi, J. I., 2004. Sporiolides A and B, new cytotoxic twelve-membered macrolides from a marine-derived fungus *Cladosporium* species. *Mar. Drugs* 2, 164-169. DOI: 10.3390/md204164
- Smetanina, O. F., Yurchenko, A. N., Ivanets, E. V., Kirichuk, N. N., Khudyakova, Y. V., Yurchenko, E. A., Afiyatullo, S. S., 2016. Metabolites of the marine fungus *Penicillium citrinum* associated with a brown alga *Padina* sp. *Chem. Nat. Compd.* 52, 111-112. DOI: 10.1007/s10600-016-1560-4
- Sobolevskaya, M. P., Leshchenko, E. V., Hoai, T. P. T., Denisenko, V. A., Dyshlovoy, S. A., Kirichuk, N. N., Khudyakova, Y. V., Kim, N. Y., Berdyshev, D. V., Pisyagin, E. A., Kuzmich, A. S., Gerasimenko, A. V., Popov, R. S., von Amsberg, G., Antonov, A. S., Afiyatullo, S. S., 2016. Pallidopenillines: Polyketides from the alga-derived fungus *Penicillium thomii* Maire KMM 4675. *J. Nat. Prod.* 79, 3031-3038. DOI: 10.1021/acs.jnatprod.6b00624
- Son, B. W., Jensen, P. R., Kauffman, C. A., Fenical, W., 1999. New cytotoxic epidithiodioxopiperazines related to verticillin A from a marine isolate of the fungus *Penicillium*. *Nat. Prod. Lett.* 13, 213-222. DOI: 10.1080/10575639908048788
- Stierle, A. A., Stierle, D. B., Mitman, G. G., Snyder, S., Antezak, C., Djaballah, H., 2014. Phomopsolides and related compounds from the alga-associated fungus, *Penicillium clavigerum*. *Nat. Prod. Commun.* 9, 87-90. DOI: 10.1177/1934578X1400900126
- Sun, H.-F., Li, X.-M., Meng, L., Cui, C.-M., Gao, S.-S., Li, C.-S., Huang, C.-G., Wang, B.-G., 2012. Asperolides A-C, tetranorlabdane diterpenoids from the marine alga-derived endophytic fungus *Aspergillus wentii* EN-48. *J. Nat. Prod.* 75, 148-152. DOI: 10.1021/np2006742
- Takahashi, C., Minoura, K., Yamada, T., Numata, A., Kushida, K., Shingu, T., Hagishita, S., Nakai, H., Sato, T., Harada, H., 1995a. Potent cytotoxic metabolites from a *Leptosphaeria* species: Structure determination and conformational analysis. *Tetrahedron* 51, 3483-3498. DOI: 10.1016/0040-4020(95)00102-E
- Takahashi, C., Numata, A., Ito, Y., Matsumura, E., Araki, H., Iwaki, H., Kushida, K., 1994a. Leptosins, antitumour metabolites of a fungus isolated from a marine alga. *Perkin Trans. 1*, 1859-1864. DOI: 10.1039/P19940001859
- Takahashi, C., Numata, A., Matsumura, E., Minoura, K., Eto, H., Shingu, T., Ito, T., Hasegawa, T., 1994b. Leptosins I and J, cytotoxic substances produced by a *Leptosphaeria* sp. Physico-chemical properties and structures. *J. Antibiot.* 47, 1242-1249. DOI: 10.7164/antibiotics.47.1242
- Takahashi, C., Numata, A., Yamada, T., Minoura, K., Enomoto, S., Konishi, K., Nakai, M., Matsuda, C., Nomoto, K., 1996. Penostatins, novel cytotoxic metabolites from a *Penicillium* species separated from a green alga. *Tetrahedron Lett.* 37, 655-658. DOI: 10.1016/0040-4039(95)02225-2
- Takahashi, C., Takai, Y., Kimura, Y., Numata, A., Shigematsu, N., Tanaka, H., 1995b. Cytotoxic metabolites from a fungal adherent of a marine alga. *Phytochemistry* 38, 155-158. DOI: 10.1016/0031-9422(94)00582-E
- Tan, L. T., Cheng, X. C., Jensen, P. R., Fenical, W., 2003. Scytlidamides A and B, new cytotoxic cyclic heptapeptides from a marine fungus of the genus



## APPENDIX

- Scytalidium*. J. Org. Chem. 68, 8767-8773. DOI: 10.1021/jo030191z
- Tan, Y., Yang, B., Lin, X., Luo, X., Pang, X., Tang, L., Liu, Y., Li, X., Zhou, X., 2018. Nitrobenzoyl sesquiterpenoids with cytotoxic activities from a marine-derived *Aspergillus ochraceus* fungus. J. Nat. Prod. 81, 92-97. DOI: 10.1021/acs.jnatprod.7b00698
- Tsuda, M., Kasai, Y., Komatsu, K., Sone, T., Tanaka, M., Mikami, Y., Kobayashi, J. i., 2004. Citrinadin A, a novel pentacyclic alkaloid from marine-derived fungus *Penicillium citrinum*. Org. Lett. 6, 3087-3089. DOI: 10.1021/ol048900y
- Usami, Y., Aoki, S., Hara, T., Numata, A., 2002. New dioxopiperazine metabolites from a *Fusarium* species separated from a marine alga. J. Antibiot. 55, 655-659. DOI: 10.7164/antibiotics.55.655
- Wang, F.-W., 2012. Bioactive metabolites from *Guignardia* sp., an endophytic fungus residing in *Undaria pinnatifida*. Chin. J. Nat. Medicines 10, 72-76. DOI: 10.1016/S1875-5364(12)60016-8
- Wang, S., Li, X. M., Teuscher, F., Li, D. L., Diesel, A., Ebel, R., Proksch, P., Wang, B. G., 2006. Chaetopyranin, a benzaldehyde derivative, and other related metabolites from *Chaetomium globosum*, an endophytic fungus derived from the marine red alga *Polysiphonia urceolata*. J. Nat. Prod. 69, 1622-1625. DOI: 10.1021/np060248n
- Wijesekara, I., Li, Y.-X., Vo, T.-S., Van Ta, Q., Ngo, D.-H., Kim, S.-K., 2013. Induction of apoptosis in human cervical carcinoma HeLa cells by neoechinulin A from marine-derived fungus *Microsporium* sp. Process Biochem. 48, 68-72. DOI: 10.1016/j.procbio.2012.11.012
- Wijesekara, I., Zhang, C., Van Ta, Q., Vo, T.-S., Li, Y.-X., Kim, S.-K., 2014. Physcion from marine-derived fungus *Microsporium* sp. induces apoptosis in human cervical carcinoma HeLa cells. Microbiol. Res. 169, 255-261. DOI: 10.1016/j.micres.2013.09.001
- Xu, K., Guo, C., Meng, J., Tian, H., Guo, S., Shi, D., 2019. Discovery of natural dimeric naphthopyrones as potential cytotoxic agents through ROS-mediated apoptotic pathway. Mar. Drugs 17, 207. DOI: 10.3390/md17040207
- Yamada, T., Iwamoto, C., Yamagaki, N., 2004. Leptosins O-S, cytotoxic metabolites of a strain of *Leptosphaeria* sp. isolated from a marine alga. Heterocycles 63, 641-653. DOI: 10.3987/COM-03-9967
- Yamada, T., Iwamoto, C., Yamagaki, N., Yamanouchi, T., Minoura, K., Yamori, T., Uehara, Y., Andoh, T., Umemura, K., Numata, A., 2002. Leptosins M-N<sub>1</sub>, cytotoxic metabolites from a *Leptosphaeria* species separated from a marine alga. Structure determination and biological activities. Tetrahedron 58, 479-487. DOI: 10.1016/S0040-4020(01)01170-X
- Yurchenko, A. N., Smetanina, O. F., Ivanets, E. V., Kalinovsky, A. I., Khudyakova, Y. V., Kirichuk, N. N., Popov, R. S., Bokemeyer, C., Von Amsberg, G., Chingizova, E. A., Afiyatullo, S. S., Dyshlovoy, S. A., 2016. Pretrichodermamides D-F from a marine algicolous fungus *Penicillium* sp. KMM 4672. Mar. Drugs 14, 122. DOI: 10.3390/md14070122
- Zhang, P., Li, X.-M., Mao, X.-X., Mándi, A., Kurtán, T., Wang, B.-G., 2016. Varioloid A, a new indolyl-6,10b-dihydro-5aH-[1]benzofuro[2,3-b]indole derivative from the marine alga-derived endophytic fungus *Paecilomyces variotii* EN-291. Beilstein J. Org. Chem. 12, 2012-2018. DOI:10.3762/bjoc.12.188
- Zhang, P., Li, X.-M., Wang, J.-N., Li, X., Wang, B.-G., 2015. Prenylated indole alkaloids from the marine-derived fungus *Paecilomyces variotii*. Chin. Chem. Lett. 26, 313-316. DOI: 10.1016/j.ccllet.2014.11.020
- Zhao, D.-L., Yuan, X.-L., Du, Y.-M., Zhang, Z.-F., Zhang, P., 2018. Benzophenone derivatives from an algal-endophytic isolate of *Penicillium chrysogenum* and their cytotoxicity. Molecules 23, 3378. DOI: 10.3390/molecules23123378
- Zhu, T. J., Du, L., Hao, P. F., Lin, Z. J., Gu, Q. Q., 2009. Citrinal A, a novel tricyclic derivative of citrinin, from an algicolous fungus *Penicillium* sp. i-1-1. Chin. Chem. Lett. 20, 917-920. DOI: 10.1016/j.ccllet.2009.03.009

APPENDIX

APPENDIX

**2. Strain list and MN data for Chapter 1**

**Table S1.** Identification of 87 fungal strains isolated from *Fucus vesiculosus* and its surrounding environment (sediment and seawater). Identification was done according to Sanger sequencing comparison of the ITS1-5.8S rRNA gene-ITS2 fragment to NCBI GenBank nucleotide database using BLASTn (incl. respective assigned Genbank accession numbers). The 3 first BLAST hits incl. respective accession numbers are given. WM: Modified Wickerham medium, PDM: Potato Dextrose medium, GCM: Glucose Casein medium, GYP: Glucose Yeast Peptone medium. SE: sediment. SA: seawater. FVE: *F. vesiculosus* endophytic fungi. FVS: *F. vesiculosus* surface epiphytic fungi. \*Strain could not be identified to genus level but only to higher taxa (order) level.

Series no.	I.D.	Source	Isolation Medium	Sequence length	Closest relative in NCBI GenBank	NCBI accession number	Order	Sequence similarity %	Accession number
1*	1	FVE	WM	297	<i>Pyrenochaetopsis</i> sp. HKU62 <i>Pyrenochaetopsis</i> sp. CBS:119739 Uncultured <i>Leptosphaeria</i> sp.2KK-2015	LC158605.1 LT623227.1 KP747710.1	Pleosporales	100	MH881440
2	2	SE	PDM	172	<i>Fusarium lateritium</i> 3821 <i>Fusarium tricinctum</i> IBL277f <i>Fusarium avenaceum</i> SFC101774	MG066631.1 MF162319.1 MF186082.1	Hypocreales	100	MH881441
3	6	SE	GCM	261	<i>Fusarium culmorum</i> F165 <i>Fusarium graminearum</i> PGTU1018S <i>Fusarium culmorum</i> Ba4	KU891563.1 MF497389.1 MH361213.1	Hypocreales	100	MH881442
4	8	SE	PDM	270	<i>Penicillium sanguifluum</i> IG103 <i>Penicillium</i> sp. S1a1 <i>Penicillium sanguifluum</i> 17_3N1	MG973279.1 KY784181.1 KY859378.1	Eurotiales	100	MH881443
5*	10	SE	GYP	426	<i>Pyrenochaetopsis microspora</i> MUT4941 <i>Roussoellaceae</i> sp. MUT4859 <i>Phoma</i> sp. MUT 5462	LT623227.1 KR014355.1 KU314985.1	Pleosporales	100	MH881444
6	11	FVS	GCM	385	<i>Gibellulopsis</i> sp. MYf203 <i>Gibellulopsis</i> sp. P2 <i>Gibellulopsis nigrescens</i> LG1401	KX079890.1 KY465972.1 KX359602.1	Hypocreales	100	MH881445
7	12	FVE	WM	400	<i>Acremonium furcatum</i> MUT1194 <i>Acremonium antarcticum</i> AY913 <i>Acremonium antarcticum</i> CBS	KR709189.1 LT549083.1 JX158422.1	Hypocreales	99	MH881446

APPENDIX

8	13	FVE	WM	301	987.87				
					<i>Trichoderma gamsii</i> SCAU130	MF061792.1	Hypocreales	100	MH881447
					<i>Trichoderma koningii</i> ACCC32855	MF780862.1			
9	14	SE	WM	306	<i>Trichoderma koningii</i> ACCC32853	MF780861.1			
					<i>Penicillium</i> sp. L2-3C	MG813426.1	Eurotiales	100	MH881448
					<i>Penicillium</i> sp. UCD161305F	MG686509.1			
10	15	SE	WM	227	<i>Penicillium thomii</i> MUT<ITA>:2257	MG813165.1			
					<i>Penicillium</i> sp. L2-3C	MG813426.1	Eurotiales	100	MH881449
					<i>Penicillium</i> sp. UCD161305F	MG686509.1			
11	16	SE	PDM	358	<i>Penicillium thomii</i> MUT<ITA>:2257	MG813165.1			
					<i>Penicillium glabrum</i> KAS5827	KY469043.1	Eurotiales	100	MH881450
					<i>Penicillium glabrum</i> SFC101259	MF185992.1			
12	20	SE	PDM	287	<i>Penicillium spinulosum</i> Su-XII-4	MF475933.1			
					<i>Penicillium</i> sp. L2-3C	MG813426.1	Eurotiales	100	MH881451
					<i>Penicillium</i> sp. UCD161305F	MG686509.1			
13	24	SE	GCM	376	<i>Penicillium thomii</i> MUT<ITA>:2257	MG813165.1			
					<i>Penicillium murcianum</i> PM1	MF668969.1	Eurotiales	100	MH881452
					<i>Penicillium nucicola</i> KAS 2101	KT887846.1			
14	25	SE	GYP	482	<i>Penicillium</i> sp. SFC102007	MF186110.1			
					<i>Cladosporium sloanii</i> DTO:130-D5	MF473253.1	Eurotiales	98	MH881453
					<i>Cladosporium psychrotolerans</i> DTO:307-H2	MF473224.1			
15	26	SE	GCM	232	<i>Cladosporium psychrotolerans</i> DTO:305-G3	MF473223.1			
					<i>Penicillium</i> sp. EMA-2011d	JF429677.1	Eurotiales	99	MH881454
					<i>Penicillium thomii</i> MUT<ITA>:2257	MG813165.1			
16	27	SE	GYP	352	<i>Penicillium glabrum</i> SFC101259	MF185992.1			
					<i>Penicillium coralligerum</i> YK247	LC214562.1	Eurotiales	99	MH881455
					<i>Penicillium atrovenetum</i> bqw5	MF599167.1			
17	29	SE	GYP	430	<i>Penicillium</i> sp. 8	KY401130.1			
					<i>Penicillium glabrum</i> KAS5827	KY469043.1	Eurotiales	100	MH881456
					<i>Penicillium glabrum</i> SFC10125	MF185992.1			
18	30	SE	GYP	375	<i>Penicillium glabrum</i> SYPF 6991	MH279474.1			
					<i>Penicillium glabrum</i> KAS5827	KY469043.1	Eurotiales	100	MH881457
					<i>Penicillium glabrum</i> SFC10125	MF185992.1			
					<i>Penicillium glabrum</i> SYPF 6991	MH279474.1			

APPENDIX

19	31	SE	GYP	338	<i>Penicillium brevicompactum</i> KX965655.1 GIBI220	Eurotiales	100	MH881458
					<i>Penicillium sp.</i> M_FA_V8 MH137760.1			
20	32	FVE	PDM	366	<i>Penicillium brevicompactum</i> MH047201.1 <i>Penicillium brevicompactum</i> MF503895.1 MERVA5	Eurotiales	100	MH881459
					<i>Penicillium brevicompactum</i> MH047201.1			
					<i>Penicillium brevicompactum</i> KY469047.1 KAS5854			
21	33	FVE	PDM	318	<i>Penicillium atroveneretum</i> bqw5 MF599167.1 <i>Penicillium atroveneretum</i> CBS 243.56 KP016835.1	Eurotiales	100	MH881460
					<i>Penicillium sp.</i> MT152 MH109377.1			
22	34	FVE	GYP	468	<i>Penicillium atroveneretum</i> bqw5 MF599167.1 <i>Penicillium coralligerum</i> YK-247 LC214562.1	Eurotiales	100	MH881461
					<i>Penicillium antarcticum</i> SFC101809 MF186085.1			
23	35	FVE	GYP	323	<i>Cadophora malorum</i> M7 MG813381.1 <i>Cadophora malorum</i> VKM F-4744 MF494613.1	Incertae sedis	100	MH881462
					<i>Cadophora malorum</i> VKM F-4747 MF494620.1			
24*	37	FVE	GYP	304	<i>Emericellopsis sp.</i> SNT1-23 KY379579.1 <i>Acremonium zonatum</i> CSR1-21 KY379556.1	Hypocreales	99	MH881463
					<i>Sarocladium kiliense</i> 11-84 KX815337.1			
25	38	FVE	WM	328	<i>Penicillium biourgeianum</i> UWR031 KX426968.1 <i>Penicillium bialowiezense</i> MF186021.1 SFC101475	Eurotiales	100	MH881464
					<i>Penicillium bialowiezense</i> KAS5860 KY469051.1			
26	39	FVE	WM	224	<i>Penicillium brevicompactum</i> KX426968.1 UWR031	Eurotiales	100	MH881465
					<i>Penicillium bialowiezense</i> KAS5860 KY469051.1			
					<i>Penicillium brevicompactum</i> 82 KY401133.1			
27	40	FVE	WM	347	<i>Penicillium sp.</i> 86 KY401137.1 <i>Penicillium atroveneretum</i> BQW5 MF599167.1	Eurotiales	100	MH881466
					<i>Penicillium sp.</i> 8 KY401130.1			
28	42	FVE	GYP	517	<i>Penicillium brevicompactum</i> F27-02 KX664363.1 <i>Penicillium brevicompactum</i> KY469047.1 KAS5854	Eurotiales	100	MH881467
					<i>Penicillium brevicompactum</i> KY469041.1			

APPENDIX

29	43	SE	WM	228	KAS5812	MG813426.1	Eurotiales	100	MH881468
					<i>Penicillium</i> sp. L2-3C				
30	44	SE	PDM	206	<i>Penicillium</i> sp. UCD161305F	MG686509.1	Hypocreales	100	MH881469
					<i>Penicillium thomii</i> MUT<ITA>:2257	MG813165.1			
31	46	SE	PDM	355	<i>Fusarium chlamydosporum</i>	KY860655.1	Eurotiales	100	MH881470
					<i>Fusarium oxysporum</i> f. sp. momordicae GuangX26	MF445489.1			
32	47	SE	PDM	372	<i>Fusarium chlamydosporum</i> Ng30	MH141316.1	Eurotiales	100	MH881471
					<i>Penicillium glabrum</i> KAS5827	KY469043.1			
33	48	SE	PDM	365	<i>Penicillium glabrum</i> SFC101259	MF185992.1	Eurotiales	100	MH881472
					<i>Penicillium glabrum</i> SFC101229	MF185985.1			
34	49	SE	GYP	307	<i>Penicillium glabrum</i> KAS5767	KY469033.1	Eurotiales	100	MH881473
					<i>Penicillium glabrum</i> SFC101259	MF185992.1			
35	50	FVE	PDM	507	<i>Penicillium glabrum</i> PO6	KY463488.1	Eurotiales	100	MH881474
					<i>Penicillium jensenii</i> P6342	MH063657.1			
36	52	SE	WM	322	<i>Penicillium sp.</i> 1217_476	MG917754.1	Eurotiales	100	MH881475
					<i>Penicillium canescens</i> 3S.106	KY458474.1			
37*	53	FVS	GYP	314	<i>Penicillium jensenii</i> P6342	MH063657.1	Eurotiales	100	MH881476
					<i>Penicillium sp.</i> 1217_476	MG917754.1			
38	54	FVS	GCM	337	<i>Penicillium canescens</i> 3S.106	KY458474.1	Eurotiales	100	MH881477
					<i>Penicillium sp.</i> 86	KY401137.1			
39	55	FVE	PDM	300	<i>Penicillium sanguifluum</i> IG103	MG973279.1	Eurotiales	100	MH881478
					<i>Penicillium sp.</i> 8	KY401131.1			
37*	53	FVS	GYP	314	<i>Penicillium sp.</i> L2-3C	MG813426.1	Eurotiales	100	MH881475
					<i>Penicillium sp.</i> UCD161305F	MG686509.1			
38	54	FVS	GCM	337	<i>Penicillium thomii</i> MUT<ITA>:2257	MG813165.1	Eurotiales	100	MH881477
					<i>Phoma</i> sp. MUT5465	KU314987.1			
39	55	FVE	PDM	300	<i>Roussoellaceae</i> sp. MUT 4859	KR014355.1	Eurotiales	100	MH881478
					<i>Phoma</i> sp. MUT 5462	KU314985.1			
37*	53	FVS	GYP	314	<i>Penicillium brevicompactum</i> F27-02	KX664363.1	Eurotiales	100	MH881476
					<i>Penicillium sp.</i> UCD160901G3	MG686505.1			
38	54	FVS	GCM	337	<i>Penicillium brevicompactum</i>	KY469047.1	Eurotiales	100	MH881477
					KAS5854				
39	55	FVE	PDM	300	<i>Penicillium glabrum</i> ND70	MG659664.1	Eurotiales	100	MH881478
					<i>Penicillium thomii</i> MUT<ITA>:2257	MG813165.1			

APPENDIX

40	56	FVE	WM	523	<i>Penicillium glabrum</i> SFC101229	MF185985.1	Eurotiales	100	MH881479
					<i>Penicillium coralligerum</i> YK-247	LC214562.1			
					<i>Penicillium</i> sp. 86	KY401137.1			
41	57	FVE	GYP	331	<i>Penicillium</i> sp. 76	KY401126.1	Eurotiales	100	MH881480
					<i>Penicillium atrovenetum</i> FO.1	KT587349.1			
					<i>Penicillium antarcticum</i> SFC101809	MF186085.1			
42	58	FVE	WM	258	<i>Penicillium coralligerum</i> YK-247	LC214562.1	Hypocreales	96	MH881481
					<i>Fusarium graminearum</i> WF1	KY985465.1			
					<i>Fusarium graminearum</i> PGTU11	MF497390.1			
43*	59	FVE	WM	231	<i>Fusarium graminearum</i> PGTU10	MF497389.1	Glomerellales	100	MH881482
					<i>Gibellulopsis nigrescens</i> LG1402	KY459202.1			
					<i>Plectosphaerella</i> sp. sedF4	KX359602.1			
44	60	FVE	WM	310	Uncultured <i>Verticillium</i> JB40C25 (MOTU06)	HG935585.1	Eurotiales	100	MH881483
					<i>Penicillium coralligerum</i> YK-247	LC214562.1			
					<i>Penicillium atrovenetum</i> bqW5	MF599167.1			
45	61	FVE	PDM	514	<i>Penicillium</i> <i>brevicompactum</i> TCDFvLDB1814	MH71548.1	Eurotiales	100	MH881484
					<i>Penicillium</i> <i>brevicompactum</i> Asa3SNA1	KY558614.1			
					<i>Penicillium</i> <i>brevicompactum</i> KAS5854	KY469047.1			
46	62	FVE	PDM	324	<i>Penicillium brevicompactum</i> F27-02	KX664363.1	Eurotiales	100	MH881485
					<i>Penicillium</i> <i>brevicompactum</i> KAS5854	KY469047.1			
					<i>Penicillium</i> <i>brevicompactum</i> KAS5812	KY469041.1			
47	63	FVE	PDM	334	<i>Penicillium brevicompactum</i> F27-02	KX664363.1	Eurotiales	100	MH881486
					<i>Penicillium</i> <i>brevicompactum</i> KAS5854	KY469047.1			
					<i>Penicillium</i> <i>brevicompactum</i> KAS5812	KY469041.1			
48	64	FVE	PDM	341	<i>Penicillium brevicompactum</i> MERV5	MF503895.1	Eurotiales	100	MH881487
					<i>Penicillium</i> <i>brevicompactum</i> SFC102216	MF186137.1			

APPENDIX

49	65	SA	PDM	247	<i>Penicillium brevicompactum</i> 2-Z-30	MH310820.1	Saccharomycetales	99	MH881488
					<i>Candida</i> sp. KJS-2016	LC155354.1			
					<i>Candida pseudolambica</i> yHRM77	KM384061.1			
50	66	SE	PDM	182	<i>Candida pseudolambica</i> yHRM67	KM384060.1	Hypocreales	100	MH881489
					<i>Fusarium lateritium</i> 3821	MG066631.1			
					<i>Fusarium tricinctum</i> SFC101814	MF186086.1			
51	67	FVE	WM	250	<i>Fusarium avenaceum</i> SFC101774	MF186082.1	Glomerellales	100	MH881490
					<i>Gibellulopsis nigrescens</i> STAF302	KU214559.1			
					<i>Gibellulopsis nigrescens</i> LG1401 GL11A	KX359602.1			
52	68	FVE	WM	316	<i>Gibellulopsis nigrescens</i> STAF302	KU314961.1	Eurotiales	100	MH881491
					<i>Penicillium atrovenerum</i> bqw5	MF599167.1			
					<i>Penicillium coralligerum</i> YK-247	LC214562.1			
53	69	FVE	PDM	329	<i>Penicillium antarcticum</i> SFC101809	MF186085.1	Eurotiales	100	MH881492
					<i>Penicillium brevicompactum</i> MERV5	MF503895.1			
					<i>Penicillium brevicompactum</i> SFC102216	MF186137.1			
54	72	FVE	WM	204	<i>Penicillium brevicompactum</i> 2-Z-30	MH310820.1	Eurotiales	100	MH881493
					<i>Penicillium coralligerum</i> YK-247	LC214562.1			
					<i>Penicillium atrovenerum</i> bqw5	MF599167.1			
55	73	FVE	GYP	321	<i>Penicillium antarcticum</i> SFC101809	MF186085.1	Eurotiales	98	MH881494
					<i>Penicillium brevicompactum</i> MERV5	MF503895.1			
					<i>Penicillium brevicompactum</i> SFC102216	MF186137.1			
56	77	SE	PDM	249	<i>Penicillium brevicompactum</i> 2-Z-30	MH310820.1	Eurotiales	100	MH881495
					<i>Penicillium</i> sp. L2-3C	MG813426.1			
					<i>Penicillium</i> sp. UCD161305F	MG686509.1			
57	78	FVE	PDM	509	<i>Penicillium thomii</i> MUT:2257	MG813165.1	Eurotiales	100	MH881496
					<i>Penicillium glabrum</i> DTO313-D4	MF803957.1			
					<i>Penicillium glabrum</i> DTO313-C1	MF803952.1			
58	81	FVE	WM	227	<i>Penicillium camemberti</i> ISSFR-016	KT832784.1	Wallemiales	100	MH881497
					<i>Wallemia muriae</i> KK18.3	KY322648.1			
					<i>Wallemia muriae</i> KAS 6011	KX911859.1			
59	82	FVE	WM	328	<i>Wallemia muriae</i> KAS 5869	KX911850.1	Hypocreales	99	MH881498
					<i>Emericellopsis terricola</i> CCF3815	J430737.1			
					<i>Emericellopsis minima</i>	KT290876.1			



APPENDIX

					OUCMBII111121					
					Uncultured	<i>Emericellopsis</i>	HG936806.1			
					10J50C67 (MOTU75)					
60*	84	FVE	WM	323	<i>Stilbella fimetaria</i> voucher AF3-097G		KX446764.1	Hypocreales	100	MH881499
					<i>Emericellopsis salmosynnemata</i>		AY632666.1			
					CBS382.62					
					<i>Stilbella fimetaria</i> D99026		AY952467.1			
61	85	SE	PDM	260	<i>Stereum hirsutum</i> P2A		KX838369.2	Russulales	100	MH881500
					<i>Stereum hirsutum</i> gap67		KX578081.1			
					<i>Stereum hirsutum</i> Wi-XI-1.1		MF476012.1			
62	86	FVE	PDM	323	<i>Emericellopsis terricola</i> CCF3815		FJ430737.1	Hypocreales	99	MH881501
					<i>Emericellopsis terricola</i>		U57676.1			
					<i>Emericellopsis minima</i> A11		KY775297.1			
63*	87	FVE	WM	279	<i>Phoma</i> sp. MUT 5465		KU314987.1	Pleosporales	99	MH881502
					<i>Pleosporales</i> sp. AT60		KX953409.1			
					<i>Pyrenochaetopsis microspora</i> CBS 119739		LT623227.1			
64	89	FVE	WM	395	<i>Trichoderma paraviridescens</i>		MG646337.1	Hypocreales	100	MH881503
					<i>Trichoderma viride</i> IMF51186		LC317804.1			
					<i>Trichoderma koningiopsis</i> ACCC32904		MF871558.1			
65	91	FVE	GCM	473	<i>Penicillium spathulatum</i> AS3.15328		KC427190.1	Eurotiales	100	MH881504
					<i>Penicillium spathulatum</i> CBS 116977		JX313162.1			
					<i>Penicillium</i> sp. DF-2		KT121500.1			
66	92	FVS	PDM	330	<i>Penicillium coralligerum</i> YK-247		LC214562.1	Eurotiales	100	MH881505
					<i>Penicillium</i> sp. MT152		MH109377.1			
					<i>Penicillium</i> sp. MT57		MH109376.1			
67	95	FVE	PDM	350	<i>Penicillium coralligerum</i> YK-247		LC214562.1	Eurotiales	100	MH881506
					<i>Penicillium</i> sp. MT152		MH109377.1			
					<i>Penicillium</i> sp. MT57		MH109376.1			
68	96	FVS	GYP	502	<i>Penicillium brevicompactum</i> BEOFB1102m		MH630035.1	Eurotiales	100	MH881507
					<i>Penicillium brevicompactum</i> TCDFvLDB1814		MH714548.1			
					<i>Penicillium brevicompactum</i> 1		MH047201.1			

APPENDIX

69	97	SE	GYP	428	<i>Fusarium culmorum</i> S68 <i>Fusarium culmorum</i> F150 <i>Fusarium asiaticum</i> G84	MH681156.1 MH681154.1 MH681153.1	Eurotiales	100	MH881508
70	99	FVS	GCM	315	<i>Penicillium brevicompactum</i> KAS5854 <i>Penicillium brevicompactum</i> KAS5812 <i>Penicillium brevicompactum</i> KAS5776	KY469047.1 KY469041.1 KY469037.1	Eurotiales	100	MH881509
71	101	FVE	GCM	326	<i>Penicillium brevicompactum</i> KG_6i <i>Penicillium brevicompactum</i> Asa3SNA1 <i>Penicillium brevicompactum</i> Cch1SNA3	MG686505.1 KY558614.1 KY558611.1	Eurotiales	100	MH8815010
72	102	FVE	W	349	<i>Penicillium</i> sp. 86 <i>Penicillium atrovenetum</i> BQW5 <i>Penicillium</i> sp. 8	MF599167.1 KY401137.1 MF599167.1	Eurotiales	100	MH881511
73	104	FVS	WM-S	318	<i>Penicillium chrysogenum</i> DCMAF01BCI <i>Penicillium brevicompactum</i> SFC102216 <i>Penicillium brevicompactum</i> 2-Z-30	KY401130.1 MF186137.1 MH310820.1	Eurotiales	100	MH881512
74	105	FVS	GCM	377	<i>Penicillium</i> sp. 86 <i>Penicillium atrovenetum</i> BQW5 <i>Penicillium</i> sp. 8	KY401137.1 MF599167.1 KY401130.1	Eurotiales	100	MH881513
75	107	FVE	PDM	415	<i>Penicillium</i> sp. 86 <i>Penicillium atrovenetum</i> BQW5 <i>Penicillium</i> sp. 8	KY401137.1 MF599167.1 KY401130.1	Eurotiales	100	MH881514
76	108	FVS	WM	305	<i>Penicillium</i> sp. 86 <i>Penicillium atrovenetum</i> BQW5 <i>Penicillium</i> sp. 8	KY401137.1 MF599167.1 KY401130.1	Eurotiales	100	MH881515
77	109	FVS	GCM	291	<i>Penicillium</i> sp. 86 <i>Penicillium atrovenetum</i> BQW5 <i>Penicillium</i> sp. 8	KY401137.1 MF599167.1 KY401130.1	Eurotiales	100	MH881516
78	111	FVE	GYP	312	<i>Penicillium</i> sp. 86 <i>Penicillium atrovenetum</i> BQW5	KY401137.1 MF599167.1	Eurotiales	100	MH881517

APPENDIX

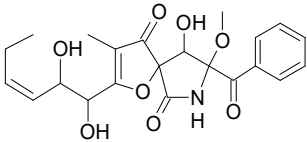
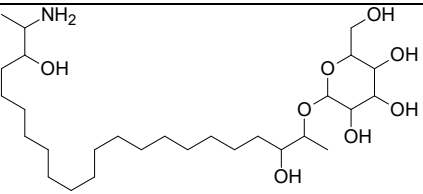
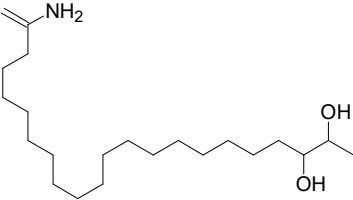
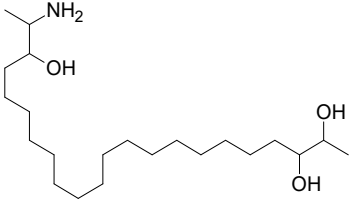
79	112	FVE	GCM	367	<i>Penicillium</i> sp. 8	KY401130.1	Eurotiales	100	MH881518
					<i>Penicillium glabrum</i> R2EK05	KR091814.1			
					<i>Penicillium glabrum</i> SFC101259	MF185992.1			
80*	113	SE	GCM	296	<i>Penicillium glabrum</i> SFC101229	MF185985.1	Hypocreales	100	MH881519
					<i>Nectria inventa</i> MUT1135	KR709185.1			
					<i>Acrostalagmus luteoalbus</i> P6424	MH063783.1			
81	114	FVS	PDM	300	<i>Acrostalagmus luteoalbus</i> H35	KX375795.1	Eurotiales	100	MH881520
					<i>Penicillium brevicompactum</i> KAS5871	KY469055.1			
					<i>Penicillium brevicompactum</i> SFC102216	MF186137.1			
82	115	SA	PDM	124	<i>Penicillium brevicompactum</i> 2-Z-30	MH310820.1	Eurotiales	100	MH881521
					<i>Penicillium coralligerum</i> YK247	LC214562.1			
					<i>Penicillium atrovenetum</i> bqw5	MF599167.1			
83	117	SE	PDM	434	<i>Penicillium</i> sp. 8	KY401130.1	Pleosporales	100	MH881522
					<i>Phoma</i> sp. MUT 5465	KU314987.1			
					<i>Phoma</i> sp. MUT 5462	KU314985.1			
84	121	FVE	GCM	287	<i>Phoma</i> sp. MUT 5460	KU314983.1	Eurotiales	100	MH881523
					<i>Penicillium canescens</i> 3S.106	KY458474.1/			
					<i>Penicillium murcianum</i> KK19.1	KY322566.1			
85	122	FVE	GCM	376	<i>Penicillium jensenii</i> P6342	MH063657.1	Eurotiales	100	MH881524
					<i>Penicillium brevicompactum</i> KAS5871	KY469055.1			
					<i>Penicillium brevicompactum</i> SFC102216	MF186137.1			
86	123	SE	GCM	102	<i>Penicillium brevicompactum</i> 2-Z-30	MH310820.1	Eurotiales	100	MH881525
					<i>Penicillium denovo</i> 13735	KR266650.1			
					<i>Penicillium</i> sp. SF1	KX011018.1			
87	124	SE	GCM	309	<i>Neosartorya</i> sp. BAB-4715	KU571518.1	Eurotiales	100	MH881526
					<i>Penicillium coralligerum</i> YK247	LC214562.1			
					<i>Penicillium atrovenetum</i> bqw5	MF599167.1			
					<i>Penicillium</i> sp. 8	KY401130.1			

## APPENDIX

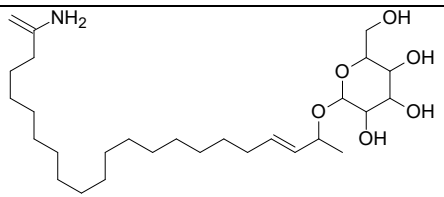
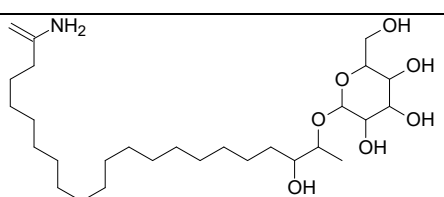
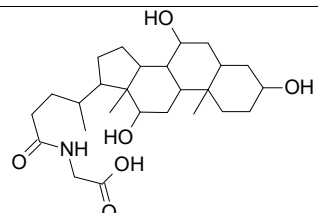
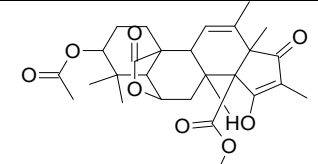
**Table S2.** Putatively identified compounds from 40 liquid culture extracts and 40 solid culture extracts. Dereplication of the compounds was based on GNPS, UNPD-ISDB, and manual dereplication by using several databases such as DNP, Scifinder and Chempidder.

Comp. No.	tr (min)	Culture regime (medium)	Precursor <i>m/z</i>	Putative ID (chemical family)	Chemical structure	Molecular formula (change in $\Delta$ ppm)	MS/MS fragmentation	Strain number
1	0.70	Solid (SYM)	204.1113 [M+H] <sup>+</sup>	Acetylcarnitine (amino acid derivative)		C <sub>9</sub> H <sub>17</sub> NO <sub>4</sub> (-59.3)*	145.1231; 85.9665	1
2	1.66	Liquid (WM)	189.1130 [M+H] <sup>+</sup>	Aspinonene (pentaketide)		C <sub>9</sub> H <sub>16</sub> O <sub>4</sub> (0)	-	68
3	2.24	Solid (PDM, SYM, Cza, WM)	239.1592 [M+H] <sup>+</sup>	Lysergine (indole alkaloid)		C <sub>16</sub> H <sub>18</sub> N <sub>2</sub> (-7.5)	197.1551; 141.9877	37
4	3.04	Solid (Cza)	245.1508 [M+H] <sup>+</sup>	Cyclo(L-Phe-D-Pro) (diketopiperazine)		C <sub>14</sub> H <sub>16</sub> N <sub>2</sub> O <sub>2</sub> (1.9)	217.1613; 154.1008; 120.1105	35
5	4.15	Liquid (PDM)	301.0852 [M+H] <sup>+</sup>	Questinol (dihydroxyanthraquinone)		C <sub>16</sub> H <sub>12</sub> O <sub>6</sub> (-0.5)	286.0602; 257.0612	50

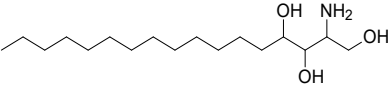
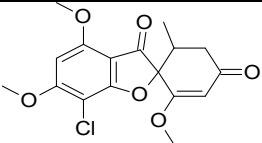
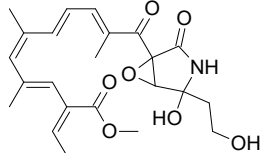
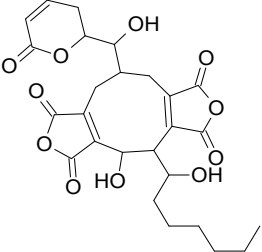
APPENDIX

6	4.18	Solid (WM)	454.1482 [M+Na] <sup>+</sup>	Pseurotin A (amide alkaloid)		C <sub>22</sub> H <sub>25</sub> NO <sub>8</sub> (-0.9)	422.1124; 370.0889; 261.0882; 216.0832	78
		Liquid (SYM)						35
7	5.19	Liquid (Cza) Solid (Cza)	536.4123 [M+H] <sup>+</sup>	2-(21-amino-3, 20-dihydroxydocosan-2-yl)oxy-6-(hydroxymethyl)oxane-3, 4, 5-triol (aminoglycolipid)		C <sub>28</sub> H <sub>57</sub> NO <sub>8</sub> (-1.9)	518.4053; 500.3958; 482.3873; 374.3875; 338.3654; 320.3527	59
8	5.19	Liquid (Cza) Solid (Cza)	356.3711 [M+H] <sup>+</sup>	21-aminodocos-21-ene-2,3-diol (aminolipid)		C <sub>22</sub> H <sub>45</sub> NO <sub>2</sub> (0.5)	338.3616; 320.3527	59
9	5.20	Liquid (Cza) Solid (Cza)	374.3796 [M+H] <sup>+</sup>	21-aminodocosane-2,3,20-triol (aminolipid)		C <sub>22</sub> H <sub>47</sub> NO <sub>3</sub> (42.2) *	356.3704; 338.3615; 320.3528	59

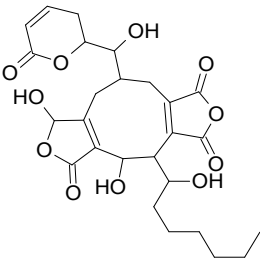
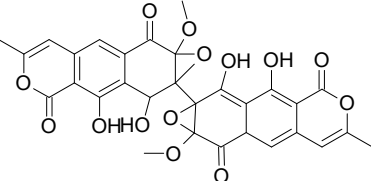
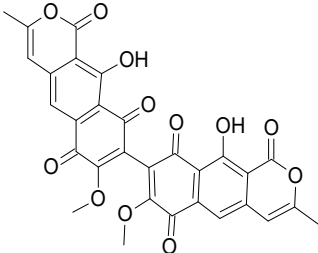
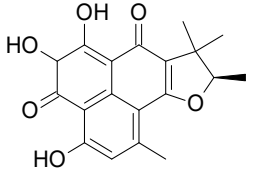
APPENDIX

10	5.21	Liquid (Cza) Solid (Cza)	500.3968 [M+H] <sup>+</sup>	( <i>E</i> )-2-((21-aminodocosa-3,21-dien-2-yl)oxy)-6-(hydroxymethyl)tetrahydro-2 <i>H</i> -pyran-3, 4, 5-triol (aminolipid)		C <sub>28</sub> H <sub>53</sub> NO <sub>6</sub> (3.2)	482.3876; 374.3875; 356.3695; 338.3606; 320.3527	59
11	5.23	Liquid (Cza) Solid (Cza)	518.4051 [M+H] <sup>+</sup>	2-(21-amino-3-hydroxydocos-21-en-2-yl)oxy)-6-(hydroxymethyl)tetrahydro-2 <i>H</i> -pyran-3, 4, 5-triol (aminoglycolipid)		C <sub>28</sub> H <sub>55</sub> NO <sub>7</sub> (-1.7)	500.3958; 482.3873; 356.3700; 338.3612; 320.3526	59
12	5.47	Solid (WM)	466.3 170 [M+H] <sup>+</sup> <hr/> 488.2 957 [M+Na] <sup>+</sup>	Glycocholic acid (bile acid)		C <sub>26</sub> H <sub>44</sub> NO <sub>6</sub> (0.2)	412.2906; 337.2691; 319.2593; <hr/> 227.1693 470.2871; 412.2914	59
13	6.32	Liquid (Cza, SYM) Solid (SYM, WM, PDM)	501.2903 [M+H] <sup>+</sup>	Citreohybridonol (sesterterpenoid)		C <sub>28</sub> H <sub>36</sub> O <sub>8</sub> (-0.3)	486.2682; 409.2138; 381.2216; 363.2131; 335.2205; 217.1520; 179.1021	68

## APPENDIX

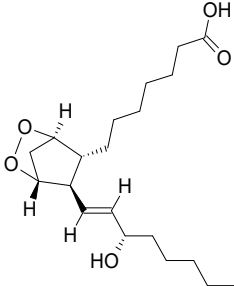
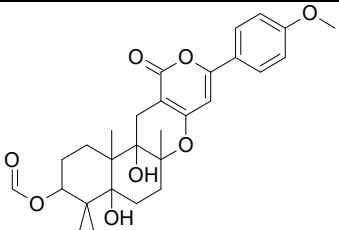
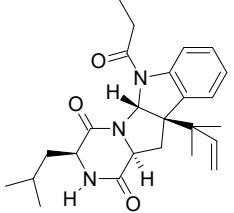

14	6.45	Solid (SYM)	318.3213 [M+H] <sup>+</sup>	Phytosphingosine (sphingolipid)		C <sub>18</sub> H <sub>39</sub> NO <sub>3</sub> (6.5)	300.3127; 282.3036; 270.3043; 264.2945; 240.2946;	56
15	6.52	Liquid (WM)	353.0795 [M+H] <sup>+</sup>	Griseofulvin (tetrahydrofuranone polyketide)		C <sub>17</sub> H <sub>17</sub> ClO <sub>6</sub> (0.8)	285.0648; 215.0305; 165.0792	68
16	6.70	Liquid (Cza) Solid (WM)	454.1801 [M+Na] <sup>+</sup>	Fusarin C (polyene)		C <sub>23</sub> H <sub>29</sub> NO <sub>7</sub> (-10.4)	413.2605; 335.1281; 290.1098	58
17	6.78	Liquid (Cza, PDM)	519.1832 [M+H] <sup>+</sup>	Rubratoxin B (bis-anhydride)		C <sub>26</sub> H <sub>30</sub> O <sub>11</sub> (-4.0)	501.1757; 451.1306; 271.1122	50

APPENDIX

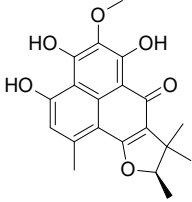
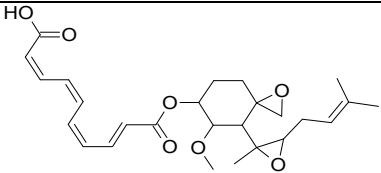
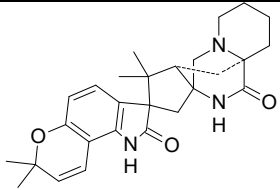
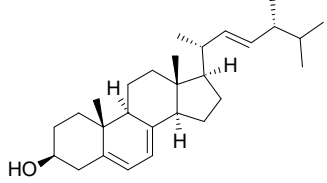
18	6.99	Liquid (Cza, PDM)	521.1890 [M+H] <sup>+</sup>	Rubratoxin A (bis-anhydride)		C <sub>26</sub> H <sub>32</sub> O <sub>11</sub> (-5.0)	503.1911; 435.1422; 283.1126; 271.1121	50
19	7.14	Liquid (PDM)	589.0890 [M+H- H <sub>2</sub> O] <sup>+</sup>	Xanthoepocin (binaphthoquinone)		C <sub>30</sub> H <sub>22</sub> O <sub>14</sub> (-10.6)	571.0801; 483.0744; 470.0672; 441.0686; 413.0764; 313.0562	59
20	7.16	Liquid (PDM)	571.0803 [M+H] <sup>+</sup>	Bisdehydroxanthomegn in (binaphthoquinone)		C <sub>30</sub> H <sub>18</sub> O <sub>12</sub> (-12.6)	511.0682; 483.0735; 469.0599; 286.0680; 257.0700	59
21	7.46	Liquid (SYM, PDM, Cza)	343.1276 [M+H] <sup>+</sup>	Atrovenetin (aromatic polyketide)		C <sub>19</sub> H <sub>18</sub> O <sub>6</sub> (24.30)	287.0714; 255.0495	68



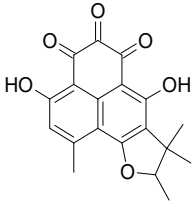
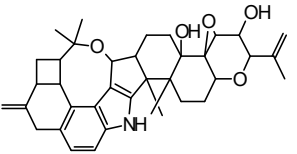
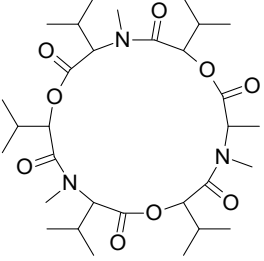
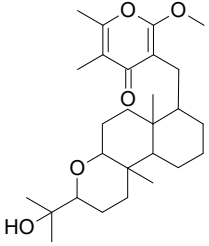
## APPENDIX

22	7.55	Solid (SYM, Cza)	337.2900 [M+H- H <sub>2</sub> O] <sup>+</sup>	Prostaglandin H <sub>1</sub> (fatty acid derivative)		C <sub>20</sub> H <sub>34</sub> O <sub>5</sub> (8.6)	263.2607; 123.1482; 109.1327	78
23	7.58	Solid (WM, Cza)	513.2470 [M+H] <sup>+</sup>	Arisugacin D (dihydroxanthone derivative)		C <sub>29</sub> H <sub>36</sub> O <sub>8</sub> (-3.9)	495.2372; 395.1965; 209.1114	50
24	7.67	Solid (SYM, Cza)	446.2421 [M+Na] <sup>+</sup>	Brevicompanine E (diketopiperazine alkaloid)		C <sub>25</sub> H <sub>33</sub> N <sub>3</sub> O <sub>3</sub> (-0.4)	386.2237; 328.1892; 130.0972; 358.1982	68
25	8.05	Solid (WM, SYM, PDM, Cza)	357.1544 [M+H] <sup>+</sup>	Deoxyherquenone (aromatic polyketide)		C <sub>20</sub> H <sub>20</sub> O <sub>6</sub> (5.4)	342.1268; 327.1049; 301.0910	50

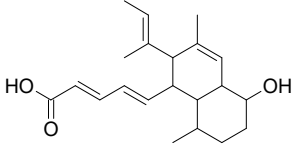
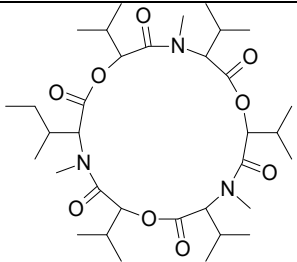
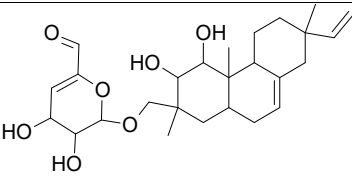
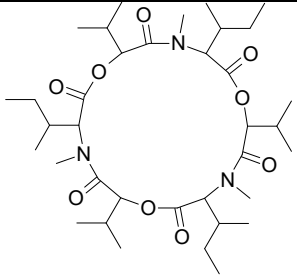
APPENDIX

		Liquid (SYM, PDM, Cza, WM)						68
26	8.12	Liquid (SYM)	481.2016 [M+Na] <sup>+</sup>	Fumagillin (meroterpenoid)		C <sub>26</sub> H <sub>34</sub> O <sub>7</sub> (-3.8)	329.2926	35
27	8.88	Solid (SYM)	448.2588 [M+H] <sup>+</sup>	Marcfortine C (indole alkaloid)		C <sub>27</sub> H <sub>33</sub> N <sub>3</sub> O <sub>3</sub> (-2.7)	406.2837; 330.2077; 182.1254	68
28	9.16	Liquid (SYM)	379.3 329 [M+H- H <sub>2</sub> O] <sup>+</sup>	Ergosterol (steroid)		C <sub>28</sub> H <sub>44</sub> O (-9.3)	309.2665; 295.2521; 253.2106; 213.1840; 199.1696; 159.1414	35

APPENDIX

29	9.35	Liquid (WM, Cza, PDM)	341.1123 [M+H] <sup>+</sup>	Atrovenetinone (aromatic polyketide)		C <sub>19</sub> H <sub>16</sub> O <sub>6</sub> (27.9)	313.7212; 287.0724	68
30	9.78	Solid (SYM)	584.3291 [M+H] <sup>+</sup>	Penitrem B (indole diterpenoid)		C <sub>37</sub> H <sub>46</sub> NO <sub>5</sub> (-14.2)	566.3217; 514.2602; 497.2591; 480.2563; 478.2471 304.1931; 260.1345	68
31	10.16	Liquid (PDM, Cza)	640.3732 [M+H] <sup>+</sup>	Enniatin B (cyclic depsipeptide)		C <sub>33</sub> H <sub>57</sub> N <sub>3</sub> O <sub>9</sub> (-53.4) *	527.3075; 427.2713; 314.2042; 214.1643; 195.1562; 186.1716	35
		Liquid (PDM, Cza)	662.3557 [M+Na] <sup>+</sup>				549.2864; 336.1829	
32	10.30	Solid (Cza)	481.2922 [M+Na] <sup>+</sup>	Candelalide C (diterpenoid pyrone)		C <sub>28</sub> H <sub>42</sub> O <sub>5</sub> (-1.7)	355.2387; 283.2012; 240.2581; 133.1116	50

APPENDIX

33	10.61	Liquid (SYM)	331.2302 [M+H] <sup>+</sup>	Phomopsidin (trimethylated nonaketide)		C <sub>21</sub> H <sub>30</sub> O <sub>3</sub> (6.5)	293.0333; 273.8689; 250.8805' 192.8811; 165.0659	87
34	10.66	Liquid (WM, PDM)	654.3968 [M+H] <sup>+</sup>	Enniatin B <sub>1</sub> (cyclic depsipeptide)		C <sub>34</sub> H <sub>59</sub> N <sub>3</sub> O <sub>9</sub> (-55.3) *	541.3203; 441.2848; 328.2178; 314.2042; 210.1696; 196.1553 563.2997	35
		Liquid (WM, PDM, Cza, SYM)	676.3968 [M+Na] <sup>+</sup>					
35	10.95	Liquid (PDM, Cza, WM)	463.2682 [M+H] <sup>+</sup>	Virescoside E (diterpene glycoside)		C <sub>26</sub> H <sub>38</sub> O <sub>7</sub> (-5.2)	355.2312	1
36	11.67	Liquid (PDM, WM)	704.3914 [M+Na] <sup>+</sup>	Enniatin A (cyclic depsipeptide)		C <sub>36</sub> H <sub>63</sub> N <sub>3</sub> O <sub>9</sub> (48.5) *	577.3101	35

\*Peak ions of low intensity (molecular formula prediction with high  $\Delta$  ppm).

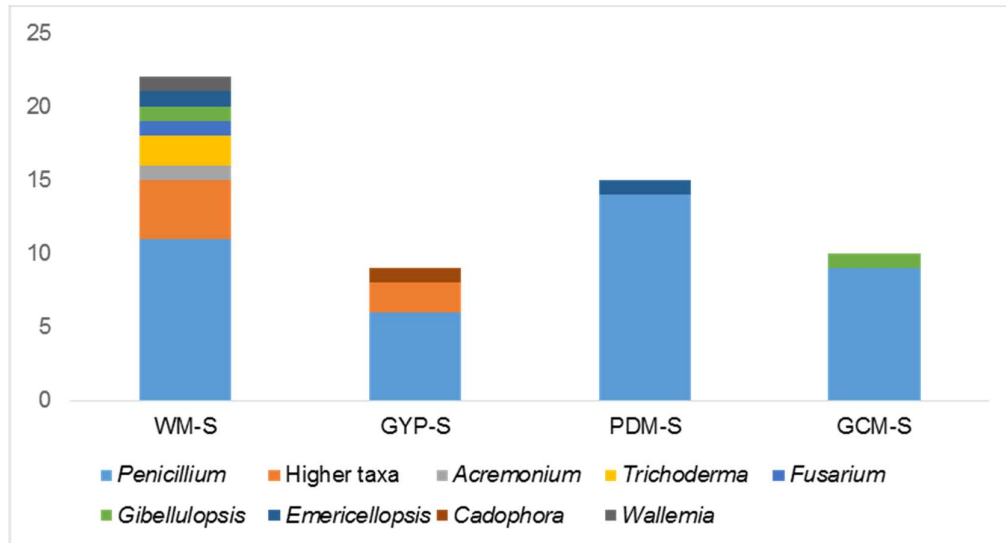


**Figure S1.** Comparison of 55 *F. vesiculosus* – derived fungi in diversity and distribution according to solid (S) isolation media. WM-S = modified Wickerham medium, PDM-S = Potato Dextrose medium, GCM-S = Glucose Casein medium, GYP-S = Glucose Yeast Peptone medium. Height of the column represents the total number of isolates derived from each media – WM-S: 21 isolates; PDM-S: 15 isolates, GCM-S: 10 isolates. GYP-S: 9 isolates.

APPENDIX

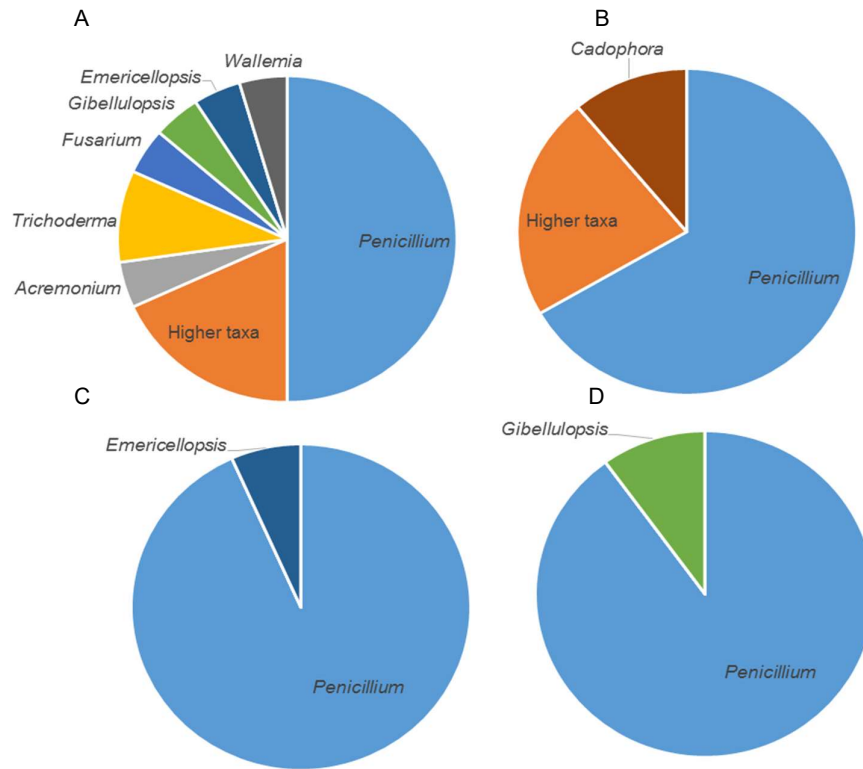


**Figure S2.** Pie chart showing the diversity of 55 *Fucus vesiculosus* – derived fungal community obtained by different isolation media. Strains that could not be identified to genus level are indicated as ‘Higher taxa’. **(A).** Fungal isolates obtained from the WM-S medium that were identified as 10 *Penicillium* sp., 1 *Emericellopsis* sp., 1 *Gibellulopsis* sp., 1 *Fusarium* sp., 2 *Trichoderma* sp., 1 *Acremonium* sp., 1 *Wallemia* sp. and 4 ‘Higher taxa’. **(B).** Fungal isolates obtained from the GYP-S medium that were identified as 6 *Penicillium* sp., 2 ‘Higher taxa’, and 1 *Cadophora* sp. **(C).** Fungal isolates obtained from the PDM-S medium that were identified as 14 *Penicillium* sp. and 1 *Emericellosis* sp. **(D).** Fungal isolates obtained from the GCM-S medium that were identified as 9 *Penicillium* sp. and 1 *Gibellulopsis* sp.

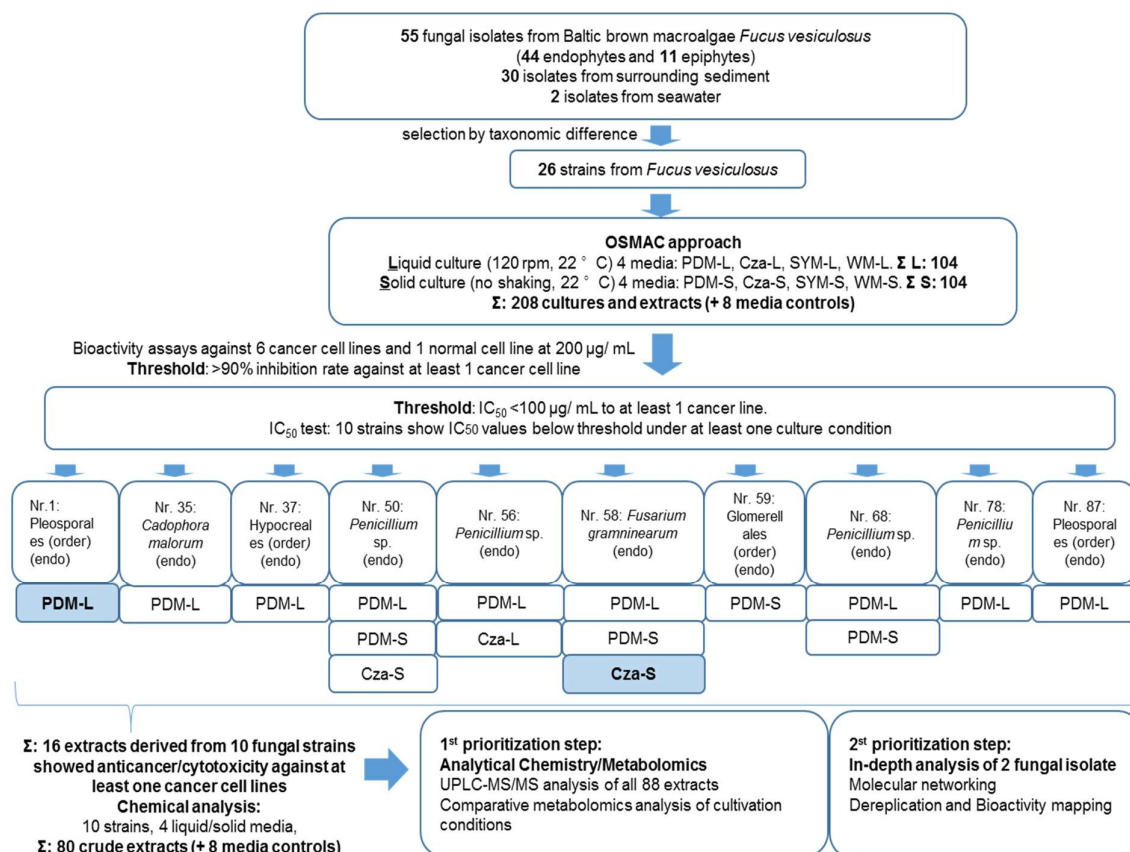


**Figure S3.** Workflow for the OSMAC study based on the 55 fungal isolates derived from *F. vesiculosus*. 26 isolates were selected for small-scale fermentation. The OSMAC approach was designed using 4 different media and 2 culture regimes. In total 208 culture extracts were tested for anticancer activity and the bioactive samples were further tested for IC<sub>50</sub> determination. 10 strains showed IC<sub>50</sub> values below 100  $\mu$ g/mL against at least one cancer cell line. In the end, all 80 culture extracts derived from 10 strains were analysed by an integrated metabolomics approach.

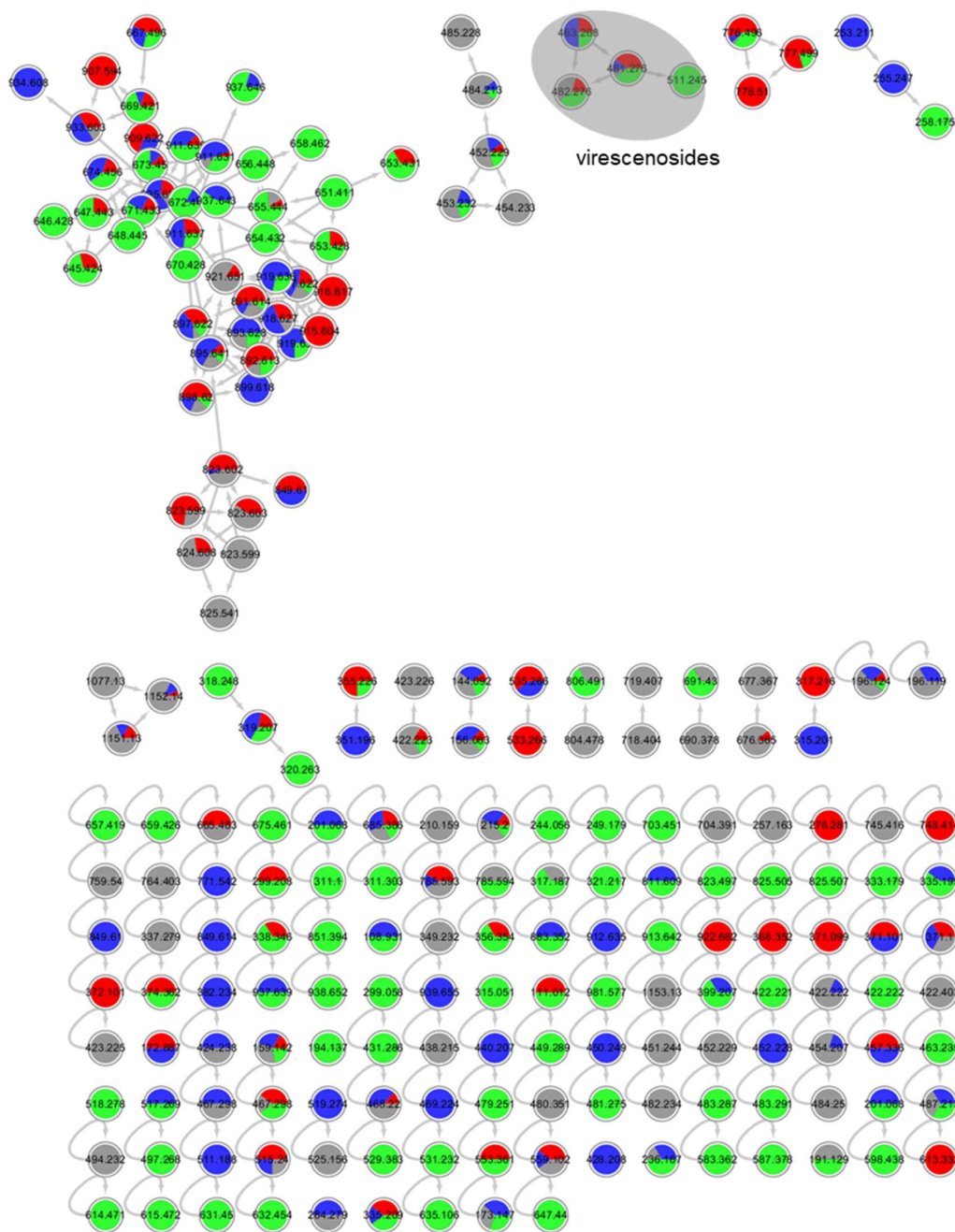


**Figure S4.** Molecular network for strain 1 (order Pleosporales) liquid culture extracts in PDM-L (**blue**), Cza-L (**red**), SYM-L (**green**), WM-L (**grey**). Annotated peak ions of putatively known compounds are highlighted by a grey loop.



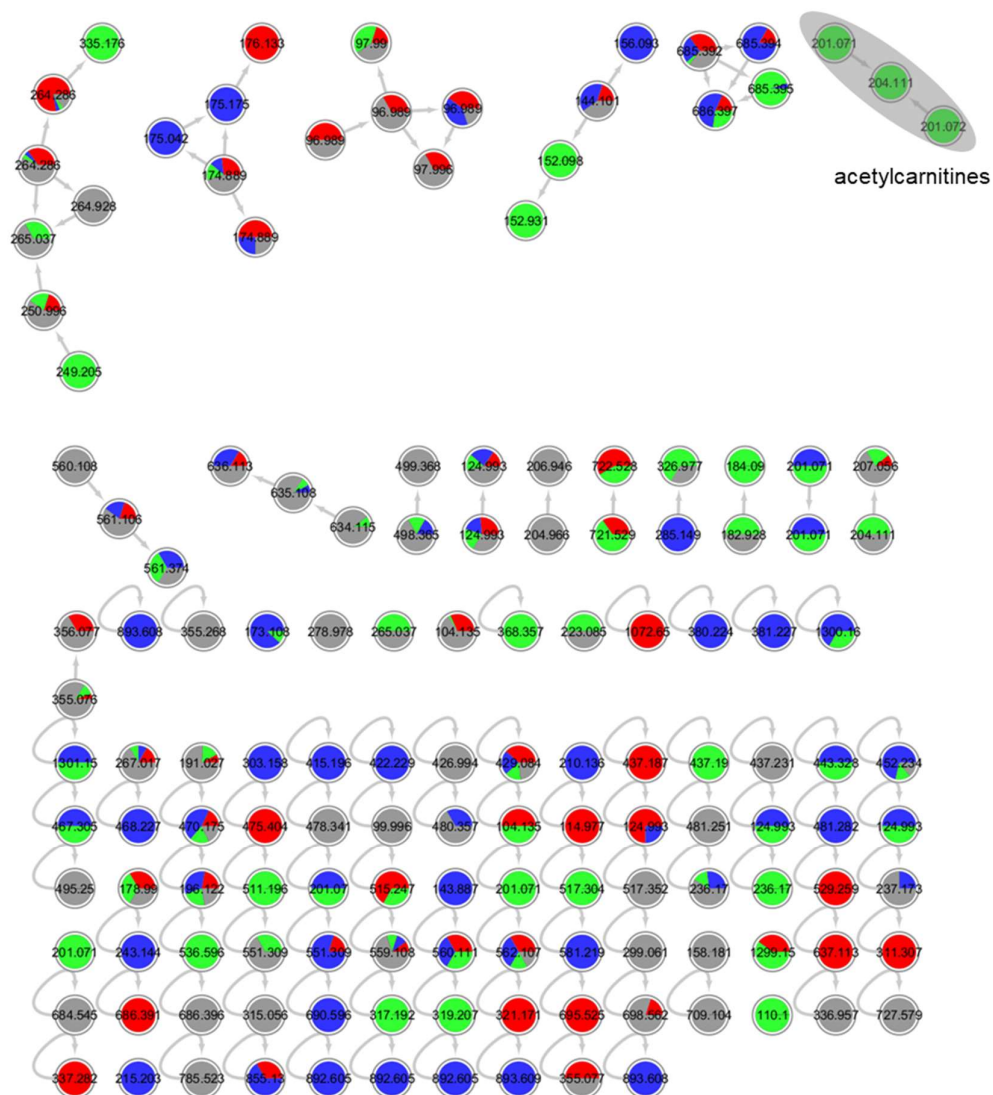


**Figure S5.** Annotated molecular network for strain 1 (order Pleosporales) solid culture extracts in PDM-S (**blue**), Cza-S (**red**), SYM-S (**green**), WM-S (**grey**). Annotated peak ions of putatively known compounds are highlighted by a grey loop.

APPENDIX

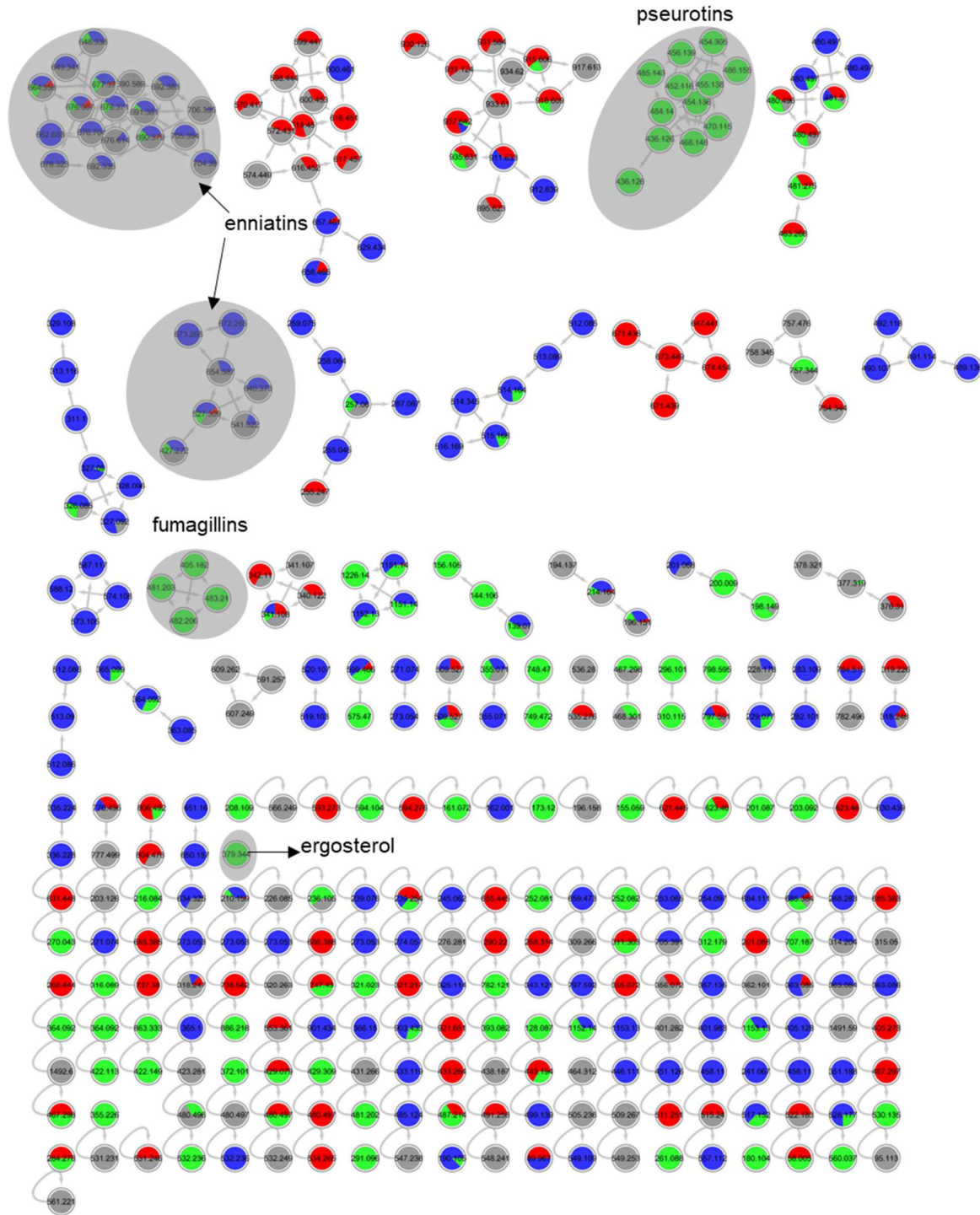


**Figure S6.** Annotated molecular network for strain 35 (*Cadophora malorum*) liquid culture extracts in PDM-L (blue), Cza-L (red), SYM-L (green), WM-L (grey). Annotated peak ions of putatively known compounds are highlighted by a grey loop.

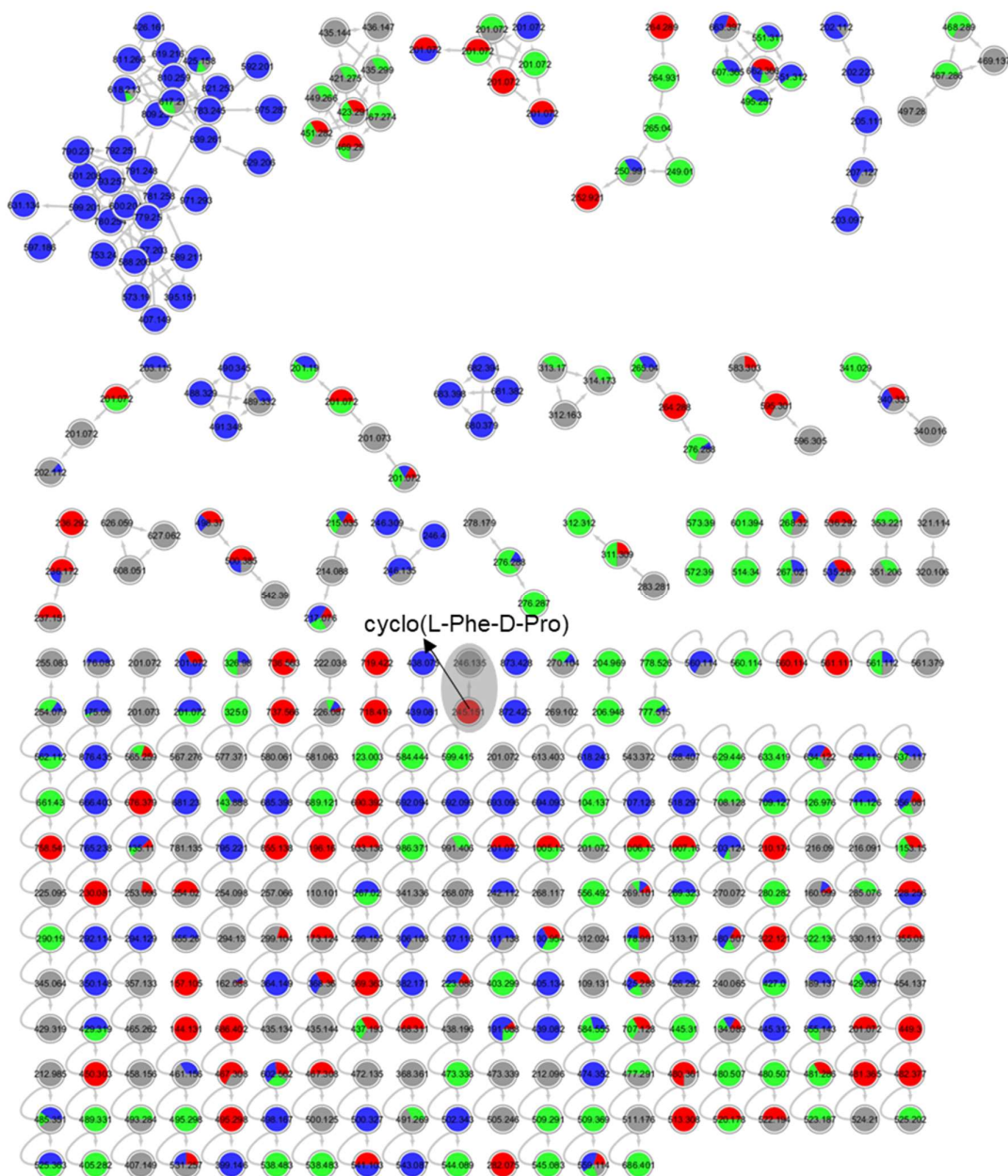


**Figure S7.** Annotated molecular network for strain 35 (*Cadophora malorum*) solid culture extracts in PDM-S (blue), Cza-S (red), SYM-S (green), WM-S (grey). Annotated peak ions of putatively known compounds are highlighted by a grey loop.

APPENDIX

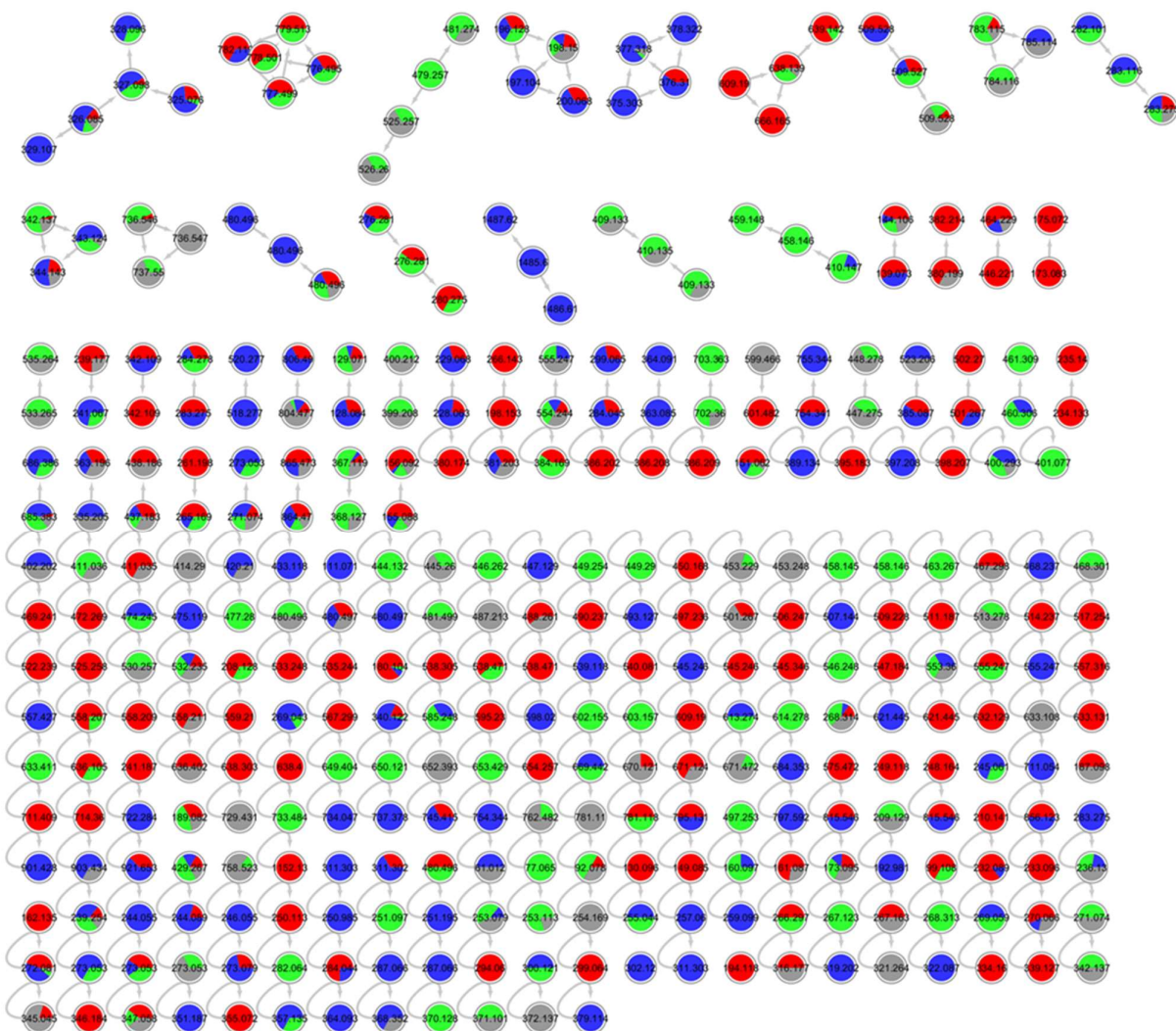


**Figure S8.** Annotated molecular network for strain 37 (order Hypocreales) liquid culture extracts in PDM-L (blue), Cza-L (red), SYM-L (green), WM-L (grey).

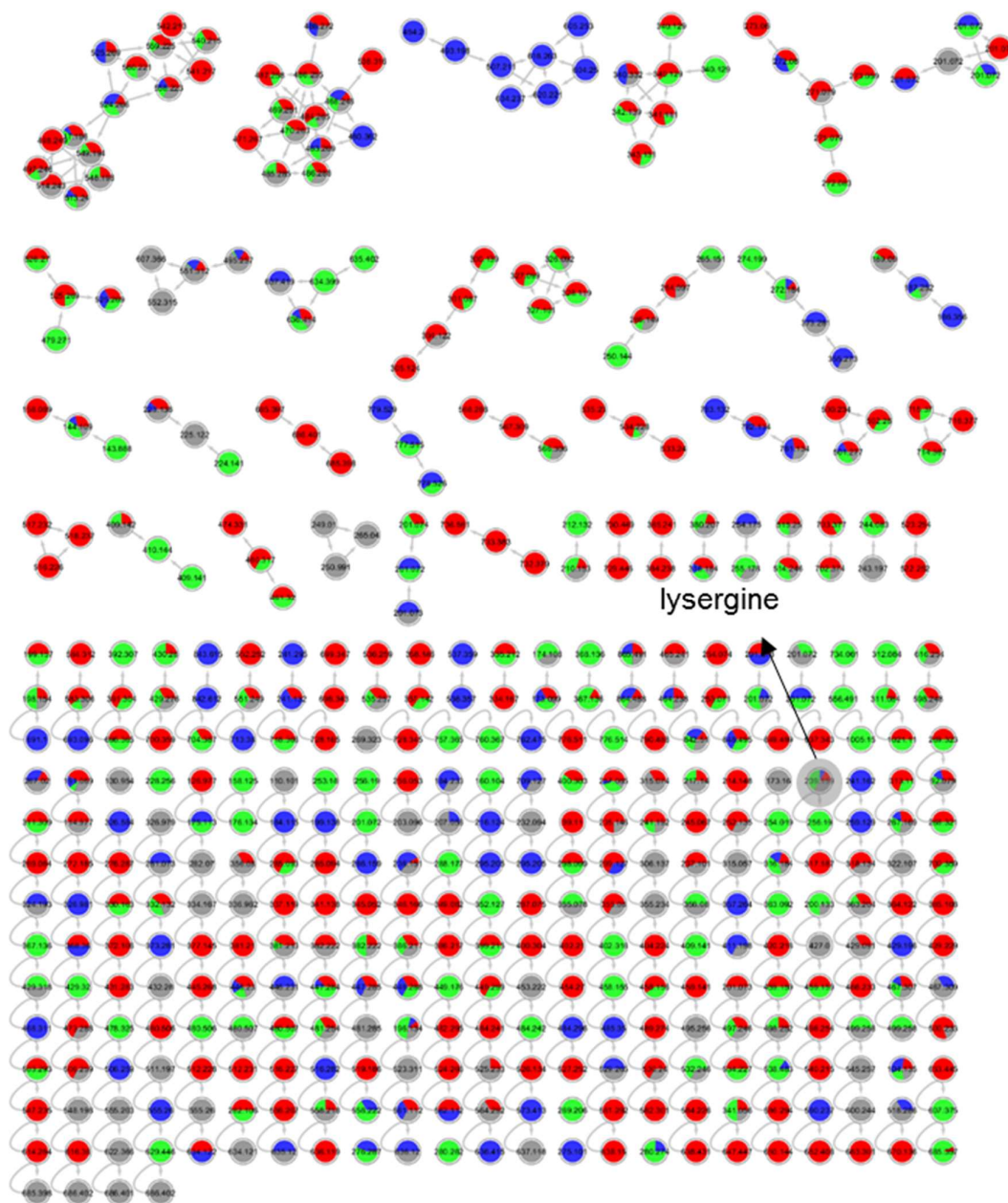


**Figure S9.** Annotated molecular network for strain 37 (order Hypocreales) solid culture extracts in PDM-S (**blue**), Cza-S (**red**), SYM-S (**green**), WM-S (**grey**). Annotated peak ions of putatively known compounds are highlighted by a grey loop.

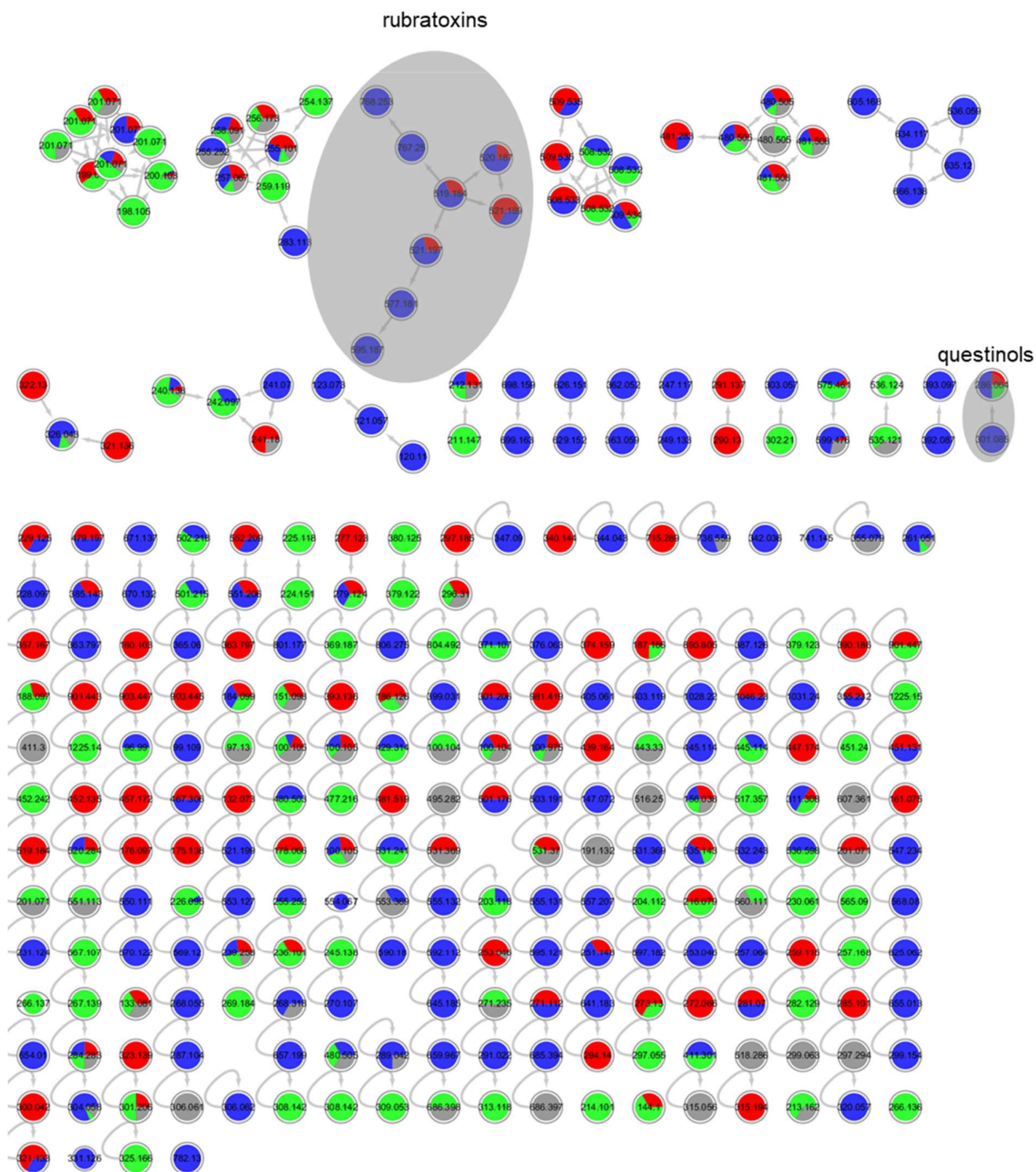


**Figure S10.** Annotated molecular network for strain 50 (*Penicillium* sp.) liquid culture extracts in PDM-L (blue), Cza-L (red), SYM-L (green), WM-L (grey). Annotated peak ions of putatively known compounds are highlighted by a grey loop.

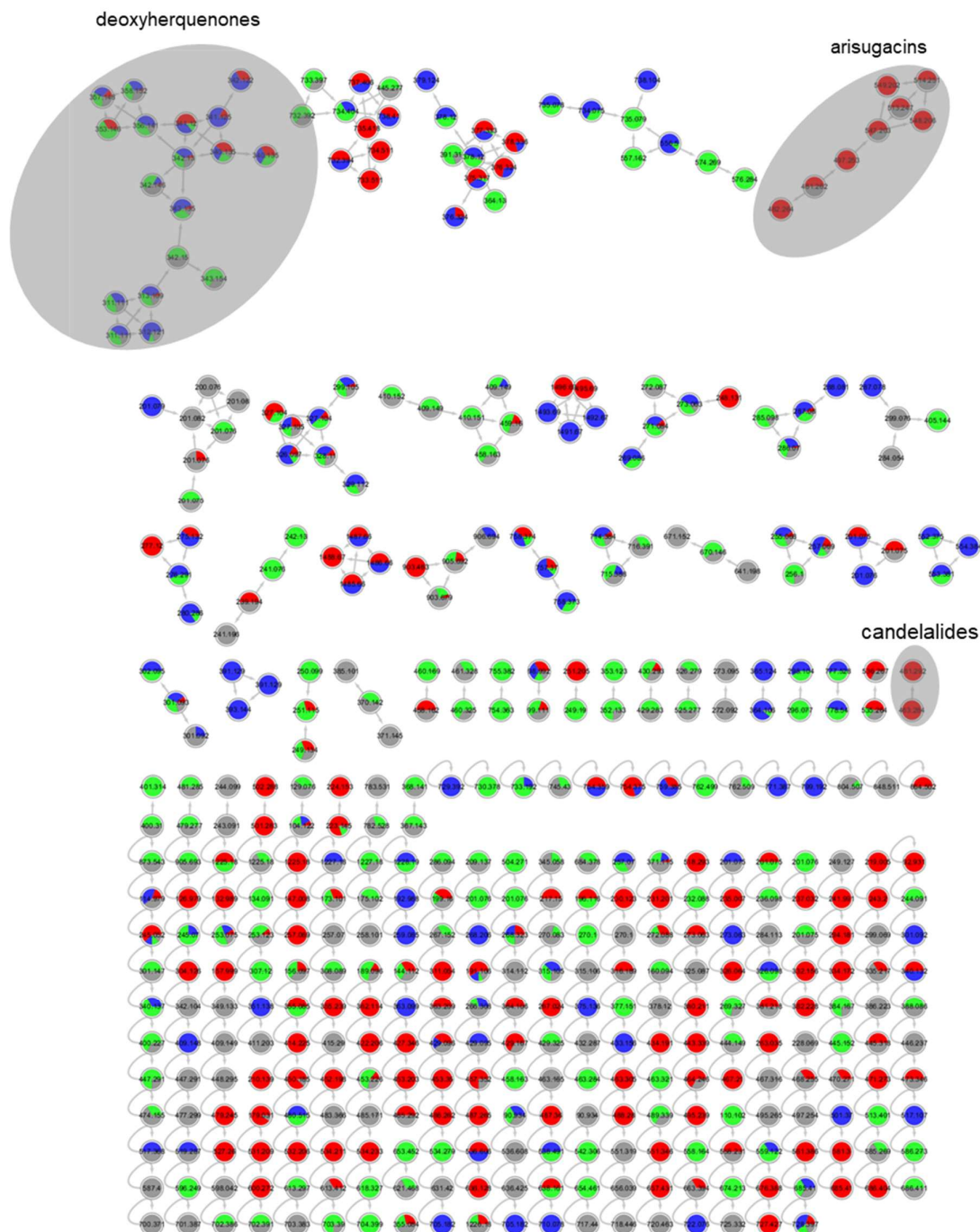


**Figure S11.** Annotated molecular network for strain 50 (*Penicillium* sp.) solid culture extracts in PDM-S (blue), Cza-S (red), SYM-S (green), WM-S (grey). Annotated peak ions of putatively known compounds are highlighted by a grey loop.

APPENDIX

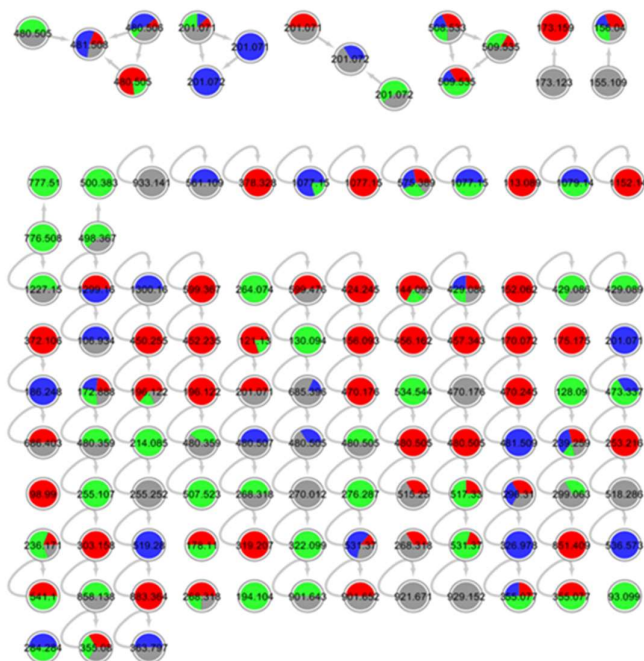


**Figure S12.** Annotated molecular network for strain 56 (*Penicillium* sp.) liquid culture extracts in PDM-L (**blue**), Cza-L (**red**), SYM-L (**green**), WM-L (**grey**).



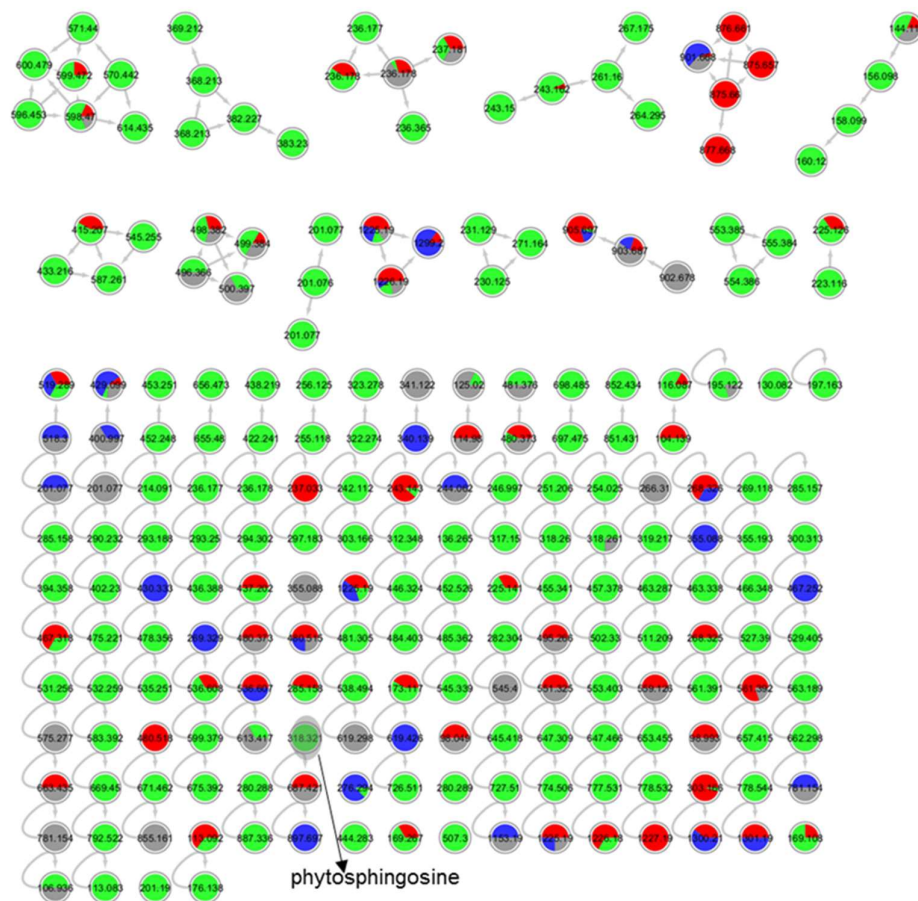


**Figure S13.** Annotated molecular network for strain 56 (*Penicillium* sp.) solid culture extracts in PDM-S (blue), Cza-S (red), SYM-S (green), WM-S (grey). Annotated peak ions of putatively known compounds are highlighted by a grey loop.

APPENDIX

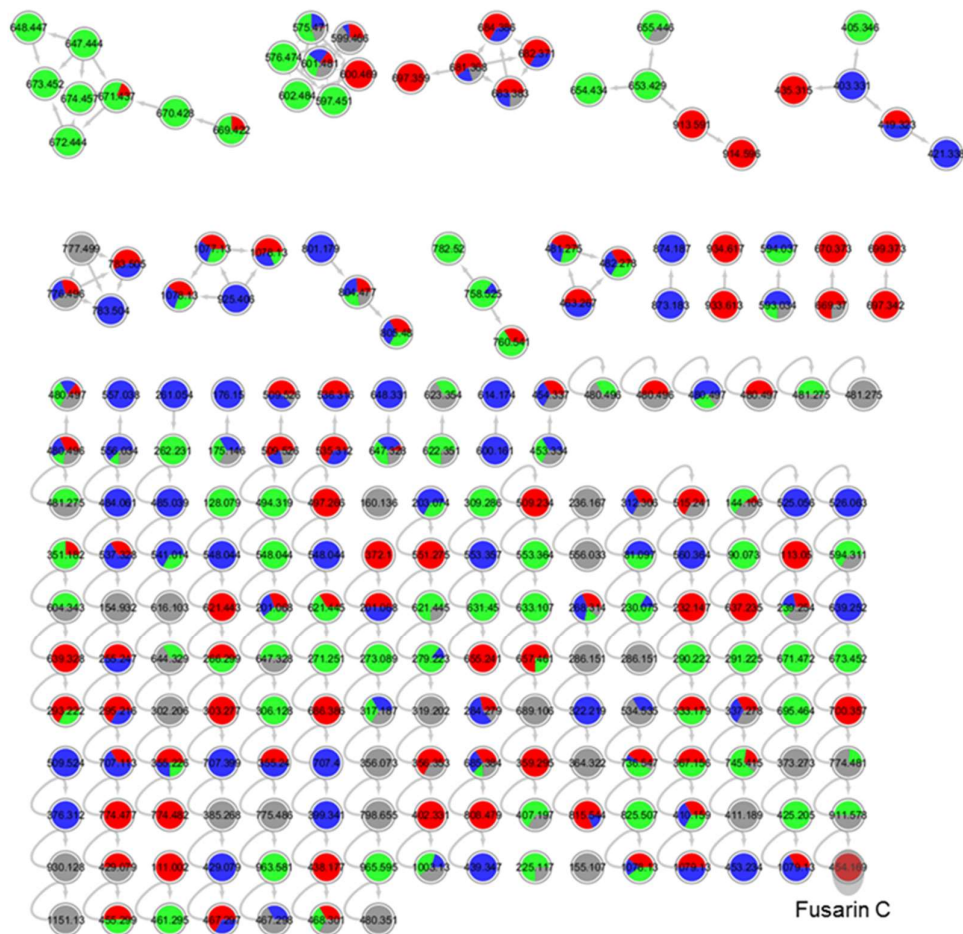


**Figure S14.** Annotated molecular network for strain 58 (*Fusarium graminearum*) liquid culture extracts in PDM-L (blue), Cza-L (red), SYM-L (green), WM-L (grey). Annotated peak ions of putatively known compounds are highlighted by a grey loop.

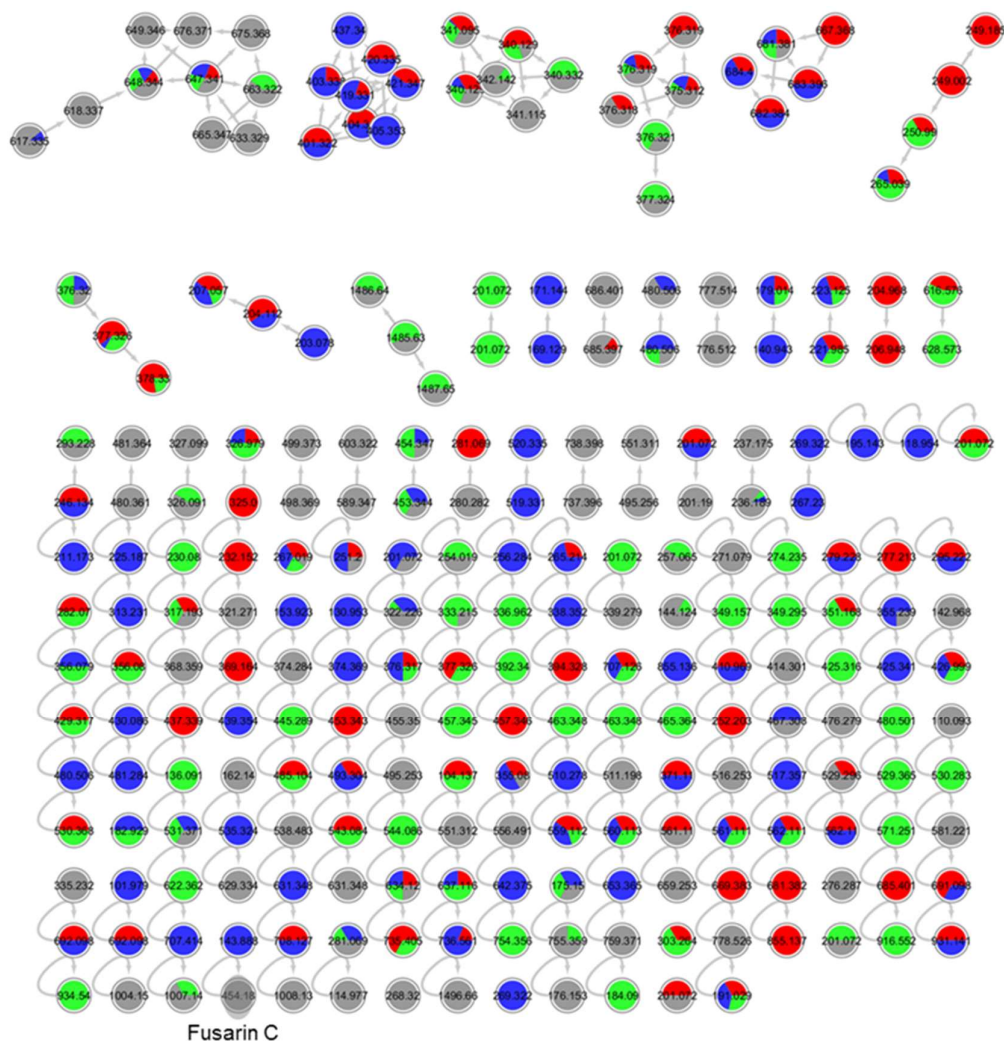


**Figure S15.** Annotated molecular network for strain 58 (*Fusarium graminearum*) solid culture extracts in PDM-S (blue), Cza-S (red), SYM-S (green), WM-S (grey). Annotated peak ions of putatively known compounds are highlighted by a grey loop.

APPENDIX

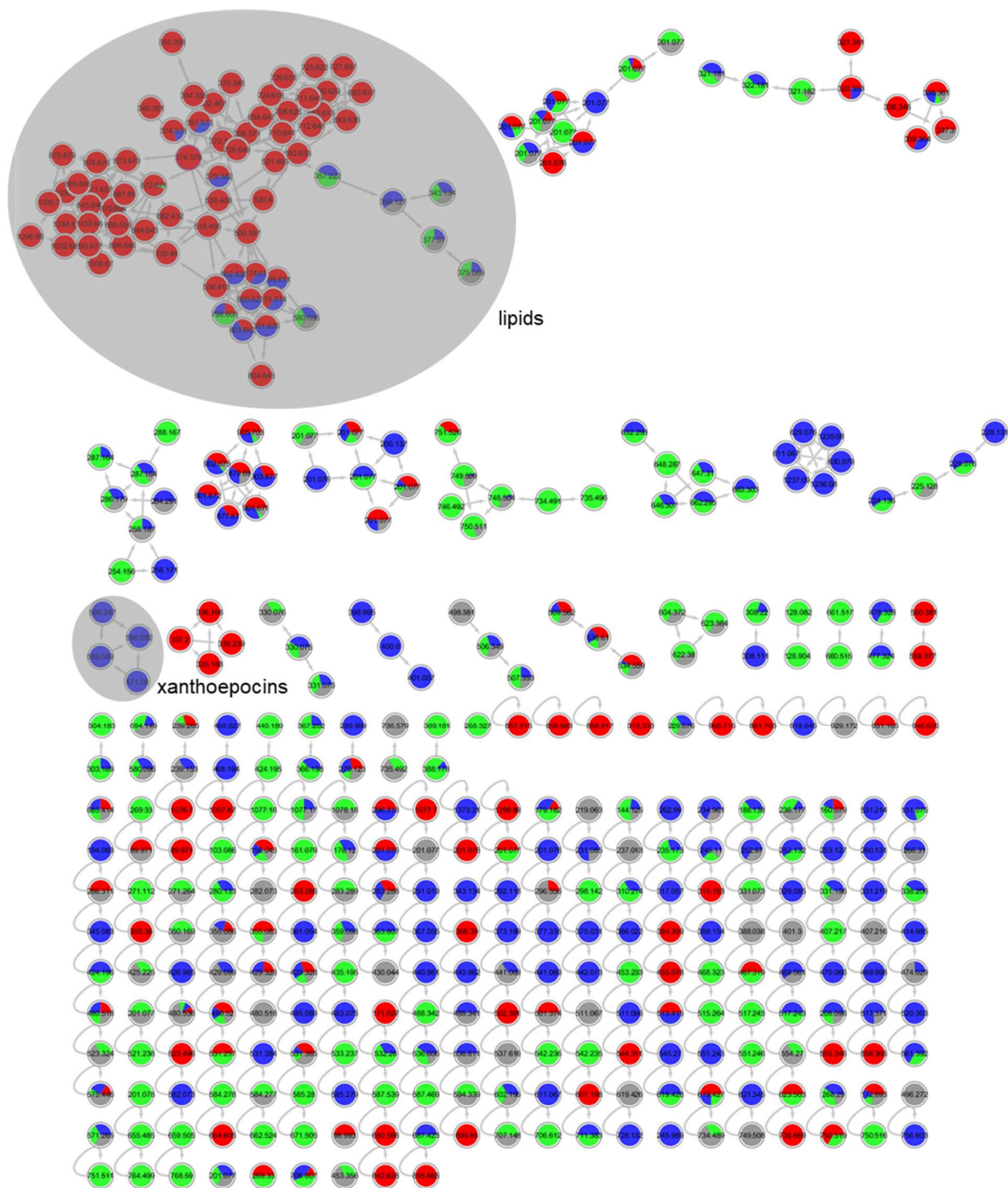


**Figure S16.** Annotated molecular network for strain 59 (order Glomerellales) liquid culture extracts in PDM-L (blue), Cza-L (red), SYM-L (green), WM-L (grey). Annotated peak ions of putatively known compounds are highlighted by a grey loop.

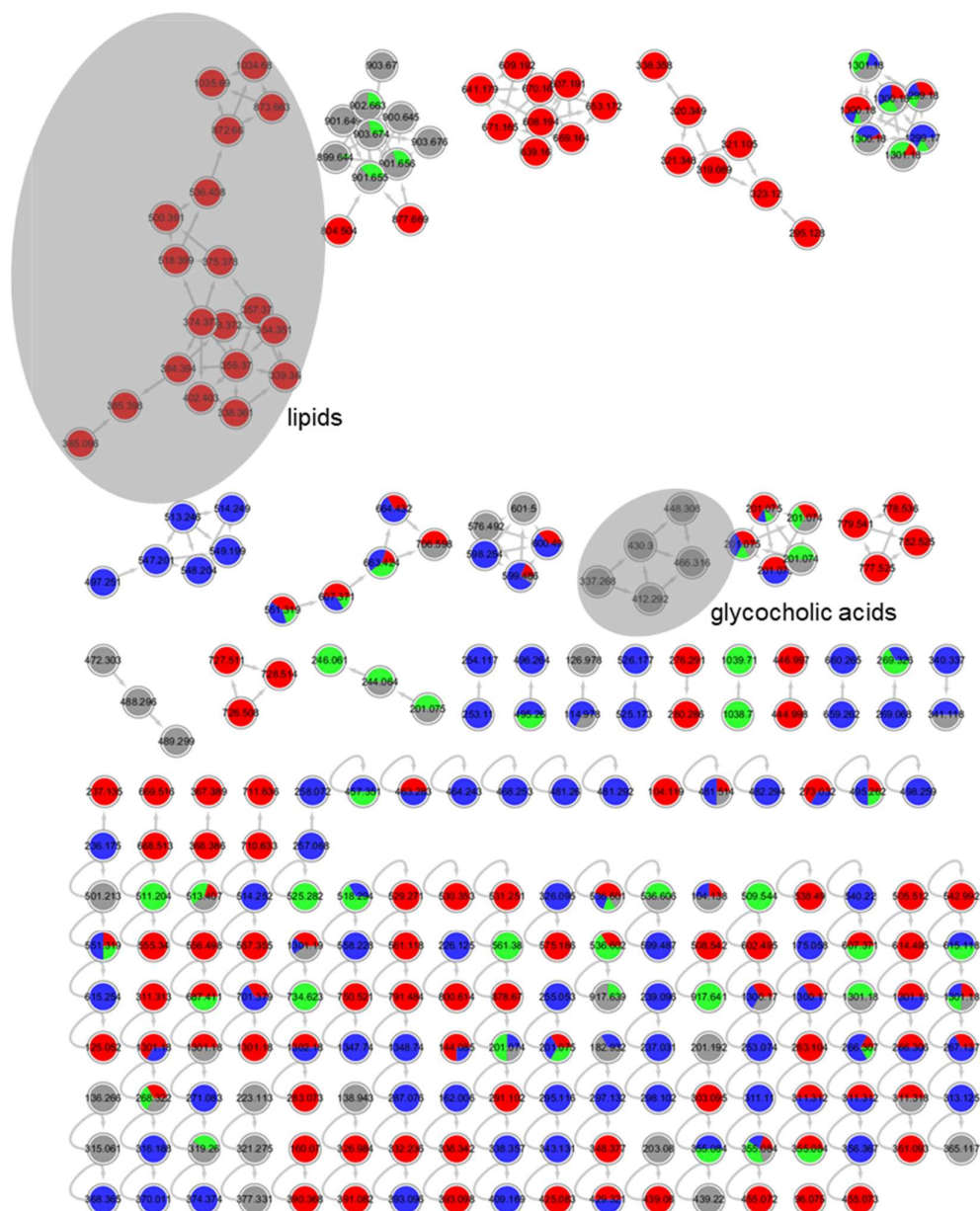


**Figure S17.** Annotated molecular network for strain 59 (order Glomerellales) solid culture extracts in PDM-S (**blue**), Cza-S (**red**), SYM-S (**green**), WM-S (**grey**). Annotated peak ions of putatively known compounds are highlighted by a grey loop.

APPENDIX

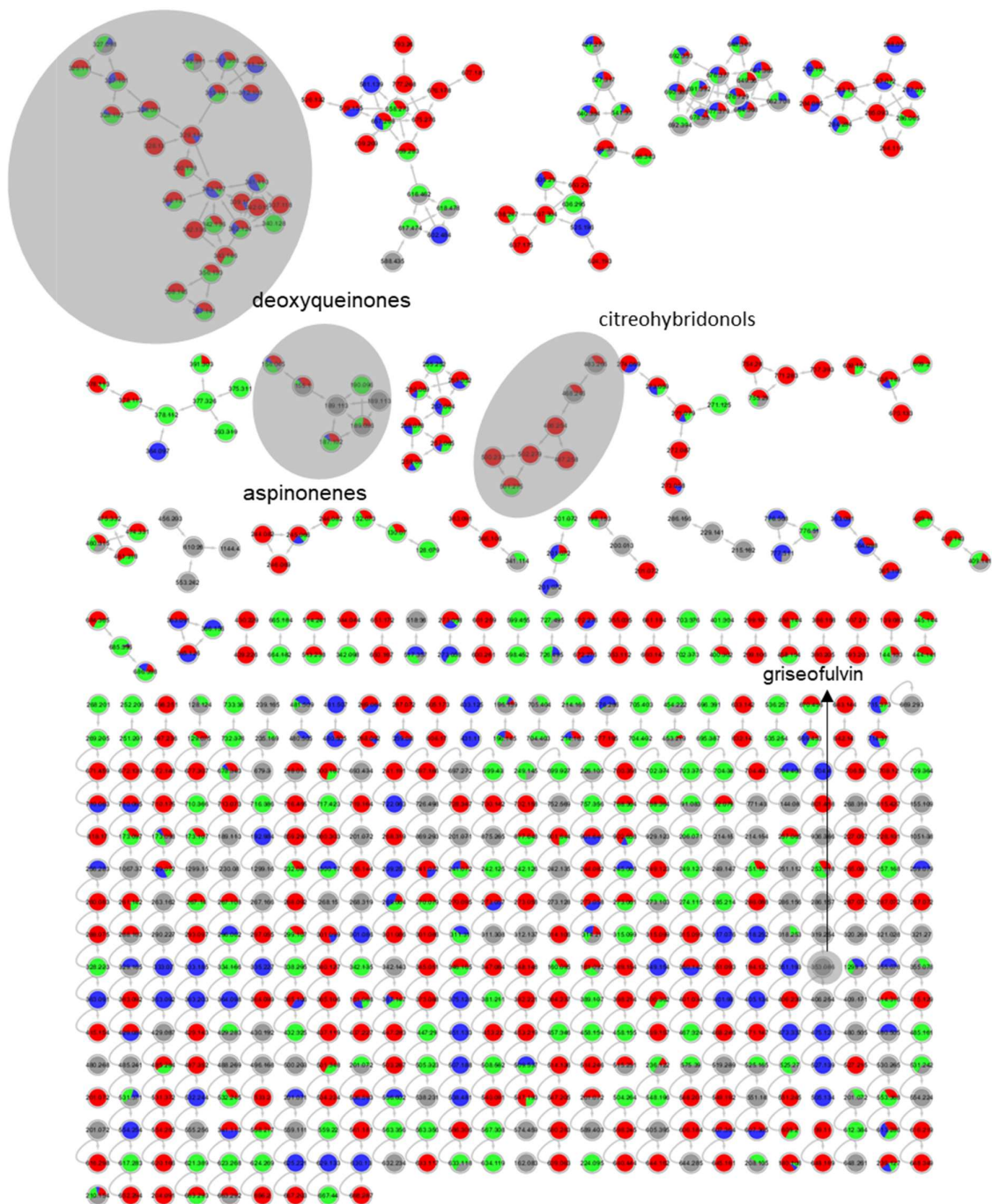


**Figure S18.** Annotated molecular network for strain 68 (*Penicillium* sp.) liquid culture extracts in PDM-L (blue), Cza-L (red), SYM-L (green), WM-L (grey). Annotated peak ions of putatively known compounds are highlighted by a grey loop.

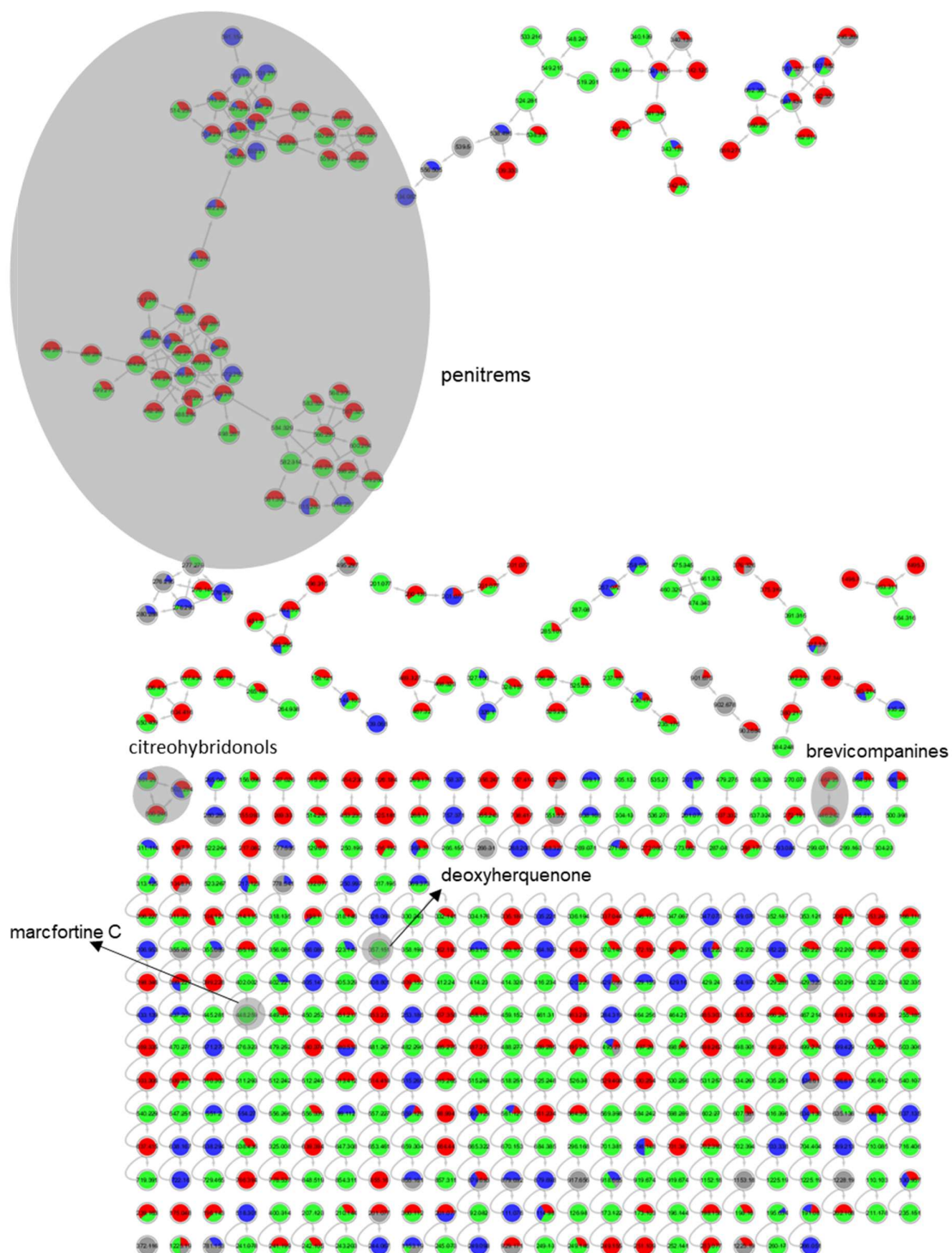


**Figure S19.** Annotated molecular network for strain 68 (*Penicillium* sp.) solid culture extracts in PDM-S (blue), Cza-S (red), SYM-S (green), WM-S (grey). Annotated peak ions of putatively known compounds are highlighted by a grey loop.

APPENDIX

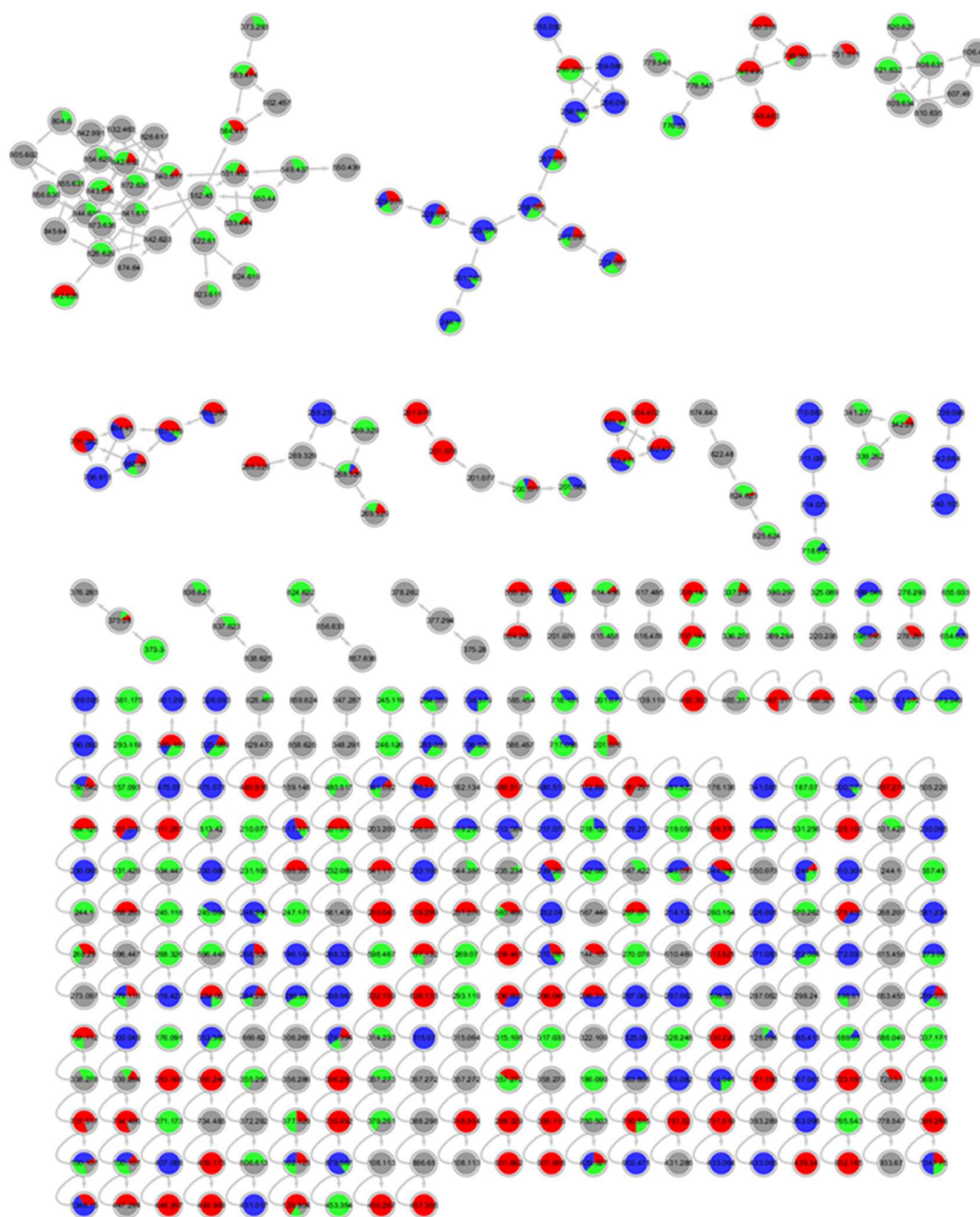


**Figure S20.** Annotated molecular network for strain 78 (*Penicillium* sp.) liquid culture extracts in PDM-L (blue), Cza-L (red), SYM-L (green), WM-L (grey).





APPENDIX

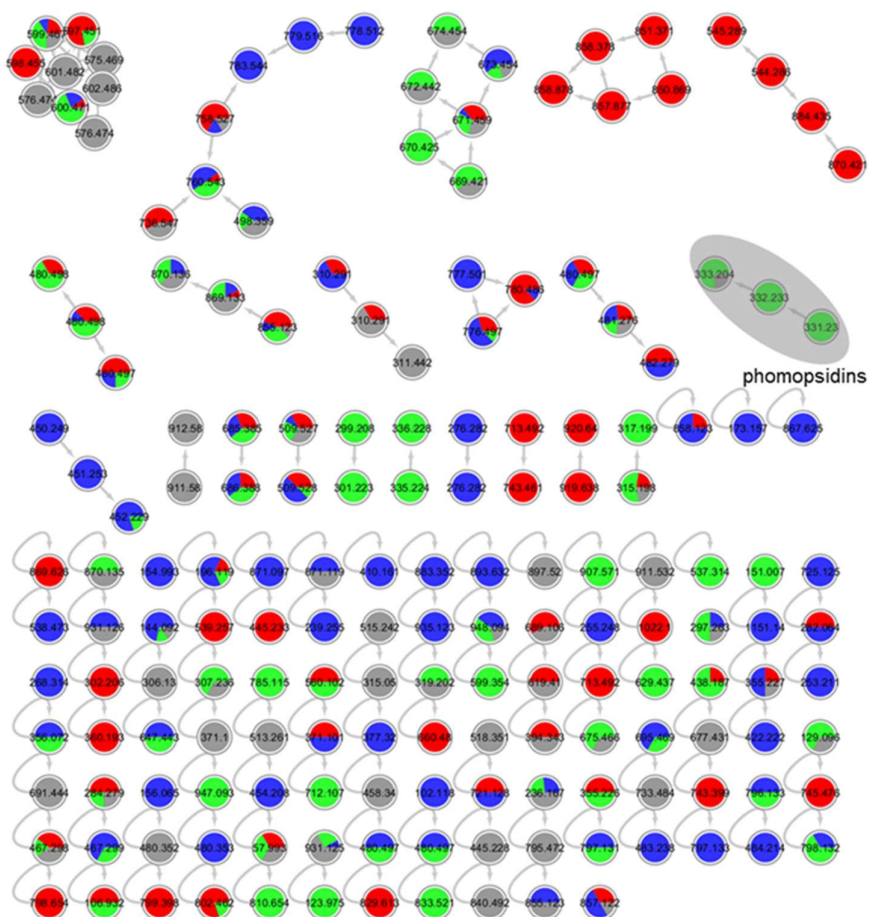


**Figure S22.** Annotated molecular network for strain 87 (order Pleosporales) liquid culture extracts in PDM-L (**blue**), Cza-L (**red**), SYM-L (**green**), WM-L (**grey**). Annotated peak ions of putatively known compounds are highlighted by a grey loop.

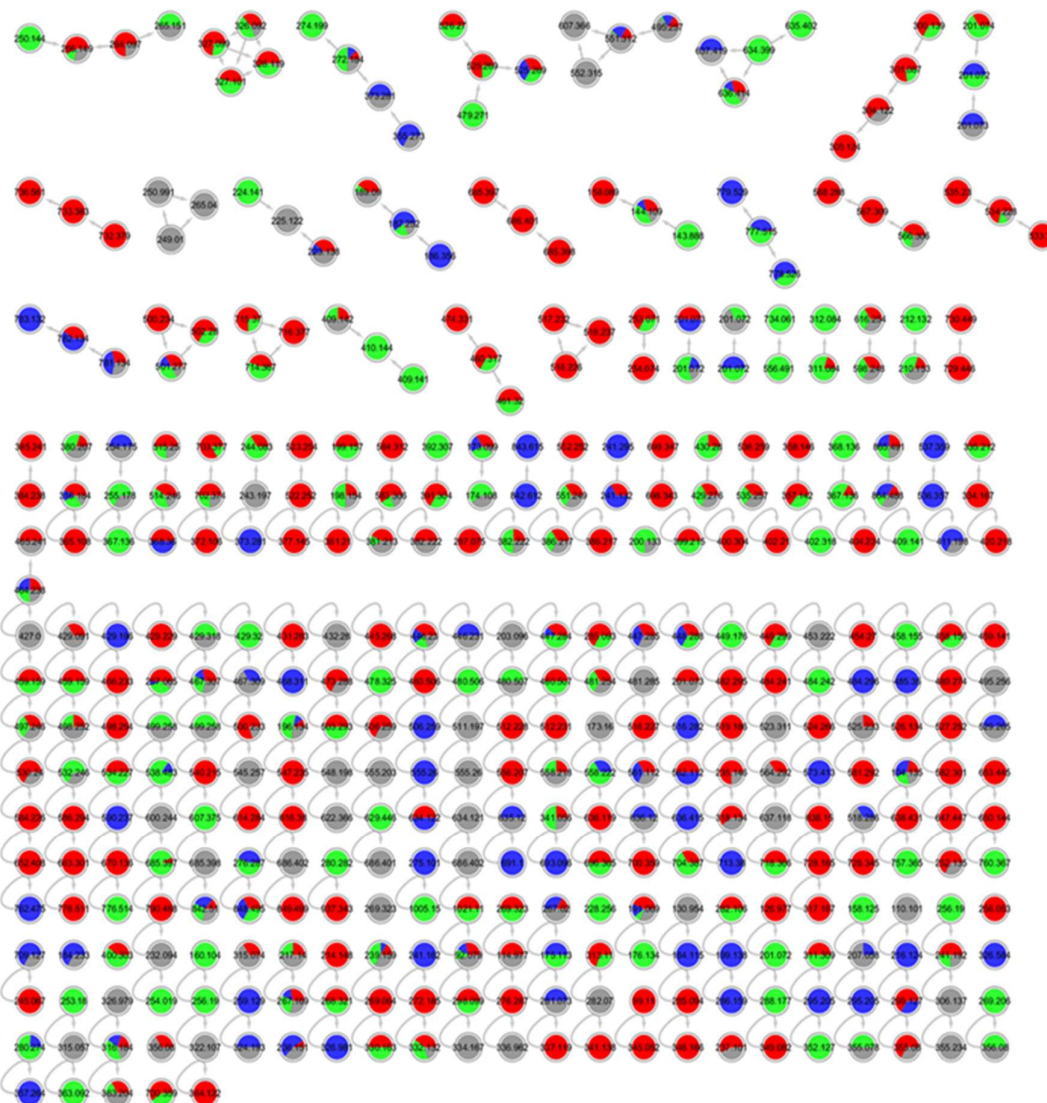


**Figure S23.** Annotated molecular network for strain 87 (order Pleosporales) solid culture extracts in PDM-S (**blue**), Cza-S (**red**), SYM-S (**green**), WM-S (**grey**).

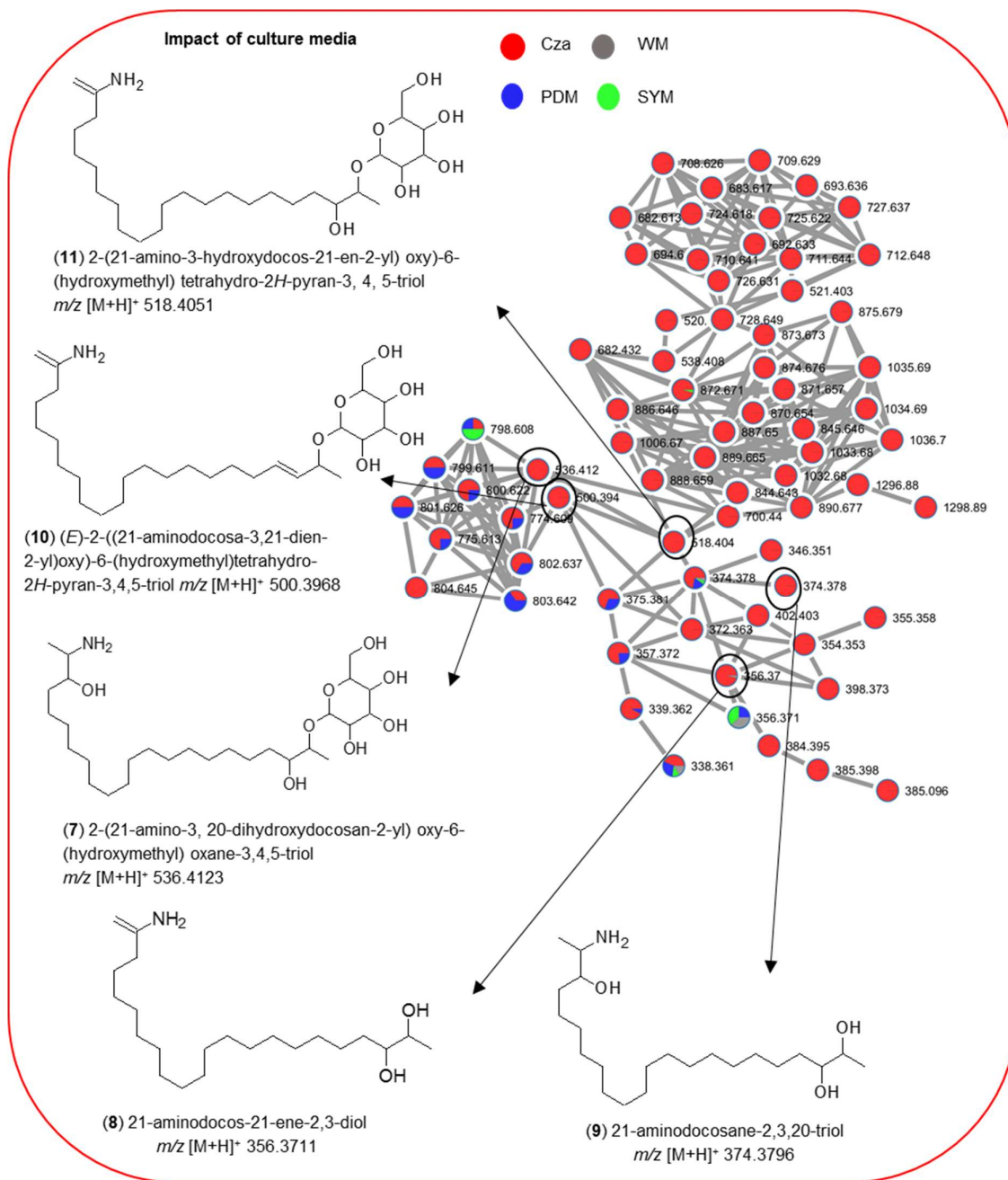


**Figure S24.** Molecular network of the aminolipid family detected in strain 59 (order Glomerellales) extracts. **Red nodes:** Ions detected in Cza extracts. **Blue nodes:** Ions detected in PDM extracts. **Green nodes:** Ions detected in SYM extracts. **Grey nodes:** Ions detected in WM extracts.

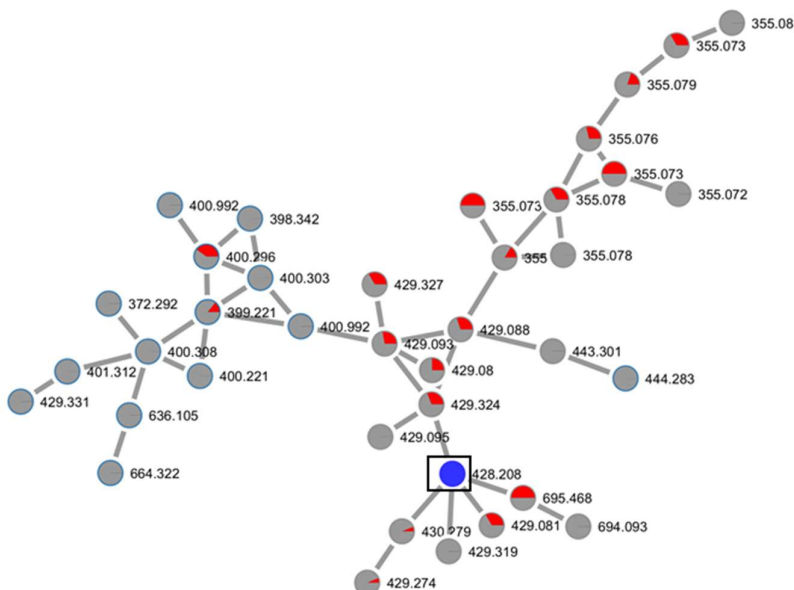


**Figure S25.** Molecular network of an unannotated cluster containing specific node ( $m/z$  [M+H]<sup>+</sup> 428.2081) generated from the global MN (Figure 7A). **Black square:** node exclusive to the bioactive 1PDM-L extract. **Red nodes:** Ions detected in toxic samples. **Grey nodes:** Ions detected in inactive samples. **Blue nodes:** Ions detected in bioactive samples.

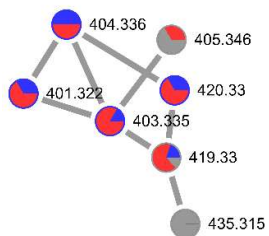


**Figure S26.** Molecular network of an unannotated cluster containing 3 specific nodes ( $m/z$  [M+H]<sup>+</sup> 401.3221, [M+H]<sup>+</sup> 403.3355, [M+H]<sup>+</sup> 419.3300) generated from the global MN (Figure 7A). **Red nodes:** Ions detected in toxic samples. **Grey nodes:** Ions detected in inactive samples. **Blue nodes:** Ions detected in bioactive samples.

### 3. Bioactivity data and NMR spectral data of Chapter 2

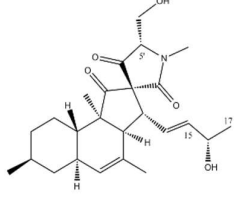
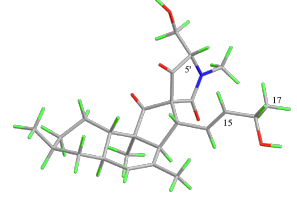
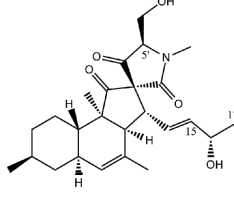
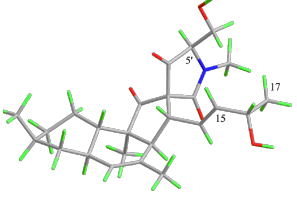
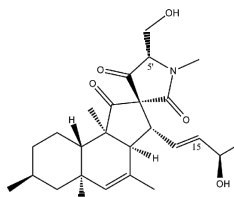
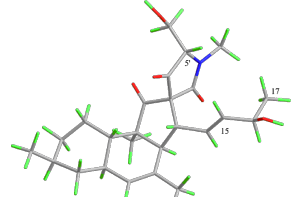
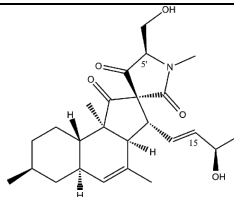
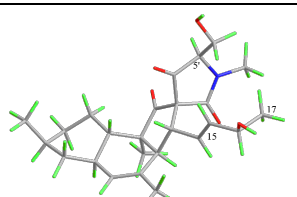
**Table S1.** In vitro anticancer activity (%) of Kupchan subextracts (KH, KC, KM) and SPE fractions against cancer cell lines (A-375, A-549, HT-29, HCT-116, MB-231) and non-cancerous HaCaT cell line.

	Cell growth inhibition (%)					
	A-375 (100 µg/ml)	A-549 (100 µg/ml)	HT-29 (100 µg/ml)	HCT-116 (100 µg/ml)	MB-231 (100 µg/ml)	HaCaT (100 µg/ml)
KH	31	0	29	0	0	31
KC	98	99	99	76	99	66
KM	0	0	0	0	0	0
KC Fr.0	0	0	0	0	0	0
KC Fr.1	0	0	0	0	0	0
KC Fr.2	0	0	0	0	0	0
KC Fr.3	0	0	0	0	0	0
KC Fr.4	0	0	0	0	0	0
KC Fr.5	85	54	99	0	63	44
KC Fr.6	99	99	99	99	99	99
KC Fr.7	99	99	99	99	99	99
KC Fr.8	43	0	0	0	0	0
KC Fr.9	0	0	0	0	0	0
KC Fr.10	0	0	0	0	0	0

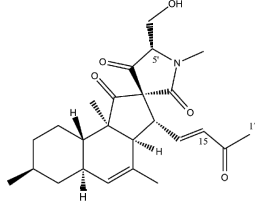
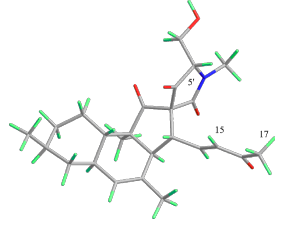
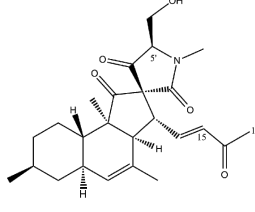
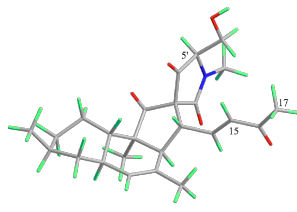
**Table S2.** The  $\Delta\delta(\delta_S-\delta_R)$  data for the *S*- and *R*-MTPA esters **6–9** in  $^1\text{H}$  NMR ( $\text{CDCl}_3$ , 500 MHz).

C	6 (S)	7 (R)	$\Delta\delta_{S-R}$	8 (S)	9 (R)	$\Delta\delta_{S-R}$
	$\delta_{\text{H}}$ , mult ( <i>J</i> in Hz)	$\delta_{\text{H}}$ , mult ( <i>J</i> in Hz)		$\delta_{\text{H}}$ , mult ( <i>J</i> in Hz)	$\delta_{\text{H}}$ , mult ( <i>J</i> in Hz)	
13	3.39, m	3.35, dd (11.5, 9.5)	0.04	3.27, dd (11.3, 9.7)	3.28, dd (11.4, 9.4)	-0.01
14	5.92, dd (15.5, 9.5)	5.84, dd (15.4, 9.8)	0.08	6.09, dd (14.8, 9.7)	6.10, dd (15.3, 9.7)	-0.01
15	5.65, dd (15.5, 6.4)	5.58, dd (15.4, 6.4)	0.07	5.39, dd (14.9, 7.8)	5.52, dd (15.3, 7.6)	-0.13
16	5.46, m	5.45, m	0.01	5.34, m	5.38, m	-0.04
17	1.22, d (6.5)	1.30, d (6.5)	-0.08	1.31, d (6.3)	1.27, d (6.5)	0.04

**Table S3.** The distance (Å) between protons H-5', H-15 and H<sub>3</sub>-17 in the tetramic acid portion of the compounds 1-3. The red marking indicates the assigned relative stereochemistry based on measured the distances allowing observable NOE correlations (up to 4 Å) between relevant protons.

Compd	2D Structure	3D model	H-5' orientation	Distance	NOE	Distance	NOE
				H-5'/H-15	H-5'/H-15	H-5'/H <sub>3</sub> -17	H-5'/H <sub>3</sub> -17
1 (5'-β)			β	2.96 Å	YES	3.28 Å	YES
1 (5'-α)			α	4.83 Å		5.07 Å	
2 (5'-β)			β	2.88 Å		3.33 Å	
2 (5'-α)			α	5.14 Å	NO	6.84 Å	NO

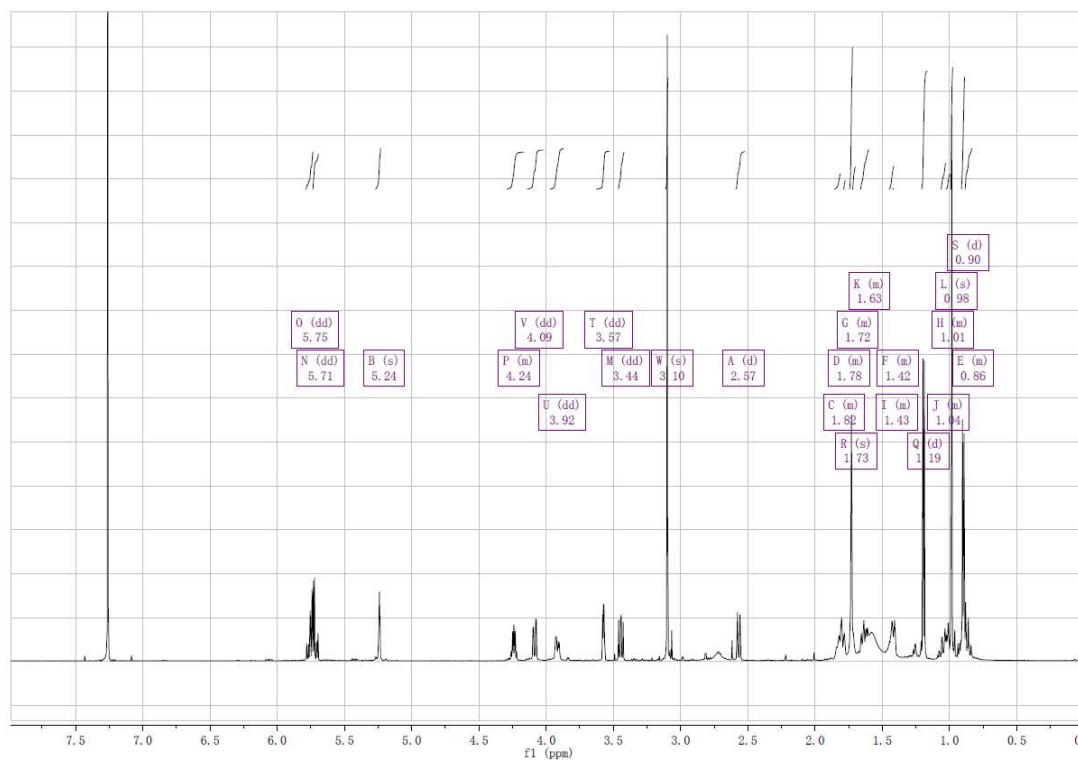
APPENDIX

<p>3 (5'-<math>\beta</math>)</p>			<p><math>\beta</math></p>	<p>3.80 Å</p>		<p>5.11 Å</p>	
<p>3 (5'-<math>\alpha</math>)</p>			<p><math>\alpha</math></p>	<p>5.41 Å</p>	<p>NO</p>	<p>6.77 Å</p>	<p>NO</p>

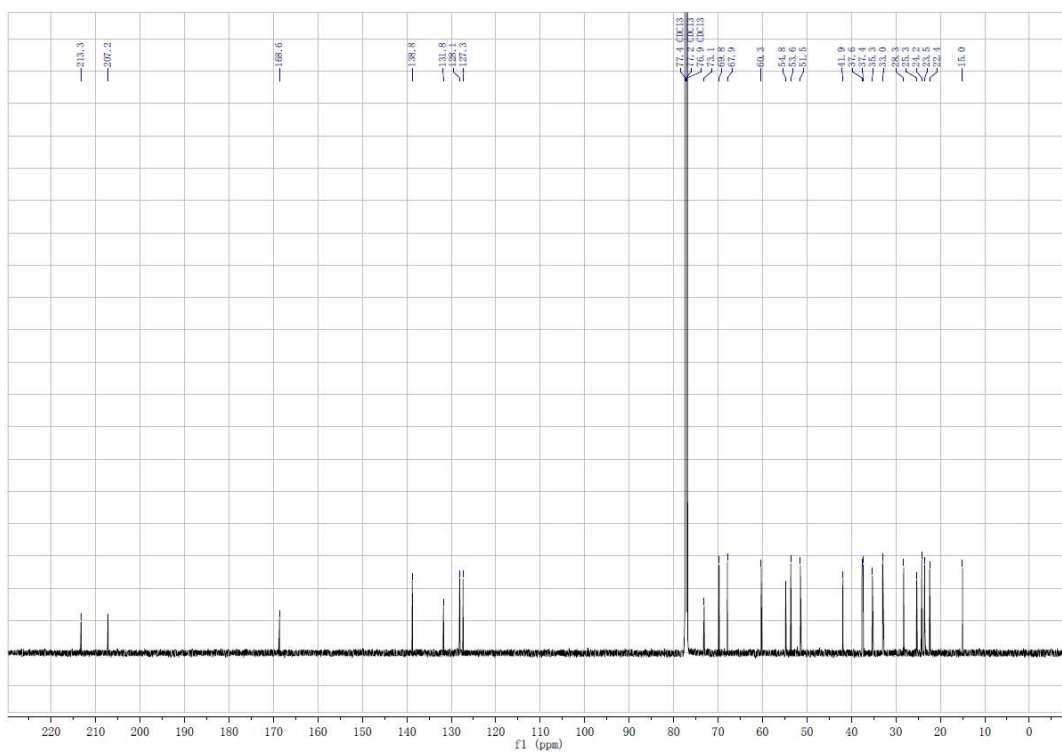


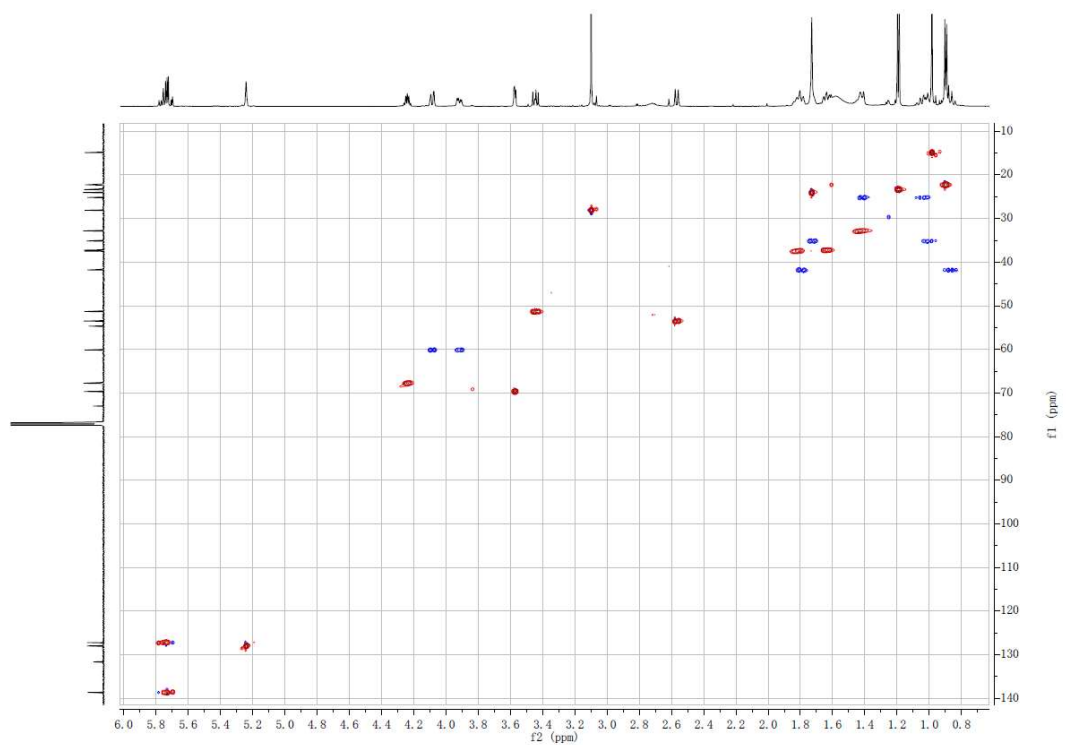
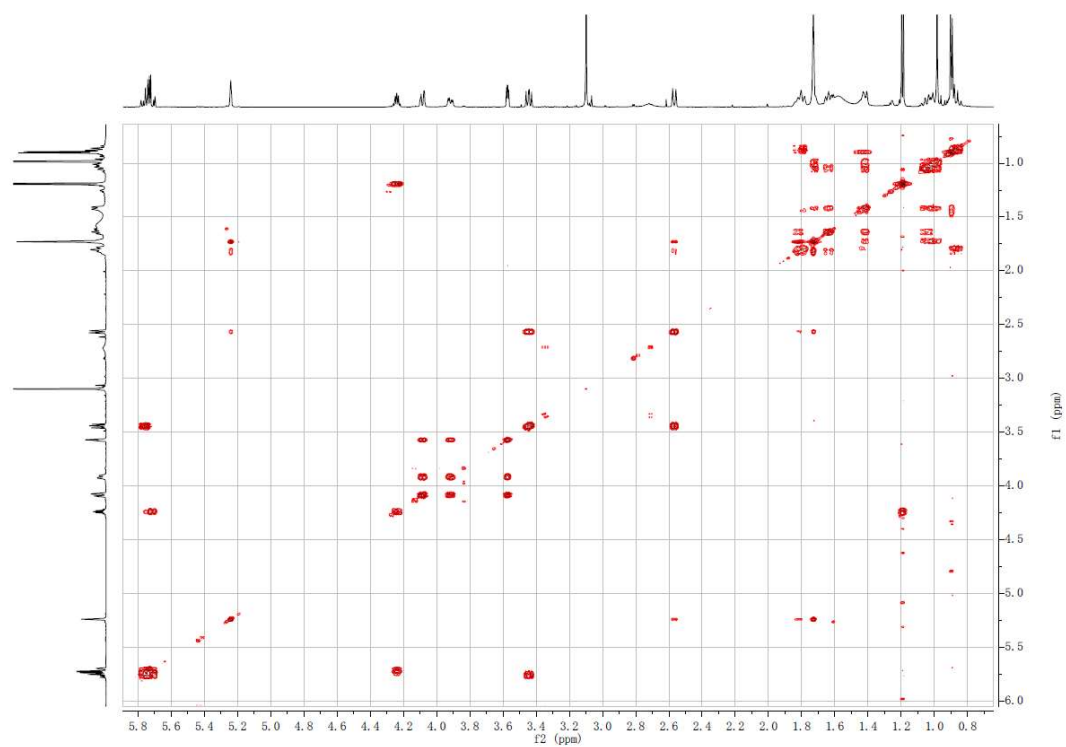
APPENDIX

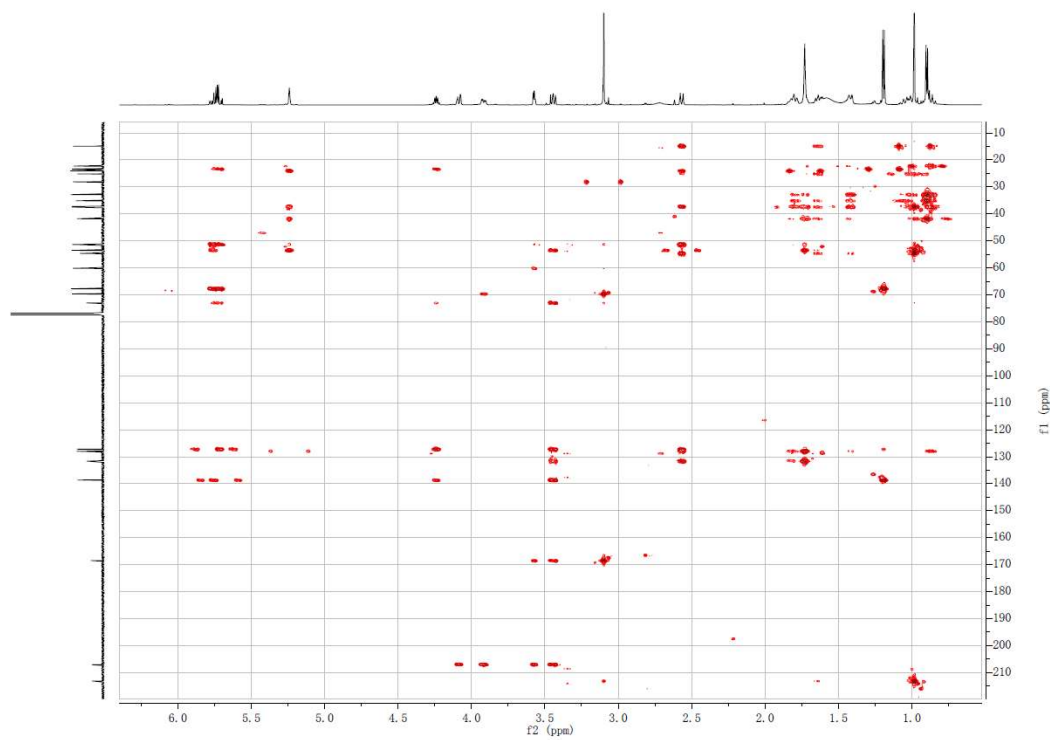
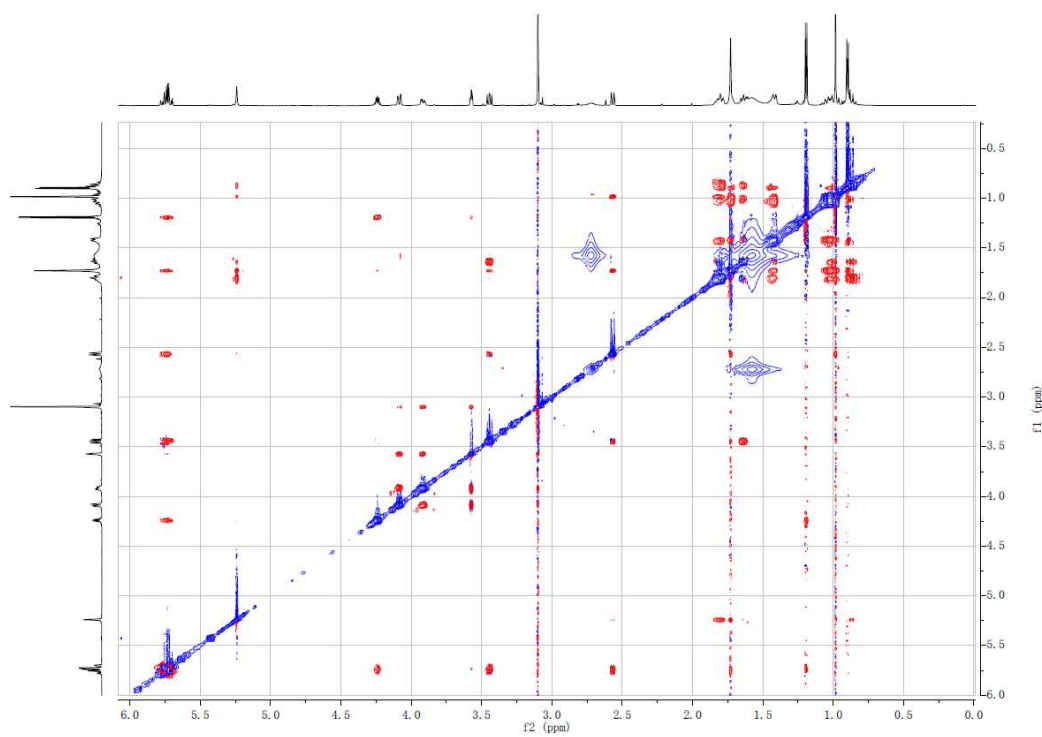
**Figure S1.**  $^1\text{H}$  NMR spectrum of compound **1** (600 MHz,  $\text{CDCl}_3$ ).



**Figure S2.**  $^{13}\text{C}$  NMR spectrum of compound **1** (150 MHz,  $\text{CDCl}_3$ ).



**Figure S3.** DEPT-HSQC spectrum of compound **1** (600 MHz, CDCl<sub>3</sub>).**Figure S4.** COSY spectrum of compound **1** (600 MHz, CDCl<sub>3</sub>).

**Figure S5.** HMBC spectrum of compound **1** (600 MHz, CDCl<sub>3</sub>).**Figure S6.** NOESY spectrum of compound **1** (600 MHz, CDCl<sub>3</sub>).

APPENDIX

Figure S7. HR-ESIMS spectrum of compound 1.

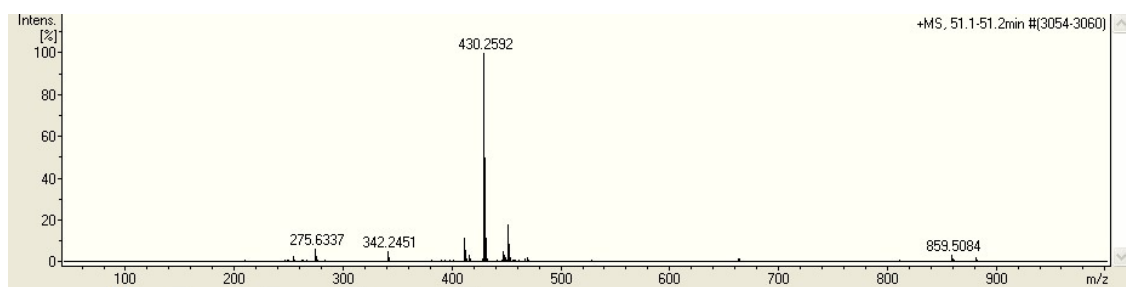


Figure S8. FT-IR spectrum of compound 1.

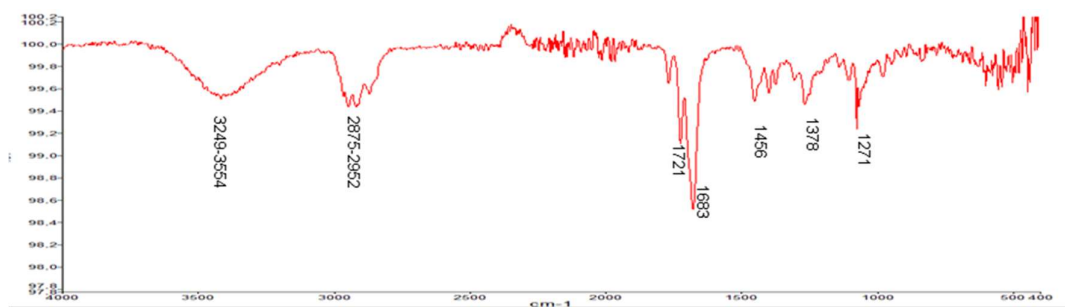
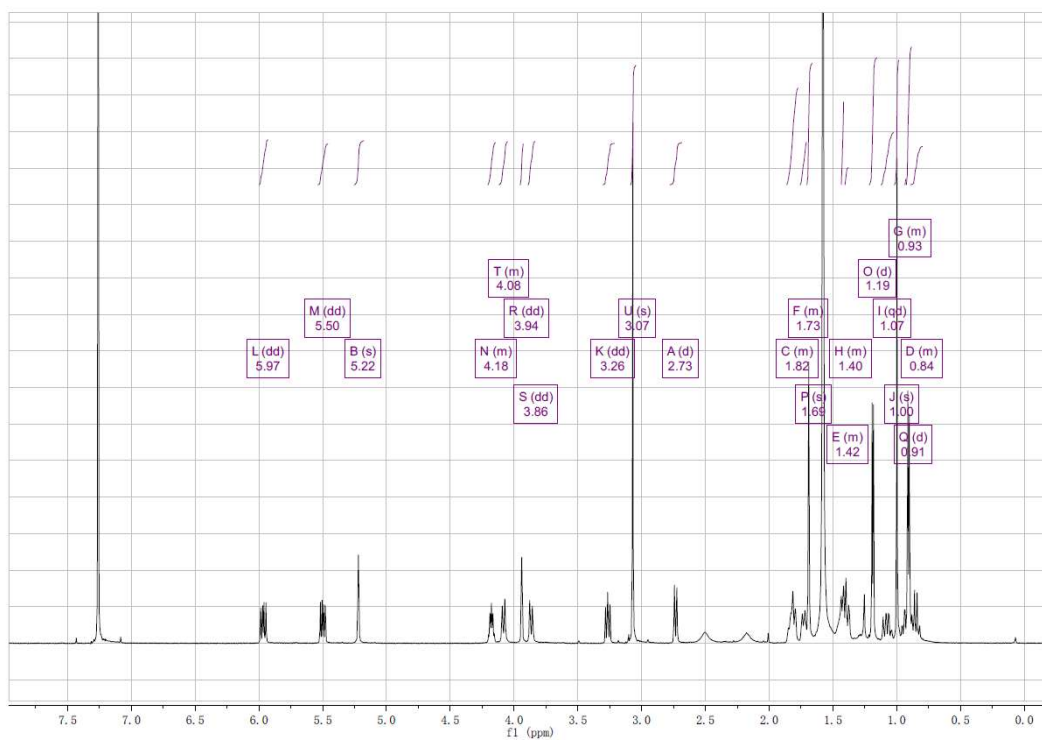
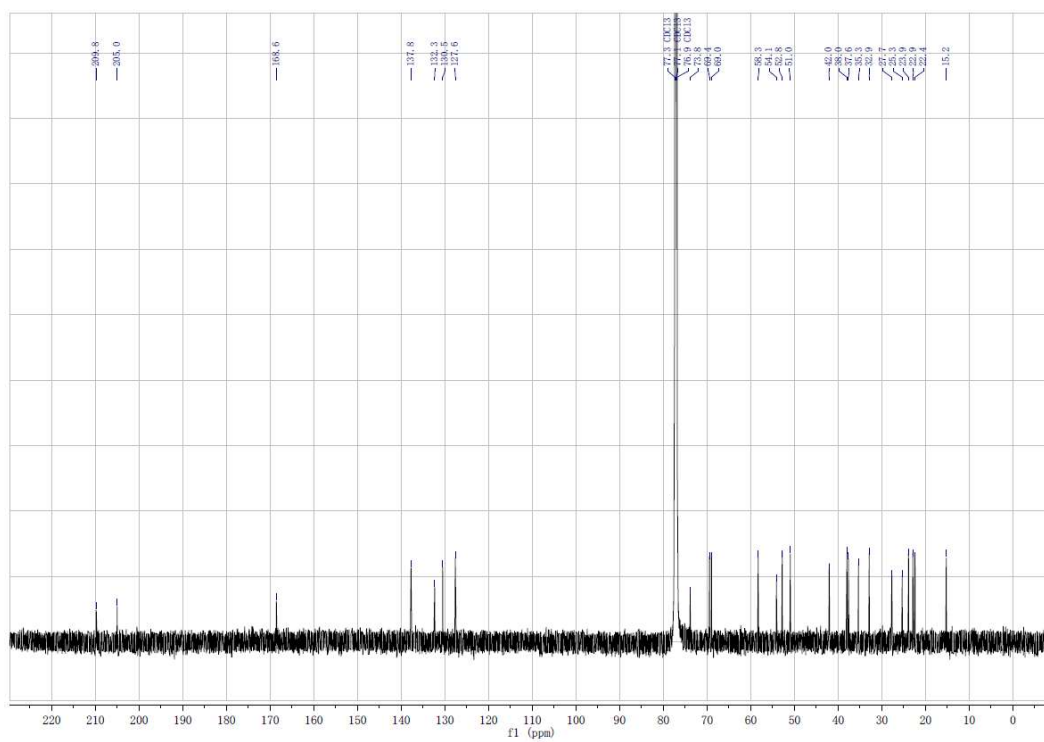
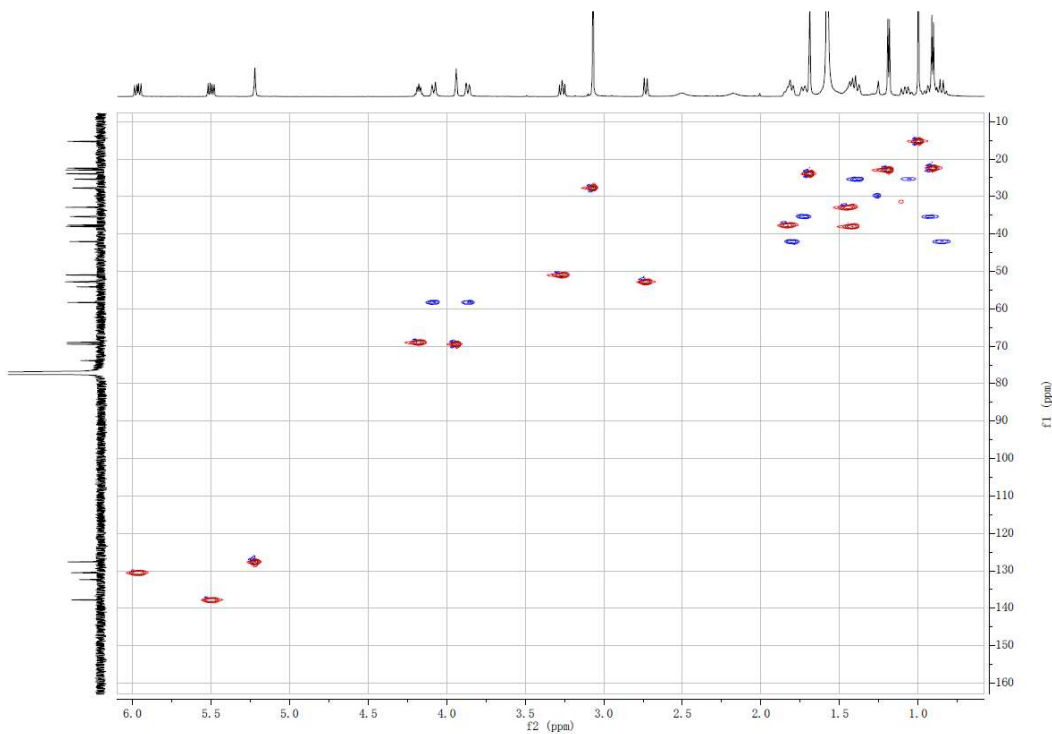
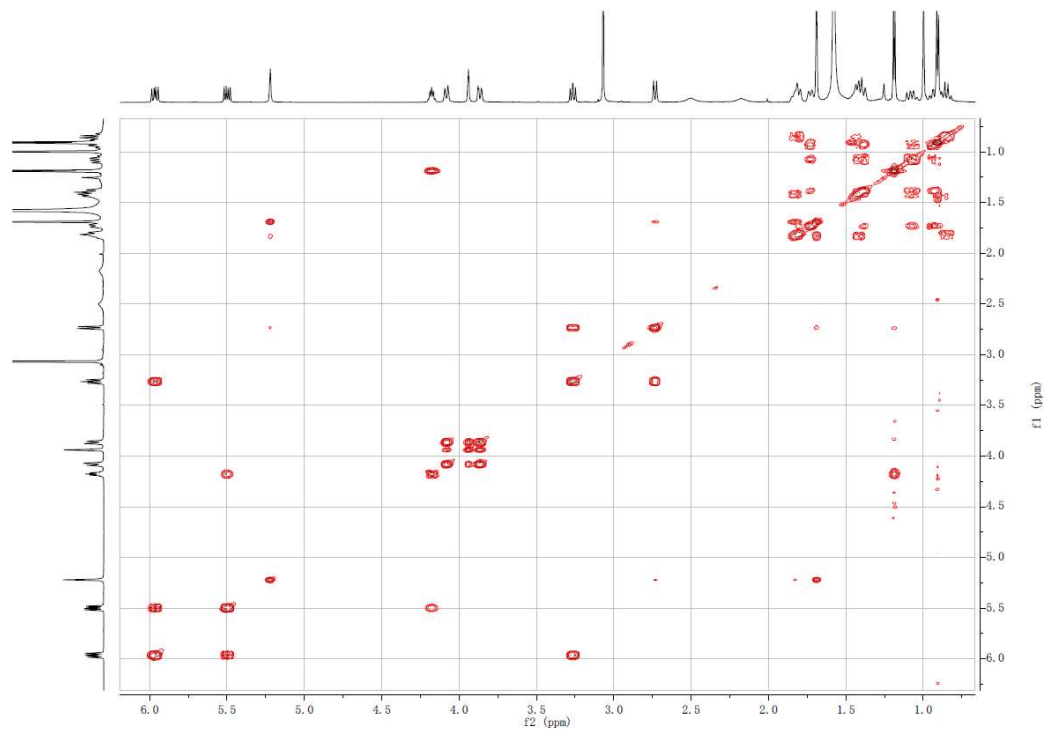
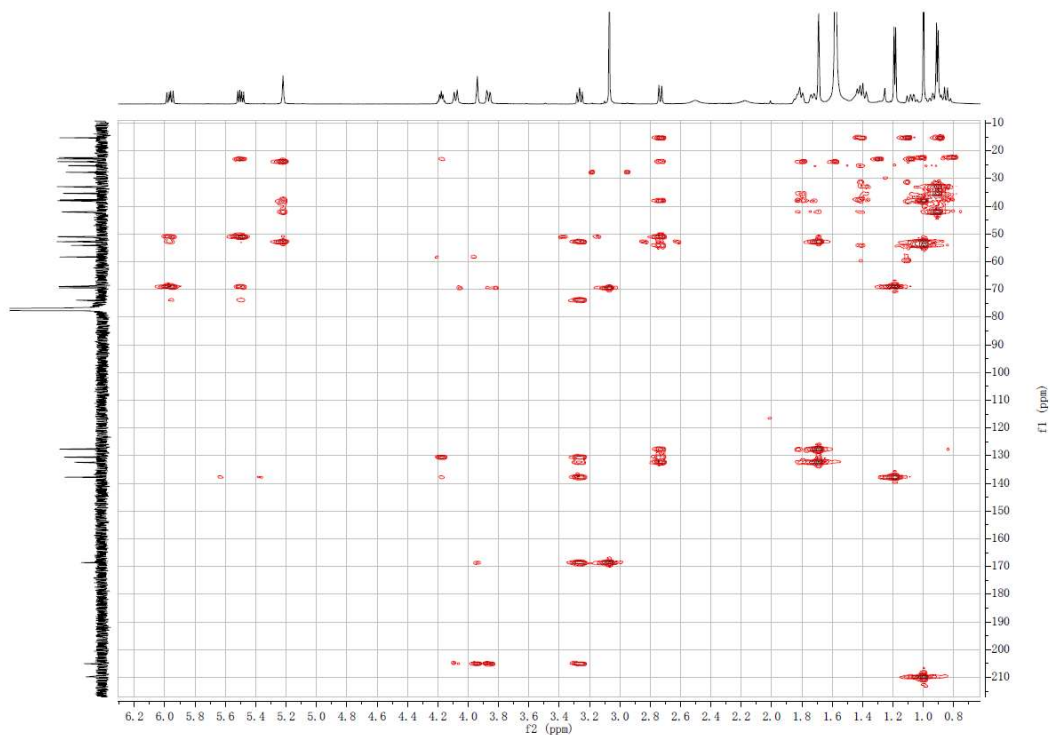
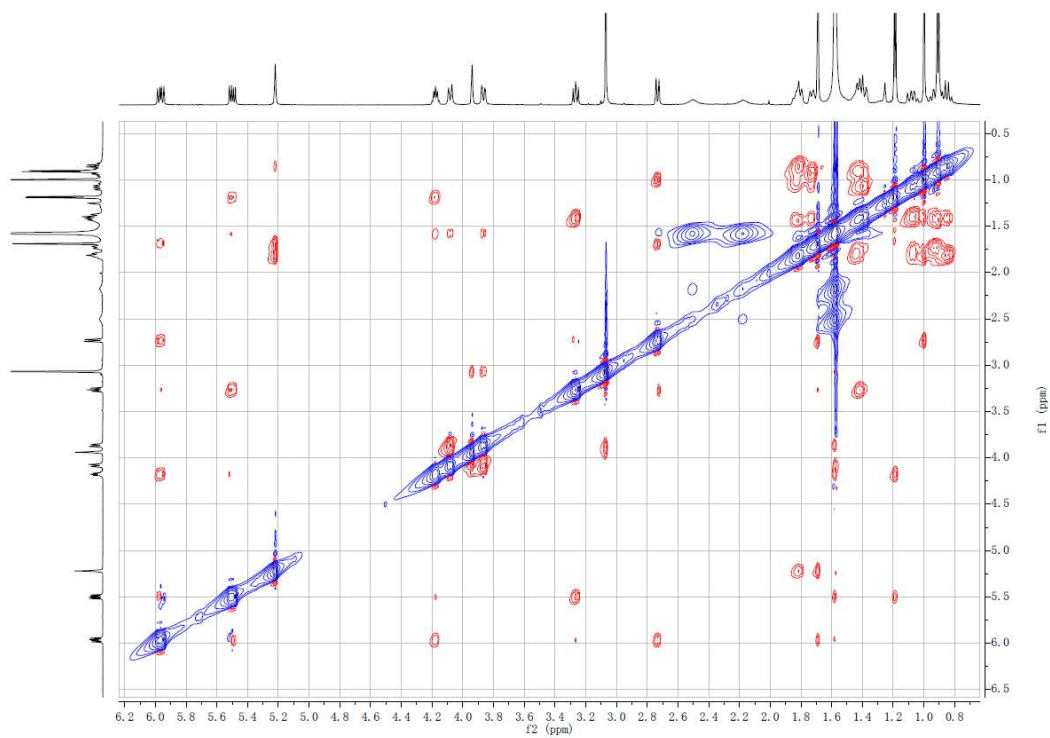
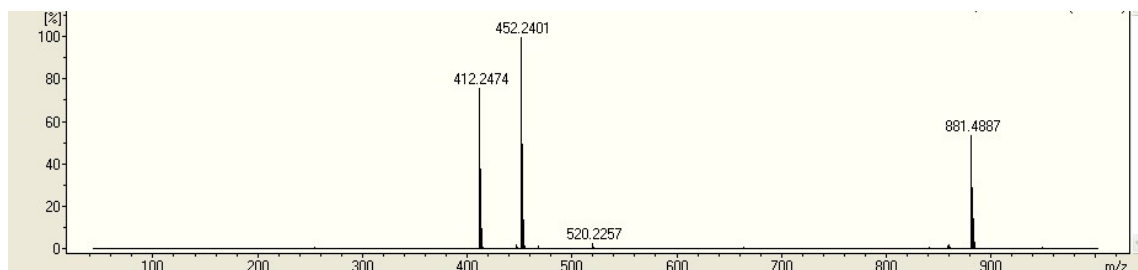
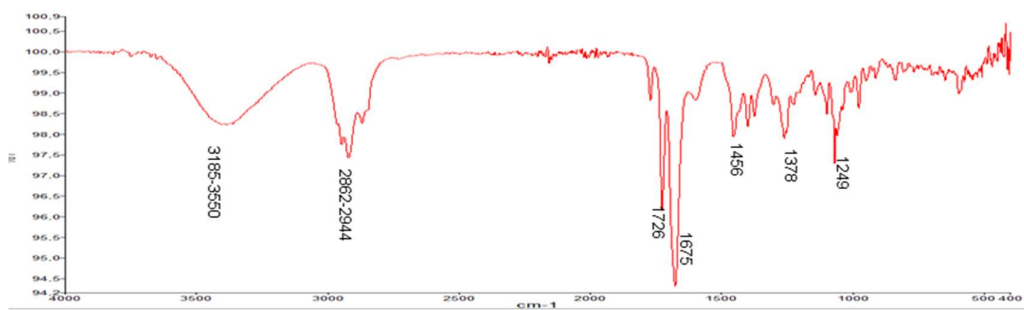


Figure S9. <sup>1</sup>H NMR spectrum of compound 2 (600 MHz, CDCl<sub>3</sub>).



**Figure S10.**  $^{13}\text{C}$  NMR spectrum of compound **2** (150 MHz,  $\text{CDCl}_3$ ).**Figure S11.** DEPT-HSQC spectrum of compound **2** (600 MHz,  $\text{CDCl}_3$ ).

**Figure S12.** COSY spectrum of compound **2** (600 MHz, CDCl<sub>3</sub>).**Figure S13.** HMBC spectrum of compound **2** (600 MHz, CDCl<sub>3</sub>).

**Figure S14.** NOESY spectrum of compound 2 (600 MHz, CDCl<sub>3</sub>).**Figure S15.** HR-ESIMS spectrum of compound 2.**Figure S16.** FT-IR spectrum of compound 2.

APPENDIX

Figure S17.  $^1\text{H}$  NMR spectrum of compound 3 (600 MHz,  $\text{CDCl}_3$ ).

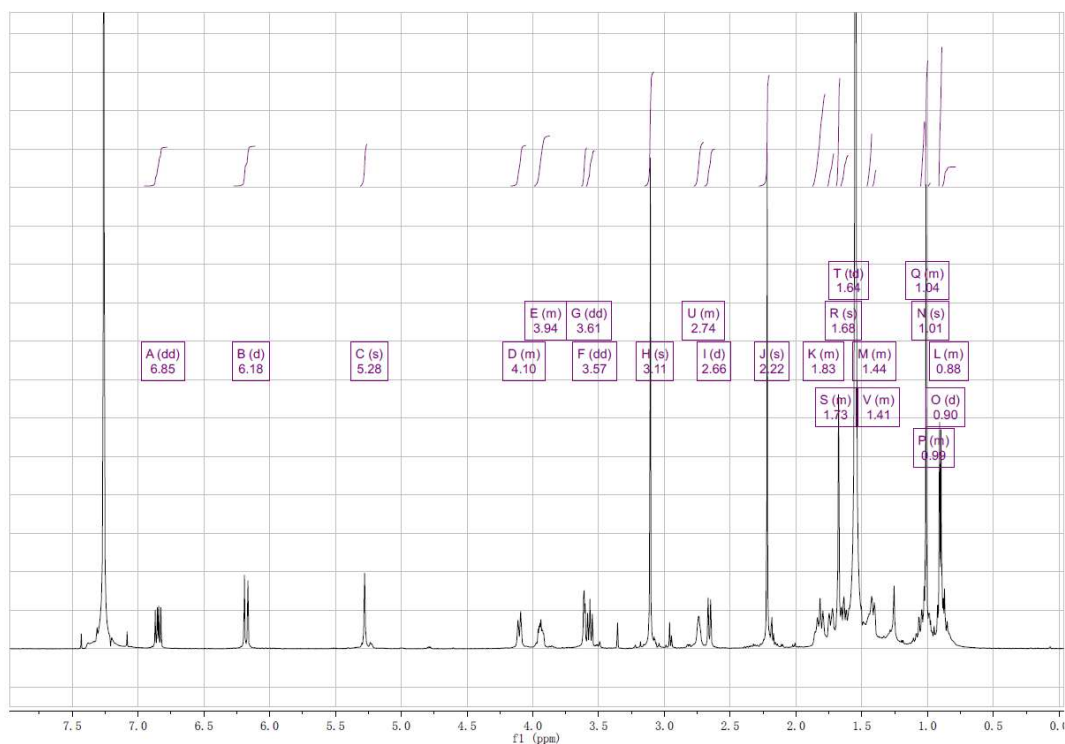
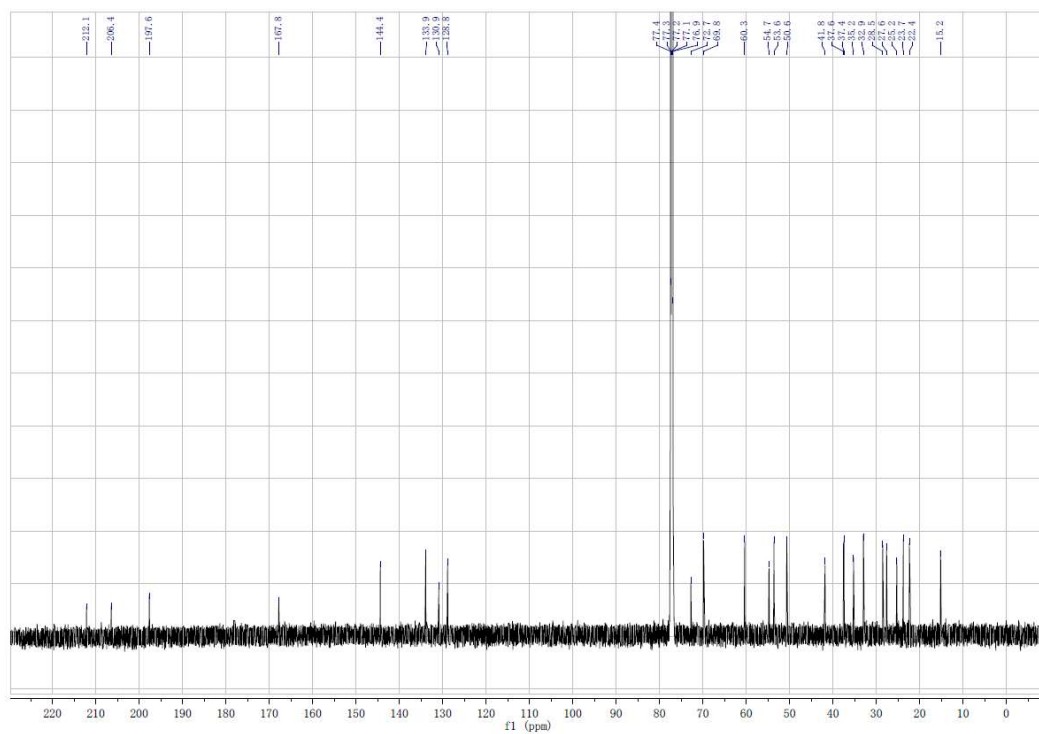


Figure S18.  $^{13}\text{C}$  NMR spectrum of compound 3 (150 MHz,  $\text{CDCl}_3$ ).





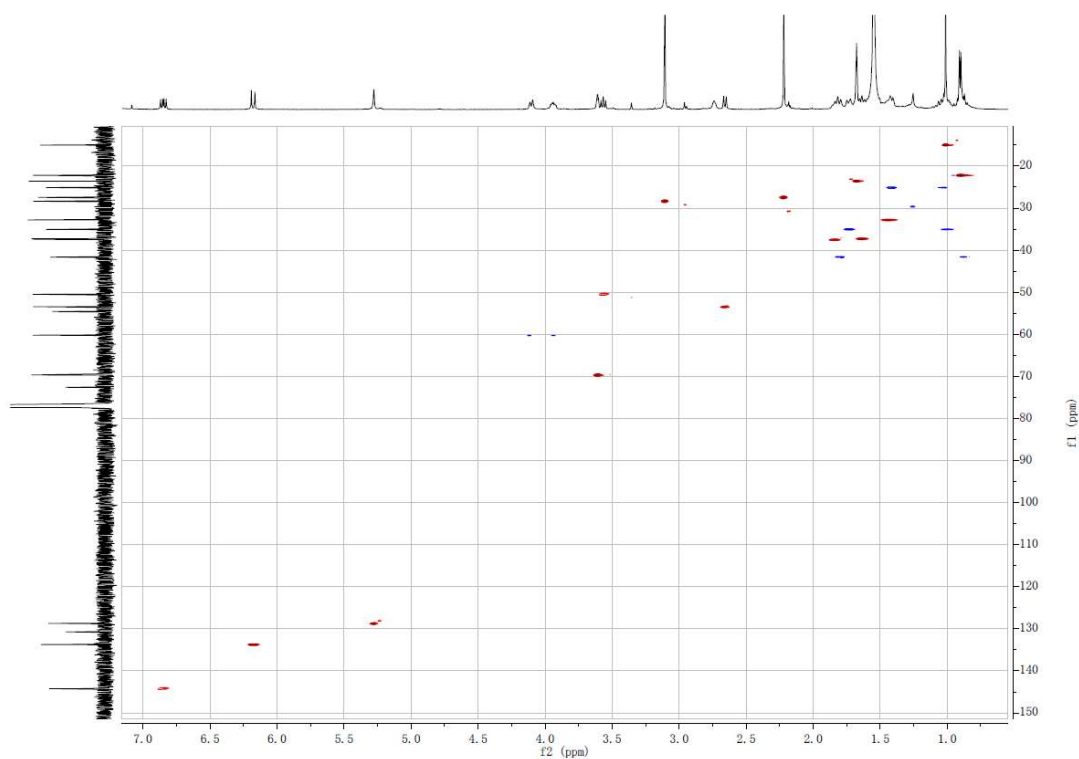
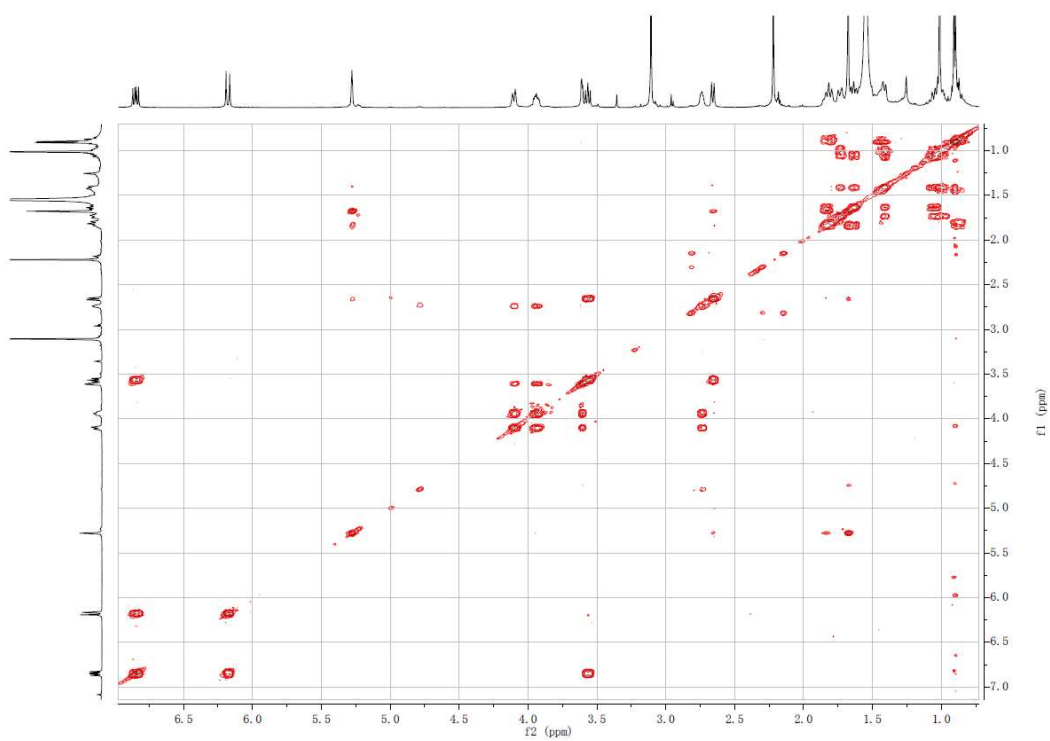
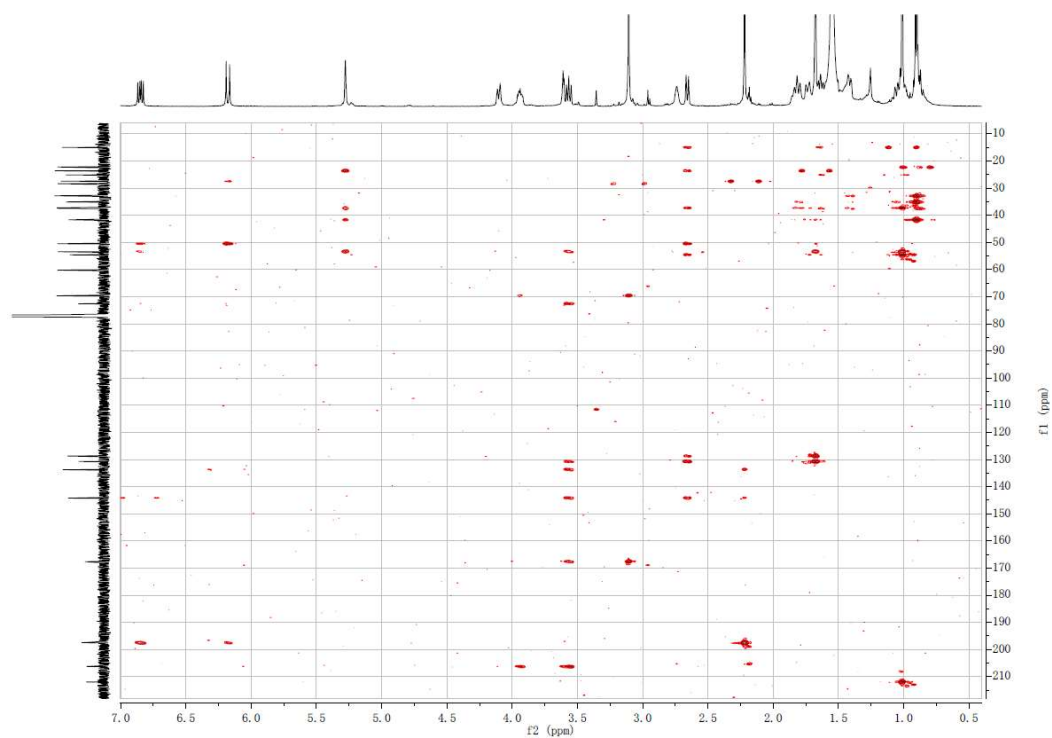
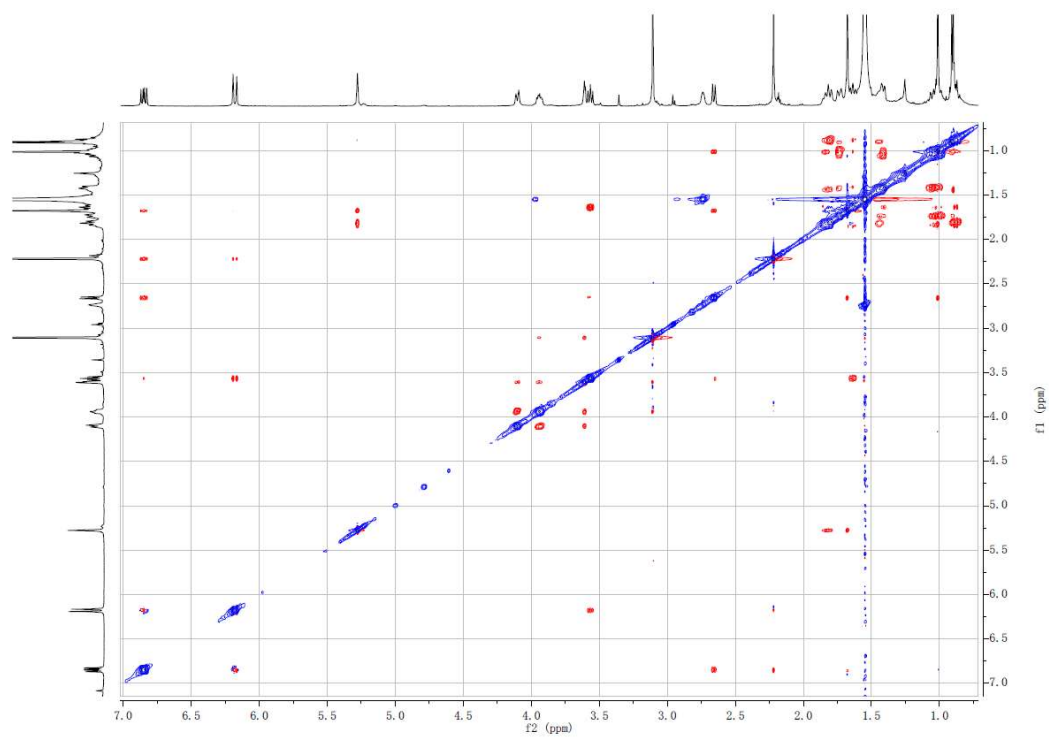
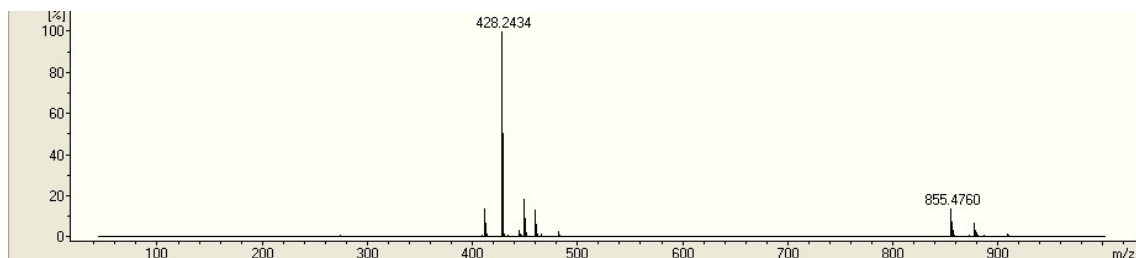
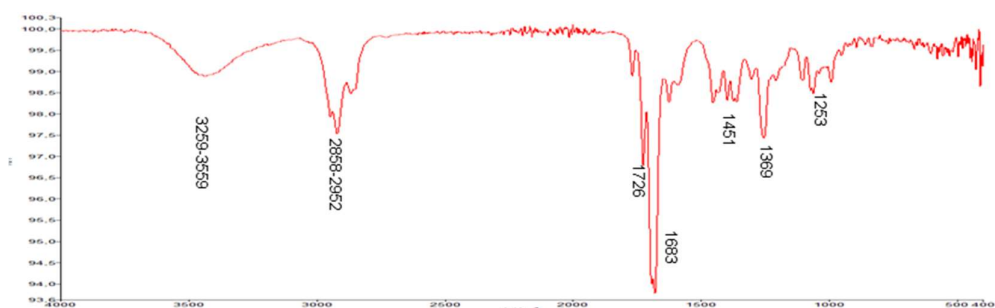
**Figure S19.** DEPT-HSQC spectrum of compound **3** (600 MHz, CDCl<sub>3</sub>).**Figure S20.** COSY spectrum of compound **3** (600 MHz, CDCl<sub>3</sub>).

Figure S21. HMBC spectrum of compound 3 (600 MHz, CDCl<sub>3</sub>).Figure S22. NOESY spectrum of compound 3 (600 MHz, CDCl<sub>3</sub>).

**Figure S23.** HR-ESIMS spectrum of compound 3.**Figure S24.** FT-IR spectrum of compound 3.

APPENDIX

Figure S25. <sup>1</sup>H NMR spectrum of 16-(*S*)-MTPA ester **6** (500 MHz, CDCl<sub>3</sub>).

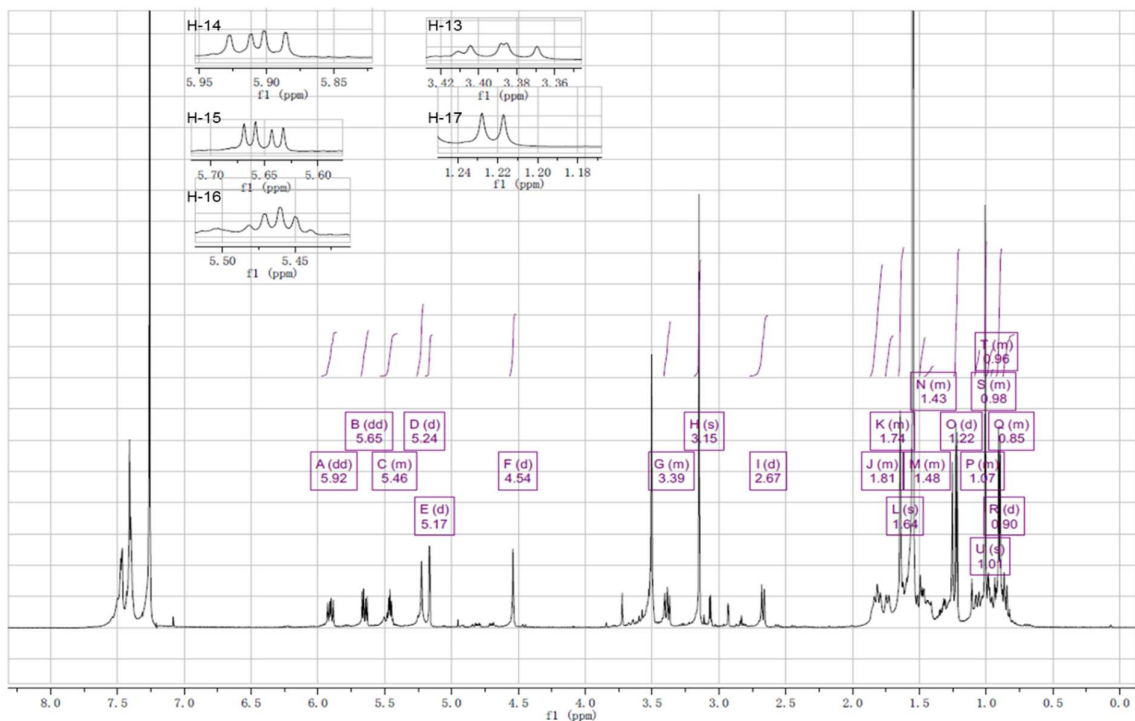


Figure S26. <sup>1</sup>H NMR spectrum of 16-(*R*)-MTPA ester **7** (500 MHz, CDCl<sub>3</sub>).

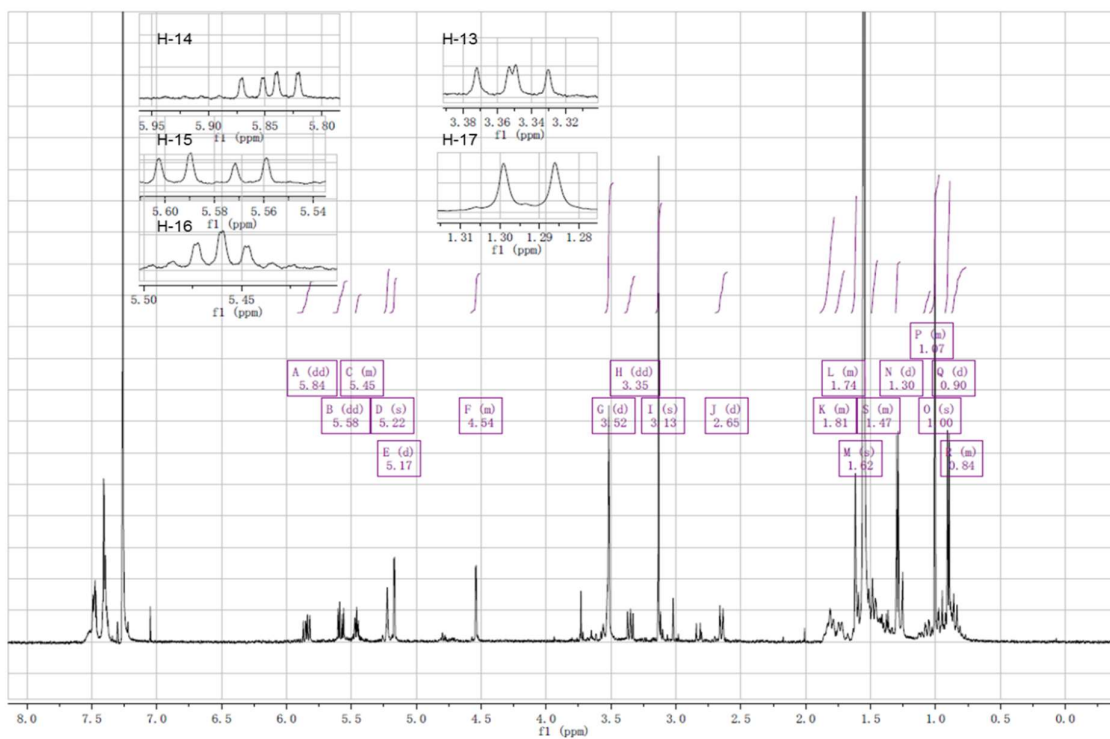
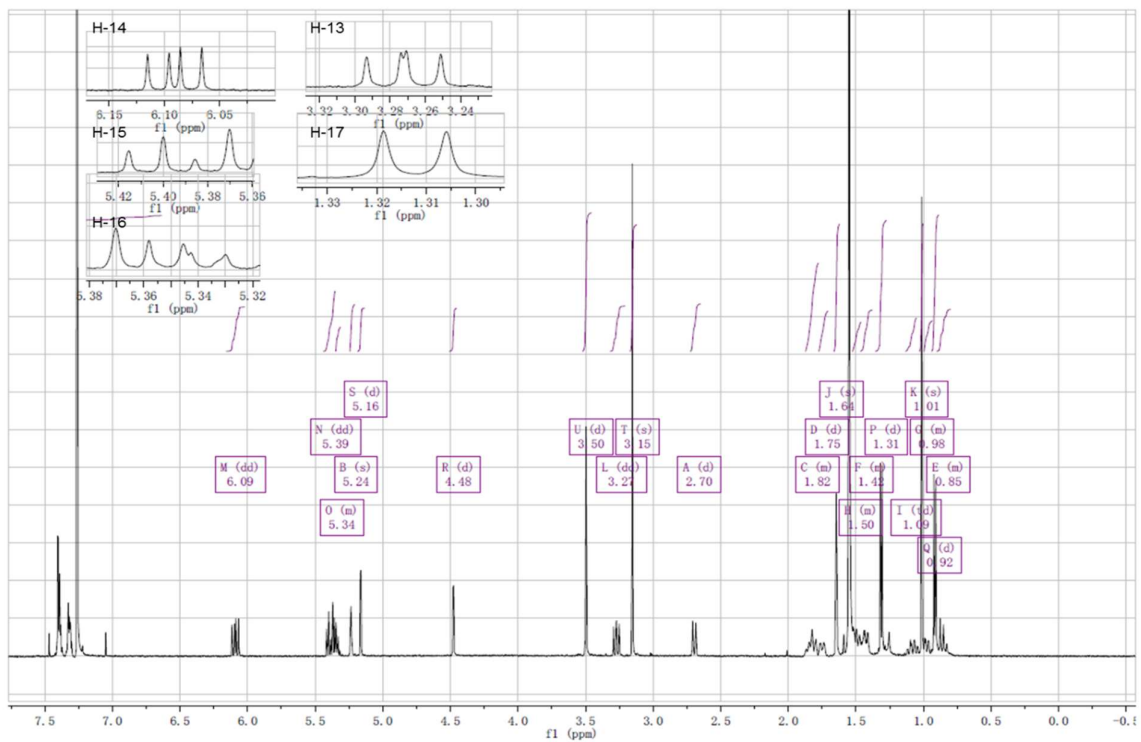
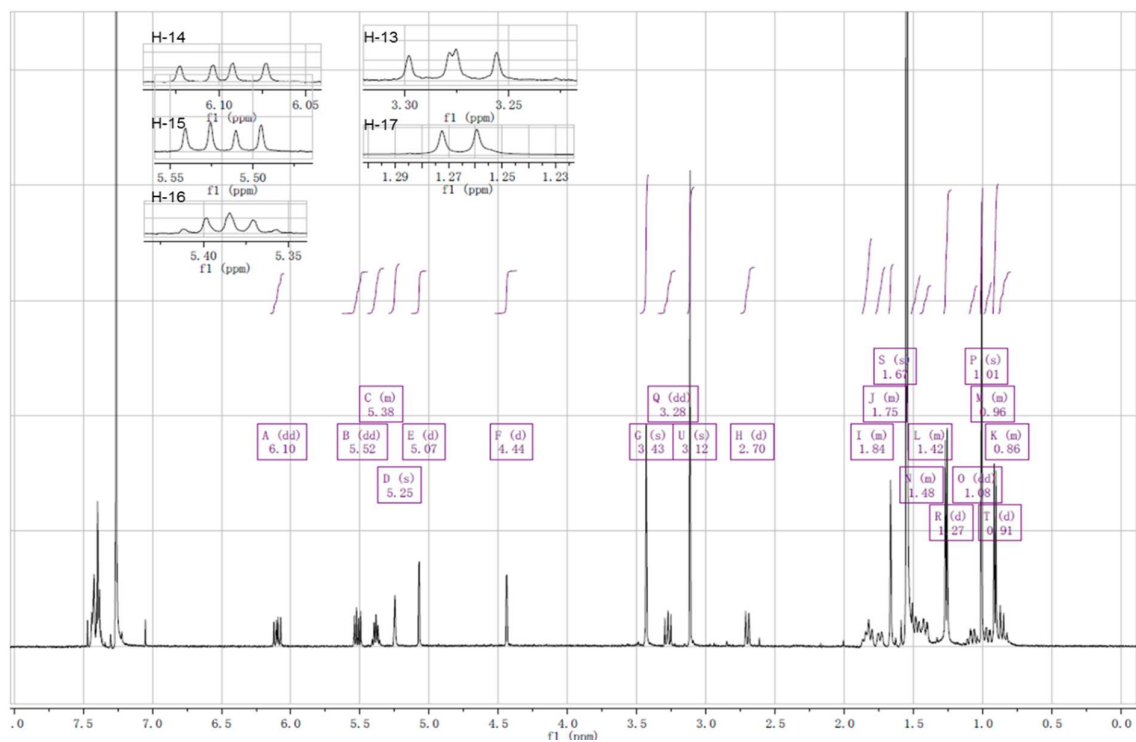
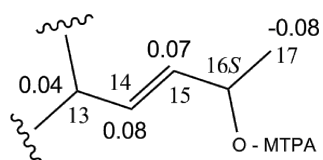


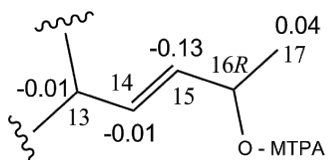
Figure S27.  $^1\text{H}$  NMR spectrum of 16-(*S*)-MTPA ester **8** (500 MHz,  $\text{CDCl}_3$ ).Figure S28.  $^1\text{H}$  NMR spectrum of 16-(*R*)-MTPA ester **9** (500 MHz,  $\text{CDCl}_3$ ).

APPENDIX

**Figure S29.**  $\Delta\delta(\delta_S-\delta_R)$  values (ppm) obtained from 16-MTPA esters (**6** and **7**) of compound **1**.

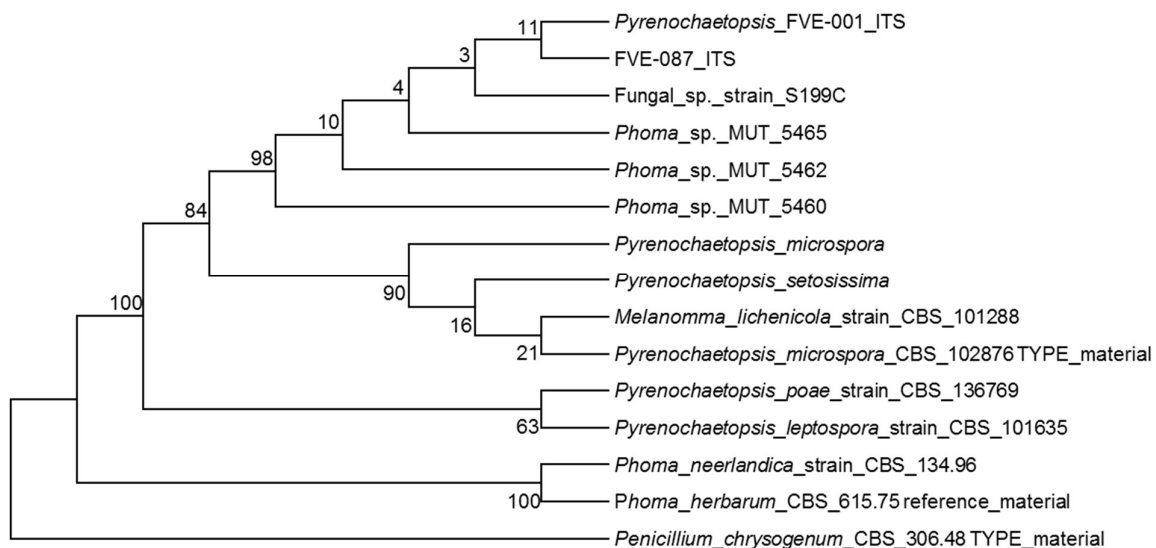


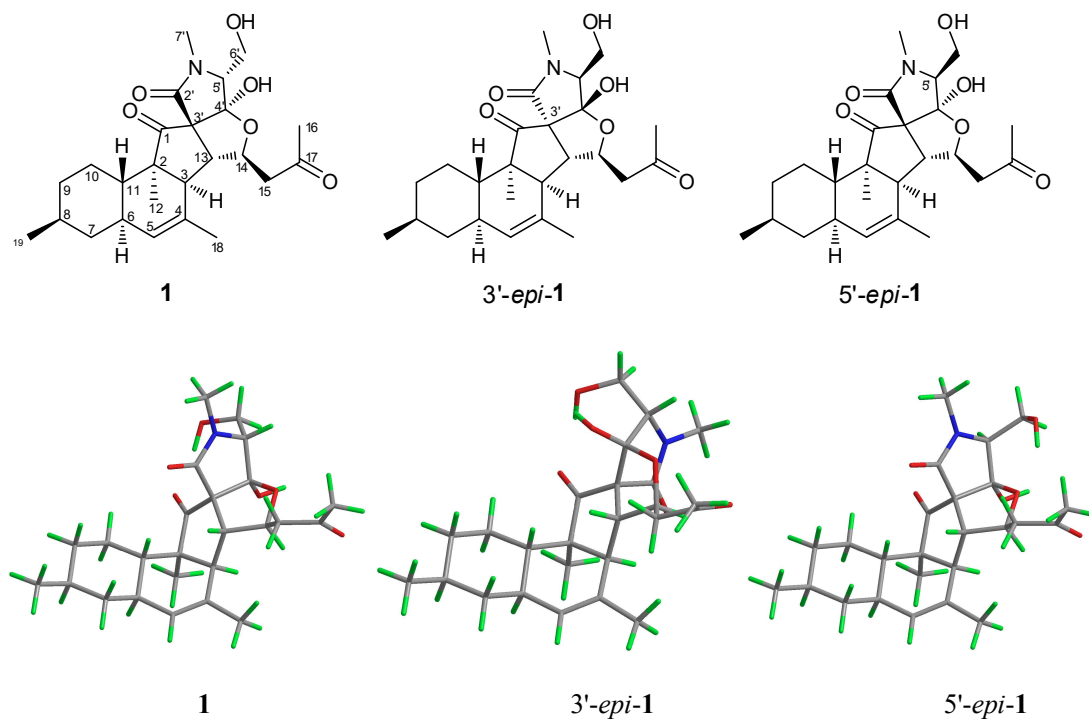
**Figure S30.**  $\Delta\delta(\delta_S-\delta_R)$  values (ppm) obtained from 16-MTPA esters (**8** and **9**) of compound **2**.



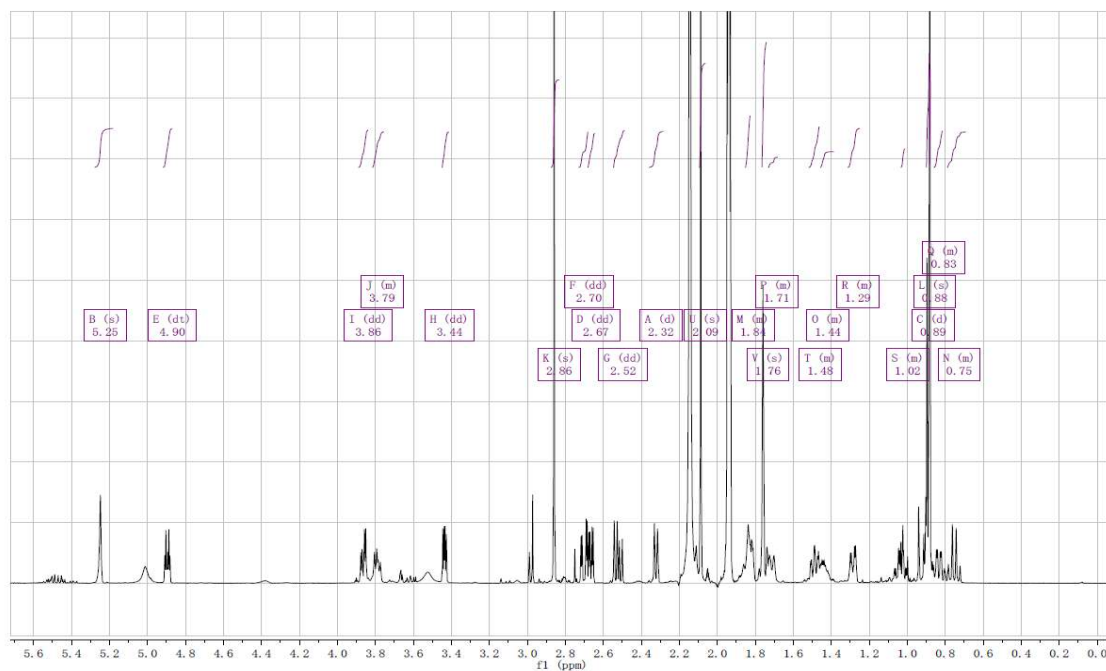
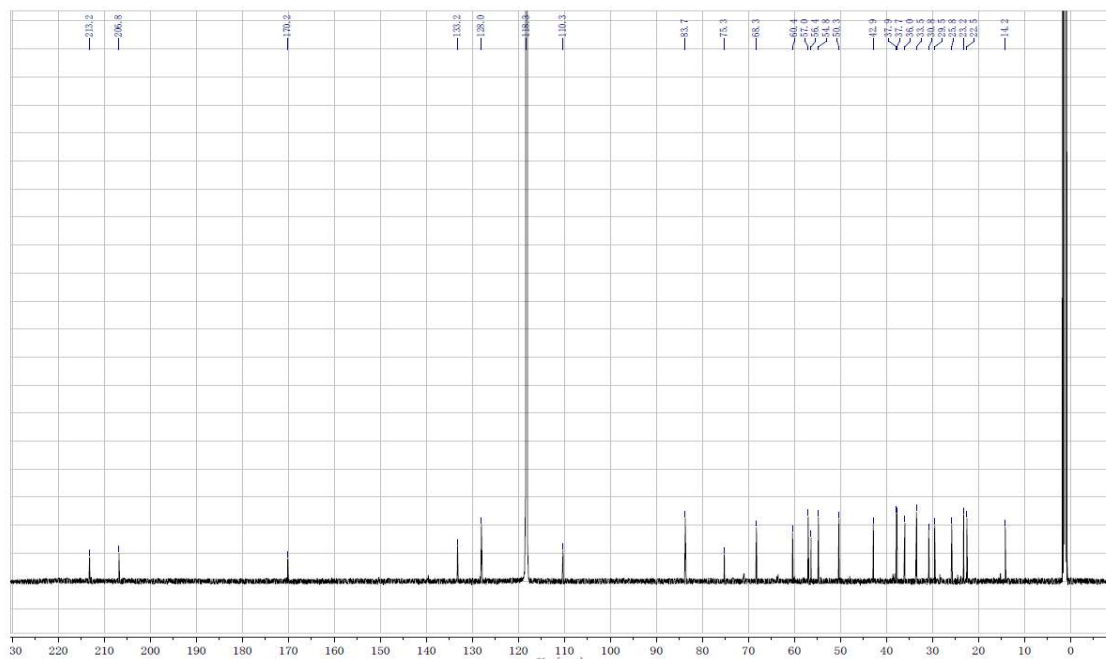
## 4. NMR spectra and DFT calculation tables of Chapter 3

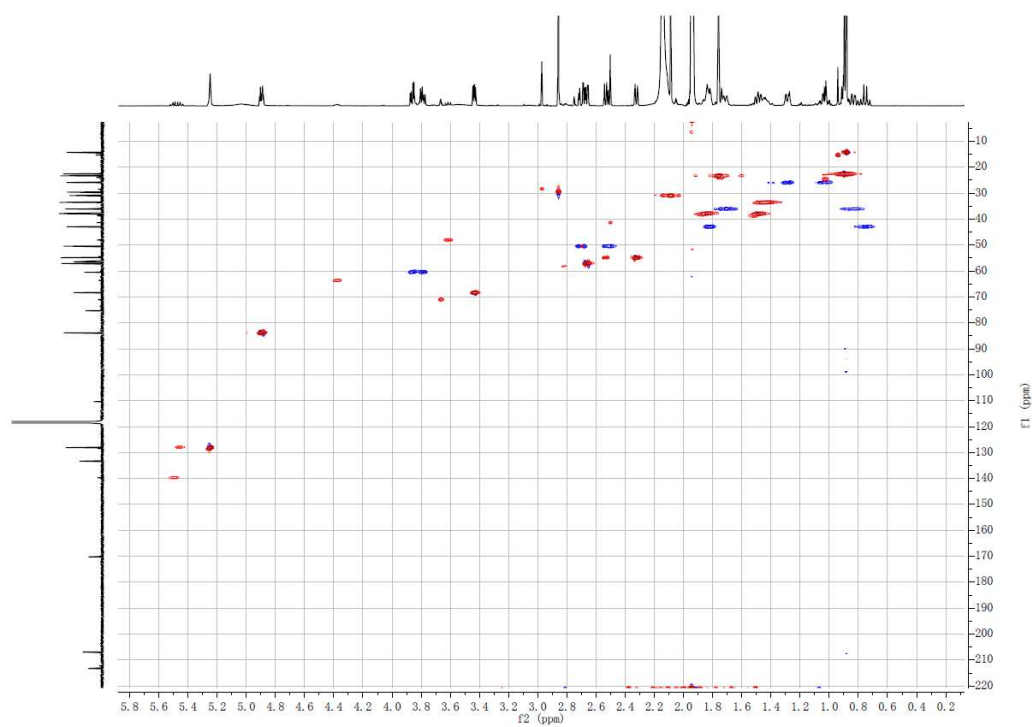
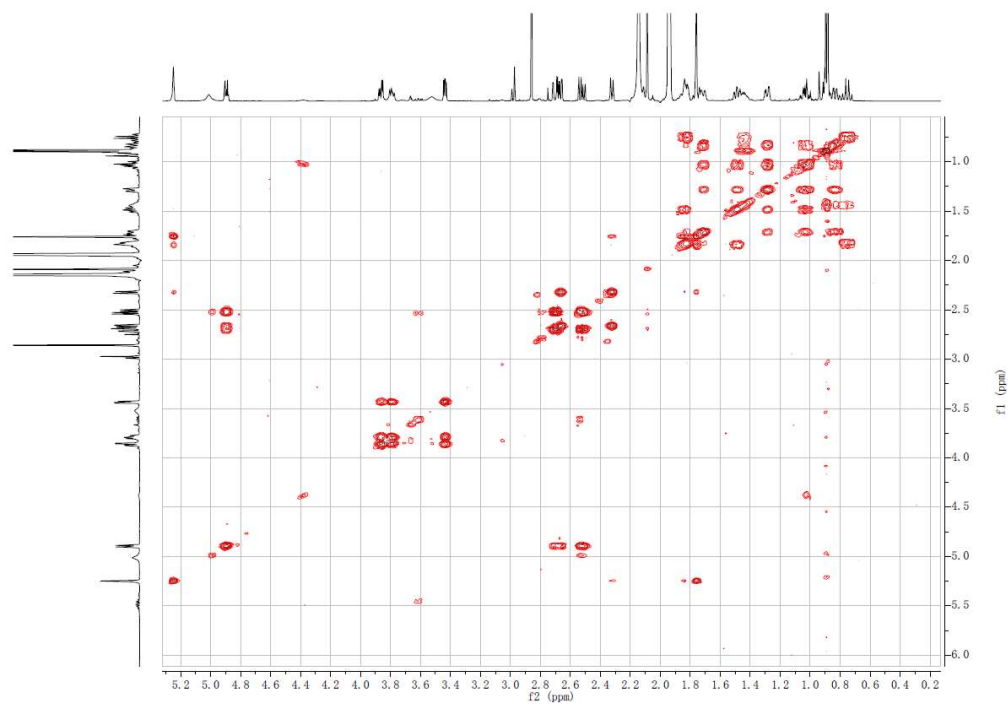
**Figure S1.** Molecular phylogenetic analysis of *Pyrenochaetopsis* sp. FVE-087 by maximum likelihood method

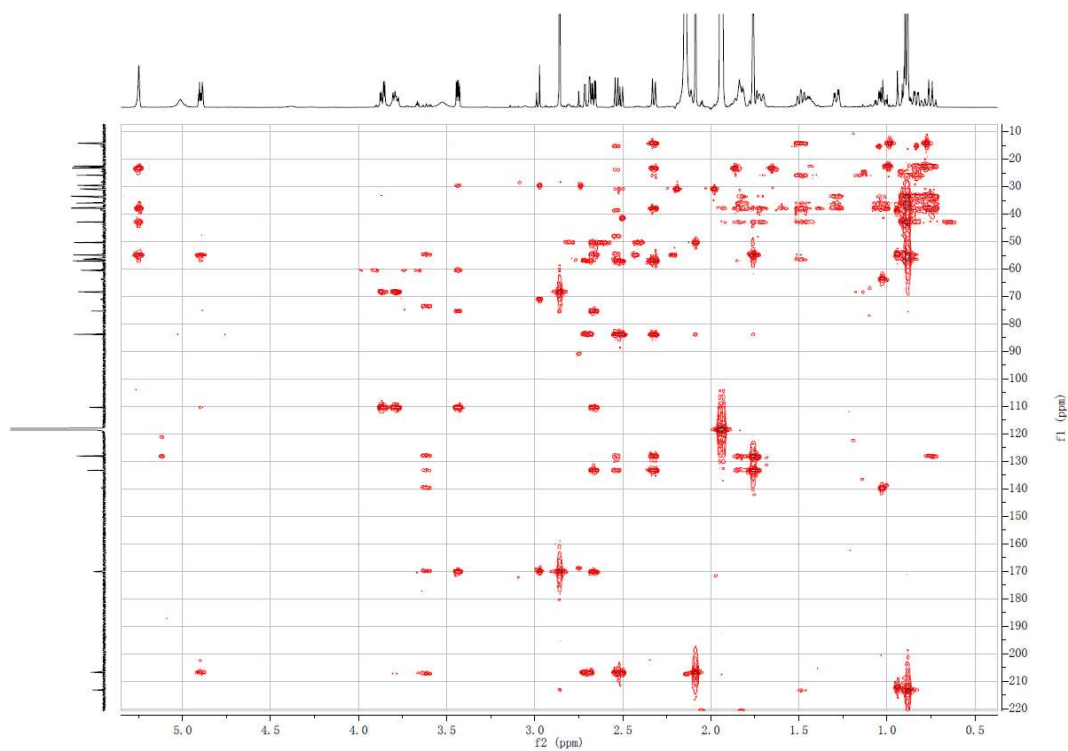
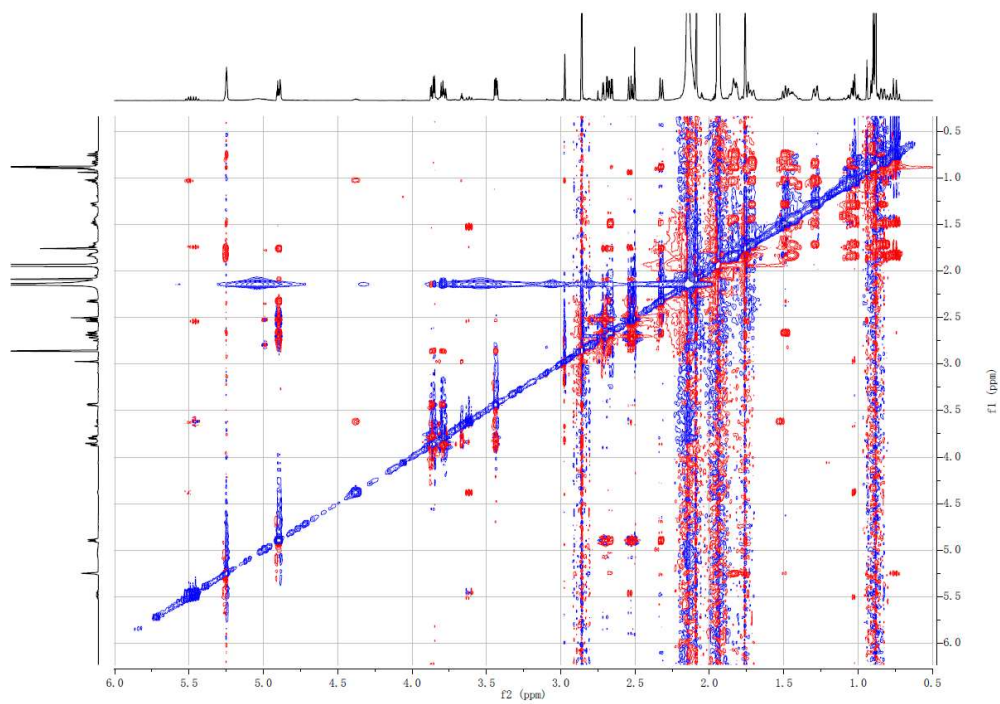


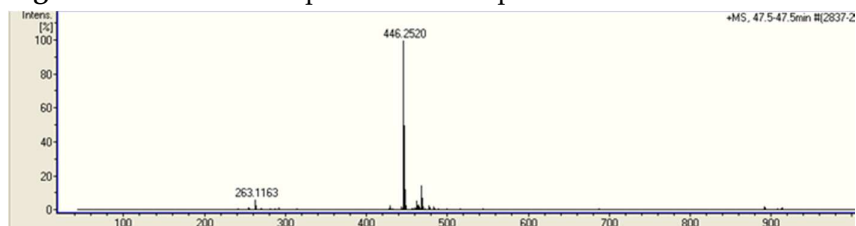
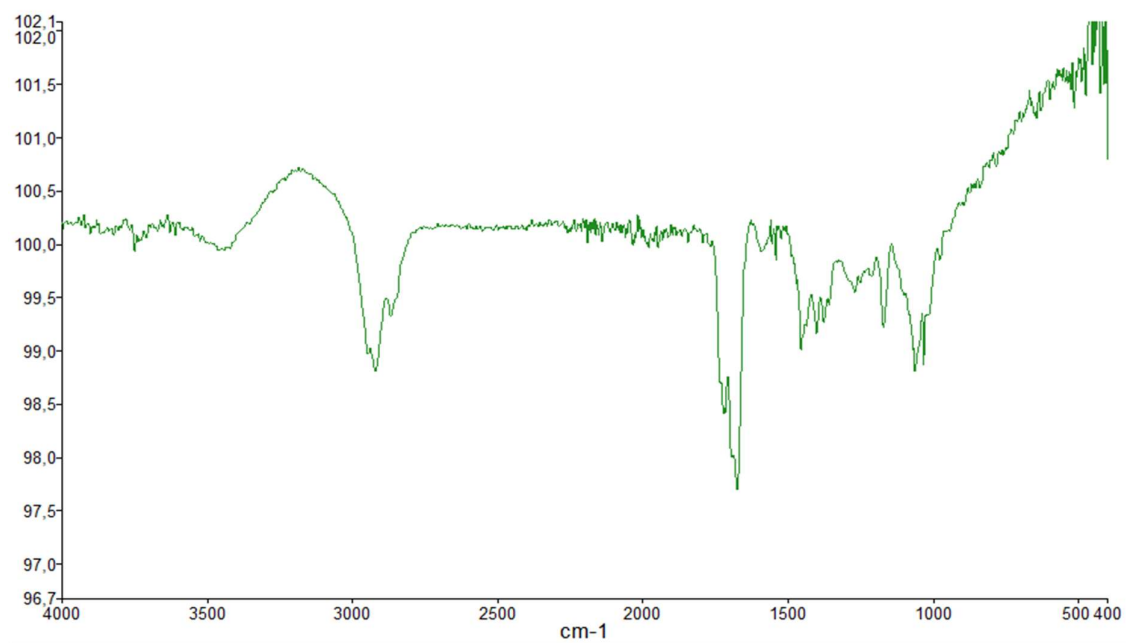
**Figure S2.** Structures of compounds **1**, **3'-epi-1**, and **5'-epi-1**.**Figure S3.** (A) Errors of predicted  $^{13}\text{C}$  chemical shifts of compounds **1** and **5'-epi-1**. (B) Errors of predicted  $^1\text{H}$  chemical shifts of compounds **1** and **5'-epi-1**.



**Figure S4.**  $^1\text{H}$  NMR spectrum of compound **1** (600 MHz,  $\text{CD}_3\text{CN}$ )**Figure S5.**  $^{13}\text{C}$  NMR spectrum of compound **1** (150 MHz,  $\text{CD}_3\text{CN}$ )

**Figure S6.** DEPT-HSQC spectrum of compound **1** (600 MHz, CD<sub>3</sub>CN).**Figure S7.** COSY spectrum of compound **1** (600 MHz, CD<sub>3</sub>CN)

**Figure S8.** HMBC spectrum of compound 1 (600 MHz, CD<sub>3</sub>CN)**Figure S9.** NOESY spectrum of compound 1 (600 MHz, CD<sub>3</sub>CN)

**Figure S10.** HR-ESIMS spectrum of compound **1**.**Figure S11.** FT-IR spectrum of compound **1**

**Table S1.** Cartesian coordinates, energies, population at 298 K, and calculated optical rotations of significantly populated conformers of compound **1**. Conformers were optimized at the B3LYP/TZVP/SMD(ACN) level; optical rotation were calculated at the B3LYP/TZVP/SMD(MeOH) level.

Conformer 1				Conformer 2				Conformer 3			
Relative energy (kcal/mol)	0.00			Relative energy (kcal/mol)	0.65			Relative energy (kcal/mol)	0.74		
Population (%)	38.7			Population (%)	13.0			Population (%)	11.1		
Calcd. [ $\alpha$ ] <sub>D</sub>	-98.0			Calcd. [ $\alpha$ ] <sub>D</sub>	-152.0			Calcd. [ $\alpha$ ] <sub>D</sub>	-60.4		
C	0.37784	-1.20880	-0.98624	C	0.37737	-1.34617	-0.78471	C	0.35542	-1.14535	-1.01927
C	1.33882	-0.08551	-1.33146	C	1.37491	-0.30065	-1.27162	C	1.33359	-0.02559	-1.32422
C	0.45876	1.18190	-1.15193	C	0.56788	1.02286	-1.17951	C	0.48067	1.24912	-1.07753
C	1.24501	2.45527	-0.93746	C	1.41977	2.26895	-1.09615	C	1.29449	2.49540	-0.81247
C	2.53958	2.42724	-0.61405	C	2.72472	2.20334	-0.82419	C	2.59215	2.42770	-0.50819
C	3.35147	1.18120	-0.41803	C	3.48534	0.93837	-0.55724	C	3.38191	1.15875	-0.38199
C	4.32704	1.29607	0.76509	C	4.51929	1.10627	0.56884	C	4.37750	1.20042	0.78932
C	5.21728	0.05475	0.90231	C	5.35369	-0.16229	0.78398	C	5.24396	-0.06322	0.85540
C	4.35852	-1.21443	0.97161	C	4.43776	-1.37302	1.00300	C	4.36028	-1.31658	0.88309
C	3.35848	-1.31982	-0.18571	C	3.38476	-1.52863	-0.10000	C	3.34058	-1.35035	-0.26141
C	2.47423	-0.06913	-0.25011	C	2.55732	-0.24590	-0.24396	C	2.48191	-0.08034	-0.25754
C	1.86943	-0.24438	-2.75773	C	1.83571	-0.61807	-2.69606	C	1.84483	-0.12901	-2.76270
C	-0.55980	0.83623	-0.01905	C	-0.43369	0.83119	0.00427	C	-0.53360	0.87107	0.04871
C	-1.98247	1.41987	-0.18158	C	-1.81931	1.49899	-0.16331	C	-1.94702	1.48727	-0.06764
C	-2.45554	2.27802	0.97645	C	-2.21757	2.42274	0.97299	C	-2.39456	2.27987	1.15445
C	-3.77482	2.99401	0.74569	C	-3.50296	3.19879	0.74446	C	-3.81767	2.80414	1.09308
C	-4.51511	3.42281	1.98304	C	-4.22431	3.65889	1.98177	C	-4.23732	3.57082	-0.13357
C	0.51531	3.75152	-1.15882	C	0.74028	3.57998	-1.38200	C	0.58697	3.81391	-0.96099
C	6.15879	0.16582	2.10008	C	6.35140	0.00623	1.92836	C	6.20706	-0.02508	2.04055
C	-0.84124	-1.41805	1.24444	C	-0.89885	-1.31350	1.40301	C	-0.85371	-1.43353	1.20845
C	-0.75917	-0.68759	-0.10454	C	-0.73838	-0.67206	0.02261	C	-0.76521	-0.64284	-0.10595
C	-2.18283	-0.87773	-0.67354	C	-2.16172	-0.79884	-0.57539	C	-2.19456	-0.78054	-0.67527
C	-2.80892	-2.07556	0.08954	C	-2.85945	-1.92895	0.21799	C	-2.84053	-1.99858	0.03727
C	-2.88131	-3.41574	-0.65426	C	-2.94460	-3.26561	-0.52439	C	-2.94570	-3.30142	-0.76670
C	-2.37211	-2.93405	2.43375	C	-2.54761	-2.68736	2.61863	C	-2.40826	-2.97090	2.33776
H	-0.12109	1.30449	-2.07339	H	-0.03405	1.09814	-2.09214	H	-0.10452	1.42561	-1.98690
H	3.07329	3.36918	-0.50804	H	3.30456	3.12376	-0.81325	H	3.14495	3.35345	-0.36446
H	3.97157	1.04415	-1.31573	H	4.05524	0.69293	-1.46507	H	3.98576	1.05097	-1.29458
H	4.95028	2.18666	0.63544	H	5.17841	1.94799	0.33302	H	5.01669	2.08356	0.69002
H	3.75698	1.44097	1.69102	H	3.99978	1.36335	1.50027	H	3.82481	1.31404	1.73000
H	5.83037	-0.00954	-0.00608	H	5.92244	-0.34017	-0.13806	H	5.84074	-0.09894	-0.06535
H	5.00535	-2.09702	0.98169	H	5.04061	-2.28398	1.06915	H	4.98849	-2.21169	0.84363
H	2.75047	-2.21773	-0.05821	H	2.74056	-2.37921	0.12962	H	2.71567	-2.24031	-0.16344
H	3.90434	-1.43933	-1.12652	H	3.88378	-1.75770	-1.04665	H	3.86959	-1.43970	-1.21506
H	1.97802	0.02137	0.72247	H	2.11040	-0.04308	0.73627	H	1.99982	-0.02327	0.72473
H	-0.13990	1.10696	0.94886	H	0.03535	1.13788	0.93867	H	-0.09989	1.08856	1.02385
H	-2.06179	1.98174	-1.11336	H	-1.87302	2.03912	-1.10999	H	-2.01649	2.10286	-0.96658
H	-2.51088	1.68464	1.89221	H	-2.27928	1.86723	1.91159	H	-2.29231	1.67150	2.05402
H	-1.71996	3.06696	1.17065	H	-1.43670	3.17899	1.11597	H	-1.73835	3.15047	1.25686
H	-3.83546	-1.80564	0.35429	H	-3.87411	-1.60745	0.47296	H	-3.85966	-1.72039	0.32126
H	3.80935	-1.21881	1.92105	H	3.93099	-1.26313	1.96969	H	3.82600	-1.35190	1.84033
H	-3.53414	-4.08251	-0.08734	H	-1.96150	-3.56818	-0.88199	H	-3.60765	-3.97995	-0.22496
H	-3.36820	-3.24042	-1.62118	H	-3.32557	-4.04035	0.14355	H	-3.43720	-3.07330	-1.72033
H	-3.06706	-0.99854	-2.39789	H	-2.88286	-1.56220	-2.20896	H	-3.09080	-0.83832	-2.39739
H	-0.95802	-3.48604	-1.11486	H	-4.70422	-3.08324	-1.39746	H	-1.02698	-3.38904	-1.24375
H	2.43069	-1.17081	-2.87490	H	0.97986	-0.64703	-3.37356	H	1.00842	-0.10117	-3.46401
H	1.04130	-0.26202	-3.46914	H	2.52603	0.14149	-3.06432	H	2.50812	0.70257	-3.00120
H	2.52197	0.58669	-3.02585	H	2.33441	-1.58561	-2.74710	H	2.38910	-1.05817	-2.92803
H	-3.83573	3.90313	2.69138	H	-3.52488	4.11319	2.68792	H	-5.18898	4.06871	0.04471
H	-4.91523	2.53372	2.48053	H	-4.65775	2.78704	2.48192	H	-4.35030	2.88327	-0.97655
H	-5.33387	4.09463	1.73058	H	-5.01626	4.36228	1.72972	H	-3.47692	4.30207	-0.41604
H	-0.31954	3.87513	-0.46380	H	-0.05128	3.79501	-0.65889	H	-0.23523	3.91801	-0.24803
H	1.18373	4.60464	-1.03296	H	1.45250	4.40608	-1.35284	H	1.27290	4.64762	-0.80350
H	0.09087	3.79356	-2.16719	H	0.26689	3.56909	-2.36911	H	0.14977	3.91289	-1.95989
H	6.81545	-0.70566	2.16988	H	7.02337	0.84994	1.74895	H	6.84595	-0.91221	2.06047
H	5.59588	0.23366	3.03606	H	6.96685	-0.88900	2.05237	H	5.66090	0.01255	2.98809
H	6.79153	1.05456	2.02724	H	5.83438	0.18793	2.87559	H	6.85743	0.85275	1.99630
H	-3.41590	-2.73956	2.68660	H	-1.84470	-2.51324	3.42958	H	-1.77118	-2.75145	3.19127
H	-2.25282	-3.99943	2.22405	H	-3.52620	-2.28894	2.89689	H	-3.44803	-2.77013	2.60175
H	-1.74127	-2.66826	3.27866	H	-2.64013	-3.76216	2.45426	H	-2.30664	-4.02813	2.08241
N	-1.98783	-2.12896	1.29210	N	-2.05679	-2.01472	1.43059	N	-2.01361	-2.12362	1.23048
O	0.47161	-2.35688	-1.36631	O	0.43925	-2.53561	-0.98741	O	0.42465	-2.27738	-1.44897
O	-2.87210	0.27548	-0.26463	O	-2.77919	0.41487	-0.20496	O	-2.85904	0.36860	-0.20966
O	-4.19404	3.23058	-0.37004	O	-3.90959	3.45683	-0.37123	O	-4.58024	2.63000	2.02411
O	0.00013	-1.34143	2.12953	O	-0.10148	-1.20589	2.32405	O	-0.00527	-1.41430	2.08956

## APPENDIX

O	-2.15440	-1.00219	-2.07051	O	-2.14733	-0.97330	-1.96157	O	-2.17621	-0.84004	-2.07525
O	-1.65110	-4.09637	-0.80252	O	-3.78253	-3.14652	-1.68401	O	-1.73110	-3.99924	-0.95714
Conformer 4				Conformer 5				Conformer 6			
Relative energy (kcal/mol)			0.76	Relative energy (kcal/mol)			0.92	Relative energy (kcal/mol)			0.98
Population (%)			10.8	Population (%)			8.2	Population (%)			7.5
Calcd. [a] <sub>p</sub>			-111.8	Calcd. [a] <sub>p</sub>			-134.2	Calcd. [a] <sub>p</sub>			-102.5
C	0.37220	-1.29118	-0.80190	C	0.37633	-1.34379	-0.79126	C	0.38064	-1.20497	-0.99324
C	1.33991	-0.21319	-1.25885	C	1.37416	-0.29718	-1.27527	C	1.34843	-0.08390	-1.33319
C	0.48420	1.08014	-1.16423	C	0.56767	1.02622	-1.17922	C	0.47186	1.18668	-1.15649
C	1.29087	2.35354	-1.05048	C	1.42012	2.27176	-1.09312	C	1.25791	2.45719	-0.92672
C	2.59371	2.32923	-0.76237	C	2.72497	2.20493	-0.82089	C	2.55137	2.42491	-0.59955
C	3.39466	1.08826	-0.50145	C	3.48498	0.93906	-0.55660	C	3.36094	1.17619	-0.41056
C	4.40955	1.27879	0.63831	C	4.51791	1.10351	0.57093	C	4.33542	1.28413	0.77417
C	5.28407	0.03706	0.84947	C	5.35192	-0.16581	0.78324	C	5.22144	0.03963	0.90926
C	4.40689	-1.20519	1.04853	C	4.43567	-1.37717	0.99750	C	4.35831	-1.22673	0.97454
C	3.37229	-1.38640	-0.06797	C	3.38357	-1.52918	-0.10686	C	3.36027	-1.32610	-0.18499
C	2.50487	-0.13033	-0.21097	C	2.55646	-0.24587	-0.24729	C	2.48015	-0.07246	-0.24847
C	1.83215	-0.49741	-2.68043	C	1.83496	-0.61065	-2.70054	C	1.88338	-0.24270	-2.75793
C	-0.53206	0.83492	-0.00365	C	-0.43333	0.83170	0.00460	C	-0.55815	0.84018	-0.03459
C	-1.93709	1.45110	-0.19166	C	-1.81883	1.50014	-0.16106	C	-1.97626	1.42854	-0.20252
C	-2.39233	2.34883	0.94340	C	-2.21588	2.42390	0.97570	C	-2.46537	2.24758	-0.97715
C	-3.70166	3.07816	0.69693	C	-3.49994	3.20215	0.74656	C	-3.77677	2.97894	0.74901
C	-4.44859	3.52257	1.92469	C	-4.22431	3.65848	1.98344	C	-4.53642	3.36813	1.98751
C	0.57016	3.64397	-1.32889	C	0.74144	3.58367	-1.37676	C	0.52664	3.75534	-1.13056
C	6.26489	0.22773	2.00489	C	6.34818	-0.00084	1.92940	C	6.16182	0.14475	2.10848
C	-0.90867	-1.35683	1.35898	C	-0.89337	-1.31702	1.39904	C	-0.85011	-1.39406	1.23357
C	-0.77744	-0.67894	-0.00522	C	-0.73821	-0.67167	0.01993	C	-0.76168	-0.68032	-0.12467
C	-2.20779	-0.85370	-0.61255	C	-2.16347	-0.79746	-0.57348	C	-2.19354	-0.88632	-0.70641
C	-2.86520	-2.02289	0.17413	C	-2.86159	-1.92538	0.22421	C	-2.81703	-2.06006	0.08716
C	-3.05784	-3.32799	-0.60523	C	-2.96150	-3.25846	-0.51073	C	-2.88395	-3.42301	-0.61527
C	-2.45441	-2.87013	2.52651	C	-2.53205	-2.70018	2.61694	C	-2.40109	-2.86178	2.45358
H	-0.10216	1.14595	-2.08749	H	-0.03476	1.10415	-2.09133	H	-0.09767	1.31862	-2.08459
H	3.14109	3.26879	-0.73234	H	3.30524	3.12505	-0.80785	H	3.08458	3.36553	-0.48035
H	3.98252	0.87260	-1.40525	H	4.05567	0.69600	-1.46459	H	3.98140	1.04195	-1.30839
H	5.04179	2.14492	0.41809	H	5.17744	1.94578	0.33819	H	4.96162	2.17315	0.64802
H	3.87139	1.50811	1.56635	H	3.99754	1.35802	1.50259	H	3.76453	1.42814	1.69973
H	5.86690	-0.11287	-0.06870	H	5.92180	-0.34092	-0.13863	H	5.83542	-0.02454	0.00146
H	5.03862	-2.09635	1.11369	H	5.03842	-2.28838	1.06129	H	5.00206	-2.11158	0.98390
H	2.75455	-2.25990	0.14843	H	2.73907	-2.38039	0.11962	H	2.74888	-2.22222	-0.06087
H	3.88940	-1.59116	-1.01032	H	3.88325	-1.75533	-1.05388	H	3.90785	-1.44536	-1.12482
H	2.03693	0.04805	0.76395	H	2.10939	-0.04594	0.73343	H	1.98106	0.01687	0.72273
H	-0.09518	1.14829	0.94403	H	0.03613	1.13628	0.93948	H	-0.14376	1.10774	0.93644
H	-1.99734	1.99335	-1.13628	H	-1.87324	2.04058	-1.10755	H	-2.03972	2.02739	-1.11281
H	-2.45040	1.78391	1.87669	H	-2.27892	1.86784	1.91385	H	-2.53838	1.62338	1.87084
H	-1.64325	3.13225	1.10706	H	-1.43396	3.17891	1.11930	H	-1.72864	3.02559	1.20889
H	-3.85919	-1.70114	0.49795	H	-3.87331	-1.60026	0.48218	H	-3.84536	-1.77967	0.33217
H	3.88599	-1.12040	2.01016	H	3.92804	-1.27035	1.96407	H	3.80738	-1.23117	1.92296
H	-3.24122	-4.14388	0.09872	H	-1.98316	-3.56440	-0.88787	H	-3.52438	-4.07696	-0.01999
H	-3.94508	-3.22852	-1.23054	H	-3.33477	-4.02740	0.16956	H	-3.37468	-3.27884	-1.58290
H	-2.06139	-1.92684	-2.21866	H	-2.89700	-1.55459	-2.20296	H	-2.05193	-0.35024	-2.57399
H	-1.13036	-3.56895	-1.05014	H	-3.90497	-3.85524	-2.13640	H	-0.96622	-3.49256	-1.09899
H	2.48950	0.29834	-3.03154	H	2.52593	0.14946	-3.06644	H	1.05786	-0.25777	-3.47267
H	2.37688	-1.43945	-2.73456	H	2.33296	-1.57841	-2.75438	H	2.53873	0.58706	-3.02328
H	0.98631	-0.55870	-3.36824	H	0.97918	-0.63689	-3.37828	H	2.44252	-1.17045	-2.87434
H	-5.26075	4.19792	1.66061	H	-4.65897	2.78515	2.47991	H	-4.94783	2.46442	2.44804
H	-3.77078	4.00438	2.63367	H	-5.01556	4.36275	1.73165	H	-5.34836	4.05164	1.74459
H	-4.85801	2.64051	2.42711	H	-3.52646	4.11056	2.69261	H	-3.86710	3.82137	2.72286
H	1.25430	4.49273	-1.28434	H	-0.05038	3.79776	-0.65367	H	-0.30926	3.86652	-0.43436
H	0.10630	3.62799	-2.32038	H	1.45406	4.40937	-1.34570	H	1.19356	4.60743	-0.99082
H	-0.23420	3.82497	-0.61064	H	0.26852	3.57488	-2.36412	H	0.10342	3.81222	-2.13874
H	6.90944	1.09541	1.83986	H	6.96338	-0.89650	2.05152	H	5.59793	0.21228	3.04390
H	6.90919	-0.64735	2.12593	H	5.82995	0.17807	2.87650	H	6.79763	1.03154	2.03853
H	5.73344	0.38241	2.94891	H	7.02048	0.84333	1.75341	H	6.81545	-0.72909	2.17706
H	-2.63623	-3.91945	2.29265	H	-1.86004	-2.47507	3.44155	H	-3.45459	-2.68338	2.67488
H	-1.68255	-2.80573	3.28903	H	-3.53759	-2.35316	2.86464	H	-2.25313	-3.93026	2.28032
H	-3.37913	-2.43094	2.91074	H	-2.56011	-3.78114	2.46836	H	-1.79723	-2.55641	3.30487
N	-2.00520	-2.14977	1.34966	N	-2.05207	-2.01650	1.43070	N	-2.00850	-2.08193	1.29734
O	0.48061	-2.47961	-1.02570	O	0.43789	-2.53252	-0.99784	O	0.46947	-2.35182	-1.37882
O	-2.85618	0.33009	-0.25689	O	-2.77924	0.41673	-0.20180	O	-2.87086	0.29328	-0.35009
O	-4.10678	3.31339	-0.42420	O	-3.90286	3.46488	-0.36937	O	-4.17385	3.25838	-0.36490
O	-0.13103	-1.21252	2.29168	O	-0.09167	-1.21365	2.31674	O	-0.00581	-1.31619	2.11586
O	-2.26024	-0.99411	-2.00757	O	-2.15383	-0.97380	-1.95920	O	-2.29130	-1.14870	-2.07984
O	-1.99073	-3.66369	-1.49627	O	-3.88953	-3.05829	-1.59046	O	-1.64556	-4.09589	-0.74690
Conformer 7				Conformer 8				Conformer 9			
Relative energy (kcal/mol)			1.33	Relative energy (kcal/mol)			1.46	Relative energy (kcal/mol)			1.71

Population (%)				Population (%)				Population (%)				
Calcd. [α] <sub>p</sub>				Calcd. [α] <sub>p</sub>				Calcd. [α] <sub>p</sub>				
-76.9				-96.3				-59.0				
C	0.34991	-1.22227	-0.87249	C	0.36284	-1.28187	-0.84506	C	0.36200	-1.15414	-1.00456	
C	1.32822	-0.13394	-1.27793	C	1.36952	-0.22429	-1.28392	C	1.35317	-0.04510	-1.31565	
C	0.49317	1.16400	-1.09939	C	0.58086	1.10254	-1.11377	C	0.51058	1.24033	-1.08720	
C	1.32193	2.41638	-0.92508	C	1.45091	2.33103	-0.97296	C	1.32837	2.48155	-0.81260	
C	2.62603	2.35551	-0.64834	C	2.75661	2.23362	-0.71443	C	2.62497	2.40668	-0.50603	
C	3.40860	1.08967	-0.46158	C	3.50180	0.94646	-0.51996	C	3.40719	1.13306	-0.37872	
C	4.43156	1.19827	0.68157	C	4.54526	1.03913	0.60591	C	4.40487	1.17538	0.79081	
C	5.28812	-0.06677	0.81431	C	5.36445	-0.24991	0.74370	C	5.26043	-0.09487	0.86723	
C	4.39336	-1.30570	0.94471	C	4.43421	-1.45896	0.90378	C	4.36538	-1.33962	0.90850	
C	3.34951	-1.40515	-0.17359	C	3.37059	-1.54035	-0.19708	C	3.34581	-1.37569	-0.23594	
C	2.50116	-0.12984	-0.23622	C	2.55981	-0.24083	-0.26439	C	2.49785	-0.09850	-0.24543	
C	1.80487	-0.34202	-2.71749	C	1.81575	-0.46936	-2.72707	C	1.86851	-0.16846	-2.75145	
C	-0.50946	0.86759	0.06139	C	-0.41108	0.85987	0.06881	C	-0.52211	0.87915	0.02664	
C	-1.91073	1.50678	-0.06800	C	-1.79067	1.55068	-0.04386	C	-1.92338	1.51393	-0.10097	
C	-2.33570	2.34252	1.13278	C	-2.16531	2.40233	1.16331	C	-2.39893	2.22838	1.15911	
C	-3.75116	2.88689	1.07012	C	-3.56338	2.99101	1.12585	C	-3.81751	2.76410	1.09451	
C	-4.17806	3.60898	-0.18070	C	-3.99101	3.72313	-0.11900	C	-4.19300	3.63117	-0.07849	
C	0.62108	3.73118	-1.13001	C	0.78849	3.66405	-1.18815	C	0.62198	3.80264	-0.94363	
C	6.27697	0.04095	1.97358	C	6.37340	-0.15761	1.88691	C	6.22601	-0.05351	2.05023	
C	-0.88025	-1.39283	1.31019	C	-0.88918	-1.35085	1.35643	C	-0.89938	-1.38929	1.20447	
C	-0.77426	-0.64137	-0.01725	C	-0.73582	-0.63852	0.01035	C	-0.77156	-0.62879	-0.12456	
C	-2.21766	-0.77108	-0.60285	C	-2.16541	-0.71922	-0.57997	C	-2.19885	-0.76980	-0.73598	
C	-2.87422	-1.96889	0.14026	C	-2.87349	-1.87491	0.16764	C	-2.87305	-1.94599	0.01261	
C	-3.10760	-3.22886	-0.69929	C	-2.99465	-3.17055	-0.62891	C	-2.97380	-3.28277	-0.73486	
C	-2.41159	-2.95945	2.42633	C	-2.53593	-2.77332	2.51625	C	-2.51940	-2.83567	2.35825	
H	-0.10425	1.29031	-2.00928	H	-0.02828	1.23408	-2.01528	H	-0.05803	1.42263	-2.00744	
H	3.18882	3.28327	-0.57234	H	3.34911	3.14440	-0.66089	H	3.18053	3.32931	-0.35345	
H	3.98902	0.91697	-1.37929	H	4.06279	0.74264	-1.44349	H	4.00821	1.01632	-1.29195	
H	5.07600	2.06615	0.50875	H	5.21368	1.88416	0.41176	H	5.05129	2.05223	0.68309	
H	3.90151	1.38076	1.62448	H	4.03569	1.25067	1.55408	H	3.85442	1.30186	1.73117	
H	5.86432	-0.17075	-0.11434	H	5.92336	-0.38391	-0.19168	H	5.85512	-0.14484	-0.05421	
H	5.01196	-2.20833	0.95278	H	5.02529	-2.37990	0.91483	H	4.98512	-2.24095	0.87847	
H	2.71979	-2.28052	-0.00430	H	2.71653	-2.39337	-0.00808	H	2.71279	-2.25889	-0.12956	
H	3.85739	-1.56187	-1.13009	H	3.85891	-1.72440	-1.15901	H	3.87465	-1.47923	-1.18822	
H	2.04213	-0.00194	0.75069	H	2.12318	-0.08593	0.72909	H	2.01370	-0.02853	0.73503	
H	-0.05609	1.12585	1.01778	H	0.07029	1.11168	1.01311	H	-0.09334	1.09494	1.00420	
H	-1.97337	2.09884	-0.98307	H	-1.83902	2.14839	-0.95654	H	-1.95776	2.19439	-0.95406	
H	-2.23256	1.76242	2.05084	H	-2.06461	1.82055	2.08060	H	-2.32307	1.56204	2.01939	
H	-1.66470	3.20560	1.19916	H	-1.46518	3.24320	1.21564	H	-1.73821	3.08503	1.33063	
H	-3.85443	-1.64979	0.50586	H	-3.87901	-1.54922	0.44787	H	-3.89497	-1.63955	0.52521	
H	3.87915	-1.27062	1.91298	H	3.93651	-1.39563	1.87928	H	3.83080	-1.35974	1.86603	
H	-3.29170	-4.07549	-0.03283	H	-2.02072	-3.47557	-1.01797	H	-3.64143	-3.93513	-0.16849	
H	-4.00574	-3.08224	-1.29924	H	-3.38308	-3.96308	0.01472	H	-3.44805	-3.09221	-1.70261	
H	-2.12157	-1.76595	-2.26199	H	-2.91107	-1.39830	-2.23740	H	-2.00303	-0.18787	-2.58432	
H	-1.19422	-3.47611	-1.19879	H	-3.94536	-3.67719	-2.28117	H	-1.05314	-3.39782	-1.19867	
H	2.33529	-1.28697	-2.83040	H	2.30445	-1.43740	-2.83398	H	1.03495	-0.14193	-3.45644	
H	0.95278	-0.35164	-3.40027	H	0.95445	-0.45388	-3.39809	H	2.53896	0.65526	-2.99709	
H	2.47128	0.46312	-3.02762	H	2.51068	0.30243	-3.05940	H	2.40564	-1.10374	-2.90471	
H	-4.31704	2.88821	-0.99144	H	-3.21091	4.40964	-0.45522	H	-3.41952	4.37622	-0.27683	
H	-3.41012	4.31384	-0.50653	H	-4.91537	4.26759	0.06661	H	-5.14688	4.12126	0.10926	
H	-5.11789	4.13082	-0.00829	H	-4.15789	3.00617	-0.92770	H	-4.28369	3.01452	-0.97721	
H	-0.17780	3.88530	-0.39955	H	0.00292	3.85237	-0.45120	H	1.31024	4.63344	-0.78132	
H	1.31868	4.56546	-1.04225	H	1.51201	4.47791	-1.11997	H	0.17795	3.91377	-1.93818	
H	0.15415	3.77626	-2.11923	H	0.31149	3.71007	-2.17255	H	-0.19502	3.89900	-0.22290	
H	6.93477	0.90637	1.85577	H	7.05565	0.68549	1.74802	H	6.88422	0.81790	1.99585	
H	6.90750	-0.84985	2.04030	H	6.97727	-1.06651	1.95654	H	6.85688	-0.94613	2.07799	
H	5.75212	0.14905	2.92770	H	5.86642	-0.02101	2.84704	H	5.68203	-0.00125	2.99832	
H	-3.36026	-2.58115	2.81575	H	-2.55954	-3.84673	2.31905	H	-1.92225	-2.57311	3.22836	
H	-2.53839	-4.00701	2.15031	H	-1.86572	-2.58282	3.35100	H	-3.57080	-2.63162	2.56631	
H	-1.65109	-2.88709	3.19956	H	-3.54287	-2.44122	2.77757	H	-2.39987	-3.90265	2.15621	
N	-1.98783	-2.16944	1.28526	N	-2.05754	-2.03446	1.36267	N	-2.08356	-2.03408	1.23243	
O	0.43244	-2.39593	-1.17116	O	0.40575	-2.45875	-1.11371	O	0.42660	-2.29217	-1.41920	
O	-2.84447	0.40350	-0.17810	O	-2.76413	0.48513	-0.14577	O	-2.84567	0.42447	-0.36307	
O	-4.50172	2.76341	2.01893	O	-4.30001	2.89372	2.08873	O	-4.61178	2.51776	1.98162	
O	-0.07500	-1.31239	2.22687	O	-0.07842	-1.30531	2.27070	O	-0.06135	-1.37474	2.09576	
O	-2.29994	-0.84149	-2.00105	O	-2.16825	-0.82600	-1.97178	O	-2.28232	-0.98935	-2.11672	
O	-2.06549	-3.53692	-1.62906	O	-3.91627	-2.90553	-1.70047	O	-1.75552	-3.98990	-0.87465	
<b>Conformer 10</b>												
Relative energy (kcal/mol)			2.05									
Population (%)			1.2									
Calcd. [α] <sub>p</sub>			-140.5									
C	0.38068	-1.34104	-0.80083									
C	1.37588	-0.28871	-1.27685									
C	0.56395	1.03100	-1.18390									

## APPENDIX

C	1.41015	2.28011	-1.08607
C	2.71397	2.21764	-0.80838
C	3.47835	0.95400	-0.54624
C	4.50676	1.11947	0.58529
C	5.34438	-0.14739	0.79778
C	4.43148	-1.36214	1.00680
C	3.38408	-1.51592	-0.10176
C	2.55327	-0.23511	-0.24299
C	1.84450	-0.59799	-2.70059
C	-0.44310	0.82974	-0.00706
C	-1.82520	1.49747	-0.17543
C	-2.24553	2.39134	0.97507
C	-3.53455	3.16170	0.74606
C	-4.25403	3.62373	1.98322
C	0.72546	3.59054	-1.36192
C	6.33629	0.01878	1.94752
C	-0.89815	-1.30730	1.39884
C	-0.74083	-0.67707	0.01141
C	-2.16569	-0.80464	-0.57634
C	-2.85428	-1.94084	0.21323
C	-2.86829	-3.30386	-0.48972
C	-2.55569	-2.64682	2.63695
H	-0.03171	1.10983	-2.10036
H	3.28966	3.14044	-0.78708
H	4.05280	0.71586	-1.45309
H	5.16404	1.96456	0.35652
H	3.98226	1.37014	1.51566
H	5.91783	-0.31882	-0.12256
H	5.03693	-2.27148	1.07118
H	2.74178	-2.36973	0.12119
H	3.88808	-1.73887	-1.04720
H	2.10132	-0.03872	0.73616
H	0.02138	1.13365	0.93036
H	-1.87607	2.05541	-1.11088
H	-2.31332	1.81709	1.90191
H	-1.47133	3.14952	1.14151
H	-3.88482	-1.65146	0.43541
H	3.91994	-1.25864	1.97165
H	-1.85744	-3.56672	-0.81367
H	-3.20186	-4.05923	0.22237
H	-2.83653	-0.41480	-2.35133
H	-3.43412	-2.75082	-2.25281
H	2.53187	0.16729	-3.06233
H	2.34904	-1.56231	-2.75352
H	0.99164	-0.62894	-3.38177
H	-3.55417	4.07882	2.68832
H	-4.68745	2.75249	2.48446
H	-5.04624	4.32658	1.73061
H	-0.06756	3.79600	-0.63738
H	1.43418	4.41925	-1.32457
H	0.25325	3.58646	-2.34965
H	6.95410	-0.87504	2.06993
H	5.81437	0.19412	2.89326
H	7.00630	0.86555	1.77531
H	-2.51597	-3.73270	2.53036
H	-1.93213	-2.35354	3.47822
H	-3.58823	-2.35069	2.83130
N	-2.07184	-1.97695	1.44454
O	0.44701	-2.52764	-1.01545
O	-2.78733	0.40455	-0.25755
O	-3.94482	3.41158	-0.37007
O	-0.08968	-1.20399	2.31113
O	-2.16626	-1.01045	-1.98308
O	-3.78795	-3.34180	-1.57421

**Table S2.** Cartesian coordinates, energies, and population at 298 K of significantly populated conformers of compound 5'-*epi*-1. Conformers were optimized at the B3LYP/TZVP/SMD(ACN) level.

Conformer 1			Conformer 2			Conformer 3					
Relative energy (kcal/mol)	0.00		Relative energy (kcal/mol)	0.05		Relative energy (kcal/mol)	0.32				
Population (%)	22.7		Population (%)	22.0		Population (%)	13.1				
C	-0.57638	-1.28034	1.10568	C	-0.57215	-1.20718	1.13624	C	-0.56244	-1.10536	1.25696
C	-1.54097	-0.12372	1.34556	C	-1.54821	-0.05054	1.32877	C	-1.54621	0.04987	1.36668
C	-0.65721	1.12854	1.09419	C	-0.68628	1.20025	1.00447	C	-0.67292	1.27833	0.98842



C	-1.43090	2.38102	0.75084	C	-1.47824	2.41699	0.58184	C	-1.45753	2.47382	0.49787
C	-2.71846	2.33053	0.40342	C	-2.77033	2.33067	0.25950	C	-2.74208	2.37014	0.15099
C	-3.53159	1.07468	0.29540	C	-3.57068	1.06246	0.24594	C	-3.54213	1.10135	0.18235
C	-4.48502	1.09868	-0.91118	C	-4.54886	1.00609	-0.93969	C	-4.49178	0.97930	-1.02112
C	-5.37641	-0.14774	-0.97001	C	-5.42314	-0.25318	-0.91122	C	-5.36565	-0.27863	-0.94331
C	-4.52026	-1.41948	-0.92411	C	-4.54650	-1.50787	-0.81545	C	-4.49142	-1.52569	-0.76053
C	-3.54429	-1.43624	0.25808	C	-3.54892	-1.44702	0.34661	C	-3.51938	-1.40074	0.41803
C	-2.65547	-0.18708	0.24454	C	-2.67800	-0.18857	0.25006	C	-2.64992	-0.14627	0.27242
C	-2.10257	-0.17825	2.76813	C	-2.08945	-0.03924	2.76078	C	-2.11443	0.14215	2.78429
C	0.40101	0.69782	0.02779	C	0.38326	0.72861	-0.03196	C	0.40022	0.75082	-0.01803
C	1.80684	1.32449	0.17331	C	1.77842	1.38115	0.08765	C	1.81042	1.36680	0.10596
C	2.32058	2.02183	-1.07118	C	2.32417	1.92616	-1.23604	C	2.37901	1.87956	-1.22155
C	3.61355	2.79724	-0.88957	C	3.74167	2.44193	-1.08556	C	3.80671	2.36395	-1.06809
C	4.34710	3.15388	-2.15353	C	3.91632	3.90208	-0.78576	C	4.01502	3.82353	-0.79104
C	-0.69680	3.68859	0.86906	C	-0.75465	3.73590	0.58167	C	-0.73227	3.79074	0.45725
C	-6.29369	-0.12770	-2.19143	C	-6.36653	-0.31248	-2.11122	C	-6.28265	-0.40449	-2.15850
C	0.82057	-1.68712	-0.95854	C	0.84782	-1.69549	-0.89116	C	0.73218	-1.70156	-0.83447
C	0.62115	-0.79887	0.27383	C	0.62722	-0.74986	0.29200	C	0.60183	-0.72627	0.33842
C	1.98632	-0.89175	0.98008	C	1.98288	-0.78571	1.02502	C	1.98914	-0.80979	1.03237
C	2.62397	-2.20902	0.48507	C	2.69150	-2.07511	0.55019	C	2.64526	-2.10940	0.50691
C	4.14963	-2.20656	0.36214	C	4.21317	-1.97486	0.35926	C	4.15529	-2.02481	0.23061
C	2.31487	-3.50492	-1.68359	C	2.38812	-3.50528	-1.52865	C	2.19936	-3.54601	-1.53757
H	-0.10773	1.32678	2.02098	H	-0.14501	1.46451	1.91985	H	-0.13797	1.58497	1.89441
H	-3.24399	3.26172	0.20303	H	-3.30701	3.24074	0.00037	H	-3.27375	3.26621	-0.16168
H	-4.16859	1.01145	1.18948	H	-4.18798	1.04382	1.15565	H	-4.18103	1.12938	1.07685
H	-5.10766	1.99786	-0.86328	H	-5.18281	1.89854	-0.92843	H	-5.12684	1.86952	-1.07300
H	-3.89698	1.17052	-1.83452	H	-3.98073	1.03410	-1.87774	H	-3.90219	0.95725	-1.94594
H	-6.00785	-0.14118	-0.07193	H	-6.03520	-0.20675	-0.00099	H	-5.99732	-0.18362	-0.05044
H	-5.16934	-2.29942	-0.87954	H	-5.18050	-2.39372	-0.71114	H	-5.12795	-2.40502	-0.62222
H	-2.93732	-2.34236	0.21580	H	-2.92987	-2.34565	0.34231	H	-2.89759	-2.29674	0.47300
H	-4.11048	-1.47956	1.19357	H	-4.09771	-1.44703	1.29339	H	-4.08784	-1.35380	1.35188
H	-2.14064	-0.17196	-0.72320	H	-2.17767	-0.21928	-0.72518	H	-2.12708	-0.23006	-0.68714
H	0.00574	0.86388	-0.97375	H	-0.00782	0.83976	-1.04259	H	0.02849	0.85171	-1.03674
H	1.83953	2.00974	1.02054	H	1.77314	2.17333	0.83871	H	1.81934	2.16994	0.84555
H	2.42883	1.31126	-1.89486	H	2.31812	1.12830	-1.98051	H	2.35910	1.07113	-1.95439
H	1.57662	2.75436	-1.40476	H	1.66522	2.72931	-1.56897	H	1.74167	2.69296	-1.57121
H	2.36840	-2.99185	1.20732	H	2.52053	-2.84922	1.30617	H	2.51543	-2.89078	1.26536
H	-3.95222	-1.49768	-1.85927	H	-3.99535	-1.62471	-1.75632	H	-3.91983	-1.69539	-1.68116
H	4.56408	-1.94504	1.34478	H	4.64127	-1.55518	1.27834	H	4.63310	-1.60114	1.12102
H	4.48990	-3.21747	0.13481	H	4.60967	-2.98699	0.26254	H	4.53552	-3.04182	0.11878
H	2.74024	-0.81258	2.76862	H	2.69281	-0.69453	2.83144	H	1.57539	-1.55653	2.79331
H	4.26461	-0.49320	-0.51859	H	4.42150	-0.33169	-0.71330	H	4.40899	-0.37626	-0.83184
H	-2.65535	-1.10090	2.94286	H	-2.76444	0.80259	2.91812	H	-2.66944	-0.75642	3.05186
H	-1.29162	-0.13086	3.49775	H	-2.62944	-0.95748	2.98985	H	-1.30614	0.26398	3.50841
H	-2.77118	0.66176	2.95853	H	-1.26912	0.05362	3.47531	H	-2.78204	0.99842	2.88377
H	4.78094	2.24377	-2.57955	H	3.27465	4.19750	0.04852	H	5.05779	4.03194	-0.55877
H	5.14120	3.87031	-1.94972	H	3.59035	4.48367	-1.65378	H	3.37166	4.14893	0.03068
H	3.65748	3.55553	-2.89979	H	4.95618	4.13229	-0.56101	H	3.71276	4.39759	-1.67260
H	-1.35569	4.53006	0.64932	H	-0.30835	3.94063	1.56007	H	-0.32534	4.04550	1.44118
H	-0.29465	3.82174	1.87867	H	0.06243	3.75134	-0.14555	H	0.11433	3.76635	-0.23496
H	0.15465	3.74275	0.18500	H	-1.43280	4.55477	0.33670	H	-1.39755	4.59631	0.14278
H	-6.92536	0.76479	-2.19973	H	-7.01223	0.56894	-2.15330	H	-6.92764	0.47233	-2.26215
H	-6.95125	-1.00117	-2.20749	H	-7.01044	-1.19502	-2.06570	H	-6.92701	-1.28429	-2.07907
H	-5.71205	-0.13248	-3.11840	H	-5.80492	-0.35885	-3.04929	H	-5.70089	-0.50067	-3.08037
H	2.36816	-4.45790	-1.15177	H	2.49971	-4.41944	-0.94076	H	1.39154	-3.69623	-2.24958
H	1.56806	-3.57769	-2.47051	H	1.62521	-3.66082	-2.28763	H	3.12251	-3.34020	-2.80092
H	3.28707	-3.29505	-2.13204	H	3.33746	-3.27894	-2.01582	H	2.33071	-4.45582	-0.94705
N	1.92300	-2.44601	-0.77523	N	1.97067	-2.41203	-0.67403	N	1.85078	-2.43778	-0.67088
O	-0.71023	-2.41586	1.49357	O	-0.70175	-2.32840	1.56397	O	-0.63132	-2.16538	1.83686
O	2.70371	0.21430	0.46908	O	2.67565	0.34132	0.54471	O	2.68100	0.31613	0.58776
O	4.01892	3.12915	0.20672	O	4.69406	1.68978	-1.19643	O	4.74199	1.58729	-1.15949
O	0.07534	-1.71141	-1.92869	O	0.09731	-1.79464	-1.85329	O	-0.07095	-1.79799	-1.75362
O	1.85503	-0.81134	2.37267	O	1.81606	-0.71736	2.41829	O	1.97642	-0.74706	2.44358
O	4.66350	-1.36471	-0.65783	O	4.64377	-1.27383	-0.78985	O	4.52284	-1.33466	-0.94676
<b>Conformer 4</b>				<b>Conformer 5</b>				<b>Conformer 6</b>			
Relative energy (kcal/mol)			0.36	Relative energy (kcal/mol)			0.58	Relative energy (kcal/mol)			0.59
Population (%)			12.4	Population (%)			8.5	Population (%)			8.4
C	-0.57953	-1.23719	1.07885	C	-0.58549	-1.28230	1.08274	C	-0.56595	-1.15379	1.25033
C	-1.55622	-0.08567	1.30800	C	-1.55312	-0.12902	1.33582	C	-1.53098	0.01320	1.38559
C	-0.69838	1.17567	1.01220	C	-0.67439	1.12940	1.09490	C	-0.63038	1.23564	1.05151
C	-1.49018	2.39775	0.60428	C	-1.44764	2.37907	0.73972	C	-1.39429	2.46452	0.61291
C	-2.78519	2.31799	0.29259	C	-2.78598	2.32671	0.39591	C	-2.67654	2.39451	0.24887
C	-3.58795	1.05172	0.26869	C	-3.54938	1.07042	0.29617	C	-3.49506	1.13761	0.21648
C	-4.58150	1.02021	-0.90517	C	-4.51016	1.09482	-0.90476	C	-4.42828	1.07451	-1.00428
C	-5.45437	-0.24008	-0.89417	C	-5.39759	-0.15430	-0.96401	C	-5.32369	-0.17064	-0.98290
C	-4.57501	-1.49506	-0.83921	C	-4.53647	-1.42281	-0.92831	C	-4.47409	-1.43877	-0.82966

APPENDIX

C	-3.56425	-1.45996	0.31239	C	-3.55573	-1.44099	0.24965	C	-3.51606	-1.37074	0.36517
C	-2.69526	-0.19869	0.23625	C	-2.67063	-0.18905	0.23788	C	-2.62468	-0.12686	0.27300
C	-2.08469	-0.11313	2.74505	C	-2.10959	-0.19792	2.76003	C	-2.11288	0.07365	2.79882
C	0.38158	0.72821	-0.02458	C	0.39706	0.70679	0.03857	C	0.43297	0.72007	0.02640
C	1.77032	1.38242	0.11560	C	1.79768	1.33621	0.19483	C	1.86053	1.29320	0.17890
C	2.37230	1.83062	-1.22209	C	2.34490	1.96565	-1.07180	C	2.40784	1.97935	-1.05730
C	3.75892	2.41458	-1.04446	C	3.64084	2.73861	-0.89927	C	3.71642	2.72389	-0.85587
C	3.87036	3.90586	-0.92799	C	4.41777	3.00674	-2.15880	C	4.48542	3.04831	-2.10718
C	-0.76181	3.71404	0.60140	C	-0.70864	3.68597	0.83296	C	-0.65694	3.77465	0.65797
C	-6.41335	-0.27266	-2.08281	C	-6.32130	-0.13241	-2.18055	C	-6.22305	-0.23939	-2.21579
C	0.88319	-1.65951	-0.93261	C	0.83820	-1.64998	-0.97258	C	0.67457	-1.70805	-0.88936
C	0.63127	-0.75115	0.27295	C	0.62025	-0.78788	0.27534	C	0.59169	-0.77584	0.32473
C	1.97680	-0.80752	1.05336	C	1.98287	-0.90136	1.01202	C	1.99140	-0.93024	0.97538
C	2.71279	-2.05394	0.51927	C	2.63104	-2.19131	0.47383	C	2.54810	-2.27250	0.44728
C	4.23443	-1.90774	0.35705	C	4.15785	-2.16110	0.37501	C	4.06207	-2.31069	0.22490
C	2.46749	-3.41585	-1.60749	C	2.36389	-3.42606	-1.73186	C	2.05392	-3.59142	-1.66900
H	-0.16867	1.43226	1.93838	H	-0.14010	1.33766	2.03033	H	-0.08820	1.49584	1.96744
H	-3.32047	3.23207	0.04506	H	-3.25964	3.25665	0.18533	H	-3.19461	3.31187	-0.02216
H	-4.19268	1.01612	1.18623	H	-4.17993	1.00568	1.19460	H	-4.14755	1.14261	1.10168
H	-5.21560	1.91175	-0.86601	H	-5.13536	1.99179	-0.85009	H	-5.04816	1.97637	-1.03393
H	-4.02535	1.06961	-1.84952	H	-3.92747	1.17206	-1.83106	H	-3.82538	1.07492	-1.92074
H	-6.05445	-0.21560	0.02487	H	-6.02425	-0.15405	-0.06258	H	-5.96806	-0.09505	-0.09728
H	-5.20619	-2.38441	-0.74846	H	-5.18178	-2.30557	-0.88488	H	-5.12811	-2.31040	-0.72965
H	-2.94442	-2.35730	0.28059	H	-2.94618	-2.34494	0.20181	H	-2.90981	-2.27871	0.39690
H	-4.10272	-1.48268	1.26478	H	-4.11832	-1.48955	1.18703	H	-4.09579	-1.34637	1.29293
H	-2.20342	-0.20612	-0.74392	H	-2.15858	-0.16830	-0.73137	H	-2.09187	-0.18701	-0.68253
H	-0.00439	0.85903	-1.03471	H	0.00827	0.87848	-0.96439	H	0.06749	0.86671	-0.98916
H	1.73701	2.23251	0.79895	H	1.81027	2.06991	1.00121	H	1.91657	1.96934	1.03261
H	2.43185	0.97435	-1.89601	H	2.46257	1.21522	-1.85783	H	2.51050	1.26603	-1.87935
H	1.70508	2.57654	-1.65597	H	1.61421	2.68834	-1.45359	H	1.68781	2.72970	-1.40210
H	2.55167	-2.86191	1.24072	H	2.37858	-2.99970	1.16828	H	2.32647	-3.04913	1.18914
H	-4.03489	-1.59110	-1.78914	H	-3.97226	-1.49440	-1.86632	H	-3.89270	-1.58814	-1.74765
H	4.63069	-1.48529	1.28702	H	4.54712	-1.92617	1.37261	H	4.54070	-2.04573	1.17517
H	4.65907	-2.90828	0.25605	H	4.51830	-3.15685	0.11468	H	4.36259	-3.33141	-0.01385
H	1.68912	-0.06899	2.82938	H	1.77257	-0.10926	2.77928	H	1.59566	-1.60710	2.76652
H	4.51278	-0.22883	-0.66132	H	4.28712	-0.40604	-0.41726	H	4.19052	-0.60162	-0.66159
H	-2.62703	-1.03493	2.95289	H	-2.77692	0.64060	2.96141	H	-2.68843	-0.82145	3.03288
H	-1.25720	-0.04529	3.45457	H	-2.66178	-1.12210	2.92783	H	-1.31029	0.15696	3.53466
H	-2.75349	0.72748	2.93274	H	-1.29558	-0.15833	3.48704	H	-2.76458	0.93954	2.91775
H	4.88644	4.20305	-0.67509	H	4.85789	2.06757	-2.50855	H	5.29207	3.74774	-1.89390
H	3.16898	4.28035	-0.17772	H	5.21058	3.73038	-1.97680	H	3.82197	3.45777	-2.87270
H	3.58037	4.35862	-1.88134	H	3.75629	3.36144	-2.95280	H	4.90608	2.12314	-2.51355
H	-1.44254	4.53693	0.37829	H	-0.29139	3.83110	1.83470	H	-0.27001	3.97045	1.66332
H	-0.29287	3.90926	1.57104	H	0.13258	3.72942	0.13494	H	0.20541	3.78180	-0.01444
H	0.03826	3.73295	-0.14467	H	-1.36881	4.52607	0.61210	H	-1.30853	4.60263	0.37459
H	-5.86391	-0.29703	-3.02890	H	-6.95635	0.75770	-2.18192	H	-5.62815	-0.31367	-3.13127
H	-7.06015	0.60885	-2.09632	H	-6.97563	-1.00830	-2.19680	H	-6.85184	0.65126	-2.29911
H	-7.05596	-1.15668	-2.04914	H	-5.74445	-0.13126	-3.11051	H	-6.88295	-1.11035	-2.17692
H	3.42171	-3.15869	-2.06900	H	3.34048	-3.19546	-2.15999	H	1.25053	-3.65935	-2.39835
H	2.58383	-4.34672	-1.04717	H	2.41870	-4.39296	-1.22588	H	2.99634	-3.41786	-2.19051
H	1.72087	-3.55865	-2.38487	H	1.62920	-3.48336	-2.53125	H	2.12072	-4.53406	-1.12079
N	2.01806	-2.35774	-0.72558	N	1.94997	-2.39622	-0.80030	N	1.75763	-2.50392	-0.75758
O	-0.71578	-2.37293	1.46475	O	-0.72218	-2.42333	1.45357	O	-0.63855	-2.21923	1.82046
O	2.63843	0.39028	0.71510	O	2.68825	0.24864	0.58740	O	2.71986	0.15079	0.46521
O	4.74010	1.69258	-0.98952	O	4.01500	3.13532	0.18652	O	4.10605	3.05774	0.24540
O	0.14592	-1.74381	-1.90673	O	0.10028	-1.66130	-1.94872	O	-0.12812	-1.72497	-1.81266
O	1.90509	-0.93459	2.45163	O	1.95857	-0.98615	2.41158	O	2.03576	-0.83510	2.38045
O	4.66021	-1.18338	-0.77866	O	4.67293	-1.27360	-0.60634	O	4.52597	-1.49235	-0.83793
<b>Conformer 7</b>				<b>Conformer 8</b>				<b>Conformer 9</b>			
Relative energy (kcal/mol)		1.04		Relative energy (kcal/mol)		1.06		Relative energy (kcal/mol)		1.12	
Population (%)		3.9		Population (%)		3.8		Population (%)		3.4	
C	0.53511	-1.31115	-1.01725	C	0.50115	-1.32546	-0.97172	C	0.50291	-1.32818	-0.96691
C	1.49303	-0.16839	-1.33745	C	1.47704	-0.20983	-1.33187	C	1.47711	-0.21184	-1.32970
C	0.62477	1.09597	-1.09413	C	0.63532	1.07771	-1.11286	C	0.63399	1.07509	-1.11237
C	1.41654	2.35561	-0.82661	C	1.45492	2.32759	-0.88688	C	1.45204	2.32631	-0.88826
C	2.71679	2.31048	-0.52912	C	2.75669	2.26444	-0.59923	C	2.75412	2.26527	-0.60161
C	3.52880	1.05488	-0.40969	C	3.54465	0.99645	-0.45224	C	3.54390	0.99853	-0.45369
C	4.52975	1.11539	0.75624	C	4.55525	1.06720	0.70481	C	4.55565	1.07236	0.70217
C	5.41765	-0.13312	0.82266	C	5.41869	-0.19674	0.79791	C	5.42077	-0.19034	0.79640
C	4.55485	-1.40073	0.85591	C	4.53126	-1.44563	0.86981	C	4.53492	-1.44017	0.87127
C	3.53213	-1.45333	-0.28497	C	3.49934	-1.50721	-0.26223	C	3.50199	-1.50488	-0.25965
C	2.64985	-0.19947	-0.28041	C	2.64203	-0.23627	-0.28387	C	2.64301	-0.23509	-0.28260
C	1.99677	-0.27515	-2.77848	C	1.96585	-0.36326	-2.77366	C	1.96508	-0.36725	-2.77158
C	-0.39066	0.70897	0.02923	C	-0.37412	0.73813	0.03052	C	-0.37499	0.73600	0.03155
C	-1.80188	1.33204	-0.08739	C	-1.77984	1.37562	-0.08245	C	-1.78129	1.37220	-0.08180
C	-2.26669	2.08208	1.14593	C	-2.21193	2.18348	1.12619	C	-2.21396	2.17888	1.12743

C	-3.57127	2.84115	0.98337	C	-3.50580	2.95876	0.95048	C	-3.50840	2.95325	0.95335
C	-4.27346	3.22006	2.25881	C	-4.21568	3.34863	2.21829	C	-4.21361	3.34798	2.22237
C	0.68357	3.66234	-0.95971	C	0.74708	3.64486	-1.04903	C	0.74221	3.64248	-1.05084
C	6.38381	-0.07565	2.00454	C	6.39418	-0.12814	1.97150	C	6.39747	-0.11860	1.96879
C	-0.76309	-1.63954	1.11920	C	-0.79658	-1.55893	1.19033	C	-0.80076	-1.55984	1.19258
C	-0.62343	-0.79520	-0.15157	C	-0.63633	-0.76479	-0.11206	C	-0.63643	-0.76696	-0.11034
C	-2.02128	-0.91066	-0.78946	C	-2.04526	-0.86560	-0.73296	C	-2.04381	-0.86858	-0.73499
C	-2.65187	-2.19045	-0.19941	C	-2.65998	-2.14710	-0.13428	C	-2.65541	-2.15187	-0.13781
C	-4.15728	-2.06953	0.05701	C	-4.17843	-2.09149	0.00332	C	-4.16941	-2.10749	-0.00958
C	-2.20971	-3.44307	1.97217	C	-2.29859	-3.27473	2.12328	C	-2.30598	-3.27414	2.12401
H	0.03844	1.26453	-2.00435	H	0.04208	1.23396	-2.02071	H	0.04046	1.22937	-2.02038
H	3.25331	3.24541	-0.38234	H	3.31307	3.19198	-0.48256	H	3.30930	3.19372	-0.48638
H	4.12906	0.95700	-1.32578	H	4.13596	0.86235	-1.36959	H	4.13439	0.86383	-1.37147
H	5.15370	2.00889	0.65212	H	5.19613	1.94494	0.57307	H	5.19528	1.95070	0.56833
H	3.97961	1.22243	1.69930	H	4.01432	1.20979	1.64851	H	4.01556	1.21579	1.64621
H	6.01202	-0.16136	-0.09994	H	6.00578	-0.26072	-0.12755	H	6.00692	-0.25513	-0.12959
H	5.19777	-2.28544	0.81647	H	5.15627	-2.34372	0.84904	H	5.16099	-2.33754	0.85138
H	2.92326	-2.35374	-0.18637	H	2.87346	-2.39236	-0.13590	H	2.87738	-2.39062	-0.13136
H	4.06007	-1.53300	-1.24024	H	4.01828	-1.62204	-1.21887	H	4.02017	-1.62055	-1.21660
H	2.17350	-0.14775	0.70554	H	2.17490	-0.14942	0.70406	H	2.17659	-0.14718	0.70561
H	0.04364	0.91348	1.00722	H	0.07527	0.95798	0.99836	H	0.07452	0.95686	0.99911
H	-1.86373	1.98404	-0.95952	H	-1.85002	1.99205	-0.97995	H	-1.85116	1.98964	-0.97869
H	-2.33801	1.40608	2.00177	H	-2.28036	1.54375	2.00932	H	-2.28169	1.53855	2.01024
H	-1.51579	2.83332	1.41682	H	-1.44579	2.93361	1.35412	H	-1.44828	2.92931	1.35596
H	-2.47706	-3.01254	-0.90027	H	-2.40769	-2.98310	-0.79635	H	-2.39794	-2.98567	-0.79969
H	4.02445	-1.44285	1.81519	H	4.00710	-1.45234	1.83343	H	4.01172	-1.44592	1.83542
H	-4.57520	-3.05281	0.27303	H	-4.55621	-3.00917	0.45847	H	-4.54035	-3.03345	0.43877
H	-4.34452	-1.41989	0.91399	H	-4.47692	-1.24741	0.62266	H	-4.47969	-1.26443	0.61035
H	-2.84565	-1.11596	-2.53074	H	-2.94171	-1.00234	-2.42454	H	-2.93550	-1.04364	-2.42361
H	-4.76282	-0.61865	-1.09288	H	-4.85694	-2.75293	-1.71821	H	-5.59678	-1.73742	-1.31219
H	1.15721	-0.25074	-3.47622	H	1.12074	-0.34107	-3.46477	H	2.49011	-1.31139	-2.91458
H	2.65918	0.55508	-3.02537	H	2.64153	0.44752	-3.04785	H	1.11951	-0.34690	-3.46217
H	2.54014	-1.20537	-2.94239	H	2.49030	-1.30754	-2.91791	H	2.63998	0.44355	-3.04761
H	-3.56678	3.64030	2.97840	H	-5.01207	4.06192	2.01218	H	-5.00966	4.06176	2.01665
H	-4.69051	2.31640	2.71433	H	-3.51091	3.76676	2.94117	H	-3.50609	3.76719	2.94189
H	-5.07694	3.92793	2.06182	H	-4.64239	2.45007	2.67493	H	-4.64026	2.5141	2.68299
H	-0.13676	3.74577	-0.24140	H	-0.06256	3.76541	-0.32394	H	1.43166	4.47868	-0.92432
H	1.35519	4.50715	-0.79920	H	1.43739	4.48004	-0.92049	H	0.28519	3.72120	-2.04261
H	0.23825	3.76201	-1.95493	H	0.29174	3.72526	-2.04146	H	-0.06641	3.76278	-0.32454
H	7.01912	0.81295	1.95603	H	7.03002	-1.01685	2.01058	H	7.03443	-1.00646	2.00864
H	7.03771	-0.95178	2.02474	H	5.85807	-0.06094	2.92316	H	5.86235	-0.05044	2.92094
H	5.84013	-0.04472	2.95377	H	7.04734	0.74543	1.89527	H	7.04949	0.75563	1.89036
H	-2.33479	-4.39657	1.45397	H	-3.24110	-3.02015	2.61099	H	-2.39265	-4.26160	1.66423
H	-1.39579	-3.52894	2.68813	H	-2.39662	-4.25922	1.65934	H	-1.52697	-3.30044	2.88218
H	-3.13069	-3.21181	2.51069	H	-1.51217	-3.31050	2.87340	H	-3.25510	-3.02314	2.60064
N	-1.87636	-2.40096	1.01944	N	-1.93725	-2.28472	1.12679	N	-1.94127	-2.28615	1.12686
O	0.64922	-2.46007	-1.37024	O	0.58918	-2.48536	-1.29783	O	0.59359	-2.48895	-1.28912
O	-2.70914	0.21724	-0.29672	O	-2.70514	0.26676	-0.22292	O	-2.70544	0.26301	-0.22423
O	-4.01004	3.14639	-0.10796	O	-3.92830	3.27023	-0.14542	O	-3.93543	3.26026	-0.14208
O	0.02936	-1.63765	2.05092	O	-0.00303	-1.54138	2.12079	O	-0.01030	-1.54110	2.12550
O	-1.96120	-0.91311	-2.19031	O	-2.02527	-0.86734	-2.13475	O	-2.02426	-0.87219	-2.13592
O	-4.82857	-1.58321	-1.10744	O	-4.76506	-1.89216	-1.28930	O	-4.66131	-1.97152	-1.34933
<b>Conformer 10</b>				<b>Conformer 11</b>							
Relative energy (kcal/mol)			1.62	Relative energy (kcal/mol)			1.68				
Population (%)			1.5	Population (%)			1.3				
C	-0.49020	-1.26136	1.00801	C	-0.49127	-1.25839	1.01136				
C	-1.47724	-0.14140	1.32118	C	-1.47671	-0.13624	1.32180				
C	-0.65503	1.14435	1.02912	C	-0.65297	1.14775	1.02611				
C	-1.49288	2.37088	0.74874	C	-1.48956	2.37435	0.74218				
C	-2.79752	2.27760	0.48387	C	-2.79425	2.28173	0.47729				
C	-3.57105	0.99448	0.41278	C	-3.56924	0.99929	0.40985				
C	-4.60093	0.99673	-0.72939	C	-4.59894	0.99920	-0.73252				
C	-5.44867	-0.28081	-0.74696	C	-5.44808	-0.27747	-0.74637				
C	-4.54533	-1.51977	-0.77593	C	-4.54614	-1.51753	-0.77128				
C	-3.49514	-1.51526	0.34090	C	-3.49618	-1.51069	0.34573				
C	-2.65486	-0.23365	0.29044	C	-2.65445	-0.23020	0.29137				
C	-1.94826	-0.22844	2.77463	C	-1.94767	-0.21867	2.77552				
C	0.34760	0.75945	-0.10541	C	0.34943	0.75852	-0.10719				
C	1.74276	1.42555	-0.04744	C	1.74612	1.42179	-0.05057				
C	2.15915	2.12770	-1.33401	C	2.16357	2.12265	-1.33760				
C	3.56921	2.68884	-1.32934	C	3.57469	2.68094	-1.33179				
C	3.97827	3.56413	-0.17377	C	3.98206	3.56067	-0.17891				
C	-0.79865	3.70264	0.83062	C	-0.79400	3.70560	0.82072				
C	-6.44524	-0.28044	-1.90479	C	-6.44434	-0.27967	-1.90446				
C	0.82504	-1.59039	-1.13420	C	0.82258	-1.59346	-1.13109				
C	0.63955	-0.72762	0.12050	C	0.63895	-0.72827	0.12248				

## APPENDIX

C	2.04498	-0.76556	0.75608	C	2.04479	-0.76780	0.75767
C	2.68925	-2.06578	0.23393	C	2.68175	-2.07228	0.23781
C	4.20770	-1.98752	0.10617	C	4.19554	-2.00940	0.11445
C	2.37133	-3.32036	-1.96288	C	2.36562	-3.32711	-1.95876
H	-0.05578	1.35395	1.92220	H	-0.05368	1.35931	1.91873
H	-3.36686	3.19122	0.32706	H	-3.36254	3.19554	0.31778
H	-4.14606	0.89846	1.34513	H	-4.14453	0.90674	1.34239
H	-5.25096	1.87188	-0.62911	H	-5.24803	1.87536	-0.63505
H	-4.07732	1.10030	-1.68779	H	-4.07502	1.09926	-1.69113
H	-6.01867	-0.30841	0.19090	H	-6.01836	-0.30156	0.19142
H	-5.15719	-2.42417	-0.70332	H	-5.15902	-2.42102	-0.69594
H	-2.85905	-2.39696	0.24546	H	-2.86110	-2.39342	0.25325
H	-3.99778	-1.59248	1.30990	H	-3.99911	-1.58426	1.31487
H	-2.20215	-0.18780	-0.70697	H	-2.20165	-0.18794	-0.70617
H	-0.11504	0.91706	-1.07900	H	-0.11263	0.91456	-1.08132
H	1.79674	2.11748	0.79533	H	1.80166	2.11418	0.79183
H	2.06423	1.44741	-2.18138	H	2.06806	1.44179	-2.18444
H	1.47901	2.97080	-1.49622	H	1.48488	2.96671	-1.50060
H	2.44692	-2.86821	0.93986	H	2.43488	-2.87035	0.94615
H	-4.03652	-1.56424	-1.74672	H	-4.03719	-1.56565	-1.74183
H	4.60800	-2.92324	-0.28835	H	4.58441	-2.95460	-0.27424
H	4.49570	-1.17696	-0.56106	H	4.49587	-1.20076	-0.55433
H	2.93081	-0.80194	2.45769	H	2.93122	-0.83913	2.45673
H	4.89610	-2.53128	1.86514	H	5.61207	-1.55332	1.40181
H	-1.09603	-0.16479	3.45425	H	-2.62718	0.59981	3.01503
H	-2.62867	0.58861	3.01638	H	-2.46240	-1.15831	2.97444
H	-2.46200	-1.16919	2.97085	H	-1.09531	-0.15409	3.45489
H	4.12104	2.94862	0.71894	H	3.20423	4.29266	0.04857
H	3.19944	4.29319	0.05972	H	4.91860	4.06669	-0.40742
H	4.91283	4.07340	-0.40313	H	4.12017	2.94900	0.71719
H	-1.50106	4.52236	0.67192	H	0.00143	3.79377	0.07551
H	-0.32681	3.83948	1.80904	H	-1.49533	4.52560	0.65873
H	-0.00419	3.79399	0.08472	H	-0.32317	3.84489	1.79929
H	-7.10877	0.58739	-1.85816	H	-7.10696	0.58901	-1.86079
H	-7.06950	-1.17804	-1.89063	H	-7.06956	-1.17657	-1.88761
H	-5.92655	-0.25149	-2.86796	H	-5.92536	-0.25438	-2.86758
H	3.31315	-3.07125	-2.45471	H	2.47011	-4.28540	-1.44427
H	2.48483	-4.27708	-1.44730	H	1.59067	-3.41144	-2.71681
H	1.59313	-3.41144	-2.71686	H	3.31160	-3.08303	-2.44516
N	1.98009	-2.28713	-1.02283	N	1.97638	-2.29244	-1.01961
O	-0.56317	-2.40583	1.38743	O	-0.56595	-2.40186	1.39333
O	2.68761	0.35148	0.18711	O	2.68898	0.34625	0.18392
O	4.33045	2.45518	-2.24859	O	4.33845	2.44132	-2.24744
O	0.03779	-1.64144	-2.06847	O	0.03511	-1.64435	-2.06509
O	2.01591	-0.68717	2.15436	O	2.02069	-0.68826	2.15529
O	4.77659	-1.69856	1.39027	O	4.67596	-1.78367	1.44633

**Table S3.** Isotropic shieldings of significantly populated conformers of compound **1**, average isotropic shieldings over conformers, linearly scaled calculated chemical shifts, experimental chemical shifts, and errors.

Atom	Isotropic shieldings											Chemical shifts		
	1	2	3	4	5	6	7	8	9	10	Average	Calcd.	Exp.	Error
C-1	-37.0	-32.5	-36.8	-39.2	-33.0	-36.7	-38.8	-32.7	-36.5	-31.3	-36.1	215.1	213.2	1.9
C-2	125.4	126.7	125.4	125.8	126.8	125.7	125.8	126.8	126.0	126.8	125.8	58.9	56.4	2.5
C-3	128.8	129.0	128.6	128.9	129.0	126.5	128.8	128.9	126.4	128.2	128.6	56.2	54.8	1.4
C-4	46.0	45.3	47.0	45.5	45.2	46.8	46.3	46.0	47.7	46.2	46.0	135.9	133.2	2.7
C-5	51.9	52.4	51.0	52.4	52.5	51.4	51.5	51.5	50.4	51.6	51.9	130.2	128.0	2.2
C-6	146.3	146.4	146.3	146.6	146.4	146.5	146.5	146.2	146.5	146.5	146.4	39.1	37.7	1.4
C-7	143.5	143.4	143.6	143.5	143.4	143.7	143.5	143.4	143.7	143.5	143.5	41.8	42.9	-1.1
C-8	151.2	151.2	151.1	151.3	151.2	151.3	151.2	151.0	151.1	151.2	151.2	34.4	33.5	0.9
C-9	150.7	150.6	150.7	150.7	150.6	150.8	150.7	150.5	150.8	150.7	150.7	34.9	36.0	-1.1
C-10	160.2	160.3	160.2	160.4	160.3	160.3	160.5	160.4	160.3	160.4	160.3	25.7	25.8	-0.1
C-11	148.3	147.4	148.4	147.4	147.4	148.4	147.7	147.6	148.3	147.6	148.0	37.5	37.9	-0.4
C-12	172.7	172.8	172.7	172.8	172.7	172.2	172.9	172.8	172.1	172.4	172.7	13.7	14.2	-0.5
C-13	127.1	128.0	126.2	128.6	127.9	127.8	127.6	127.0	127.0	128.3	127.4	57.3	57.0	0.3
C-14	100.7	102.0	97.4	100.1	102.1	101.2	97.1	99.2	97.8	99.3	100.3	83.5	83.7	-0.2
C-15	137.2	137.1	133.2	137.0	137.1	136.8	133.0	133.1	132.7	137.4	136.3	48.8	50.3	-1.5
C-16	-24.2	-24.1	-24.1	-23.6	-24.0	-23.9	-24.5	-24.7	-23.7	-24.3	-24.1	203.5	206.8	-3.3
C-17	155.8	155.6	159.4	155.7	155.6	155.8	159.3	159.3	159.5	155.7	156.5	29.3	30.8	-1.5
C-18	161.6	161.7	161.5	161.7	161.7	161.7	161.6	161.5	161.6	161.8	161.6	24.4	23.2	1.2
C-19	164.4	164.4	164.5	164.5	164.4	164.5	164.5	164.5	164.5	164.4	164.4	21.7	22.5	-0.8

C-2'	14.2	11.8	14.8	12.8	11.7	14.1	13.6	12.4	14.8	13.5	13.5	167.2	170.2	-3.0
C-3'	107.0	106.2	107.1	104.1	106.0	105.9	104.3	106.2	106.2	106.3	106.3	77.8	75.3	2.5
C-4'	72.7	72.6	72.5	71.1	72.6	72.3	71.0	72.3	71.7	71.7	72.3	110.5	110.3	0.2
C-5'	114.7	118.1	115.1	115.9	119.7	114.5	116.1	120.1	114.7	116.6	116.0	68.4	68.3	0.1
C-6'	126.6	123.1	126.6	126.4	123.5	127.5	126.4	123.3	127.4	124.2	125.8	58.9	60.4	-1.5
C-7'	158.6	158.6	158.6	159.1	158.5	158.7	159.1	158.5	158.7	158.5	158.7	27.2	29.5	-2.3
H-3	29.69	29.68	29.63	29.67	29.68	29.87	29.62	29.62	29.82	29.63	29.69	2.25	2.32	-0.07
H-5	26.49	26.50	26.43	26.50	26.50	26.47	26.44	26.45	26.42	26.50	26.48	5.34	5.25	0.09
H-6	30.10	30.09	30.09	30.08	30.09	30.11	30.08	30.11	30.09	30.10	30.10	1.85	1.84	0.01
H-7eq	30.22	30.23	30.19	30.24	30.23	30.22	30.19	30.19	30.19	30.23	30.22	1.74	1.82	-0.08
H-7ax	31.18	31.20	31.17	31.19	31.20	31.17	31.19	31.21	31.17	31.20	31.18	0.80	0.75	0.05
H-8	30.57	30.58	30.55	30.57	30.58	30.57	30.56	30.56	30.55	30.58	30.57	1.40	1.44	-0.04
H-9eq	30.39	30.41	30.36	30.39	30.41	30.39	30.38	30.39	30.35	30.41	30.39	1.57	1.71	-0.14
H-9ax	31.08	31.15	31.09	31.13	31.15	31.08	31.13	31.15	31.09	31.14	31.11	0.88	0.83	0.05
H-10eq	30.78	30.70	30.79	30.73	30.71	30.77	30.75	30.74	30.77	30.71	30.75	1.22	1.29	-0.07
H-10ax	30.98	31.02	30.98	31.00	31.03	30.98	31.02	31.04	30.97	31.02	31.00	0.99	1.02	-0.03
H-11	30.20	30.49	30.25	30.42	30.48	30.18	30.38	30.48	30.27	30.47	30.31	1.65	1.48	0.17
H-13	29.31	29.40	29.30	29.31	29.40	29.30	29.29	29.39	29.28	29.34	29.33	2.59	2.67	-0.08
H-14	26.89	26.91	26.94	26.82	26.91	26.88	26.87	26.97	26.91	26.75	26.89	4.94	4.90	0.04
H-15a	29.06	29.17	29.65	29.10	29.16	29.07	29.65	29.73	29.68	29.10	29.21	2.70	2.70	0.00
H-15b	29.41	29.50	29.12	29.44	29.50	29.43	29.13	29.17	29.17	29.44	29.38	2.55	2.52	0.03
H-5'	28.60	28.64	28.57	28.49	28.52	28.56	28.49	28.49	28.53	28.61	28.57	3.32	3.44	-0.12
H-6'a	28.19	28.00	28.19	27.79	27.79	28.23	27.78	27.78	28.24	27.82	28.06	3.81	3.86	-0.05
H-6'b	28.06	27.85	28.08	28.28	27.84	27.88	28.27	27.84	27.88	28.31	28.03	3.84	3.79	0.05
H <sub>3</sub> -12 <sup>b</sup>	31.02	31.03	31.01	31.02	31.03	31.02	31.02	31.03	31.01	31.01	31.02	0.96	0.88	0.08
H <sub>3</sub> -17 <sup>b</sup>	29.75	29.76	29.65	29.75	29.76	29.75	29.61	29.63	29.65	29.75	29.73	2.20	2.09	0.11
H <sub>3</sub> -18 <sup>b</sup>	30.25	30.26	30.10	30.24	30.26	30.25	30.10	30.11	30.10	30.26	30.22	1.73	1.76	-0.03
H <sub>3</sub> -19 <sup>b</sup>	31.05	31.06	31.04	31.06	31.06	31.05	31.05	31.06	31.04	31.06	31.05	0.93	0.89	0.04
H <sub>3</sub> -7' <sup>b</sup>	29.03	29.06	29.04	29.06	29.05	29.02	29.06	29.06	29.03	29.05	29.04	2.87	2.86	0.01

<sup>a</sup> Isotropic shieldings for <sup>13</sup>C were calculated at the mPW1PW91/6-311+G(2d,p) level; isotropic shielding for <sup>1</sup>H were calculated at the WP04/aug-cc-pVDZ/PCM(ACN) level.

<sup>b</sup> Isotropic shieldings of methyl protons are the arithmetic mean of the shieldings of the three protons of each methyl group.

## APPENDIX

**Table S4.** Isotropic shieldings of significantly populated conformers of compound 5'-*epi*-1, average isotropic shieldings over conformers, linearly scaled calculated chemical shifts, experimental chemical shifts, and errors.

Atom	Isotropic shieldings <sup>a</sup>												Chemical shifts		
	1	2	3	4	5	6	7	8	9	10	11	Average	Calcd.	Exp.	Error s
C-1	-30.9	-30.6	-36.7	-30.4	-30.6	-36.9	-30.8	-31.4	-31.1	-31.2	-30.9	-32.0	211.7	213.2	-1.5
C-2	127.0	127.6	126.3	128.5	127.6	125.5	127.0	126.7	126.8	126.8	126.8	127.1	57.9	56.4	1.5
C-3	129.1	129.0	128.8	127.3	126.7	128.7	129.1	129.2	129.2	129.1	129.1	128.6	56.5	54.8	1.7
C-4	46.2	47.1	47.1	47.9	47.0	46.6	45.7	45.2	45.3	46.3	46.3	46.7	135.5	133.2	2.3
C-5	51.8	50.7	51.0	50.0	51.1	51.7	52.0	52.4	52.3	51.6	51.5	51.2	131.2	128.0	3.2
C-6	146.2	146.4	146.6	146.7	146.6	146.5	146.4	146.3	146.3	146.2	146.2	146.4	39.2	37.7	1.5
C-7	143.5	143.6	143.8	143.6	143.6	143.8	143.3	143.2	143.2	143.4	143.4	143.6	42.0	42.9	-0.9
C-8	151.2	151.1	151.1	151.1	151.3	151.1	151.2	151.2	151.1	151.0	151.0	151.2	34.7	33.5	1.2
C-9	150.4	150.5	150.8	150.5	150.5	150.8	150.4	150.4	150.4	150.3	150.3	150.5	35.3	36.0	-0.7
C-10	160.4	160.4	159.9	160.5	160.5	159.8	160.5	160.5	160.4	160.3	160.3	160.3	25.8	25.8	0.0
C-11	147.3	147.5	148.8	147.2	147.3	148.7	147.4	147.5	147.5	147.5	147.5	147.7	38.0	37.9	0.1
C-12	172.8	172.7	173.0	172.0	172.2	173.1	172.9	173.0	173.0	172.9	172.9	172.7	13.8	14.2	-0.4
C-13	129.0	127.2	127.4	128.2	129.9	129.4	128.6	128.2	128.2	127.4	127.4	128.3	56.7	57.0	-0.3
C-14	100.3	98.2	97.2	99.0	100.5	98.7	101.1	101.7	101.9	98.6	98.7	99.3	84.8	83.7	1.1
C-15	137.1	137.0	136.6	137.3	136.8	136.9	137.0	137.3	137.1	133.2	133.2	136.9	48.4	50.3	-1.9
C-16	-24.3	-28.0	-28.3	-28.6	-24.2	-23.5	-24.7	-23.9	-24.3	-24.8	-25.2	-26.1	205.9	206.8	-0.9
C-17	156.1	156.6	156.7	156.4	156.0	156.1	156.0	155.9	155.9	159.3	159.3	156.4	29.6	30.8	-1.2
C-18	161.7	161.8	161.9	161.7	161.8	161.8	161.6	161.6	161.7	161.5	161.5	161.7	24.4	23.2	1.2
C-19	164.3	164.4	164.5	164.5	164.4	164.4	164.4	164.4	164.4	164.5	164.4	164.4	21.9	22.5	-0.6
C-2'	12.9	13.4	13.9	13.5	13.0	13.4	12.7	11.7	11.6	12.5	12.3	13.1	168.0	170.2	-2.2
C-3'	106.7	106.6	104.9	106.1	105.8	104.7	106.6	106.6	106.8	106.8	107.0	106.1	78.2	75.3	2.9
C-4'	71.4	71.9	71.7	70.1	70.0	71.4	72.9	73.5	73.6	73.0	73.1	71.5	111.6	110.3	1.3
C-5'	119.0	116.7	114.5	118.3	120.9	117.1	119.8	119.3	121.7	119.4	121.6	118.0	66.7	68.3	-1.6
C-6'	127.5	128.0	127.9	127.9	126.9	127.1	121.7	123.3	123.4	123.3	123.3	127.0	58.0	60.4	-2.4
C-7'	160.3	159.9	159.7	159.6	160.1	160.2	159.9	160.0	160.0	159.9	159.9	160.0	26.1	29.5	-3.4
H-3	29.60	29.65	29.73	29.85	29.85	29.72	29.65	29.65	29.65	29.58	29.59	29.69	2.24	2.32	-0.08
H-5	26.47	26.45	26.46	26.42	26.44	26.47	26.48	26.50	26.50	26.46	26.46	26.46	5.35	5.25	0.10
H-6	30.09	30.10	30.13	30.10	30.09	30.14	30.12	30.13	30.12	30.13	30.13	30.11	1.84	1.84	0.00
H-7eq	30.22	30.21	30.20	30.21	30.21	30.20	30.21	30.21	30.21	30.20	30.21	30.21	1.74	1.82	-0.08
H-7ax	31.18	31.17	31.13	31.19	31.19	31.13	31.21	31.22	31.22	31.21	31.21	31.17	0.81	0.75	0.06
H-8	30.57	30.56	30.56	30.56	30.57	30.57	30.57	30.57	30.57	30.55	30.55	30.57	1.40	1.44	-0.04
H-9eq	30.37	30.34	30.36	30.33	30.37	30.38	30.38	30.38	30.38	30.34	30.33	30.36	1.60	1.71	-0.11
H-9ax	31.12	31.14	31.11	31.14	31.13	31.10	31.14	31.14	31.14	31.13	31.13	31.13	0.86	0.83	0.03
H-10eq	30.69	30.69	30.84	30.65	30.68	30.87	30.74	30.74	30.73	30.76	30.76	30.73	1.25	1.29	-0.04
H-10ax	31.00	30.98	30.97	30.98	30.99	30.98	31.03	31.03	31.03	31.01	31.01	30.99	0.99	1.02	-0.03
H-11	30.54	30.64	30.37	30.66	30.57	30.28	30.48	30.47	30.48	30.54	30.54	30.53	1.44	1.48	-0.04
H-13	29.35	29.30	29.30	29.30	29.35	29.33	29.39	29.40	29.40	29.35	29.35	29.33	2.59	2.67	-0.08
H-14	26.81	27.30	27.28	27.28	26.76	26.77	26.85	26.86	26.86	26.90	26.91	27.03	4.80	4.90	-0.10
H-15a	29.30	28.92	28.92	29.05	29.35	29.28	29.34	29.40	29.39	29.13	29.12	29.15	2.77	2.70	0.07
H-15b	29.02	29.87	29.84	29.88	29.04	29.01	29.03	29.08	29.08	29.67	29.67	29.44	2.49	2.52	-0.03
H-5'	28.37	28.41	28.65	28.47	28.44	28.61	28.10	28.20	28.14	28.19	28.12	28.42	3.46	3.44	0.02
H-6'a	27.92	27.95	27.87	27.85	27.82	27.85	28.06	27.84	27.83	27.85	27.83	27.90	3.97	3.86	0.11
H-6'b	28.20	28.22	28.24	28.23	28.21	28.24	28.27	28.23	28.01	28.26	28.05	28.21	3.66	3.79	-0.13
H <sub>3</sub> -12 <sup>b</sup>	31.06	31.05	31.05	31.06	31.05	31.07	31.06	31.06	31.06	31.04	31.04	31.06	0.93	0.88	0.05
H <sub>3</sub> -17 <sup>b</sup>	29.76	29.59	29.57	29.57	29.77	29.74	29.74	29.74	29.75	29.62	29.62	29.67	2.26	2.09	0.17
H <sub>3</sub> -18 <sup>b</sup>	30.26	30.12	30.12	30.11	30.25	30.27	30.24	30.24	30.24	30.08	30.08	30.19	1.77	1.76	0.01
H <sub>3</sub> -19 <sup>b</sup>	31.04	31.04	31.05	31.04	31.04	31.04	31.05	31.05	31.05	31.05	31.05	31.04	0.94	0.89	0.05
H <sub>3</sub> -7' <sup>b</sup>	28.96	28.94	28.95	28.93	28.96	28.99	29.14	29.15	29.14	29.14	29.13	28.98	2.93	2.86	0.07

<sup>a</sup> Isotropic shieldings for <sup>13</sup>C were calculated at the mPW1PW91/6-311+G(2d,p) level; isotropic shielding for <sup>1</sup>H were calculated at the WP04/aug-cc-pVDZ/PCM(ACN) level.

<sup>b</sup> Isotropic shieldings of methyl protons are the arithmetic mean of the shieldings of the three protons of each methyl group.

**Table S5.** Selected coupling constants of compounds **1** and **5'-epi-1** calculated at the B3LYP/6-31G(d,p) level and relative intensities of the corresponding HMBC peaks.

Compound <b>1</b>						
Conformer	Population	H-5'/C-2'	H-5'/C-3'	H-5'/C-4'	H-5'/C-6'	H-5'/C-7'
1	38.7%	4.8	1.7	-5.3	4.0	0.9
2	13.0%	3.7	1.6	-4.7	-2.3	1.5
3	11.1%	4.8	1.7	-5.4	4.0	0.9
4	10.8%	2.7	1.2	-5.6	4.4	1.8
5	8.2%	3.8	1.7	-4.8	-3.1	1.5
6	7.5%	5.5	1.5	-5.9	3.2	0.8
7	4.1%	2.6	1.2	-5.7	4.4	1.8
8	3.3%	3.8	1.7	-4.9	-3.2	1.5
9	2.2%	5.6	1.5	-5.9	3.2	0.8
10	1.2%	4.6	2.2	-5.1	-2.9	1.4
<b>Average coupling (Hz)</b>		<b>4.3</b>	<b>1.6</b>	<b>-5.3</b>	<b>2.2</b>	<b>1.2</b>
Compound <b>5'-epi-1</b>						
Conformer	Population	H-5'/C-2'	H-5'/C-3'	H-5'/C-4'	H-5'/C-6'	H-5'/C-7'
1	22.7%	0.4	-0.2	-2.7	3.8	0.0
2	21.0%	0.8	-0.3	-2.6	3.9	0.2
3	13.1%	0.9	-0.4	-2.2	2.9	0.2
4	12.4%	0.8	-0.4	-2.8	2.8	0.2
5	8.5%	0.4	-0.3	-2.7	3.0	0.1
6	8.4%	0.5	-0.3	-2.2	3.0	0.1
7	3.9%	0.7	-0.2	-2.4	-0.5	0.4
8	3.8%	0.2	-0.1	-2.2	-2.5	0.2
9	3.4%	0.2	-0.1	-2.3	-3.0	0.2
10	1.5%	0.2	-0.1	-2.1	-2.6	0.2
11	1.3%	0.2	-0.1	-2.1	-3.1	0.2
<b>Average coupling (Hz)</b>		<b>0.6</b>	<b>-0.3</b>	<b>-2.5</b>	<b>2.6</b>	<b>0.2</b>
HMBC experiment (optimized for $J_{CH} = 8$ Hz)						
Relative peak intensity	H-5'/C-2'	H-5'/C-3'	H-5'/C-4'	H-5'/C-6'	H-5'/C-7'	
	<b>0.822</b>	<b>0.149</b>	<b>1.000</b>	<b>0.177</b>	<b>0.072</b>	

**Table S6.** Bioactivity of Kupchan subextracts (KM, KC, KH) and C18 SPE fractions (F0-F10) obtained from *Pyrenochaetopsis* FVE-087 against cancer cell lines (A-375, A-549, HT-29, HCT-116, MB-231) and HaCaT cells. The activity is expressed as % inhibition at 100  $\mu$ g/mL test concentration. Reference compound: Doxorubicin.

Sample	A-375	A-549	HT-29	HCT-116	MB-231	HaCaT
KM	0	0	0	0	0	0
KC	99	99	84	99	99	98
KH	69	35	99	34	0	64
F0	0	0	0	0	0	0
F1	0	0	0	0	0	0
F2	0	0	0	0	0	0
F3	0	0	0	0	0	0
F4	0	0	0	0	23	0
F5	0	0	0	0	43	20
F6	43	0	0	0	33	45
F7	<b>98</b>	99	99	99	99	98
F8	<b>95</b>	49	74	67	68	78
F9	<b>98</b>	99	99	99	99	98
F10	27	0	0	28	66	25
Reference	88	73	63	90	84	91